CENTRO INTERNACIONAL DE ESTUDOS
DE DOUTORAMENTO E AVANZADOS
DA USC (CIEDUS)

TESIS DOCTORAL

APPLICATION OF TWO ORTHOGONAL CLICK-TYPE REACTIONS FOR THE PREPARATION OF CYCLIC PEPTIDES WITH ANTIBACTERIAL AND ANTICANCER ACTIVITY

Eva González Freire

ESCUELA DE DOCTORADO INTERNACIONAL

PROGRAMA DE DOCTORADO EN CIENCIA Y TECNOLOGÍA QUÍMICA

SANTIAGO DE COMPOSTELA

AÑO 2019

USC
UNIVERSIDADE
DE SANTIAGO
DE COMPOSTELA

DECLARACIÓN DEL AUTOR DE LA TESIS

APPLICATION OF TWO ORTHOGONAL CLICK-TYPE REACTIONS FOR THE PREPARATION OF CYCLIC PEPTIDES WITH ANTIBACTERIAL AND ANTICANCER ACTIVITY

D.ª Eva González Freire

Presento mi tesis, siguiendo el procedimiento adecuado al Reglamento, y declaro que:

1) La tesis abarca los resultados de la elaboración de mi trabajo.
2) De ser el caso, en la tesis se hará referencia a las colaboraciones que tuvo este trabajo.
3) La tesis es la versión definitiva presentada para su defensa y coincide con la versión enviada en formato electrónico.
4) Confirmo que la tesis no incurre en ningún tipo de plagio de otros autores ni de trabajos presentados por mí para la obtención de otros títulos.

En Santiago de Compostela, ... de ..... de 2019

Fdo.

USC
UNIVERSIDADE
DE SANTIAGO
DE COMPOSTELA

AUTORIZACIÓN DEL DIRECTOR/ TUTOR DE LA TESIS

APPLICATION OF TWO ORTHOGONAL CLICK-TYPE REACTIONS FOR THE PREPARATION OF CYCLIC PEPTIDES WITH ANTIBACTERIAL AND ANTICANCER ACTIVITY

D. Juan Ramón Granja Guillán
D. Manuel Amorín López

INFORMAN:

Que la presente tesis se corresponde con el trabajo realizado por D.ª Eva González Freire, bajo nuestra dirección, y autorizamos su presentación, considerando que reúne los requisitos exigidos en el Reglamento de Estudios de Doctorado de la USC, y que como directores de esta no incurre en las causas de abstención establecidas en la Ley 40/2015.

En Santiago de Compostela, ... de ..... de 2019

Fdo. Juan R. Granja

Fdo. Manuel Amorín

USC
UNIVERSIDADE
DE SANTIAGO
DE COMPOSTELA

Agradecimientos

En primer lugar, me gustaría dar las gracias a los directores de esta tesis doctoral, Juan R. Granja y Manuel Amorín, por brindarme la oportunidad de participar en este proyecto. Por ser buenos directores y buenas personas. También, por todo el apoyo profesional y personal a lo largo de estos años, por todo lo aprendido, y por toda vuestra dedicación.

Al profesor Rafael Seoane y a Antonio Pérez Estévez, por haber sido como unos directores de estas tesis. Por enseñarme todo lo que se de trabajar con bacterias y por todo vuestro apoyo.

A Luis Castedo, Javier Montenegro y Rebeca Fandiño, por su consejos y apoyo a lo largo de todo este trabajo. Además, agradecer a Rebeca y Martin por los estudios computacionales realizados para este trabajo.

A las instituciones que han financiado esta investigación, al Ministerio de Economía y Competitividad (CTQ2013-43264-R, CTQ2016-78423-R), a la Xunta de Galicia y al Fondo Europeo de Desarrollo Regional (EM2014/011, ED413 2017/25). Además, agradecer de nuevo a la Xunta de Galicia por mi beca predoctoral (ED481A-2017/044). Y a la fundación Barrié por haberme dado la oportunidad de realizar una estancia predoctoral.

Al profesor Toni Davis, por haberme dado la oportunidad de realizar una estancia predoctoral en la Universidad de Bristol, y a todos los miembros de su grupo, por su cariño y buena acogida, en especial a Robert y Ashley por ayudarme en el laboratorio. Y a Alberto, por su amistad dentro y fuera del laboratorio.

A la profesora Margarida Bastos y a Barbara Claro, así como al resto de su grupo de investigación en la Universidad de Porto, por sus estudios biofísicos de varios de los péptidos preparados en esta tesis, además de por su excelente trabajo y su gran compañerismo.

A la profesora Concepción Bello y a la doctora Verónica Prado por la síntesis del gamma-aminoácido dihidroxilado utilizado en la síntesis de péptidos que incorporan dicho residuo en el esqueleto peptídico.

A la profesora Ana Otero y a la doctora Andrea Muras por enseñarme a usar y facilitarme el uso del equipo xCELLigence®.

A la profesora Mabel Loza, Jose Manuel Brea y Jose Manuel Santamaría, así como a los miembros de su grupo, por los ensayos de los péptidos con doxorrubicina.

Al doctor Juan J. Reina y a Alicia Rioboo por la síntesis de los sacáridos derivados con un grupo aldehído utilizados en esta tesis.

A la doctora Federica Novelli, con quien compartí este proyecto en el último año. Gracias por todo el trabajo realizado, por todo lo que me has enseñado, pero sobre todo por tu apoyo y amistad.

A la RIAIDT de la Universidad de Santiago de Compostela por poner a mi disposición sus medios técnicos para el desarrollo de este proyecto. Quiero destacar a los miembros del CIQUS, en especial a los técnicos que facilitan nuestra labor a diario. También al servicio técnico de RMN, a Ramón y Mencha. A María, porque sin ella no podríamos hacer todo lo que hacemos. A Patricia, que solventa todos nuestros problemas administrativos y que además lo hace con el

todo el cariño y con la mejor sonrisa. Y, en especial, a Arcadio, que además de ser un excelente técnico, ha sido compañero de laboratorio, mentor y amigo durante todos estos años.

A todas las personas con las que he compartido tantas horas en el CIQUS, en especial a mis compañeros de laboratorio: Noel, Jorge, Nuria, Lionel, Juanillo, Marta, Iván, Lamas, Ale, Héctor, Alfonso, Angel, Ezequiel, Marcos, Guilia, Iría, Julián, Nacho, Rebeca, Sandra, Victoria, Irene, Geert, Ghibom y Richard. Y, por último, a Marisa y a Alberto, con los que empecé esta aventura hace tantos años y en la que me han ayudado tanto.

A Esteban, a Álvaro y a Renata, por vuestra amistad, aunque no compartamos laboratorio.

A todos los miembros de la panadería Leal, por su apoyo en todos los momentos difíciles y por ser ya una parte de mi familia.

A mi profesora de lengua, Lourdes, por creer en mi cada día y por tu cariño todos estos años. A Carmiña y al grupo de costura, por todo su cariño durante tantos años.

A Ana, mi compañera de piso y mi amiga.

A mis amigos, Ana y Javi, por todas las horas de biblioteca compartidas, por las risas, por los buenos momentos y por los momentos difíciles que pasamos juntos. Por todos los momentos que vinieron después y espero que sigan llegando.

Al resto de mis amigos, Maika, Diego, Toño, Migui, Ana, Aitor, Hugo, Andrea, Toste y Majo, por haberme aceptado tal como soy y por el apoyo recibido. A Charlie, por estar siempre ahí. A Mely, Sonia y María, por ser como sois.

A todos aquellos de los que me haya podido olvidar, y que hayan contribuido de algún modo en la elaboración de este trabajo.

A Javi, por todos estos años compartidos, por tu apoyo, paciencia, comprensión. Te podría escribir mil líneas, pero me conformo con citar a gritando en silencio: “porque no hay guerras civiles si echamos el pestillo, y aunque siga siendo cutre, el mundo ya no es un ladrillo, setecientos treinta y tantos días de tu sonrisa, haciendo que la vida no sea papel de lija.”

A Marisé, Milucho y Jacobo, por acogerme en vuestra familia.

A mi familia, que ha estado a mi lado incondicionalmente. A mi abuelo que ya no está y a mi abuela Rosita. A mis tíos Juanjo y Ángeles y mis primos Juanjo y Paula por su cariño. A mis tíos Fran y Carmen, por todas las tardes de café, los momentos compartidos y por todo el apoyo y cariño. A mi prima Marta, a su mujer, Iría, y a la pequeña Olivia, por romper barreras y enseñarnos a todos como es la felicidad. A mis padres, que me han priorizado siempre la educación de sus hijos y que me han ensañado a perseguir mis sueños, hoy son reales gracias a vosotros. A mi hermano Dani y a Patri por enseñarme cada día a ser mejor. Y, por último, a mi hermana Lucía, siempre serás mi “one for all”.

A mis padres

USC
UNIVERSIDADE
DE SANTIAGO
DE COMPOSTELA

Index

Abbreviations

Aas	amino acids
Aiha	α-amino-β-[4´-(2´-iminoimidazolidinyl)]-β-hydroxypropionic acid
AIPs	autoinducer peptides
AMP	antimicrobial peptide
BHB	Bushnell Haas broth
BHI	brain heart infusion broth
Boc	*tert*-butoxycarbonyl
c-di-GMP	3´,5´-cyclic diguanylic acid
CAC	critical aggregation concentration
CA-MRSA	community-associated methicillin resistance *Staphylococcus aureus*
CF	cystic fibrosis
CFU	colony-forming unit
CNTs	carbon nanotubes
CP	cyclic peptide
CPP	cell-penetrating peptide
CSLM	confocal laser scanning microscope
CTC	Chlorotrityl chloride resin
CuAAC	Cu^{I}-catalysed azide/alkyne cycloaddition
DIEA	*N*,*N*-diisopropylethylamine
DMAP	4-dimethylaminopyridine
DPA	2,3-diaminopropionic acid
DNA	deoxyribonucleic acid
DOX	doxorubicin
DSC	differential scanning calorimetry
ED	effective dose
EDC·HCl	*N*-(3-dimethylaminopropyl)-*N´*-ethylcarbodiimide hydrochloride
eDNA	extracellular deoxyribonucleic acid
EPS	exopolysaccharides
ESI-MS	electrospray ionization mass spectrometry

FBS	fetal bovine serum
FDA	Food and Drug Administration
Fmoc	Fluorenylmethyloxycarbonyl
FRET	Fluorescence Emission Energy Transfer process
FTIR	Fourier-transform infrared spectroscopy
^{1}H-NMR	proton nuclear magnetic resonance
HCD	high cell density
HD	hemolytic dose
HD_{50}	50% of hemolytic dose
HDP	host defense peptides
HER	human epidermal receptor
HFIP	1,1,1,3,3,3-hexafluoroisopropanol
HOBt	hydroxybenzotriazole
HP	homing peptides
HPLC	high-performance liquid chromatography
HSV	herpes simplex virus
Lac	lactic acid
LCD	low cell density
LD	lethal dose
LPS	lipopolysaccharide
MBC	minimal bactericidal concentration
MD	molecular dynamics
Mephe	β-methylphenylalanine
MHB	Muller-Hilton Broth
MIC	minimal inhibitory concentration
MIC_{50}	50% of minimal inhibitory concentration
MBIC	minimal biofilm inhibitory concentration
MRSA	methicillin resistance *Staphylococcus aureus*
MS	mass spectrometry
M_w	molecular weight
Mtt	4-methyltrytil (protecting group)

MTT	3-(4,5-dimethylthiazol-2-yl)-2,5-diphenyltetrazolium bromide
*N*AcGlc	*N*-acetylglucosamine
N-HATU	Hexafluorophosphate Azabenzotriazole Tetramethyl Uronium
N-HBTU	Hexafluorophosphate Benzotriazole Tetramethyl Uronium
N-TBTU	2-(1H-benzotriazol-1-yl)-1,1,3,3-tetramethyluronium tetrafluoroborate
Orn	ornithine
PBP	penicillin-binding proteins
PC	phosphatidyl choline
PE	phosphatidyl ethanolamine
PEG	poly(ethylene glycol)
PG	phosphatidyl glycerol
PMA	polymeric anhydride
Pra	proparlgylglycine
PRSA	penicillin-resitant *Staphylococcus aureus*
PS	phosphatidyl serine
PyAOP	(7-azabenzotriazol-1-yloxy)tripyrrolidinophosphonium hexafluorophosphate
QS	quorum sensing
RBC	red blood cell (human erythrocytes)
Redox	reduction-oxidation
RNA	ribonucleic acid
SCPNs	self-assembling cyclic peptide nanotubes
SM	sphingomyelin
SMAMPs	synthetic mimics of antimicrobial peptides
SPPS	solid phase peptide
STEM	scanning transmission electron microscopy
TBTA	Tris[(1-benzyl-1H-1,2,3-triazol-4-yl)methyl]amine
TEM	transmission electron microscopy
TFA	trifluoroacetic acid
TFE	2,2,2-trifluoroethanol
TIS	triisopropylsilane
TLC	thin-layer chromatography

TNBC	triple negative breast cancer
TOCSY	total correlation spectroscopy
VISA	vancomycin intermediate-resistant *Staphylococcus aureus*
VRE	vancomycin resistant enterococci
VRSA	vancomycin resistant *Staphylococcus aureus*
WHO	world health organization

Summary

The discovery of penicillin in 1928 and later appearance of cephalosporins, quinolones, macrolides and tetracyclines gave rise to "golden era of antibiotics". The distribution of this antibiotics generated the popular believe that the battle against bacteria was won. However, bacteria managed to develop new defence mechanism, leading to useless antibiotic. This is what is known as bacterial resistance, which appeared few years after the distribution of each antibiotic (or even before as in the case of penicillin). Nowadays, there are bacteria stains that are resistant to multiple drugs, superbugs, which treatment is very difficult.

Generally, antibiotics can be classified by its structure (penicillins, cephalosporins, etc.), by its evolution from the original drug (1^{st}, 2^{nd}, 3^{rd} generation, etc.) or by its action mechanism. Those can be: i) inhibition of the cell wall biosynthesis, ii) inhibition of protein biosynthesis, iii) inhibition of DNA and RNA biosynthesis, iv) folic acid metabolism inhibition, and v) cell membrane attachment. There is one type of resistant for each mechanism. Thus, the most famous one is the development of *β*-lactamases, enzymes able to open the *β*-lactam ring of the penicillin.

The first strain to show resistance to penicillin was *Staphylococcus aureus*, which infection was treated with methicillin, antibiotic used against penicillin-resistant Gram-positive bacteria. However, after long exposure time, the bacteria developed immunity against this antibiotic, leading to the methicillin-resistant *S. aureus* (MRSA). MRSA, resistant to penicillin and methicillin, is nowadays also resistant to other antibiotics, leading to very few options for treatment. Currently, MRSA is treated with vancomycin, considering a last resort antibiotic, although it has been detected resistance to this antibiotic since 2002.

The resistance to antibiotics problem is increasing by biofilm formation. Previously, it was believed that infection was caused by planktonic bacteria cells, in other words, bacteria acting in an isolated and independently way. However, since 80s and 90s, it was demonstrated that bacteria are organized in a kind of community. Biofilm is formed by a organized community of bacteria that are enclosed in a self-produced polymeric matrix. The most famous biofilm is the one that is generated in the mouth, known as bacterial plaque. The biofilm protects the bacteria in hostile environments, acting as a barrier which is an intrinsic way of resistance. Usually, antibiotics destroy planktonic bacteria that are releasing from the biofilm, but they are not able to destroy the biofilm itself. In other words, antibiotics kill the bacteria that generate the infection but not the source of the infection, being necessary to repeat the process several times, which can also lead into a resistance. The study of biofilms as well as the searching for antibiotics that can remove them has gained huge relevance in recent years.

Despite the "use of antibiotic" regulation has been a key factor to slow down the development of resistant strains, the world health organization (WHO) communicated the worrying situation about the lack of efficiency antibiotics in 2014, which has been called the pot-antibiotic era since 2016. In 2017, the world health organization published a list of priority pathogens for what is urgent to develop new antibiotics. This list includes Gram-positive bacteria, such as resistant to methicillin and vancomycin *S. aureus*, as well as Gram-negative bacteria, such as carbapenem-resistant *Pseudomonas aeruginosa*. Nowadays, the lack of antibiotics caused 700.000 deaths per year, but it is expected to reach 10 million deaths every year in 2050. The problem is increased by the cost of developing a drug, which limits that the drug reaches the last clinical phases for its approval.

At the present time, there are two pathways to obtain an antibiotic: the modification of already known antibiotics or the development of new compounds. This last one is the most promising due to it involves the discovery of new mechanisms of action for which the bacteria are not yet ready. However, this strategy is more tedious and costly because it requires going through all stages of pre-clinical and clinical studies. A hybrid strategy has been developed with antimicrobial peptides, in which certain natural structures are employed and transformed into completely different structures. Antimicrobial peptides exist in nature and act as first line of defence against microorganisms in different species as insects, plants and animals, including humans. There are hundreds of distinct antimicrobial peptides, which generally share a number of characteristics. They are small peptides (with less than 50 amino acids), positively charged and composed by hydrophilic and hydrophobic amino acids, which results in an amphipathic structure. Moreover, these peptides have a well-defined secondary structure, whether is a α-helix or a β-sheet. The more accepted mechanism for these compounds relies on the electrostatic interaction between the positive charges of the antimicrobial peptides with the negative charges of the cell membrane, in such a way that the peptide is placed on the top of the membrane in a carpet-like mechanisms. When the peptide reaches the bacterial membrane is able to generate a pore and cause the death of the cell by breaking the ionic balance or releasing the cell content.

Our group is pioneer in the synthesis and study of cyclic peptides that present the property of assembly to form peptide nanotubes. This self-assembly is due the alternating chirality of the amino acids that constituted the cyclic peptide, resulting in a planar disposition of the cyclic peptide. In this conformation, the carbonyl and amide groups are oriented perpendicular to the plane of the ring, so each cyclic peptide can interact by both faces of the ring with another cyclic peptide through the hydrogen bond interaction, achieving the nanotube structure. The properties of the nanotube can be modified by the selection of the amino acid that constitute the cyclic peptide. Furthermore, the number of amino acids used in the structure determines the diameter of the nanotube, so the properties can also be modulated by the number of amino acids that are present in the cyclic peptide. Thus, the control of the diameter allows the formation of structures with the ability of encapsulate molecules in its inside. The use of only hydrophobic amino acids can lead into nanotubes with the ability of forming pores in lipidic membranes, while the use of hydrophobic and hydrophilic amino acids leads to amphipathic structures, which can have antimicrobial properties when present a positive charge.

There has been prepared several cyclic peptides with antimicrobial properties, with 6 or 8 amino acids, using lysine, histidine or arginine in the hydrophilic side and mostly tryptophan and leucine in the hydrophobic side. Although at the beginning the proposed peptides present a higher hydrophobic side, with 5 amino acids, the reduction to 3 amino acids results in good results against bacteria as well. The relevant characteristic of these compounds was the reduction of toxicity presented in the haemolysis assays, where the toxicity was reduced until 4 folds compare with the 5 hydrophobic amino acid cyclic peptides. The introduction of different saccharides in the structure increase the selective of the cyclic peptides towards bacteria instead of human cells. Between all the peptides with saccharides in their structures, it is worth to mention the mannopeptimycin family. These compounds have been widely studied and some of their derivatives has been shown amazing activities. However, it seems that this family of compounds has not been further developed.

The objective of these thesis approaches the development of a new synthetic strategy that lets the obtention of a peptide library in an easy and fast way for its study as potential antimicrobial agents. This strategy has been focused in the design of cyclic peptides with two anchor points that allow their modification in the last steps of the synthesis. These anchor points were used alternatively for the introduction of aliphatic tails of different lengths and the post incorporation of diverse saccharides. Specifically, the cyclic peptides were constituted by 8 amino acids with no more than 3 hydrophobic residues. The propargylglycine amino acid was introduced as one of the anchor points due to the [3+2] cycloaddition reaction catalysed by copper (click reaction) allows the conjugation in a chemo-selective manner of the azide substituents. The other anchor point was the introduction of an alkoxyamine in the side chain of a lysine to get an oxime bond. Depending on the position of these two reactive groups in the hydrophilic or in the hydrophobic side of the cyclic peptide, two platforms were design. Thus, two different cyclic peptides were proposed as a model, **CP-A** (with the alkyne in the hydrophobic side) and **CP-B** (where it was in the centre of the hydrophilic side). The antimicrobial activity of these peptides was tested against Gram-positive bacteria, *S. aureus* and *S. epidermidis*, and Gram-negative bacteria, *E. coli*. Once the most active platform was determined, the effects of the different substituents were studied to determine their effects on the antimicrobial activity. Moreover, the most active peptides would be tested against *S. aureus* biofilm. The last objective of this work is the study of these compounds as possible anticancer agents, taking advantage of the alkoxyamine in the structure to anchor anticancer compounds and rise a combine therapy.

In the first chapter of this thesis we have developed the synthetic methodology for the preparation of these compounds, optimizing the solid phase synthesis of the cyclic peptides, the [3+2] cycloaddition reaction, the incorporation of the alkoxyamine and the oxime bond formation. Furthermore, for the synthetic alternative in which the triple bond is in the hydrophilic side, a *D*-mannose derivative with an azide was synthesized to carry out the [3+2] cycloaddition reaction. On the other hand, for the alternative where the alkoxyamine is the anchor point of the hydrophilic side, the methyl-alkoxyamine was synthesized to attach the saccharide in a close conformation. However, we would not be able to carry out the condensation reaction between the sugar and the methyl alkoxyamine in an efficient manner, so we decided to carry out the reaction with the commercial saccharide, leading to an open conformation, or with the aldehyde derivative (prepared in the group for another project), leading to the close conformation. The synthetic obstacles found in this chapter was solved by carrying out the [3+2] cycloaddition reaction as well as the introduction of the alkoxyamine in the solid support. Both reactions can be done indistinctively, first the introduction of the alkoxyamine and then the [3+2] cycloaddition reaction or vice versa. However, the introduction of the saccharide was carried out in solution in the last step of the synthesis.

In this chapter we also optimized the conditions to test the activity of the compounds against bacteria. After the optimization process, the compounds derived from **CP-B**, where the alkoxyamine is in the hydrophobic side of the peptide ring, were tested. The results showed that these compounds present a low activity compared with **CP-A**, so we decided to dismiss the platform **CP-B**. The position of the alkoxyamine in **CP-A** was also tested, leading to the conclusion that the difference was too small to distinguish between then. Finally, we decide to work just with **CP-A1** and **CP-A2** in next chapter.

In the second chapter, a library of compounds was synthesised. Firstly, different aliphatic tails were introduced in the peptide backbone derived from **CP-A**. The study of these compounds as antimicrobial agents determined that the optimal length to achieve the maximum activity was ten and fourteen carbon atoms. The next step, the introduction of the saccharide, was carried out with two of the peptides that show the best antimicrobial activities, **CP-A1$_{14}$** and **CP-A2$_{10}$**. These peptides were condensate with the aldehydes derivates from *D*-glucose, *D*-mannose, *D*-galactosamine and *D*-maltose. All the peptides with the saccharides showed lower activity than the peptides without them. Nevertheless, the toxicity of peptide **CP-A1$_{14}$** was completely reduced in the presence of the saccharide at the maximum concentration tested. Peptide **CP-A2$_{10}$** did not show toxicity at any concentration tested, neither its derivates with saccharides.

Our next step in the optimization of the peptide was the substitution of central residue of hydrophilic side, which seems to be a key position in platform **CP-A** biological activity. For this purpose, we decided to change the lysine with the alkoxyamine in **CP-A1** for other basic residues, such as arginine, ornithine and 2,3-diaminopropionic acid. The good results obtained with these compounds derived with the aliphatic chains, with MIC values around to one milligram per millilitre that are similar to those obtained with the best AMPs, leaded us to a more exhaustive study, in which the nanotube formation could be determined by different techniques, such as fluorescence and/or STEM. Among a large characterization, these cyclic peptides were tested against other bacteria to see the scope of their activity. The mechanism of action studies confirmed a fast-bactericidal activity (15-20 min), that suggest that the modo of action is not based on a therapeutic target. These results confirmed the activity against Gram-positive bacteria that can significantly vary depending on the type of bacteria. Finally, some of them were use in the activity assay against biofilms. Two assays were carried out with *S. aureus* biofilms. On the one hand, the bactericidal activity was measured against a mature biofilm. Interestingly, most of the compounds showed high activity against biofilms, reaching a MBIC values of 20 folds the MIC. On the other hand, the inhibition of the formation of the biofilm was also measured. Despite the peptides do not present a specific mechanism against the formation of the biofilm, the quick action of the peptide demonstrates to kill the planktonic bacteria before the biofilm is created, which means the cyclic peptides can be used to prevent the formation of the biofilm.

Lastly, we decide to prepare a series of compounds were the saccharide is inside the cyclic peptide skeleton. The first studies shown a low activity compared to their analogue without the saccharide, although further studies are necessary to determine the validity of this strategy.

In the third chapter, we decided to explore the anticancer properties or as vehicles for other drugs with the most active compounds. There are several structures with the ability to transport a drug to its target, known as drug delivery systems. Between all the systems studied, it is worthy to mention the cell penetrating peptides (CPPs) are worth to mention. These peptides present an amphipathic structure similar to the antimicrobial peptides. Therefore, we thought that our cyclic peptides could be an analogue behaviour. For this chapter, we decide to carry out cytotoxicity assays for the peptides prepared before and for those conjugated with doxorubicin, which is a widely used drug as a model in many cell studies due to its biological activity and spectroscopic properties. Between all type of cancer, we choose breast cancer due to the high number of patients that are recorded every year, which is the second in the most diagnostic cancer in the world, and ovarium cancer, which present a high mortality rate (over a 62% of the affected patients) even though it is not one of the most diagnosticated one. Current

breast cancer options belong to a family of compounds known as anthracyclines and its cardiotoxicity is so high that the used of the drug is limited and treatment is interrupt in some cases. To reduce the toxicity of these family of compounds, nanocarriers have been design and develop to encapsulate the drug and deliver it to their action points, reducing their side effects. A way of releasing a drug is through an external stimulus, which can be a changed in the temperature or in the pH. The dynamic covalent bonds, such as imines, hidrazones and oximes, allow the release of the drug at acid pH. Several compounds that attach doxorubicin through this kind of bond has been reported. The release takes places at the endosome, where the pH is around 4-5.

Specifically, we proposed to study the combined therapy of doxorubicin with those peptides, linked by an oxime bond. The synthesis of these compounds was carried out in solid phase, in the same way that in the previous chapter. The doxorubicin was introduced in the last step of the synthesis, carrying out the reaction in solution. The compounds were tested against breast and doxorubicin-resistant ovarium cancer cells. The obtaining results, as expected from the previous studies in mammalian cells, confirmed the previous observed selectivity, as neither of the compounds without the doxorubicin showed anticancer activity. The cyclic peptides with doxorubicin showed lower toxicity values than free doxorubicin, which indicates that our cyclic peptides could act as carriers for the drug to the cell with less side effects. However, the release of the drug could take place in a very slow manner inside the endosome or inside the cell. The kinetic studies about the stability of the oxime bond at pH 4 confirmed its high stability. The change of the dynamic bond for a hizdrazone system should be an interesting option for the drug release.

USC
UNIVERSIDADE
DE SANTIAGO
DE COMPOSTELA

Resumen

El descubrimiento de la penicilina en 1928 y la posterior aparición de las cefalosporinas, quinolonas, macrólidos y tetraciclinas dio lugar a lo que se conoce como la era dorada de los antibióticos. La comercialización de estos antibióticos generó la creencia popular de que la batalla contra las infecciones estaba ganada. Sin embargo, las bacterias consiguieron desarrollar mecanismos de defensa, haciendo inútil a estos antibióticos. Esto es lo que se conoce como resistencia (bacteriana), que apareció pocos años después de la comercialización de cada antibiótico (o incluso antes en el caso de la penicilina). Hoy en día existen cepas resistentes a múltiples fármacos, "superbugs", lo que hace muy difícil su tratamiento.

Los antibióticos generalmente se clasifican por su estructura (penicilinas, cefalosporinas, etc.), por el número de evoluciones del fármaco original (1ª, 2ª, 3ª generación, etc.) o por su modo de acción. Estos últimos pueden ser: i) inhibición de la síntesis de la pared celular, ii) inhibición de la síntesis de proteínas, iii) inhibición de la síntesis de ADN y/o ARN, iv) actuar en la ruta del ácido fólico y v) actuar sobre la membrana celular. Para cada mecanismo existe un tipo de resistencia. Así, el más conocido es el desarrollo de las β-lactamasas, que son enzimas capaces de romper el anillo β-lactámico de las penicilinas.

La primera cepa en mostrar resistencia a la penicilina fue el *Staphylococcus aureus*, cuya infección causada por la cepa resistente empezó a tratarse con meticilina, antibiótico usado contra bacterias Grampositivas. Sin embargo, con el tiempo, estas bacterias consiguieron inmunizarse también contra este antibiótico, derivando en una cepa resistente comúnmente abreviada como MRSA (meticilina-resistente *S. aureus*). Esta bacteria, resistente tanto a penicilina como a meticilina, es también resistente a otros antibióticos, dejando muy pocas opciones para su tratamiento hoy en día. En la actualidad, MRSA se trata con vancomicina, considerado un antibiótico de último recurso, a pesar de que desde 2002 se han detectado casos de resistencia a vancomicina para esta especie.

El problema de la resistencia a los antibióticos se incrementa con la formación de biofilms. Previamente se creía que una infección estaba causada por bacterias planctónicas, es decir, bacterias que actuaban de forma aislada o independiente. Sin embargo, a partir de los años 80 y sobre todo en los 90, se demostró que las bacterias se organizan formando una especie de comunidad. Los biofilms se forman por un conjunto de bacterias que segregan una matriz extracelular que las envuelve y protege del entorno. El biofilm más conocido es el que se genera en la boca, conocido como placa bacteriana, que puede derivar en sarro. El biofilm es una barrera que protege a las bacterias en medios hostiles, lo que ya de por si se considera un método de resistencia a los antibióticos. Normalmente, los antibióticos destruyen las bacterias planctónicas que se liberan del biofilm al medio, pero son incapaces de destruir el propio biofilm. Es decir, se tratan las bacterias que generan la infección, pero no se destruye el foco de infección, siendo necesario repetir el tratamiento varias veces, lo que en muchos casos deriva también en la resistencia a ese antibiótico. Por todo ello, el estudio de los biofilms así como la búsqueda de antibióticos que puedan destruirlos ha cobrado una gran relevancia en los últimos años.

La regulación del uso de antibióticos ha sido clave para frenar el desarrollo de cepas resistentes. Aun así, en 2014, la organización mundial de la salud comunicó la preocupante situación respecto a la falta de eficacia de los antibióticos, que en 2016 empezó a llamarse la "era post-antibióticos". De nuevo, en 2017, la organización mundial de la salud publicó una

lista de patógenos para los cuales es urgente el desarrollo de nuevos antibióticos. En esta lista de patógenos se incluyen tanto bacterias Grampositivas (por ejemplo, *S. aureus* resistente a meticilina y vancomicina) como Gramnegativas (*Pseudomonas aeruginosa* resistente a carbapenem). La falta de antibióticos cuesta en la actualidad 700.000 muertes al año y se espera que la cifra alcance un valor de 10 millones de muertes al año en 2050. El problema se agrava por el coste de desarrollo de un fármaco que limita que compuestos viables alcancen las últimas fases clínicas para su aprobación.

En la actualidad existen dos vías de obtención de antibióticos: la modificación de los antibióticos ya existentes o el desarrollo/descubrimiento de nuevos compuestos; siendo esta última las más prometedora ya que supone el descubrimiento de nuevos mecanismos de acción para él que las bacterias no están aún preparadas. Sin embargo, esta estrategia es más tediosa y costosa porque requiere pasar por todas las etapas de los estudios preclínicos y clínicos. Una estrategia hibrida se está desarrollando con los péptidos antimicrobianos (AMP) en la que se emplean determinadas estructuras naturales que se transforman en otras completamente diferentes. Los péptidos antimicrobianos existen en la naturaleza y actúa como primera línea de defensa contra los microorganismos en diferentes especies de insectos, plantas y animales, incluyendo los humanos. Existen cientos de diferentes péptidos antimicrobianos, que generalmente cumplen una serie de características. Son péptidos pequeños (con un numero de aminoácidos inferior a 50) y cargados positivamente, que suelen estar compuestos por aminoácidos hidrofílicos e hidrofóbicos, por lo que presentan una estructura anfipática. Además, estos péptidos tienen una estructura secundaria definida, ya sea como hélice α o lamina β. El mecanismo más aceptado para estos compuestos se basa en la interacción electrostática entre las cargas positivas de los péptidos antimicrobianos con las cargas negativas presentes en las membranas bacterianas, de forma que el péptido se sitúa a lo largo de la membrana en un mecanismo llamado tipo “alfombra”. Cuando el péptido alcanza la membrana bacteriana es capaz de generar un poro y provocar la muerte de la bacteria al romper el balance iónico o liberar el contenido celular.

Nuestro grupo es pionero en la síntesis y estudio de péptidos cíclicos que tienen la propiedad de ensamblarse para formar nanotubos peptídicos. Este auto-ensamblaje se debe a la quiralidad alternante de los amino ácidos que lo forman, dando lugar a una disposición plana del anillo. En esta conformación, los grupos carbonilo y amino quedan orientados perpendicularmente al plano del anillo por lo que cada péptido cíclico interactúa por cada una de las caras del ciclo con otro péptido cíclico mediante enlaces de hidrógeno, apilándose y dando lugar a un nanotubo. Las propiedades de los nanotubos peptídicos se pueden modificar mediante la selección de los aminoácidos que lo forman. Además, el número de aminoácidos utilizados determina el diámetro del nanotubo, por lo que sus propiedades también se pueden modular en función de cuantos aminoácidos compongan el péptido cíclico. Así, el control del diámetro permite la formación de estructuras capaces de albergar moléculas en su interior. El uso exclusivo de aminoácidos hidrofóbicos da lugar a nanotubos que generan poros en membranas lipídicas mientras que el uso de aminoácidos hidrofóbicos e hidrofílicos dan lugar a estructuras anfipáticas, que cuando presentan carga neta positiva pueden tener propiedades antimicrobianas.

Se han preparado numerosos péptidos cíclicos con propiedades antimicrobianas, ya sean compuestos por 6 u 8 aminoácidos, alternando el uso de lisinas, histidinas y argininas en la parte hidrofílica del péptido y el uso mayoritario de triptófanos y leucinas en la parte hidrofóbica. Aunque en un principio se propusieron péptidos con mayor carácter hidrofóbico

que hidrofílico, 5 aminoácidos hidrofóbicos frente a 3 hidrofílicos, la reducción de 5 a 3 aminoácidos hidrofóbicos también dio buenos resultados frente a bacterias. Lo curioso de estos compuestos fue la reducción que presentaban en los valores de toxicidad obtenidos de los ensayos de hemolisis, que se reducía hasta 4 veces frente a los péptidos cíclicos de 5 aminoácidos hidrofóbicos. La introducción de diferentes azucares en la estructura consiguió aumentar la selectividad de los péptidos cíclicos hacia las bacterias frente a las células humanas. Entre los péptidos con azucares en su estructura, cabe destacar la familia de las mannopeptimicinas. Estos compuestos naturales han sido ampliamente estudiados y algunos de sus derivados han mostrado actividades realmente asombrosas. Sin embargo, esta familia de compuestos no parece haber seguido desarrollándose en estos últimos años.

El objetivo de esta tesis doctoral plantea el desarrollo de una nueva estrategia sintética que permita la obtención de una librería de péptidos de forma rápida y sencilla para su estudio como potenciales agentes antimicrobianos. Esta estrategia se enfocó en el diseño de péptidos cíclicos con dos puntos de anclaje que permiten su modificación en las últimas etapas de la síntesis. Estos puntos de anclaje se usaron de forma alternativa para la introducción de cadenas alifáticas de distintos tamaños y la posterior incorporación de diferentes sacáridos. En concreto, los péptidos cíclicos se compusieron de 8 aminoácidos en el que únicamente dos residuos eran hidrofóbicos. Como uno de los puntos de anclaje se incorporó una propargilglicina, ya que las reacciones de adición [3+2] catalizadas por Cu tipo "clic" permiten la conjugación de forma quimio-selectiva con los sustituyentes deseados portadores de un grupo azida. El otro punto de anclaje se llevó a cabo mediante la formación de un enlace oxima, para lo cual una lisina del péptido cíclico se modificó con una alcoxiamina. Dependiendo de la ubicación de estos grupos reactivos en la zona hidrofílica o hidrofóbica del compuesto se diseñaron dos plataformas diferentes. Así, en un primer momento, se plantearon dos péptidos cíclicos como modelo, **CP-A** (con el alquino en el entorno hidrofóbico) y **CP-B** (con dicho grupo en el centro de la zona hidrofílica). La actividad antibacteriana de estos péptidos se probó contra *S. aureus* y *S. epidermidis* como ejemplos de bacteria Grampositivas y contra *E. coli* como ejemplo de bacteria Gramnegativa. Una vez determinada la plataforma más activa, sobre ella se estudiaría los efectos de la incorporación de diferentes grupos sobre los centros reactivos para determinar su efecto sobre la actividad antimicrobiana. Además, los péptidos más activos se estudiarían contra el biofilm obtenido a partir de *S. aureus*. El último objetivo de este trabajo es el estudio de estos compuestos como posibles agentes anticancerígenos, aprovechando la presencia de la hidroxilamina en la estructura para anclar compuestos con propiedades anticancerígenas y alcanzar una terapia combinada.

En el primer capítulo de esta tesis se desarrolló la metodología sintética necesaria para la preparación de estos compuestos, optimizando la síntesis en fase solida de los péptidos, la reacción de adición [3+2], la incorporación de la alcoxiamina y la posterior formación de la oxima. Además, para la alternativa sintética donde el triple enlace formaba parte del entorno hidrofílico, se llevó a cabo la síntesis de un derivado azida de *D*-manosa para la reacción de adición [3+2]. Por otro lado, para la alternativa sintética donde la hidroxilamina era el punto de anclaje de la parte hidrofílica, se llevó a cabo la síntesis de la hidroxilamina metilada para el acoplamiento del azúcar en una conformación cerrada. Sin embargo, la reacción de condensación entre el azúcar y la hidroxilamina metilada no consiguió llevarse a cabo de forma eficiente, por lo que se optó por utilizar azucares en su conformación abierta o derivados glicosídicos que portan un grupo aldehído (preparados para el desarrollo de otro proyecto en nuestro grupo de investigación). Las dificultades de síntesis encontradas en este capítulo se solventaron realizando tanto la reacción de adición [3+2] como la incorporación de la

alcoxiamina en el soporte sólido. Se determinó que ambas reacciones se podían llevar a cabo de forma indistinta, es decir, primero la incorporación de la hidroxilamina y después la reacción de adición [3+2] o viceversa. No obstante, en el caso de la introducción del azúcar, esta se llevó a cabo en disolución en el último paso de la síntesis.

En este capítulo también se optimizaron las condiciones para llevar a cabo los estudios de actividad frente a bacterias. Tras el proceso de optimización, se testaron los compuestos derivados de la plataforma **CP-B**, donde la hidroxilamina se sitúa en la parte hidrofóbica del anillo peptídico. Los resultados de estos compuestos mostraron una actividad muy baja respecto a la plataforma **CP-A**, por lo que decidimos descartar la plataforma **CP-B** en los siguientes estudios. También se estudió la posición más adecuada de la hidroxilamina en la plataforma **CP-A**, llegando a la conclusión de que la diferencia entre los compuestos resultantes era muy pequeña, por lo que se decidió simplificar el número de plataformas a **CP-A1** y **CP-A2** en el siguiente capítulo.

En el segundo capítulo, se llevó a cabo la síntesis de una librería de compuestos y se estudiaron sus propiedades antimicrobianas. En primer lugar, se insertaron las cadenas alifáticas a las dos estructuras peptídicas derivadas de la plataforma **CP-A**. Los estudios de estos compuestos como agentes antibacterianos determinaron que el tamaño óptimo de la cadena alifática para alcanzar la máxima actividad era de diez y catorce carbonos. El siguiente paso, la incorporación del azúcar, se llevó a cabo sobre dos de los péptidos que presentaban mejores actividades, **CP-A1$_{14}$** y **CP-A2$_{10}$**. Estos péptidos se condensaron con los glicosialdehídos derivados de *D*-glucosa, *D*-manosa, *D*-galactosamina y *D*-maltosa. Todos los péptidos con azúcar mostraron una menor actividad antimicrobiana respecto al péptido sin azúcar. No obstante, la toxicidad del péptido **CP-A1$_{14}$** se redujo completamente con la presencia de los azucares en la máxima concentración evaluada en estos ensayos. El péptido **CP-A2$_{10}$** no mostró efectos de toxicidad en ninguna de las concentraciones testadas, así como tampoco ninguno sus derivados con azucares.

Nuestro siguiente paso en la optimización del péptido fue la sustitución del resido central en el entorno hidrofílico, que los estudios anteriores parecían indicar que en la plataforma **CP-A** jugaba un papel importante en la actividad biológica. Para ello planteamos la sustitución de este residuo en **CP-A1** por otros residuos básicos como arginina, ornitina y el ácido 2,3-diaminopropionico. Los buenos resultados obtenidos con estos compuestos al derivar con las cadenas alifáticas, con valores de MIC en torno a un microgramo por mililitro que son similares a los obtenidos con los mejores AMP, nos llevaron a un estudio más exhaustivo de los mismos, en los que se pudo determinar la formación de nanotubos mediante diferentes técnicas, como fluorescencia o STEM. Además de esta extensa caracterización, también se han estudiado contra otras bacterias para ver el alcance de su actividad. Los estudios del mecanismo de acción de estos péptidos confirman una rápida acción bactericida (15-20 min), que sugieren que el modo de acción no está basado en una diana terapéutica proteica. Estos estudios confirman la actividad preferente contra bacterias grampositivas y que sus actividades varían de forma significativa dependiendo del tipo de bacterias. Finalmente, algunos de ellos se usaron en el estudio de actividad frente a biofilms. Se llevaron a cabo dos ensayos distintos sobre el biofilm formado por *S. aureus*. Por un lado, se midió la capacidad bactericida frente a un biofilm maduro. De forma altamente gratificante, la mayoría de los compuestos tenían una alta actividad contra biofilms, alcanzando valores de máxima inhibición de 20 veces la MIC. También, se midió la capacidad de los péptidos para inhibir la formación del biofilm. Estos mostraban que a pesar de que el péptido no tiene un mecanismo propio contra la formación del

biofilm, es capaz de matar a las bacterias antes de que lo generen, por lo que pueden usarse en la prevención de formación de biofilm gracias a su rápida acción bactericida contra células planctónicas.

Por último, decidimos preparar una serie de compuestos donde el azúcar se incluyese dentro del esqueleto del péptido cíclico. Los primeros estudios mostraron una baja actividad respecto a sus análogos sin azúcar, aunque es necesario un estudio más profundo para determinar la validez de esta estrategia.

En el tercer capítulo, nos planteamos explorar las propiedades anticancerígenas o como vehículos de otros fármacos con los compuestos más activos. Existen diversas estructuras capaces de transportar un fármaco a su destino denominados vehículos moleculares. De entre todos los estudiados caben destacar los péptidos penetrantes de membrana (CPPs). Estos péptidos presentan una estructura anfipática similar a los péptidos antimicrobianos por lo que pensamos que nuestros péptidos podrían tener un comportamiento análogo. Para este capítulo decidimos realizar estudios de citotoxicidad de los péptidos anteriormente preparados y conjugados con doxorrubicina, un fármaco muy utilizado como modelo en muchos estudios celulares por su actividad biológica y por sus propiedades espectroscópicas. De entre todos los tipos de cáncer a estudiar, elegimos el cáncer de mama debido al alto número de pacientes que se registran cada año, el segundo cáncer más diagnosticado en el planeta, y el cáncer de ovario debido a que, a pesar de no ser un cáncer muy diagnosticado, sigue teniendo una alta mortalidad (que alcanza un valor del 62% de las pacientes afectadas). La mayoría de los tratamientos actuales del cáncer de pecho pertenecen a la familia de las antraciclinas y presentan una elevada cardiotoxicidad que limita el uso del fármaco, llegando a interrumpirse el tratamiento en algunos casos. Para reducir la toxicidad de estos compuestos, se han diseñado transportadores que son capaces de envolver al fármaco y llevarlo a su punto de acción, reduciendo sus efectos secundarios. Una forma de liberar el fármaco es a través de un estímulo externo, ya sea un cambio de temperatura o pH. Los enlaces dinámicos covalentes como las iminas, hidrazonas o oximas permiten la liberación del fármaco a pH ácido. Se han reportado varios ejemplos de compuestos que anclan doxorrubicina a su estructura a través de un enlace de este estilo y lo liberan en el endosoma (pH 4-5).

En concreto, nos propusimos estudiar la terapia combinada de doxorrubicina con dichos péptidos, unidos a través de un enlace oxima. La síntesis de estos compuestos se llevó a cabo en fase sólida, al igual que en el capítulo anterior. La doxorrubicina se incorporó en el último paso de la síntesis, llevándose a cabo la reacción en disolución. Los compuestos se estudiaron con células cancerosas de pecho y de ovario resistente a la doxorrubicina. Los resultados obtenidos, al igual que en los anteriores estudios de toxicidad en células mamíferas, confirmaron las selectividades observadas anteriormente, ya que ninguno de los péptidos sin doxorrubicina tenía actividad anticancerígena. Los péptidos con la doxorrubicina anclada a la estructura mostraron valores de toxicidad más bajos que los de la doxorrubicina libre, lo que nos indicaba que nuestros péptidos transportar el fármaco a la célula con menos efectos secundarios. Sin embargo, la liberación del fármaco debe tener lugar de forma lenta en el endosoma o en el interior celular. Los estudios cinéticos sobre la estabilidad de este enlace a pH 4 confirmaron su alta estabilidad. El cambio del enlace dinámico a un enlace hidrazona sería una opción interesante para optimizar la liberación del fármaco.

USC
UNIVERSIDADE
DE SANTIAGO
DE COMPOSTELA

Introduction

USC
UNIVERSIDADE
DE SANTIAGO
DE COMPOSTELA

1. Antibiotics vs resistance.

There is probably no chemotherapeutic drug to which in suitable circumstances the bacteria cannot react by in some way acquiring 'fastness' (resistance)

Alexander Fleming (1946)

1.1. History of antibiotics.

Despite many people believe that the history of antibiotics starts with Alexander Fleming and the discovery of the penicillin, the true is that this story started a little bit early. The English physician John Tyndall had noticed in 1876 that 'in a fight between bacteria and *Penicillum* fungi, fungi are always the winner and bacteria end dead at the bottom of the test tube'.[1] In 1882, Robert Koch (Nobel prize in Medicine and Physiology in 1905) demonstrated that bacteria can cause infections.[2] From 1899 to 1901, Paul Ehrlich (Nobel prize in Medicine in 1908) stablished the correct structural formula of atoxyl, which was knowing to be active against trypanosomiases, and synthesized 606 analogues based on its structure.[3] The latest compound '606' had succeeded in treating rabbits that were previously infected with syphilis. After hundreds of experiments in which repeatedly proved its efficacy against syphilis, Ehrlich announced it under the name 'Salvarsan' (1909). Further work on this subject was carried out, finding a new analogue (compound 914) that was presented as 'Neosalvarsan'. Although this new arsenical substance presented less curative effect, better solubility, easier manufacture and administration was achieved. After this, the development of what the scientist had called 'chemotherapy' was paused during the First World War (1914-1918).

In 1928, Alexander Fleming (Nobel prize in Medicine in 1945) observed a dish in which *Staphylococcus aureus* was contaminated with *Penicillum notatum* where the fungi colonies inhibited the growing of the bacteria. This phenomenon was previously observed by Tyndall, but unlike him, Fleming decide to study it. This moment was considered the official discovery of the penicillin.[4] Fleming proof the inhibition activity of the *Penicillum* against different bacteria strains, such as *Staphylococcus*, *pneumococcus*, *streptococci*, *meningococcus* and *gonococcus*. He also demonstrates that *Penicillum* has not activity against *bacilli* and it was not toxic in rabbits or mice.

In 1939, René J. Dubos discovered gramidicin as a crude complex together with a second peptide antibiotic known as tyrocidin.[5,6] The mixture of both antibiotics was called tyrothricin. Tyrothricin was the first antibiotic utilized in clinical practice. However, this antibiotic causes severe haemolysis when it is administered parentally. It can not be administered orally due to digestion destroyed it. Thus, their use was restricted to topical administration. It is used in various creams, ointment, lotion and/or solution and can be combined with another antibiotics.[5]

---

[1] a) Acuña, G., *Revista Médica Clínica Las Condes*, **2002**, Vol. 13, Num. 1 b) Tindall, J., *Philosophical Transactions of the Royal Society*, **1876**, 166, 27.
[2] Koch, R., *Berliner Klinische Wochenschrift*, **1882**, 19, 221-230.
[3] https://www.nobelprize.org/prizes/medicine/1908/ehrlich/biographical/
[4] Fleming, A., *British Journal of Experimental Pathology*, **1929**, 10, 226-236.
[5] Brewer, G. A., *Anal. Prof. Drug Subs*., **1979**, 8, 179-218.
[6] Dubos, R. J., *J. Exper. Med*., **1939**, 70, 1-10.

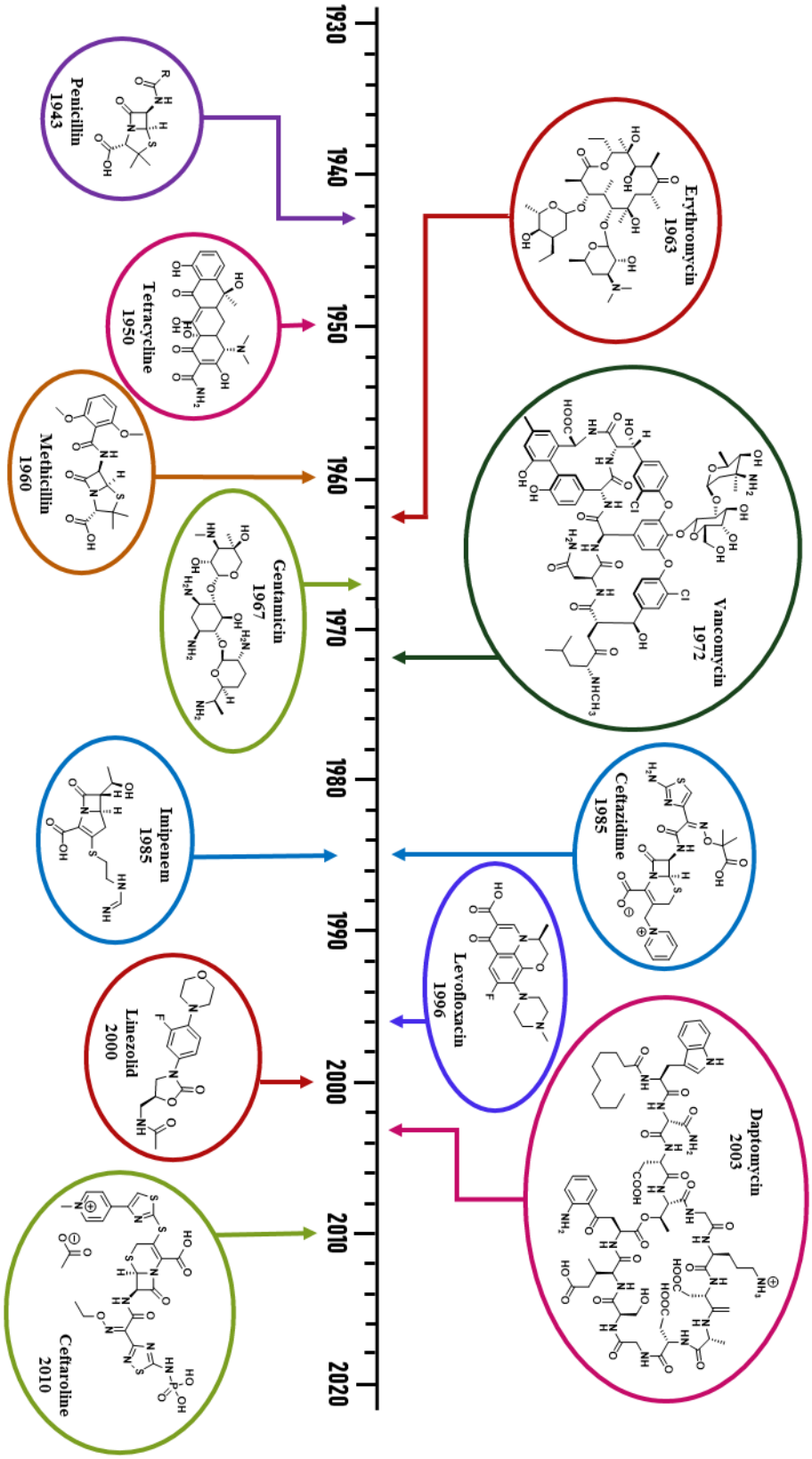

Figure 1. *Regulatory approvals of new classes of antibiotics bring novel mechanisms of attack.*

The penicillin had changed the way of treating infectious diseases. Many antibiotics appeared after penicillin (Figure 1)[7], giving rise to what is now known as 'Golden age of antibiotics'. Death caused by infections decrease more than a 90% in the 20th century, increasing life expectancy in almost 30 years.[8] It was taken for granted that any infectious disease was curable by antibiotic therapy, being manufactured at an estimated scale of about 100,000 tons of antibiotics annually worldwide in 2009, and their use had a profound impact on the life of bacteria on earth.[9] However, it is worth to mention that most of these antibiotics (73% of antibiotics developed between 1981 and 2005) were synthesized from 'the antibiotics of first generation'. There are five different basic structures: penicillins, cephalosporins, quinolones, macrolides and tetracyclines (Figure 2).[10] Only one antibiotic belonging to a new class, the narrow-spectrum daptomycin, was discovered and made it into clinical practice in the last years (Figure 1).[11] Although the term 'antibiotic' was introduced to denote chemical substances produced by microorganism, semisynthetic modifications of natural products have produced a large variety of antimicrobial agents, that are also called antibiotics (such as *β*-lactams antibiotics and macrolides).[12] This definition distinguishes antibiotics from antibacterial agents, totally synthesized by the chemist. These purely synthesized antibacterial agents are also treated as antibiotics in this work.

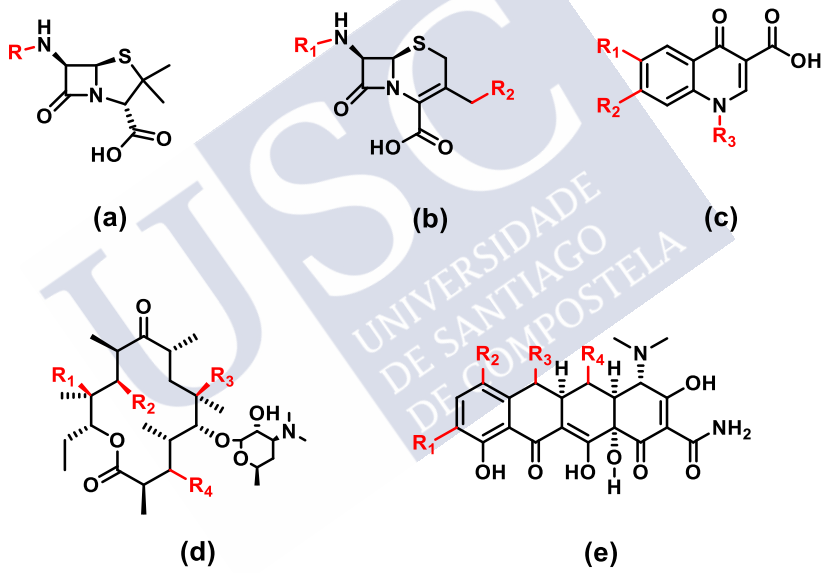

***Figure 2**. (a) Penicillin, (b) Cephalosporins, (c) Quinolones, (d) Macrolides and (e) Tetracyclines. Commun structure is shown in black and modifications of the structures are show in red.*

Antibiotics can be classified considering the effects they exert on bacteria: bacteriostatic and bactericidal. Bacteriostatic agents prevent the growth of bacterial cells, while bactericidal agents kill bacteria, as exemplified by penicillin.[12] To understand how antibiotics work, we will carry out a brief description of the targets of the main classes of antibiotics: (i) cell wall

[7] Hede, K., *Nature*, **2014**, 509, S2-3.
[8] Raviña, E., 'Medicamentos, Un viaje a lo largo de la evolución histórica del descubrimiento de fármacos', Vol. 1, Universidade de Santiago de Compostela, Santiago de Compostela, **2008**.
[9] Nikaido, H., *Annu. Rev. Biochem*., **2009**, 78, 119-146.
[10] Fischbach, M. A., Walsh, C.T., *Science*, **2009**, 325, 1089-1093.
[11] Lewis, K., *Nature*, **2012**, 485, 439-440.
[12] Yoneyama, H.; Katsumata, R., *Biosci. Biotechnol. Biochem*., **2006**, 70, 1060-1075.

synthesis, (ii) protein biosynthesis, (iii) DNA and RNA biosynthesis, (iv) folate biosynthesis and (v) cell membranes (Figure 3).[12,13]

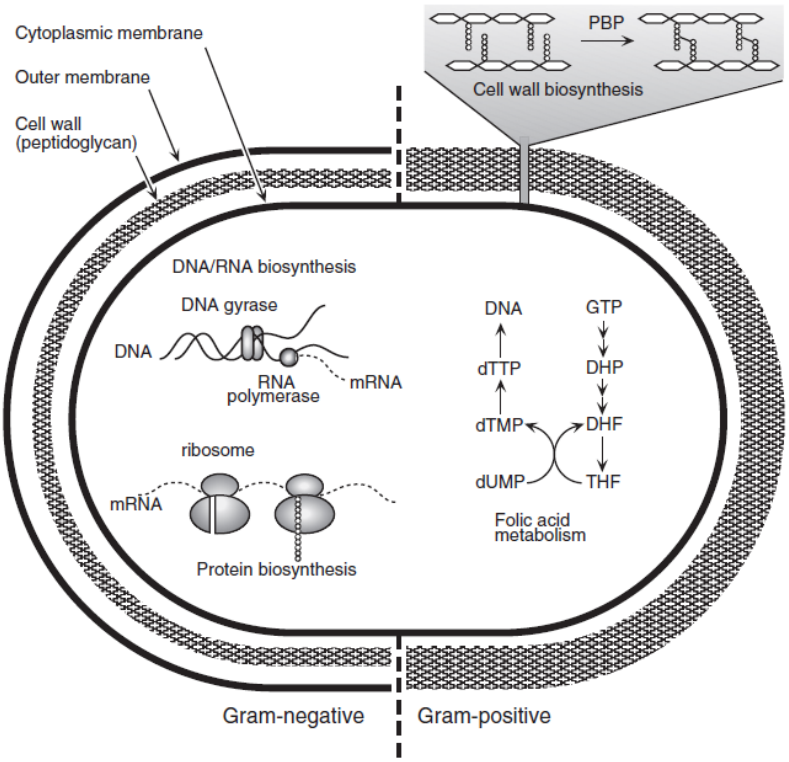

Antibiotic Category	Examples	Mode of action
β-lactams	Penicillin Cephalosporin Cetoximes Carbapenems	Inhibition of cell wall synthesis
Aminoglycosides	Streptomycin Gentamycin Tobramycin Amikacin	Inhibition of protein synthesis
Quinolones	Ciprofloxacin Ofloxacin Norfloxacin	Inhibition of DNA biosynthesis
Glycopeptides	Vancomycin	Inhibition of cell wall synthesis
Tetracyclines	Tetracycline	Inhibition of translation
Rifamycins	Rifamycin	Inhibition of transcription
Streptogramins	Virginamycins Quinupristin Dalfoprisitin	Inhibition of cell wall synthesis
Oxazolidinones	Linezolid	Inhibition of formation of 70S ribosomal complex

***Figure 3**. (Top) Major targets of antibiotics[12] and (bottom) mode of action of some antibiotics.[14]*

[13] Walsh, C., *Nat. Rev. Microbiol.*, **2003**, 1, 65-70.
[14] Ahmed, M., *IntechOpen*, **2012**, DOI: 10.5772/30161.

(i) **Inhibition of bacterial cell wall biosynthesis.** Bacteria present a high intracellular pressure, where a rigid peptidoglycan protect them from osmolysis. The peptidoglycan layer in Gram-positive bacteria (outer layer) is generally much thicker than that in Gram-negative bacteria. The peptidoglycan is crosslinked to the glycan strands by the action of transglycosidases, and the peptide strands by the action of transpeptidases. Penicillin and cephalosporins (known as β-lactams) targets enzymes with both transglycosidase and transpeptidase domains in their structures. β-lactams acylate the active site of the transpeptidase, leading to inactivation of the enzymes.

(ii) **Inhibition of protein biosynthesis.** The biosynthesis of proteins is a central process in cellular function, which is catalysed by ribosomes. The effectiveness and selective toxicity of many antibiotics is due to the mechanism of biosynthesis of proteins in prokaryotes differs substantially from the eukaryotes. There are different steps that can be blocked in a selective manner (during the initiation, elongation and/or termination step).

(iii) **Inhibition of DNA and RNA biosynthesis.** DNA replication is an essential process in cell division for all organisms. The enzyme involved in these processes are called topoisomerases, and they are classified into tipe I and tipe II. Tipe I topoisomerase break one strand of the DNA while tipe II breaks both strands at the same time. Some antibiotics, such as quinolones, can stabilize the interaction between the DNA and the topoisomerase in an irreversible manner.

The genetic information is decoded from DNA and RNA in a process known as transcription, which is also an essential process that occurs in all organism. RNA polymerase of bacteria is composed of different subunits with a stoichiometry of $\alpha_2\beta\beta'\omega$. Rifampicin inhibits RNA polymerase by binding to the β subunit of the enzyme at an allosteric site. This kind of inhibition is used principally in the treatment of tuberculosis and leprosy.

(iv) **Folic acid metabolism**. This inhibition of this metabolic pathway take place by the combination of two drugs that inhibit distinct steps in the folic acid metabolism, sulfamethoxazole and trimethoprim. Sulfamethoxazole competes with the natural product, *p*-aminobenzoic acid, for the interaction with the dihydropteroate synthase enzyme, involved in the biosynthetic pathway of folate. As the affinity for the antibiotic is stronger, the resulting product can not be a substrate for the next enzyme, dihydrofolate synthase (not present in humans). Trimethoprim inhibits dihydrofolate reductase, a key enzyme involved in the synthesis of purine nucleotides and amino acids glycine and methionine. The combination of both antibiotics shows a synergistic effect compare with each drug alone.

(v) **Cell membranes**. The integrity of cell membranes is essential to all organisms. Cationic peptides attach the cytoplasmic membrane of Gram-positive and Gram-negative bateria, and the outer membrane of Gram-negative bacteria as well. The interaction disrupts membrane organization, inducing the permeabilization of the cell components, which leads to cell-killing. However, the toxicity of antibiotics like polymyxin B restricts its use to topical applications.

1.2. Resistance to antibiotics.

Only a few years after the introduction of penicillin intro clinical practice, *S. aureus* developed resistance caused by a plasmid gene that code a *β*-lactamase.[9] Although this problem was solved by the introduction of methicillin and similar compounds that resist the enzymatic hydrolysis, some strains become also resistant to them. Methicillin-resistant *Staphylococcus aureus* (MRSA) is resistant not only to methicillin but usually also to aminoglycosides, macrolides, tetracycline, chloramphenicol, and lincosamides.[9,15] MRSA is the major source of hospital-acquired infections and is treated with vancomycin nowadays, even though the first case of fully vancomycin-resistant *S. aureus* was already discovered in 1997.[12] Although *S. aureus* was the first bacteria to present resistance to penicillin, the spread of antibiotic-resistant pathogens continues unabated (Figure 4). [7,11] Resistance appear extremely fast with antibiotics like Levofloxacin, ceftaroline or linezolid, whereas the resistance of vancomycin took 16 years to develop. This can be explained as vancomycin was always use as last resort antibiotic, so their use, compare with the others, was limited. The most serious resistance in bacteria is caused by Gram-negative pathogens, like *Pseudomonas aeruginosa* and *Acinetobacter baumanii*, due to lack of no agents that could be used against these strains.[9] Other of the greatest threat to public health is the multi-drug resistant tuberculosis.[14] Moreover, the use of antibiotics for prophylaxis, chemotherapy, and grown promotion in animals (about 50%) makes the problem even more complicated. There is evidence that antibiotic use in animals plays a role in the development of resistant in human pathogens. Interestingly, the European Union banned the use of avoparcin in 1997, on the basis of the 'Precautionary Principle', closely follow by the banning of bacitracin (a polypeptide), spiramycin and tylosin (macrolides) and virginiamycin (a streptogramin combination) (all of them are growth promoters).[16] The ban of these antibiotics didn´t lead to a decrease in the use of antibiotics in animals, only to use therapeutic antibiotics, which are identical to those used in human medicine.

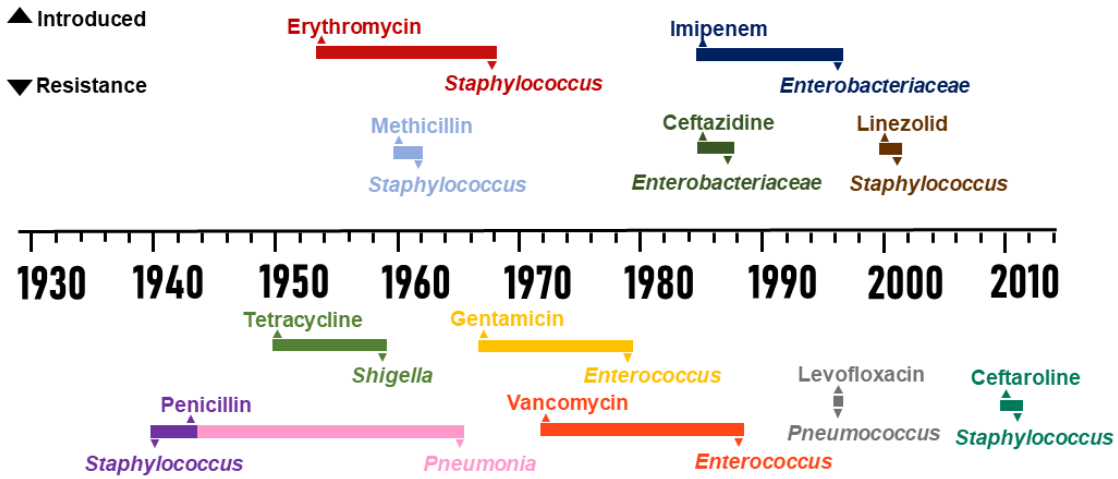

***Figure 4**. Appearance of resistance. As new antibiotics come to the market (upward arrows), resistance develops (downward arrows).*

[15] de Lencastre, H., *Curr. Opin. Microbiol*., **2007**, 10, 428-435.
[7] Hede, K., *Nature*, **2014**, 509, S2-3.
[9] Nikaido, H., *Annu. Rev. Biochem*., **2009**, 78, 119-146.
[16] Casewell, M.; Friis, C.; Marco, E.; McMullin, P.; Phillips, I., *J. Antimicrob. Chemother.*, **2003**, 159-161.

According to the WHO, a resistant microbe is one which is not killed by an antimicrobial agent after a standard course of treatment.[14] Antibiotic resistance can be either intrinsic (natural) or acquired. Intrinsic resistance mechanisms are natural characteristics of the genetic constitution of the organisms. These inherited properties of a species are due to the lack of either the antimicrobial target site or accessibility to the target site. For example, obligate anaerobes are resistant to aminoglycosides as they lack electron transport system essential for their uptake. Gram-negative bacteria are resistant to macrolides and certain β-lactams as the drugs are too hydrophobic to traverse the outer bacterial membrane. Furthermore, Gram-negative bacteria have a lower proportion of anionic phospholipids in the cytoplasmic membrane than Gram-positive bacteria, which reduces the efficiency of the Ca^{2+}-mediated insertion of daptomycin into the cytoplasmatic membrane. They are also intrinsic resistant to vancomycin, due to it can not cross the outer membrane and access the peptidoglycan cell wall.[17] Between Gram-negative bacteria, *Pseudomonas aeruginosa* is a particular case. It has been demonstrated that this intrinsic resistance is a combination of unusually restricted outer membrane permeability (like the other Gram-negative bacteria) and other natural resistance mechanisms such as energy-dependent multidrug efflux pumps and chromosomally encoded β-lactamase.[18] More recently, it has been shown that instead of an active efflux pump, the resistance is due to the carriage of an insensitive allele of *fabI* that encodes an additional 'enoyl-ACP reductase' enzyme, that target for triclosan in sensitive species.[15]

Acquired resistance occur by many different mechanisms: a) Mutational alteration of the target protein, b) enzymatic inactivation of the drug, c) acquisition of genes for less susceptible target proteins from other species, d) bypassing of the target and e) preventing drug access to targets.[9,14,19]

a) Mutational alteration of the target protein: This mechanism is mainly for man-made compounds and it is considered a spontaneous mutation. Fluoroquinolone resistance is mainly caused by the mutation in the target enzyme, DNA topoisomerases.[20] Although the mutation of the enzyme does not make the bacteria completely resistant, the mutants will become more prevalent after a few bacteria replications. Furthermore, the resistance of this type is easily transferred to other cells on plasmids. In the presence of prolonged, non-lethal amount of antibiotic, a small population of bacteria enters in a brief state of high mutation rate, known as hypermutation. When the cell is in a hypermutation state, it acquires a mutation that relieves the selective pressure, it grows, reproduces and exits the state of high mutation rate. Studies have shown that the

[17] Blair, J. M. A.; Webber, M. A.; Baylay, A. J.; Ogbolu, D. O.; Piddock, L. J. V., *Nat. Rev. Microbiol*., **2015**, 13, 42-51.
[18] a) Normark, B. H; Normark, S., *J. Int. Med*., **2002**, 252, 91-106. b) Hancock, R. E.; Speert, D.P., *Drug Resist. Updat.*, **2000**, 3, 247-55.
[19] Alekshun, M. N; Levy, S. B., *Cell*, **2007**, 128, 1037-1050.
[20] Hooper, D. C., *Clin. Infect. Dis*., **2000**, 31 (Suppl 2), S24-S28.

hypermutators play a significant role in the evolution of antibiotic resistance and may also be responsible for the multiresistant phenotype.[21]

b) Enzymatic inactivation of the drug: This is the common mechanism for antibiotics of natural origin, such as aminoglycosides (kanamycin, tobramycin…), which are inactivated by enzymatic phosphorylation, acylation, or adenylation (Figure 5a); and *β*-lactams (penicillins, cephalosporins…), which are inactivated by enzymatic hydrolysis by *β*-lactamases (Figure 5b).

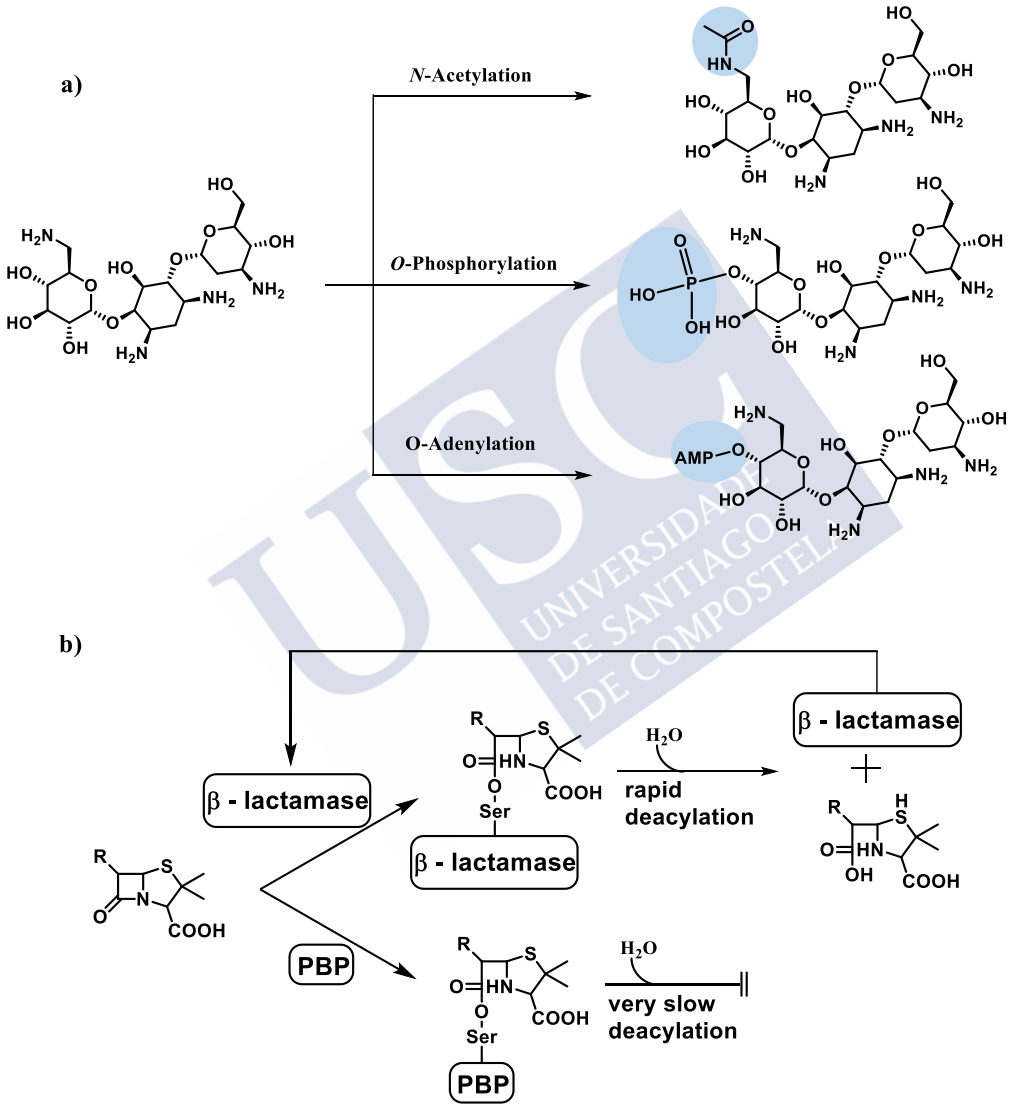

***Figure 5**. a) Inactivation of aminoglycosides by acetylation. b) Inactivation of penicillin by β-lactamases.*[12]

[21] a) Martinez, J.L.; Baquero, F., *Antimicrob. Agents Chemother*., **2000**, 44, 1771-1777. b) Giraud, A.; Matic, I.; Radman, M.; Fons, M.; Taddei, F., *Antimicrob. Agents Chemother*., **2002**, 46, 863-865. c) Chopra, I.; O´Neill, A. J.; Miller, K., *Drug Resist. Updates*, **2003**, 6, 137-145. d) Blanquez, J., *Clin. Infect. Dis*., **2003**, 37, 1201-1209.

- **Aminoglycosides**. They are inactivated by modifications that reduce the net positive charges on these polycationic antibiotics. There are now many aminoglycoside-modifying enzymes known; for example, APH (3´)-I, which is present in 46% of the aminoglycoside-resistant Gram-negative bacteria and is a plasmid code aminoglycoside phosphorylase that is strongly related to a chromosomally coded enzyme in *Streptomyces fradiae*; or AAC(3)-II, a plasmid-coded enzyme present in more than 60% of aminoglycoside-resistant Gram-negative bacteria examined.[22]

- ***β*-Lactams**. It was mentioned above the case that *S. aureus* developed resistance to penicillin due to a *β*-lactamase. Another enzyme, TEM *β*-lactamase, was reported in Gram-negative bacteria. Whereas methicillin was used to solve this problem in Gram-positive bacteria, it is useless in Gram-negative bacteria because they are pump out efficiently by the multidrug efflux pump (mechanism e).
  β-Lactamases are classified in three families. Class A includes both the *S. aureus* and TEM enzymes, whereas Class C represents chromosomally coded enzymes (e. g. Amp C) that are present in many Gram-negative bacteria. These two classes are both similar to serine proteases in their mechanism, whereas Class B enzymes are metalloenzymes that hydrolize carbapenems efficiently.
  First-generation cephalosporins, such as cephaloridine and cefazolin, were developed in order to resist *β*-lactams action. Although they were rapidly hydrolysed by both TEM and AmpC, cephamycins (such as cefoxitin) and the third-generation cephalosporins (such as cefotaxime) were initially reported to resist both types of enzymes. However, they were inactive against some Gram-negative bacteria, such as *Enterobacter* and *Serratia*.

c) Adquisition of genes for less susceptible Target Proteins from other species: Sequencing the genes coding for the targets of penicillin allow to determine that penicillin resistance among *Streptococcus pneumoniae* was due to the production of mosaic proteins, parts of which came from other organisms.[23] In other words, *S. pneumoniae* is an organism capable of import foreign DNA.

d) Bypassing of the target: Vancomycin binds the lipid-linked dissacharide-pentapeptide, a precursor of cell wall peptidoglycan. Study of the resistance mechanism showed that the end of the pentapeptide, *D*-Ala-*D*-Ala, was replaced by *D*-Ala-*D*-lactic acid (ester structure), which is not bound by vancomycin. Production of this altered structure requires the participation of several imported genes (Figure 6).[24]

[22] Shaw, K. J.; Rather, P. N.; Hare, R. S.; Miller, G. H., *Microbiol. Rev*. **1993**, 57, 138-163.
[23] Spratt, B. G., *Science*, **1994**, 264, 388-393.
[24] a) Courvali, P., *Clin. Infect. Dis*. **2006**, 42(Supp. 1): S25-S34. b) Williams, D.H. and Bardsley, B., *Angew. Chem. Int. Ed.* **1999**, 38, 1172-1193.

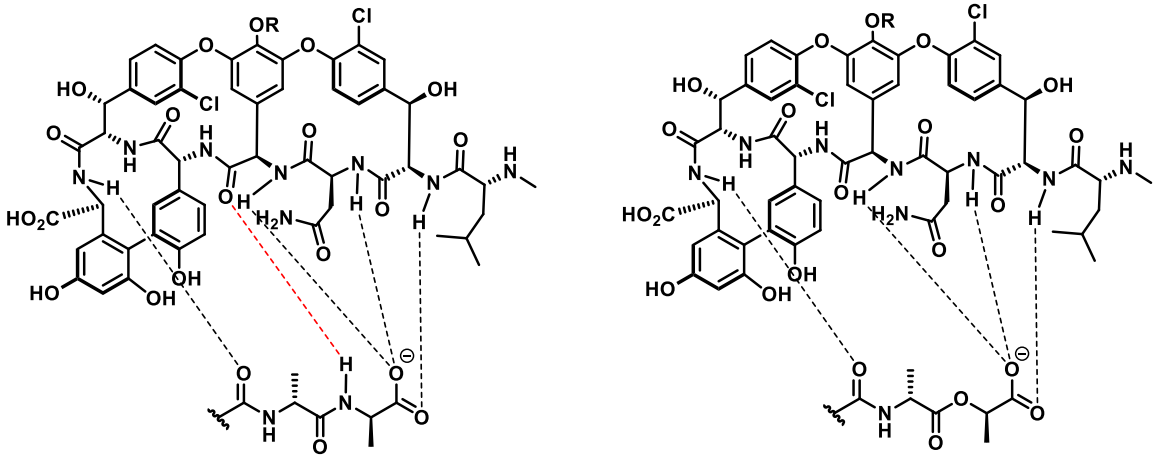

***Figure 6**. Binding site of the vancomycin with the D-Ala-D-Ala dimer and the resistance binding site D-Ala-D-lactic acid.*

e) **Preventing drug access to targets (also known as exclusion from the internal environment):** The access of the drug can be reduced locally by an active efflux process. In Gram-negative bacteria, the access is reduced by decreasing the influx across the outer membrane barrier. There are three mechanisms that prevent the access of the drug: local inhibition of the drug access (by changing the common conformation of the enzyme. Usually needs an extra agent that binds other site of the enzyme), drug-specific efflux pumps (pump out the drug from the cell) and nonspecific inhibition of drug access (decreasing outer membrane permeability. It is a last resort resistance due to the nutrient influx is also reduce).

1.3 *Staphylococcus aureus* resistance.

As it was mentioned above, *S. aureus* was the first strain to show resistance against penicillin. It is the pathogen of greatest concern because of its intrinsic virulence, its ability to cause a diverse of infections and its capacity to adapt to different environmental conditions.[25,26] *S. aureus* is continually evolving under our eyes. Therefore, a short explanation of its resistance is presented.[15]

A fundamental property of this pathogen is its ability to asymptomatically colonize healthy individuals. Approximately 30% of humans are asymptomatically nasal carriers of *S. aureus*, which it is part of the normal floral.[27,28] The primary mode of transmission is by direct contact, usually skin-to-skin contact, although contact with infected objects and surfaces can be another

[25] a) Lowy, F. D., *N. Engl. J. Med*., **1998**, 339, 520-532. b) Waldvogel, F. A., In *Principles and practice of infectious diseases*, **2000**, 2069-2092, Churchill Livingstone, Philadelphia, Pennsylvania, USA.
[26] Lowy, F. D. *J. Clin. Invest*., **2003**, 111, 1265-1273.
[27] Chambers, H. F.; DeLeo, F. R., *Nat. Rev. Microbiol*, **2009**, 7, 629-641.
[28] a) Kluytmans, J.; van Belkum, A.; Verbrugh, H., *Clin. Microbiol. Rev*., **1997**, 10, 505-520. b) Gorwitz, R. J. *et al*, *J. Infect. Dis*., **2008**, 197, 1226-1234.

way of contagion.[25a,29] The mortality remains approximately 20-40% despite the availability of effective antimicrobials.[30] *S. aureus* is now leading nosocomial infections and, as more patients are treated outside the hospital setting, is an increasing concern in the community.[31]

A timeline illustrating emergence of antibiotics and *S. aureus* resistance to them in is summarized in Figure 7.

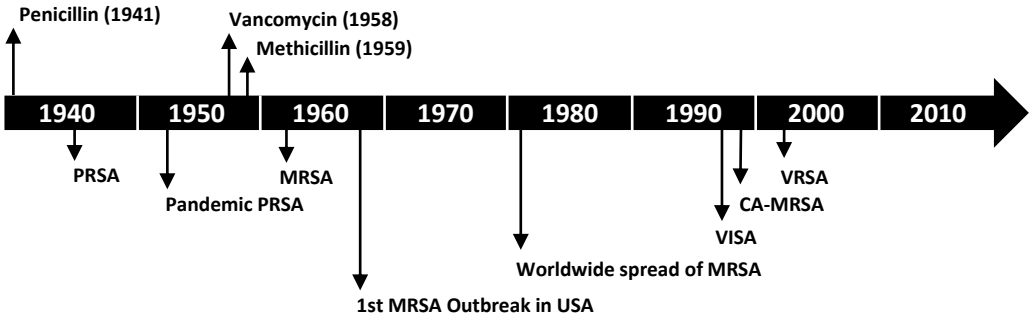

***Figure 7**. S. aureus drug resistance and epidemics.*[32]

Antibiotic	**Resistance gene**	**Gene product(s)**	**Mechanism(s) of resistance**
β-lactams	1) *bla*Z	1) *β*-Lactamase	1) Enzymatic hydrolysis of *β*-lactam nucleus
	2) *mec*A	2) PBP2a	2) Reduced affinity for PBP
Glycopeptides		1) Altered peptidoglycan	1) Trapping of vancomycin in the cell wall
		2) *D*-Ala-*D*-Lac	2) Synthesis of dipeptide with reduced affinity for vancomycin
Quinolones	1) *par*C	1) ParC (or GrlA component of topoisomerase IV	1,2) Mutations in the QRDR region, reducing affinity of enzyme-DNA complex for quinolones
	2) *gyr*A *or gyr*B	2) *gyr*A *or gyr*B components of gyrase	
Oxazolidinones	*rrn*	23S rRNA	Mutations in domain V of 23S rRNA component of the 50S ribosome. Interferes with ribosomal binding
Quinupristin-dalfopristin (Q-D)	1) Q: *erm*A, *erm*B, *erm*C	1) Ribosomal methylases	1) Reduce binding to the 23S ribosomal subunit
	2) D: *vat*, *vat*B	2) Acetyltransferases	2) Enzymatic modification of dalfopristin

***Table 1**. Mechanism of S. aureus resistance to antimicrobials.*

[29] a) Miller, L. G., Diep, B. A., *Clin. Infect. Dis*., **2008**, 46, 752-760. b) Kazakova, S. V. *et al, N. Engl. J. Med*., **2005**, 468-475.
[30] Mylotte, J. M.; McDermott, C.; Spooner, J. A., *Rev. Infect. Dis*., **1987**, 9, 891-907.
[31] Diekema, D. J. *et al*, *Clin. Infect. Dis*., **2001**, 32, (Suppl. 2): S114-S132.
[32] McGuiness, W. A.; Malachowa, N.; DeLeo, F. R., *Yale J. Biol. Med.*, **2017**, 90, 269-281.

1.3.1 Penicillin resistance.

• **History and epidemiology.** The mortality of patients with *S. aureus* in the pre-antibiotic era exceeded the 80% of infections.[33] Penicillin was truly a miracle drug: uniformly fatal infections could be cure. However, as early as 1942, resistance to penicillin had appeared, first in hospital and subsequently in the community.[34] By the late 1960s, more than 80% of staphylococcal isolates were resistant to penicillin. The first well-characterized pandemic of antibiotic-resistant *S. aureus*, that is attributable to a single clone, was caused by phage type 80/81 strains and it was responsible of both hospital and community outbreaks on a global scale.[35]

• **Mechanism of resistance.** Staphylococcal resistance to penicillin is mediated by *blaZ*, the gene that encodes *β*-lactamase (Table 1). The *blaZ* gene is part of a transposable element located on a large plasmid, often with additional antimicrobial resistance genes. *β*-lactamase is synthesized when staphylococci are exposed to *β*-lactam antibiotics, hydrolysing the *β*-lactam ring, leading to an inactive antibiotic. *blaZ* is controlled by two regulatory genes, the antirepressor *blaR1* and the repressor *blaI*.[36]

1.3.2 Methicillin resistance.

- **History and epidemiology.** Methicillin, a semi-synthetic *β*-lactam antibiotic, was introduced in the late 1950s as a therapy for penicillin-resitant *S. aureus* (PRSA) infections. Despite efficacy of methicillin for treatment of PRSA infections, the first methicillin-resistant *S. aureus* (MRSA) strains were reported within two years of clinical use.[37] Among the earlies MRSA clinical isolates was the archetypal MRSA strain COL, isolated in the UK in 1960. Outbreaks of infections caused by MRSA strains were reported in hospitals in the United States in the late 1970s, and by the mid-1980s these strains were endemic,[38] leading to the worldwide pandemic of MRSA in hospitals that continues to the present time. Currently, MRSA accounts for a large proportion of hospital-associated *S. aureus* infections and is associated with significant morbidity and mortality.[39] The overall burden of staphylococcal disease is increasing in many countries in both health care and community settings. The rapidity and extent of the spread of community-associated MRSA (CA-MRSA) strains have been reported in the United States, Canada, Asia, South America, and Australia, as well as throughout Europe, including countries that historically have a low prevalence of MRSA (Norway, Netherlands, Denmark and Finland).[40] They have been identified

[33] Skinner, D.; Keefer, C. S., *Arch. Intern. Med*., **1941**, 68, 851-875.
[34] Rammelkamp, C. H.; Maxon, T., *Proc. Royal Soc. Exper. Biol. Med*., **1942**, 51, 386-389.
[35] Robison, D. A. *et al*, *Lancet*, **2005**, 365, 1256-1258.
[36] Kernodle, D. S., *Am. Soc. Microbiol.*, **2000**, 609-620 (Fischetti, V. A.; Novick, R. P.; Ferretti, J. J.; Portnoy, D. A.; Rood, J. I., editors. Washington, DC, USA).
[37] Jevons, M. P., *BMJ*, **1961**, 1 (5219), 124-125.
[38] a) Crossley, K.; Landesman, B.; Zaske, D., *J. Infect. Dis*., **1979**, 139, 280-287. b) Peacock, J. E. Jr.; Marsik, F. J.; Wenzel, R. P., *Ann. Intern. Med*., **1980**, 93, 526-532.
[39] a) Dantes, R. *et al*, *JAMA Intern Med*, **2013**, 173(21), 1970-1978. b) Jarvis, W. R.; Schlosser, J.; Chinn, R. Y.; Tweeten, S.; Jackson, M., *Am. J. Infect. Control*, **2007**, 35(10), 631-637. c) Klein, E.; Smith, D. L.; Laxminarayan, R., *Emerg. Infect. Dis*., **2007**, 13(12), 1840. d) Klevens, R. M. *et al*, *Clin. Infect. Dis*., **2006**, 42(3), 389-391.
[40] a) Laupland, K. B.; Ross, T.; Gregson, D. B., *J. Infect. Dis*., **2008**, 198, 336-343. b) Larsen, A. R. *et al*, *J. Clin. Microbiol*., **2008**, 46, 62-68. c) Stam-Bolink, E. M.; Mithoe, D.; Baas, W. H.; Arends, J. P.; Moller, A. V., *Eur. J.*

a considerable number of different CA-MRSA strains all around the world. Between 2001 and 2004, a study in US shown an increase from 0.8% to 1.5% for MRSA[28b] strains and an increase from 7% to 24.2% for CA-MRSA.[41] Despite a lack of rigorous clinical studies, the agents for the treatment of CA-MRSA that are recommended include clindamycin, long-acting tetracyclines (doxycycline and minocycline) and trimethoprim-sulphamethoxazole, as well as rifampin and fusidic acid as adjunctive agents to be used in combination.[42]

The *mecA* gene (responsible for methicillin resistance) is encode on a mobile genetic element know as cassette chromosome *mec* (SCC*mec*).[43],[44] There are eight SSC*mec allotypes*, designated SCCmecI-SCCmecVIII, varying in size from 21 to 67 kb.[45] *mecA* was discovered more than twenty years after the first reported case of MRSA.[37,39] The emergence of 'epidemic' MRSA clones was in part the result of a successful horizontal transfer of the mec gene into an ecologically fit and transmission-efficient methicillin-sensitive *S. aureus* (MSSA) clone. This horizontal transfer leads to a limited number of clones responsible for infection of MRSA, in contrast to the multiple different strains of MSSA that cause infections.[46]

- **Mechanisms of resistance.** Resistance to methicillin confers resistance to all *β*-lactam agents, including cephalosporins.[47] Methicillin resistance requires the presence of the *mecA* gene, which controls the synthesis of proteins capable of binding penicillin, such as protein binding penicillin 2a (PBP2a; also called PBP2´).[48] A crystal structure determined that the active site of PBP2a blocks *β*-lactam binding sites but allows the transpeptidation reaction (as it is a membrane-bound enzyme).[49] The active site is similar to serine proteases.

  Phenotypic expression of methicillin is variable, and each MRSA strain has a characteristic profile. There is no homologue of *mecA* in MSSA, thus it has been

Clin. Microbiol. Infect. Dis., **2007**, 26, 723-727. d) Nimmo, G. R.; Coombs, G. W., *Int. J. Antimicrob. Agents*, **2008**, 31, 401-410. e) Kanerva, M. *et al*, *J. Clin. Microbiol*., **2009**, 7, 2655-2657. f) Gardella, N. *et al*, *Diagn. Microbiol. Infect. Dis*., **2008**, 62, 343-347.

[41] Tenover, F. C. *et al*, *J. Clin. Microbiol*., **2008**, 46, 2837-2841.

[42] a) Barton, M. *et al*, *Can. J. Infect. Dis. Med. Microbiol*., **2006**, 17 (Suppl. C), 4-24. B) Nathwani, D. *et al*., *J. Antimicrob. Chemother*., **2008**, 61, 976-994.

[43] Katayama, Y.; Ito, T.; Hiramatsu, K., *Antimicrob. Agents Chemother*., **2000**, 44, 1549-1555.

[44] a) Ubukata, K.; Nonoguchi, R.; Matsuhashi, M.; Konno, M., *J. Bacteriol*., **1989**, 171, 2882-2885. b) Ito, T.; Katayama, Y.; Hiramatsu, K., *Antimicrob. Agents Chemother*., **1999**, 43, 1449-1458.

[45] a) Hiramatsu, K.; Cui, L.; Kuroda, M.; Ito, T., *Trends Microbiol*., **2001**, 9, 486-483. b) Deurenberg, R. H.; Stobberingh, E. E., *Infect. Genet. Evol*., **2008**, 8, 747-763. c) Ma, X. X. *et al*, *Antimicrob. Agents Chemother*., **2002**, 46, 1147-1152. d) Oliveira, D. C.; Milheirico, C.; de Lencastre, H, *Antimicrob. Agents Chemother*., **2006**, 50, 3457-3459. e) Higuchi, W.; Takano, T.; Teng, L. J.; Yamamoto, T., *Biochem. Biophys. Res. Commum*., **2008**, 377, 752-756. f) Zhang, K.; McClure, J. A.; Elsayed, S.; Conly, J. M., *Antimicrob. Agents Chemother*., **2009**, 53, 531-540.

[46] a) Enright, M. C. *et al*, *Proc. Natl. Acad. Sci. U. S. A*., **2002**, 99, 7687-7692. b) Oliveira, D. C.; Tomasz, A.; de Lencastre, H., *Microb. Drug Resist*., **2001**, 7, 349-361. C) Crisostomo, M I.; *et al*, *Proc. Natl. Acad. Sci. U. S. A.*, **2001**, 98, 9865-9870.

[47] Ghuysen, J. M., *Trends Microbiol*., **1994**, 2, 372-380.

[48] a) Hartman, B. J.; Tomasz, A., *J. Bacteriol*., **1984**, 158, 513-516. b) Utsui, Y.; Yokota, T., *Antimicrob. Agents Chemother*., **1985**, 28, 397-403. c) Song, M. D.; Wachi, M.; Doi, M.; Ishino, F.; Matsuhashi, M, *FEBS lett.*, **1987**, 221, 167-171.

[49] Lim, D.; Strynadka, N. C., *Nat. Struct. Biol*., **2002**, 9, 870-876.

assumed that the gene *mecA* was adquired from other species.[50] The *mecA* has also been identified in the *S. sciuri*, with an 88% of the amino acid sequence in common with the MRSA gene, but also might come from another coagulase-negative staphylococcus.[51]

1.3.3 Quinolone resistance.

- **History and epidemiology.** Fluoroquinolones were initially introduced to treat Gram-negative infections in the 1980s. However, as they present a high Gram-positive spectrum, they have been used to treat infections of pneumococci and staphylococci as well. Quinolone resistance in *S. aureus* emerged quickly, more prominently in MRSA strains. The resistance of the fluoroquinolones was developed as a result of a mutation of the topoisomerase IV (which separates concatenated DNA strands) or DNA gyrase (which relieves DNA supercoiling), or by the induction of a multidrug efflux pump. As *S. aureus* is part of the common flora of the skin or mucosal surface, when a subject is treated for another infection, the bacteria is exposed to a subtherapeutic antibiotic concentration, with the risk of becoming resistant mutans.[52]

- **Mechanisms of resistance.** Resistance to quinolones results from chromosomal mutations. As we mentioned above, quinolones act on DNA gyrase and topoisomerase IV. Amino acid changes in critical regions of the enzyme-DNA complex (quinolone resistance-determining region [QRDR]) reduce quinolone affinity for both of its targets. The ParcC subunit (GrlA in *S. aureus*) of topoisomerase IV and the GyrA subunit in gyrase are the most common sites of resistance mutations. The mutations of the topoisomerase IV are the most critical because this is the primary drug target in staphylococci.[53,53]

1.3.4 Vancomycin resistance.

- **History and epidemiology.** Staphylococcal resistance to vancomycin was first reported in *Staphylococcus haemolyticus*.[54] In 1997, in Japan, took place the first report of vancomycin intermediate-resistant *S. aureus* (VISA), and additional cases were subsequently reported from other countries.[55] The VISA isolates were all MRSA and were not clonal. The first vancomycin-resistant *S. aureus* (VRSA) was isolated in the United States in 2002.[56] Since then, there have been a total of 14 isolates reported in the United States.[57]

---

[50] Archer, G. L.; Niemeyer, D. M., *Trends Microbiol*., **1994**, 2, 343-347.
[51] Couto, I.; Wu, S. W.; Tomasz, A.; de Lencastre, H., *J. Bacteriol*., **2003**, 185, 645-653.
[52] Hooper, D. C.; *Lancet Infect*., **2002**, 2, 530-538.
[53] Ng, E. Y.; Trucksis, M.; and Hooper, D. C., *Antimicrob. Agents Chemother.*, **1996**, 35, 1881-1888.
[54] Schwalbe, R. S.; Stapleton, J. T.; Gilligan, P. H., *N. Engl. J. Med*., **1987**, 316, 927-931.
[55] a) Hiramatsu, K. *et al*, *J. Antimicrob. Chemother*., **1997**, 40, 135-136. b) Smith, T. L.; *et al*, *N. Engl. J. Med*., **1999**, 340, 493-501.
[56] b) Chang, S. *et al*, *N. Engl. J. Med*., **2003**, 348, 1342-1347.
[57] Walters, M. S. *et al*, *MMWR (Morb. Mortal Wkly Rep.)*, **2015**, 64, 1056.

VISA is typically associated with hospitalization, persistent infection, prolonged vancomycin treatment and/or treatment failure. The majority of cells of VISA have little resistance to vancomycin (MIC ≥ 4 μg/mL).[58] Complete vancomycin resistance in *S. aureus* (VRSA, MIC ≥ 16 μg/mL) is conferred by the *vanA* operon encoded on transposon Tn*1546*, originally a part of a vancomycin-resistant enterococci (VRE) conjugative plasmid.[59] The resistance is maintained by retaining an original enterococcal plasmid or by a transposition of Tn*1546* from the VRE plasmid into a staphylococcal resident plasmid.[60]

- **Mechanism of resistance.** Two forms of *S. aureus* resistance to vancomycin have now been identified.[61] One form has been identified in the VISA strains, which have MICs to vancomycin between 8 and 16 μg/mL.[55a] The reduced of the affinity to vancomycin appears to result from changes in the peptidoglycan synthesis. The VISA strains present irregularly shaped of the peptidoglycan and thickened cell wall. There is also decreased cross-linking of peptidoglycan strands, which leads to the exposure of more *D*-Ala-*D*-Ala residues.[62] As result, more vancomycin is trap in the *D*-Ala-*D*-Ala residues available.[63]

  The second form of vancomycin resistance has resulted from the probable conjugal transfer of the *vanA* operon from a vancomycin-resistant *E. faecalis*.[64] The vancomycin resistance is based on two key events mediated by the *vanA* operon: 1) Hydrolysis of dipeptide *D*-Ala-*D*-Ala peptidoglycan precursors (anchor point of vancomycin), and 2) synthesis of *D*-Ala-*D*-Lactate peptidoglycan precursors, which can not bind vancomycin.

1.4 Biofilms.

In the 1970s, we began to appreciate that bacteria in the biofilm (known as sessile bacteria) constitute a major component of the bacterial biomass in many environments.[65,66] It was not until the 1980s and 1990s that we began to appreciate that attached bacteria were organized in elaborate ways.[65,67] Furthermore, different bacteria can coaggregate with multiple partnerts to form a dense bacterial plaque when they attach to a surface,[68] emphasizing that biofilms could adhere to surfaces and interfaces and to each other. So, biofilms are defined as ‘a structure

[58] Howden, B. P.; Davies, J. K.; Johnson, P. D. R.; Stinear, T. P.; Grayson, M. L., *Clin. Microbiol. Rev.*, **2010**, 23, 99-139.
[59] Arthur, M.; Molinas, C.; Depardieu, F.; Courvalin, P., *J. Bacteriol.*, **1993**, 175, 117-127.
[60] a) Périchon, B.; Courvalin, P., *Antimicrob. Agents Chemother.*, **2009**, 53, 4580-4587. B) Zhu, W. *et al*, *Antimicrob. Agents Chemother.*, **2010**, 54, 4314-4320.
[61] Walsh, T. R.; Howe, R. A., *Annu. Rev. Microbiol.*, **2002**, 56, 657-675.
[62] a) Hanaki, H. *et al*, *J. Antimicrob. Chemother.*, **1998**, 42, 315-320. b) Hanaki, H. *et al*, J. Antimicrob. Chemother., 1998, 42, 199-209.
[63] Sieradzki, K.; Roberts, R. B.; Haber, S. W.; Tomasz, A., *N. Engl. J. Med*, **1999**, 340, 517-523.
[64] Showsh, S. A.; de Boever, E. H.; Clewell, D. B., *Antimicrob. Agents Chemother.*, **2001**, 45, 2177-2178.
[65] a) Costerton, J. W.; Stewart, P. S.; Greenberg, E. P., *Science*, **1999**, 284, 1318-1322. b) Donlan, R. M., Costerton, J. W., *Clin. Microbiol. Rev.*, **2002**, 15, 167-193.
[66] Costerton, J. W.; Geesey, G. G.; Cheng, K. J., *Sci. Am.*, **1978**, 238, 86-95.
[67] Lawrence, J. R.; Korber, D. R.; Hoyle, B. D.; Costerton, J. W.; Caldwell, D. E., *J. Bacteriol.*, **1991**, 173, 6558-6567.
[68] Whittaker, C. J.; Klier, C. M.; Kolenbrander, P. E., *Annu. Rev. Microbiol.*, **1996**, 50, 513-552.

community of bacterial cells enclosed in a self-produced polymeric matrix and adherent to inert or living surfaces'.[69]

Advances in light microscopy and microelectrode technology (such as scanning electron microscope or confocal laser scanning microscope, CLSM) have led to an appreciation that bacterial biofilms consist of microcolonies on a surface, in which the bacteria are organized into a community with functional heterogeneity.[65b] The scanning electron microscope utilizes alcohol, acetone and xylene to gradually dehydrate the specimen prior to examination, since water is not compatible with the technique. This dehydration process results in significant sample distortion: the extracellular polymeric sustances, which are approximately 95% water, will appear more as fibres than as a thick gelatinous matrix surrounding the cells (Figure 8).

Biofilms constitute a protected mode of growth that allows the survival of the bacterial in hostile environments. The structures that form biofilms contain channels in which nutrients can circulate[70], and cells in different regions of a biofilm exhibit different patterns of gene expression.[71] It is not surprising that an impressive number of chronic bacterial infections involve bacterial biofilms, which are not easily eradicated by conventional antibiotic therapy.

These biofilm infections might be caused by a single species or by a mixture of species of bacteria or fungi (Table 2).[65] Biofilm infections share clinical characteristics, such as the preference for developing in inert surfaces (medical devices) or on dead tissue (sequestrum dead bone).[72] They grow slowly, in one or more locations.[73] Antibiotic therapy treats the planktonic cells released from the biofilm, which produce the symptoms of the infection, but fails to kill the biofilm.[74] Thus, although the infection is treated with the antibiotic, the biofilm stays intact, leading to new episodes of infection. Usually, the infection appears after stopping the treatment, which is treat again with antibiotic (not necessary the same antibiotic). These pattern of repeating the treatment several times also induce the antibiotic resistance. Moreover, most previous pharmacodynamic and pharmacokinetic studies of antibiotics have been performed on planktonic cells, and extrapolation of the results on biofilms is problematic as bacterial biofilms differ from planktonic cells in terms of growth rate, gene expression, and metabolism. Usually, bacterial biofilms are resistant to antibiotics, disinfectant chemicals and to phagocytosis and other components of the innate and adaptative inflammatory defence system of the body.[75] For this reason, biofilm infections show recurring symptoms until the sessile population is surgically removed from the body.[76]

[69] Ha, D. G.; O´Toole, G. A., *Microbiol. Spectr.*, **2015**, MB-0003-2014.
[70] de Beer, D.; Stoodley, P.; Lewandowski, Z., *Biotechnol. Bioeng.*, **1994**, 44, 636-641.
[71] Davies, D. G.; Chakrabarty, A. M.; Geesey, G. G., *Appl. Environ. Microbiol*., **1993**, 59, 1181-1186.
[72] Lambe, D. W. Jr.; Fergeson, K. P.; Mayberry-Carson, K. J.; Tober-Meyer, B.; Costerton, J. W., *Clin. Orthop. Relat. Res*., **1991**, 266, 285-294.
[73] Ward, K. H.; Olson, M. E.; Lam, K; Costerton, J. W., *J. Med. Microbiol*., **1992**, 36, 406-413.
[74] Marrie, T. J.; Nelligan, J.; Costerton, J. W., *Circulation*, **1982**, 66, 1339-1341.
[75] a) Frieri, M.; Kumar, K.; Boutin, A., *J. Infect. Public Health*, **2017**, 10, 369-378. b) Hoiby, N. *et al*, *Int. J. Oral Sci*., **2011**, 3, 55-65.
[76] Costerton, J. W. *et al*., *Annu. Rev. Microbiol*., **1995**, 49, 711-745.

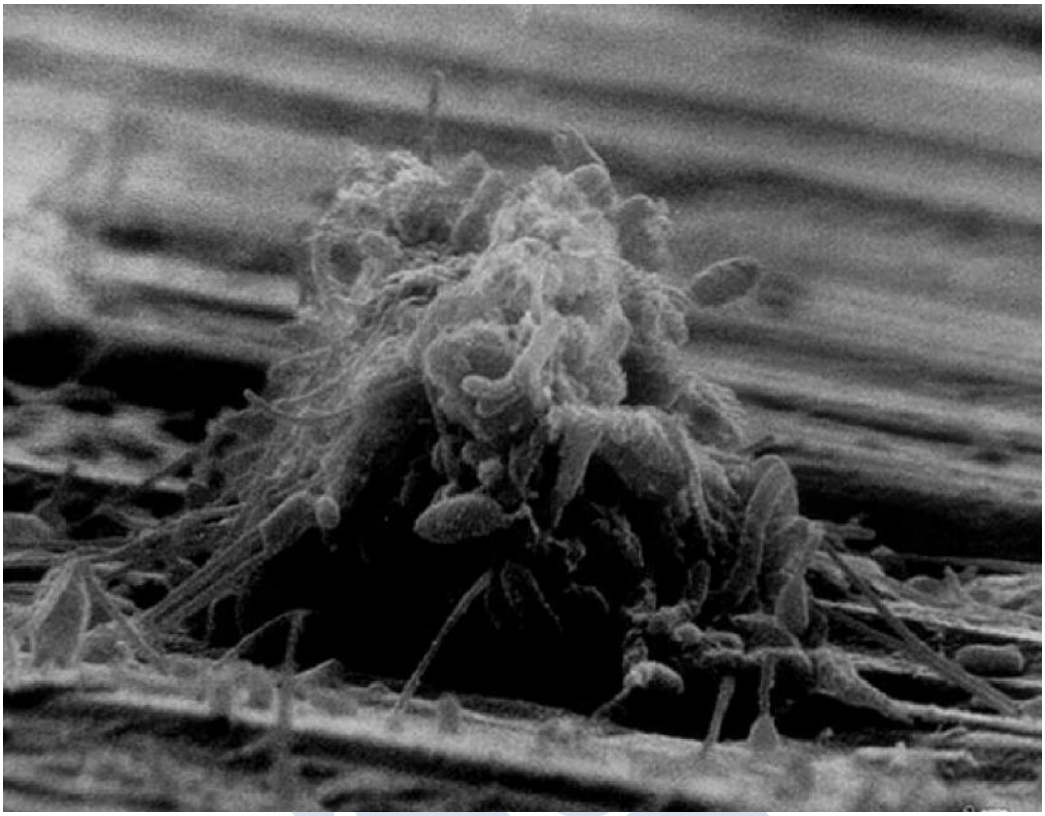

Figure 8. *Scanning electron micrograph of a biofilm on a metal surface.*[65b]

To destroy a biofilm, their physical properties has also been studied. In general, biofilms display viscoelastic properties. They undergo both reversible elastic responses and irreversible deformation, depending strongly on the forces acting on the matrix. Compression experiments with *P. aeruginosa* biofilms revealed that in response to pressure the biofilms go through a phase of elastic behaviour until a break point is reached, after which the biofilm behaves like a viscous fluid.[77] However, the measurements of the mechanical parameters of a biofilm is a challenge process due to the biofilm is a living material and their characteristic change over time, depending strongly on the growing environment. For this reason, the scientific community need to reach and agree on the parameters for each of the microbiological issues.[77b]

[77] a) Körsteng, V.; Flemming, H. C.; Wingender, J.; Borchard, W., *Water Sci. Technol*., **2001**, 43, 49-57. b) Boudarel, H.; Mathias, J. D.; Blaysat, B.; Grédiac, M., *NPJ Biofilms Microbiomes*., **2018**, 4, 17.

Infection or disease	Common biofilm bacterial species
Dental caries	Acidogenic Gram-positive cocci (e. g. Streptococcus)
Periodontitis	Gram-negative anaerobic oral bacteria
Otitis media	Nontypable strains of *Haemophilus influenzae*
Musculoskeletal infections	Gram-positive cocci (e. g. staphylococci)
Necrotizing fasciitis	Group A streptococci
Biliary tract infection	Enteric bacteria (e. g. *Escherichia coli*)
Osteomyelitis	Various bacterial and fungal species – often mixed
Bacterial prostatitis	*E. coli* and other Gram-negative bacteria
Native valve endocarditis	Viridans group streptococci
Cystic fibrosis pneumonia	*P. aeruginosa* and *Burkholderia cepacian*
Meloidosis	*Pseudomonas pseudomallei*
Nosocomial infections	
ICU pneumonia	Gram-negative rods
Sutures	*Staphylococcus epidermidis* and *S. aureus*
Exit sites	*S. epidermidis* y *S. aureus*
Arteriovenous shunts	*S. epidermidis* y *S. aureus*
Schleral buckles	Gram-positive cocci
Contact lens	*P. aeruginosa* and Gram-positive cocci
Urinary catheter cystitis	*E. coli* and other Gram-negative rods
Peritoneal dialysis (CAPD) peritonitis	A variety of bacteria and fungi
IUDs	*Actinomyces israelii* and many others
Endotracheal tubes	A variety of bacteria and fungi
Hickman catheters	*S. epidermidis* and C. albicans
Central venous catheters	*S. epidermidis* and others
Mechanical heart valves	*S. aureus* and *S. epidermidis*
Vascular grafts	Gram-positive cocci
Biliary stent blockage	A variety of enteric bacteria and fungi
Orthopedic devices	*S. aureus* and *S. epidermidis*
Penile prostheses	*S. aureus* and *S. epidermidis*

***Table 2**. Partial list of human infections involving biofilms.*

1.4.1 Formation of a biofilm.

Research in the 1990s has begun to reveal information about the molecular and genetic basis of biofilm development. Biofilms involving several different bacterial species have been studied,[75] but perhaps none more intensively than biofilms of *Pseudomonas aeruginosa*, which biofilm produce the recessive genetic disease cystic fibrosis (CF).

To explain the process of biofilm formation, we will focus on the *P. aeruginosa* biofilm.[69] In this case, the intracellular second messenger molecule 3´,5´-cyclic diguanylic acid (or c-di-GMP, Figure 9B) is implicated in biofilm formation, as many cellular functions as regulation of cell cycle, differentiation, motility and virulence. The current general model associates high intracellular levels of c-di-GMP with biofilm formation or sessile lifestyle. The low levels are related with a mobile or planktonic existence. Moreover, the *P. aeruginosa* biofilm is dependent on a multitude of cellular factors and coordinated pathways. Flagellar motility, twitching motility and the production of exopolysaccharides are prerequisites to form the biofilm.

In the laboratory, biofilm formation is a cyclical process wherein a free-swimming planktonic cell encounters a surface and initiates cell-to-surface attachment (Figure 9A).[69]

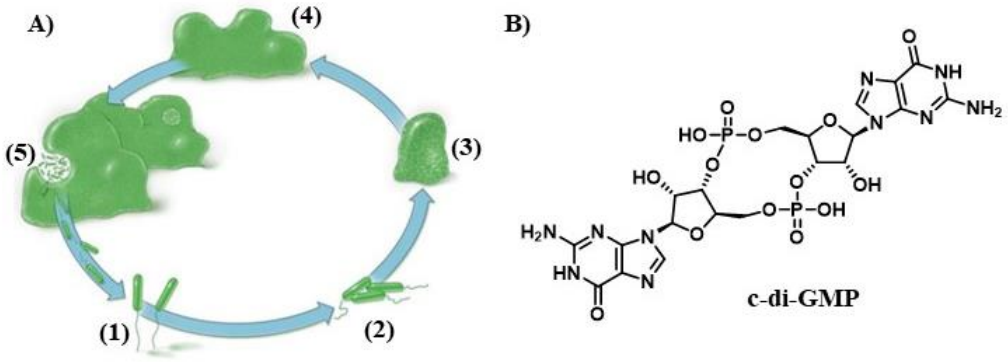

***Figure 9**. A) Steps of biofilm formation: (1) reversible attachment, (2) irreversible attachment, (3) microcolony formation, (4) macrocolony formation and (5) dispersion. B) Structure of the c-di-GMP.*[69]

1) **Reversible attachment.** It is the first step in biofilm formation, a step wherein a bacterium made a first contact with the surface. To overcome surface repulsion, *P. aeruginosa* utilizes flagellar-mediated swimming motility. It appears to be two distinct mechanisms that control flagellar motility during early biofilm formation in response to increasing intracellular c-di-GMP: the FleQ-c-di-GMP complex represses transcription of the genes required for flagellar assembly, while YcgR forms a complex with c-di-GMP that modulates flagellar rotation. The suppression of flagellar function stabilizes the interaction between the bacteria and the surface and promotes the transition to irreversible attachment.

2) **Irreversible attachment.** The irreversible attachment requires the production of exopolysaccharides (EPSs), that is believed to serve as an adhesin. These secreted polysaccharides, together with nucleic acids, proteins, extracellular DNA and additional factors, comprise the matrix of the mature biofilm. There are three possible mechanisms for this step: a) twitching, b) swarming and c) irreversible attachment.

    a. The bacteria can move using twitching motility, powered by type IV pili, which extend and retract to tug bacterial cells across the surface.

    b. *P. aeruginosa* has another form of motility known as swarming, which utilizes the flagellum as well as surfactants, to migrate on a substratum.

    c. The bacteria can attach 'irreversibly' via the long axis of the cell. This attachment is much more stable than the reversible attachment and it is the first committed step in biofilm formation and is typically associated with the so-called monolayer stage of biofilm formation.

3) **Microcolony formation.** The current model postulates that the formation of microcolonies and macrocolonies, and thus mature biofilms, requires the production of the EPS component of the matrix. For example, there are three different sugars as a central binding block for the *P. aeruginosa* biofilm: alginate, Pel and Psl (Figure 10). Psl is a neutral, branched polysaccharide with a five-sugar repeat unit composed of three *D*-mannose, one *L*-rhamnose and one *D*-glucose and there are not modifications in the molecule after polymerization.[78] The exact structure of Pel is currently unknown, but it is believed to be glucose rich.[79] EPSs appear to play roles in two discrete steps in biofilm formation: irreversible attachment and biofilm maturation. However, the regulation is due to two different proteins: RoeA acts in the early step while WspR participates in later stages in biofilm formation. The contact with the solid surface seems to be sufficient to trigger regulation trough the WspR system.[80]

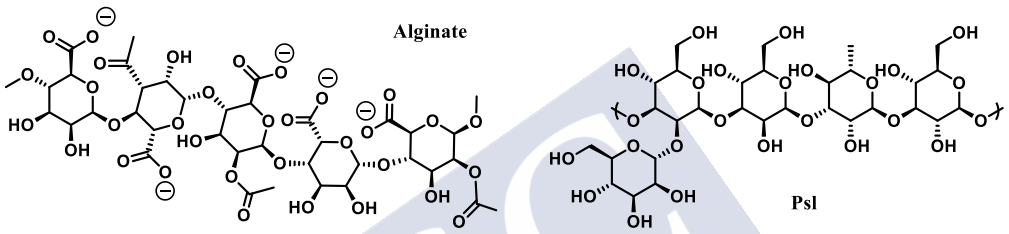

Figure 10. *Estructure of alginate (left) and Psl (right).*[81]

4) **Macrocolony formation**. The transition from microcolonies to macrocolonies is still poorly understood. The mechanism may be just continued development of microcolony over time. Alternatively, perhaps maturation of the biofilm is driven by a combination of genetic determinants for microcolony formation intersecting with (and/or modified by) physiological factors.

Examining the localization of Psl during the maturation of a biofilm by the strain *P. aeruginosa* PAO1 illustrates how microcolonies and macrocolonies may be distinct. Microcolonies of PAO1 probed with antiPsl antibodies showed a uniform distribution of the polysaccharide across the biofilm.[82] However, in the larger macrocolonies, the expression profile of Psl is much less uniform, being mainly expressed on the periphery of the structure. This differential expression of Psl may be attributed to relatively higher metabolic activity observed in the periphery and the lack of necessary energy to make Psl in the heart of the biofilm.[83] The loss of Psl production together with other

[78] Rozeboom, H. J. *et al*, *J. Biol. Chem*., **2008**, 283, 23819-23828.
[79] a) Friedman, L.; Kolter, R., *Mol. Microbiol*., 2004, 51, 675-690. b) Ma, L. *et al*, *Environ. Microbiol*., **2012**, 14, 1995-2005.
[80] a) Huangyutitham, V.; Güvener, Z. T.; Harwood, C. S., *mBio*, **2013**, 4, e00242-13. b) Güvener, Z. T.; Harwood, C. S., *Mol. Microbiol*, **2007**, 66, 1459-1473.
[81] Franklin, M. J.; Nivens, D. E.; Weadge, J. T.; Howell, P. L., *Front. Microbiol*., **2011**, 2, 167.
[82] Ma, L. *et al*, *PLoS Pathog*., **2009**, 5, e1000354.
[83] a) Rani, S. A. *et al*, *J. Bacteriol*., **2007**, 189, 4223-4233. b) Werner, E. *et al*, *Appl. Environ. Microbiol*., **2004**, 70, 6188-6196.

contributing factors may enable the formation and maintenance of channels between macrocolonies, which seems necessary for transporting nutrients, metabolites and waste.[84]

5) **Dispersion.** Under appropriate conditions, the dispersal of planktonic bacteria enables a controlled release from a mature biofilm structure to planktonic cells. Several signals have been identified that trigger dispersal of biofilm cells back to the planktonic state, such as nitrous oxide[85] and glutamate. Sodium nitroprusside is a known NO donor, and upon addition to *P. aeruginosa* biofilms (conc. 500 nM), induces dispersion and reduces biofilm surface coverage by approximately 68% compare to wild type.[86] Glutamate induces release of planktonic cells from the biofilm in a process called nutrient-induced dispersion.[87]

1.4.2 The biofilm matrix.

One common tactic that bacteria use to adapt to their surroundings is to grow as a multicellular community or biofilm.[88] As it was explain before, the formation of the biofilm begins with the attachment to a surface, followed by bacterial aggregation and secretion of self-produced polymeric substances, which form a matrix that encapsulates and protects the bacteria.[89] Living, fully hydrated biofilms are composed of cells (±15% by volume), located in the matrix-enclosed 'towers' and 'mushrooms' (Figure 11a), and of matrix material (±85% by volume). [65b]

The matrix can almost be considered as an immobilized enzyme system in which the environment and the enzyme activities are constantly changing and evolving.[84a] The nature of the matrix, is thus dependent on both intrinsic and extrinsic factors. Intrinsic factors arise in accordance with the specific bacteria that form the biofilm and extrinsic factors include the physico-chemical environment in which the biofilm and its matrix are located, which is constantly influenced by solute transport and solute diffusion gradients. Bacteria form biofilms in nearly all environments[90] and are implicated in contamination of surfaces as diverse as the International Space Station,[91] ship hulls[92] and oil storage and transfer infrastructure.[93] Biofilms are also of major concern in medical settings, where they are responsible for the chronic infection of burn wounds, eye and skin lacerations and pneumonia in cystic fibrosis patients.[94]

[84] a) Sutherland, I. W., *Trends Microbiol*., **2001**, 9, 222-227. b) Davey, M. E.; Caiazza, N. C.; O´Toole, G. A., *J. Bacteriol*., **2003**, 185, 1027-1036.
[85] Webb, J. S. *et al*, *J. Bacteriol*., **2003**, 185, 4585-4592.
[86] a) Barraud, N. *et al*, *J. Bacteriol*., **2006**, 188, 7344-7353. b) Barraud, N. *et al*, *J. Bacteriol*., **2009**, 191, 7333-7342.
[87] Sauer, K. *et al*, *J. Bacteriol*., **2004**, 186, 7312-7326.
[88] Whitfield, G. B.; Marmont, L. S.; Howell, P. L., *Front. Microbiol*., **2015**, 6, 471.
[89] a) Ohman, D. E., *Eur. J. Clin. Microbiol*., **1986**, 5, 6-10. b) Allensen-Holm, M. *et al*, *Mol. Microbiol*., **2006**, 59, 1114-1128.
[90] Bjarnsholt, T.; Ciofu, O.; Molin, S.; Givskov, M.; Høiby, N., *Nat. Rev. Drug Discov*., **2013**, 12, 791-808.
[91] Kim, W. *et al*, *PLoS ONE*, **2013**, 8:e62437. doi: 10.1371/journal.pone.0062437.
[92] Schultz, M. P.; Bendick, J. A.; Holm, E. R.; Hertel, W. M., *Biofouling*, **2011**, 27, 87-98.
[93] Lenhart, T. R. *et al*, *Biofouling*, **2014**, 30, 823-835.
[94] Lyczak, J. B.; Cannon, C. L.; Pier, G. B., *Microbes Infect*., **2000**, 2, 1051-1060.

The contamination of medical devices such as catheters, prosthetic joints and ventilators has also been well documented.[95]

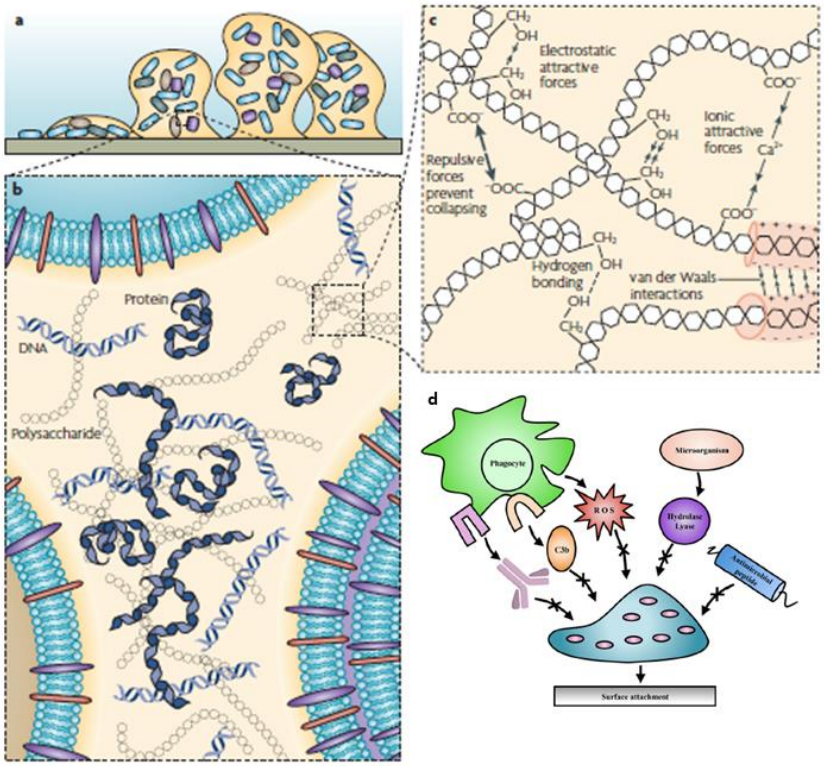

Figure 11. *EPS. a) Model of bacterial biofilm attach to a solid surface (towers´ shape). b) The major matrix components, polysaccharides, proteins and DNA, are distributed in a non-homogeneous pattern. c) The classes of weak physicochemical interactions that dominate the stability of the EPS matrix.*[96] *d) modifications of EPS contribute to the protection of the bacteria.*

In most biofilms, the microorganisms account for less than 10% of the dry mass, whereas the matrix account for over 90%.[97] The matrix consists on a conglomeration of different types of exopolysaccharides that forms the scaffold for the three-dimensional architecture of the biofilm. The matrix is responsible for adhesion to surfaces and for cohesion in the biofilm. The formation of the biofilm allows an entirely different lifestyle from the planktonic state. EPS have been called 'the dark matter of biofilms' due to the large range of matrix biopolymers and the challenge of analysing them.[98] EPS were initially denoted 'extracelullar polysaccharides' but were renamed, due to contain proteins, nucleic acids, lipids and other biopolymers.[98] Several functions of EPS have been determined (Table 3), demonstrating a wide range of advantages for the biofilm mode of life. They immobilize biofilm cells and keep them in close proximity, thus allowing for intense interactions, including cell-cell communication. The matrix

[95] Veerachamy, S.; Yarlagadda, T.; Manivasagam, G.; Yarlagadda, P. K., *Proc. Inst. Mech. Eng. H.*, **2014**, 228, 1083-1099.
[96] Mayer, C. *et al*, *J. Biol. Macromol*., **1999**, 26, 3-16.
[97] Flemming, H. C.; Wingender, J., *Nat. Rev. Microbiol*., **2010**, 8, 623-633.
[98] Flemming, H. C.; Neu, T. R.; Wozniak, D., *J. Bacteriol*., **2007**, 189, 7945-7947.

also protects organisms against desiccation, oxidizing or charged biocicles, some antibiotics and metallic cations, ultraviolet radiation and host immune defences.

The formation and maintenance of biofilm communities crucially depend on the production and quantity of EPS.[84a] The concentration, cohesion, charge, sorption capacity, specificity and nature of the individual components of EPS, as well as the three dimensional architecture of the matrix (pores, channels…) determine the mode of life in a biofilm. The morphology of the biofilm can be smooth and flat, rough, fluffy or filamentous, and it can also vary in the porosity degree. All these morphologies provide very diverse habitats on a small scale, favouring biodiversity.

The use of microelectrodes (to monitor oxygen levels, for example) revealed spatial heterogeneity in biofilms on a micrometre scale (Figure 11b).[99] The EPS matrix provides a physical structure that segregates microdomains.[100]

[99] de Beer, D.; Stoodley, P.; Roe, F.; Lewandoski, Z., *Biotechnol. Bioeng*., **1994**, 43, 1131-1138.
[100] Lawrence, J. R.; Swerhone, G. D. W., Kuhlicke, U.; Neu, T. R., *Can. J. Microbiol*., **2007**, 53, 450-458.

Function	Relevance for biofilms	EPS components involved
Adhesion	Allows the initial biofilm formation step, and the long-term attachment of whole biofilms to surface	Polysaccharides, proteins, DNA and amphiphilic molecules
Aggregation of bacterial cells	Enables bridging between cells, the temporary immobilization of bacterial populations, the development of high cell densities and cell-cell recognition	Polysaccharides, proteins and DNA
Cohesion of biofilms	Forms the biofilm matrix, mediating the mechanical stability of biofilms and through the EPS structure, determining biofilm architecture, as well as allowing cell-cell communication	Neutral and charged polysaccharides, proteins (such as amyloids and lectins) and DNA
Retention of water	Maintains a highly hydrated microenvironment around biofilm organisms, leading to their tolerance of desiccation in water-deficient environments	Hydrophilic polysaccharides and proteins
Protective barrier	Confers resistance to nonspecific and specific host defences during infection, and confers tolerance to various antimicrobial agents, as well as protecting cyanobacterial nitrogenase from the harmful effects of oxygen and protecting against some grazing protozoa	Polysaccharides and proteins
Sorption of organic compounds	Allows the accumulation of nutrients from the environment and the sorption of xenobiotics (thus contributing to environmental detoxification)	Charged or hydrophobic polysaccharides and proteins
Enzymatic activity	Enables the digestion of exogenous macromolecules for nutrient acquisition and the degradation of structural EPS, allowing the release of cells from biofilms	Proteins
Nutrient source	Provides a source of carbon-, nitrogen- and phosphorus-containing compounds for utilization by the biofilm community	Potentially all EPS components
Exchange of genetic information	Facilities horizontal gene transfer between biofilm cells	DNA
Electron donor or acceptor	Permits redox activity in the biofilm matrix	Proteins and biopolymers
Export of cell components	Releases cellular material as a result of metabolic turnover	Membrane vesicles containing nucleic acids, enzymes, lipopolysaccharides and phospholipids
Binding of enzymes	Results in the accumulation, retention and stabilization of enzymes through their interaction with polysaccharides	Polysaccharides and enzymes

Table 3*. Functions of extracelular polymeric substances in bacterial biofilms.*

- **Exopolysaccharides.**

Biosynthesis of EPS begins in the cytoplasm with the generation of activated precursor sugars.[88] In Gram-negative bacteria, the polymer is transported across the inner membrane to the periplasm during synthesis; whereas in Gram-positive bacteria the polymer is transported directly to the extracellular space. Modifications to the polymer can occur in the cytoplasm[101] or the periplasm[102] prior to export across the outer membrane, and in the excellular space in both Gram-positive and Gram-negative bacteria.[103] Bacterial EPS are usually composed of hexose sugars, but pentose sugars have also been identified. They can be as short as dimers and trimers, as well as being constituted by thousands of saccharide repeat units.[104] In same cases, EPS can even form fibers.[105]

Many known exopolysaccharides are polyanionic, such as alginate, xanthan and colanic acid. Polycationic exopolysaccharides can be used as an intercellular adhesin, which they are mainly composed by *β*-1,6-linked *N*-acetylglucosamine with partly deacetylated residues. This adhesin was discovered in important nosocomial pathogens such as *S. aureus* and *S. epidermidis*, which can colonize medical implants and lead to biofilm-related infections.[106] More recently, this adhesin was also detected in a range of other bacteria.[107]

As it was mentioned above, *P. aeruginosa* produces at least three distinct exopolysaccharides (in the microcolony formation) that contribute to biofilm development and architecture: alginate, Pel and Psl.

a) **Alginate**. Is one of the most extensively studied exopolysaccharides. It has a high-molecular-mass due to the presence of unbranched heteropolymer formed by1,4-linked uronic residues of β-*D*-mannuronate and α-*L*-guluronate.

In mucoid strains, alginate is involved in the establishment of microcolonies, but it is also responsible for the mechanical stability of mature biofilms.[108] However, in non-mucoid strains, alginate is not expressed, and Pel and Psl are involved in the establishment of biofilms.

b) **Pel and Psl**. Unlike alginate, Pel and Psl are primarily associated with non-mucoid biofilm establishment. Pel is essential for the biofilm formation and attachement to a surface, whereas Psl is involved in the adherence to biotic surfaces and in the maintenance of biofilm architecture.

---

[101] Atkin, K. E.; Macdonals, S. J.; Brentall, A. S.; Potts, J. R.; Thomas, G. H., *FEBS lett*., **2014**, 588, 1869-1872.
[102] a) Colvin, K. M. *et al, J. Bacteriol*., **2013**, 195, 2329-2339. b) Baker, P. *et al, PLoS Pathog*., **2014**, 10:e1004334. c) Little, D. J. *et al, Proc. Natl. Acad. Sci. U. S. A*., **2014**, 111, 11013-11018. d) Wolfram, F. *et al, J. Biol. Chem*., **2014**, 289, 6006-6019.
[103] Little, D. J. *et al, J. Biol. Chem*., **2014**, 289, 35907-35917.
[104] González, J. E.; Semino, C. E.; Wang, L. X.; Castellano-Torres, L. E.; Walker, G. C., *Proc. Natl. Acacd. Sci. U. S. A*., **1998**, 95, 13477-13482.
[105] Benziman, M.; Haigler, C. H.; Brown, R. M.; White, A. R.; Cooper, K. M., *Proc. Natl. Acacd. Sci. U. S. A.*, **1980**, 77, 6678-6682.
[106] Götz, F., *Mol. Microbiol*., **2002**, 43, 1367-1378.
[107] Jefferson, K. K., *Current Innovations and Future Trends*, **2009**, 175-186, Caister Academic, Norfolk, UK.
[108] a) Marcus, H.; Baker, N. R., *Infect. Immun*., **1985**, 47, 723-729. b) Doig, P.; Smith, N. R.; Todd, T.; Irvin, R. T., *Infect. Immun*., **1987**, 55, 1517-1522. c) Ramphal, R.; Guay, C.; Pier, G. B., *Infect. Immun*., **1987**, 55, 600-603.

In many bacteria, exopolysaccharides are indispensable for biofilm formation, and mutants that can not synthesize them are severely compromised or unable to form mature biofilms.[82,109] However, in mixed-species biofilms, the presence of a species that produces exopolysaccharides may lead to the integration of other species that do not synthesize matrix polymers.[83]

- **The other components of the matrix: extracellular proteins and DNA, surfactants, lipids and water.**

The biofilm matrix can contain considerable amounts of proteins that can far exceed the polysaccharide content, on a mass basis.[110, 111] Various extracellular enzymes have been detected in biofilms, many of which are involved in the degradation of biopolymers.[112] The substrates of these extracellular enzymes include water-soluble polymers (such as polysaccharides, proteins and nucleic acid) and water-insoluble compounds (such as cellulose, chitin and lipids), as well as organic particles that are trapped in biofilms.[113] There are non-enzymatic proteins in the matrix, such as the extracellular carbohydrate-binding proteins that are associated with the cell surface (called lectins). They are involved in the formation and stabilization of the polysaccharide matrix network and constitute a link between the bacterial surface and extracellular EPS. Examples include the galactose-specific lectin LenA and fucose-specific lectin LenB[114] of *P. aeruginosa*, both of which are implicated in biofilm formation.

Extracellular DNA (eDNA) is a major structural component in the biofilm matrix of *S. aureus*, whereas it is only a minor component of *S. epidermidis* biofilm.[115] eDNA is also a major matrix component of *P. aeruginosa* biofilm, in which functions as an intercellular connector.[116] It can also be used as an adhesin like in *Bacillus cereus* biofilm[117] or act as an antimicrobial compound, causing lysis by chelating cations that stabilize lipopolysaccharides and the bacteria outer membrane.[118]

Lipids are also found in the matrix.[119] Lipopolysaccharides are crucial for the adherence of *Thiobacillus ferrooxidants* to pyrite surfaces,[120] and *Serratia marcescens* produces extracellular lipids with surface-active properties (known as 'serrawettins').[121]

---

[109] a) Watnik, P. I.; Kolter, R., *Mol. Microbiol*., **1999**, 34, 586-595. b) Danese, P. N.; Pratt, L. A., Kolter, R., *J. Bacteriol*., **2000**, 182, 3593-3596.
[110] Frølund, B.; Palmgren, R.; Keiding, K.; Nielsen, P. H., *Water Res*., **1996**, 30, 1749-1758.
[111] Conrad, A. *et al*, *Lipids*, **2003**, 38, 1093-1105.
[112] a) Ude.S.; Arnold, D. L.; Moon, C. D.; Timms-Wilson, T.; Spiers, A. J., *Environ. Microbiol*., **2006**, 8, 1997-2011. b) Laue, H. *et al*, *Microbiology*, **2006**, 152, 2909-2918.
[113] Wingender, J.; Jaeger, K. E.; Flemming, H. C., in *Microbial Extracellular polymeric substances*, **1999**, 231-251, Springer, Heidelberg.
[114] a) Tielker, D. *et al*, *Microbiology*, **2005**, 151, 1313-1323. b) Diggle, S. P. *et al*, *Environ. Microbiol*., **2006**, 8, 1095-1104.
[115] Izano, E. A., Amarante, M. A., Kher, W. B.; Kaplan, J. B., *Appl. Environ. Microbiol*., **2008**, 74, 470-476.
[116] Yang, L. *et al*, *Microbiology*, **2007**, 153, 1318-1328.
[65] b) Donlan, R. M., Costerton, J. W., *Clin. Microbiol. Rev*., **2002**,15, 167-193.
[117] Vilain, S.; Pretorius, J. M.; Theron, J.; Broezel, V. S., *Appl. Environ. Microbiol*, **2009**, 75, 2861-2868.
[118] Mulcahy, H.; Charron-Mazenod, L.; Lewenza, S., *PLoS Pathog*., **2008**, 4, e1000213.
[119] Socolofsky, M. D.; Wyss, O., *J. Bacteriol*., **1961**, 81, 946-954.
[120] Sand, W.; Gehrke, T., *Res. Microbiol*., **2006**, 157, 49-56.
[121] Matsuyama, T.; Nakagawa, Y., *J. Microbiol. Methods*, **1996**, 25, 165-175.

Biosurfactants can have antibacterial and antifungal properties and are important for bacterial attachment and detachment from oil droplets.[122]

Water is by far the largest component of the matrix. Many EPS are hygroscopic and seem to retain water entropically rather than through specific water-binding mechanisms. When embedded in EPS, the cyanobacterium *Nostoc commune* maintains its phosphosynthetic activity during drying and rehydration.[123] Bacteria actively respond to desiccation by producing EPS.[124] Desiccation concentrates EPS, increasing the number of non-specific binging sites that can react with each other and reducing the biofilm volume.

1.4.3 Resistance to antimicrobial agents.

The nature of the biofilm structure confers an inherent resistance to antimicrobial agents, whether these antimicrobial agents are antibiotics, disinfectants or germicides. The efficiency of an antibiotic against planktonic cells and sessile cells are dramatically different (Table 4). Mechanisms responsible for resistance may be delayed the penetration of the antimicrobial agent through the biofilm matrix, altered growth rate of biofilm organisms, and other physiological changes due to the biofilm mode of growth (and/or a combination of them).[65b]

Bacteria	Antibiotic	MIC or MBC (μg/mL)	Conc. Effective against biofilm (μg/mL)
S. aureus NCTC 8325-4	Vancomycin	2 (MBC)	20[a]
P. aeruginosa ATCC 27853	Imipenem	1 (MIC)	>1,024[b]
E. coli ATCC 25922	Ampicillin	2 (MIC)	512[b]
P. pseudomallei	Ceftazidime	8 (MBC)	800[c]
S. sanguis 804	Doxycycline	0.063 (MIC)	3.15[d]

[a] Concentration required for 99% reduction. [b] Minimal biofilm eradication concentration. [c] Conc. required for ~ 99% reduction. [d] Conc. Required for > 99.9% reduction.

***Table 4**. Susceptibility of planktonic and biofilm bacteria to selected antibiotics.*

a) Delayed penetration of the antimicrobial agent.

The antimicrobial agent must diffuse through the biofilm matrix to inactivate the encased cells. The substance that constitutes the matrix present a diffusional barrier for these molecules by influencing either the rate of transport of the molecule to the interior of the biofilm or the reaction of the antimicrobial substance with the matrix material. Ciprofloxacin presents a delayed penetration in *P. aeruginosa* biofilms, from 40 s for a sterile surface to 21 min for a biofilm-containing surface.[125] Totramycin is 15 times more effective in planktonic *P.*

[122] Ron, E. Z.; Rosenberg. E., *Environ. Microbiol*., **2001**, 3, 229-236.
[123] Tamaru, Y.; Takami, Y.; Yoshida, T.; Sakamoto, T., *Appl. Environ. Microbiol*, **2005**, 71, 7327-7333.
[124] Roberson, E. B.; Firestone, M. K., *Appl. Environ. Microbiol*, **1992**, 58, 1284-1291.
[125] Suci, P. A.; Mittelman, M. W.; Yu, F. P.; Geesey, G. G., *Antimicrob. Agents Chemother*., **1994**, 38, 2125-2133.

aeruginosa cells than in sessile ones.[126] A suspension of 2% alginate inhibited the diffusion of gentamicin and tobramycin, although it can be reversed by using alginate lyase.[127]

Another study examined the diffusion of several antimicrobial agents (ceftazidime, cefsulodin, piperacillin, gentamicin and tobramycin) through synthetic and naturally produced alginate gels and found that β-lactam antibiotics diffuse more rapidly into the matrix than aminoglycosides.

b) Altered growth rate of biofilm organisms.

Biofilm-associated cells grow significantly more slowly than planktonic cells and, as a result, take up antimicrobial agents more slowly. The slowest growing *E. coli* cells (in biofilms) are the most resistant to cetrimide.[128] Another example is the *S. epidermidis* susceptibility for the growth rate: the fast the rate of cell growth, the more rapid inactivation by ciprofloxacin.[129]

1.4.4. Human infections involving biofilm.

Some diseases are strongly associated with biofilm: native valve endocarditis, chronic bacterial prostatitis, cystic fibrosis and periodontitis.

- **Native valve endocarditis (NVE).** It is a condition that results from the interaction between the vascular endothelium, generally of the mitral, aortic, tricuspid and pulmonic valves of the heart, and bacteria or fungi circulating in the bloodstream.[130] The diversity of organisms causing NVE is quite extensive: streptococci, staphylococci, gram-negative bacteria and fungi (*Aspergillus* spp. and *Candida*). These organisms gain access to the bloodstream primarily via the oropharynx, gastrointestinal tract and genitourinary tract. Biofilms on native heart valves may result in valve tissue damage or production of emboli.[131]

- **Chronic Bacterial Prostatitis.** The prostate gland may become infected by bacteria that once is in the prostatic duct can multiply rapidly and induce a host response. As long as the infection is in the early stages, the bacteria can be eradicated with antibiotic therapy.[132] If the bacteria persist, they can form biofilms that adhere to the epithelial cells of the duct system. Organisms isolated in cases of chronic bacterial prostatitis include *E. coli* (the most common isolate), *Klebsiella*, enterobacteria, *Proteus*, *Serratia*, *P. aeruginosa* and *E. faecalis*.[133] The treatment usually fails probably as a result of the local environment surrounding the infecting organisms and the fact that these organisms have produced a biofilm.

[126] Hoyle, B. D.; Wong, C. K. W.; Costerton, J. W., *Can. J. Microbiol*., **1992**, 38, 1214-1218.
127 Hatch, R. A.; Schiller, N. L., *Antimicrob. Agents Chemother*., **1998**, 42, 974-977.
[128] Evans, D. J.; Allison, D. G.; Brown, M. R. W.; Gilbert, P., *J. Antimicrob. Chemother*., **1990**, 26, 473-478.
[129] DuGuid, I. G.; Evans, E.; Brown, M. R. W.; Gilbert, P., *J. Antimicrob. Chemother*., **1990**, 30, 791-802.
[130] Thiene, G.; Basso, C., *Cardiovasc. Pathol*., **2006**, 15, 256-263.
[131] a) Ferguson, D. J.; McColm, A. A.; Ryan, D. M.; Acred, P., *J. Exp. Pathol*., **1986**, 67, 679, 686. b) Rohmann, S.; Erthel, R.; Darius, H., Makowski, T.; Meyer, *J., Clin. Cardiol*., **1997**, 20, 132-140.
[132] Nickel, J. C.; Costerton, J. W.; McLean, R. J. C.; Olson, M., *J. Antimicrob. Chemother*., **1994**, 33, 33-41.
[133] Domingue, G. J.; Hellstrom, W. J. G., *Clin. Microbiol. Rev*., **1998**, 11, 604-613.

- **Cystic Fibrosis.** It is a chronic disease of the respiratory system and is the most common inherited disease. In CF, there is a net deficiency of water, which impedes the upward flow of the mucus layer. *S. aureus* is usually the first pulmonary isolate from these patients,[134] and it can be controlled by antibiotics. *S. aureus* and *H. influenzae* infections usually predispose the CF-affected lung to colonization with *P. aeruginosa*.[135] The possibilities for successful treatment of CF may depend upon an early antimicrobial treatment to prevent or delay chronic infection with *P. aeruginosa*. The early treatment with oral ciprofloxacin and inhaled colistin could postpone chronic infections with *P. aeruginosa* for several years.[136] It has also been suggested that a vaccine against this organism might be effective in preventing initial colonization of the lungs of patients with CF.

- **Periodontitis**. Periodontal diseases are infections involving the supporting tissues of teeth. They range from mild and reversible inflammations of the gums (known as gingiva) to chronic destruction of periodontal tissues (such as the alveolar bone).[137] The channel between the tooth root and the gingiva is the primary site of periodontal infection and will extend into a periodontal pocket with the progression of the disease. *Porphyromonas gingivalis* is the primary agent responsible for periodontitis.[137,138] The predominant microflorae of active lesions in subgingival areas were *Fusobacterium nucleatum*, *Wolinella recta*, *Bacteroides intermedius*, *Bacteroides forsythus*, and *Bacteroides gingivalis* (*Porphyromonas gingivalis*).[139] The predominant flora is highly diverse, though periodontitis is clearly a polymicrobic infection.

  Plaque that becomes mineralized with calcium and phosphate ions is termed calculus or tartar. As the plaque mass increase, the beneficial buffering and antimicrobial properties of the saliva are less able to penetrate and protect the tooth enamel, leading to dental caries or periodontal disease. The control of supragingival plaque by professional tooth cleaning and personal efforts would prevent gingival inflammation and adult periodontitis.

[134] May, T. B. *et al*, *Clin. Microbiol. Rev*., **1991**, 4, 191-206.
[135] Govan, J. R.; Deretic, V., *Microbiol. Rev*., **1996**, 60, 539-574.
[136] Kock, C.; Hoiby, N., *Lancet*, **1993**, 341, 1065-1069.
[137] Lamont, R. J.; Jenkinson, H. F., *Microbiol. Mol. Biol. Rev*., **1998**, 62, 1244-1263.
[138] Socransky, S. S.; Haffajee, A. D., *J. Periodontol*., **1992**, 63, 322-331.
[139] Dzink, J. L.; Socransky, S. S., Haffajee, A. D., *J. Clin. Periodontol*., **1988**, 15, 316-323.

2. The post – antibiotic era. The discovery of novel antibacterial drugs.

In 2014, the WHO published a report in which revealed a worrying reality: antimicrobial resistance is a globalized phenomenon and constitutes a threat to public health.[140,141] They also stablished that infectious diseases produced by multi-resistant bateria increases every month. Currently, infectious diseases caused 700.000 deaths per year, but it is expected to reach 10 million deaths every year in 2050.[142]

The post-antibiotic era was evidenced in May 2016, when a strain of *E. coli* was isolated encoding a colistin resistance gene. Colistin is considered the last line of treatment for multi-resistant Gram-negative bacteria and the last therapeutic resource available.[143] In 2017, the WHO published a list of priority pathogens, composed of the 12 most dangerous bacterial species to human health (Table 5).[144] It is clear that we are in a race to develop new antimicrobials to supplement our decreasing antibiotic arsenal for combating the growing emergence of antibiotic resistant strain, and, currently, we are losing this race. The major contributor to this deteriorating situation is excessive and imprudent use of antibiotics in healthcare settings and animal production sector.[145] Moreover, during the last two decades, the development of antimicrobial compounds changes as the focus moved from MRSA to *Clostridium difficile* and most recently to Gram-negative bacteria.[146]

Priority	Pathogens
Critical	Carbapenem-resistant *Acinetobacter baumannii*
	Carbapenem-resistant *Pseudomonas aeruginosa*
	Carbapenem-resistant and ESBL-producing *Enterobacteriaceae*
High	Vancomycin-resistant *Enterococcus faecium*
	Methicillin-resistant, vancomycin-intermediate and resistant *Staphylococcus aureus*
	Clarithromycin-resistant *Helicobacter pylori*
	Fluoroquinolone-resistant *Campylobacter spp*
	Fluoroquinolone-resistant *Salmonellae*
	Fluoroquinolone-resistant and cephalosporin resistant *Neisseria gonorrhoeae*
Medium	Penicillin-non-susceptible *Streptococcus pneumoniae*
	Ampicillin-resistant *Haemophilus influenzae*
	Fluoroquinolone-resistant *Shigella spp.*

***Table 5**. WHO priority pathogens list for drug development of new antibacterial agents.*

[140] Campanini-Salinas, J.; Andrades-Lagos, J.; Mella-Raipan, J.; Vásquez-Velásquez, D., *Curr. Top. Med. Chem.*, **2018**, 18, 1188-1202.
[141] WHO, **2014**, Antimicrobial resistance: global report on surveillance. https://www.who.int/drugresistance/documents/surveillancereport/en/
[142] O´Neill, J., *Rev. Antimicrob. Resist.*, **2014**, 1-16.
[143] McGann, P. *et al*, *Antimicrob. Agents Chemother*., **2016**, 60, 4420-4421.
[144] https://www.who.int/news-room/detail/27-02-2017-who-publishes-list-of-bacteria-for-which-new-antibiotics-are-urgently-needed
[145] a) Bragg, R. R.; Meyburgh, C. M.; Lee, J. Y.; Coetzee, M., *Adv. Exp. Med. Biol*., **2018**, 1052, 51-61. b) Kennedy, D., *Science*, **2013**, 342, 777.
[146] Jackson, N.; Czaplewski, L.; Piddock, L. J. V., *J. Antimicrob. Chemother*., **2018**, 73, 1452-1459.

Concern about resistance has escalated in the past 15-20 years, with reports by the UK Department of Health, the European Commission, WHO, and an inter-agency force in the USA, among others.[147] These reports all argue for reduced antibiotic use, for better-tailored use (i. e., appropriate drug, dose and duration), and for better infection control.[148] After these reports, around the 23% of the community use of antibiotics has fallen in UK since 1997. Antimicrobial prescription to ambulatory patients in the USA has declined over 20% and the use of antibiotics as growth promoters in animal husbandry has been banned in the EU.[149] Even with more appropriate prescribing, antibacterial resistance continues to accumulate in many pathogens and settings, especially in hospitals. Respiratory infections account for over half of all community antibiotic prescribing, much of it inappropriate. The size of this market explains why many of the developmental antibiotics are tailored against respiratory infections but the medical need for new agents is much less here than in the context of nosocomial infection. In the community, multi-resistance is complicating the treatment of urinary tract infections, gonorrhoea and tuberculosis, apart from the nosocomial infections mention before. In the annual reports of new systemic drugs approved by the FDA, in the 2007-2016 period, there is only ten new antibacterial drugs were introduced (Table 6), but most of them are for skin infections treatment.

Clinicians have already seen pan-resistance to antibiotics in isolates of *P. aeruginosa* and *Acinetobacter spp*., and *Enterobacteriaceae* is not pan-resistance only due to the continued efficacy of the carbapenems.[148] If carbapenemases do spread widely, we will face a situation where many nosocomial Gram-negative infections become effectively untreatable. It is here (against Gram-negative pathogens) where the medical need for new agents is most acute. Moreover, while new treatments are becoming available for multi-resistant Gram-positive infections, the goal of finding a drug that is effective against MRSA remains elusive.

[147] a) UK Standing Medical Advisory Committee (SMAC). 'The Path of Least Resistance'. Department of Health, London, **1998**. b) European Commission BD. Opinion of the Scientific Steering Committee on Antimicrobial Resistance, Brussels, **2003**. c) WHO, 'Global strategy for containment of antimicrobial resistance', **2001**. d) Interagency Task Force on Antimicrobial Resistance. 'A public health plan to combat antimicrobial resistance', **2003**.

[148] Livermore, D. M., *Clin. Microbiol. Infect*., **2004**, 10, 1-9.

[149] a) Livermore, D. M., *Clin. Infect. Dis*., **2003**, 36, S11-S23. b) Gruneberg, R. N., *J. Chemother*., **2002**, 14, 9-16.

Year	Commercial Name	Active Principle	FDA Aprroved Indication
2017	Vabomere®	Meropenem - vaborbactam	Complicated urinary tract infection
	Baxdela®	delafloxacin	Acute bacterial skin infections
2016	**No Antibacterial Drugs Approvals Reported**		
2015	Avycaz®	Ceftazidime - avibactam	Complicated intra-abdominal infections in combination with metronidazole, and complicated urinary tract infections, including pyelonephritis.
2014	Zerbaxa®	Ceftolozane - tazobactam	Complicated intra-abdominal infections in combination with metronidazole, and complicated urinary tract infections, including pyelonephritis.
	Orbactiv®	Oritavancin	Skin infections.
	Sivextro®	Tedizolid phosphate	Skin infections.
	Dalvance®	Dalbavancin	Skin infections.
2013	**No Antibacterial Drugs Approvals Reported**		
2012	**No Antibacterial Drugs Approvals Reported**		
2011	Dificid®	Difaxomicin	Clostridium difficile-associated diarrhea.
2010	Zinforo®	Ceftaroline fosamil	Complicated skin and soft tissue infections and Community-acquired pneumonia.
2009	Vibativ®	Telavancin	Complicated skin and skin structure infections.
2008	**No Antibacterial Drugs Approvals Reported**		
2007	Doribax®	Doripenem	Complicated intra-abdominal infections and complicated urinary tract infections, including pyelonephritis.

***Table 6**. Chronology of the antibacterial drugs approvals in the last decade. Information extracted from FDA reports "Novels Drugs summary" years 2007-2017.*[140]

2.1. Current strategies to Combat Antimicrobial Resistance.

Today, the development of novel antibacterial drugs continues to represent an unattractive investment for big pharma.[150] The decline in antibacterial research by large pharmaceutical industries can be explained by several factors, such as the low ratio of Return On Investment (ROI) or the appearance of resistance, which occurs beforehand or shortly after the release of the new drug to the market. Moreover, trovafloxacin, temafloxacin and telithromycin antimicrobial agents, which were approved between 1990 and early 2000, had to be withdrawn from the market due to numerous reports of serious adverse reactions. Phase III clinical trials (those with a large group of patients) of an antibiotic in a single disease indication cost about US$70 million.[151] The unfavourable economics of antibiotic development have had a chilling effect on industrial discovery programs, and policy-based efforts to reverse this decline deserve attention.

[150] a) Kresse, H.; Belsey, M. J.; Rovini, H., *Nat. Rev. Drug Discov*., **2007**, 6, 19-20. b) Projan, S. J.; Bradford, P. A., *Curr. Opin. Microbiol*., **2007**, 10, 441-446.
[151] Cooper, M. A.; Shlaes, D., *Nature*, **2011**, 472, 32.

For those pharmaceuticals that are still developing new antibiotics, the main strategy has been the modification of existing antibiotics, such as the second- and third generation molecules of the best-selling antibiotic groups of β-lactams, macrolides, and fluoroquinolones.[12,11] The 68% of antibacterial agents found in clinical phases II and III follow this strategy, and the remaining 32% are compounds that have a new mechanism.[140] The problem is that this strategy brings the potential risk that these new antibacterial drugs will rapidly develop resistance since they continue to act on the same targets susceptible to mutation.

Another obstacle in the development of new antibiotics is the current system of regulatory requirements that discriminate against their approval.[152,153] In US, companies must demonstrate that a new antibiotic present superior activity than existing antibiotics. However, existing agents are so effective against drug-sensitive strains that a new antibiotic is unlikely to be much better than an older one. Moreover, testing new antibiotics against antibiotic-resistant bacteria is exceptionally hard, as patients with resistant infections have usually been treated with other antibiotics before resistance is documented.[152]

As it was already mentioned, the strategies applied by pharmaceuticals are the improvement of already known structures, but there is no longer any reason to confine the development of drugs to those that inhibit the synthesis of protein, nucleic acids, cell walls and folate simply because such drugs were so successful once.[173] Another broad set of targets are the enzymes of core metabolism (intermediary metabolism, energy generation and micronutrient acquisition) in the bacteria. Another target can be the enzymes that enable the pathogen to resist the defences of the host. The key aspect of the potential targets is that they are essential for bacterial growth or viability and are expressed under the conditions of the infection process.[12,154] There is now some evidence suggesting that the expression pattern of pathogens during infection can be quite different from that in culture medium.[152, 154a, 155] Several new techniques detect and monitor gene expression during infection. *In vivo* expression technology allows identification of genes specifically induced in the host, and it has been applied successfully to several pathogens.[156] A similar technique, differential fluorescence induction, utilizes promoter fusions with green fluorescent protein to identify active promoters *in vivo*.[156b, 157] Signature-tagged mutagenesis is another technique that identifies the genes required for the infection process and viability *in vivo*.[156b, 158] This is the reason why it is believed that contemporary structural, computational and chemical biology should be able to engineer compounds that can harm the pathogen without harming the host.[159]

[12] Yoneyama, H.; Katsumata, R., *Biosci. Biotechnol. Biochem*., **2006**, 70, 1060-1075.
[13] Walsh, C.; *Nat. Rev. Microbiol*., **2003**, 1, 65-70.
[152] Nathan, C., *Nature*, **2004**, 431, 899-902.
[153] a) Projan, S. J., *Curr. Opin. Microbiol*., **2003**, 6, 427-430. b) Coates, A.; Hu, Y.; Bax, R.; Page, C. *Nat. Rev. Drug Discov*., **2002**, 1, 895-910.
[154] a) McDevitt, D.; Rosenberg, M., *Trends Microbiol*., **2001**, 9, 611-617. b) Allsop, A., *Curr. Opin. Microbiol*., **1998**, 1, 530-534.
[155] Alksne, L. E.; Projan, S. J., *Curr. Opin. Biotechnol*., **2000**, 11, 625-636.
[156] a) Mahan, M. J.; Slauch, J. M.; Mekalanos, J. J., *Science*, **1997**, 277, 2007-2011. b) Chiang, S. L.; Mekalanos, J. J.; Holden, D. W., *Annu. Rev. Microbiol*., **1999**, 53, 129-154.
[157] Valdivia, R. H.; Falkow, S., *Science*, **1997**, 277, 2007-2011.
[158] Hensel, M. *et al*, *Science*, **1995**, 269, 400-403.
[159] Fidock, D. A.; Rosenthal, P. J.; Croft, S. L., Brun, R.; Nwaka, S., *Nat. Rev. Drug Discov*., **2004**, 126, 12809-12819.

New antibiotics should be approved if they meet three tests: 1) safety profile, 2) effectiveness against antibiotic-sensitive bacteria in patients, 3) effectiveness *in vitro* against antibiotic-resistant bacteria. After a new antibiotic is approved, its clinical efficacy should be monitored in patients who are infected with bacteria resistant to previously approved antibiotics.[152] It is important to understand that as a new antibiotic moves into clinical use, the clock starts ticking down on its useful lifetime. Basic studies to estimate the potential for developing resistance (such as determining the MIC), resistance frequencies and exploring the consequences of resistance mechanisms should be done in the early stages of drug discovery.[146,160]

2.2. Modification of existing antimicrobial compounds.

Members of each antibiotic class share a common core structure, or scaffold. Usually, the core of the antibiotic is left intact to preserve its activity while the chemical groups at its periphery are modified to improve the drug´s properties. New generations are often designed to be active against pathogens that have become resistant to the previous generation.[10]

- **Cephalosporins.** There are now at least four recognized generations of the cephalosporins (Figure 12), which are differentiated by their efficacy and activity spectrums rather than by structural similarity.[161] First-generation cephalosporins have activity against Gram-positive cocci; second-generation compounds maintain this activity and also display activity against Gram-negative organisms; third-generation compounds have decreased activity against Gram-positive organisms but increased against Gram-negative bacteria. Fourth-generation cephalosporins show an increased activity profile against both Gram-positive and Gram-negative organisms and also show activity against strains that produce some β-lactamase enzymes. Fifth-generation are effective against MRSA.[162]

- **Vancomycin-like structures.** Vancomycin became the first antibacterial glycopeptide to be introduced to the clinic in 1959.[163] They present high activity against Gram-positive bacteria but have not activity against Gram-negative bacteria, probably due to the size of the molecule, which is not able to penetrate the outer membrane. Vanc-1 and Vanc-2 (Figure 13) are synthetic compounds that present activity against vancomycin-resistant bacteria. Replacing the amide functionality with an amidine group (Vanc-2) resulted in significantly improved binding characteristics for both ligands, *D*-Ala-*D*-Ala and *D*-Ala-*D*-Lac residues at the termini of peptidoglycan.[164] The binding affinity of Vanc-1 is only around 2-fold less than vancomycin itself. Vanc-2 binding affinity for *D*-Ala-*D*-Ala was 15-fold greater than vancomycin and 600-fold greater for *D*-Ala-*D*-Lac, which suggest that the amidine group can function as a hydrogen-bond acceptor for the amide in the

[10] Fischbach, M. A., Walsh, C.T., *Science*, **2009**, 325, 1089-1093.
[160] Silver, L. L., *Clin. Microbiol. Rev*., **2011**, 24, 71-109.
[161] Page, M. G., *Expert. Opin. Invest. Drugs*, **2004**, 13, 973-985.
[162] a) Laudano, J. B.; *J. Antimicrob. Chemother*., **2011**, 66, iii11-iii18. b) Widmer, A. F., *Clin. Infect. Dis*., **2008**, 46, 656-658. c) Hebeisen, P. *et al*, *Antimicrob. Agents Chemother*., **2001**, 45, 825-836. d) Chong, Y. P. *et al*, *Diagn. Microbiol. Infect. Dis.* **2012**, 73, 264-266. e) Saravolatz, L. D.; Stein, G. E.; Johnson, L. B., *Clin. Infect. Dis*., **2011**, 52, 1156-1163. f) Ishikawa, T. *et al*, *Bioorg. Med. Chem. Lett*., **2003**, 11, 2427-2437.
[163] Nicolau, K. C.; Boddy, C. N. C.; Brase, S.; Winssinger, N., *Angew. Chem. Int. Ed*., **1999**, 38, 2096-2152.
[164] a) Xie, J.; Pierce, J. G.; James, R. C.; Okano, A.; Boger, D. L., *J. Am. Chem. Soc*., **2011**, 133, 13946-13949. b) Xie, J. *et al*., *J. Am. Chem. Soc*., **2012**, 134, 1284-1297.

ligand and so act as an isostere for the amide group of vancomycin. Vanc-2 displayed very potent antimicrobial activity against VRE BM4166 with an MIC_{50} value of 0.31 μg/mL, which is comparable to the activity displayed by vancomycin susceptible strains (MIC_{50} = 0.3 μg/mL).

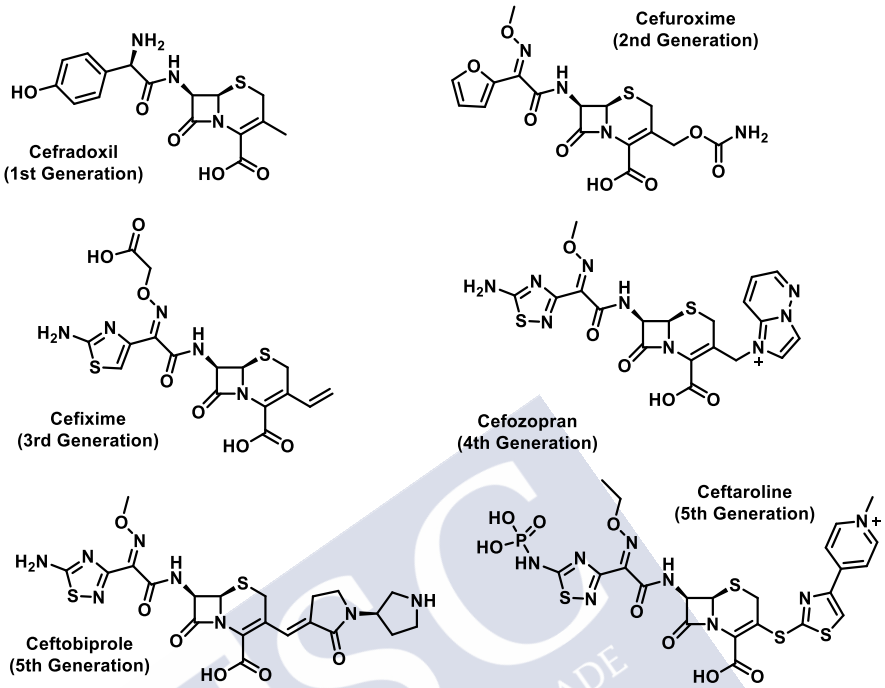

***Figure 12**. Different generations of cephalosporins.*

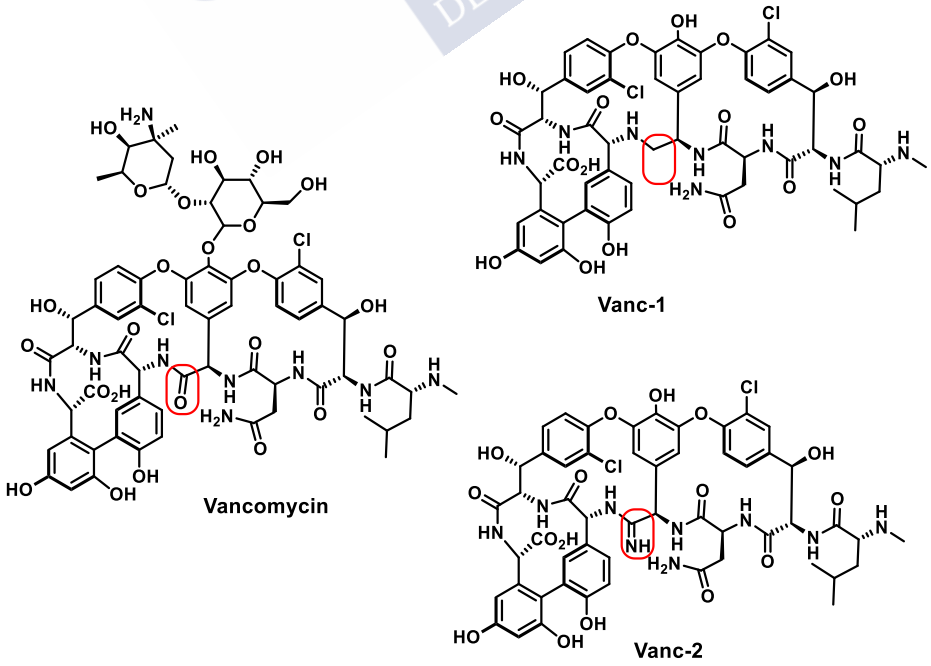

***Figure 13**. Vancomycin aglycon analogues structures.*

It has been proposed that the mechanism of action of vancomycin is based on the dimerization upon recognition of the dipeptide motif. Therefore, there are efforts on the introduction of structural elements on the glycopeptides that either promote dimerization of the antibacterial or improve affinity for the bacterial cell membrane, such as hydrophobic side chains in naturally teicoplanin (Figure 14).[165] This compound has a similar core to vancomycin, but differs in the saccharides attach to it. Following the idea that both dimerization and cell-membrane anchoring enhance the activity, three semisynthetic glycopeptides have progressed to clinical trials following similar strategies: oritavancin, dalbavancin, and telavancin. Oritavancin is the 4-chlorobiphenylmethyl analogue of chloroeremomycin, a glycopeptide produced by *Amycolatopsis orientalis*. The addition of this substituent has a profound effect on the ability of oritavancin to form dimers. The dimerization constant is four orders of magnitude higher than vancomycin.[166] The biphenyl substituent also serves to improve the membrane-anchoring ability of oritavancin. In combination, these two effects appear to override the loss of binding efficacy encountered with the substitution of *D*-Ala-*D*-Ala for *D*-Ala-*D*-Lac, and consequently improve against VanA-resistant organisms.

Dalbavancin is a close analogue of teicoplanin and displays a similar activity profile. It shows activity against many Gram-positive bacteria and is generally slightly more potent than vancomycin. However, it lacks activity against VanA-resistant strains.[167] Telavancin is the youngest of the semisynthetic variants and the first to be approved for clinical use. It was approved by the FDA for the treatment of complicated skin and skin-structure infections in 2009. Telavancin has been described as a multifunctional lipoglycopeptide and its potency has been attributed to a dual mode of action.[168] It maintains the common glycopeptide mechanism of inhibiting cell-wall biosynthesis, but additionally appears to be able to disrupt the integrity of the cell-wall, thus leading to depolarization, leakage and cell death.

[165] Allen, N. E.; LeTourneau, D. L.; Hobbs, J. N., *J. Antibiot*., **1997**, 50, 677-684.
[166] Allen, N. E.; Nicas, T. I.; *FEMS Microbiol. Rev*., **2003**, 26, 511-532.
[167] Streit, J. M.; Fritsche, T. R.; Sader, H. S.; Jones, R. N., *Diagn. Microbiol. Infect. Dis*., **2004**, 48, 137-143.
[168] a) Higgins, D. L. *et al*, *Antimicrob. Agents Chemother*., **2005**, 49, 1127-1134. b) Lunde, C. S. *et al*, *Antimicrob. Agents Chemother*., **2009**, 53, 3375-3383.

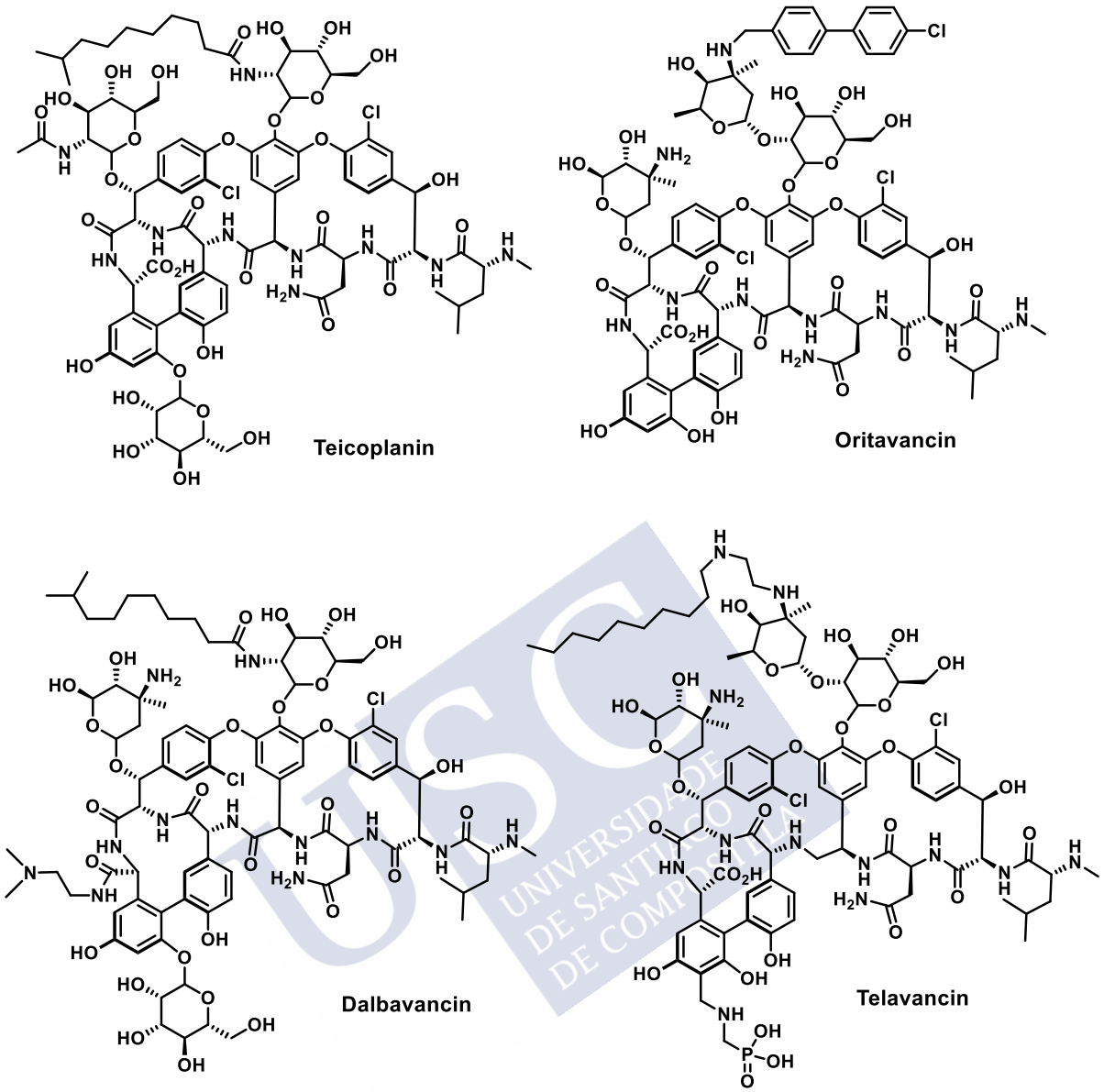

***Figure 14**. Semisynthetic glycopeptides.*

- **Combinatorial therapy.** This strategy is about treating the infections with a set of drugs rather than individual therapy (monotherapy), fusing of two (or more) antimicrobial agents with distinct mode of action to produce a single bifunctional entity.[169] Dual mode of action would make the emergence of the bacteria slower than monotherapy. The difficulty of this methodology it that the hybrid agents must prove to be more effective than the sum of their parts. There are three different ways to combine the drugs: a) combination drugs acting on different targets in different

[169] Moellering, R. C., *Int. J. Antimicrob. Agents*, **2011**, 37, 2-9.

pathways, b) combination drugs acting on different targets in same pathway, c) combination drug acting on single target, but in different proportions.[170]

a) Combination drugs acting on different targets in different pathways. The classical example is the treatment against Mycobacterium tuberculosis, by combining four drugs: Rifampicin (RNA polymerase inhibitor), Isoniazid (enoylreductase subunit of fatty acid synthase), Ethambutol (an inhibitor of arabinosyl transferases involved in cell wall biosynthesis) and Pyrazinamide (mechanism of action poorly understood) (Figure 15).[171] Assuming that the bacterium got a change to develop resistance by changing one target, this combination regimen will still be effective against at least other two pathways, minimizing the chances of bacterial propagation.

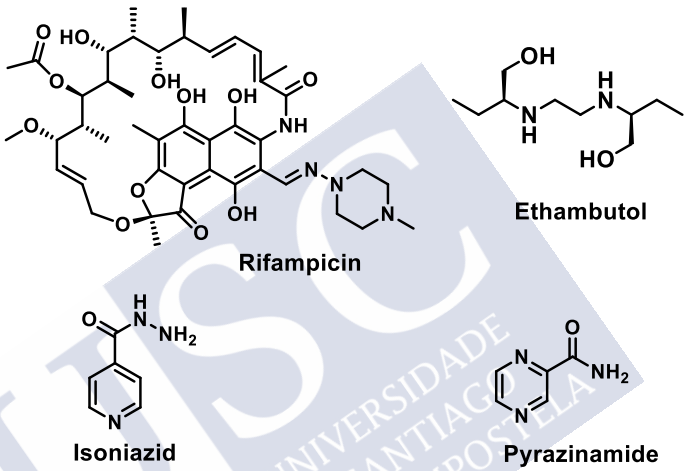

Figure 15. *Combination of drugs to treat tuberculosis: Rifampicin, Isoniazid, Ethambutol and Pyrazinamide.*

b) Combination drugs acting on different targets in same pathways. The classical example is the amoxicillin (*β*-lactam) and clavulanic acid (*β*-lactamase enzyme inhibitor).

c) Combination drugs acting on simple target, but in different proportions. Streptogramins is a mixture of two active molecules such as quinupristin and dalfopristin. These two molecules - one a nonribosomal peptide and the other a polypeptide-nonribosomal peptide hybrid- bind in adjacent sites in the 50S ribosomal subunit, near the peptidyl transferase center.[172]

[170] Kaur, I., *J. Infect. Dis. Ther*., **2016**, 4, 1000292. (ISSN: 2332-0877).
[171] Ginsberg, A. M.; Spigelman, M., *Nat. Med*., **2007**, 13, 290-294.
[172] a) Hansen, J. L.; Moore, P. B.; Steitz, T. A., *J. Mol. Biol*., **2003**, 330, 1061-1075. b) Tu, D.; Blaha, G.; Moore, P. B.; Steitz, T. A., *Cell*, **2005**, 121, 257-270.

An alternating approach is the mixture of an antimicrobial with an agent that either enhances its activity or stimulate it to reach its site of action more efficiently. An interesting example of this approach is the combination of an antibacterial with an iron(III)-chelating siderophore group. These siderophore-drug conjugates may find utility in the treatment of Gram-negative pathogens such as *P. aeruginosa*, which are resistant to many classes of antibacterials. Gram-negative bacteria actively transport Fe^{III}-siderophore complexes into the cell via specific receptors.[173] By attaching an antibacterial to a siderophore, it is hoped that the resulting compound would be able to cross the membrane and deliver the drug in its site of action.[174] Penicillin antibacterial attach to an artificial tris(catecholate) siderophore was tested against *P. aeruginosa*, proving that whereas the parents compounds were initially inactive against the strain, the conjugate frequently attained values of < 0.5 μM (Figure 16).[175]

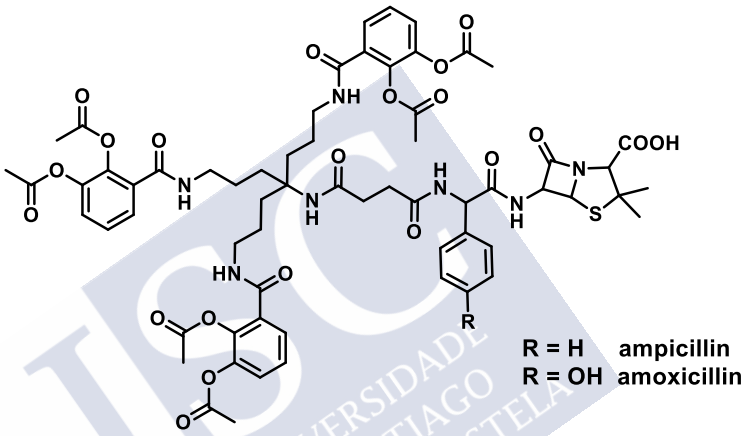

Figure 16. *Penicillin attach to a tris(catecholate) siderophore.*[175]

2.3. New antibacterial compounds from Natural products.

Antibacterial compounds are obtained from two sources: de novo chemical synthesis and natural products. Most of the antibacterial substances introduced during the golden age (1940s – 1960s) were discovered as a result of screening natural products obtained from microbial fermentations.[176] However, nowadays, natural product screening tends to result in the rediscovery of compounds rather than the procuration of new ones.[146]

Natural products exhibit remarkable characteristics such as extraordinary chemical diversity, chemical and biological properties with macromolecular specificity and less toxicity, apart from low side effects and low price.[177] Although the most easily accessible compounds have been discovered, there is still value in this approach. Recent efforts to search new

[146] Jackson, N.; Czaplewski, L.; Piddock, L. J. V., *J. Antimicrob. Chemother*., **2018**, 73, 1452-1459.
[173] Hider, R. C.; Kong, X., *Nat. Prod. Rep*., **2010**, 27, 637-657.
[174] Ji, C.; Juarez-Hernandez, R. E.; Miller, M. J., *Future Med. Chem*., **2012**, 4, 297-313.
[175] Ji, C.; Miller, P. A.; Miller, M. J., *J. Am. Chem. Soc*., **2012**, 134, 24, 9898-9901.
[176] Spring, D. R. *et al*, *Angew. Chem. Int. Ed*., **2013**, 52, 10706-10733.
[177] Siddiqui, A. A.; Iram, F.; Siddiqui, S, Sahu, K., *Int. J. Drug Dev. Res*., **2014**, 6, 172-204.

modalities – underexplored ecological niches and/or the genomes of even well studied bacteria – have yield novel molecules.[178]

- **Abyssomicins.** They were isolated in 2004 from a actinomycete found in deep sea sediment samples, as one of the unexplored niche is the marine bacteria.[175,179] Abyssomicin C (Figure 17), which show promising activity against MRSA (MIC = 4 μg/mL) and VRSA (13 μg/mL), acts by preventing the conversion of chorismite into *ρ*-aminobenzoic acid (*ρ*-ABA), a precursor in tetrahydrofolate biosynthesis. *ρ*-ABA is found in many microorganisms but not in humans, what make the inhibition of *ρ*-ABA biosynthesis an attractive target for antibacterials.[180]

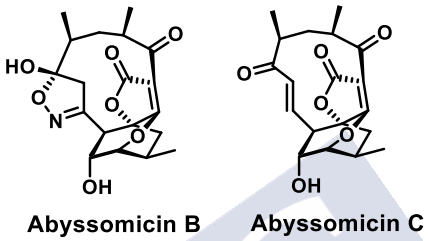

Figure 17. *Examples of Abyssomicins.*

- **Pantocins.** It is stimated that the number of species successfully cultured and evaluated from soil represent less than 1% of the total population[181], probably because many organisms are unculturable under standard laboratory conditions. Therefore, they were historically unavaiblable for investigation.[182] However, technology nowadays allows mimicking the natural environment of the bacteria.[183] Pantocin A and B (Figure 18) could not be identified until their biosynthetic genes were expressed by recombinant DNA methods in *E. coli*.[184] It has been proved that Pantocin A and Pantocin B inhibit the histidine and the arginine biosynthesis, respectively.

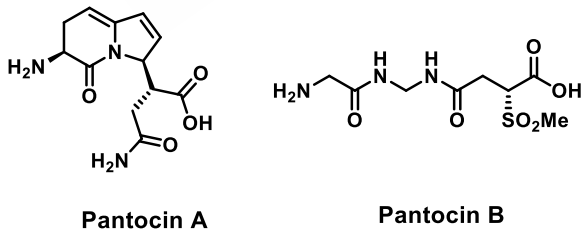

Figure 18. *Examples of Pantomicins.*

[178] Clardy, J.; Fischbach, M. A.; Walsh, C. T., *Nat. Biotechnol*., **2006**, 24, 1541-1550.
[179] a) Bister, B. *et al*, *Angew. Chem. Int. Ed*., **2004**, 43, 2574-2576. b) Bister, B. *et al*, *Angew. Chem. Int. Ed*., **2004**, 116, 2628-2630.
[180] Riedlinger, J. *et al*, *J. Antibiot*., **2004**, 57, 271-279.
[181] MacNeil, I. A. *et al*, *J. Mol. Microbiol. Biotechnol*., **2001**, 3, 301-308.
[182] Bull, A. T.; Ward, A. C.; Goodfellow, M., *Microbiol. Mol. Biol. Rev*., **2000**, 64, 573-606.
[183] Lewis, K.; Epstein, S.; D´Onofrio, A.; Ling, L. L., *J. Antibiot*., **2010**, 63, 468-476.
[184] Jin, M; Liu, L.; Wright, S. A. I.; Beer, S. V.; Clardy, J., *Angew. Chem. Int. Ed*., **2003**, 42, 2898-2901.

- **Metagenomics**. It is called to the direct extraction and analysis of DNA from the entire microbial population within an environmental sample.[185] Metagenomics involves the extraction of DNA, subsequent purification, and insertion into vectors such as plasmids, cosmids, or bacterial artificial chromosomes, and finally, propagation of the DNA in hosts such as *E. coli*.[186,187] The resulting complex DNA library can then be screened functionally to test for the production of novel antibacterials or other biologically interesting secondary metabolites. One example is the discovery of the antibacterial turbomycin (A and B) (Figure 19), which have activity against a range of Gram-positive and Gram-negative bacteria such as *Erwinia herbicola*, *Streptococcus pyogenes* and *Staphylococcus aureus*.

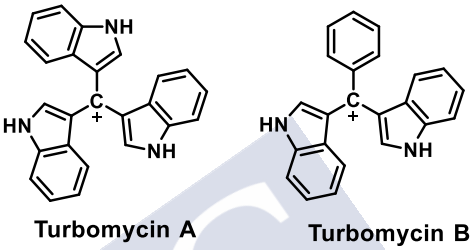

Figure 19. *Examples of Turbomycins.*

- **Lantibiotics.** They are peptidic toxins, a subclass of bacteriocins, produced by bacteria to inhibit the growth of closely related bacteria.[188] They are synthesized in the ribosomes, so they go through a high amount of post-translational modification that leads to the formation of multiple macrocyclic rings within their 3D structure. The macrocycles are generated from a linear peptide sequence by formation of lanthionine and methyllanthionine bridges, through a process of dehydration and cyclization typically involving cysteine and serine/threonine residues (Figure 20).[188c,189]

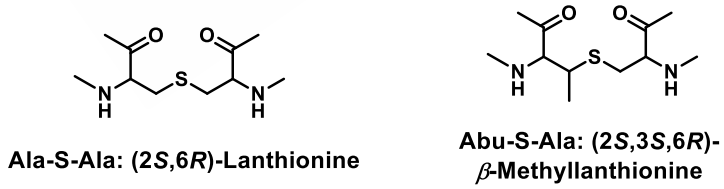

Figure 20. *Lanthionine and methyllanthionine brigdes.*

[185] Banik, J. J.; Brady, S. F., *Curr. Opin. Microbiol*., **2010**, 13, 603-609.
[186] a) Srinivas, N. *et al*, *Science*, **2010**, 327, 1010-1013. b) Vetterli, S. U.; Moehle, K.; Robinson, J. A., *Bioorg. Med. Chem*., **2016**, 24, 6332-6339. c) Shankaramma, S. C. *et al*, *ChemBioChem*, **2002**, 3, 1126-1133.
[187] Handelsman, J.; Rondon, M. R.; Brady, S. F.; Clardy, J.; Goodman, R. M., *Chem. Biol*., **1998**, 5, R245-R249.
[188] a) McAuliffe, O.; Ross, R. P.; Hill, C., *FEMS Microbiol. Rev*., **2001**, 25, 285-308. b) Chatterjee, C.; Paul, M.; Xie, L.; van der Donk, W. A., *Chem. Rev.*, **2005**, 105, 633-683. c) Willey, J. M.; van der Donk, W. A., *Annu. Rev. Microbiol*., **2007**, 61, 477-501.
[189] Wang, H.; van der Donk, W. A., *ACS Chem. Biol*., **2012**, 7, 1529-1235.

Novel lanbiotics structures have been discovered, isolated and reported: actagardine (Figure 21),[190] deoxyactagardine B,[191] entianin,[192] curvopeptin,[193] prochlorosins,[194] catenulipeptin,[189] erythreapeptin,[195] avermipeptin,[195] griseopeptin,[195] and labyrinthopeptins.[196]

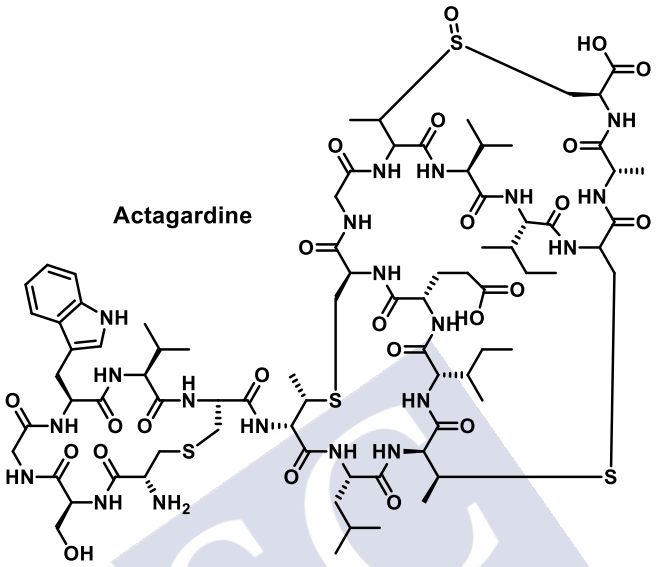

Figure 21. *Estructure of Actagardine.*

2.4. Antibacterial agents with new mechanism of action.

Modern medicine must address the inescapable fact that the supply of available, effective antibiotics is being rapidly exhausted. The development of new classes of antimicrobials utilizing novel antimicrobial mechanisms is the only solution to counteract emerging multiple drug resistance.[197]

- One new approach is the use of vaccines, that reduces the occurrence of antimicrobial resistance by various mechanisms.[198] The emergence of recombinant DNA and genome sequencing technology heralded a new era in the field of vaccinology.[199] This approach,

[190] a) Vértesy, L. *et al*, *J. Antibiot*., **1999**, 52, 730-741. b) Shi, Y.; Bueno, A.; van der Donk, W. A., *Chem. Commun*., **2012**, 48, 10966-10968.
[191] Boakes, S.; Appleyard, A. N.; Cortes, J.; Dawson, M. J., *J. Antibiot*., **2010**, 63, 351-358.
[192] Fuchs, S. W. *et al*, *Appl. Environ. Microbiol*., **2011**, 77, 1698-1707.
[193] Krawczyk, B.; Voller, G. H.; Voller, J.; Ensle, P.; Sussmuth, R. D., *ChemBioChem*, **2012**, 13, 2065-2071.
[194] Tang, W.; van der Donk, W. A., *Biochemistry*, **2012**, 51, 4271-4279.
[195] Völler, G. H. *et al*, *ChemBioChem*, **2012**, 13, 1174-1183.
[196] Meindl, K. *et al*, *Angew. Chem. Int. Ed*., **2010**, 49, 1151-1154.
[197] Spellberg, B.; Powers, J. H.; Brass, E. P.; Miller, L. G.; Edwars, J. E., *Clin. Infect. Dis*., **2004**, 38, 1279-1286.
[198] Mishra, R. P. N.; Oviedo-Orta, E.; Prachi, P.; Rappuoli, R.; Bagnoli, F., *Curr. Opin. Microbiol*., **2012**, 15, 596-602.
[199] Rappuoli, R., *Vaccine*, **2001**, 19, 2688-2691.

termed reverse vaccinology, utilizes full genome sequence data and bioinformatics to identify potential antigens that hold promise as vaccine targets.

- Another approach is the bacteriophage therapy. Bacteriophages are viruses that target bacterial cells.[200] One of the advantages of bacteriophage to fight infections is their high level of host specificity, which translate to a very low probability of a population of bacteria developing resistance. The ability of bacteriophages to exclusively target pathogenic bacteria ensures that the micriobiota of the host is not affected, thereby reducing the risk of secondary or opportunistic infections occurring. Bacteriophage therapy is nontoxic and administration rarely results in allergic reactions.[201] The major bacterial resistance mechanisms are listed in the Table 7. Phages are capable of evolving to infect completely resistant host populations and have risen to the challenge of adaptive immunity.[202]

Resistance mechanism	Description
Adsorption Resistance	Absence of receptor molecules on bacterial surfaces prevents binding of phage to host cell
Immunity to superinfection	Inhibition of phage replication by recognition of a phage-associated motif
Abortive infection	Inhibition of phage replication by the suicide of infected bacteria
Restriction/modification enzymes	Restriction enzymes cleave incoming foreign DNA at specific sequences
CRISPRs-Cas proteins	Phage DNA is integrated into CRISPR loci and transcribed into short, noncoding RNAs. These RNAs and Cas proteins recognize and silence foreign genetic elements

***Table 7**. Bacterial mechanisms of resistance to phage infection.*

- Another attractive options that are increasingly explored is targeting bacterial virulence. The conventional concept of virulence is defined by the ability of a pathogen to cause disease or cause damage to host tissues.[203] Anti-virulence drugs disrupt the process of infection, but in contrast to antibiotics, they do not directly affect bacterial growth or viability.[204] The earliest examples of the antivirulence approach include inactivation of bacterial toxins, such as tetanus and diphteria.[205]Some of the most attractive antivirulence strategies include inhibition of quorum sensing and virulence regulation,[206] virulence factor secretion and function,[207] and bacterial adhesion and colonization.[208]

[200] Elbreki, M. *et al*, *J. Viruses*, **2014**, 1-20.
[201] Slopek, S.; Weber-Dabrowska, B.; Dabrowski, M.; Kucharewicz-Krukowska, A., *Arch. Immunol. Ther. Exp. (Warsz)*, **1987**, 35, 569-583.
[202] Buckling, A.; Rainey, P. B., *Proc. R. Soc*., **2002**, 269, 931-936.
[203] Clatworthy, A. E.; Pierson, E.; Hung, D. T., *Nat. Chem. Biol*., **2007**, 3, 541-548.
[204] Neville, N.; Jia, Z., *Molecules*, **2019**, 24, 378-394.
[205] a) Keller, M. A.; Stiehm, E. R., *Clin. Microbiol. Rev*., **2000**, 13, 602-614. b) Schmitt, C. K.; Meysick, K. C.; O´Brien, A. D., *Emerg. Infect. Dis*., **1999**, 5, 224-234.
[206] Kalia, V. C., *Biotechnol. Adv*., **2013**, 31, 224-245.
[207] Baron, C., *Curr. Opin. Microbiol*., **2010**, 13, 100-105.
[208] Cusumano, C. K.; Hultgren, S. J., *IDrugs*, **2009**, 12, 699-705.

Only three antivirulence therapeutics have gained US Food and Drug Administration (FDA) approval, all of which are antibody-based.[209]

- A new target that is being explored is the inhibition of the fatty acid synthesis.[210] FabI, an enoyl-ACP reductase, is implicated in the last step in the fatty acid biosynthetic pathway. This biosynthetic cycle results in elongation of the fatty acid by two carbons, an acetate unit, during each cycle. The FabI inhibition prevents elongation of the acyl chain, disrupting both saturated and unsaturated fatty acid biosynthesis and preventing bacterial growth.[211] In *S. aureus* and *E. coli* this enzyme has been shown to be the antibacterial target of triclosan and diazaborines, thereby demonstrating the essentiality of FabI in these organisms.[212]

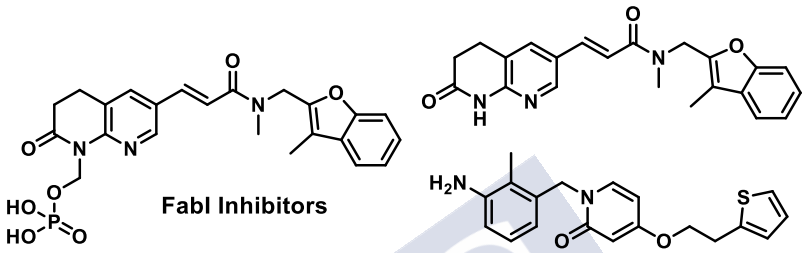

Figure 22. *Examples of FabI inhibitors.*

- Another strategy being used for the discovery of new antibacterial drugs is to mimic innate defense structures, and in particular antimicrobial peptides called defensines (further explain in antimicrobial peptides section).[213] Brilacidine (Figure 23) is a non-peptidic foldamer that possesses bactericidal activity on Gram-positive and Gram-negative bacteria. The folding ability is essential for its high antimicrobial potency and low toxicity. Members of this class of foldamers have been found to have low MIC but high haemolysis values toward eukaryotic cells.[214] The mechanisms studies suggest that the arylamide inserts into the lipid membrane just below the headgroups nearly perpendicular to the bilayer surface and the long axis parallel to the bilayer. In this manner, the antimicrobial arylamide destroys the barrier function of the microbial cell membrane mainly by altering its electrical potential.[215] Its action is in the cell membrane, and consequently, it has been propose that is the reason why these compounds do not exhibit toxicity on the mammalian cell membrane.

[209] Dickey, S. W.; Cheung, G. Y. C.; Otto, M., *Nat. Rev. Drug Discov*., **2017**, 16, 457-471.
[210] Karlowsky, J. A.; Kaplan, N.; Hafkin, B.; Hoban, D. J.; Zhanel, G. G., *Antimicrob. Agents Chemother.*, **2009**, 53, 3544-3548.
[211] Bergler, H.; Fuchsbichler, S.; Hogenauer, G.; Turnowsky, F., *Eur. J. Biochem*., **1996**, 242, 689-694.
[212] Miller, W. H., *J. Med. Chem*., **2002**, 45, 3246-3256.
[213] Scott, R. W.; Tew, G. N., *Curr. Top. Med. Chem.*, **2017**, 17, 576-589.
[214] a) Tew, G. N.; Scott, R. W.; Klein, M. L.; Degrado, W. F., *Acc. Chem. Res*., **2010**, 43, 30-39. b) Scott, R. W.; DeGrado, W. F.; Tew, G. N., *Curr. Opin. Biotechnol*., **2008**, 19, 620-627.
[215] Su, Y.; DeGrado, W. F.; Hong, M., *J. Am. Chem. Soc*., **2010**, 132, 9197-9205.

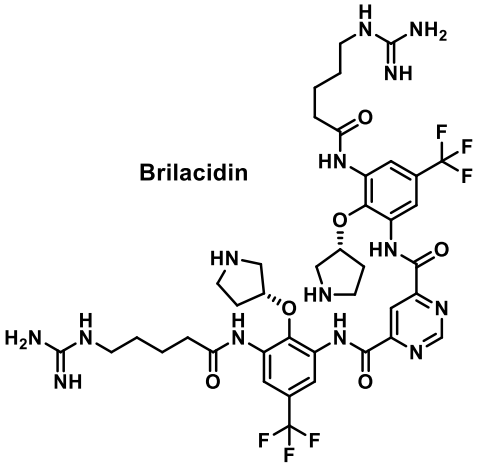

Figure 23. *Structure of Brilacidin.*

- Antibiotics acting on outer membrane proteins are a new class of antibacterial drugs with activity on Gram-negative bacteria. Murepavadin (Figure 24) is a peptidomimetic engineered from the cationic antimicrobial peptide protegin I.[216] It is a macrocyclic structure based on *β*-hairpin conformation, stablished by *D*-proline-*L*-proline sequence, that it is critical for its activity.[217] The binding of murepavidin with the LptD protein causes lipopolysaccharide alterations in the outer membrane of the bacterium and, ultimately, cell death.[218] It has specific activity against *P. aeruginosa* but it has not activity against other Gram-negative bacteria. Actually, intravenous murepavidin is recruiting patients for Phase III study for the treatment of different types of pneumonia due to *P. aeruginosa* (NCT03409679).

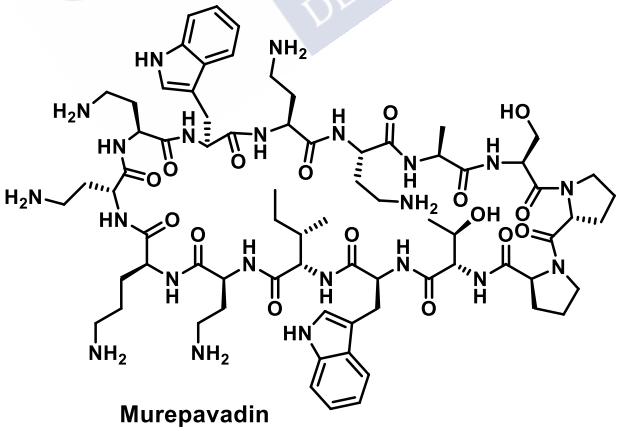

Figure 24*. Structure of Murepavadin*

[216] Robinson, J. A., *Bioorg. Med. Chem.*, **2005**, 13, 2055-2064.
[217] Werneburg, M. *et al*, *ChemBioChem*, **2012**,13, 1767-1775.
[218] Martin-Loeches, I.; Dale, G. E.; Torres, A., *Expert Rev. Anti. Infect. Ther*., **2018**, 16, 259-268.

- Antivirulence strategies by quorum sensing (QS) inhibition. Quorum sensing is a cell-cell signalling phenomenon utilized by bacteria cells within a given population to collectively coordinate gene expression. Gram-positive bacteria utilize oligopeptides as quorum sensing signals and are commonly referred as autoinducer peptides (AIPs). The detection of this AIP by bacterial cells consists of a two-component receptor/response system including a membrane-associated receptor histidine kinase protein (AgrC) and an intracellular response regulator protein (AgrA).[219] Some of the virulence phenotypes regulated by the AIP signalling system include: extracellular toxins, cell-surface, adhesion factors, tissue degrading enzymes, and exoproteins.[220]

  Four different autoinducer peptides (I-IV, Figure 25) has been proposed for *S. aureus*.[221] The natural product hamamelitannin inhibits MRSA infections in vivo without affecting growth, which indicates that it may be inhibiting QS (Figure 25).[222] Ambuic acid (Figure 25) has been shown to reduce *agr* gene expression in *S. aureus*.[223] It has been proposed that the mechanism of action is based on the inhibition of the AIP biosynthesis pathway as deduced by the observed abolishment of AIP products. Further studies of the mode of action are necessary, as they could lead to novel strategies for inhibiting QS in *S. aureus*.

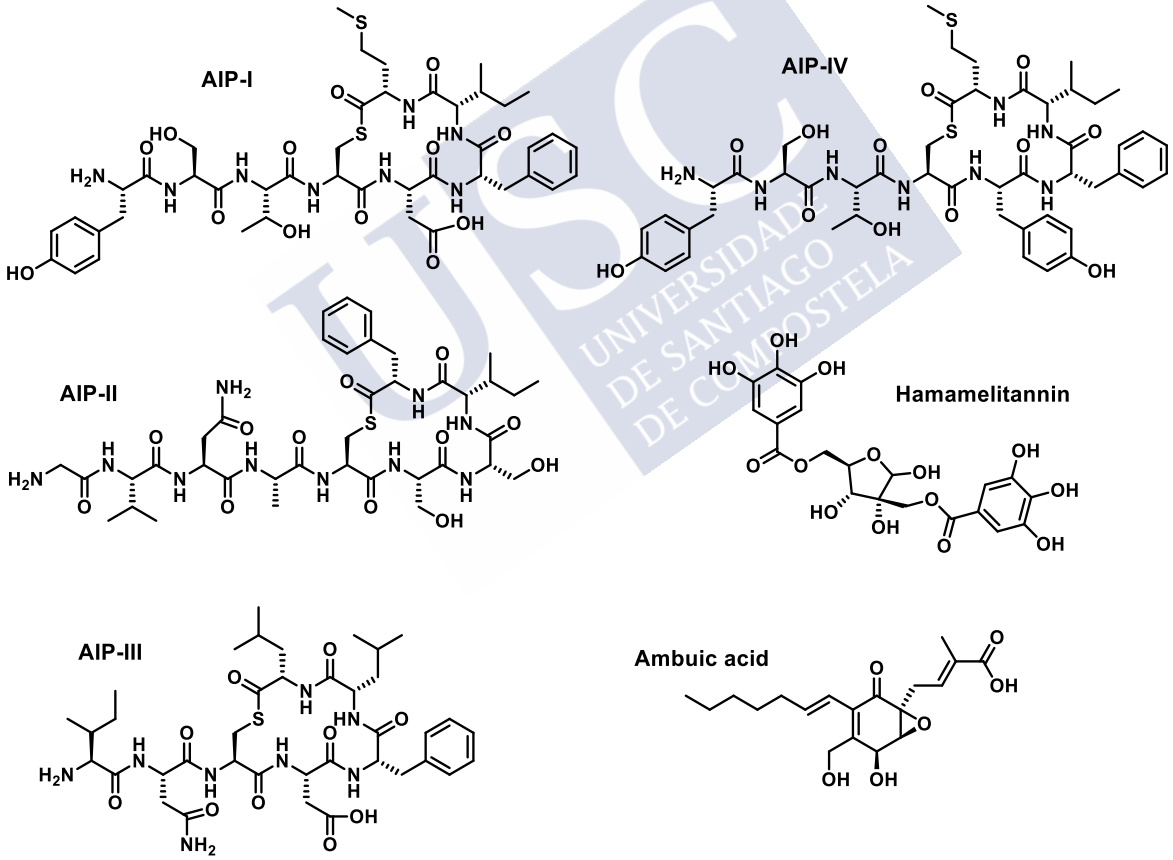

***Figure 25**. Chemical structure of the four AIP, Hamamelitannin and ambuic acid.*

[219] Lina, G. *et al*, *Mol Microbiol*., **1998**, 28, 655-662.
[220] Oogai, Y. *et al*, *Appl. Environ. Microbiol*., **2011**, 77, 8097-8105.
[221] Ji, G.; Beavis, R.; Novick, R. P., *Science*, **1997**, 276, 2027-2030.
[222] Kiran, M. D. *et al*, *Mol. Pharmacol*., **2008**, 73, 1578-1586.
[223] Nakayama, J. *et al*, *Antimicrob. Agents Chemother*., **2009**, 53, 580-586.

2.5 Antimicrobial peptides. Novel strategy for natural and synthetic compounds.

The innate immune system is the first line of defense against microorganisms that are quite conserved among invertebrate and vertebrate animals. It is recognized as the most ancient arm of the immune system and its effectiveness is characterized by a rapid and effective response, intended to quickly eliminate threats.

Antimicrobial peptides (AMPs), also known as host defense peptides (HDPs), have the potential to be developed as a new generation of antimicrobials.[224] They are released by practically every eukaryotic life form, from insect and plants to human beings, as part of the innate immune response to infections.[225] AMPs are an abundant and diverse group of molecules, where more than 1200 HDPs were identified or predict and approximately 940 of them were found in eukaryotic systems.[224d] In fact, over 600 HDPs have been reported to kill pathogenic microorganisms including Gram-positive and Gram-negative bacteria, viruses, protozoa, and fungi, and also to be involved in promoting and regulating the immune response (Table 8).[226] AMPs also mediate chemotaxis, apoptosis, immunomodulatory effects, and wound healing.[227] Although their structures are extremely diverse, the AMPs share a number of important characteristics. They are relatively small (less than 50 amino acid) and positively charge, and they also present a substantial number of hydrophobic residues. As a consequence of this distribution of hydrophilic and hydrophobic amino acids, the peptides are able to adopt amphipathic structures, often as a result of interacting with their microbial targets, which are fundamental to their mechanism of action.[228] This represents a class of antimicrobials with broad spectrum activity against bacteria, mycobacterial, enveloped viruses, fungi and even transformed or cancerous cells.[229] Due to the mechanism based on the membrane interactions with AMPs, it is theoretically and clinically difficult for the pathogen to acquire resistance to AMPs. Additionally, certain cationic HDPs at sub-inhibitory concentration can also prevent bacterial biofilm formation, which is strongly implicated in the development of chronic infections.

Normally, AMPs are short peptides, ranging from 10 to 50 amino acid, although shorter AMPs are preferred to reduce production costs. Most of the short AMPs exhibit antibacterial potency against clinical isolates like those of longer AMPs. For example, the hexapeptide MP196 (RWRWRW-NH_2) shows robust activity against *E. coli* and *S. aureus* with a MIC of 5 μg/mL.[230] However, peptides with excessively short lengths show a decrease tendency to form amphipathic secondary structures, which is associated with reduction of activity potency.[231]

---

[224] a) Wang, J. *et al*, *Med. Res. Rev*., **2019**, 39, 831-859. b) Van´t Hof, W., Veerman, E. C.; Helmerhorst, E. J.; Amerongen, A. V., *Biol. Chem*., **2001**, 382, 597-619. c) Afacan, N. J.; Yeung, A. T. Y.; Pena, O. M.; Hancock, R. E. W., *Curr. Pharm. Des.*, **2012**, 18, 807-819.
[225] Zasloff, M., *Nature*, **2002**, 415, 389-395.
[226] a) Marr, A. K.; Gooderham, W. J.; Hancock, R. E. W., *Curr. Opin. Pharmacol*., **2006**, 6, 468-472. b) Jenssen, H.; Hamill, P.; Hancock, R. E. W., *Clin. Microbiol. Rev*., **2006**, 19, 491-511.
[227] Zhong, G, *et al*, *Adv. Healthc Mater*., **2017**, 6, 1601134.
[228] a) Lai, Y.; Gallo, R. L., *Trends Immunol*., **2009**, 30, 131-141. b) Yeaman, M. R.; Yount, N. Y., *Pharmacol. Rev*., **2003**, 55, 27-55. c) Brogden, K. A., *Nat. Rev. Microbiol*., **2005**, 3, 238-250.
[229] Reddy, K. V.; Yedery, R. D.; Aranha, C., *Int. J. Antimicrob. Agents*, **2004**, 24, 536-547.
[230] Domalaon, R.; G. Zhanel, G.; Schweizer, F., *Curr. Top. Med. Chem*, **2016**, 16, 1217-1230.
[231] Phambu, N. *et al*, *Biophys. Chem*., **2017**, 227, 8-13.

Several approaches have been applied to AMPs to improve their bactericidal activity and reduce their hemolytic activity, including modifications to the sequence, cyclization, and synthesis of multivalent constructs.

Classes	Representatives	Sequences
α-helix	Melittin	GIGAVLKVLTTGLPALISWIKRKRQQ
	Magainin-1	GIGKFLHSAGKFGKAFVGEIMKS
	LL-37	LLGDFFRKSKEKIGKEFKRIVQRIKDFLRNLVPRTES
β-sheet	HNP-1	AC[1]YC[2]RIPAC[3]IAGGRRYGTC[2]IYGGRKWAFC[3]C[1]
	HBD-1	DHYNC[1]VSSGGQC[2]LYSAC[3]PIFTKIQGTC[2]YRGKAKC[1]C[3]K
	Protegin 1	RGGRLC[1]YC[2]RRRFC[2]VC[1]VGR
Extended	Indolicidin	ILPWKWPWWPWRR
	Tritrpticin	VRRFPWWWPFLRR
	PR-39	RRRPRPPYLPRPRPPPFFPPRLPPRIPPGFPPRFPPRFP

[1], [2] and [3] are disulfide bonds intramolecularly formed by Cys residues in one peptide.

***Table 8**. Classification of natural antimicrobial peptides by their secondary structure.*

2.5.1. Composition and secondary structure of antimicrobial peptides.[232]

- **Amino acid composition**: AMPs mainly include two types of amino acids: cationic and hydrophobic residues. In naturally AMPs, the cationic residues are Arg, Lys, and His,[233] while hydrophobics are mainly aliphatic and aromatic amino acids. In addition, Cys and Pro residues are conserved in natural AMPs. It is generally accepted that positively charged residues of AMPs directly interact with the negatively charged components of bacterial cells. Then, the hydrophobic residues get incorporated into lipid bilayers to mediate membrane permeabilization and disruption, which lead to rapid cell death.
  - Proline-rich peptides. They can penetrate the bacterial cytosol through outer membrane protein channels, which can modulate the immune system via cytokine activity or angiogenesis.[234] Therefore, they are considered to be a potential type of cell-penetrating peptides with the capability of internalizing membranes.
  - Cysteine-rich peptides. Cys residues are able to form disulphide bonds to stabilize β-hairpin or sheet structures.[235] The presence of disulphide bridges is a prerequisite for pore formation in a membrane, and subsequent studies have confirmed that antimicrobial activity is highly associated with the stability of β-hairpin conformations.

[232] a) Takahashi, D.; Shukla, S. K.; Prakash, O.; Zhang, G., *Biochimie*, **2010**, 92, 1236-1241. b) Brogden, K. A.; Ackermann, M.; McCray, P. B. Jr., Tack, B. F., *Int. J. Antimicrob. Agents*, **2003**, 22, 465-478. c) Hancock, R. E. W.; Lehrer, R., *Trends Biotechnol*., **1998**, 16, 82-88. d) Powers, J. P. S., Hancock, R. E. W., *Peptides*, **2003**, 24, 1681-1691.
[233] Mi, G.; Shi, D.; Herchek, W.; Webster, T. J., *J. Biomed. Mater. Res. A*., **2017**, 105, 1046-1054.
[234] Li, W. *et al*, *Amino Acids*, **2014**, 46, 2287-2294.
[235] Sonderegger, C. *et al*, *PLOS One*, **2017**, 12, e0169920.

- Glycine-rich peptides. The use of small amino acids, such as Gly, can improve the activities of AMPs.[236] Gly-rich peptides usually destroy fungi, Gram-positive bacteria, and cancer cells.[237]
- Aromatic amino acid-rich peptides. Trp residues are frequently chosen for their tendency to stablish Trp-Trp interactions, that leads to a distinctive cross-strand contact and stable tertiary structures.[238] AMPs containing Trp penetrate a microbial cell membrane and efficiently disrupt it.[239] Trp-rich peptides analogs are effective against several isolated antibiotic-resistant bacteria.[240] Phe is usually chosen for its high hydrophobicity and Phe-rich AMPs exhibit potent antimicrobial activity against Gram-positive and negative bacteria as well as yeast without hemolytic activity.[241]

A general trend for the charged side chains indicates that Arg has higher activity against Gram-negative bacteria when compared to His and Lys. For the nonpolar side chains, Trp and Tyr display higher activity than Phe, with Trp being more potent than Tyr.[242]

- **Secondary structures**:
  - α-helixes. Most of the AMPs present an active form based on an α-helix conformation. They are mainly derived from different species, including insects, fish, amphibians, mammalians, and plants. The formation of the α-helix results in an amphipathic structure that is recognized as a prerequisite for AMPs to act on membranes.[232,243] Electrostatic interactions between the positively charged residues of AMPs and negatively charged components of bacterial membranes have been widely reported to be the primary antimicrobial mechanism of most AMPs, and the nonpolar face can penetrate further into the membrane. Due to the importance of the secondary structure, many studies have focused on the studies on magainins[244] and the *novo* design of short α-helical peptides with potent activity.[245]

[236] Tripathi, A. K. *et al*, *Sci. Rep*., **2017**, 7, 3384.
[237] a) De Souza Cândido, E. *et al*, *Peptides*, **2014**, 55, 65-78. b) Ilić, N. *et al*, *Biochim. Biophys. Acta*., **2013**, 1828, 1004-1012.
[238] a) Cochran, A. G.; Skelton, N. J.; Starovasnik, M. A., *Proc. Natl. Acad. Sci. U. S. A*., **2001**, 98, 5578-5583. b) Chou, S. *et al*, *Acta Biomater*., **2016**, 30, 78-93.
[239] a) Yu, H. Y. *et al*, *Biochim. Biophys. Acta*, **2013**, 1828, 2720-2728. b) Haney, E. F. *et al*, *Biochim. Biophys. Acta*, **2013**, 1828, 1802-1813. c) Zhu, X.; Ma, Z.; Wang, J.; Chou, S.; Shan, A., *PLOS One*, **2014**, 9, e114605.
[240] a) Jacob, B. *et al*, *Amino Acids*, **2014**, 46, 187-198. b) Sharma, R. K.; Reddy, R. P.; Tegge, W.; Jain, R., *J. Med. Chem*., **2009**, 52, 7421-7431.
[241] a) Lee, E. *et al*, *PLOS One*, **2014**, 9, e114453. b) Konai, M. M.; Ghosh, C.; Yarlagadda, V.; Samaddar, S.; Haldar, J., *J. Med. Chem.*, **2014**, 57, 9409-9423. c) Lee, J. K.; Park, S. C.; Hahm, K. S.; Park, Y., *Biomaterials*, **2014**, 35, 1025-1039. d) Tripathi, A. K. *et al*, *Acta Biomater*., **2017**, 57, 170-186.
[242] Young, A. W. *et al*, *Med. Chem. Commun*, **2011**, 2, 308-314.
[243] Uggerhøj, L. E. *et al*, *ChemBioChem*, **2015**, 16, 242-253.
[244] Matsuzaki, K., *Biochimica et Biophysica Acta*, **1999**, 1462, 1-10.
[245] a) Kim, H; Jang, J. H.; Kim, S. C.; Cho, J. H., *J. Antimicrob. Chemother*., **2014**, 69, 121-132. b) Faccone, D. *et al*, *Eur. J. Med. Chem*., **2014**, 71, 31-35. c) Saravanan, R. *et al*, *Biotechnol. Bioeng*., **2014**, 111, 37-49. d)Maccari, G.; Di Luca, M.; Nifosi, R., *Methods Mol. Biol*., **2015**, 1268, 195-219. e) Ma, Q. Q. *et al*, *Amino acids*, **2013**, 44, 1215-1224.

- β-sheets. Despite the big number of α-helix AMPs, β-sheets are another principal secondary structure of AMPs that can be induced by a membrane-like environment. They usually change from an unstructured conformation in aqueous solution to β-sheets structures in contact to with membranes.[246] Generally, β-sheets peptides consist of 2 to 10 Cys residues that form 1 to 5 disulfide bridges as conformational constraints for stabilizing their bioactive conformation. Most natural β-sheets AMPs play important roles in the innate immune system and are categorized as defensins that can kill invading pathogens or regulate immune responses. Defensins are well-known for their characteristic six to eight Cys residues in defined positions that are evolutionarily conserved across most multicellular organisms. Additionally, the disulphide bridge between conserved Cys residues is crucial to stabilize the defensins structure, although these covalent bonds are not directly associated with antimicrobial activity. Tachyplesins are another representative group of β-sheet peptides.[244]

  The α-helix AMPs possesses similar antimicrobial activity compare with the β-sheet structure with equal hydrophobicity and charge, but β-sheet structure present a greater cell selectivity. Despite the difficulty for short peptides to addopt robust β-structures, several rational designed synthetic β-sheet folding peptide amphiphiles with broad-spectrum and highly selective antimicrobial activities have been reported.[247]

- **Charge**: The net positive charge is one of the main characteristics of AMPs. Most AMPs present a net charge ranging from +2 to +9 due to the interaction between AMPs and cell membranes mainly relies on electrostatic attraction.[248] The enhancement of the total positive charge often results in increased affinity for the microbial membrane and greater antimicrobial activity. However, the continuous increase of the number of positive charges may no longer improve the antimicrobial activity.[249]

  There are some anionic AMPs (rich in Gln and Asp) that have been shown to participate in the eukaryotic innate immune response.[250] These peptides have net charges ranging from -1 to -2 and they generally require cations, for example Zn^{2+}, as cofactors for their biocidal activity.[251]

- **Hydrophobicity**: AMPs with high hydrophobicity can damage the membrane structure, which results in cell lysis or the formation of temporary pores, and the transport of peptides inside the cell; this property enables them to interact with intracellular targets.[252] Studies have shown that hydrophobicity is strongly correlated with antimicrobial and haemolytic activities.[253] In red blood cell membranes, the increase of hydrophobicity induces peptides to penetrate deeper into the hydrophobic core.[254]

---

[246] a) Dong, N. *et al*, *Antimicrob. Agents Chemother*, **2012**, 56, 2994-3003. b) Liu, Y.; Xia, X.; Xu, L.; Wang, Y., *Biomaterials*, **2013**, 34, 237-250.
[247] a) Dong, N. *et al*, *Biomaterials*, **2014**, 35, 8028-8039. b) Ong, Z. Y.; Gao, S. J.; Yang, Y. Y., *Adv. Funct. Mater*., **2013**, 23, 3682-3692. c) Ong, Z. Y. *et al*, *Biomaterials*, **2014**, 35, 1315-1325.
[248] Wang, X. *et al*, *Biochim. Biophys. Acta*, **2017**, 1859, 1350-1361.
[249] a) Mcphee, J. B.; Hancock, R. E. W., *J. Pept. Sci*., **2005**, 11, 677-687. b) Dong, N. *et al*, *Protein Pept. Lett.*, **2012**, 19, 1212-1219.
[250] Leite, N. B. *et al*, *Amino Acids*, **2011**, 40, 91-100.
[251] Dashper, S. G. *et al*, *Antimicrob. Agents Chemother*., **2005**, 49, 2322-2328.
[252] Schmidtchen, A.; Pasupuleti, M.; Malmsten, M., *Adv. Colloid Interface Sci*., **2014**, 205, 265-274.
[253] Sun, J.; Xia, Y.; Li, D.; Du, Q.; Liang, D., *Biochim. Biophys. Acta*, **2014**, 1838, 2985-2993.
[254] Wood, S. J. *et al*, *Int. J. Pept. Res. Ther*., **2014**, 20, 519-530.

- **Amphipathicity**: Results from the segregation of hydrophobic and polar residues at opposite faces of the molecular framework and has been recognized as the most important phycicochemical and structural parameter for the activity of AMPs. However, some studies suggest that perfect amphipathicity often results in a simultaneous increase in both bactericidal activity and cytotoxicity.[255]

A net positive charge and hydrophobicity are essential for peptides to act as antibacterial agents. Additionally, flexibility has a great influence on the bacterial activity of AMPs as it permits peptides to transform conformations from an aqueous solution to a membrane-mimicking environment. In response to environment stimuli, changes in the peptide secondary structure can cause more efficient membrane leakage.[256]

2.5.2. Mechanism of antimicrobial peptides.

The antimicrobial mechanism of AMPs is extremely complex. It is difficult to characterize the mode of action of each AMP, and one AMP may act on multiple targets to protect against pathogens.[257] Increasing membrane permeability may not be sufficient alone to cause cell death.[258] In addition to membrane permeabilization, AMPs cause cell death by targeting not only intracellular contents for inhibiting transcription,[259] translation,[260] or other processes,[261] but also precursors and/or essential intermediates in peptidoglycan, lipopolysaccharides or other biosynthetic pathways for interfering with the functional synthesis of the cell wall and impairing subsequent bacterial replication.[262]

[255] Hollmann, A. *et al*, *Colloids Surf. B. Diointerfaces*, **2016**, 141, 528-536.
[256] Strömstedt, A. A.; Pasupuleti, M.; Schmidtchen, A.; Malmsten, M., *Antimicrob. Agents Chemother.*, **2009**, 53, 593-602.
[257] Brogden, K. A., *Nat Rev Microbiol*., **2005**, 3, 238-250.
[258] Fjell, C. D.; Hiss, J. A.; Hancock, R. E. W., *Nat. Rev. Drug Discovery*, **2012**, 11, 37-51.
[259] a) Zhang, J.; Wu, X.; Zhang, S. Q., *Biotechnol. Lett*., **2008**, 30, 2157-2163. b) Lan, Y. *et al*, *Biochim. Biophys. Acta*, **2010**, 1798, 1934-1943.
[260] Kragol, G. *et al*, *Biochemistry*, **2001**, 40,3016-3026.
[261] a) Patrzykat, A.; Friedrich, C. L.; Zhang, L.; Mendoza, V.; Hancock, R. E., *Antimicrob. Agents Chemother.*, **2002**, 46, 605-614. b) Hsu, S. T. D. *et al*, *Nat. Struct. Mol. Biol*., **2004**, 11, 963-967.
[262] Schneider, T. *et al*, *Science*, **2010**, 328, 1168-1172.

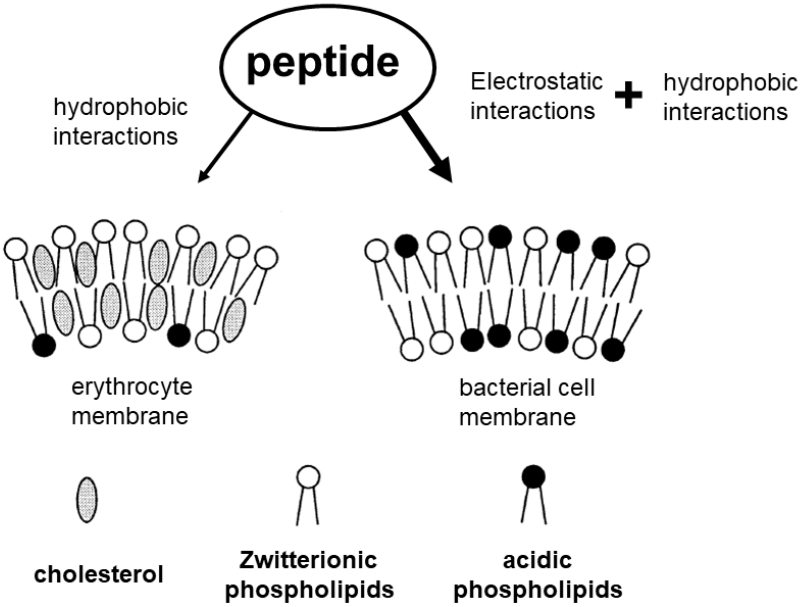

Figure 26. *Molecular basis for membrane discrimination by antimicrobial peptides.*[269]

In general, biological membranes are constructed from phospholipid constituents such as phosphatidyl choline (PC), phosphatidyl ethanolamine (PE), phosphatidyl serine (PS), phosphatidyl glycerol (PG) and sphingomyelin (SM).[263] Due to the differences in their biochemical properties, only PS and PG are negatively charged at physiological pH, while the others form zwitterionic species. The outer monolayer of mammalian cells is fundamentally composed by PC and SM, sequestering the negative charge from PS within the inner monolayer. In contrast the same PS constituent is found largely on the outer layer of most microbial plasma membranes (Figure 26). In addition to the plasma membrane, microbes are also different from mammalian cells in their outer envelope, which provides mechanical stability to microbial cells when facing harsh osmotic imbalances encountered in the extracellular environment. Moreover, the envelope is different in Gram-positive than in Gram-negative bacteria. Briefly, in Gram-positive bacteria, there is a thick peptiglycan layer (~20-80 nm) makes up for almost 90% of the cell wall. Moreover, a negatively charged teichoic acid (a polymer stitching peptidoglycan mesh from different layers together) is attached to the phospholipid bilayer which projects outwardly across the peptidoglycan layer (Figure 27). In Gram-negative bacteria, the peptidoglycan is relatively thin (~10 nm) and only makes up about 15-20% of their cell wall components. Furthermore, the teichoic acid is not found, and the peptidoglycan layer is buried under an additional phospholipid bilayer known as the outer membrane (Figure 27). Instead of the peptidoglycan, the yeast family of microbes have their cell wall constructed from a thick layer of chitin and glucan cross-linked polymer network (~140 nm) and an outer mananprotein (glycoprotein) layer containing phosphodiester linkages, which confers a homogenously dispersed anionic complex at physiological pH (Figure 27).[264]

[263] Engler, A. C. *et al*, *Nano Today*, **2012**, 7, 201-222.
[264] Ruiz-Herrera, J.; Elorza, M. V.; Valentín, E.; Sentadreu, R., *FEMS Yeast Research*, **2006**, 6, 14-29.

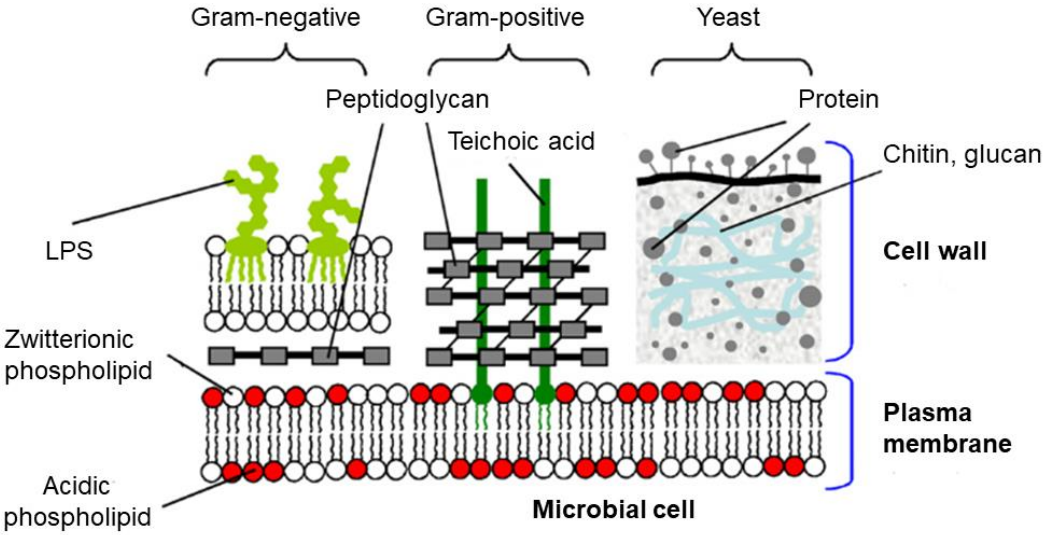

***Figure 27**. Scheme of the major differences between Gram-positive, Gram-negative bacteria and yeast.*

As it was mentioned before, AMPs are thought to be unstructured in an aqueous environment and turn into their final amphipathic conformation upon interaction with an anionic membrane environment (Figure 26).[265] They mainly target the phospholipid membranes of bacterial cells due to they are heavily populated with anionic phosphate head groups. These negatively charged groups provide an electrostatic attraction to the cationic peptides, thereby causing them to congregate at the membrane surface, and thus allowing them to exert their antimicrobial effects.[266] In the case of Gram-positive bacteria, the AMPs interacts with teichoic and teichuronic acids and in the case of Gram-negative bacteria, the initial action of peptides involves the competitive displacement of LPS-associated divalent cations, Mg^{2+} and Ca^{2+}. In this way, peptides can transit across the outer membrane by self-promoted uptake[267] and gain access to both outer and inner membranes. The outer membrane surface of eukaryotic cells is generally neutral, which results in a reduced affinity for the cationic peptides. In these membranes, the negatively charged groups are instead oriented inwards towards the cell cytoplasm. The presence of collagen in eukaryotic membranes also increases their stability and has a protective effect against host-defence-type peptides (Figure 26).

Once the peptides are aggregated at the membrane surface, they are able to insert into the membrane and consequently exert their antibacterial effects. For that, peptides must reach a certain concentration at the target surface that is described as the minimum threshold concentration.[268] Below this threshold concentration, peptides tend to interact and concentrate at the level of the lipid headgroup, fold simultaneously and remain adsorbed parallel to the lipid bilayer.[258] As the concentration increases, the peptides begin to orient themselves perpendicular

[265] a) Zhu, X. *et al*, *Acta Biomater*., **2014**, 10, 244-257. b) Xu, W., Zhu, X.; Tan, T.; Li, W.; Shan, A., *PLOS One*, **2014**, 9, 298935.
[266] a) Travkova, O. G.; Brezesinski, G., *Chem. Phys. Lipids*, **2013**, 167-168, 43-50. b) Wang, Y.; Schlamadinger, D. E.; Kim, J. E.; Mccammon, J. A., *Biochim. Biophys. Acta*, **2012**, 1818, 1402-1409.
[267] Hancock, R. E. W.; Chapple, D. S., *Antimicrob. Agents Chemother*., **1999**, 43, 1317-1323.
[268] Ma, Q. *et al*, *Chem. Biol. Drug Des*., **2014**, 84, 348-353.

to the membrane, insert and partition into the hydrophobic core of the bilayer (pore formation or disintegration is achieve above the threshold concentration).

Following the initial attachement, peptides insert into the bacterial membrane to form transmembrane pores (membrane permeabilization and lysis).[269] A number of mechanisms have been suggested by which antimicrobial peptides disrupt membrane function.[270] The peptides can orient themselves perpendicular to the membrane to form either 'barrel-stave' (pore formation) or 'toroidal' transmembrane pores. Alternatively, the peptides can orient themselves parallel to the membrane as in the 'carpet model' (detergent-like action) (Figure 28). Independently of the mechanism, AMPs lead to complete disintegration of the cell membrane, and the death of the cell.

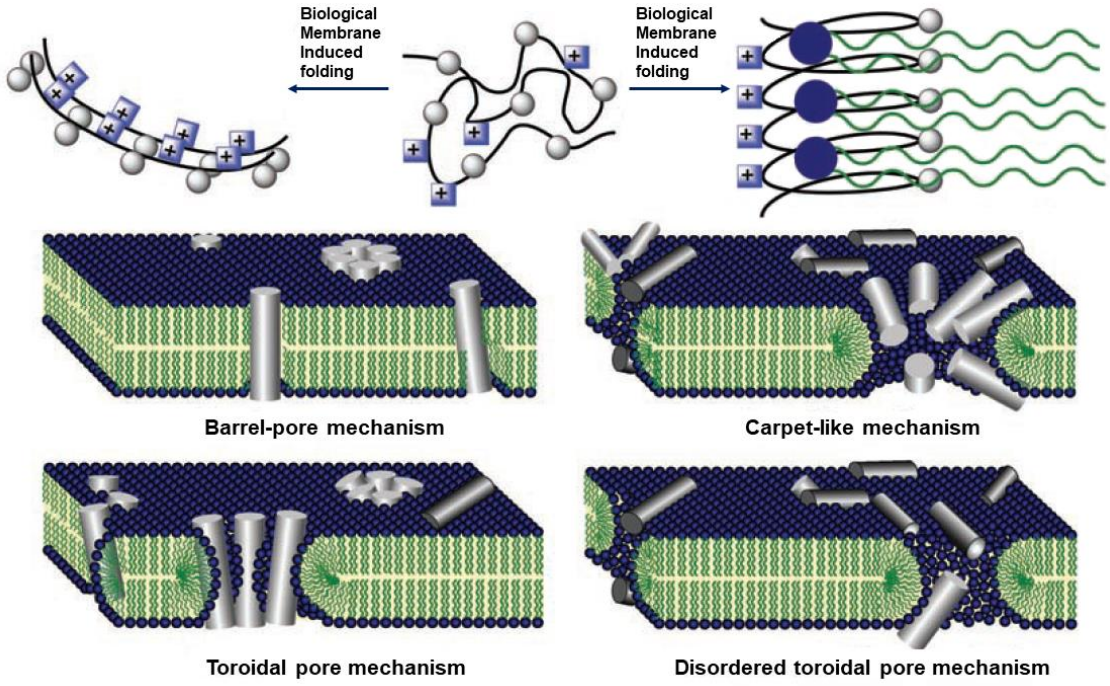

***Figure 28**. Mode of action of antimicrobial peptides.*[271]

In some cases, AMPs may kill bacteria by other antimicrobial mechanisms rather than by inducing membrane damage. AMPs have been found to attenuate a wide range of cytoplasmic processes, including nucleic acid synthesis, protein synthesis, cell-wall synthesis, and protein folding.[272] Interestingly, AMPs often appear to modulate several targets with similar, moderate potency, thus providing a sharp contrast to most clinically developed antibacterials, where the preference has been for high-affinity binding to a single target.

The activity of AMPs may be the result of their ability to act at multiple sites simultaneously, including the cell membrane as well as intra- and extracellular targets, thereby

[269] Dong, N. *et al*, *Amino acids*, **2014**, 46,2137-2154.
[270] Shai, Y., *Biopolymers*, **2002**, 66, 236-248.
[271] Rodriguez-Vazquez, N. *et al*, *Curr. Top. Med. Chem.*, **2014**, 14, 2647-2661.
[272] Yeung, A. T. Y.; Gellatly, S. L.; Hancock, R. E. W., *Cell. Mol. Life Sci*., **2011**, 68, 2161-2176.

exposing the cell to many stresses that cumulatively cause the cell to die. Antimicrobial peptides act by multiple modalities includes:[273]

a) Lipopolysaccharide neutralization or disaggregation.

b) Induction of membrane permeability.

c) Inhibition of cytoplasmic proteins related to cell division or survival.

d) Inhibition of macromolecular synthesis through interaction with nucleic acids.

e) Anti-biofilm activity of antimicrobial peptides against biofilm of multi-drug resistant bacteria.

2.5.3. Antimicrobial peptides therapy.

These therapies may offer a number of advantages over more traditional antibacterials. While it is inevitable that AMPs will (and do) induce resistance, there is a considerable amount of evidence to suggest that the onset of such resistance is slower than for conventional treatments. This slow development of resistance has been attributed to a combination of the interaction of the AMPs with the cell membrane and their ability to act at multiple targets. It has been postulated that a mutation capable of furnishing resistance by the reorganization of the cell membrane may often prove to be too metabolically expensive for survival. Additionally, if multiple cellular targets can be affected with similar potency, then resistance to a single mode of action will not necessarily confer complete resistance to the AMP. It is worth mentioning that resistance mechanisms against native host-defense peptides have been observed, and another possible strategy for chemotherapy would be to target these mechanisms, thereby removing the pathogens´ defence against endogenous AMPs.[274] The fact that they are frequently bactericidal rather than bacteriostatic is also viewed positively.

Apart from the antibacterial action of AMPs, they can also be antifungal, antiviral, anticancer and antiparasitic compounds:

- Antifungal activity. Despite the antibacterial activity of AMPs, the number of studies on antifungal peptides has increased.[275] Astacidin 1 (FKVQNQHGQVVKIFHH) is a novel antibacterial peptide that was isolated from *Pacifastacus leniusculus* and that exhibited antifungal activity against *Candida albicans, Trichosporon beigelii, Malassezia furfur* and *Trichophyton rubrum*.[276] Moreover, 14-helical hydrophobic *β*-peptides are able to prevent the formation of *C. albicans, C. glabrata, C. parapsilosis* and *C. tropicalis* biofilms.[277] Peptides that primarily exhibit antifungal activity, such as many of those isolated from plants,

[273] Park, S. C.; Park, Y.; Hahm, K. S., *Int. J. Mol. Sci*., **2011**, 12, 5971-5992.
[274] Gruenheid, S.; Le Moual, H., *FEMS Microbiol. Lett*., **2012**, 330, 81-89.
[275] Rautenbach, M.; Troskie, A. M.; Vosloo, J. A., *Biochimie*, **2016**, 130, 132-145.
[276] Choi, H.; Lee, D. G., *Biochimie*, **2014**, 105, 58-63.
[277] Raman, N.; Lee, M. R.; Lynn, D.; Palecek, S., *Pharmaceuticals*, **2015**, 8, 483-503.

tend to be relatively rich in polar and neutral amino acids, suggesting a unique structure-activity relationship.[278]

- Antiviral activity. Many AMPs have shown the ability to inhibit a wide spectrum of virus infections, including those caused by enveloped RNA and DNA viruses, feline calicivirus and echovirus.[279] Some α-helical peptides, such magainins, dermaseptin and melittin, have shown potent anti- herpes simplex virus (HSV) activity.[280] Additionally, some β-sheet peptides, such as defensins, tachyplesin, protegrins and the β-turn peptide lactoferricin, have all shown high activity against HSV.[380c,281]

- Antitumor activity. Currently, cancer is the third leading cause of human death. Some cationic AMPs exhibit a broad spectrum of cytotoxic activity against tumour cells, which could provide a new class of anticancer drugs. Most tumour cells carry a net negative charge on the membrane due to the overexpression of various anionic molecules, such as phosphatidylserine.[282] AMPs mainly act on target cell membranes through a non-receptor-mediated pathway, for which it is more difficult for tumour cells to develop resistance compared to conventional chemotherapeutic agents.[283] Several tumour-targeting drug delivery systems have been established by conjugating targeting domains of epidermal growth factor receptor family with nanoparticles or cell penetrating peptides (CPPs).[284] Several tumour-homing cell-penetrating peptides (HP-CPPs) have been successfully developed by means of conjugating HPs with CPPs.[285] AMPs with ideal antitumor activity should meet at least three conditions: 1) high net positive charge, leading to the electrostatic attraction between the negatively charged components of tumour cells and the positively charged AMPs;[286] 2) high structural flexibility (as it was explain before, to allow conformation changes); and 3) high oligomerization, as AMPs should be easily clustered on the membrane surface of a tumour cell so that they can form a pore on the tumour cell membrane.[287]

- Antiparasitic activity. Protozoan parasites cause millions of deaths annually worldwide. AMPs that show good activity against parasites include melittin,

[278] Lustig, F. *et al*, *Biochemistry*, **1996**, 35, 12077-12085.
[279] a) Jenssen, H.; Hamill, P.; Hancock, R. E. W., *Clin. Microbiol. Rev*., **2006**, 19, 491-511. b) Bastian, A.; Schäfer, H., *Regul. Rept*., **2001**, 101, 157-161. c) Horne, W. S. *et al*, *Bioorg. Med. Chem*., **2005**, 13, 5145-5153. d) Pietrantoni, A. *et al*, *Antiviral Res*., **2006**, 69, 98-106.
[280] a) Albiol Matanic, V. C.; Castilla, V., *Int. J. Antimicrob. Ag*., **2004**, 23, 382-389. b) Belaid, A. *et al*, *J. Med. Virol*., **2002**, 66, 229-234. c) Yasin, B. *et al*, *Eur. J. Clin. Microbiol. Infect. Dis*., **2000**, 19, 187-194.
[281] a) Andersen, J. H.; Jenssen, H.; Gutteberg, T. J., *Antiviral Res*., **2003**, 58, 209-215. b) Daher, K. A.; Selsted, M. E.; Lehrer, R. I., *J. Virol*., **1986**, 60, 1068-1074. c) Jenssen, H.; Andersen, J. H.; Uhlinhansen, L.; Gutterberg, T. J.; Rekdal, Ø., *Antiviral. Res*. **2004**, 61, 101-109. d) Lehrer, R. I.; Szklarek, D.; Ganz, T.; Selsted, M. E., *Infection & Immunity*, **1985**, 49, 207-211. e) Sinha, S.; Cheshenko, N.; Lehrer, R. I.; Herold, B. C., *Antimicrob. Agents Chemother*., **2003**, 47, 494-500.
[282] Dobrzyńska, I.; Szachowicz-Petelska, B.; Sulkowski, S.; Figaszewski, Z., *Mol Cell Biochem*., **2005**, 276, 113-119.
[283] a) Hoskin, D. W.; Ramamoorthy, A., *Biochim. Biophys. Acta*, **2008**, 1778, 357-375. b) Mader, J. S.; Hoskin, D. W., *Expert Opin. Investig. Drugs*, **2006**, 15, 933-946.
[284] Nguyen, L. T. *et al*, *Amino Acids*, **2015**, 47, 997-1006.
[285] Svensen, N.; Walton, J. G. A.; Bradley, M., *Trends Pharmacol. Sci*., **2012**, 33, 186-192.
[286] Harris, F.; Dennison, S. R.; Singh, J.; Phoenix, D. A., *Med. Res. Rev*., **2013**, 33, 190-234.
[287] Kao, F. S.; Pan, Y. R.; Hsu, R. Q.; Chen, H. M., *Biochim. Biophys. Acta*, **2012**, 1818, 2927-2935.

cecropin, magainin, bovine myeloid antimicrobial peptide 18 (BMAP-18), BMAP-27 and PG-1.

- Immunomodulatory activity. AMPs have a diverse range of functions in modulating immunity.[288] The immunomodulatory properties of AMPs include reduction in the levels of proinflammatory cytokines produced in response to microbial signature molecules; modulation of the expression of chemokines; stimulation of angiogenesis; enhanced wound healing; and macrophage and leukocyte differentiation.[289]

Despite their favourable properties, few AMPs have been approved for clinical use, such as polymyxins, cationic lipopeptides obtained from the Gram-positive bacterium *Bacillus polymyxa*. Polymyxin E (known as colistin, Figure 29) is currently used as a drug of last resort for some multidrug-resistant *P. aeruginosa* infections.[290] Colistin is generally administered topically to treat diseases such as wound infections, while its prodrug colomycin, in which the acidic groups are neutralized by methane sulfonation, is used systemically for the treatment of pulmonary infections in cystic fibrosis patients.[291]

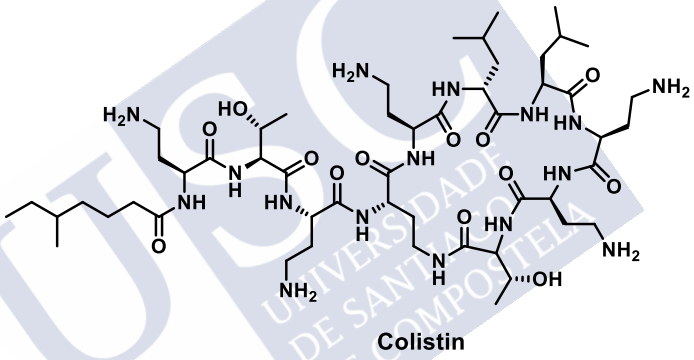

Figure 29. *Structure of Colistin.*

The unfavourable history of AMPs as therapeutics has been attributed to several factors.[292] The most important factor is the high cost of peptide synthesis, which is unappealing from manufacturing point of view. Additionally, they display short half-lives *in vivo* as a result of their susceptibility to proteolytic enzymes and can present issues with toxicity. For these reasons there is a great deal of interest in the development of peptidomimetics to mitigate some of these difficulties.[293] Polymers appears as interesting peptidomimetics due to the presence of a positive charge (typically quaternary ammonium salts) and an amphipathic structure (with long hydrophobic alkyl chains). They also kill pathogens through a membrane disruption

[288] Brown, K. L.; Hancock, R. E., *Curr. Opin. Immunol.*, **2006**, 18, 24-30.
[289] Dong, W.; Mao, X.; Guan, Y.; Kang, Y.; Shang, D., *Sci. Rep.*, **2017**, 7, 40228.
[290] Falagas, M. E.; Grammatikos, A. P.; Michalopoulos, A., *Expert Rev. Anti-Infect. Ther.*, **2008**, 6, 593-600.
[291] Conway, S. P. *et al*, *Thorax*, **1997**, 52, 987-993.
[292] Brogden, N. K.; Brogden, K. A., *Int. J. Antimicrob. Agents*, **2011**, 38, 217-225.
[293] a) Giuliani, A.; Rinaldi, A. C., *Cell. Mol. Life Sci.*, **2011**, 68, 2255-2266. b) Rotem, S.; Mor, A., *Biochim. Biophys. Acta Biomembr.*, **2009**, 1788, 1582-1592.

mechanism. These polymers found applications in textiles, water purification, disinfecting surfaces, etc.

It is hoped that the novel AMPs would overcome some of the challenges currently faced with natural AMPs, such as ease of synthesis, increased stability, and reduced toxicity. One approach was the logical synthesis of linear peptides with sequence $(XXYY)_n$, where n is the number of repeat units, X are hydrophobic and Y are hydrophilic amino acids. In this way, the peptide is able to fold in a α-helical structure.[294] Control change of amino acids in pair allow a logical improved of the peptides instead of a random optimization (as it has been done with natural products). The α-helical synthetic mimics of antimicrobial peptides (SMAMPs) with three repeat units show the best results.

A more promising strategy is the use of acyllysine oligomers to mimic the effects of naturally occurring peptides.[295] These peptidomimetics are deliberately designed to have an alternating acyl chain (A) and a cationic amino acid (K) structure, to preclude the formation of stable secondary structure in the resulting oligo-AKs (OAKs). $C_{12}K\text{-}7_{\alpha 8}$ (Figure 30) was found to be rapidly bactericidal, displaying potent activity (MIC = 1.6 – 12.5 μM) against a range of Gram-negative bacteria, including strains of *Acinetobacter Klebsiella* and pseudomonas. The mechanism of action adopted by the OAK would vary between strains. The concentration of AMP also had an impact on the mechanism adopted. With low concentrations, there is an intracellular mechanism, while high concentrations of AMP led to rapid killing rates, thereby indicating there was enough amounts of the peptide to inhibit cell-wall or membrane synthesis.[296]

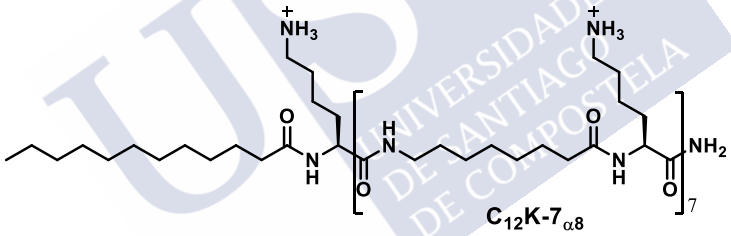

***Figure 30**. Structure of colistin and $C_{12}K\text{-}7_{\alpha 8}$.*

An alternative approach for the development of novel AMPs is based on the concept of disrupting the bacterial cell membrane with tubular structures.[297] Potent antibacterial activity was achieved with a series of six- and eight-residues cyclic peptides, which self-assemble into hollow tubular open-ended structures within bacterial cell membranes and lead to an increased permeability and bacterial death. In the bacterium cell membrane, the cyclic peptides stack together with the amide backbone through the formation of hydrogen bonds between the rings and create the tubular structure. The nature of the R group was essential for achieving potency, as these interact with the bacterial membrane.

[294] Wiradharma, N. *et al*, *Biomaterials*, **2011**, 32, 2204-2212.
[295] a) Sarig, H.; Rotem, S.; Ziserman, L.; Danino, D.; Mor, A., *Antimicrob. Agents Chemother*., **2008**, 52, 4308-4314. b) Radzishevsky, I. S. *et al*, *Chem. Biol*., **2008**, 15, 354-362.
[296] Epand, R. F. *et al*, *J. Mol. Biol*., **2008**, 379, 38-50.
[297] a) Kim, H. S.; Hartgerink, J. D.; Ghadiri, M. R., *J. Am. Chem. Soc*., **1998**, 120, 4417-4424. b) Fernandez-Lopez, S. *et al*, *Nature*, **2001**, 412, 452-456.

3. Cyclic peptide nanotubes.

The interest for antimicrobial peptides started long time ago, as for example the gramicidin A (Figure 31), whose antimicrobial activity was reported in 1941.[298,299] It is a linear polypeptide composed of alternating *D*- and *L*- amino acids (HCO-*L*-Val-Gly-*L*-Ala-*D*-Leu-*L*-Ala-*D*-Val-*L*-Val-*D*-Val-*L*-Trp-*D*-Leu-*L*-Trp-*D*-Leu-*L*-Trp-$NHCH_2CH_2OH$)[300] that forms transmembrane channels by folding into tubular structures (by a *β*-helical structure).[301] The active form of gramicidin A is able to span the lipid bilayer wider than 35 Å, thanks to the formation of head to head dimeric structure facilitated by the amino ethanal group.[302]

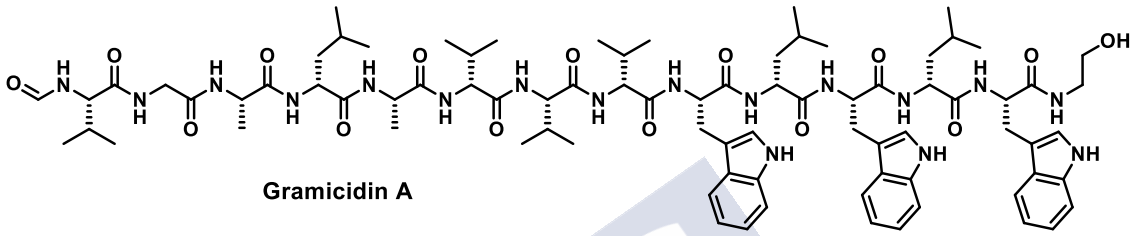

Figure 31. *Structure of Gramicidin A.*

In 1974 it was postulated that cyclic peptides with an even number of amino acids of *D*,*L*-alternating chirality could adopt a flat conformation in which the NH and CO groups would be oriented perpendicular to the plane of the structure. The stacking of this disc-shaped form would generate a hollow cylindrical structure (Figure 32) related to the *β*-helical conformation adopted by linear *D*,*L*-peptides (in the same way that gramicidin A).[303] The side chain of the amino acids should be oriented outwards of the tubular structure.

First peptide nanotubes were obtained in 1993.[304] They were constituted by an eight-residue cyclic peptide *c*-[(*L*-Gln-*D*-Ala-*L*-Glu-*D*-Ala)$_2$]. The formation of the nanotube was modulated (or controlled) by changing the pH of the medium. At alkaline pH, the repulsive interaction between the charged carboxylate side chains of the glutamic acid disfavour ring stacking while increasing the solubility in aqueous media. As consequence, this octa-cyclic peptide was soluble in aqueous media at basic pH, but acidification induces the self-assembly process, leading to the nanotube formation. Moreover, the neutral form of glutamic acid side chain facilitates hydrogen bond formation between these side chains. It was also proposed that at neutral pH,

---

[298] Bong, D. T.; Clark, T. D.; Granja, J. R.; Ghadiri, M. R., *Angew. Chem. Int. Ed*., **2001**, 40, 988-1011.
[299] Hotchkiss, R. D., *J. Biol. Chem*., **1941**, 141, 171.
[300] a) Ishi, S. I.; Witkop, B., *J. Am. Chem. Soc*., **1963**, 85, 1832-1834. b) Synge, R. L. M., *Biochem. J*., **1945**, 39, 355. c) Sarges, R.; Witkop, B., *J. Am. Chem. Soc*., **1964**, 86, 1861-1862. d) Sarges, R.; Witkop, B., *J. Am. Chem. Soc*., **1964**, 86, 1862-1863.
[301] a) Ketchem, R. R.; Hu, W.; Cross, T. A., *Science*, **1993**, 261, 1457-1460. b) Hladky, S. B.; Haydon, D. A., *Nature*, **1970**, 225, 451 ± 453.
[302] Urry, D. W., *Proc. Natl. Acad. Sci. U. S. A.*, **1971**, 3, 672-673.
[303] a) DeSantis, P.; Morosetti, S.; Rizzo, R., *Macromolecules*, **1974**, 7, 52-58. b) Hartgerink, J. D.; Ghadiri, M. R., *Proc. 2nd OUMS*, **1996**, 181-188 (Osuka, Japan). c) Hartgerink, J. D.; Clark, T. D.; Ghadiri, M. R., *Chem. Eur. J*., **1998**, 4, 1367-1372. d) Buriak, J. M.; Ghadiri, M. R., *Mater. Sci. Eng. C*, **1997**, 4, 207-212. e) Ghadiri, M. R., *Adv. Mater*., **1995**, 7, 675-677.
[304] Ghadiri, M. R.; Granja, J. R.; Milligan, R. A.; McRee, D. E.; Khazanovich, N., *Nature*, **1993**, 366, 324-327.

the no-protonated cyclic peptide would be less soluble in water, contributing to the self-assembly process.

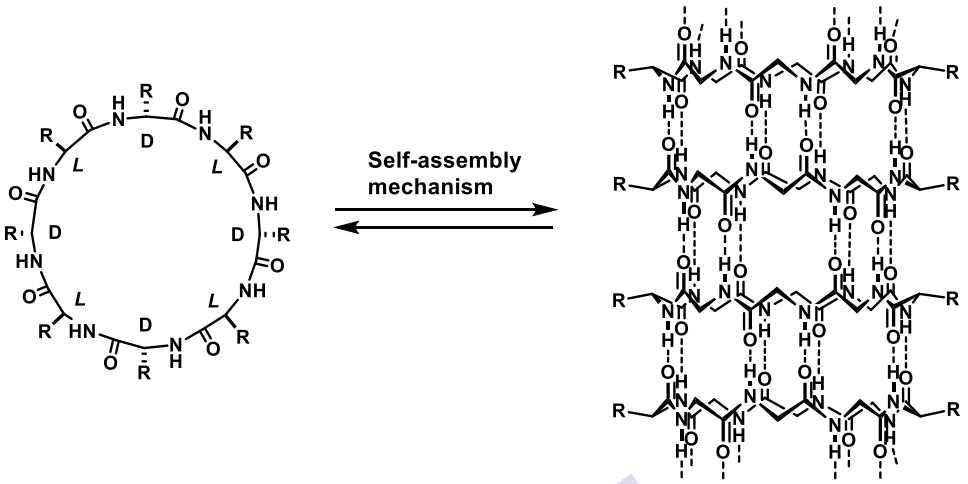

Figure 32. *Self-assembly process to obtain a peptide nanotube.*

The self-assembly operation presents several inherent advantages over covalent syntheses due to its high synthetic convergence, the built-in error-correction and high efficiency process.[298,305] The peptide nanotubes are obtained as rod-shaped crystals that could be analysed by different techniques. Transmission electron microscopy (TEM) showed that the crystal was formed by hundreds of tightly packed nanotubes, with an average length of 10-30 μm and diameters ranging from 100 to 500 nm. Electron diffraction pattern provided a distance between cyclic peptides of 4.7 Å, which can only be achieved with the proposed flat conformation with all the side chains pointing outside to avoid steric interactions. FTIR experiments were also carried out to confirm the structure. In alkaline solutions, the cyclic peptide backbone presents an amide-I band at 1,632 cm^{-1}, and the typical solvent-exposed carbonyl stretching frequencies for glutamate and glutamine side-chain functionalities, 1,568 and 1,670 cm^{-1}. However, when the self-assembly process takes place at acidic pH, the peptide nanotube displays characteristic features of a hydrogen-bonded *β*-sheet structure (amide-I bands at 1,628 and 1,688 cm^{-1}, amide-II band at 1,540 cm^{-1}) and also it is observed the N-H stretching frequency at 3,277 cm^{-1} that supports the formation of a tight network backbone-backbone inter-subunit interaction.

Following the same pH strategy, the nanotube formed by different subunits of *c*-[(*L*-Gln-*D*-Ala-*L*-Glu-*D*-Ala)$_3$] was obtained.[306] Again, the formation of the tubular structure was supported by cryo-electron microscopy, electron diffraction and FTIR, which allow to determine a value of 13 Å van der Waals pore diameter, demonstrating that the internal diameter of the peptide nanotube can be controlled simply by adjusting the ring size of the cyclic peptide subunit. In other words, the properties of the outer surface and the internal diameter of the peptide nanotube can be adjusted simply by the choice of the amino acid (type and number)

[305] Philip, D.; Stoddart, J. F., *Angew. Chem. Int. Ed*., **1996**, 1154-119.
[306] Khazanovich, N.; Granja, J. R.; McRee, D. E.; Milligan, R. A.; Ghadiri, M. R., *J. Am. Chem. Soc*., **1994**, 116, 6011-6012.

employed in the cyclic peptide component (which represents an advantage with respect to their *β*-helical counterparts).[307]

The remarkable stability of the peptide nanotubes can be attributed to the highly cooperative nature of the self-assembled structure which simultaneously reinforces multiple noncovalent interactions throughout the network. In this way, once the peptide nanotube is formed, it exhibits good mechanical stability to centrifugation and vortex mixing, strongly acidic and basic pH, and long-term stability in most common polar and nonpolar organic solvents.[307]

To determine the energetic constants involved in the nanotube formation, it was designed a simple system.[308] Cyclic peptides with all the residues of the same chirality were synthesized, such as c-[(*L*-Phe-*D*-^{Me}N-Ala-)$_4$]. The methyl groups block the formation of hydrogen bond in one face of the ring, and only dimers can be formed. The dimeric structure was determined by X-ray crystallography studies that corroborated the flat conformation of the cyclic peptide as well as the amide and CO involved in the hydrogen bond were disposed parallel to the tube axis. Moreover, partially disordered water molecules were observed in the internal cavity of the dimer, probing the hydrophilic nature of the pore. Further studies using the ^{1}H-NMR technique, combining c-[(*L*-Phe-*D*-^{Me}N-Ala-)$_4$] and its enantiomer, c-[(*D*-Phe-*L*-^{Me}N-Ala-)$_4$] (Figure 33),[309] confirmed that the antiparallel *β*-sheet structure was about 0.8 kcal/mol more stable than the parallel one. The synthesis of c-[(*L*-Phe-*D*-^{Me}N-Ala-*L*-Leu-*D*-^{Me}N-Ala)$_2$] demonstrated that the interactions between the side chains of Phe and Leu did not contribute to the *β*-sheet stability, concluding that in this case, the self-assembly process was independent of the amino acid sequence and, therefore, they were not responsible of the higher stability of the antiparallel packing.

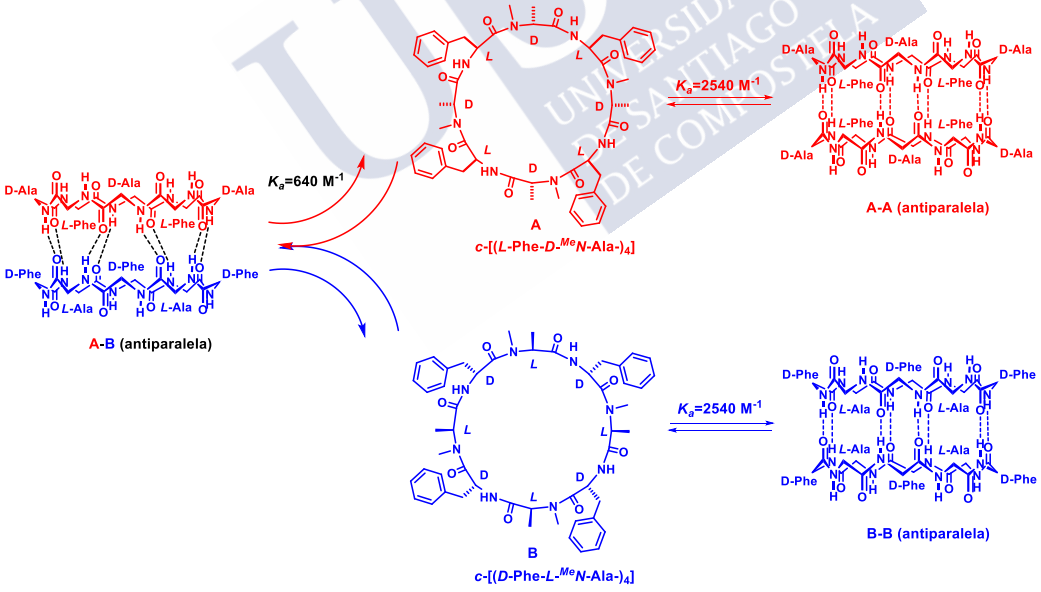

***Figure 33**. Homodimer (A-A and B-B) and heterodimer (A-B) formation.*

[307] Hartgerink, J. D.; Granja, J. R.; Milligan, R. A.; Ghadiri, M. R., *J. Am. Chem. Soc*., **1996**, 118, 43-50.
[308] Ghadiri, M. R.; Kobayashi, K.; Granja, J. R.; Chadha, R. K.; McRee, D. E., *Angew. Chem. Int. Ed.*, **1995**, 34, 93-95.
[309] Kobayashi, K.; Granja, J. R.; Ghadiri, M. R., *Angew. Chem. Int. Ed.*, **1995**, 34, 95-98.

However, the self-assembly process is influenced by the size of the cyclic peptide.[307] *N*-methylated cyclic peptides with the same sequence but different number of residues present different assembly properties. Cyclic peptides with less than six residues have conformational restrictions that did not allow the nanotube formation, because adopting the flat conformation would require high energy cost. The formation of nanotubes with six-residue cyclic peptide was also prepared, and in general, they have low dimerization constants, although it seems highly dependent of the peptide sequence.[310] Conversely, too large cyclic peptide structures are too flexible to maintain the flat conformation required for the self-assembly process.

3.1. Classification of cyclic peptides.

The self-assembly process of cyclic peptides is not exclusive for peptides constituted by α-aa. In fact, there are so many examples that, usually, the classification is based on the type of residues that form the cyclic peptide: *α*-Aas[304], *β*-Aas[311], *α*,*β*-Aas[312], *α*,*γ*-Aas[313], *δ*-Aas[314], *α*,*δ*-Aas (Figura 36)[315] and *α*-*ε*-Aas[316] (Figure 34). Additional cyclo-ureas have also being used in nanotube formation based on the stacking of flat rings.[317]

[310] Sun, X.; Lorenzi, G. P.; *Helv. Chim. Acta*, **1994**, 77, 1520-1526.
[311] a) Seebach, D. *et al*, *Helv. Chim. Acta*, **1997**, 80, 173-182. b) Clark, T. D.; Buehler, L. K.; Ghadiri, M. R., *J. Am. Chem. Soc*., **1998**, 120, 651-656.
[312] Karle, I. L.; Handa, B. K.; Hassall, C. H.; *Acta Crystallogr. Sect. B*, **1975**, 31, 555-560.
[313] Amorín, M.; Castedo, L.; Granja, J. R.; *J. Am. Chem. Soc*., **2003**, 125, 2844-2845.
[314] a) Gauthier, D.; Baillargeon, P.; Drouin, M.; Dory, Y. L., *Angew. Chem. Int. Ed*. **2001**, 40, 4635-4638. b) Leclair, S. *et al*, *Angew. Chem. Int. Ed.* **2004**, 43, 349-353.
[315] Lamas, A.; Guerra, A.; Amorín, M.; Granja, J. R., *Chem. Sci.*, **2018**, 9, 8228-8233.
[316] Horne, W. S.; Stout, C. D.; Ghadiri, M. R., *J. Am. Chem. Soc*., **2003**, 125, 9372-9376.
[317] Semetey, V.; Didierjean, C.; Briand, J.P.; Aubry, A.; Guichard, G.; *Angew. Chem. Int. Ed*., **2002**, 41, 1895-1898.

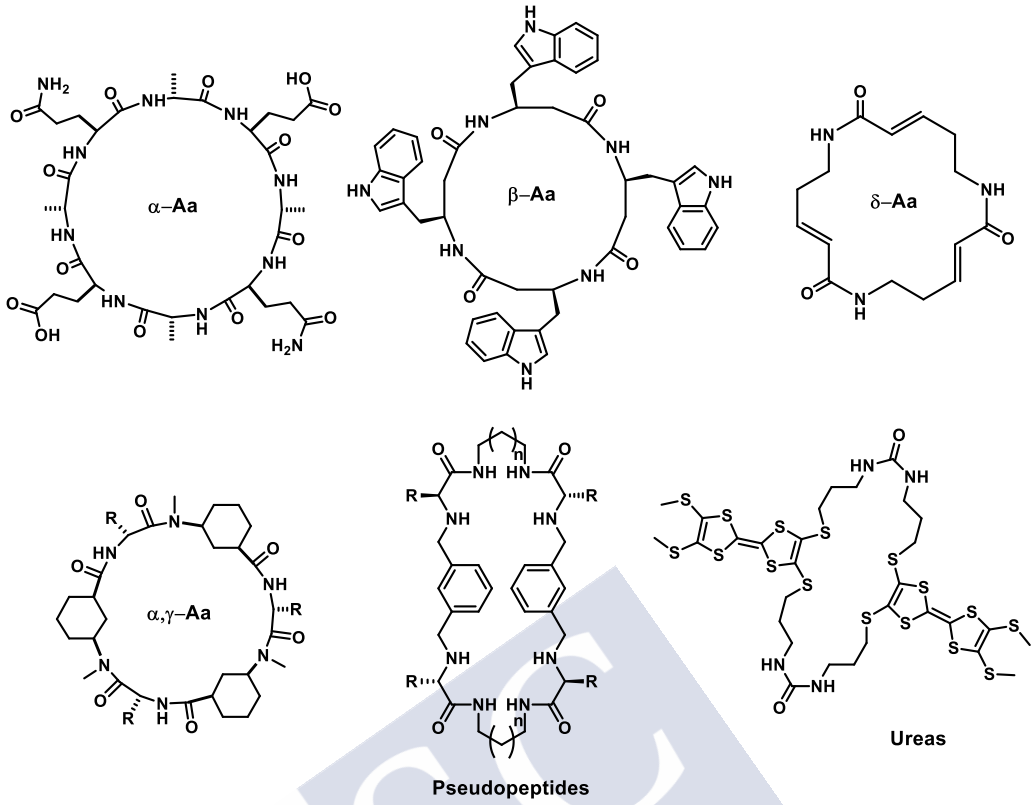

***Figure 34**. Examples of cyclic peptides that are able to self-assemble in peptide nanotubes.*

As mentioned before, the flat conformation in cyclic α-peptides can only be achieved by the alternation of amino acids of opposite configuration and using an even number of residues. In this conformation, the hydrogen bond interactions between different subunits can be stablish because of the complementary of both donor (NH) and acceptor (CO) groups in each face of the cyclic peptide. It has been proposed that nanotubes are formed by antiparallel *β*-sheet, although recent studies by Perrier have shown that the parallel arrangement is also possible.[318] The self-assembly properties of cyclic β-peptides were similar to those of cyclic *D,L*- α-peptides, with the amino acid side chain radiating equatorially from the peptide ring, although the additional methylene group provide some flexibility and the chirality of the residues seems not so important. [311] The cyclic *α,γ*-peptides are another class of self-assembling cyclic peptide that differs from both cyclic *D,L*- *α*-peptides and *β*-peptides due to the alternation of *α* and *γ* residues. In the flat conformation, all the amide groups (NH and CO) of the *α*-residues are pointing towards one face of the ring while the other face is decorated with these groups but from the *γ*-residues. Consequently, we can define two faces for each residue, the *α* and *γ* faces. Due to the different separation of each NH and carbonyl of each face (*α* or *γ*), it has been proposed that *α*-faces interact with *α*-faces and *γ* -faces with *γ*-faces. Therefore, each nanotube is formed by two different hydrogen bonding patterns: *γ*-*γ* and *α*-*α* interactions (Figure 35).[313] The cyclic *δ*-peptides are more rigid structures that form the nanotubes in a parallel *β*-sheet conformation in a similar manner that cyclic *β*-peptides due to their donor and acceptor groups

[318] Silk, M. R. *et al*, *Chem. Comm*., **2017**, 53, 6613-6616.

are pointing to opposite sides of the ring. Recently our group has shown the trans-4-amino-cyclohexanecarboxilic acid (Figure 36) could be intercalate in *α-D,L*-CPs (Figure 36), forming cyclic peptides that assembly into nanotubes. The rigidity of this group allows large ring to maintain the flat conformation. The resulting nanotubes have a cavity with hydrophobic properties that can encapsulate fullerene moieties.[315]

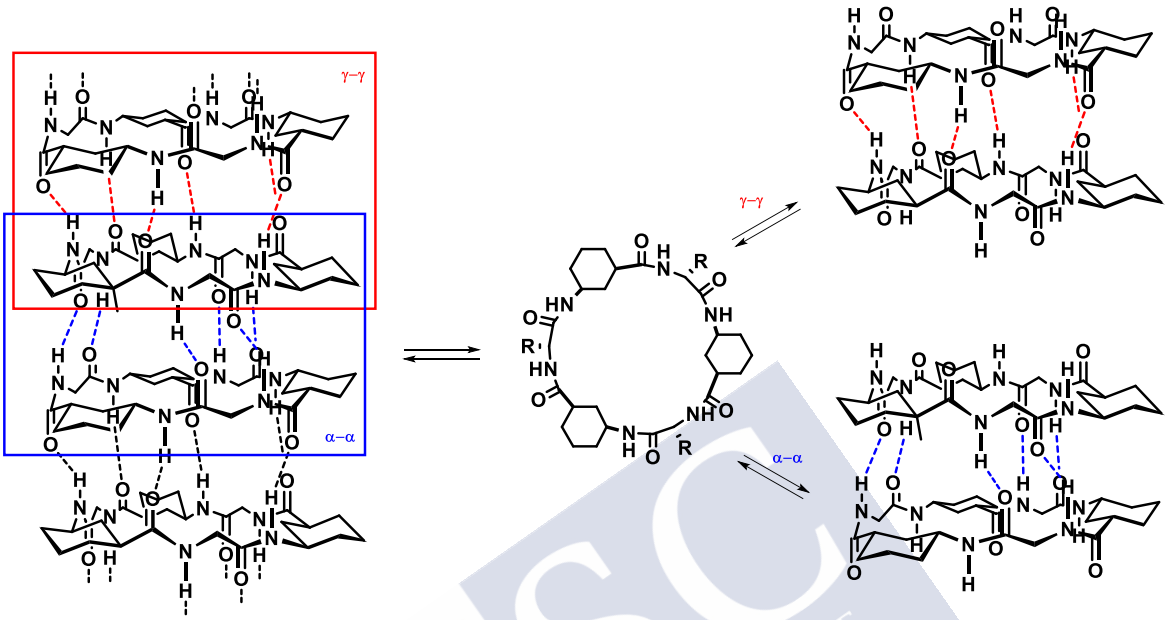

Figure 35*.Scheme of γ-γ and α-α interactions.*

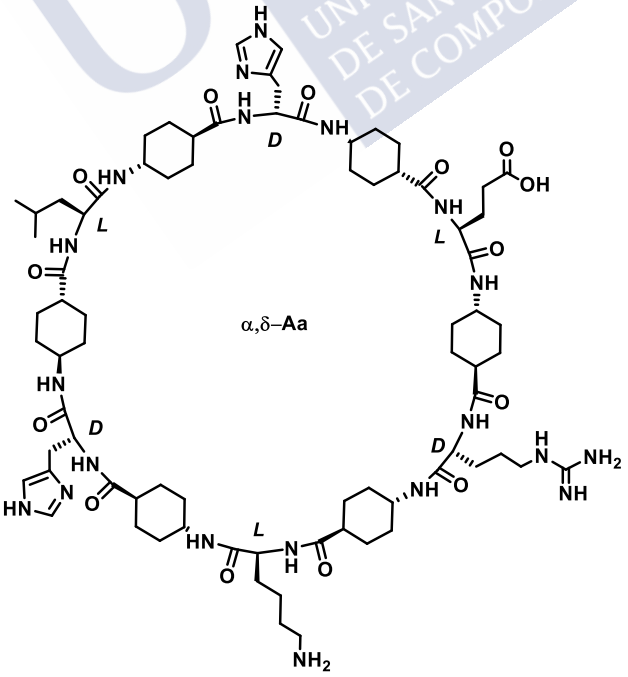

Figure 36*. Example of α,δ-cyclic peptide.*

3.2. Application of cyclic peptide nanotubes.

The formation of ion channels was the first application found for cyclic peptide nanotubes, as a consequence of controlling the external surface properties by changing the amino acid side chains that constituted each cyclic peptide. It was envisaged that hydrophobic peptides would solubilize in membrane media and would form nanotubes that would facilitate the diffusion of ions. In 1994, it was reported the first cyclic peptide bearing hydrophobic side chains: the eight-residue cyclic peptide *c*-[(*L*-Trp-*D*-Leu)$_3$-*L*-Gln-*D*-Leu-], that was able to self-assembling in a lipid bilayer and create an ion channel (Figure 37).[319] These tubular structure has the same length that the hydrophobic part of the membrane. The formation of the transmembrane channel provided a highly efficient proton transport activity, but also, and more important, display transport activities for K^+ and Na^+ greater than 10^7 ions/s, three times faster than the ion-channel created by gramicidin A. Additionally, small polar molecules were also transported through the lumen of the tube. In this case, the selectivity of the transport is based on the relative size of the transported molecules. For example, glucose needs a pore about 9 Å of size, so it can not pass through a cyclic octapeptide (which size is about 7 Å in diameter). The cyclic decapeptide c-[L-Gln-(D-Leu-L-Trp)4-D-Leu-], with an internal diameter of 10 Å, was efficiently able of transporting glucose, glutamic acid and other polar substances in a very efficient way.[320]

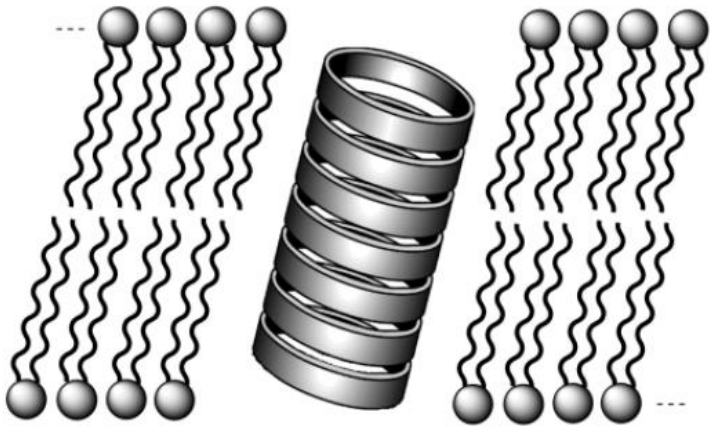

***Figure 37**. Self-assembled nanotube embedded in a lipid bilayed membrane.*

Ion-channel pores were also obtained with *β*-CP. The membrane nanotube derived from *β*-CP showed similar behaviour to their *α*-CP analogues, transporting more than 1.9 x 10^7 K^+ ions/s (higher values than gramicidin A at the same conditions). More recently, CP constituted by *α,γ*-Aas were able to insert into the membrane and form ion-channels as well, leading to the transport of alkali ions despite having a partially hydrophobic cavity.[321]

[319] Ghadiri, M. R.; Granja, J. R.; Buehler, L. K., *Nature*, **1994**, 369, 301-304.
[320] a) Shanchez-Quesada, J.; Kim, H. S.; Ghadiri, M. R., *Angew. Chem. Int. Ed*., **2001**, 40, 2503-2506. b) Granja, J. R.; Ghadiri, M. R., *J. Am. Chem. Soc*., **1994**, 116, 10785-10786.
[321] García-Fandiño, R.; Amorín, M.; Castedo, L.; Granja, J. R., *Chem. Sci*., **2012**, 3, 3280-3285.

Peptide nanotubes were also used as sensors in redox process due to their capability at transporting ions of determined size. Modified cyclic peptides were able to form nanotubes on a gold-surface covered with an alkyl-thiol and they showed selective redox properties for small ions as $[Fe(CN)_6]^{3+}$ compared to large ions as $[Mo(CN)_8]^{4+}$.[322]

The preparation of novel materials based on CPs was also evaluated. For this purpose, CPs were combined with polymers, leading to hybrid compounds. After the formation of the nanotube, polymerization process was triggered on the surface of the nanotube, leading to porous materials, which size of the pore was determined by the size of the internal diameter of the cyclic peptide.[323] In a similar way, CPs were combined with block copolymers to obtain polymeric porous membranes.[324] Porous liquid crystals were also prepared using *α,γ*-CP modified with mesogens dendrons on their side chain (Figure 38).[325]

Another new class of synthetic redox active biomaterials were prepared from *D,L-α*-CPs that were bond to 1,4,5,8-naphthalenetetracarboxylic diimide (NDI). The self-assembly process is induced by the excitation of the NDI. The resulting biomaterials presented a delocalized charge state.[326]

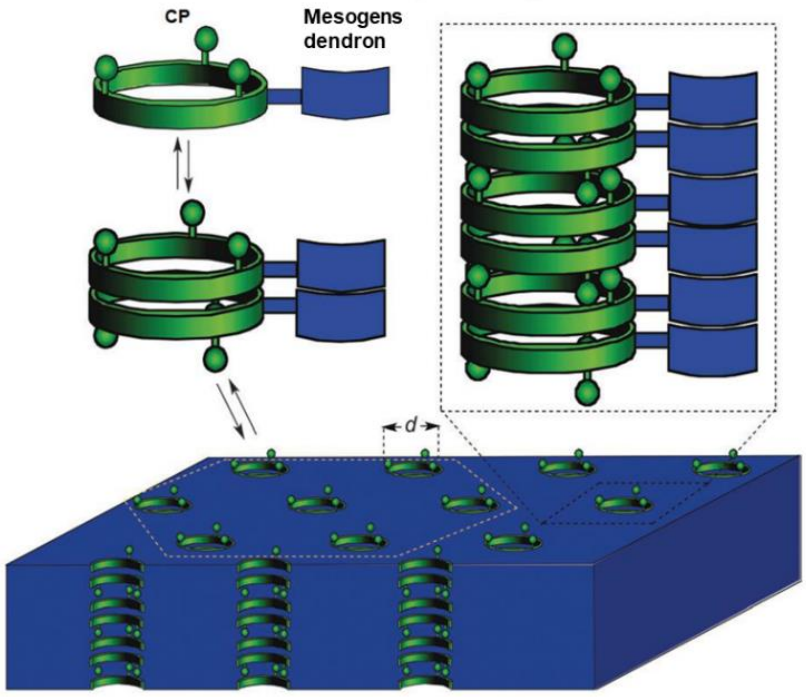

***Figure 38**. Porous liquid crystals obtained from α,γ-CP modified with mesogens dendrons.*

[322] Motesharei, K.; Ghadiri, M. R.; *J. Am. Chem. Soc*., **1997**, 119, 11306-11312.
[323] a) Couet, J. *et al*, *Angew. Chem. Int. Ed*., **2005**, 44, 3297-3301. b) Gokhale, R.; Couet, J.; Biesalski, M., *Phys. Status. Solidi A*, **2010**, 207, 878-883.
[324] Xu, T. *et al*, *ACS Nano*, **2011**, 5, 1376-1384.
[325] Amorín, M. *et al*, *Chem. Commun*., **2014**, 50, 688-690.
[326] a) Horne, W. S.; Ashkenasy, N.; Ghadiri, M. R., *Chem. Eur. J*., **2005**, 11, 1137-1144. b) Ashkenasy, N.; Horne, W. S.; Ghadiri, M. R., *Small*, **2006**, 2, 99-102.

Recently, it has been successfully synthesized the first example of supramolecular capsules based on stacked metal peptides (the diameter of the cyclic peptide determines the size of the capsule). A porphyrin cap was attached to the entrance of the CP cavity to drive the interaction with the guest. In this way, the metallic ion determine which ligands would be introduced inside the capsule. One of the most relevant characteristic of this approach is the union by dynamic covalent bonds between both components (Figure 39).[327] Three different interactions are involved in the formation of the capsule: hydrogen bond for the assembly of the cyclic peptide to form the dimer, hydrazone bond to link the CP and the porphyrin and a metal coordination for the recognition and encapsulation of specific ligands.

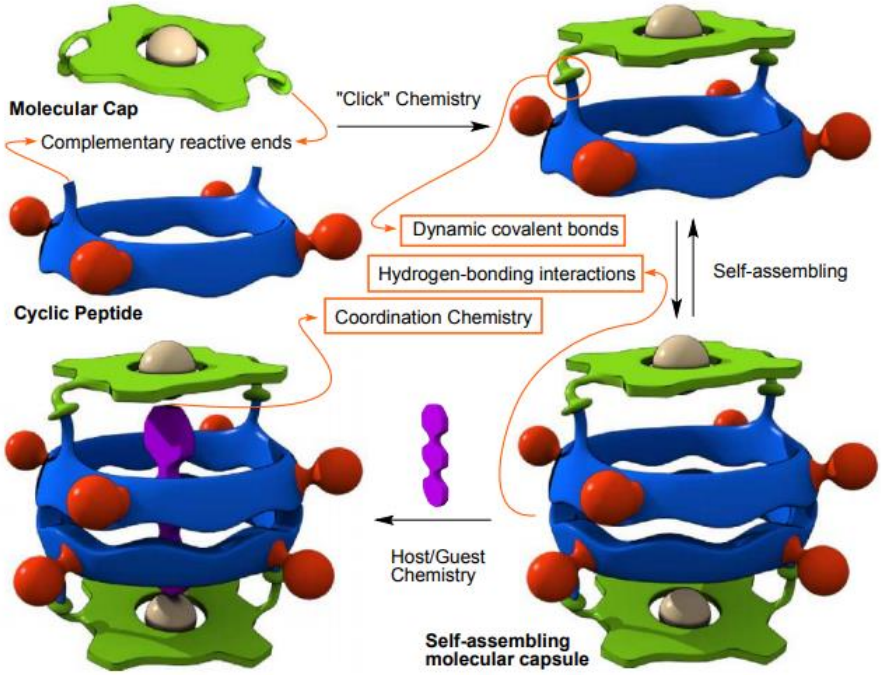

***Figure 39**. Scheme of the different dynamic covalent bonds involved in the formation of the capsule.*

These peptide structures are also applied in medicinal chemistry, involving in the release of a drug. Hydrophobic peptides were synthesized to transport the 5-fluorouracil antitumor drug, observing an improvement of its antitumor activity.[328] In the same way, cyclic peptides have been used to deliver doxorubicin in the treatment of breast cancer.[329] In this process, the authors used a peptide that contained a cysteine, where a PEG moiety was attached to increase the solubility of the CP in water. Additionally, glutamic acid residues at the opposite side was used to attach the DOX. These supramolecular aggregates, loading with DOX, showed an enhancement of the antitumor properties of the drug (cytotoxicity, absorption and intracellular distribution). One interesting example of a novel drug delivery system is the case of a dimeric structure that was modified with two carboxylate moiety projected towards the lumen of the dimer to coordinate Pt(II) complexes. This hybrid is constituted by α,γ-Aas, where one of the methylenes of the γ-residues was functionalized to attach the cargo. In this design, the dimer

[327] Ozores, H. L.; Amorín, M.; Granja, J. R., *J. Am. Chem. Soc*., **2017**, 139, 776-784.
[328] a) Liu, H.; Chen, J.; Shen, Q.; Fu, W.; Wu, W., *Mol. Pharmaceut*., **2010**, 7, 1985-1994. b) Cheng, J. *et al*, *Nanoscale*, **2016**, 8, 7126-7136.
[329] Wang, Y. *et al*, *J. Biomed. Nanotechnol*., **2014**, 10, 445-454.

acts as bidentate ligand of the platinum. Cytotoxicity assays shows that the compound present selectivity against ovarian cancer.[330]

Moreover, the cyclic *D,L*-α-peptides have also been studied as antiviral agents. The eight-residue cyclic peptide *c*-[*L*-Ser-*D*-His-*L*-Lys-*D*-Arg-*L*-Lys-*D*-Trp-*L*-Leu-*D*-Trp] (Table 9, entry 1), with a IC_{50} of 5 μM against type-A influenza viral activity, acts by preventing Hela cells from forming low-pH endocytic vehicles and further inhibiting viral escape from endosomes.[279c] It seems that the amphiphilic character and the amino acid sequence strongly affects the antiviral activities (see Table 9).[331] Furthermore, peptide sequences of entries 4 and 5 are *N*-methylated analogues of entry 6, *c*-[WLWSENSK], designed to prevent peptide stacking and nanotube formation through intermolecular hydrogen bonding. The IC_{50} increased for the *N*-methylated compounds, thus suggesting that the supramolecular structure is required for the antiviral activity.

Entry	Cyclic Peptide Sequence	Anti-Virus Activity		
		IC_{50} (μM)		LD_{50} (μM)
		Type-A influenza	Hepatitis C	Hela Cell
1	c-[SHKRKWLW]	5	ND	57
2	*c*-[WLWKRKHS]	5	ND	35
3	*c*-[SHKRKWLW]	7	ND	63
4	*c*-[WL^{Me}WSENS^{Me}K]	ND	> 50	ND
5	*c*-[WL^{Me}WS^{Me}ENSK]	ND	> 50	ND
6	*c*-[WLWSENSK]	ND	7	> 100
7	*c*-[WLWSEQSK]	ND	3	65
8	*c*-[WLWSEKNS]	ND	8	> 100
9	*c*-[WLWXEQEX]	ND	7	80
10	*c*-[WLWRESQK]	ND	3	90
11	*c*-[WLWOSNES]	ND	8	> 100

ND = Non-detected; Me = *N*-methylation; O = Ornithine X = 2,3-diaminopropionic acid; HD = Hemolytic dose. Underling represents *D*-amino acids.

***Table 9**. In vitro antiviral activity of several cyclic D,L-α-peptides.*

3.3. Cyclic peptides as antimicrobial agents.

Cyclic peptide nanotubes possess unique structural features not found in the natural class of peptide antibiotics.[297b] Perhaps, the most interesting characteristic of these tubular structures is the ability to modify its properties by changing the amino acids sequence of the basic building block. The optimal ring size for taking place the self-assembly process are CPs with six- or eight-amino acids. Also, the appropriated design should be able to self-assemble and form *β*-sheet structures in contact with the bacteria membrane, increasing the membrane permeability while would remain as monomer, and less toxic, in the aqueous media (following the same mechanism that antimicrobial peptides describe above). In 2001, it was presented a series of

[330] Rodriguez-Vazquez, N. *et al*, *Org. Lett.*, **2017**, 19, 10, 2560-2563.
[331] Montero, A. *et al*, *Chem. Biol.*, **2011**, 18, 1453-1462.

amphiphilic cyclic peptides composed of three consecutive hydrophilic residues and a repeating *L*-Trp and *D*-Leu motif that were able to self-assemble in synthetic membranes into tubular structures.[297b] Furthermore, these nanotubes allow a highly efficient transport of ion and small species (with relative mass less than 10,000 of M_w) across lipid bilayers, which was demonstrated by vesicular ion and molecular transport assays, conductance measurements in planar lipid bilayers and RTIR analyses. These cyclic peptides were constituted by six and eight-amino acids, where each peptide include at least one basic residue to enhance its target specificity towards negatively charged bacterial membranes (Table 10). The antibacterial activity were testes against MRSA, as representative of Gram-positive bacteria and due to the general interest for treating this kind of infections, and *E. coli* as Gram-negative bacteria.

		MIC (μg/mL)		HD_{50} (μg/mL)
Entry	**Peptides**	**MRSA***	***E. coli*** **	**Haemolysis**
1	*c*-[SKSWLWLW]	10	100	30
2	*c*-[THSWLWLW]	100	100	100
3	*c*-[RGDWLWLW]	100	100	100
4	***c*-[KQRWLWLW]**	**6**	**80**	**45**
5	*c*-[KQRWLWLW]	8	80	40
6	*c*-[RQRWLWLW]	18	90	25
7	*c*-[KQKWLWLW]	45	100	50
8	***c*-[KSKWLWLW]**	**5**	**40**	**100**
9	*c*-[SHKWLWLW]	10	100	35
10	*c*-[SKHWLWLW]	15	100	20
11	*c*-[SHHWLWLW]	20	100	20
12	*c*-[EKHWLWLW]	100	100	>100
13	*c*-[KKKWLWLW]	**8**	**70**	**50**
14	***c*-[RRKWLWLW]**	**6**	**15**	**50**
15	*c*-[KRKWLWLW]	10	40	50
16	*c*-[RRRWLWLW]	10	50	35
17	*c*-[HKHWLWLW]	12	15	25
18	*c*-[KHKWLWLW]	10	80	30
19	H_2N-WKKKWLWL-COOH	60	-	100
20	H_2N-KKKWLWLW-$CONH_2$	50	-	100
21	Ac-KKKWLWLW-$CONH_2$	80	-	100
22	*c*-[KKLWLW]	**10**	**17**	**80**
23	*c*-[KHLWLW]	10	100	25
24	*c*-[KSLWLW]	75	100	90
25	*c*-[RRLWLW]	**35**	**5**	**90**

Single-letter codes for amino acids. Underling represents *D*-amino acid residues. The most active and selective sequences are in bold. * ATCC 33591. ** JM109.

Table 10. *In vitro activity of cyclic D,L-α-peptides.*[297b]

The role of hydrophilic side chains was studied with the peptides *c*-[SKSWLWLW] and *c*-[THSWLWLW] (entry 1 and 2, Table 10). Entry 1 include one basic residue between two serines whereas entry 2 has it between a serine and a threonine. The substitution of these basic residue, lysine (1) for histidine (2), give rise to a significant reduction in activity (MICs from 10 μg/mL to 100 μg/mL). The introduction of a glutamic acid in the sequence present a similar behaviour, such as peptide at entrance 10 is much more active than *c*-[EKHWLWLW] (entry 12, Table 10) (MICs from 15 μg/mL to 100 μg/mL). The reduction of the activity in peptide *c*-[EKHWLWLW] may be produced by unfavourable electrostatic interactions of the carboxylate side chain with the bacterial membrane constituents. Peptides at entries 13-17 show three basic residues, instead of two as in entries 1-12, which result in a moderate activity against MRSA and peptides *c*-[RRKWLWLW] (entry 14, Table 10) and *c*-[HKHWLWLW] (entry 17, Table 10) also exhibit moderate activity against *E. coli*. However, red blood cell toxicity is also increased (lower haemolytic values). Hexapeptide *c*-[KKLWLW] (entry 22, Table 10), which has two consecutive lysine residues, displays activity against both bacteria and low haemolytic behaviour. *c*-[KHLWLW] (entry 23, Table 10) retains high activity against MRSA but it is inactive against *E. coli* due to the substitution of the lysine for histidine. The substitution of the same lysine for serine leads to inactive peptide *c*-[KSLWLW] (entry 24, Table 10). Surprisingly, the peptide 25, which present two arginines instead of lysine, displays potent and selective activity against *E. coli*, with low levels of haemolysis. The activity and membrane selectivity of the compounds represented in Table 10 highlight the effects that single amino acid substitutions have on these two properties.

Studies with the linear peptides (entries 19-21) show little *in vitro* activity against MRSA. Furthermore, the positively charged control peptide *c*-[KLKLKLKL], which is not an amphiphilic structure, is membrane inactive and lacks *in vitro* antibacterial activity.

Different experiments, such as fluorescence-based cell depolarization studies, rate of bacteria killing or attenuated total reflectance (ATR) FTIR studies in synthetic lipids, are all consistent with a membrane permeation mode of action for this class of antibacterial peptides. The possibility of a receptor/ligand-mediated mode of action in bacterial membranes is unlikely for these CPs as both enantiomeric entries 4 and 5 have similar in vitro activities. Time-killing studies with the octa-peptides *c*-[KQRWLWLW] and *c*-[KRKWLWLW] (entries 4 and 15, Table 10) and hexa-peptides *c*-[KKLWLW] and *c*-[KHLWLW] (entries 22 and 23, Table 10) show that at concentrations equal to or above the MIC, all peptides have completely bactericidal activity against MRSA within 5 (octa-CPs) and 60 min (hexa-CPs). This timescale is more consistent with membrane permeation than receptor/ligand-mediated binding/inhibition mechanism that typically takes several hours to achieve complete bactericidal or bacteriostatic activity.

Cyclic peptides at entries 9,14,22 and 25 were assayed for proteolytic susceptibility. These peptides were stable in the presence of trypsin, α-chymotrypsin, subtilisin and murine blood plasma. The mixture was analysed by HPLC, showing lack of degradation in these peptides over 72 h. However, the linear peptides (entries 19-21) were degraded in less than 10 min under similar conditions (4 h for murine blood plasma).

Peptides *c*-[KQRWLWLW], *c*-[RRKWLWLW] and *c*-[KKLWLW] (entries 4, 14 and 22, Table 10) were studied in vivo to evaluate the best route of administration, maximum tolerance dose, and blood and tissue toxicity. Studies with peptide *c*-[KQRWLWLW] (entry 4) cause signs of temporary discomfort (less than 10 min) for intravenous administration of 12 mg per kg. In contrast, there is not appreciation of toxicity at same concentration with the

intraperitoneal route of administration. Peptide *c*-[KKLWLW] (entry 22) was tolerated up to the maximum tested intraperitoneal dose (50 mg per kg), which signs of toxicity are dissipated within 2 h. Peptide 14 was tested up to 17.5 mg per kg intraperitoneal and subcutaneous doses without any apparent signs of toxicity. 300 mg per day for three consecutive days of peptide *c*-[RRKWLWLW] (entry 14) was administered to two mice intraperitoneally and two mice subcutaneously. Over four days, there are not apparent changes in the physical, social and feeding activities were observed in any of these mice.

Studies of the efficacy *in vivo* of these compounds were carried out with the peptides at entries 13, 14 and 22. Groups of mice were infected with lethal doses of MRSA (2-5 x 10^7 CFU per mouse, intraperitoneal) and then each group was treated intraperitoneally with a single dose of peptides at entries 13,14 or 22 at 45-60 min after initial infection. A single appropriate dose of peptide was enough to completely protect various groups of mice from MRSA infections. These *in vivo* studies highlight the considerable potential that this class of peptides of low molecular weight holds for the treatment of MRSA infections.

The ability of these structures to treat MSSA and MRSA was further studied.[332] A hexamer library that possess between two and four consecutive hydrophilic residues that were chosen from six amino acids (Lys, Arg, His, Glu, Asn, and Ser) but having always a lysine residue at position 1. The hydrophobic region was filled with Trp and Leu. In addition, an octamer library was prepared, but the hydrophilic core was constituted by a range of 3-5 amino acids. The hexamer peptide *c*-[LLWHSK] and the octamer peptide *c*-[KKHKWLWK] (Table 11) were isolated directly from this library. The properties of the hexameric peptide were further optimized by the incorporation of non-natural residues, leading to the compound *c*-[LLWHOK] (Table 11). Similarly, optimization of the octameric peptide leads to compounds *c*-[SWFKTKSK], *c*-[SWFKHKSK] and *c*-[SWXKNKSK].

Entry	Sequence	MIC_{90} for *S. aureus* 29213 (μg/mL)	Serum MIC for *S. aureus* 29213* (μg/mL)	MBC for *S. aureus* 29213 (μg/mL)	HD_{50} (μg/mL)	EC_{50} (μg/mL)	Tolerance at 8 mg/kg
1	*c*-[SWFKTKSK]	8	16	32	>400	>100	4
2	*c*-[SWFKTKSK]	8	16	16	>400	>100	4
3	*c*-[SWFKHKSK]	12	12	16	>400	>100	3
4	*c*-[SWXKNKSK]	2	8	4	209	63.5	2
5	*c*-[LLWHOK]	2	1	32	190	5.9	1
6	*c*-[KKHKWLWK]	2	2	32	101	29.9	0.5

* Serum MICs were determined in cation-adjusted MHB in the presence of 50% mouse serum. Underling represents *D*-amino acid residues. O = Ornithine. X = *O*-benzyltyrosine.

***Table 11**. Summary of in vitro potency and toxicity and in vivo tolerability of peptide compounds.*

[332] Dartois, V. *et al*, *Antimicrob. Agents Chemother*, **2005**, 49, 3302-3310.

The MIC_{90} was determined for 10 different strains of *S. aureus*, including MRSA ATCC 43300 and 33591. The MICs for MRSA are similar to those for *S. aureus* 29213, with values of 8 μg/mL for *c*-[SWFKTKSK] and 12 μg/mL for *c*-[SWFKHKSK]. The enantiomer *c*-[SWFKTKSK] was also synthesized and its antimicrobial properties were maintained. It is unlikely that the critical mode of action involves interaction with a specific receptor where changes in stereochemistry would be expected to have drastic consequences with regard to potency and activity. Time-kill assays were carried out to study the pharmaco-kinetics of these compounds. Compounds *c*-[SWFKTKSK] and *c*-[KKHKWLWK], and vancomycin as control, were tested against MSSA strain ATCC 25923 at four times the respectively MIC. Both peptides display much more rapid bacterial killing (about 5 min) than did vancomycin, which bactericidal action occurs by other mechanism of action and cause a reduction over an incubation period of 6 h at four times de MIC of 1.6-log CFU/mL. All these data confirm that these new molecules displayed fast bactericidal activity in an enantiomer-independent manner, which is consist with an insertion into the bacterial membrane with a subsequent increase in membrane permeability, inducing its collapse and a fast cell death (short killing times).[297b, 298,333]

The ability of *S. aureus* to develop resistance against the six peptides of the Table 11, and vancomycin and rifampicin as control, was evaluated by repeated passaging and MIC determination. S. aureus cells was incubated for 15 days introducing each day the half of the MIC to keep the bacteria in a continue exposure of the antibiotic. The MIC of rifampicin increased as much as 512-fold over 15 days; rifampicin is an agent to which resistance is known to arise quite easily by spontaneous chromosomal point mutations.[334] In contrast, the MICs of *c*-[SWFKTKSK], *c*-[SWFKHKSK] and *c*-[SWXKNKSK] (entries 2, 3 and 4, Table 11) increased twofold, while the MIC of *c*-[SWFKTKSK] (entry 1, Table 11) increased fourfold and that of *c*-[KKHKWLWK] (entry 6, Table 11) remained unchanged. Again, the results of entries 1 and 2 (Table 11) are very similar.

Haemolytic activity of the peptides was tested using a mouse RBC lysis assay. As it is summarized in the table, peptides at entries 1, 2 and 3 (Table 11) exhibited no significant haemolytic activity. Moreover, experiments in vivo were carried out. Mice were inoculated with 5.1 ± 0.1 $\log_{10}$ CFU of *S. aureus* ATCC 25923 per thigh. After 2 h of the inoculation, the drug was administered as well. Single 16-mg/kg doses of *c*-[SWFKTKSK] (entry 1, Table 11) and vancomycin produced a prolonged antibacterial effect against *S. aureus*.

Since the MRSA infections are increasing, there has been attempts to treat them with cyclic peptides of six amino acids as well.[335] The design follows the same principles than the others: cationic nature and amphiphilic properties. To simplify, Lys was use as first amino acid to attach the resin. A combinatorial screening result in 352 different peptides. First screening reduced the library to 88 were defined as 'highly active', that were rescreened at lower concentrations (10, 5, and 2.5 μM). The biological activity of the most interesting structures against two prokaryotic bacteria and two eukaryotic marine algae are presented in Table 12.

Cyclic peptides *c*-[KWFHWK] and *c*-[KWFHWK] (entries 1 and 2, Table 12) display appreciable selectivity for *E. coli* while peptides *c*-[KWFFLH] and *c*-[KWLFFK] (entries 3 and 4, Table 12) showed an opposite selectivity (activity against MRSA). It seems that the histidine

[333] Clark, T. D. *et al*, *J. Am. Chem. Soc*., **1998**, 120, 8949-8962.
[334] Schwarz, T. F.; Yeats, S. M.; Connolly, P.; McConnell, D. J., *Mol. Gen. Genet*., **1981**, 183, 181-186.
[335] Fletcher, J. T.; Finlay, J. A.; Callow, M. E.; Callow, J. A.; Ghadiri, M. R., *Chem. Eur. J*., **2007**, 13, 4008-4013.

in peptides at entrance 1 and 2 act as hydrophobic residue in its deprotonated state. Peptides *c*-[KWWFWK] and *c*-[KWFWWK] (entries 5 and 6, Table 12), which sequences can be differentiated by the position of the tryptophan and the phenylalanine, also display similar activity profiles, suggesting that side-chain properties are largely responsible for the observed biocidal behaviour (also observed in previous studies[297b,332]).

Entry	Peptide sequence	MIC [μM]		LD_{66} [μM]		HD_{50} [μM]
		MRSA	*E. coli*	*U. linza*	*N. perminuta*	
1	*c*-[KWFHWK]	30	15	10	20	> 100
2	*c*-[KWFHWK]	> 100	7.5	12.5	n. d.	n. d.
3	*c*-[KWFFLH]	10	> 100	10	> 100	> 100
4	*c*-[KWLFFK]	7.5	40	40	20	50
5	*c*-[KWWFWK]	30	100	10	40	> 100
6	*c*-[KWFWWK]	100	> 100	30	20	> 100
7	*c*-[KWFKWS]	> 100	> 100	50	30	> 100
8	*c*-[KWFKKL]	50	20	> 100	30	> 100
9	*c*-[KWFLWH]	100	> 100	> 100	40	> 100

Underling represents *D*-amino acid residues. LD_{66} = 66% lethal dose. HD50 = 50% hemolytic dose (mouse erythrocytes). n. d. = not detected.

***Table 12**. Activities of the selected sequences against bacteria, algae and red blood cells.*

Peptide *c*-[KWFHWK] (entry 1, Table 12) was chosen to further explore its potency optimization by single amino acid modification, as shown in Table 13. This study was shown to be highly sensitive towards single side-chain perturbations. It is important to note that as the result of single amino acid substitutions, the overall cationic charge and amphiphilicity may vary. In comparing the activity profiles of peptide *c*-[KWFHWK] analogues (Table 13), it seems that overall toxicity is strongly affected by the degree of amphiphilicity and not by the overall cationic charge. Sequences containing hydrophilic residues (Lys, Arg, His, or Ser) display broad-spectrum activity while those sequences containing hydrophobic Trp, Phe or Tyr substitutions were largely inactive in the concentration tested range.

Entry	Peptide sequence	MIC [μM]		LD_{66} [μM]		HD_{50} [μM]
		MRSA	*E. coli*	*U. linza*	*N. perminuta*	
1	*c*-[**K**WFHWK]	30	15	10	20	> 100
2	*c*-[**H**WFHWK]	15	20	50	20	> 100
3	*c*-[**R**WFHWK]	30	20	10	30	> 100
4	*c*-[**S**WFHWK]	10	40	5	8	> 100
5	*c*-[**L**WFHWK]	10	> 100	> 100	> 100	> 100
6	*c*-[**W**WFHWK]	> 100	> 100	> 100	> 100	> 100
7	*c*-[**Y**WFHWK]	> 100	> 100	> 100	> 100	> 100
8	*c*-[**F**WFHWK]	> 100	> 100	> 100	> 100	> 100

Underling represents *D*-amino acid residues. LD_{66} = 66% lethal dose. HD50 = 50% hemolytic dose (mouse erythrocytes). n. d. = not detected.

***Table 13**. Activities of peptides 32 and analogues against bacteria, algae and red blood cells.*

As it was mentioned in section 2.5.2, one of the proposed mechanisms for an antimicrobial activity was related to the permeabilization of the membrane that could follow two ways of interaction with membranes, pore formation and carpet-like mode of action. In general, this two structural alternatives were related with the sequence of *D*,*L*-α-amino acids. Synthetic channels resulting from the stacking of primarily hydrophobic cyclic peptides tent to partition in the lipid bilayer as single, individual transmembrane tubular structures.[297a] In contrast with α-helical AMPs, peptide nanotubes can organize as barrel staves when they procedure the pore by forming a supra-pore made of several peptide nanotube bundles. The carpet-like mode of action, which was originally proposed for amphipathic α-helical antimicrobial peptides, can be adopted by any compound that exhibits the required amphipathicity and possesses antibacterial properties.[336] The theoretical mechanism proposed for the carpet-like mode of action follows three steps: a) amphipathic peptide nanotubes anchor at the water-membrane interface to satisfy both, the hydrophobic interaction with the alkyl bilayer and the hydrophilic interacting with water phase or lipid heads, until a critical concentration is reached; b) then, the permeabilization of the bilayer proceeds through encapsulation of bundles of lipids as they progressively diffuse through the hydrophobic medium; c) the resulting lipid-nanotube aggregates are expelled, forming nanopores that modify in a irremediable fashion the permeability properties for the membrane (Figure 40).

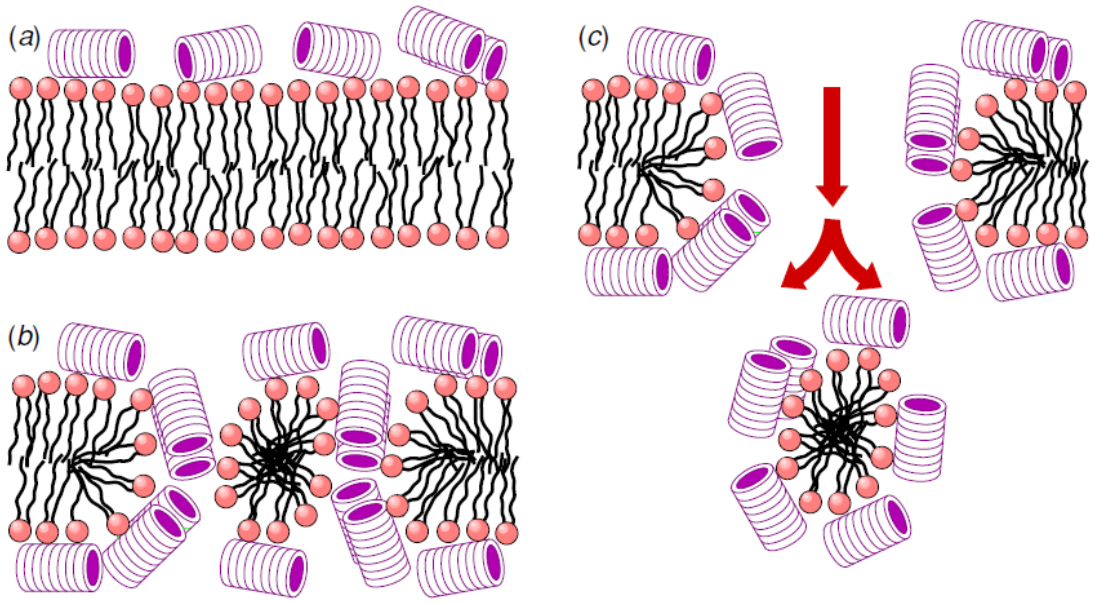

Figure 40. *Carpet-like mechanism of action of cyclic peptides.*[337]

Molecular dynamics (MD) simulations were used to examine the interactions of a peptide nanotube of biologically relevant sequence (*c*-[RRKWLWLW], table 10) with a water-membrane interface.[337] Although at the begging the nanotube appears as a hollow tubular structure, the number of water molecules sequestered inside the nanotube increase progressively up to about 24 after 4 ns. After 8.2 ns of contact between the peptide and the membrane, it can be observed that the amphipathic character of the peptide nanotube is maintained, as arginine and lysine side chains remain largely exposed to the aqueous medium

[336] Chipot, C.; Tarek, M., *Phys. Biol*., **2006**, 3, S20-S25.

and the head-group region of the lipid bilayer, while the leucine side chains are buried in its hydrophobic core. In fact, there is ample contacts between the lipid bilayer and the cyclic *D,L*-α-peptides. Specifically, the leucine and tryptophan side chains interact with the aliphatic chains of the membrane, essentially through disperse forces. Charged side chains also interact strongly with the polar moieties of the lipid units.

3.4. Cyclic glycopeptides as antimicrobial agents.

Many human proteins are co- or post-translationally modified by mono- or oligo-saccharides. Among a number of post-translational modifications, glycosylation is the most abundant form and it has been predicted that nearly 50% of all human proteins are glycosylated. Due to their complexity and structural diversity, carbohydrates and glycoconjugates play crucial roles in many key biological processes. These include pathogenic processes involving viral and bacterial infections. Many viral and bacterial pathogens employ the recognition of carbohydrates displayed on the epithelial surface of cells via pathogenic lectins to penetrate and infect their target organisms.[337]

Adhesion of viruses and bacteria to carbohydrate epitopes on the host cell is the initial step in pathogenesis. The adhesion of uropathogenic *E. coli* is mediated by FimH, which is a bacterial lectin of type 1 fimbriae that recognizes *α-D*-mannosides.[338] X-Ray studies have shown that the lectin possesses a monovalent carbohydrate recognition domain that specially recognizes *α-D*-mannose.[339] On the other hand, the adhesion of Pseudomonas aeruginosa depends on lectins LecA and LecB, which are tetrameric adhesins that are involved in the bacterial biofilm formation and specially recognize and bind to *D*-galactosides and *L*-fucosides, respectively.[340] Thereby, LecA shows a preference for α-linked terminal galactose units on longer glycans.[341] LecB exhibits a preference for α-L-fucosides over β-L-fucosides.[342] Therefore, glycoconjugates interfering with LecA or LecB binding have the potencial to lead to the development of new anti-biofilm and anti-adhesion therapies.

The first two glycopeptide antibiotics, vancomycin and ristocetin, were discovered by Eli Lilly and Abbott Laboratories from *Amycolatopsis orientalis* and *A. lurida*, respectively, in the mid-1950s.[343,344] Both glycopeptides were used clinically to treat Gram-positive infections (vancomycin was approved for use in the clinic in 1958); however, ristocetin was later withdrawn from the market as it led to lowered blood platelet counts (thrombocytopenia) in some patients.[345] Teicoplanin (Figura 14, page 44), the other natural glycopeptide in the market, is a ristocetin-type lipoglycopeptide complex first reported from *Actinoplanes teichomyceticus*

[337] Behren, S.; Westerlind, U., *Molecules*, **2019**, 24, 1004.
[338] Hartmann, M; Lindhorst, T. K., *Eur. J. Org. Chem*., **2011**, 3583-3609.
[339] a) Hung, C. S. *et al*, *Mol. Microbiol*., **2002**, 44, 903-915. b) Bouckaert, J. *et al*, *Mol. Microbiol*., **2005**, 55, 441-455. c) Wellens, A. *et al*, *PLoS ONE*, **2008**, 3, e2040.
[340] a) Garber, N.; Guempel, U.; Belz, A.; Gilboa-Garber, N.; Doyle, R. J., *Biochim. Biophys. Acta*, **1992**, 1116, 331-333. b) Imberty, A.; Wimmerová, M.; Mitchell, E. P.; Gilboa-Garber, N., *Microbes Infect*, **2004**, 6, 221-228.
[341] Chen, C. P.; Song, S. C.; Gilboa-Garber, N.; Chang, K. S.; Wu, A. M., *Glycobiology*, **1998**, 8, 7-16.
[342] Mitchell, E. *et al*, *Nat. Struct. Biol*., **2002**, 9, 918-921.
[343] Blaskovich, M. A. T. *et al*, *Infect. Dis*., **2018**, 4, 715-735.
[344] a) Butler, M. S.; Hansford, K. A.; Blaskovich, M. A.; Halai, R.; Cooper, M. A., *J. Antibiot*., **2014**, 67, 631-644. b) Levine, D. P., *Clin. Infect. Dis*., **2006**, 42, S5-S12.
[345] Jenkins, C. S. P.; Meyer, D.; Dreyfus, M. D.; Larreu, M. J., *Br. J. Haematol*., **1974**, 28, 561-578.

in 1978.[346] It was approved in EU in 1998 and is currently used in many countries, but it has never been approved for use in the US.

Over the years, there have been many semisynthetic glycopeptide derivatives made that employ a range of derivatization strategies. Comprehensive reviews of structural modifications of vancomycin-like structures,[347] their total synthesis,[348] and their biosynthesis[349] are available.

As part of a program designed to discover new classes of agents to combat the rapid increase of bacterial resistance, antibiotics discovered long time ago were re-examined.[350,351] This so-called 'look-back' program was successful in the determination of several novel antibiotics with highly diverse structures and mechanism thanks to the advance in HPLC, NMR and mass spectrometry that make possible to isolate and structurally characterize what were previously intractable molecules.[352]

One of the most promising of those was a mixture made of several compounds, known as AC98 complex,[353] which was isolated from the strain of *Streptomyces hygroscopicus* LL-AC98. The complex was initially isolated in the late 1950s and shown to be effective against Gram-positive bacteria. At that time, the chemical complexity of the mixture coupled with the lack of broad-spectrum activity reduced the prospects to further develop the antibiotic. However, under the 'look-back' program, the interest in the complex was revived because of its activity against antibiotic-resistant strains, such as MRSA, penicillin resistant *Streptococcus pneumoniae* and vancomycin resistant enterococci.[349,354] The AC98 complex result to be a mixture of mannopeptimycins α-ε (Table 14, Figure 41).[355] They are novel glycosylated cyclic hexapeptides bearing two stereoisomers of an unprecedented amino acid, α-amino-β-[4´-(2´-iminoimidazolidinyl)]-β-hydroxypropionic acid (Aiha), as a distinguishing feature. 2-D NMR data stablished the sequence for the cyclic hexapeptide core as *c*-[Ser-Gly-Mephe-Tyr-Aiha A-Aiha B].

[346] Barna, J. C. J.; Williams, D. H.; Stone, D. J. M.; Leung, T. W. C.; Doddrell, D. M., *J. Am. Chem. Soc*., **1984**, 106, 4895-4902.
[347] Malabarba, A.; Nicas, T. I., Thompson, R. C., *Med. Res. Rev*., **1997**, 17, 69-137.
[348] Okano, A.; Isley, N. A.; Boger, D. L. *Chem. Rev*., **2017**, 117, 11952-11993.
[349] a) Yim, G.; Thaker, M. N.; Koteva, K.; Wright, G., *J. Antibiot*., **2014**, 67, 31-41. b) Chen, S.; Wu, Q. H.; Shen, Q. Q.; Wang, H., *ChemBioChem*, **2016**, 17, 119-128.
[350] He, H., *Appl. Microbiol. Biotechnol*., **2005**, 67, 444-452.
[351] a) Kong, F. *et al, J. Am. Chem. Soc*., **1998**, 120, 13301-13311. b) McDonald, L. A. *et al, J. Am. Chem. Soc*., **2002**, 124, 10260-10261.
[352] Koehn, F. E., *J. Med. Chem*., **2008**, 51, 2613-2617.
[353] De Voe, S. E.; Kunstmann, M. P., Antibiotic AC98 and production, US patent 3495004, **1970**.
[354] Singh, M. P. *et al, Antimicrob. Agents Chemother*., **2003**, 47, 62-69.
[355] He, H. *et al, J. Am. Chem. Soc*., **2002**, 124, 9729-9736.

Entry	MIC (μg/mL)			ED_{50} (i. v., mg/kg)
	S. aureus	***E. faecalis***	***E. faecium***	***S. aureus* (Smith)**
1	128	> 128	> 128	20
2	64	128	32 – 128	nt
3	8	64 – 128	16 – 64	3.5
4	4 – 8	64	8 – 64	2.6
5	4	16 – 32	4 – 32	0.6

Data are presented for ranges of MICs for seven strains of *S. aureus*, including MRSA, and for five strains of *E. faecalis* and four strains of *E. faecium*, both including VREs. Vancomycin as a control exhibited an ED_{50} of 1.0 mg/kg. nt = not tested.

***Table 14**. Antimicrobial data for mannopeptimicins α-ε.*

Mannopeptimycins α-ε exhibited moderate to good antibiotic activity against Gram-positive bacteria, including methicillin-resistant streptococci and VRE. Entry 2 present only one saccharide (in the core) whereas entries 1,2,4 and 5 present an additional disaccharide together with the monosaccharide present in the core (Table 14, Figure 41). However, entry 5 (Table 14) is the one that shows the best activity of the series.[355]

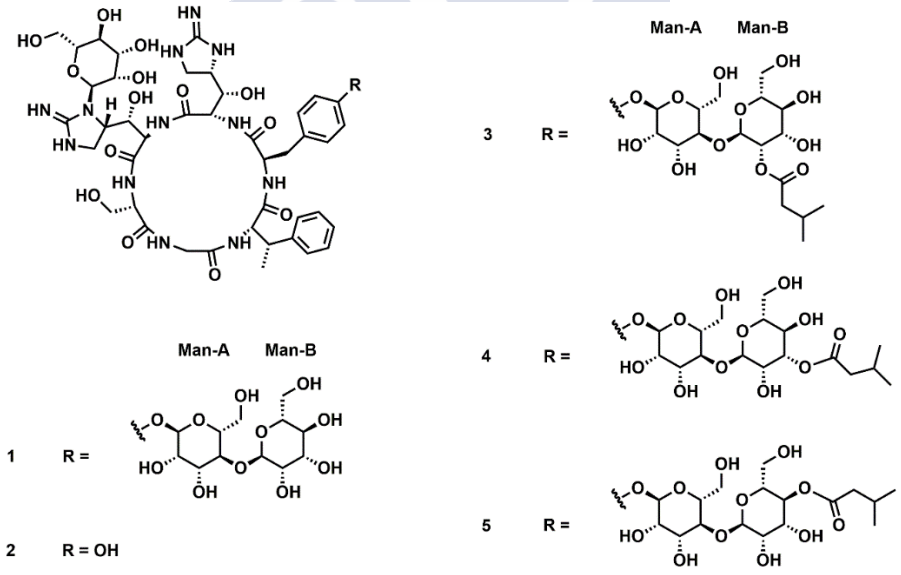

***Figure 41.** Structures of mannopeptimycins α-ε (entries 1-5, Table 15).*

In an effort to obtain more potent antibacterial agents, random acylations were prepared as the initial approach to obtain monoacylated products.[356] Several derivatives by the formation of esters were potent antibacterial agents against MRSA and VRE. However, due to it hydrolysis by esterases in mouse serum, they showed only moderated *in vivo* activity against *S.*

[356] He, H. *et al*, *Bioorg. Med. Chem. Lett.*, **2004**, 14, 279-282.

aureus infection. In contrast, acyl derivatives were stable in mouse serum and exhibited excellent in vivo efficacies.

In the process of achieving more selective hydrophobic functionalization to enhance the antibacterial activity, a method to synthesize cyclic acetal derivatives of mannopeptimycin α was developed.[357] Mannopeptimycin-α was treated with several compounds to produce predominantly a hydrophobic cyclic acetal derivative with potent activity against Gram-positive bacteria (Figure 42, Table 15).[358]

One of the most potent antibiotics obtained was the adamantyl derivative (entry 4).[353] The MICs of acetal and ketal derivatives against a spectrum of Gram-positive bacteria are shown in Table 15. These compounds displayed potent antibacterial activities against staphylococcus, streptococcal and enterococcal strains. The activities compared favourably not only with vancomycin but also with the natural mannopeptimycin esters. Entry 5 (Table 15), also called AC98-6446, was further evaluated against a variety of recent clinical Gram-positive isolates, including multiple-resistant strains.[359] It demonstrated similarly potent activities against methicillin-susceptible and resistant staphylococci and glycopeptide-intermediate staphylococcal isolates,[360] with MIC_{90}s of 0.03 – 0.06 μg/mL.

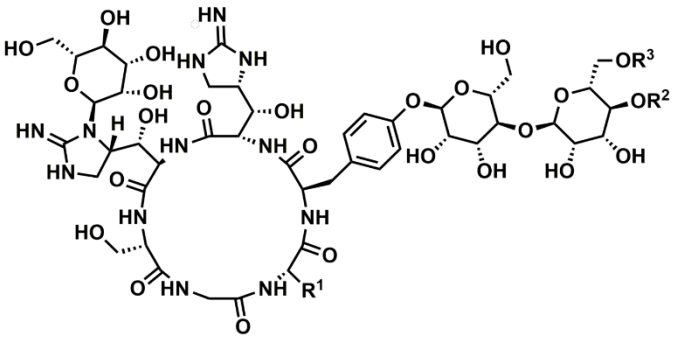

Entry	R^1	R^2, R^3	Entry	R^1	R^2, R^3
1	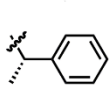	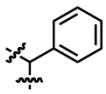	4	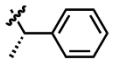	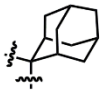
2	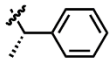	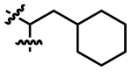	5	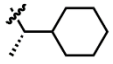	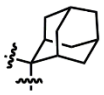
3	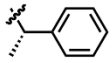	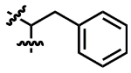			

Figure 42. *Mannopeptimycins acetals (entries 1-3 and 5) and ketals (entry 4).*

[357] Dushin, R. G. *et al*, *J. Med. Chem*., **2004**, 47, 3487-3490.
[358] Bonner, T. G., *Methods Carbohydr. Chem*., **1963**, 314-317.
[359] Petersen, P. J.; Wang, T. Z.; Dushin, R. G.; Bradford, P. A., *Antimicrob. Agents Chemother*., **2004**, 48, 739-746.
[360] Tenover, F. C., *J. Hosp. Infect*., **1999**, 43, S3-S7.

Entry	MIC (μg/mL)			ED_{50} (mg/kg)	
	Staphylococcus spp	**Streptococcus spp**	**Enterococcus spp**	***S. aureus* Smith (GC 4543)**	**E. faecalis (GC 6189)***
Vancomycin	0.5 – 2	<0.12 – 0.5	0.5 – >128	1	>32
1	0.5 – 2	<0.12 – 0.25	2 – 4	0.19	0.39
2	0.5 – 1	<0.12	0.5 – 2	0.07	0.19
3	0.5 – 2	<0.06 – 0.25	1 – 2	0.23	1.04
4	0.25 – 1	<0.06	0.5 – 1	0.04	1.80
5	0.25 – 1	<0.12 – 0.5	0.5 – 2	0.08	0.39

*Vancomycin-resistant strain.

***Table 15**. In vitro and in vivo antibacterial data for compounds 23-34.*

In a separate approach, Man-B 4,6-cyclic acetals were transformed by reductive ring-opening into Man-B 4-*O*- and 6-*O*-ether derivatives with potent antibacterial activities.[361] Both derivatives demonstrated potent in vitro activity against Gram-positive bacteria, including resistant strains of *S. aureus*, *E. faecalis* and streptococcus. Mannopeptimycins ether derivatives are generally more stable than ester, acetal and ketal derivatives, but preparation of these products requires extra reaction and purification steps.

Mannopeptimycin structures possess a cyclic peptide structure and potentially membrane-active antibacterial mode of action. However, to be best of our knowledge, there has not been published further studies of these compounds since 2004, suggesting that the compounds present more disadvantages that could be expected.

While mannopeptimycins can be hard to synthesize, cyclic *D*,*L*-α-peptides can be readily prepared and subjected to multiple rounds of sequence-activity optimizations through either parallel or combinatorial library approaches.[297b,362,363] In an attempt to obtain glycosylated analogs of cyclic *D*,*L*-α-peptides, a library of peptides were synthesized from progenitor peptide sequence *c*-[WLWKSKSK] (entry 1, Table 16). The symmetrical disposition of hydrophilic amino acids in this peptide (entry 1, Table 16) seemed appropriate for testing the effects of the position and type of *O*-glycosyl serine residue substitutions on antibacterial activity and target membrane selectivity. Glycopeptides (entries 2-4) were designed to maintain a similar overall cationic character by individually substituting each of the three lysine residues with serine (β$GlcNH_2$, X). Similarly, neutral serine residues were individually replaced with either serine (βGal, Z) or serine (αMan, U), providing glycopeptides that correspond with entries 5 and 6 or 7 and 8, respectively (Table 16, Figure 43).

[361] a) Sum, P. E. *et al*, *Bioorg. Med. Chem. Lett*., **2003**, 13, 1151-1155. b) Sum, P. E. *et al*, *Bioorg. Med. Chem. Lett.*, **2003**, 13, 2805-2808.
[362] Motiei, L.; Rahimipour, S.; Thayer, D. A.; Wong, C. H.; Ghadiri, M. R., *Chem. Commun*., **2009**, 3693-3695.
[363] Redman, J. E.; Wilcoxen, K. M.; Ghadiri, M. R., *J. Comb. Chem*., **2003**, 5, 33-40.

Entry	Peptide sequence	MIC (μM)				HD_{50} (μM)		LD50 (μM) NIH 3T3
		MRSA* (MBC)	MRSA* in FBS	*Bacillus cereus***	VRE	m-RBC	h-RBC	
1	*c*-[WLWKSKSK]	5	5	5	10	65	120	10
2	*c*-[WLWKSKSX]	5	15	10	10	65	85	20
3	*c*-[WLWKSXSK]	5 (10)	10	10	10	90	140	50
4	*c*-[WLWXSKSK]	5	5	15	10	80	150	20
5	*c*-[WLWKSKZK]	5 (10)	10	10	15	150	260	50
6	*c*-[WLWKZKSK]	5	5	5	10	105	190	25
7	*c*-[WLWKSKUK]	2.5 (5)	5	10	10	70	120	25
8	*c*-[WLWKUKSK]	2.5	10	5	5	50	105	15

**Methicillin-resistant S. aureus (ATCC33591). **ATCC11778.*

***Table 16**. In vitro actibacterial, hemolytic and cytotoxic activities of cyclic D,L-α-glycopeptides.*

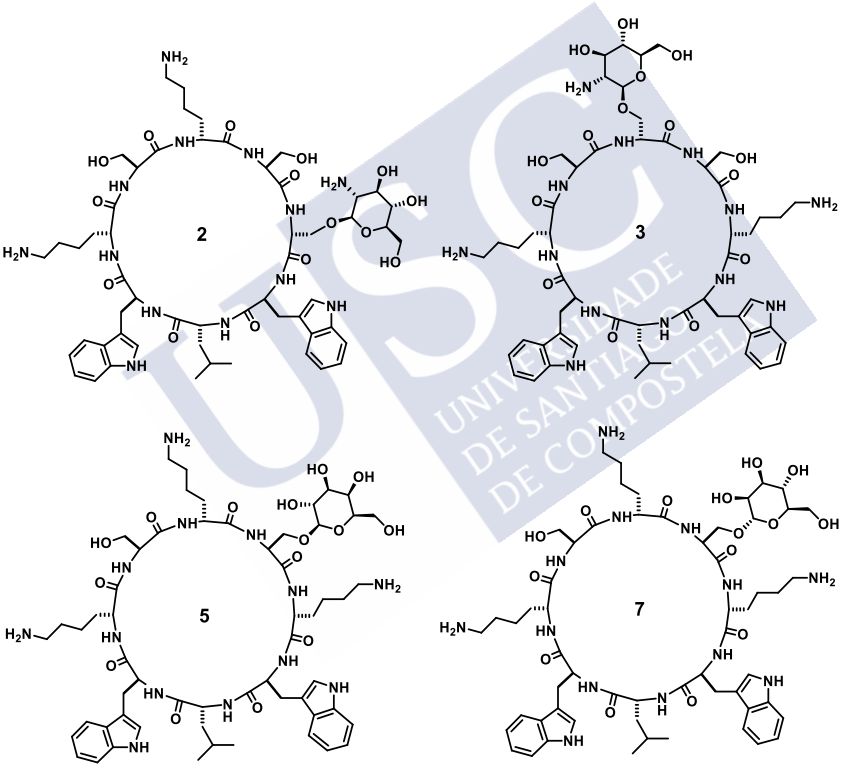

***Figure 43.** Examples of cyclic peptides with saccharides in their structure.*

In vitro antibacterial activities of glycopeptides (entries 1-8) against the Gram-positive species tested were generally in the 5 – 10 μM range, indicating that glycosylation did not adversely influence cell membrane uptake and activity. Furthermore, glycosylation also did not diminish the bactericidal activity. However, depending on the position and the type of glycosyl residue employed, glycosylation significantly attenuated the *in vitro* toxicity toward erythrocytes and mammalian cells (mouse fibroblast). Glycopeptides with the β-Gal side chain modification (5 and 6) were the most selective sequences, displaying low hemolytic activity

against human and mouse red blood cells. Of particular interest is the significant hemolytic activity differences observed between human and mouse RBCs: mouse red blood cells were more susceptible to haemolysis in all cases. Although the hemolytic activity of membrane-active antimicrobial peptides is typically used as an indicator of toxicity to mammalian cells, it has been found that several non-hemolytic antimicrobial cyclic *D,L*-α-peptides were acutely toxic in mice.[368] Therefore, in selecting promising cyclic peptide sequences for further studies, it should take into account their activity against mammalian tissue culture cells. Since *in vitro* cytotoxicity assays are performed in FBS, it is necessary to stablish if the cyclic peptides are affected by the medium. As it is shown in Table 16, the antibacterial activities of cyclic *D,L*-α-peptides were not appreciably perturbed in the presence of FBS (even at large amounts of it, 50% v/v). Moreover, glycosylation considerably reduced mammalian cell toxicity (up to approximately five-fold in the cases of entries 3 and 5) even after prolonged (48h) exposure of tissue culture cells to cyclic *D,L*-α-glycopeptides. Furthermore, the relative position of glycosylated serine side chain in the cyclic peptide sequence had up to a three-fold effect on mammalian cell membrane selectivity and toxicity.

Overview of the situation:

1. Pharmaceutical drug discovery and development is a lengthy (8-12 years) and expensive ($400-$800 million per approved agent) process.
2. In the past 4 decades have seen only two new classes of antibiotics introduced into clinical use, represent by the natural product daptomycin and the oxazolidine linezolid.
3. With few exceptions, the introduction of each new antibiotic has been followed, within a few years, by the appearance of resistance.
4. MRSA is currently a major source of hospital-acquired infections associated with significant morbidity and mortality.
5. Multidrug resistance in bacteria is generated by various mechanisms and it is not limit to bacteria; it can be observed in other pathogens including parasites, viruses, and fungi.
6. The return to a pre-antibiotic era is rapidly becoming a reality in many parts of the world.
7. The search for new antimicrobial compounds based on natural products could end in the rediscovering of already known structures.

Factors to be considered to design antibacterial compounds:

- Design for SMAMPs should consider: (i) introduction of both hydrophobic and hydrophilic functional groups to attain the desired amphiphilicity; (ii) rigid or semirigid backbone to preserve the amphiphilicity; (iii) use of highly repetitive structures to enhance activity through multiple SMAMP-lipid interactions.
- For selective toxicity and broad spectra, the peptides should target those molecules which are universal in prokaryotic cells, but rarely or never present in eukaryotic cells. For rapid killing, the site of action should preferably be the cell surface rather than the cell interior.
- AMPs are bactericidal compounds that selectively bind to and permeabilize anionic membranes. But also can present multiple targets including specific membrane molecules (LPS, Lipid II, etc…) as well as interactions inside the cell. The mechanism appears to vary from peptide to peptide. Moreover, it seems to depend on the membrane composition as well.
- Peptide-induced membrane disruption is irreversible and unrecoverable, inevitably leading to cell death. Due to their mode of action, it has been suggested that AMPs can potentially escape the multidrug resistance mechanisms.
- AMPs frequently contain Arg, Lys, His, Pro, Trp, Tyr and Phe
- High cost of peptide production reduces the number of peptides approve for therapeutic use. Thus, shorter peptides are preferred.

- Cyclic *D,L*-α-peptides present a flat conformation that can self-assembly into tubular structures (peptide nanotube). Self-assembly is driven by intermolecular forces, such as weak Van der Waals forces, hydrophobic effect, hydrogen bonding and electrostatic interactions. The best self-assembly process is achieved with 8 residues cyclic peptides.
- The introduction of saccharides can reduce the toxicity of cyclic *D,L*-α-peptides.

USC
UNIVERSIDADE
DE SANTIAGO
DE COMPOSTELA

Objective

USC
UNIVERSIDADE
DE SANTIAGO
DE COMPOSTELA

The main objective of these work is to develop a synthetic strategy that allow the preparation of amphipathic cyclic peptides with antimicrobial properties, that can be obtain from an efficient and easy manner. For these propose, we design a versatile cyclic peptide precursor as a common platform that can be modified in order to obtain a library of different peptides with potential antimicrobial properties. The analysis of these library may suggest which modifications improve the bactericidal characteristics as well as decrease the toxicity of these compounds. As a second objective, the peptides prepared by this methodology should be fully soluble in water to reduce some of the toxic effect observed in previous antimicrobial cyclic peptides. Moreover, the peptide nanotubes should only be achieved in the presence of the lipid membrane, and this should be the active form (Figure 44). Therefore, toxicity effect should only be observed for cells that facilitate the nanotube formation.

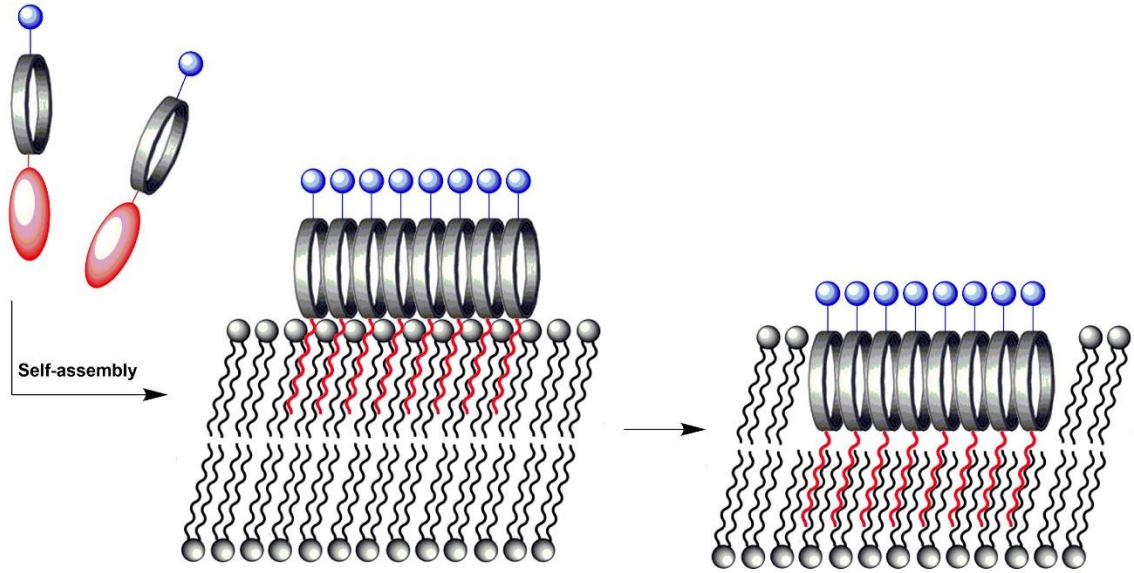

Figure 44. *Self-assembly process of cyclic peptides induced by lipid membranes to form nanotubes parallel oriented on the membrane surface like the carpet-like mechanism.*

As it was described in the introduction, cyclic peptides with antibacterial properties are cyclic *D,L-α*-peptides with an amphipathic structure. In general, these cyclic peptides are hexamer and octamers in which half of the residues were non-polar amino acids. The hydrophobic core was constituted mainly by Trp, Tyr or Phe, whereas the hydrophilic part used to have Lys, His, Arg, Ser, Glu and Asn. Moreover, these peptides present between 3 and 5 hydrophobic amino acids, leading to compounds that were not completely soluble in water. In vivo studies of intravenous injections showed drastic toxic effects that were related with peptide aggregation. These peptides used to form large cationic aggregates formed as a consequence of their low solubility and amphipatic properties.

The most effective compounds found for this goal were glycopeptides, natural or semi-synthetic, with high polar surface that leads to a good solubility in aqueous media and were unable to cross membrane barriers such as the blood-brain and intestinal barriers. In order to improve the membrane permeability, the glycopeptide structure should be either coupled to a lipid carrier or chemically modified by for example acetylation or methylation to increase the lipophilicity.[337,364] Additionally, the glycopeptide drug can be pharmaceutically formulated or

[337] Behren, S.; Westerlind, U., *Molecules*, **2019**, 24, 1004.

delivered using different carrier systems to facilitate the delivery at the target cell.[365] However, chemical and physical degradation of glycopeptide drugs are limiting factors for medical applications.

With the purpose of improving the cytotoxic effect of already known candidates, we proposed a new synthetic strategy to prepare in a simple and efficient manner new candidates with biological properties that could make them "production heads" for the development of new drugs. For this purpose, we proposed a new strategy based on a cyclic octa-peptide that present a reduce number of hydrophobic residues (2) and a large hydrophilic core. Moreover, the peptide includes two orthogonal reactive sites, one at each part of the amphipathic structure. This groups should allow the introduction of different moieties to modify the cyclic peptide properties. Based on this structure requisites, we proposed to use as the anchor points a terminal triple bond to carry out a [3+2] cycloaddition reaction. The second reactive group would be an alkoxyamine, which form an oxime with an appropriate aldehyde. This novel design should lead to the reduction of the synthetic effort required in the preparation of other glycopeptides.

Cyclic *D*,*L*-α-peptides has the ability not only to self-assembly into peptide nanotubes, but also are less prone to degradation by proteolytic enzymes. To increase the affinity of cyclic peptides for biological membranes, we considered that one of the components introduced in the peptide reactive groups could be aliphatic chains of different length. The other component should be a saccharide derivative that, as previously have been claim[262], would reduce the toxicity, which increasing the selectivity against bacteria. In principle, both components can be introduced by either of the two reactive sites, which give rise to two different platforms. The first one could have the triple bond in the hydrophilic side and the alkoxyamine in the hydrophobic one. Alternatively, the second precursor would have the triple bond would be placed at the hydrophobic core and the alkoxyamine in the hydrophilic. So, we decide to propose both possibilities (Figure 45).

[364] a) Adessi, C.; Soto, C., *Curr. Med. Chem*., **2002**, 9, 963-978. b) Di, L., *AAPS J*., **2015**, 17, 134-143.
[365] Bruno, B. J.; Miller, G. D.; Lim, C. S., *Ther. Deliv*., **2013**, 4, 1443-1467.

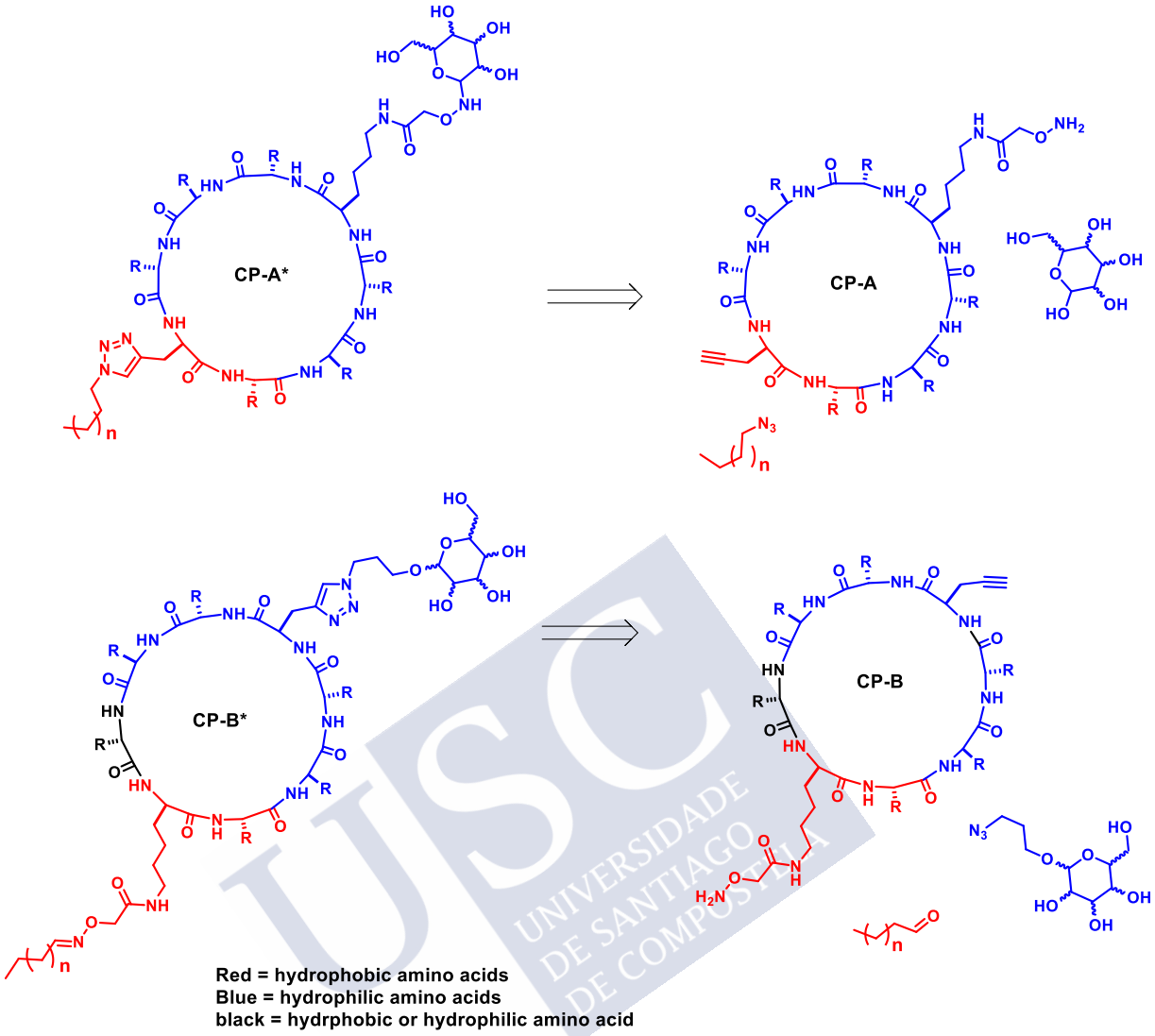

Figure 45. *The two platform propose for this work.*

More precisely, we proposed the synthesis of platform **CP-A** and **CP-B** and then evaluate the incorporation of the pendants on the reactive ends. Upon incorporation of both groups, the resulting peptides will be tested to determine the best platform for antimicrobial activity. *c*-[WLWKSKSK] (entry 1, Table 16), which one of the serine was conjugated with saccharide, showed a non-significant reduction in its antimicrobial activity but a clear reduction of toxicity. We used this cyclic peptide as a model for the generation of platforms **CP-A** and **CP-B**. In our design of **CP-B**, we substitute one of the lysines for the propargylglycine residue. Also, serine was substituted by glutamine in order to facilitate its synthesis in solid phase. The leucine of the hydrophobic core was substituted by a lysine on which an alkoxyamine would be attached by a methodology already implemented in the group.[366] **CP-A** (Figure 46) present only two hydrophobic amino acids, Trp and the terminal alkyne necessary for the attachment of different

[366] Pazo, M.; Fernández-Caro, H.; Priegue, J. M.; Lostalé-Seijo, I.; Montenegro, J., *Synlett*, **2017**, 28, 924-928.

aliphatic chains. In the hydrophilic side, we kept KSKSK of peptide *c*-[WLWKSKSK], but one serine was changed by glutamine for synthetic reasons and the alkoxyamine was planned to be introduced in a lysine. Therefore, three alternatives were proposed, in which the alkoxyamine was incorporated in one of the three positions. We considered that the lysine closer to the terminal alkyne was to close to the hydrophobic side, so this alternative was discarded. **CP-A1** has the alkoxyamine in the central lysine, and **CP-A2** on the remaining position (Figure 46). Inspired in the substitution in peptide *c*-[WLWKSKSK], where the saccharide is introduced in the middle of both lysines, we also proposed the exchang of Ser and Lys positions, leading to **CP-A3**, that would attach the saccharide in the same position than *c*-[WLWKSKUK] (entry 7, Table 16).

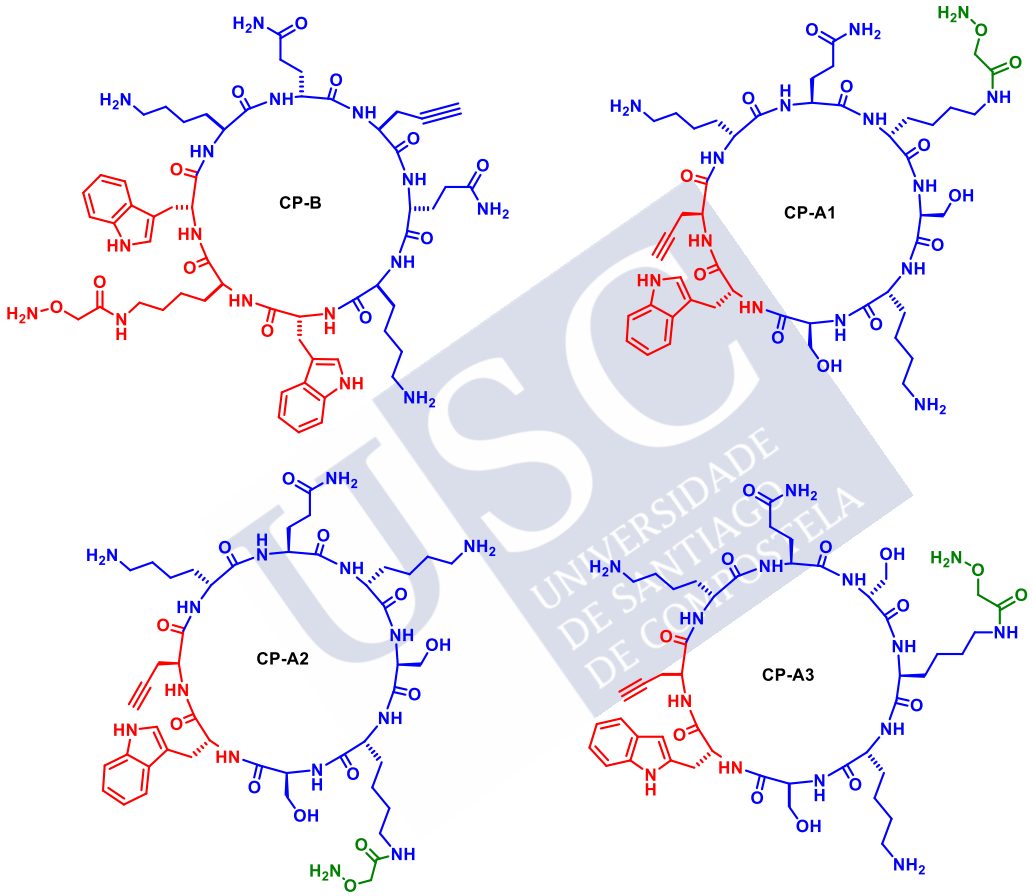

Figure 46. *Sequence of the peptides* ***CP-B***, ***CP-A1***, ***CP-A2*** *and* ***CP-A3***.

The number of infections caused by resistant strains of only two Gram-positive organisms (methicillin resistant *Staphylococcus aureus* and multidrug resistant *Streptococcus pneumoniae*) are almost twenty times more abundant than resistant Gram-negative infections, with > 1 000 000 vs < 50 000 cases, respectively. This translates into a similar imbalance in the number of deaths, with over 6-fold more deaths caused by Gram-positive bacteria (approximately 18 000 vs 3200).[343]

As it was mention in the introduction, this kind of structures present higher activity against Gram-positive bacteria than Gram-negative bacteria, due to the mechanism of action in which the peptide has to reach the cytoplasmic membrane to disrupt it. This is harder in Gram-negative bacteria compared to Gram-positive due to the presence of an additional external membrane. In this work we will focus on *S. aureus* infections, modifying the peptides to improve the activity against this strain. Although the treatment of *S. aureus* infections is our principle goal, we would also test them against one representative Gram-negative bacterium, such as *E. coli*. For the peptides with highest activities, we would carry out the antibacterial experiments with other Gram-positive bacteria in order to determine their bacteria selectivity. Therefore, *S. epidermidis*, *E. faecalis*, *S. mutans* and, of course, against *S. aureus* resistant strains, MRSA, will finally be evaluated.

Nowadays, the treatment of infections caused by bacteria´s biofilm is the most challenge goal for antibiotics, due to their inherent resistance structure. Infections produced by Gram-positive bacteria *S. epidermidis* was found in orthopaedic devices, central venous catheters, Hickman catheters, and, as well as *S. aureus*, in arteriovenous shunts and mechanical heart valves, which can cause the death of the host (Table 2 of the introduction).[65a] Due to the importance of fighting these symptoms, we also decide to study the activity against *S. epidermidis* as planktonic cells, and then, test the cyclic peptides activity against both *S. aureus* and *S. epidermidis* biofilms. In this way, our third objective will be to develop most of cyclic peptides with activity against mature biofilm, as well as to try the ability of the peptide to inhibit the biofilm formation, due to the lack of antibiotics that can treat these infections.

Many amphipathic cyclic peptides are able to internalize different cargos into the cell. These peptides are called cell penetrating peptides (CPPs).[367] CPPs have been developed in the last years due to their potential use as drug delivery systems. Recent precedents in the Granja/Montenegro group have shown that CPPs can be conjugated to the cargo through a dynamic covalent bond, sensible to pH. Consequently, the cargo can be release from endosome after the CPP induced the cell internalization. [368] Using this methodology, it is possible to reduce the toxicity and side effects of a drug. As we explained in the introduction, cyclic peptides forming dimers that encapsulate a *cis*-platin analogue as their cargo reduced cytotoxicity, as a consequence of reducing the amount of drug that circulates free in the host, while maintaining their activity in cell lines resistant to this drug.[330] Peptide nanotubes loaded with doxorubicin (DOX) by an encapsulation process was already prepared and probed to be efficient against breast cancer cells. Furthermore, the internalization of the DOX in the cell was improved.[329] However, many AMPs are also antitumor agents due to the higher amount of anionic phospholipids of cancer cell lines. Our last objective in this work is combine our platform with anticancer agents, by dynamic covalent bond, in order to improve the cytotoxic properties of antitumoral agents (Figure 47). In this strategy, we will attach the cargo to the cyclic peptide without modification of the drug structure and similar hydrolysis of the conjugate would release it in the cell.

[65] a) Costerton, J. W.; Stewart, P. S.; Greenberg, E. P., *Science*, **1999**, 284, 1318-1322.
[367] Reissmann, S., *J. Pept. Sci*., **2014**, 20, 760-784.
[368] a) Louzao, I.; García-Fandiño, R.; Montenegro, J., *J. Mater. Chem. B*, **2017**, 5, 4426-4434. c) Lostalé-Seijo, I.; Louzao, I.; Juanes, M., Montenegro, J., *Chem. Sci*., **2017**, 8, 7923-7931. d) Pazo, M.; Juanes, M.; Lostalé-Seijo, I.; Montenegro, J., *Chem. Commun*., **2018**, 54, 6919-6922. e) Gallego, I. *et al*, *ChemBioChem*, **2019**, 20, 1400-1409.

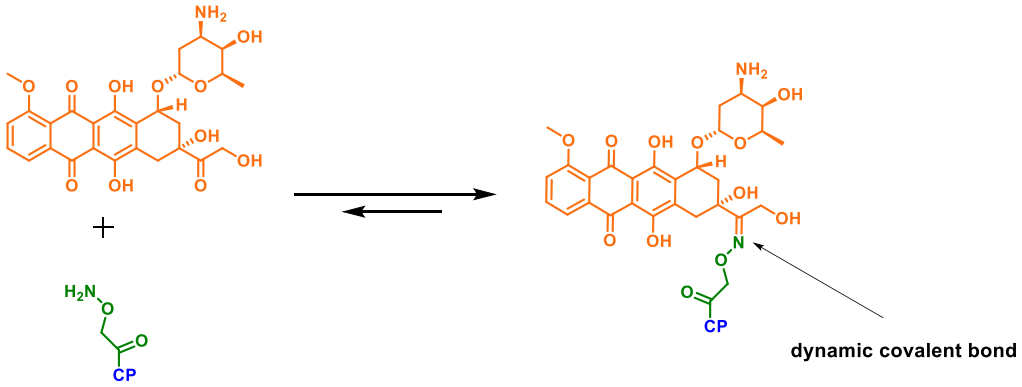

Figure 47. *Dynamic covalent bond between the doxorubicin and the alkoxyamine of the cyclic peptide.*

Chapter 1: Synthesis of the building blocks and cyclic peptides platforms

USC
UNIVERSIDADE
DE SANTIAGO
DE COMPOSTELA

The objectives of this work are focused on the preparation of several cyclic *D,L*-α-peptide units. These peptides should assembly into tubular structures under specific conditions, such as the interaction with bacterial membranes. The strategy includes the optimization of every step on the proposed methodology. The synthetic methods proposed to get the mentioned peptide will be on solid support to dismiss the solubility problems related with the large tendency to aggregate of the synthetic intermediates. In addition, this method on solid support reduce the chemo-selective problems related with the presence of a large number of basic nucleophile groups.

Solid phase peptide synthesis (SPPS) is the most common technique for the synthesis of peptides, which consist on growing the peptide chain using a solid support as a protecting group of the C-terminal end of the polypeptide. Therefore, the subsequent residues would be added to the N-terminal group of the growing chain. Prior to the development of SPPS,[369] peptides were synthesized through classical solution-phase methods, which required the purification and characterization in each step of the synthesis.[370] This was tedious and time-consuming method compare with solid phase synthesis. The development of this strategy allowed to Merrifield to be rewarded with the Nobel Prize in 1984.[371] The main advantages of the method is its simplicity and the speed with peptides can be synthesized. In this approach, the peptide is only purified at the end of the synthesis, after it is cleavage from the resin. The development of SPPS together with the development of HPLC allow the preparation of perfectly pure peptides in shorter periods of time.

In SPPS, the first amino acid of the sequence is attached to the solid support by a covalent bond between the resin functional group with one of the nucleophilic atoms of the amino acid forming, in general, amide or ester linking bonds. Usually, the attachment takes places through the carboxylic group of the amino acid,[372] although there are examples of peptides which first amino acid is attach through its side chain[321,373] or through the *N*-terminal moiety (Figure 1.1).[374] The last alternative presents more inconveniences than the other two approaches due to the high tendency of racemization/epimerization observed in the coupling reactions. Although some strategies have been developed to minimize the problem, this still represents a main drawback. [372a] Independently of the group that binds to the resin, the resulting bond must resist all the synthetic steps, deprotection, coupling and other functionalizations, but be labile enough to allow the removal of the peptide once the synthesis is completed. The selection of the resin depends on the protecting groups of the amino acids, the resin removal method and the

[369] a) Benoiton, N. L., In *Chemistry of peptide synthesis*, **2005**, 125-126 (Taylor and Francis Group; editors. Boca ratón, Florida). b) Blackburn, C.; Kates, S. A., *Methods Enzymol*., **1997**, 289, 175-198. c) Lloyd-Williams, P.; Albericio, F.; Giralt, E., *Tetrahedron*, **1993**, 49, 11065-11133. d) Stewart, J. M.; Young, J. D., *Solid phase in peptide synthesis*, 2nd edition, **1984** (Pierce Chemical Company: Rockford, Illinois). e) Merrifield, R. B., *Science*, **1965**, 150, 178-185. f) Barany, G.; Kneib-Cordonier, N.; Mullen, D. G., *Int. J. Peptide Protein Res*., **1987**, 30, 705-739.

[370] Merrifield, R. B., *J. Am. Chem. Soc*., **1963**, 85, 2149-2154.

[371] Merrifield, R. B., *Angew. Chem. Int. Ed*., **1985**, 24, 799-810.

[372] a) Hourani, R. *et al*, *J. Am. Chem. Soc*., **2011**, 133, 15296-15299. b) Marcucci, E.; Tulla-Puche, J.; Albericio, F., *Org. Lett*., **2012**, 14, 612-615. c) Bayó, N.; Jiménez, J. C.; Rivas, L.; Barany, G.; Albericio, F., *Tettrahedron Lett*., **1993**, 34, 1549-1552.

[373] a) Cherkupally, P. *et al*, *Amino Acids*, **2014**, 46, 1827-1838. b) Yan, L. Z.; Edwards, P.; Flora, D.; Mayer, J. P., *Tetrahedron Lett*., **2004**, 45, 923-925. c) Sabatino, G.; Chelli, M.; Mazzuco, S.; Ginanneschi, M.; Papini, A. M., *Tetrahedron Lett*., **1999**, 40, 809-812.

[374] a) Thieriet, N.; Guibé, F.; Albericio, F., *Org. Lett*., **2000**, 2, 1815-1817. b) Léger, R.; Yen, R.; She, M. W.; Lee, V. J.; Hecker, S. J., *Tetrahedron Lett*., **1998**, 39, 4171-4174.

protecting groups of the amino acids side chains. [375,376] The most common resin is polystyrene in which a proton of the aromatic ring is functionalized. Nowadays, often resins, polyethylene glycol and so on are also used for other different purposes.

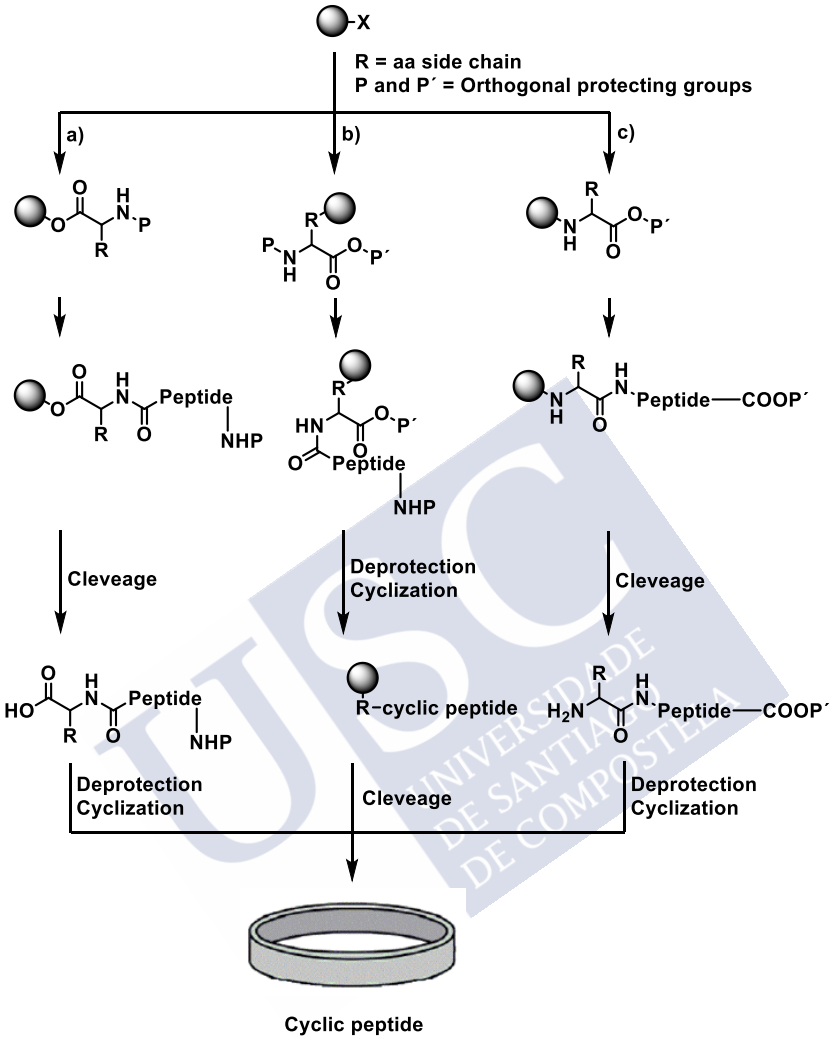

Figure 1.1. *Synthetic strategies for solid phase peptide synthesis. a) Attachment of the first amino acid through the C-terminal extreme, b) attachment through the side chain of the first amino acid, c) attachment through the N-terminal extreme.*

[375] a) Li, P.; Kolaczkowshi, E. K.; Kates, S. A., In *Drug discovery strategies and methods*, **2004**, 175-220 (Makriyannis, A.; Biegel, D.; editors. Marcel Dekker, New York). b) Van Den Nest, W.; Albericio, F., In *Optimization of solid-phase combinatorial synthesis*, **2002**, 91-108 (Yan, B.; Czarnik, A. W.; editors. Marcel Dekker, New York).

[376] a) Isidro-Llobet, A.; Álvarez, M.; Albericio, F., *Chem. Rev*., **2009**, 109, 2455-2504. b) Albericio, F., *Biopolymers*, **2000**, 55, 123-139. c) Greene, T. W.; Wuts, P. G. M., *Protective Groups in Organic Synthesis*, 3rd edition, **1999** (Wiley-Interscience, New York).

Generally, the amino acids are introduced one by one to the sequence, which required that the rest of the functional groups presented in the amino acids of the growing peptide are protected with resistant orthogonal protecting groups. Therefore, in the methods in which the peptide grows through its C-terminal side (Figure 1.1a and b), the reacting amino acid must have protected the amine group. This group should be eliminated in the next step without affecting the protecting groups of peptide side chains. Two main strategies were developed for the preparation of peptides: the Boc/Bzl and the Fmoc/^{t}Bu. In both strategies, the α-amine is protected as a carbamate because it has been probed that this group minimize the epimerization. The Fmoc group (fluorenylmethyloxycarbonyl)[377] is stable to acidic conditions, but it is easily removed by nucleophilic compounds or in basic media through two different mechanisms: β-elimination or nucleophilic attack (Figure 1.2). The most common agent employed in its removal is piperidine. The use of Fmoc as protecting group implies the use of acid labile resins, that are stable to basic conditions. The side chains are typically protected with *tert*-butyl groups, which are also stable to basic medium. In the strategy Boc/Bzl, the amine is protected by the Boc group (*tert*-butoxycarbonyl), which is stable to basic conditions but are labile to acidic environments. TFA (trifluoroacetic acid) is the typical acid used for the deprotection due to its acidity and its ability to keep the resin swelling. TFA allows short reaction times. Moreover, it is not acidic enough to cleavage the peptide from the resin. It is necessary to use a stronger acid, normally HF liquid, although trifluorosulfonic acid and others were also used, to carry out the release of the peptide from the resin. Although protocols for the safe use of hydrogen fluoride have been published, this strategy is every day less employed in conventional laboratories.[378] In this strategy, the side chains are usually protected with benzyl derivatives, although it also can be used the Alloc (allyloxy carbonyl) group, stable to basic and acidic conditions but it can be release with Pd (0) in the presence of a nucleophile.[379]

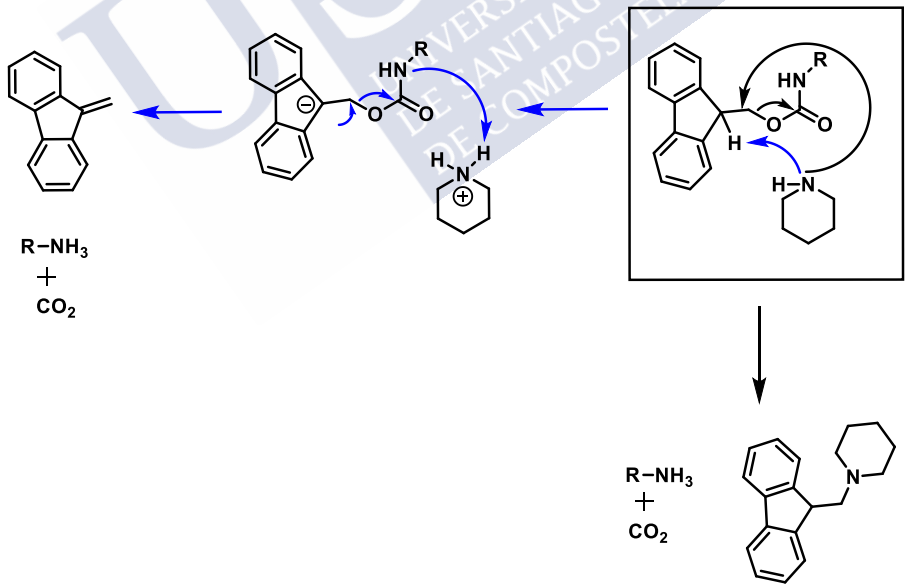

Figure 1.2. *Mechanism of Fmoc removal. Arrows in blue represent the β-elimination mechanism, where the piperidine act as a base. Arrows in black represent the nucleophilic attack of the piperidine.*

[377] Albericio, F.; Tulla-Puche, J.; Kates, S. A., In *Amino Acids, Peptides and Proteins in Organic Chemistry: Building Blocks, Catalysis and Coupling Chemistry* (Vol 3), **2011**, 349-369 (Hughes, A. B., editor. Wiley-VCH Verlag Gmb & Co. KgaA, Weinheim, Germany).
[378] Muttenthaler, M.; Albericio, F.; Dawson, P. E., *Nat. Protoc.*, **2015**, 10, 1067-1083.
[379] Thieriet, N.; Alsina, J.; Giralt, E.; Guibé, F.; Albericio, F., *Tetrahedron Lett.*, **1997**, 38, 7275-7278.

The last step of the synthesis of cyclic peptides is cyclization, which is normally carried out in solution when the peptide is attached to the resin by the C- or N-terminal groups (strategies a and c in Figure 1.1). Oxime resins were developed to allow a final step in which cyclization step is also triggering the peptide release.[380] It is very important to take into account the resin and side chain protecting groups when choosing the conditions for the peptide cleavage. The peptides should have the C-terminal and N-terminal groups deprotected and keep the side chains protected to carry out the cyclization. Once the cyclic peptide is obtained, it is necessary an extra step in order to remove all the blocking groups. However, following the scheme b in Figure 1.1, the cyclization can be carried out while the peptide is still attached to the solid support.

Due to the SPPS is a linear strategy and only one purification step is made, it is necessary to ensure high yields in each peptide bond formation. This represents the most critical point in peptides synthesis. Furthermore, the previous activation of the carboxylic acid is essential to facilitate amide bond formation under mild conditions. This is the reason why, in the last decades, huge efforts have been devoted to the development of new activation methods, both for solution as well as solid phase methods. In this way, the most powerful strategies are based on the *in situ* formation of an active ester intermediate that leads to an easier coupling with the free amine. Among all the different coupling agents developed,[381] it is worth to mention the carbodiimides (EDC, DCC DIC…) and the uranium salts, known as amidinium salts, such as *N*-HATU, *N*-TBTU, *N*-HBTU and so on.[382] It is assumed that all the amidinium process present the same mechanism (Figure 1.3), but are differentiated by the reactivity of the ester intermediate. *N*-HATU is one of the most reactive agents, tolerating the coupling even with secondary amines and/or bulky side chains in good yields.

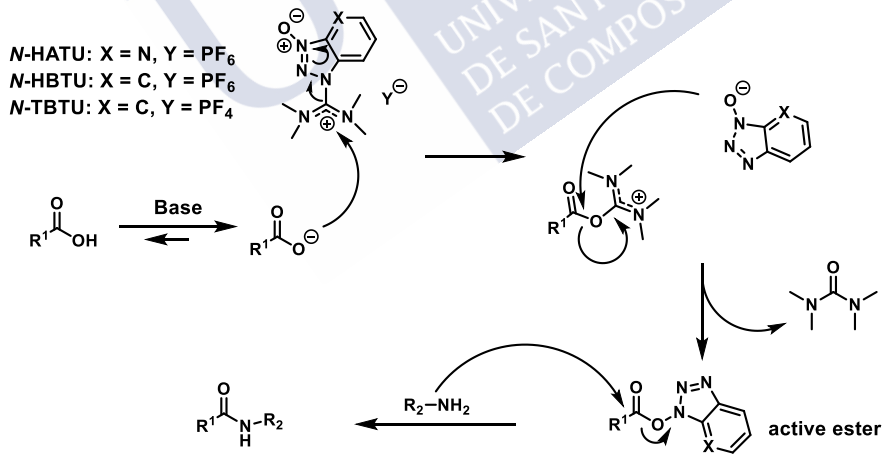

Figure 1.3. *Coupling agents in this thesis for synthesis of peptides and their proposed mechanism of activation.*

[380] Bérubé, C. Borgia, A. Voyer, N., *Org. Biomol. Chem*., **2018**, 16, 9117-9123.
[381] El-Faham, A.; Albericio, F., *Chem. Rev*., **2011**, 111, 6557-6602.
[382] a) Abdelmoty, I.; Albericio, F.; Caprino, L. A.; Foxman, B. M.; Kates, S. A., *Lett. Pept. Sci.*, **1994**, 1, 57-67. b) Bofill, J. M.; Albericio, F.; *J. Chem. Res*., **1996**, 6, 302-303.

The selected coupling agent must produce a high reactive ester in order to carry out the coupling in short period of time and good yields. Sometimes special additives, such as hydroxybenzotriazole (HOBt or HOAt), are combined with a variety of coupling agents in order to improve the yield of the reaction through the formation of their respectively esters. Although the coupling agents reduce or remove the amino acid epimerization, it is worthy to mention that this risk is not fully resolved due to the resulting increase in the acidity of the α-proton of the active ester. These epimerization processes is minimized by the employment of highly hindered bases, such as *N*,*N*-diisopropylethylamine (DIEA).

Despite the use of these excellent coupling agents, it is still necessary to employ a excess of amino acid and coupling agent (3 – 4 equiv) to carry out the coupling step in good yields. This excess of amino acid can lead to an expensive cost to the synthesis of peptides with non-natural amino acids.

1.1. Synthesis and post-modifications of peptide CP-B.[383]*

The synthesis of the peptides was carried out in solid phase, following the Fmoc/^{t}Bu strategy, and the solid support used in the synthesis was a polystyrene functionalized with an amide group (Rink Amide). The cleavage of the peptide from the resin was carried out with TFA. The group selected for the C-terminal group was an allyl ester, which can be selectively removed by treatment with Pd (0). The cyclization was carried out in the solid support as it is shown in the synthetic scheme of Figure 1.1b.

For carrying out our strategy, the non-natural propargylglycine (Pra) was used. To reduce the cost, we always used the natural configuration enantiomer as the Boc-protected derivative, and this determine the chirality of the other residues to keep the alternating chirality of the *D*,*L*-*α*-CPs. The Boc derivative was then transformed into the Fmoc-L-Pra-OH by the treatment with TFA followed by reaction with Fmoc-OSu.

The peptide was prepared following the synthetic strategy summarized in Figure 1.4. Once the resin is swollen, the deprotection of the amide was carried out in 25% piperidine/DMF (15 min). Then, the resin was repeatedly washed with DMF. The *in situ* formation of the active ester was obtained by pre-activating the amino acid (3 equiv) with *N*-HBTU (3 equiv) and DIEA (6 equiv) in DMF, which was added over the resin after mixing for 1 minute. The vessel was shaken for 40 minutes, after which the excess of the reagents was removed by filtration. Finally, the resin was washed with DMF. After each coupling, TNBS test[384] was carried out to determine the efficacy of the reaction. If the test suggests that the reaction was not fully completed (the resin became red), a new coupling step was carried out again, although we only used half number of equivalents of each reagents (1,5 equiv of amino acid and coupling agent, and 3 equiv of DIEA).

To carry out the cyclization, the protecting groups of both extremes must be detached. The allyl group was removed using Pd (0), as catalyst, in presence of a nucleophile. For this purpose

[383] González, E. "Desarrollo de agentes antimicrobianos basados en ciclopéptidos". Trabajo de fin de máster. Universidade de Santiago de Compostela (**2014**).

* **CP-B**, **CP-B-C6**, **CP-B-C10** and **CP-B-C16** were proposed during the master disertation. The activity experiments were carried out after master defense. Thus, we decided to include the most relevant data to a full view of this project.

[384] Kay, C *et al*, *Biotechnol. Bioeng*., **2000**, 71, 110-118.

we used the combination of $Pd(OAc)_2$ and triphenylphosphine to in situ generate the tetrakis(triphenylphosphine)palladium (0), $[Pd(PPh_3)_4]$. After addition of phenylsilane and 4-methylmorpholine, the mixture was transfer to the reaction vessel in which the resin was stored under argon atmosphere. A portion of peptide is cleavage for the resin (3-5 mg) using a TFA/H_2O/TIS (95:2,5:2,5) cocktail and the mixture was study by reverse phase HPLC-MS. If starting material was observed, the process would be repeated it. The N-terminal group was deprotected and the resulting resin was treated with a mixture of *N*-TBTU and DIEA. Again, the progress of the reaction was analysed by HPLC-MS by cleaving a small portion of the resin after 12 h of reaction.

The used of 4-methyltrityl (Mtt) protecting groups in the side chains of the lysine allowed the selective removal under appropriate conditions. The 4-methyltrityl protecting group was removed under soft acidic conditions, such as the mixture of DCM/HFIP/TFE/TIS (0.65:0.2:0.1:0.05).[385] The cocktail is prepared *in situ* before adding to the resin. The mixture is shaking for 6 hours and, once the lysine is deprotected, the Boc-protected aminooxy-acetic acid was coupling with *N*-HATU as activating agent. This deprotection/coupling step was repited 2/3 times until all peptide without alkoxyamine was disappear in the HPLC-MS of the crude mixture.

The cyclic peptide was removed from the resin through the treatment with the TFA cocktail [TFA/H_2O/TIS (95:2,5:2,5)]. Usually, 1 mL of this mixture was used for 50 mg of resin, and the reaction was carried out for 2 hours. Then, the solution was filtered, and added dropwise over cold diethyl ether. The precipitated containing the peptide was centrifuged and decantated. The peptide was purified by HPLC to obtain 20 mg (22% overall yield) of **CP-B**.

[385] Priegue, J. M.; Montenegro, J.; Granja, J. R., *Small*, **2014**, 10, 3613-3618.

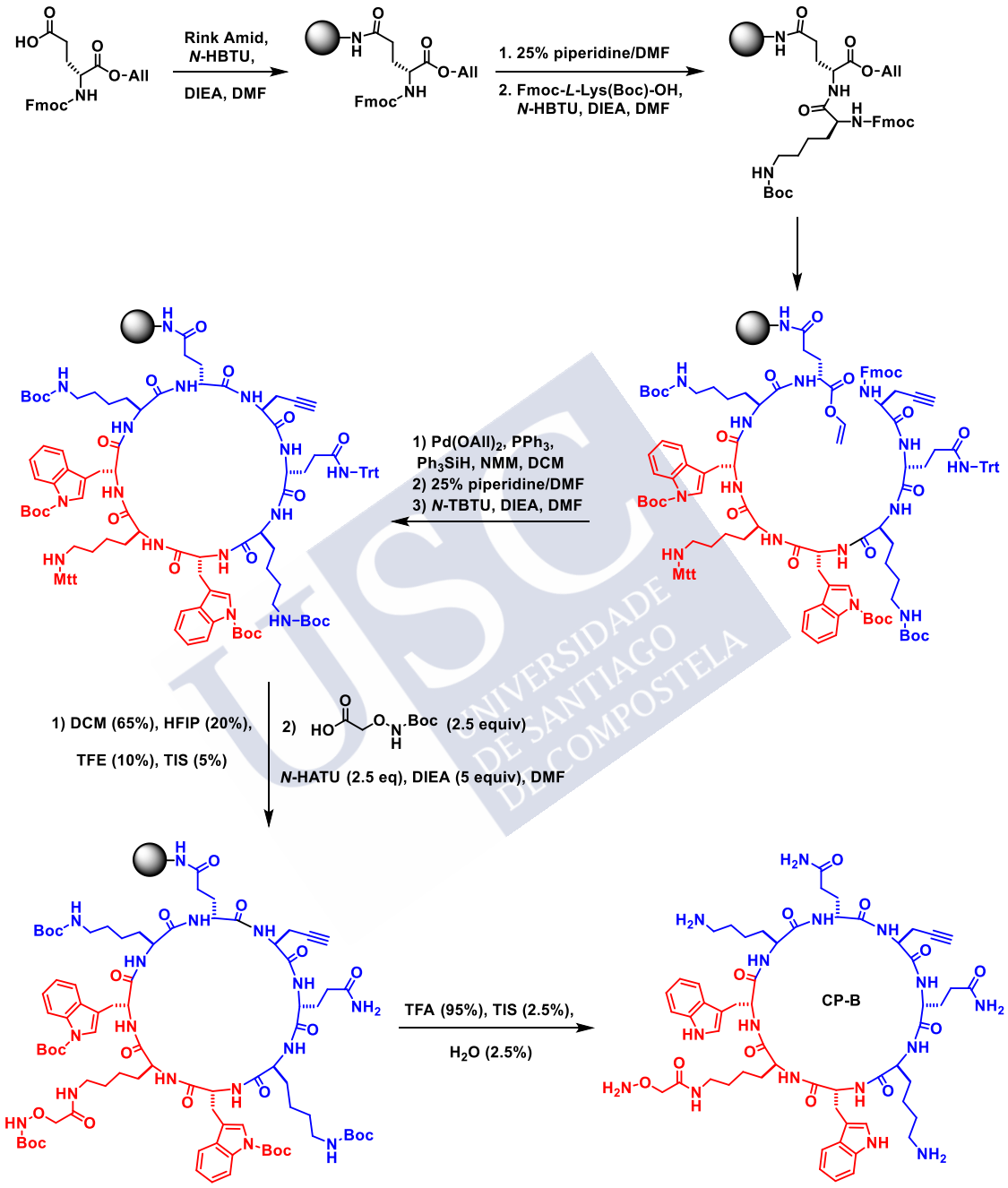

Figure 1.4. *Synthesis of* ***CP-B****.*

The diversification of **CP-B** was carried out with different aldehydes by condensation at 60 ºC with 2 equiv of each carbonyl derivatives in dry DMSO containing a 10% of acetic acid (Figure 1.5). Under this conditions, **CP-B$_6$**, **CP-B$_{10}$** and **CP-B$_{16}$**, in which the number indicates the number of carbons of alkyl chain added to the cyclic peptide, were prepared. Additional **CP-BAc**, obtained by condensation with acetone, was also prepared. This peptide was used as control for some studies.

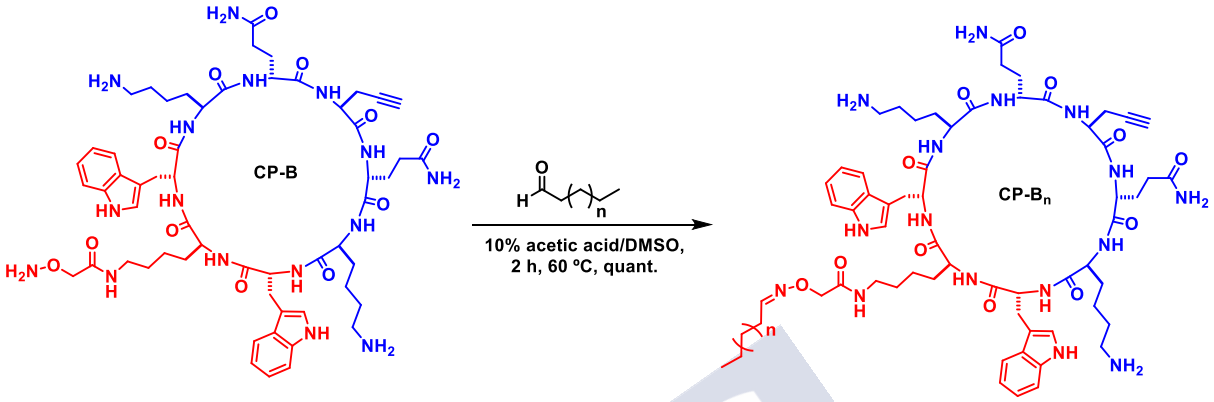

Figure 1.5. *Synthesis of the* ***CP-B$_n$*** *compounds.*

The second CP modification of **CP-B** required the synthesis of saccharide derivatives bearing an azide group. As a proof of concept, we decided to synthesis the *D*-mannose derivative **5** (Figure 1.6). As illustrated in this figure, compound **5** was prepared from *D*-mannose (**1**) in four steps and 17% overall yield following the method described by Hayes et al. [386] Key step in this method is the incorporation of the 3-bromopropan-1-ol in a stereoselective manner using boron trifluoride diethyl etherate under dry and not polar conditions. The substitution of bromide with iodine azide followed by aminolysis of resulting product provided compound **5**.

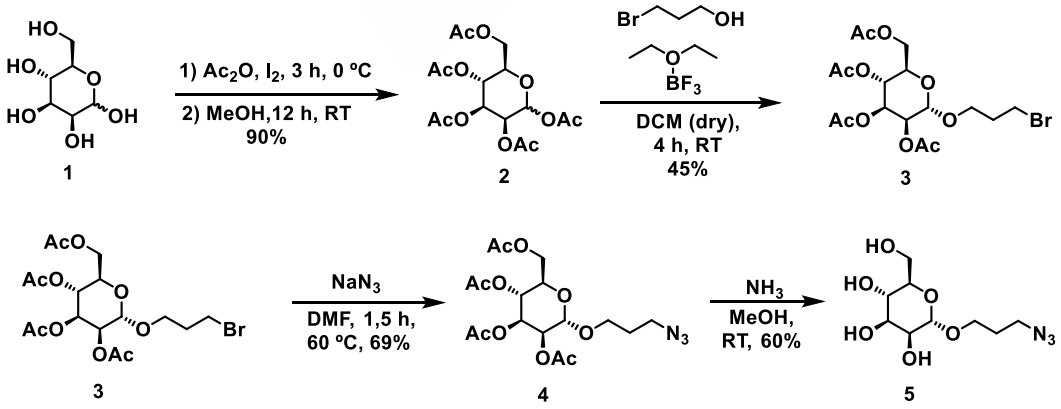

Figure 1.6. *Synthesis of the D-mannose derivative.*

[386] Hayes, W.; Osborn, H. M. I.; Osborne, S. D.; Rastall, R. A. y Romagnoli, B., *Tetrahedron*, **2003**, 59, 7983-7996.

Once the azide derivative was ready, we decide to study the click reaction (see section 1.2.2) with the peptide **CP-B** bearing the aliphatic tails. In the first attempt, we evaluate this reaction with model peptide CP-Bac. e reaction was carried out using a mixture of THF and water (azeotropic 95:5) using standard conditions.[387] After stirring overnight this mixture, the formation of a new product that was identified by MS as the saccharide derivate (**CP-BAc-Man**) was observed. The compound was obtained in 60% yield after HPLC purification.

In order to check if we could carry out both reactions independently of the order, we evaluated the click reaction with the free alkoxyamine group. We started to study the reaction in water. Unfortunately, the TBTA was not soluble. Consequently, no reaction product was observed. The mixture of THF/water used in previous experiments did not afforded the expected product even in the presence of TBTA ligand. We conclude that the free alkoxyamine might interact with the copper precluding the catalysis of the cycloaddition. Therefore, the oxime formation must be carried out before the copper-catalysed alkyne-azide cycloaddition.

Unfortunately, when we carried out the click reaction with the precursor derived from aldehydes (**CP-B$_6$** and **CP-B$_{10}$**) did not provided the expected cycloaddition product. Under these conditions, the starting product was neither isolated. These results were related with the low solubility of the starting materials. This solubility problem seems to be one of the limitations of this method. Moreover, the synthesis of saccharides is more challenging than the describe for *D*-mannose. However, as we had succeeded in synthesizing the peptides **CP-BAc-Man** and **CP-B$_6$**, we decided to test them against *S. aureus*, *S. epidermidis*, *E. faecalis* and *E. coli*. For the positive control we used *c*-[WLWKSKSK] (entry 1, Table 16) as model. We prepared *c*-[QZQKWLWK] (**CP-B-Leu**), where Z is the Pra, to evaluate the lack of activity after substitution of central lysine for a propargylglycine. The chirality of the commercially available Pra force us to prepare the enantiomeric form of *c*-[WLWKSKSK].

Peptide *c*-[KSKWLWLW] (entry 8, Table 10) was also synthesized to optimize the conditions of the bacterial studies. For this synthesis we attached the first residue through the lysine side chain to a chlorotrityl resin, as previously described (Figure 1.7).[388]

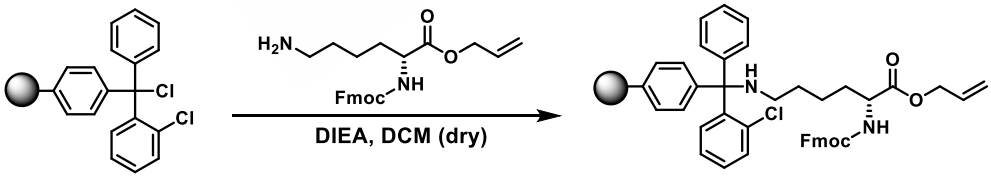

Figure 1.7. *Scheme of the first coupling in chlorotrityl resin.*

[387] Hein, J. E.; Fokin, V. V., *Chem. Soc. Rev*., **2010**, 39, 1302-1315.
[388] a) Barlos, K. *et al*, *Tetrahedron Lett*., **1989**, 30, 3947-3950. b) Barlos, K.; Gatos, D.; Schafer, W., *Angew. Chem. Int. Ed. Engl*., **1991**, 30, 590-593.

For bacteria assays we prepared a stock solution of 1 mg/mL of cyclic peptide in a solution of 9 g/L NaCl in water. The CP final concentration was calculated by UV using a ε of 5690 $M^{-1}cm^{-1}$ for tryptophane.[389] We evaluated the minimal inhibitory concentration against *S. aureus* and *E. coli* in different growth media (broths). Instead of maintaining the standard conditions, the concentration of bacteria was closer to 1 x 10^5 CFU/mL in order to appreciate better the different between peptides and/or modifications in the sequence. Shortly, the peptide was diluted in each well to achieve concentrations of 250 µg/mL, 125 µg/mL…. until 2 µg/mL, keeping the mentioned bacterial concentration (Figure 1.8), and the resulting plates were incubated overnight a 37 ºC. After that, we measure in a plate reader at 492 nm and 620 nm using at exciting light to determine which concentrations of peptides were able to inhibit the growth of the bacteria. The lowest concentration for each peptide was considered the minimal inhibitory concentration (MIC). Initial experiments were carried out using different cell media to evaluate its importance in the antimicrobial activity. The best values were obtained using Mueller-Hilton Broth (MHB) (Table 1.1). So, we selected this broth for the experiments carry out with our peptides. Peptide **CP-B-Leu** is less active than peptide *c*-[WLWKSKSK] (Table 1.1) due to the substitution of a lysine for the propargylglycine, which result in a peptide with less positive charged. To our surprise, **CP-B$_6$** was almost not active: a MIC of 125 µg/mL was observed for *S. epidermidis* and not activity was found for *S. aureus* or *E. coli*. The polarity of the alkoxyamine must interfere in the peptide activity. Even more surprising was the higher activity of **CP-BAc-Man** with MIC of 125 µg/mL against *S. aureus* and 32 µg/mL for *S. epidermidis*. This might suggest that we are also dealing with solubility problems that reduced the activity observed for the derivatives having long alkyl chains.

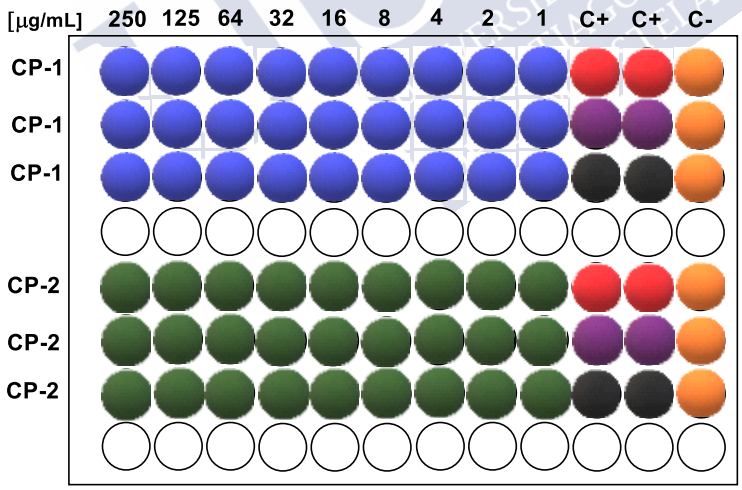

Figure 1.8. *96-well plate for the bacterial assay. The peptides (in general CP-1 and CP-2) diluted with the bacteria are represented in blue and in green. The positive controls (three bacteria without peptide) are represented in red, purple and black. The negative control (only broth) is represented in orange.*

[389] a) Edelhoch, H., *Biochemistry*, **1967**, 6, 1948-1954. b) Gill, S. C.; von Hippel, P. H., *Anal. Biochem.*, **1989**, 182, 319-326.

Code	peptide	MIC (μg/mL)		
		S. aureus	***S. epidermidis***	***E. coli***
entry 8 (t. 10)[297b]	*c*-[KSKWLWLW]	5	---	40
8*	*c*-[KSKWLWLW] (BHI broth)	32	16	250
8*	*c*-[KSKWLWLW] (MHB)	8	---	64
entry 1 (t. 16)[362]	*c*-[WLWKSKSK]	5	---	---
CP-B-Leu	*c*-[QZQKWLWK]	8	4	125
***CP-B*$_6$**	*c*-[QZQKWK^{6}WK]	ND	125	ND
CP-BAc-Man	*c*-[QZ^{Man}QKWK^{Ac}WK]	125	32	ND

ND = not detected, Z = propargylglycine, Ac = acetone, --- = not measured. * = peptide synthesis in our lab.

Table 1.1. *In vitro activity of the peptide series* ***CP-B***.[390]

1.2. Synthesis and post-modifications of peptide CP-A.

After these results we decided to move towards the second target, the **CP-A** derivatives. Those compounds should be more soluble in aqueous media thanks to the reduction of hydrophobic residues. **CP-A** was synthesized follow the same strategy that peptide **CP-B**. However, in **CP-A**, the propargyl group is near the tryptophan, being part of the hydrophobic side. In this way, we expect that the imidazole group resulting from the click chemistry would be less polar. Before introducing the alkoxyamine, we decided to test the platform **A** itself in order to determine if this would be a good candidate for the further development of new peptides. Interestingly, **CP-A** present a MIC of 32 μg/mL against *S. aureus*, representing a promising starting point. Moreover, the peptide was also activite against *S. epidermidis* (MIC = 16 μg/mL) whereas the activity against *E. coli* is low (MIC = 125 μg/mL) (Table 1.2). Considering that the activity against *S. aureus* is quite good for only two hydrophobic amino acids, we decided that platform **A** would be more interesting than **B** for further studies. Furthermore, **CP-A** presented more hydrophilic amino acid than most structures studied until now, leading to a platform that can be diversified in at least three different branches: **CP-A1**, **CP-A2** and **CP-A3** (Figure 1.6). Compare at the relative positions of tryptophan, **CP-A1** present the alkoxyamine at the opposite side of the expected nanotubes. However, the **CP-A2** would provide nanotubes in which the alkoxyamine and, consequently the saccharide, would be pointed forming a 90º angle, whereas **CP-A3** changed the lysine and the serine position to achieve almost 120º degrees with the tryptophan. The activities of the three peptides against the same three bacteria are shown in Table 1.2. The introduction of the alkoxyamine in any of each position clearly reduces. The loss in activity can be correlated with the reduction of positive charges of this CPs due to the reduced basicity of alkoxyamines compared with lysine side chains. This reduction in activity is less pronounced for **CP-A2** than for the other two.

[390] All antibacterial studies were carried out in collaboration with A. J. Perez-Estevez and Prof. Seoane (microbiology department of Medicine, USC).

Code	peptide	MIC (μg/mL)		
		S. aureus	***S. epidermidis***	***E. coli***
CP-A	*c*-[QKSKSWZK]	32	16	125
CP-A1	*c*-[QK^{Ox}SKSWZK]	125 – 64	64 – 32	ND
CP-A2	*c*-[QKSK^{Ox}SWZK]	64 – 32	64 – 32	ND
CP-A3	*c*-[QSK^{Ox}KSWZK]	125	64	ND

Ox = oxime precursor, alkoxyamine. ND = not detected. Z = propargylglycine.

Table 1.2. *Activities of the peptide derivatives from* ***CP-A*** *platform.*

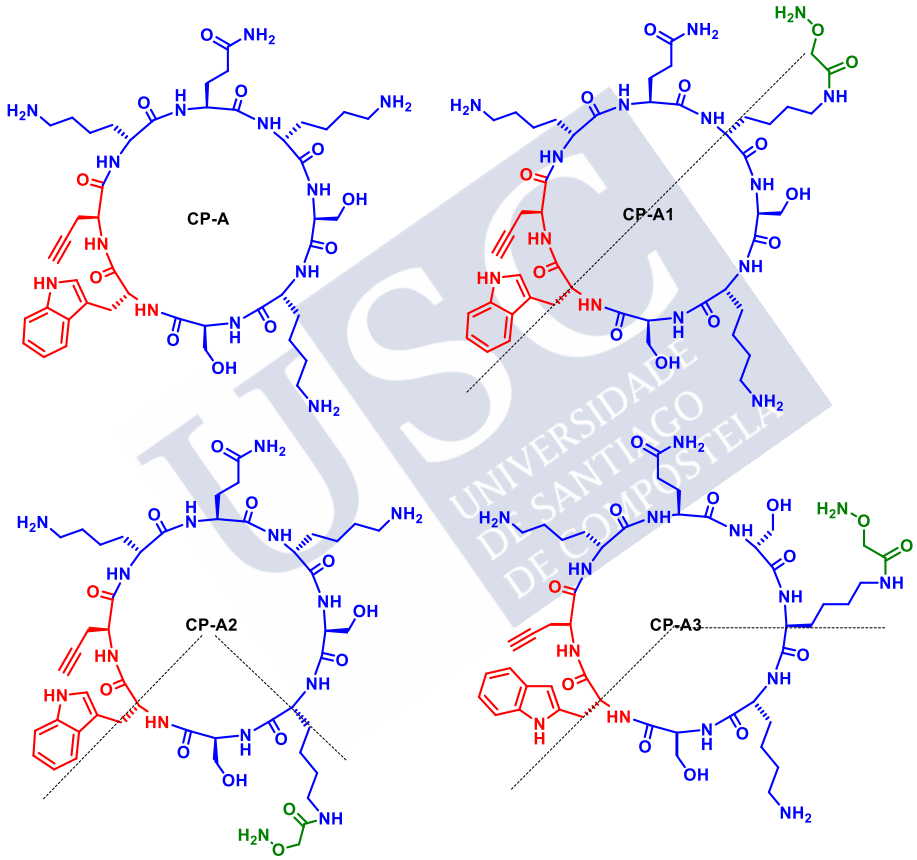

Figure 1.9. *Structural differences between* ***CP-A***, ***CP-A1***, ***CP-A2*** *and* ***CP-A3***.

1.2.1. Incorporation of the saccharide.

In nature, most of the saccharide recognized by different receptors are in the pyranose form, in other words, they are forming a six members ring, instead of the five members ring (furanose) or in an open conformation. One objective of this work is the introduction of these structures in our peptide platform in the same conformation. However, in the reaction between the alkoxyamine with commercial saccharides, it has been proposed to be a mixture of open and cyclic forms (Figure 1.10).[391] It has been described that the *N*-substituted alkoxyamine can lead to the pyranose derivatives (Figure 1.10).[392]

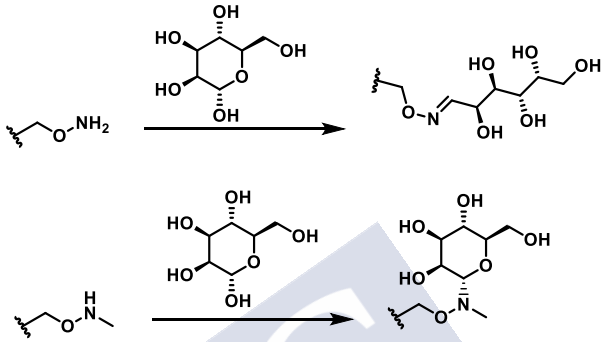

Figure 1.10. *Conformation of the D-mannose with the alkoxyamine and the methyl-alkoxyamine.*

Therefore, we evaluated the use of *N*-methyl alkoxyamines to conjugate with different aldoses to reduce the synthetic effort required for conjugation mediated by carbonyl aldehydes.

The synthesis of the *N*-methyl alkoxyamine is illustrated in Figure 1.11. The direct alkylation of the Boc-protected aminooxyacetic acid with sodium hydride in dry DMF did not provide compound **8**.[393] Thus, we decided to protect the acid, that was carryed out with EDC, HOBt and DMAP in dry MeOH. Now the reaction of compound **7** with MeI and NaH gave compound **8** in a 65% yield. Finally, the hydrolysis of methyl ester with sodium methoxide followed by treatment with amberlite resulted in compound **9** in a 90% yield.

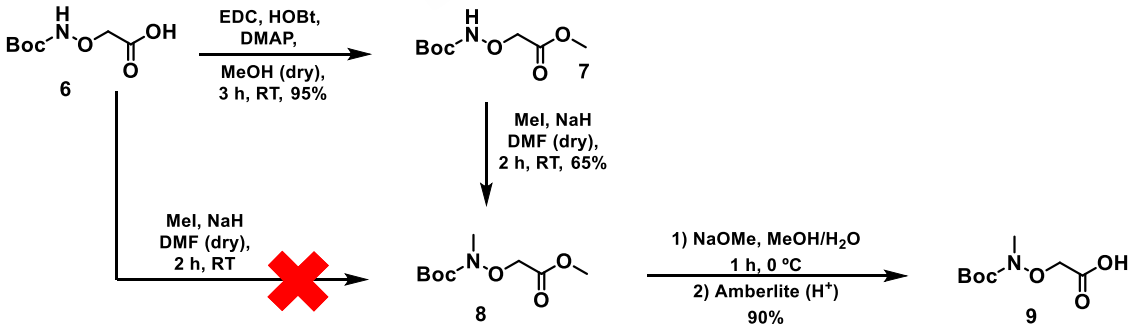

Figure 1.11. *Methyl-alkoxyamine synthesis.*

[391] a) Cervigni, S. E.; Dumy, P.; Mutter, M., *Angew. Chem. Int. Ed. Engl.*, **1996**, 35, 1230-1232. b) Zhao, Y.; Kent, S. B., Chait, B. T., *Proc. Natl. Acad. Sci. U. S. A.*, **1997**, 94, 1629-1633.
[392] Peri, F.; Dumy, P.; Mutter, M., *Tetrahedron*, **1998**, 54, 12269-12278.
[393] Niikura, K. *et al*, *Chem. Eur. J.*, **2005**, 11, 3825-3834.

The condensation of the *N*-methyl alkoxyamine with the saccharide was evaluated with this precursor. The treatment of compound **9** (0.1M) with TFA/DCM (1:1) removed the protecting group to evaluate the condensation with *N*-acetyl-*D*-glucosamine. Unfortunately, the condensation with deprotected derivative of 9 in an ammonium acetate buffer (pH 4.5) in water gave a complex mixture that was not easily to purify or to analyse the formation of the oxime derivative. in water and *N*-acetyl-*D*-glucosamine was added.[394]. So, we decided to prepare a new derivative that contain a UV visible group and at the same time is less polar. Therefore, compound **12** was prepared (Figure 1.12). This compound was prepared by condensation of the fluorenyl ester of alanine (**11**) with **9** using *N*-HBTU as coupling agent. The treatment of compound **12a** with TFA provided **12b**. Condensation of **12b** with *N*-acetyl-*D*-glucosamine in the ammonium acetate buffer (pH 4.5) did provide only a 10% of the expected product (**13**).

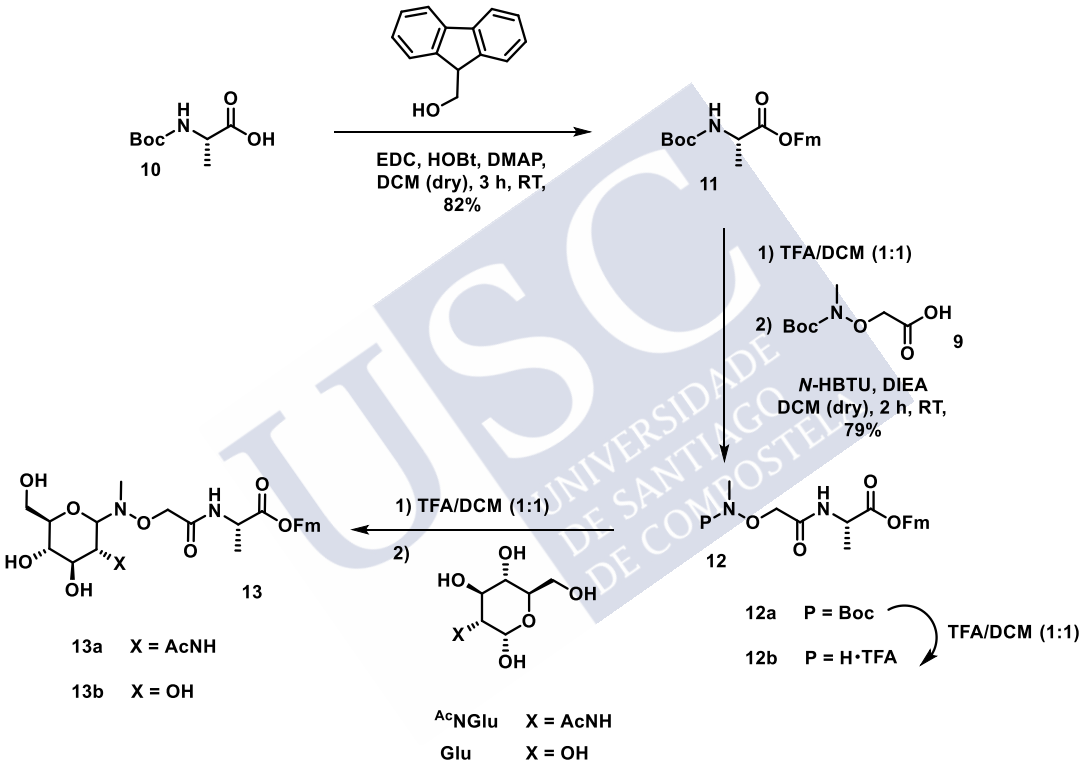

Figure 1.12. *Synthesis of compound **13**.*

The optimization of this conditions was afforded changing solvent, concentration of buffer or substrate as is illustrated in Table 1.3. [395] The aniline has been proposed to catalyse this type of reactions.[396] Therefore, this was also evaluated. The use of sodium acetate immediately provided the product formation, although in low yield (entry 2, Table 1.3). Similar results were

[394] Gudmundsdottir, A. V.; Paul, C. E.; Nitz, M., *Carbohydrate Research*, **2009**, 344, 278-284.
[395] a) Munneke, S.; Prevost, J. R. C.; Painter, G. F.; Stocker, B. L.; Timmer, M. S. M., *Org. Lett.*, **2015**, 17, 624-627. b) Wen, H. Y.; Hsu, P. H.; Chen, G. S.; Fang, J. M., *RSC adv.*, **2013**, 3, 9530-9533. c) Dasgupta, S.; Nitz, M., *J. Org. Chem.*, **2011**, 76, 1918-1921.
[396] Loskot, S. A.; Zhang, J.; Langenhan, J. M., *J. Org. Chem.*, **2013**, 78, 23, 12189-12193.

obtained with glucose. Those condensations were carried out at 60 ºC and the HPLC-MS analysis provided chromatograms that shown the formation of the products upon incrementing temperature and reaction time. The low yield and the reduce solubility of compound **12** lead us to look for more stable and soluble *N*-methyl alkoxyamine derivative. Consequently, compound **15** was prepared as is illustrated in Figure 1.13. The reaction of this compound (**15**) with glucose after addition of ammonium acetate buffer provided the compound **16** in similar yields.

Exp	12b/15	saccharide	equiv	buffer	t	T[a]	ref	%conv.
1	**12b** (0.5 M)	*N*AcGlc (0.75 M)	0.83	NH_4OAc (2 M, pH 4.5)	72 h	RT	392	0%
2	**12b** (10 M)	*N*AcGlc (0.75 M)	0.9	$NaOAc/H_2O$ (1 M)	20 h	40 ºC	395c	20% – 30%
3	**12b** (0.02 M)	*N*AcGlc (0.017 M)	0.83	NH_4OAc (0.1 M, pH 4.5), 20% MeOH, aniline (0.1 M)	12 h	60 ºC	395b	20%
4	**12b** (1 M)	*D*-Glc (0.75 M)	0.9	$NaOAc/H_2O$ (1 M)	72 h	60 ºC	395c	30%
5	**12b** (0.014 M)	*D*-Glc (0.017 M)	0.83	NH_4OAc (0.1 M, pH 4.5), 20% MeOH, aniline (0.1 M)	24 h	60 ºC	395b	10%
6	**15** (0.07 M)	*D*-Glc (0.35 M)	5	$NaOAc/H_2O$ (0.1 M)	20 h	40 ºC		60%
7	**15** (0.05 M)	*D*-Glc (0.25 M)	5	NH_4OAc (0.1 M, pH 4.5), 20% MeOH, aniline (0.1 M)	12 h	40 ºC		60%

Table 1.3. *Reaction conditions tested for the saccharide-oxime bond formation.*

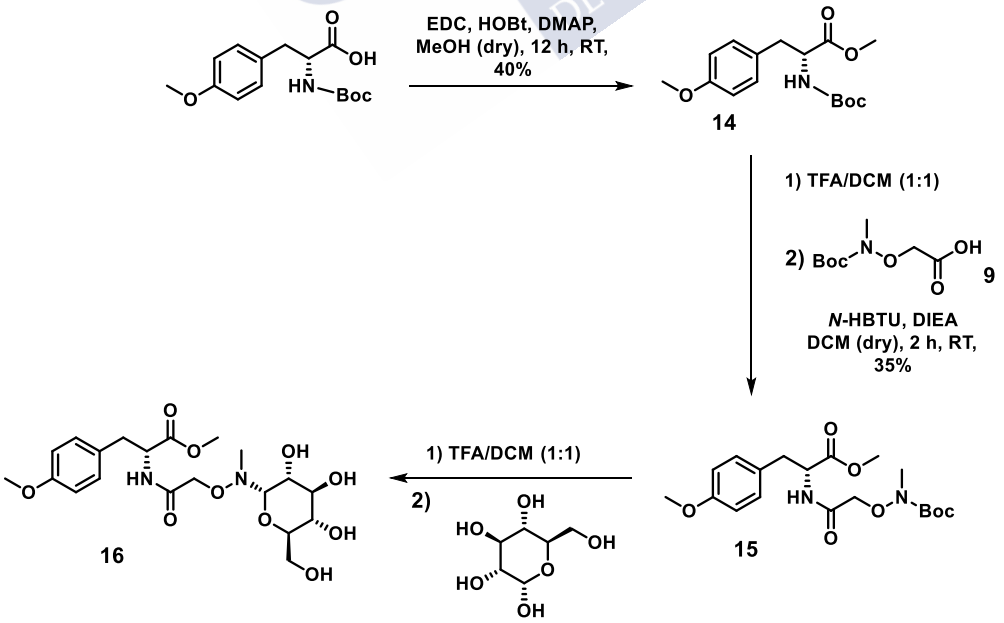

Figure 1.13. *Strategy for the synthesis of compound **16**.*

The peptide **CP-A1^{Me}** was prepared in solid phase following the same scheme than **CP-A1**. This compound was subjected under similar conditions to the previous optimized with the *N*-methyl alkoxyamine model. Under these conditions, the HPLC-MS analysis of the mixture provided a broad peak where MS corresponded with the reaction product and starting material. This mixture could not be separated by HPLC. Therefore, additional saccharide was added, and the reaction mixture was stirred for 72 h. Unfortunately, under these conditions, we were not be able to improve the conversion yields. The change of the saccharide no increase the yield neither.

After the adversity of carry out the reaction with the methyl-alkoxyamine, we thought in the possibility of use the alkoxyamine with glycosides bearing the according moiety, such as **17** (Figure 1.14). Compound **17** was prepared in the lab by Marisa Juanes to develop new protein transmembrane transports, and later optimized by Dr. Jose J. Reina and A. Rioboo.[397] Cyclic peptide **CP-A1** was mixed with 10 equivalents of *D*-mannose derivative **17** in 5% acetic acid/water at room temperature for 15 minutes to provided compound **CP-A1-17** in quantitative yield (Figure 1.14). Cyclic peptide **CP-A1** was also condensed with D-mannose to provide the mixture CP-A1-Man that, most probably, is a mixture of isomers of the open and closed oxime forms. The activity analysis of both compounds (Table 1.4) showed that the saccharide has a big impact in the CP activities, with a quite important reduction for any of the saccharide derivatives. The cyclic peptide **CP-A1-17** present less activity against *S. aureus* than the open saccharide. However, the opposite was observed in *S. epidermidis*, where **CP-A1-Man** is less active than **CP-A1-17**.

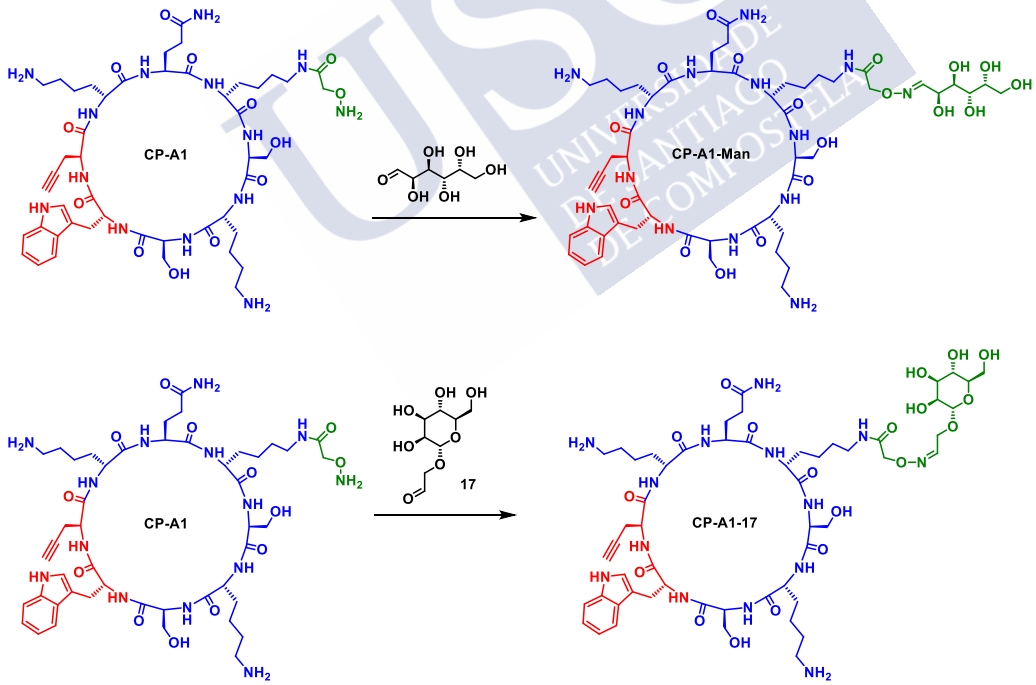

Figure 1.14. *Reaction between* ***CP-A1*** *with D-mannose and with compound* ***17****.*

[397] a) Juanes, M.; Lostalé-Seijo, I.; Granja, J. R.; Montenegro, J., *Chem. Eur. J.*, **2018**, 24, 10689-10698. b) Reina, J. J.; Rioboo, A.; Montenegro, J., *Synthesis*, **2018**, 50, 831-845.
[409] Motiei, L.; Rahimipour, S.; Thayer, D. A.; Wong, C. H.; Ghadiri, M. R., *Chem. Commun.*, **2009**, 3693-3695.

Code	peptide	MIC (μg/mL)		
		S. aureus	***S. epidermidis***	***E. coli***
CP-A1	*c*-[QK^{Ox}SKSWZK]	125 – 64	64 – 32	ND
CP-A1-17	*c*-[QK^{17}SKSWZK]	ND	125	ND
CP-A1-Man	*c*-[QK^{Man}SKSWZK]	250	250 – 125	ND

Ox = oxime precursor, alkoxyamine. ND = not detected. Z = propargylglycine.

Table 1.4. *Activities of the peptide* ***CP-A1*** *with saccharide derivatives.*

These results pront us to prepare new derivatives by condensing **CP-A1**, **CP-A2** and **CP-A3** with commercial saccharide (*D*-mannose, *N*-acetyl-*D*-glucosamine) to form the corresponding hybrids (**CP-A1-NAcGlc**, **CP-A1-Man**…) as a mixture of isomers in the open and closed form. The activity of these compounds was also analysed against the same three bacteria strains. In Table 1.5 are shown the most relevant results. No activity was observed with derivatives conjugated with *N*AcGlc. The best results were observed with the D-mannose derivatives, especially for **CP-A2**.

Code	peptide	MIC (μg/mL)		
		S. aureus	***S. epidermidis***	***E. coli***
CP-A1	*c*-[QK^{Ox}SKSWZK]	125 – 64	64 – 32	ND
CP-A1-NAcGlc	*c*-[QK^{NAcGlc}SKSWZK]	ND	250 – 125	ND
CP-A1-Man	*c*-[QK^{Man}SKSWZK]	250	250 – 125	ND
CP-A2	*c*-[QKSK^{Ox}SWZK]	125	64	ND
CP-A2-NAcGlc	*c*-[QKSK^{NAcGlc}SWZK]	ND	250	ND
CP-A2-Man	*c*-[QKSK^{Man}SWZK]	250	**125**	ND
CP-A3	*c*-[QSK^{Ox}KSWZK]	125	64	ND
CP-A3-NAcGlc	*c*-[QSK^{NAcGlc}KSWZK]	ND	250	ND
CP-A3-Man	*c*-[QSK^{Man}KSWZK]	250	125 – 64	ND

Ox = oxime precursor, alkoxyamine. ND = not detected. Z = propargylglycine.

Table 1.5. *Activities of the cyclic peptides modified with D-mannose and N-acetylglucosamine in different positions.*

The results were not very relevant because of the lack of alkyl chain and reduce hydrophobic core. However, they encourage us to continuing our studies. The next step was the introduction of the hydrophobic tail by the [3+2] cycloaddition reaction catalysed by Cu (I). To prioritize the work to be done, we decide to leave **CP-A3** in the background and continue the development of peptides **CP-A1** and **CP-A2**.

1.2.2. Incorporation of the aliphatic tail.

The most used "click" reaction is by far the Cu^{I}-catalyzed azide/alkyne cycloaddition (CuAAC).[398] The non-catalyzed azide/alkyne reaction has been known since 1893, when the first synthesis of 1,2,3-triazoles from diethyl acetylenedicarboxylate and phenyl azide was reported.[399] The reaction is known as Huisgen reaction and produces a mixture of 1,4 and 1,5-disubstitution products.[400] Instead, the CuAAC reaction of terminal alkynes is completely regioselective to form the 1,4-disubstituted triazoles. The reaction is catalysed by a variety of Cu^{I} catalysts.[401] The 1,5-disubstituted triazole isomer was also reported upon catalysis by ruthenium cyclopentadienyl complexes (RuAAC reaction).[402] The great success of the CuAAC is rooted by the fact that it is a virtually quantitative, very robust, very general, and orthogonal ligation reaction, suitable even for biomolecular ligation[403] in vivo tagging.[404] The triazole formed is essentially chemically inert to other reactive conditions, e. g. oxidation, reduction, and hydrolysis.[405]

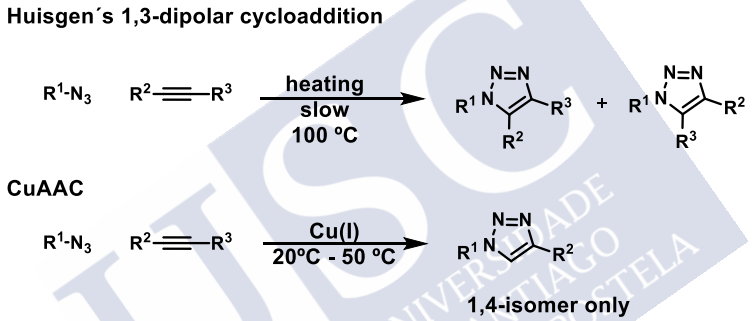

Figure 1.15. *Products of click chemistry reaction with and without catalysts.*[398a]

The first attempt to explain the mechanism suggest that only one atom of copper was involved in the formation of the imidazole ring. However, each C-C-triple bond coordinates three Cu-atoms in more than 90% of all crystal structures of Cu^{I}-alkyne complexes in the Cambridge Crystal Database.[398b] Azides, on the other hand, coordinate Cu^{I} in two different ways. Most common is the end-on coordination, in which the terminal azide nitrogen is coordinated to the central Cu atom with an 180º bond angle. The second coordination option is carried by the substituted imine nitrogen, with an 120º bond angle. In Figure 1.16, it is outlining the proposed reaction mechanism. Except for decomposition due to substrate instability, the

[398] a) Liang, L.; Astruc, D., *Coord. Chem. Rev*., **2011**, 255, 2933-2945. b) Meldal, M.; Tornøe, C. W., *Chem. Rev*., **2008**, 108, 2952-3015.
[399] Michael, A., *J. Prakt. Chem*., **1893**, 48, 94-95.
[400] Huisgen, R., *Angew. Chem. Int. Ed*., **1963**, 2, 565-598.
[401] a) Rostovtsev, V. V.; Green, L. G.; Fokin, V. V.; Sharpless, K. B., *Angew. Chem. Int. Ed*., **2002**, 41, 2596-2599. b) Tornøe, C. W.; Christensen, C.; Meldal, M., *J. Org. Chem*., **2002**, 67, 3057-3064.
[402] Zhang, L. *et al*, *J. Am. Chem. Soc*., **2005**, 127, 15998-15999.
[403] Speers, A. E.; Adam, G. C.; Cravatt, B. F., *J. Am. Chem. Soc*., **2003**, 125, 4686-4687.
[404] a) Beatty, K. E.; Xie, F.; Wang, Q.; Tirrell, D. A.; *J. Am. Chem. Soc*., **2005**, 127, 14150-14151. b) Dieters, A.; Schultz, P. G., *Bioorg. Med. Chem. Lett*., **2005**, 15, 1521-1524.
[405] Wu, P.; Fokin, V. V., *Aldrich Chim. Acta*, **2007**, 40, 7-17.

triazole-formation is essentially insensitive to steric bulk and electronic properties of the alkyne and azide, although the rates may differ, and reaction conditions may have to be optimized.

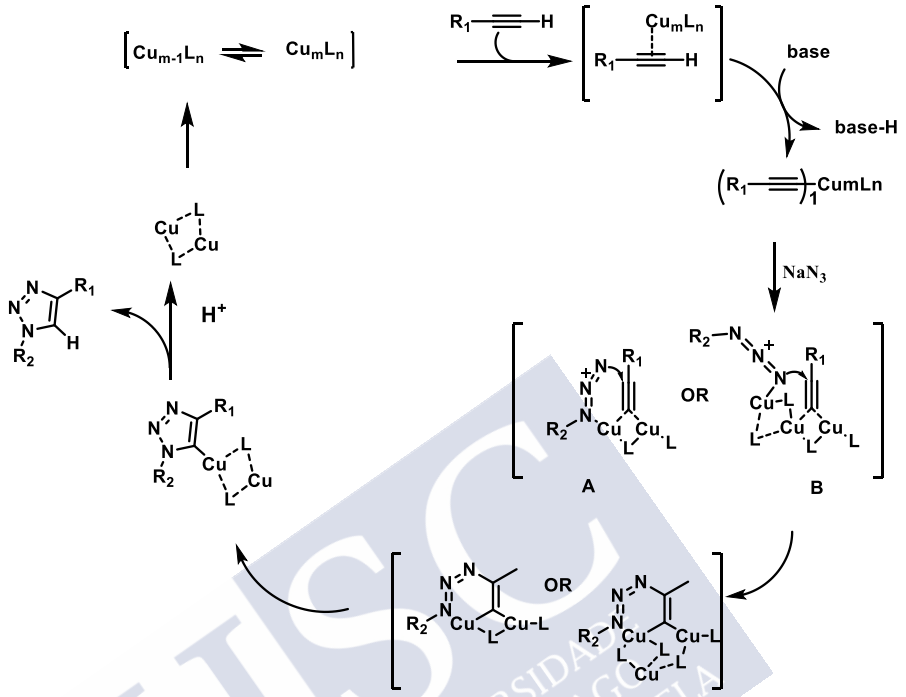

Figure 1.16. *Outline the pausible mechanism for the CuAAC reaction.*[398a]

Although the reaction is carried out with Cu^{I}, salts of Cu^{II} (usually $CuSO_4$) are commonly used because of their stability. In this case, a reducing agent, as sodium ascorbate, is also added to the reaction mixture. A base or an amine ligand can be used to avoid the aerobic oxidation to Cu^{II}. Although the reaction admits a high variety of solvents, the most common conditions are $CuSO_4$ and sodium ascorbate (10 equiv) in aqueous solvent such as water and an alcohol (t-BuOH, MeOH, or EtOH) in order to solubilize the substrate. The CuAAC reaction rate is low at room temperature, so ligands are usually added to enhance it. Tris(triazolyl)methyl amine ligands, such as TBTA or TTTA, provide faster reaction rates than pyridines.[398a]

The first step to carry out the reaction is to incorporate the reacting functional groups, i. e. the alkyne and the azide in both building blocks. In our case, the triple bond is introduced in the cyclic peptide using a propargylglycine amino acid, as we described before. There is not commercially available alkyl azides, so we have to prepare them from the corresponding aliphatic bromide. 1-Bromohexane was used to optimize the reaction conditions (Figure 1.17). As it is summarized in the Table 1.6, the reaction was studied under different mixture of solvents.[406] The best conditions were obtained in DMF, but the high boiling point of this solvent preclude to isolate the final product in high yields.

[406] a) Mamidyala, S. K.; Cooper, M. A., *Chem. Commun.*, **2013**, 49, 8407-8409. b) Nulwala, H. B. *et al*, *Green Chem.*, **2011**, 13, 3345-3349.

We changed the substrate to 1-bromodecane, that under the same conditions, provided the corresponding azide in quantitative yield. The reaction was optimized to be carried out at room temperature and only one equivalent of sodium azide. Again, isolation of the azide was not successful in high yields.

Figure 1.17. *Synthesis of 1-azidohexane in DMF.*

Exp	[C]	compound	Equiv NaN_3	solvent	t	T[a]	ref	%conv.
1	0.5 M	1-bromohexane	10	THF/H_2O (1:1)	3 h	80 ºC	406a	ND
2	0.5 M	1-bromohexane	10	EtOH/H_2O (1:1)	24 h	70 ºC		ND
3	1 M	1-bromohexane	3	DMF	24 h	RT	406b	ND
4	0.5 M	1-bromodecane	10	EtOH/H_2O (1:1)	24 h	70 ºC		0%
5	1 M	1-bromodecane	3	DMF	24 h	RT	406b	100%
6	0.5M	1-bromodecane	1	DMF	24 h	40 ºC		100%

ND = not determined

Table 1.6. *Conditions of the azide synthesis.*

In general, organic azides are more reative than the azide salt used in their preparation. Therefore, we considered that the alkyl azide does not require any purification step.[398b] So, to carry out the CuAAC reaction, we prepared the equivalents of alkyl azide necessary to carry out the next transformation. The click reaction was study with **CP-A1** derivative in which the free alkoxyamine was blocked with acetone (**CP-A1Ac**). Unfortunately, the reaction of this compound with the unpurified 1-azidodecane in a mixture of DMSO/H_2O (1:1) using standard conditions ($CuSO_4$, sodium ascorbate and TBTA) did not provided the expected product. No product was obtained using stoichiometric amount of Cu (I) or excess.

The main limitation was the different solubility of starting materials in the aqueous conditions. Recent studies have shown that the CuAAC can be carried out in the solid support.[398b] This transformation under these conditions would simplify the problem of solubility and isolation. The solid phase synthesis allows the use of different solvents and mixtures, and, all the reagents used in excess can be filtered off after the reaction takes place. It is worth to mentioned that in the solid support, the alkoxyamine is protected with the Boc group, so it is unlikely that it can interfered in the reaction. In addition, the aggregation of the peptide can be limited under these conditions.

Consequently, the optimization of CuAAC on the solid support was carried out. The resume of these studies is presented in Table 1.7. We started with conditions optimized in solution (exp. 1, Table 1.7), but the conversion was estimated around 60%. Substitution of piperidine for 2,6-lutidine reduced the conversion. The use of larger excess of alkylazide (6 equiv), sodium ascorbate (10 equiv) and reaction times provided the expected product **CP-A1$_{10}$** in quantitative yields. We also determined the best order of the two reaction, the acylation and the cycloaddition. Interestingly, both reactions can be carried out independently without affecting the cyclic peptide conversion. However, we decided to carry out always the click transformation at the end of the process for the rest of this work (Figure 1.18).

Exp	equiv				solvent	t	T[a]	%conv.
	$C_{10}H_{21}N_3$	CuI	sodium ascorbate	DIEA				
1	3	5	5	10	20%piper./DMF	5 h	RT	60%
2	3	5	5	---	20%piper./DMF	5 h	RT	50%
3	3	5	5	10	30% 2,6 lutidine/DMF	17 h	RT	0%
4	3	5	5	10	20%piper./DMF	12 h	RT	60%-70%
5	6	5	5	10	20%piper./DMF	12 h	RT	80%
6	6	5	10	10	20%piper./DMF	36 h	RT	100%

Table 1.7. *Optimization of the CuAAC reaction with the cyclic peptide in the solid support.*

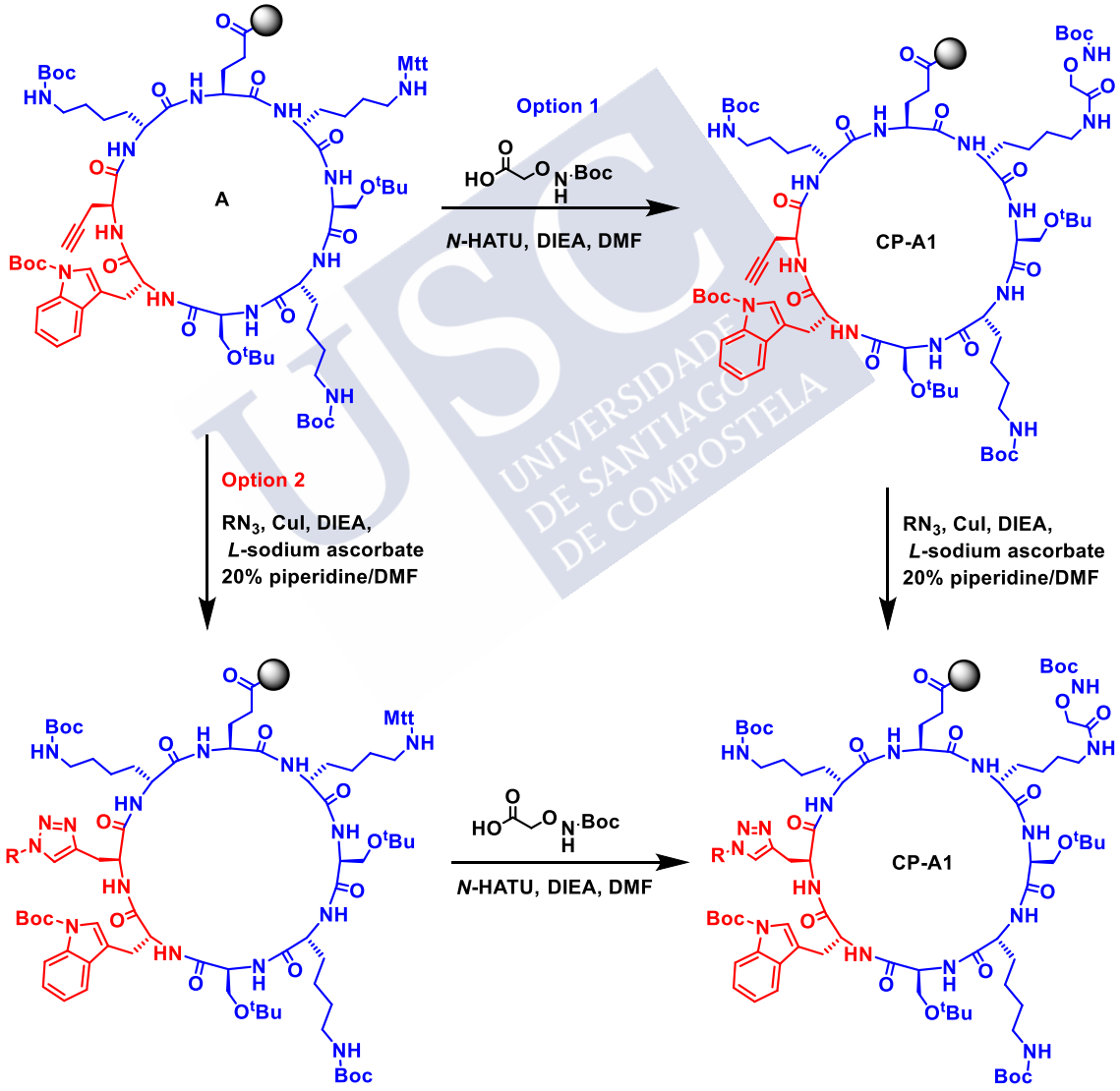

Figure 1.18. *Both options of synthesis. Option 1: introduction of the alkoxyamine follow by the introduction of the aliphatic tail. Option 2: introduction of the aliphatic tail follow by the introduction of the alkoxyamine.*

1.3. Self-assembly in lipid bilayers: cyclic peptide nanotube/membrane interaction.

Biophysical studies with model membranes have been widely used to characterize antimicrobial peptides/membrane interactions,[407] and various models have been proposed thereafter.[408] Different mechanisms have been proposed for the same peptide, depending on the specific techniques and experimental conditions used to study them.[409] Although there has been advances in the application of atomic-resolution structural techniques (X-ray and neutron diffraction and NMR spectroscopy), the structure determination of peptides, proteins and other molecules in membranes is still a challenge. At this regard, Molecular Dynamics (MD) simulations may provide a useful tool to understand the interaction between membranes/antimicrobials. The MD approach has been widely used in this area, providing very useful insight of AMPs action,[410] their effects and their location at the membrane.[411] Our group is collaborating with Prof. Bastos (CIQUP, Universidade do Porto, Portugal) to carry out studies combining the physical protocols with MD. In their studies they have compared **CP-A** comparing with peptide RRKWLWLW (entry 14, Table 10, **CP-14**).[412] In Porto, they carried out differential scanning calorimeter (DSC), dynamic light scattering (DLS) and attenuated total reflection Fourier transform infrared spectroscopy (ATR-FTIR) combining with coarse-grained molecular dynamic simulations.

Differential Scanning Calorimetry (DSC) experiments were carried out in pure DMPG, which confirmed the interaction of the two peptides with the membrane.[413] The results demonstrated that there is a strong peptide/lipid interaction, similar to those previous observed with other peptides in the same phospholipid membrane and also with mixture of this phospholipids with DMPE.[414] DSC shows that both peptides interact with negatively charged membranes, although some differences were found in the degree of interaction, with **CP-14** having stronger interaction than **CP-A**. For example, **CP-14** was able to segregate the two lipid components in the DMPE:DMPG (1:9) membranes, whereas **CP-A** is only able to segregate the two lipids in membranes enriched on DMPE.

The results obtained for DMPC are very interesting, due to DMPC has been used as a crude model for eukaryotic membranes. The studies carried out in Porto found excellent agreement between the DSC results and toxicity test.[415] It could be observed by DSC that **CP-14** interacts with DMPC, whereas **CP-A** does not.

The ATR-FTIR experiments were performed to obtain information on the possible self-assembly of the peptides at the mebrane, as well as their relative position to the membrane plane. Initially, they studied the peptides with DMPC membranes because these membranes were used by Ghadiri´s group in their initial work with this type of peptides.[332a] The results are

[407] a) Reuter, M.; Schwieger, C.; Meister, A.; Karlsson, G.; Blume, A., *Biophys. Chem*., **2009**, 144, 27-37. b) Silva, T. *et al*, *Langmuir*, **2018**, 34, 2158-2170. c) Bastos, M. *et al*, *Biophys. J*.; **2011**, 101, L20-22.
[408] Teixeira, V., Feio, M. J.; Bastos, M., *Progress in Lipid Research*, **2012**, 51, 149-177.
[409] Sevcsik, E.; Pabst, G.; Jilek, A.; Lohner, K., *Biochimica et biophysica acta*, **2007**, 1768, 2586-2595.
[410] Mika, J. T. *et al*, *Biochim. Biophys. Acta*, **2011**, 1808, 2197-2205.
[411] a) Boags, A.; Hsu, P. C.; Samsudin, F.; Bond, P. J.; Khalid, S., *The Journal of physical chemistry letters*, **2017**, 8, 2513-2518. b) Parkin, J.; Chavent, M.; Khalid, S., *Biophysical journal*, **2015**, 109, 461-468.
[412] Manuscript in preparation in collaboration with Claro, B.; Bessa, L.; Goormatight, E. and Bastos, M.
[413] Data not shown due to these experiments corresponds with Barbara Claro´s Ph.D.
[414] Abrunhosa, F. *et al*, *J. Phys. Chem. B*, **2005**, 109, 17311-17319.
[415] Silva, T. *et al*, *Biomembranes*, **2013**, 1828, 1329-1339.

represented in Figure 1.19, in which different ratios between CP and phospholipids were studied. The spectrum of **CP-C14** showed the characteristic feature of an antiparallel *β*-sheet structure.[332a] On the other hand, **CP-A** spectra had a ~ 1688 cm^{-1} band very strong and broad, suggesting that a significant fraction of the structure does not adopt a typical extended *β*-sheet structure, and 'turns' (these can contribute in the 1680 cm^{-1} region)[416] or other non-periodic structures are probably also present. All in all, **CP-A** form some *β*-sheet structure at the lipid surface, but with much less defined orientation with respect to the bilayer.

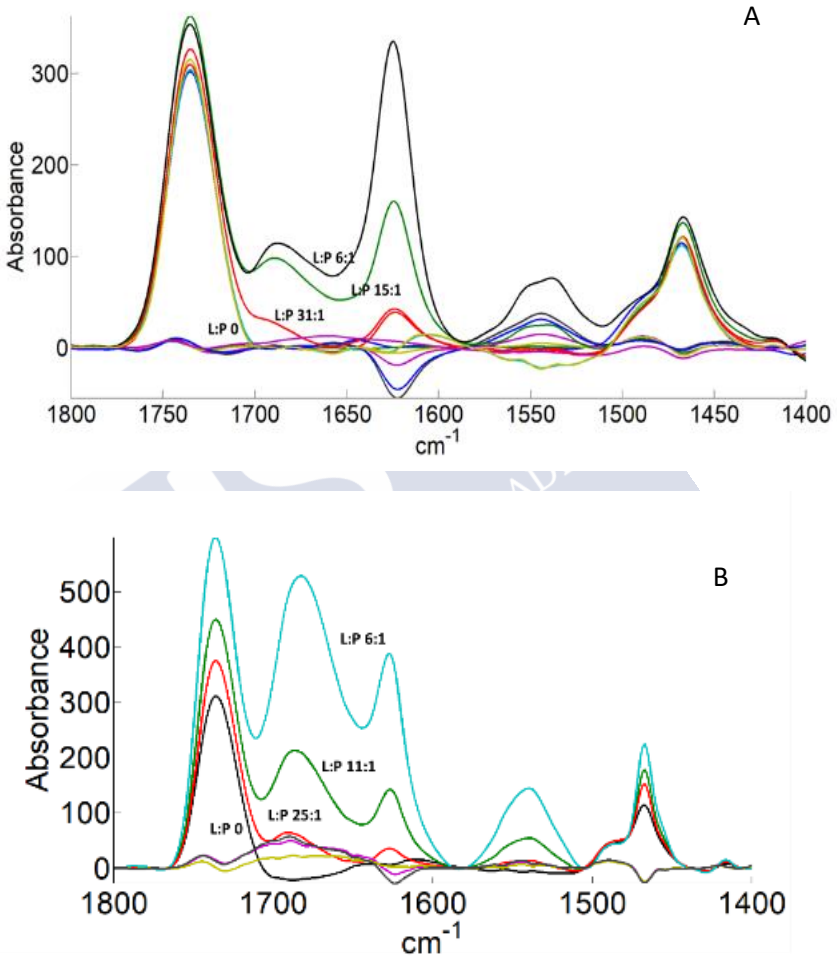

Figure 1.19. *ATR-FTIR results for DMPC and its mixtures with* ***CP-14*** *(A) and* ***CP-A*** *(B). The used molar ratios are shown in each curve (lipid:peptide, L:P). The dichroic spectra when polarizers were used at right angles (difference between the parallel and perpendicular spectra) for the various ratios are also shown, as the negative peaks at 1630* cm^{-1}.

[416] Tamm, L. K.; Tatulian, S. A., *Quarterly reviews of biophysics*, **1997**, 30, 365-429.

Negatively charged (DMPG) and mixed of DMPE:DMPG were also studied by ATR-FTIR. The spectra show that both peptides form a β-sheet structure (Figure 1.20). The band at ~1688 cm^{-1} for **CP-A** [except for the DMPE:DMPG (1:9) system], is stronger than the band at 1630 cm^{-1}. However, even in those cases, the area of the amide II band is more intense than the amide I that suggest parallel nanotubes to the membrane surface.

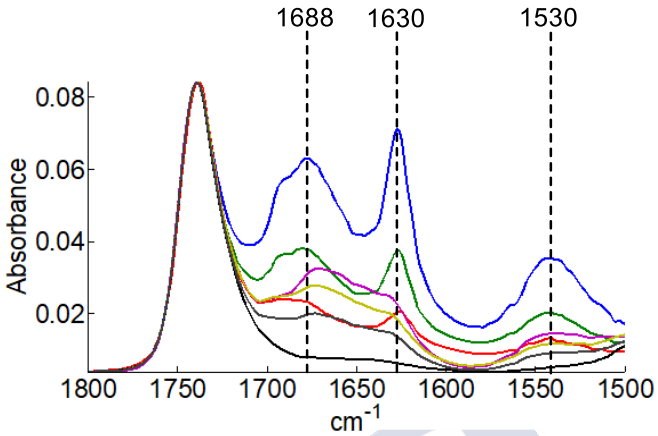

Figure 1.20. *ATR-FTIR results for DMPE:DMPG (1:9) and its mixtures with* ***CP-14*** *and* ***CP-A*** *at different lipid:peptide (L:P) molar ratios. Black, pure DMPE:DMPG (1:9);* ***CP-14****: grey, L:P = 46:1; yellow, L:P = 34:1; magenta, L:P = 24:1.* ***CP-A****: red, L:P = 37:1; green, L:P = 17:1; blue, L:P = 8:1.*

The dichroic ratio for the strong amide I band (perpendicular component) was chosen to quantitatively asses the peptide nanotube orientation, concluding that both CPs interact mainly with the polar heads of the lipids. For the amide I, the ratio values do not change significantly with peptide content. The amide I dichroic ratio is always similar to the lipid *ν* (C=O) dichroic ratio, a further indication of the parallel orientation of the nanotube with respect to the membrane.

MD were carried out using standard simulation parameters corresponding to the polarizable MARTINI force field (martini v2.2P),[417] maintain the channel morphology. This approach allows the spontaneous insertion and reorientation of the SCPN into the lipid bilayer. In the case of **CP-A**, the orientation of the resulting SCPN did not change significantly with the membrane composition. In all cases (Figure 1.21), the lysine residues are oriented towards the aqueous media, leaving the tryptophan and the alkyne moiety interacting with the lipid aliphatic chains.

[417] Bartlett, G. R., *J. Biol. Chem*., **1959**, 234, 466-468.

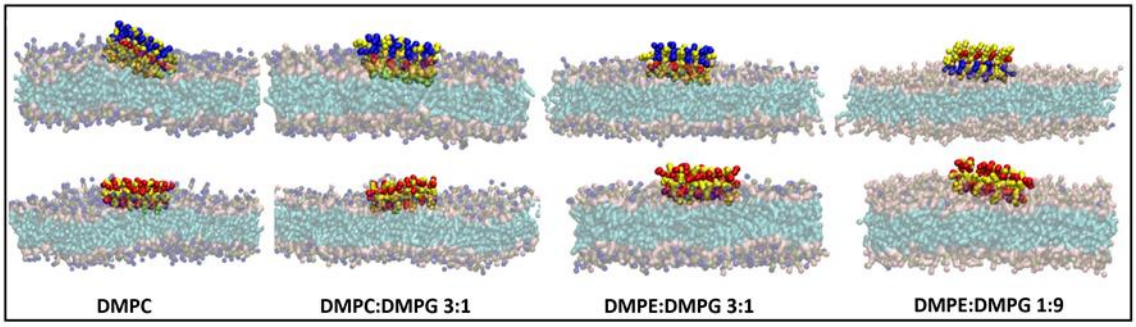

Figure 1.21. *CG-MD simulation of SCPN of* ***CP-14*** *and* ***CP-A*** *at different membrane concentrations. It can be noted that for* ***CP-14****, the arginine are directed towards the DMPE:DMPG (1:9) membrane, in contrast to what happens in the other membrane compositions. Water molecules have been removed for clarity.*

In summary, in this chapter we propose two different cyclic peptides as modulable platforms for the preparation of new antimicrobial peptides. **CP-B** required the conjugation with the saccharide through a CuAAC reaction, but the low solubility of the peptide precluded the formation of the hybrid derivatives in high yields. **CP-A** was completely soluble in water thanks to the reduced number of hydrophobic residues. The incorporation of the alkyl chain can be carried out at the solid support in high yield. We were also able to attach different saccharides to **CP-A1**, **CP-A2** and **CP-A3** in quantitative yield, although the process reduced the antimicrobial properties. Biophysical studies carried out at Porto of **CP-A** show that it can form nanotubes at the lipid membrane (as shown by ATR-FTIR). The peptide interacts with the phospholipid heads aligning the resulting nanotube parallel to the membrane surface. In addition, this organization has a limited segregation capacity (DSC).

USC
UNIVERSIDADE
DE SANTIAGO
DE COMPOSTELA

Chapter 2: Modifications and antibacterial activity of platform **CP-A**.

USC
UNIVERSIDADE
DE SANTIAGO
DE COMPOSTELA

2.1. Introduction of aliphatic tails in cyclic peptides CP-A1 and CP-A2.

In previous chapter, we described the optimization of peptide synthesis, such as the click chemistry reaction and the attachment of the saccharide. Using these conditions, we were able to prepare a library of peptides whose antimicrobial activity against *S. aureus*, *S. epidermidis and E. coli* will be discussed in these chapter.

In the activity optimization, we study the effect of the aliphatic chains. Alkyl chains of six, ten and sixteen carbons and benzyl derivative were introduced in **CP-A1** (Figure 2.1, Table 2.1) to confirm that the introduction of these chains play an important role in membrane activity.

The introduction of short aliphatic tails as the benzyl group or the six carbons tail did not improve the antimicrobial activity. However, longer chains, such as those of ten and sixteen carbons, notably improved the activity against the three bacteria strains. After this, new derivatives with alkyl chains ranging from nine to twenty carbons were prepared. Chains with odd and even number of carbons were also prepared to evaluate their effect in peptide´s activity. Finally, a derivative having a geranyl group was also prepared. The results with the activities of these peptides are shown in Table 2.1.

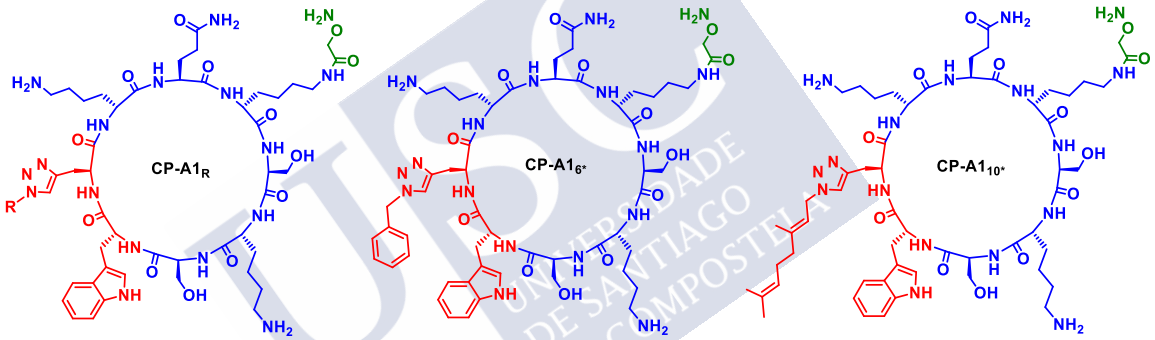

***Figure 2.1. CP-A1$_R$, CP-A1$_{6*}$** (benzyl tail) and **CP-A1$_{10*}$** (geranyl tail).*

Code	peptide	MIC (µg/mL)		
		S. aureus	***S. epidermidis***	***E. coli***
CP-A1	*c*-[QK^{Ox}SKSWZK]	125 – 64	64 – 32	ND
CP-A1$_{6*}$	*c*-[QK^{Ox}SKSWZ^{6*}K]	125 – 64	125	ND
CP-A1$_6$	*c*-[QK^{Ox}SKSWZ^{6}K]	64	64	250
CP-A1$_9$	*c*-[QK^{Ox}SKSWZ^{9}K]	32	16	64
CP-A1$_{10}$	*c*-[QK^{Ox}SKSWZ^{10}K]	**16**	32	64
CP-A1$_{10*}$	*c*-[QK^{Ox}SKSWZ^{10*}K]	250 – 125	8 – 4	125
CP-A1$_{11}$	*c*-[QK^{Ox}SKSWZ^{11}K]	64 – 32	32 – 16	64
CP-A1$_{12}$	*c*-[QK^{Ox}SKSWZ^{12}K]	62	8 – 4	125
CP-A1$_{14}$	*c*-[QK^{Ox}SKSWZ^{14}K]	32 – 16	**4**	**62 – 32**
CP-A1$_{16}$	*c*-[QK^{Ox}SKSWZ^{16}K]	32	16	125 – 64
CP-A1$_{18}$	*c*-[QK^{Ox}SKSWZ^{18}K]	64	16	125 – 64
CP-A1$_{20}$	*c*-[QK^{Ox}SKSWZ^{20}K]	64	32	125

Ox = oxime precursor, alkoxyamine. ND = not detected. 6* = benzyl group. Z = propargylglycine.

***Table 2.1.** Activity of cyclic peptides **CP-A1** with and without different aliphatic tails.*

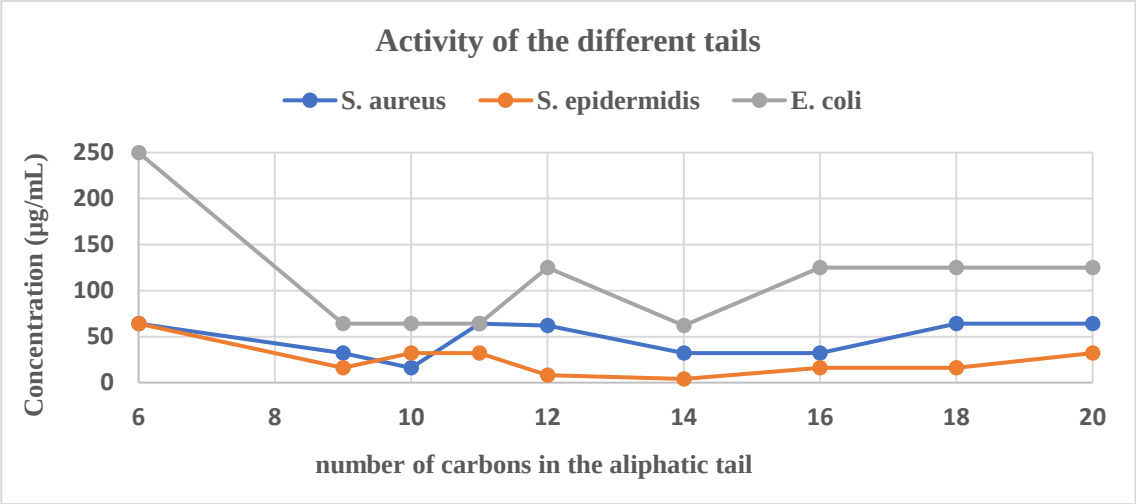

Figure 2.2. *Tendency of the peptide* ***CP-A1*** *with different aliphatic tails (****CP-A1****,* ***CP-A1$_{6*}$*** *and* ***CP-A1$_{10*}$*** *were excluded from this graph). The high values of the table were taken to represent the graph in all cases.*

In general, almost not differences were observed for the peptide having alkyl chain with odd or even number of carbons. The activity against *S. epidermidis* increase with the length of the alkyl chain, reaching a maximum for fourteen carbons chain. Then the increase in length reduced the activity. This effect can be observed in Figure 2.2. Some differences at this behaviour can be observed. For example, the activity against *S. aureus* decrease to a minimum of 16 µg/mL for **CP-A1$_{10}$**, but addition of one carbon reduce the activity (64 – 32 µg/mL), to then increase the minimal inhibitory concentration up to sixteen carbons chain to loss again the activity with longer tails (Figure 2.2). This irregular tendency is also observed in *E. coli*, in which the maximum inhibition was caused by the cyclic peptide **CP-A1$_{14}$**. However, the activity against *S. epidermidis* is less sensible to the chain length, achieving the higher activity (4 µg/mL) with **CP-A1$_{14}$**, although the analogues with similar length presented similar activities.

These peptides were studied by scanning transmission electron microscopy (STEM) in order to confirm the nanotube formation. Deposition of a solution of **CP-A1** (0.05 mg/mL) in water over a STEM grid did not show any nanotube formation (Figure 2.3), confirming that the lack of alkyl chain precluded the formation of nanotubes, at least in aqueous media.

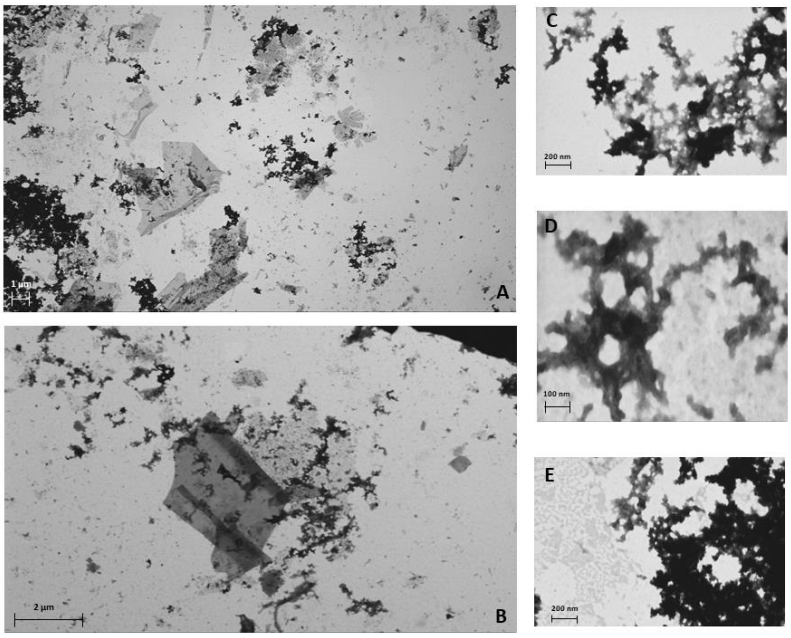

Figure 2.3. *STEM images of peptide* ***CP-A1*** *solved in water. A) and B) show the formation of sheets. C), D) and E) show aggregates without defined structure.*

Solution of **CP-A$_{16}$** in water (0.5 mg/mL) deposited over STEM grid showed no nanotubes formation. Instead, sheets where observed (Figure 2.4A). However, these structures were not observed at more diluted conditions. Other CPs with longer alkyl chains gave different type of aggregates but no nanotubes were observed, i. e. **CP-A1$_{10}$** (Figure 2.4D), **CP-A1$_{16}$** (Figure 2.4E), **CP-A1$_{20}$** (Figure 2.4F). Experiments using solutions with NaCl at concentrations similar to the solution used for the antimicrobial studies were also carried out. In these conditions, no nanotube or sheets were observed.

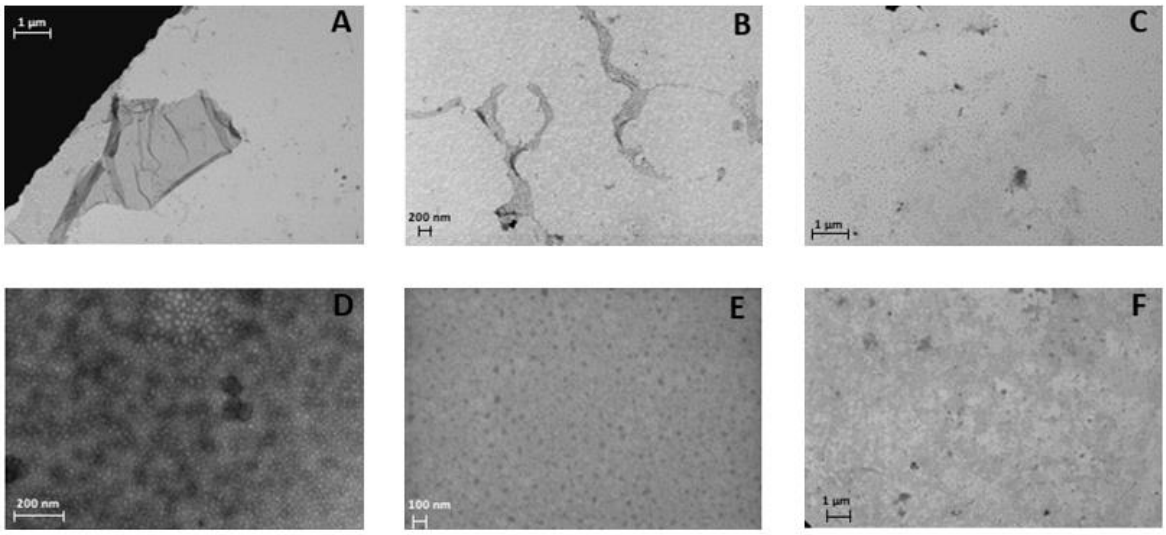

Figure 2.4. *A) and B)* ***CP-A1$_6$*** *at 0.5 mg/mL and C) at 0.05 mg/mL. D)* ***CP-A1$_{10}$*** *(0.5 mg/mL). E)* ***CP-A1$_{16}$****. F)* ***CP-A1$_{20}$****.*

After the study of **CP-A1** with different alkyl chains, we also study the derivatization of platform **CP-A2**. In this case we restricted the alkyl chains to those that have the best results with **CP-A1** derivates. These were alkyl chains with 6, 10, 12, 14, 16 and 18 carbons. The activities of these peptide nanotubes were summarized in Table 2.2. We analysed again this data as a tendency depending on the bacteria (Figure 2.5). For *S. aureus*, the activity has a large difference between the 12 carbons chain and those with 10 and 14 carbons. Surprisingly, the activity between *S. aureus* and *E. coli* is almost identical. The larger activity was found for *S. epidermidis*, being the most active the one with 14 and 18 atoms.

Code	peptide	MIC (µg/mL)		
		S. aureus	***S. epidermidis***	***E. coli***
CP-A2	*c*-[QKSK^{Ox}SWZK]	64 – 32	64 – 32	ND
CP-A2$_6$	*c*-[QKSK^{Ox}SWZ^{6}K]	64	16	125
CP-A2$_{10}$	*c*-[QKSK^{Ox}SWZ^{10}K]	**32 – 16**	16	**32**
CP-A2$_{12}$	*c*-[QKSK^{Ox}SWZ^{12}K]	125	32 – 16	125
CP-A2$_{14}$	*c*-[QKSK^{Ox}SWZ^{14}K]	62	**8**	62
CP-A2$_{16}$	*c*-[QKSK^{Ox}SWZ^{16}K]	62	16	62
CP-A2$_{18}$	*c*-[QKSK^{Ox}SWZ^{18}K]	62	**8**	62

Ox = oxime precursor, alkoxyamine. ND = not detected. Z = propargylglycine.

Table 2.2. *Activity of cyclic peptides* ***CP-A2*** *with and without different aliphatic tails.*

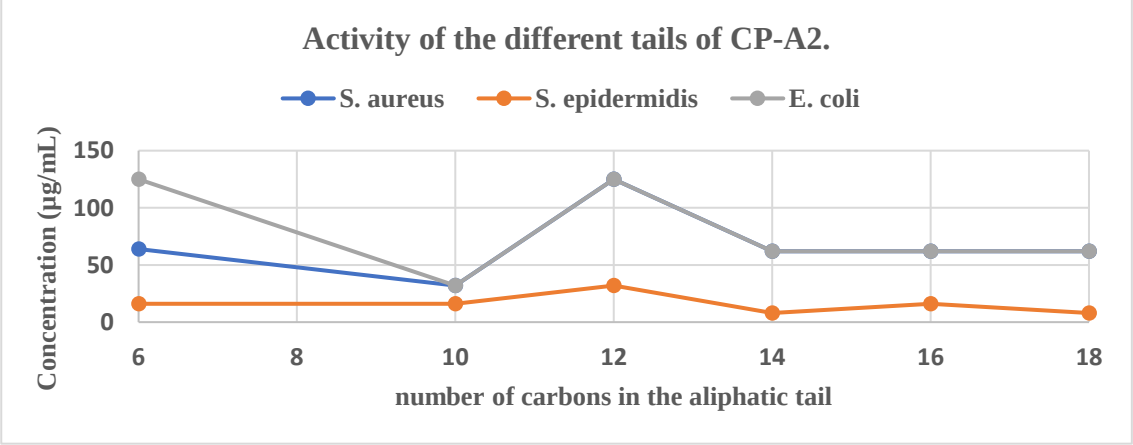

Figure 2.5. *Tendency of the peptide* ***CP-A2*** *with different aliphatic tails. The high values of the table were taken to represent the graph in all cases.*

2.2. Introduction of the saccharide derivatives.

Our next step was the introduction of saccharide derivatives in the hydrophilic core of the cyclic peptides and the evaluation of their antimicrobial potency as well as the capacity to reduce the toxicity against mammalian. Dr. Jose J. Reina prepared a battery of different saccharides with an aldehyde in the Cα, some of which were used in this work (Figure 2.4).[297b] The cyclic peptides were prepared as follow: 1) synthesis the cyclic peptide in solid phase, 2) alkoxyamine addition to Lys side chain, 3) alkyl chain incorporation on solid support, 4) cleavage/deprotection from the resin, 5) introduction of the saccharide and 6) purification of the final compound by reverse phase HPLC for antimicrobial activity evaluation. The introduction of the saccharide is so chemo-selective that can be carried out before purification without oxime hydrolysis, reducing time and cost of synthesis. However, as these saccharides requires several steps of synthesis, we decide to prepare the conjugates of only two of the most active peptides, including both platforms and the two more relevant alkyl chains (**CP-A1$_{14}$** and **CP-A2$_{10}$**). **CP-A2-C10** was chosen mainly because of its higher activity against *S. aureus* and *E. coli* for its series, while **CP-A1-C14** was selected based on its high activity against *S. epidermidis*. Four saccharide derivatives were studied, three monosaccharides (glucose, mannose and *N*-acetyl-galactosamine derivatives) and one disaccharide (maltose). The condensation was carried out mixing the cyclic peptide with the corresponding saccharide in water, which was shaken for 30 min at room temperature, to provide the corresponding oxime in good yields. The activity of these peptides is summarized in Table 2.3. Once again, the saccharide reduced the activity of the compounds independently of the position in which it was incorporated. Conjugates with glucose (**CP-A1$_{14}$-Glu** and **CP-A2$_{10}$-Glu**) present the higher potency and have similar activity against the three different bacteria, and they provide the best results against *S. aureus* compare with the other glycopeptides.

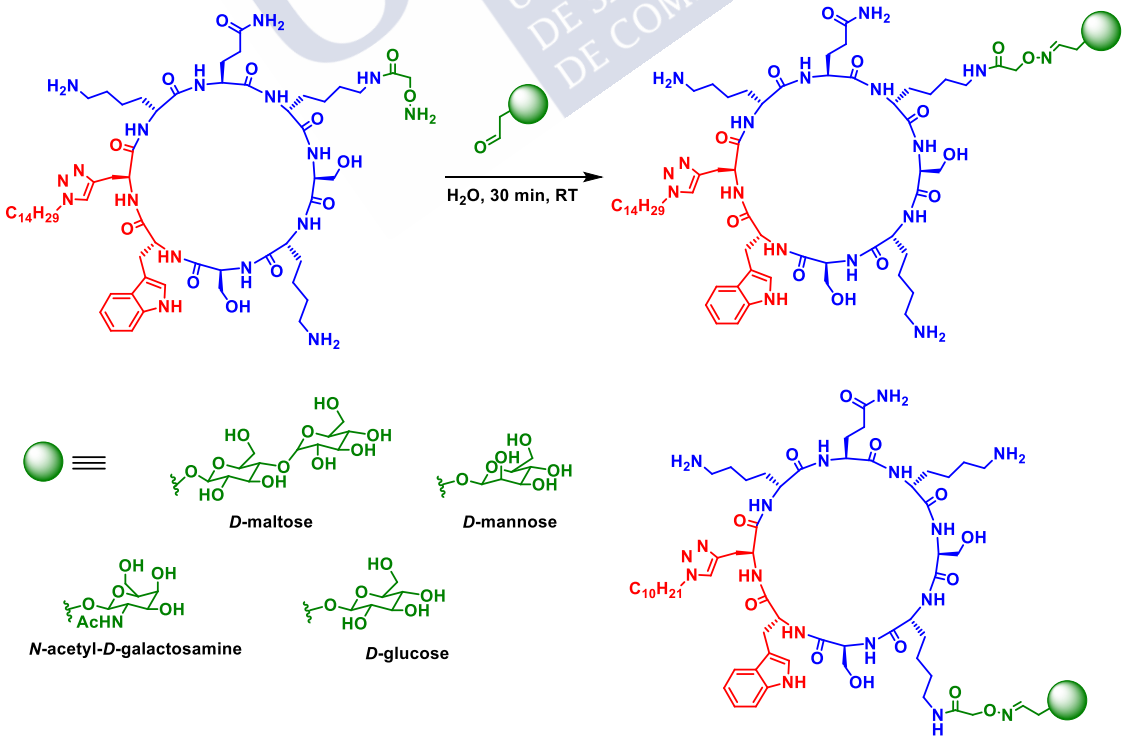

Figure 2.6. *Different saccharides used in this work for synthesis* ***CP-A1$_{14}$-saccharide*** *and* ***CP-A2$_{10}$-saccharide.***

Code	peptide	MIC (μg/mL)		
		S. aureus	***S. epidermidis***	***E. coli***
CP-A1	*c*-[QK^{Ox}SKSWZK]	125 – 64	64 – 32	ND
CP-A1$_{14}$	*c*-[QK^{Ox}SKSWZ^{14}K]	32 – 16	**4**	**64 – 32**
CP-A1$_{14}$-Glu	*c*-[QK^{Glu}SKSWZ^{14}K]	32	16	64
CP-A1$_{14}$-Man (17)	*c*-[QK^{Man}SKSWZ^{14}K]	64 – 32	32 – 16	64
CP-A1$_{14}$-Gal	*c*-[QK^{Gal}SKSWZ^{14}K]	64 – 32	32 – 16	64
CP-A1$_{14}$-Mal	*c*-[QK^{Mal}SKSWZ^{14}K]	64 – 32	32 – 16	64
CP-A2	*c*-[QKSK^{Ox}SWZK]	64 – 32	64 – 32	ND
CP-A2$_{10}$	*c*-[QKSK^{Ox}SWZ^{10}K]	**32 – 16**	16	**32**
CP-A2$_{10}$-Glu	*c*-[QKSK^{Glu}SWZ^{10}K]	32	16	64
CP-A2$_{10}$-Man (17)	*c*-[QKSK^{Man}SWZ^{10}K]	64 – 32	16	64
CP-A2$_{10}$-Gal	*c*-[QKSK^{Gal}SWZ^{10}K]	64 – 32	16	64
CP-A2$_{10}$-Mal	*c*-[QKSK^{Mal}SWZ^{10}K]	64 – 32	16	64

Ox = oxime precursor, alkoxyamine. ND = not detected. Z = propargylglycine.

Table 2.3. *Activity of the glycopeptides* ***CP-A1$_{14}$*** *and* ***CP-A2$_{10}$.***

Although the glycopeptides did not present high antibacterial potential, they could become antibiotics if they have a huge therapeutic window, in other words, if their toxicities appear at concentrations far over the MIC. The toxicity was measured by haemolysis assays. The experiment, which was carried out with human red blood cells to determine the damage of the erythrocytes after a period of incubation. The commercially available erythrocytes in Alsever´s solution (saline liquid used to prevent the coagulation of blood[418]) was diluted to an 8% erythrocytes/PBS for these experiments. The mixture with different concentrations of peptide at same concentration of erythrocytes were incubated for 1 hour at 37 ºC. A dilution of 0.1% Triton/PBS was used as positive control and PBS was used as negative control. After incubation, the plate was centrifuged, the solution was removed and transfer to a new plate to measure at 405 nm.

The result of these studies is summarized in Figure 2.7 and they were very gratifying as any of the tested peptides showed any important haemolytic activity. **CP-A1$_{14}$** did not show toxicity under 125 μg/mL, as the toxicity percentage is equal to the negative control. At 250 μg/mL, the toxicity is around the 21%, 16% more toxic than the PBS itself, and around the 25% at 500 μg/mL. The incorporation of saccharides reduced the toxicity of the peptide, although the haemolysis effects of **CP-A1** were observed only at concentrations higher than 64 μg/mL. Galactosamine is the saccharide with the smallest effect in the toxicity, whose haemolysis percentage was over 10% at 500 μg/mL. The less toxic glycopeptide is **A1-C14-Glu**, with haemolytic activity similar to the PBS. Moreover, it is the glycopeptide with the lowest MIC, leading to a therapeutic window of 15-fold the MIC.

With respect to the **CP-A2** series, they were slightly less haemolytic than the previous one. The results of these cytotoxic studies were summarized in Figure 2.8. In these series, the most toxic was the more active one (**CP-A2$_{10}$-Glu**) with 12% haemolytic activity at the maximum concentration tested. This haemolysis is even higher than the non-saccharide cyclic peptide.

[418] Alsever, J. B.; Ainslie, R. B., *N. Y. State J. Med*., **1941**, 41, 126-131.

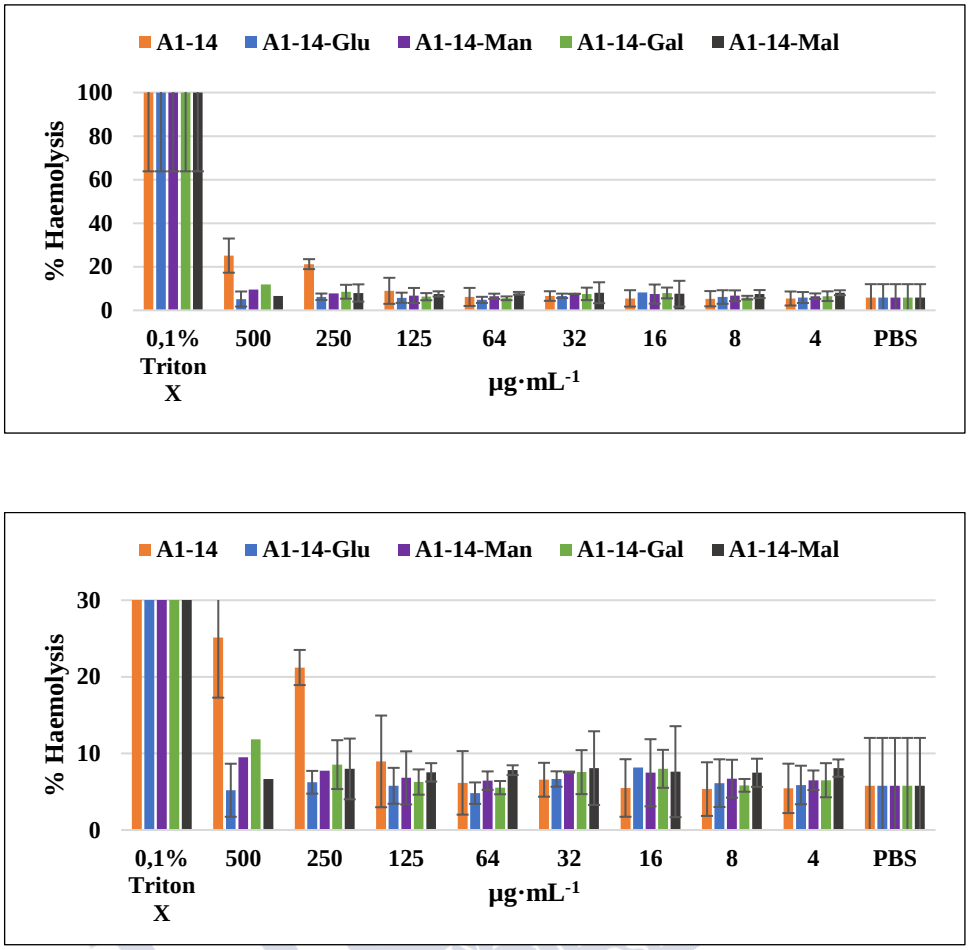

Figure 2.7. *Haemolysis assays of peptides* ***CP-A1$_{14}$-saccharide*** *compared with* ***CP-A1$_{14}$****. The complete graph is show on the top, whereas in the bottom the graph is focus on the small values to compare with the negative control. To afford space in the graphs, the acronym CP was removed from the name of the compounds.*

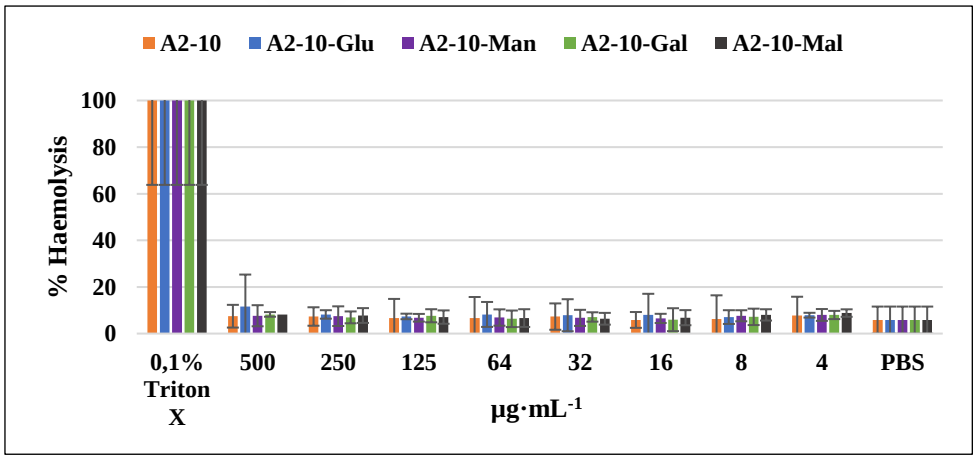

Figure 2.8. *Haemolysis assays of peptides* ***CP-A2$_{10}$-saccharide*** *compared with* ***CP-A2$_{10}$****. To afford space in the graphs, the acronym CP was removed from the name of the compounds.*

2.3. Optimization of the CP-A sequence.

The first part of this study was focussed on the optimization of the CP platform to obtain higher antibacterial activity. The results clear confirmed that the optimal alkyl chain was those having ten or fourteen carbons. From the previous studies, we deduced that changes at position 2 of **CP-A1** are more important than those carried out at position 4 of **CP-A2**. For example, the introduction of the alkoxyamine in position 2 have a higher impact in the activity. For this reason, we decide to study this position of the peptide, substituting the lysine for other cationic amino acids. In this way, Lys was substituted by arginine, ornithine and 2,3-diaminopropionic acid (Figure 2.9). All peptides were prepared in solid phase following the same strategy previously described. The antibacterial activity of the new compounds is summarized in Table 2.4. The more potent peptides were **CP-A4** and **CP-A5**, in which arginine and ornithine were used. In both cases, one-digit MIC were obtained for *S. epidermidis* strain.

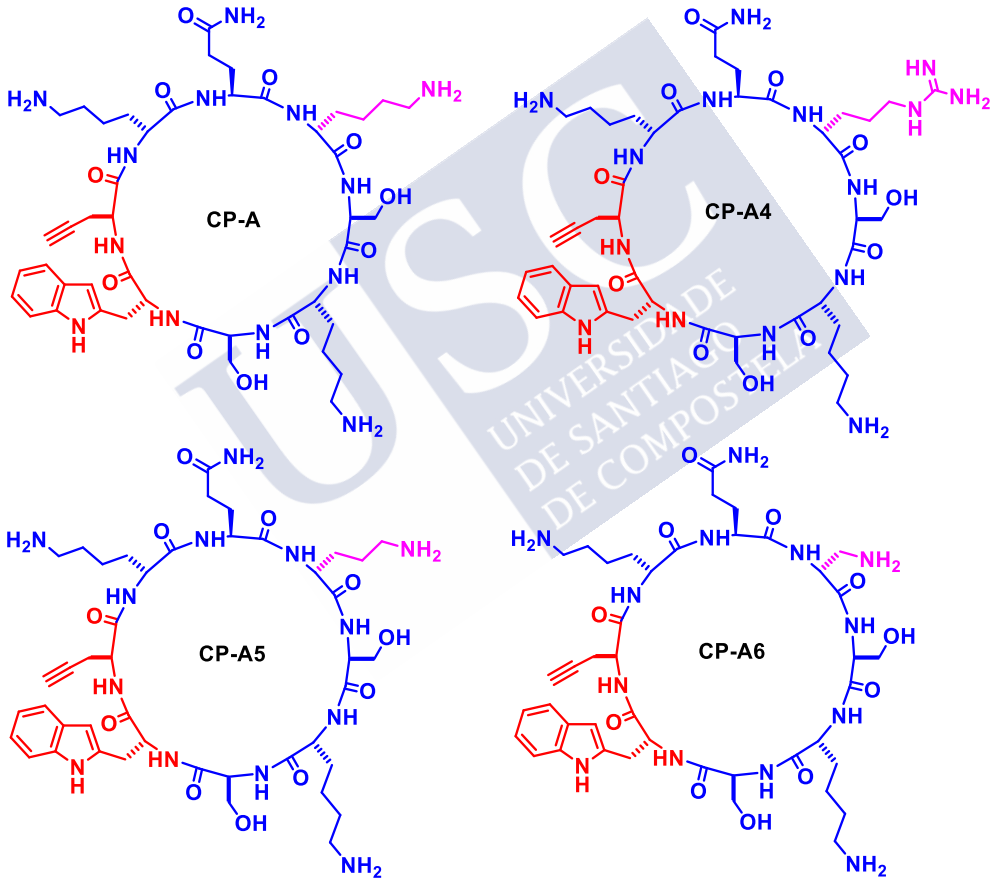

Figure 2.9. *Structures derived from* ***CP-A****:* ***CP-A4****,* ***CP-A5*** *and* ***CP-A6****.*

Code	peptide	MIC (μg/mL)		
		S. aureus	***S. epidermidis***	***E. coli***
CP-A	*c*-[QKSKSWZK]	32	16	125
CP-A4	*c*-[QRSKSWZK]	64 – 32	4	64
CP-A5	*c*-[QOSKSWZK]	64	8	125
CP-A6	*c*-[QXSKSWZK]	125	32	ND

ND = not detected. Z = propargylglycine. X = 2,3-diaminopropionic acid.

Table 2.4. *Antibacterial activity of the compounds* ***CP-A4****,* ***CP-A5*** *and* ***CP-A6*** *compared with* ***CP-A****.*

Alkyl chains with ten and fourteen carbons were also incorporated to these new peptides. The antimicrobial activity is summarized in Table 2.5. The introduction of the tails increases the activity of the three cyclic peptides. In general, the 2,3-diaminopropionic acid derivative was the most potent of all of them. Clearly, *for S. epidermidis*, the ten carbons alkyl chain provide the most active cyclic peptides with MIC of 2 μg/mL. Regarding *S. aureus*, all the peptides have similar activities, showing no differences in the substitution of Lys 2 in the presence of the hydrophobic chain. The long alkyl chain seems more important for Gram-negative bacteria, reaching MICs of 32 μg/mL with independence of the residue placed at position 2. These interesting results pront us to extend the studies to other Gram-positive bacteria, including methicillin resistant *S. aureus*. The activities are summarized in Table 2.6, that includes MRSA, *S. mutans* and *E. faecalis*. Notably, peptides **CP-A5** and **CP-A6** show low activity against these bacteria, requiring concentrations around 250 μg/mL or higher. However, when the aliphatic chain of ten carbons was introduced, the resulting peptides, **CP-A5$_{10}$** and **CP-A6$_{10}$**, achieve MICs of 16 μg/mL even for MRSA. In other words, the different between activity of the peptides with arginine, ornithine and 2,3-diaminopropionic acid is not appreciate when the aliphatic tail is included in the structure. Again, the best activities against Gram-positive bacteria are those with the ten carbons chain, being the less active the arginine derivative. Moreover, **CP-A5$_{10}$** present the same activity against MRSA than against non-methicillin resistant *S. aureus*, which suggest that the mechanism of action of these peptides is not in the peptidoglycan wall.

Code	peptide	MIC (μg/mL)		
		S. aureus	***S. epidermidis***	***E. coli***
CP-A4	*c*-[QRSKSWZK]	64 – 32	4	64
CP-A4$_{10}$	*c*-[QRSKSWZ^{10}K]	16	2 – 1	64
CP-A4$_{14}$	*c*-[QRSKSWZ^{14}K]	16	4	32
CP-A5	*c*-[QOSKSWZK]	64	8	125
CP-A5$_{10}$	*c*-[QOSKSWZ^{10}K]	16	2	64 – 32
CP-A5$_{14}$	*c*-[QOSKSWZ^{14}K]	16	8	32
CP-A6	*c*-[QXSKSWZK]	125	32	ND
CP-A6$_{10}$	*c*-[QXSKSWZ^{10}K]	8	2	64 – 32
CP-A6$_{14}$	*c*-[QXSKSWZ^{14}K]	32 – 16	4	32

ND = not detected. Z = propargylglycine. X = 2,3-diaminopropionic acid.

Table 2.5. *Activity of the compounds* ***CP-A4****,* ***CP-A5*** *and* ***CP-A6*** *with ten and fourteen carbons.*

Code	peptide	MIC (μg/mL)		
		MRSA	***S. mutans***	***E. faecalis***
CP-A4	*c*-[QRSKSWZK]	125	125	250 – 125
CP-A4$_{10}$	*c*-[QRSKSWZ^{10}K]	32	32	32
CP-A4$_{14}$	*c*-[QRSKSWZ^{14}K]	16	64 – 32	32
CP-A5	*c*-[QOSKSWZK]	250 – 125	250	250
CP-A5$_{10}$	*c*-[QOSKSWZ^{10}K]	16	16	16
CP-A5$_{14}$	*c*-[QOSKSWZ^{14}K]	32	32	64 – 32
CP-A6	*c*-[QXSKSWZK]	125	ND	250
CP-A6$_{10}$	*c*-[QXSKSWZ^{10}K]	16	16	16
CP-A6$_{14}$	*c*-[QXSKSWZ^{14}K]	32	32	32

ND = not detected. Z = propargylglycine. X = 2,3-diaminopropionic acid.

Table 2.6. *Activity of the compounds **CP-A4**, **CP-A5** and **CP-A6** with ten and fourteen carbons against MRSA, S. mutans and E. faecalis.*

In this work, in collaboration with Dr. Federica Novelli, we also evaluated the biophysical properties of these cyclic peptides. Thioflavin T (ThT) fluorescence assay was performed to determine the critical aggregation concentration (CAC) of the resulting aggregates (Figure 2.10). Thioflavin T molecule is able to interact selectively with the *β*-sheets-rich structures, being one of the assays used for amyloid detection.[419] This interaction results in an increase in the intensity of fluorescence and a shift of the maximum emission to longer wavelengths (red shift).[420] Figure 2.10 shows the fluorescence traces of the peptide solutions at different concentrations, when the samples are excited at 440 nm. In all the cases there is a clear increase in emission at 480 nm with peptide concentration higher than 25 μM. From these studies, we can estimate the CAC for each peptide reporting the normalized intensity as a function of the peptide concentration (Figure 2.11). A clear change in fluorescence emission was observed in all of them with a point in the concentration around 12 μM and 5 μM for the cyclic peptides functionalized with ten and fourteen carbons tails, respectively (Figure 2.11). The low CACs found are an index of high thermodynamic stability of the prepared nanostructures, even at high diluted conditions.

[419] a) LeVine III, H., *Methods Enzimol*., **1999**, 309, 274-284. b) Chimon, S.; Ishii, Y., *J. Am. Chem. Soc*., **2005**, 127, 13472-13473.
[420] Biancalana, M.; Koide, S., *Biochim Biophys Acta*, **2010**, 1804, 1405–1412.

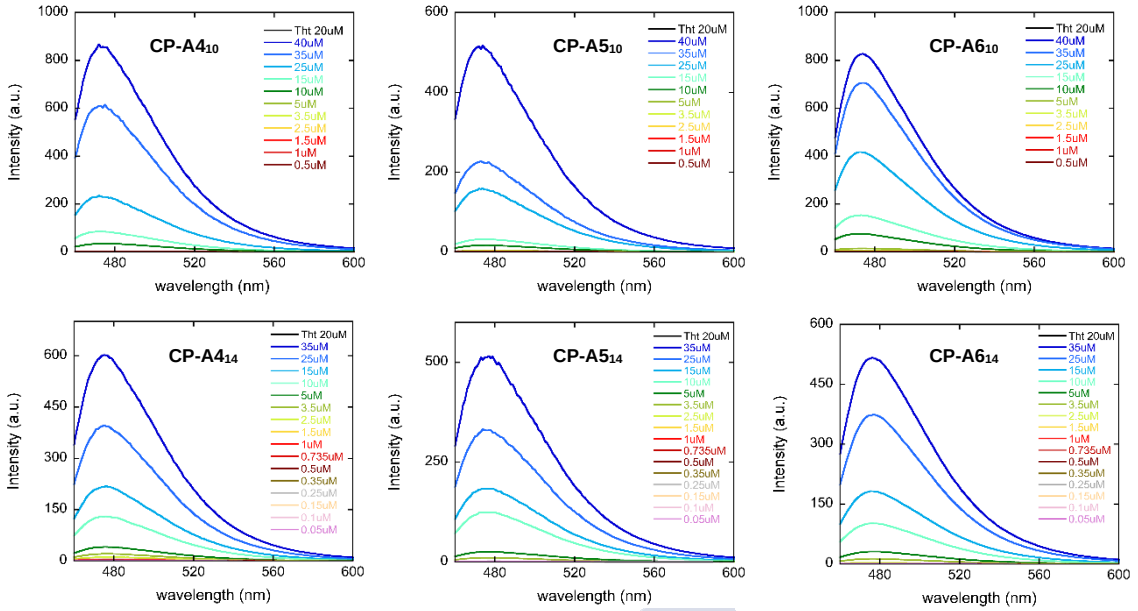

Figure 2.10. *Fluorescence ThT assays to determine the critical aggregation concentration. CPs were solubilized in a buffer composed by 10 mM Tris and 107 mM NaCl at pH 7.4. The concentration of the ThT was 20 μM and the λ_{exc} = 440 nm.*

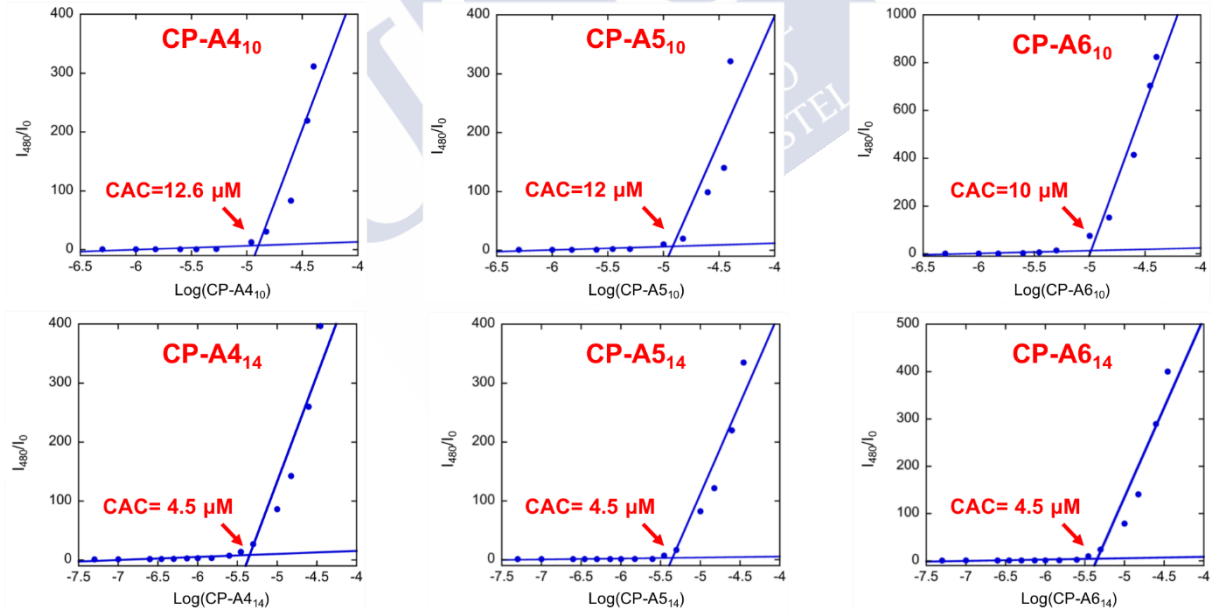

Figure 2.11. *Dependence of I_{480}/I_0 on the sample concentration for **CP-A4**, **CP-A5** and **CP-A6** with ten carbons (top) and fourteen carbons (bottom). I_{480} is the fluorescence emission intensity at 480 nm for samples containing the CP and ThT, while the I_0 is the fluorescence emission intensity at 480 nm for samples containing only ThT.*

To deeply investigate the morphology of the self-assembled peptide amphiphiles **CP-A4$_{14}$**, **CP-A5$_{14}$**, and **CP-A6$_{14}$** in aqueous solution, STEM microscopy measurements were performed at concentration over the CAC (1 mg/mL). STEM images revealed that all the peptides self-assemble in nanotubes with lengths of few micrometres and average diameters of 3-4 nm (Figure 2.12).

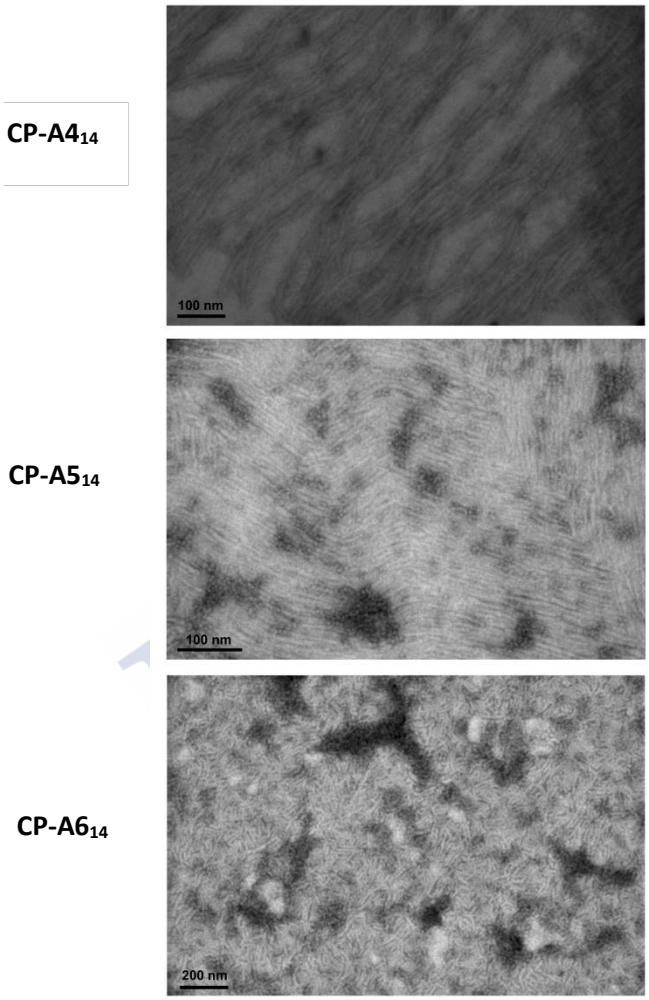

Figure 2.12. *STEM images of* ***A4-C14****,* ***A5-C14*** *and* ***A6-C14****.*

Moreover, ^{1}H-NMR expectra at 2 mM of fourteen carbons derivatives show broad bands that can be attributed to conformational equilibrium and/or formation of aggregates (Figure 2.13). Only the cyclic peptide derived from the 2,3-diaminopropionic acid residue (**CP-A6$_{14}$**) gave an NMR spectrum in which some of the amide protons are sharp and well defined. The ^{1}H-NMR of CPs with ten carbons show spectra in which the signals are sharp and well defined. In fact, the signals of amide protons (NH) are perfectly defined and can be assigned to each residue of the cyclic peptide. This is consisted with monomeric cyclic peptides (Figure 2.14).

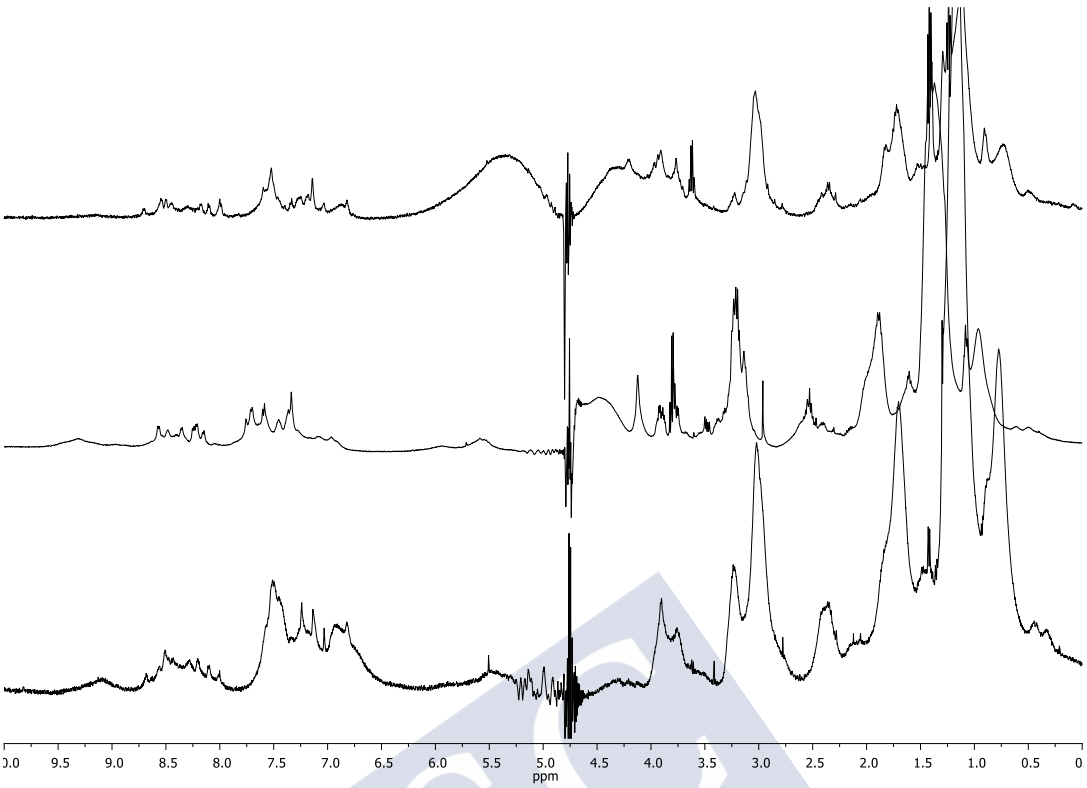

Figure 2.13. *^{1}H-NMR of* ***CP-A$_{C14}$*** *(top),* ***CP-A6$_{C14}$*** *(medium) and* ***CP-A4$_{14}$*** *(bottom).*

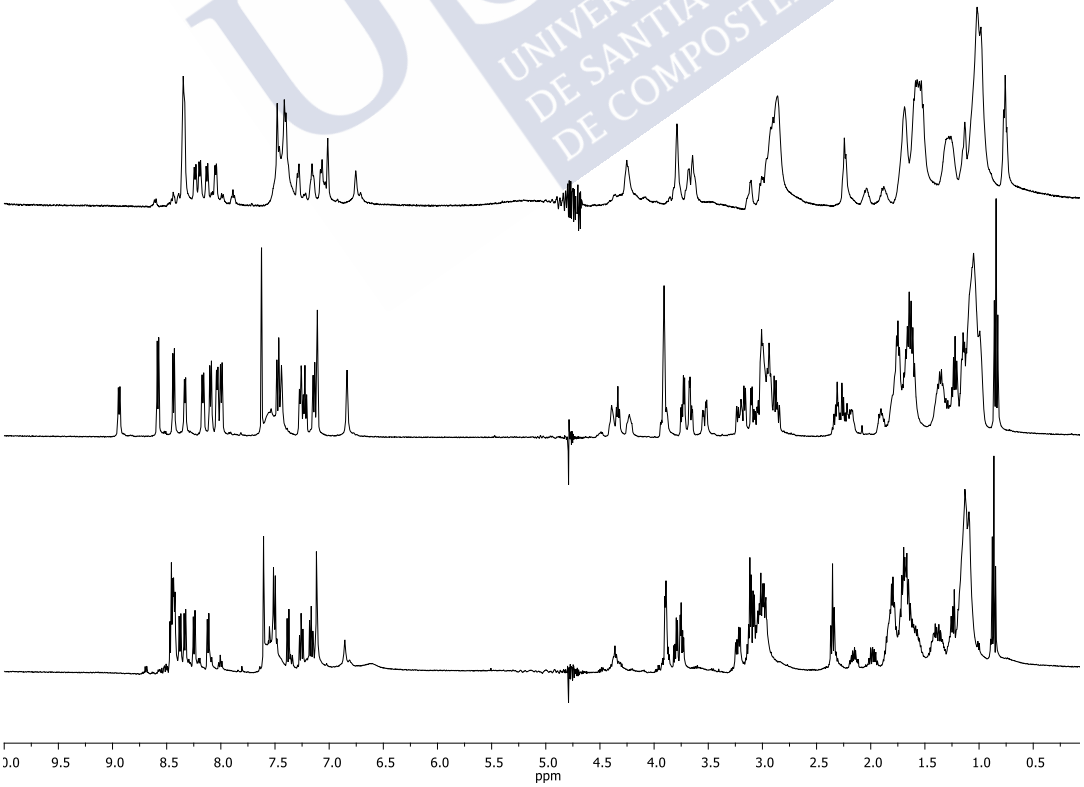

Figure 2.14. *^{1}H-NMR of* ***CP-A$_{C14}$*** *(top),* ***CP-A6$_{C14}$*** *(medium) and* ***CP-A4$_{14}$*** *(bottom).*

MTT assays of these cyclic peptides were carried out in Hela Cells by Dr. Federica Novelli (see section 2.4 and supporting information). The results show that the peptides have low toxicity in all the range of concentrations tested (0.5 to 40 µM, Figure 2.15).

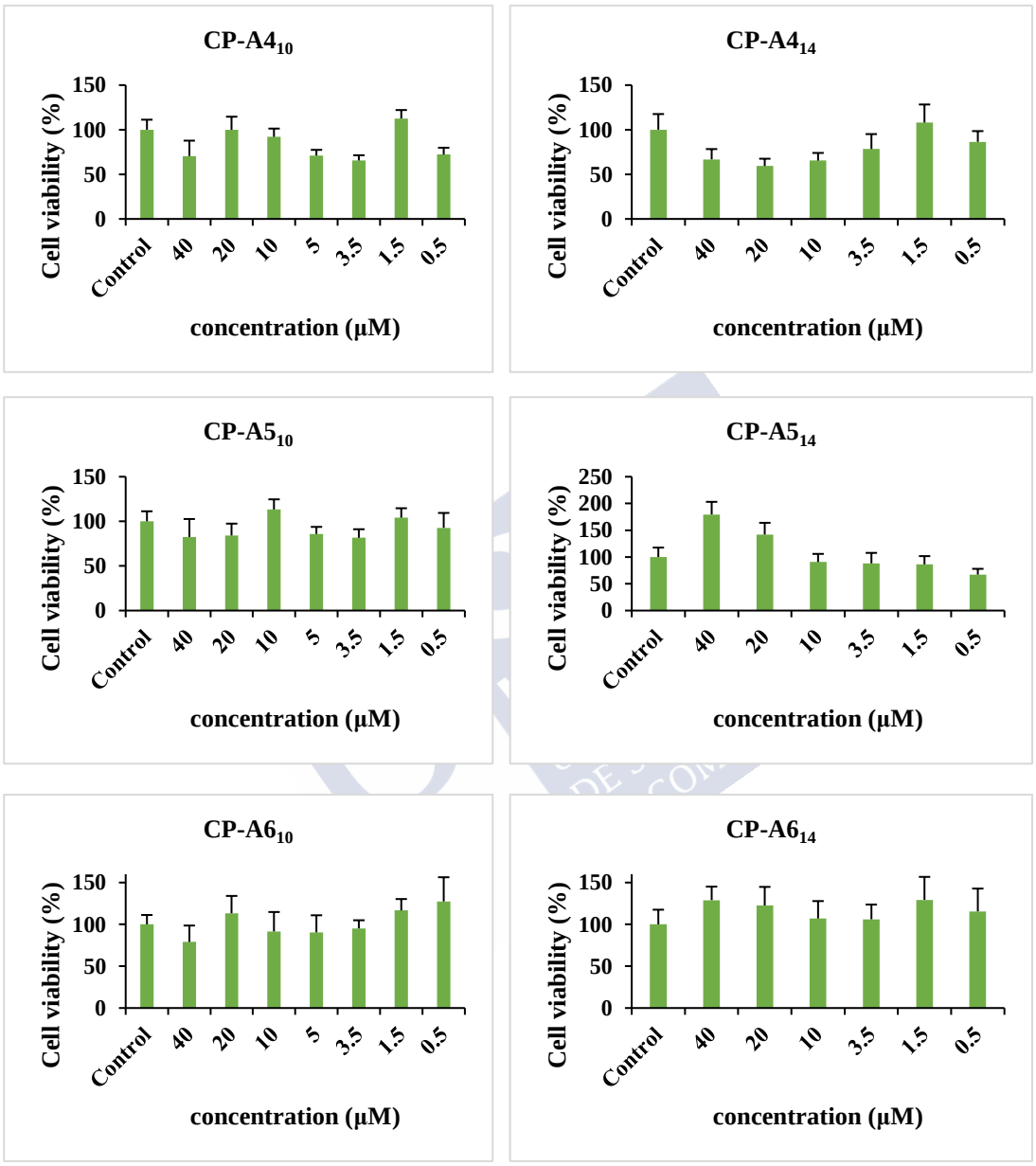

Figure 2.15. *MTT assay in HeLa Cells of the compounds* ***CP-A4-6*** *with ten carbons and fourteen carbons.*

Moreover, the haemolysis of these cyclic peptides was measured in the same way that was carried out with **CP-A1$_{14}$**, **CP-A2$_{10}$** and their derivatives. The results are summarized in bar graphs (Figure 2.16-2.18). As common tendency, cyclic peptides with longer tails are more toxic than peptides with the shorter one. **CP-A4** and **CP-A4$_{10}$** show the same haemolysis than the PBS, whereas **CP-A4$_{14}$** show a toxicity closed to the 55% at 250 µg/mL and around a 35% at 250 µg/mL. The less toxic are the peptides with the ornithine residue that shown haemolytic activity smaller than 20% at the higher concentration tested. **CP-A4$_{10}$** present the highest activity against *S. epidermidis* (MIC = 2 µg/mL) and not leak against red blood cells (same toxicity than PBS), which offers a therapeutic window of 250 fold the MIC. **CP-A6$_{10}$** present a MIC of 8 µg/mL against *S. aureus*, and also low toxicity until 250 µg/mL, leading to a therapeutic window of 30 fold the MIC.

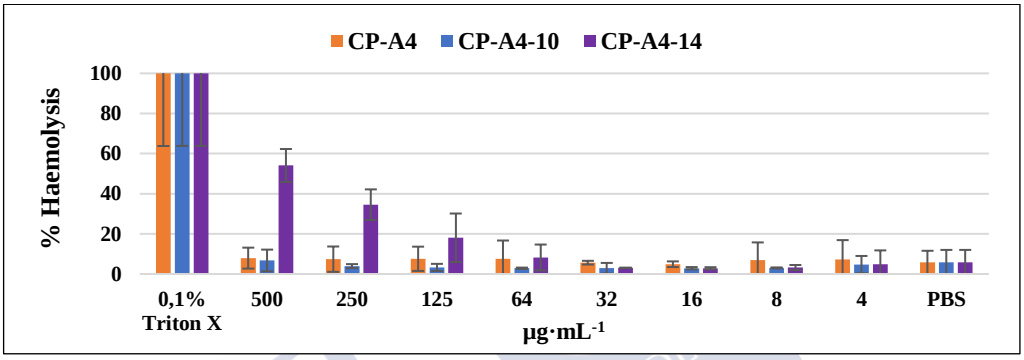

Figure 2.16. *Haemolysis assays of peptides* ***CP-A4****,* ***CP-A4$_{10}$*** *and* ***CP-A4$_{14}$****.*

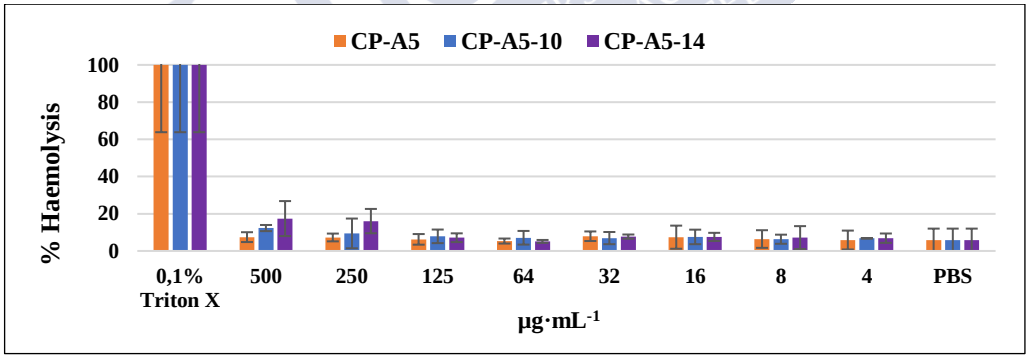

Figure 2.17. *Haemolysis assays of peptides* ***CP-A5****,* ***CP-A5$_{10}$*** *and* ***CP-A5$_{14}$****.*

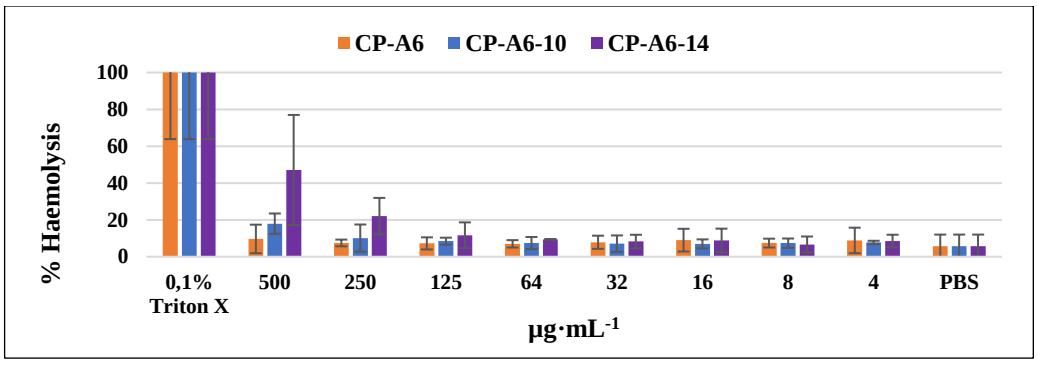

Figure 2.18. *Haemolysis assays of peptides* ***CP-A6****,* ***CP-A6$_{10}$*** *and* ***CP-A6$_{14}$****.*

With the aim of reduce the cytotoxicity of **CP-A4$_{14}$** and **CP-A5$_{14}$**, we planned the incorporation of the alkoxyamine in which the saccharide would be attached. Two alternatives were evaluated: the attachment at residue 4, as in previously **CP-A2** derivatives, or at residue 8. These two options were **CP-A4-Ox^4** and **CP-A4-Ox^8** for the peptide with the arginine in the cyclic peptide skeleton (Figure 2.19). **CP-A4$_{10}$-Ox^4** and **CP-A4$_{14}$-Ox^4**, well as **CP-A4$_{10}$-Ox^8** and **CP-A4$_{14}$-Ox^8** were prepared and their antimicrobial activity was tested (Table 2.7). The introduction of the alkoxyamine reduce the activity, maintaining the idea that the reduction of positive charges reduces the activity. Drastic reduction was observed for the cyclic peptides having the oxime at Lys-8. It seems that the peptides with longer alkyl chains are less sensitive to the alkoxyamine incorporation.

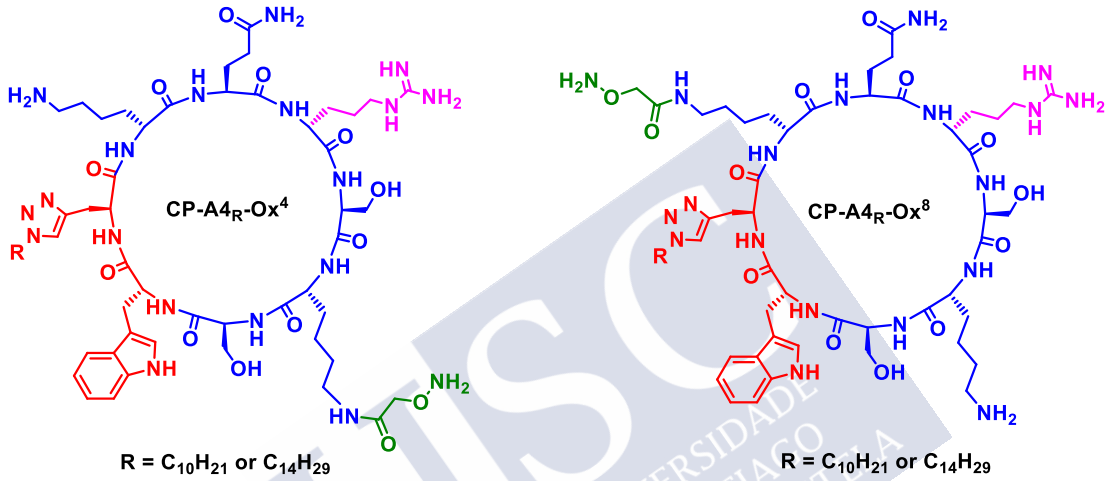

Figure 2.19. *Structure of the peptides* ***CP-A4$_R$-Ox^4*** *and* ***CP-A4$_R$-Ox^8****.*

Code	peptide	MIC (μg/mL)		
		S. aureus	***S. epidermidis***	***E. coli***
CP-A4	*c*-[QRSKSWZK]	64 – 32	4	64
CP-A4-C10	*c*-[QRSKSWZ^{10}K]	16	2 – 1	64
CP-A4-C14	*c*-[QRSKSWZ^{14}K]	16	4	32
CP-A4-C10-Ox^4	*c*-[QRSK^{Ox}SWZ^{10}K]	64 – 32	32	64
CP-A4-C14-Ox^4	*c*-[QRSK^{Ox}SWZ^{14}K]	64	125 – 64	125
CP-A4-C10-Ox^8	*c*-[QRSKSWZ^{10}K^{Ox}]	125	125	125
CP-A4-C14-Ox^8	*c*-[QRSKSWZ^{14}K^{Ox}]	64	64	125

Ox = oxime precursor, alkoxyamine. Z = propargylglycine.

Table 2.7. *Activity of the compounds* ***CP-A4-C10*** *and* ***CP-A4-C14*** *with the alkoxyamine in two different positions.*

2.4. Activity of cyclic peptides against biofilms.

One of the objectives of this work was developed peptide nanotubes with antimicrobial properties to test against *S. aureus* and *S. epidermidis* biofilms because they are involved in many chronic diseases. Throughout this work, we have been modifying platform A to achieve cyclic peptides with moderate and good activities, some of them with low toxicity and haemolytic properties. The biological studies have shown that **CP-A4$_{10}$** present good activity against *S. epidermidis* while **CP-A6$_{10}$** achieved the best toxicity against *S. aureus*. These peptides were selected for these studies. In addition, we also prepared **CP-A** due to its high activity.

Initially, we decide to repeat the experiments with planktonic cells at higher concentrations. As it was mentioned before, the standard method is usually between 1 – 5 x 10^5 CFU/mL, and we had carried out the experiments with 1 x 10^5 CFU/mL, which is the lower limit. So, we repeat the experiments using 5 x 10^5 CFU/mL. The results are summarized in Table 2.8. The MIC of **CP-A6$_{10}$** against *S. aureus* is maintained although **CP-A4$_{10}$** activity against *S. epidermidis* decrease until values compare with the other ten carbons chain cyclic peptides. Peptides obtained from **CP-A** and **CP-A4** show identical values of MIC in all cases (16 μg/mL). Only **CP-A6$_{10}$** gave MIC larger than the other peptides.

Code	peptide	MIC (μg/mL)	
		S. aureus	***S. epidermidis***
CP-A4-C10	*c*-[QRSKSWZ^{10}K]	16	16
CP-A4-C14	*c*-[QRSKSWZ^{14}K]	16	16
CP-A6-C10	*c*-[QXSKSWZ^{10}K]	8	16
CP-A6-C14	*c*-[QXSKSWZ^{14}K]	32	32
CP-A-C10	*c*-[QKSKSWZ^{10}K]	16	16
CP-A-C14	*c*-[QKSKSWZ^{14}K]	16	16

Z = propargylglycine. X = 2,3-diaminopropionic acid.

Table 2.8. *Activities of the cyclic peptides against planktonic bacteria at 5 x 10^5 CFU/mL.*

To carry out these experiments, we followed a previous described methodology for the formation of a *S. aureus* mature biofilm.[421] This is based on incubating the bacteria overnight at 37ºC, that we carried out in MHB. After incubation, the mixture was diluted 1:100 in MHB. Diluted bacteria (100 μL, aprox. 10^9 CFU/mL) were inoculated into a 96-well flat-bottom cell culture plates and incubated at 37ºC for 24h. The culture medium was removed, and wells were carefully washed with PBS to remove planktonic bacteria before refilling wells with fresh MHB. Peptides were added at different concentrations (100 μL), and plates were incubated at 37 ºC for 24 h. Then, the peptide and the medium were removed and a solution of 3-(4,5-dimethylthiazol-2-yl)-2,5-diphenyltetrazolium bromide (MTT) in PBS (0.5 mg/mL, 100 μL) was added and incubated for 2 hours until the solution turn from yellow to blue. This colour change is due to the enzymatic activity of the cells, reflecting the number of viable cells present in the wells. Finally, the solvent is removed and DMSO (100 μL) was added to dissolve the

[421] Mohamed, M. F.; Hamed, M. I.; Panitch, A.; Seleem, M. N., *Antimicrob. Agents Chemother*., **2014**, 58, 4113-4122.

MTT crystals, obtaining a purple solution in the wells where the biofilms was not destroyed by the peptides (Figure 2.20).

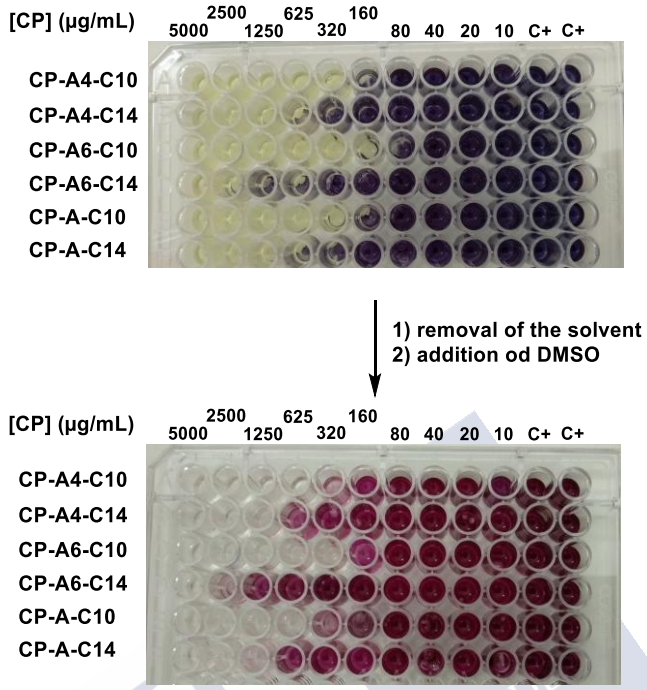

Figure 2.20. *Mtt assay of S. aureus biofilm with several peptides at different concentrations.*

This procedure was carried out to obtain mature biofilms of *S. aureus* and *S. epidermidis*, However, the low enzymatic activity of both positive controls leads us to check the growth of the biofilms. We decide to quantify the formation of the biofilm using the xCELLigence® System RTCA,[422] in which the increase in the cell adherence on the electrodes causes an increase in the electrode impedance, which is expressed into a dimensionless parameter called cell index. The bacteria in MHB (OD_{600} adjusted to 0.05, aprox. 10^7 CFU/mL) was incubated and measured by this technique. The data is represented in Figure 2.21 (left) and show a maximum value of 0.1 cell index. Usually, a mature biofilm achieved a cell index value over 0.2, so in MHB, neither *S. aureus* nor *S. epidermidis* form a proper biofilm. We decide to change the medium to BHB, however, it was necessary to add a 0.25% of glucose to achieve a value of 0.2 cell index for *S. aureus* (Figure 2.21 right). Unfortunately, the *S. epidermidis* strain used in these experiments is a not biofilm-forming strain.

[422] a) Junka, A. F. *et al*, *Pol. J. Microbiol*., **2012**, 61, 191-197. b) Cihalova, K. *et al*, *Int. J. Mol. Sci*., **2015**, 16, 24656-24672. c) Ferrer, M. D. *et al*, *J. Appl. Microbiol*., **2017**, 122, 640-650. d) Gutiérrez, D.; Hidalgo-Cantabrana, C.; Rodríguez, A.; García, P.; Ruas-Madiedo, P., *PloS One*, **2016**, 11:e0163966.

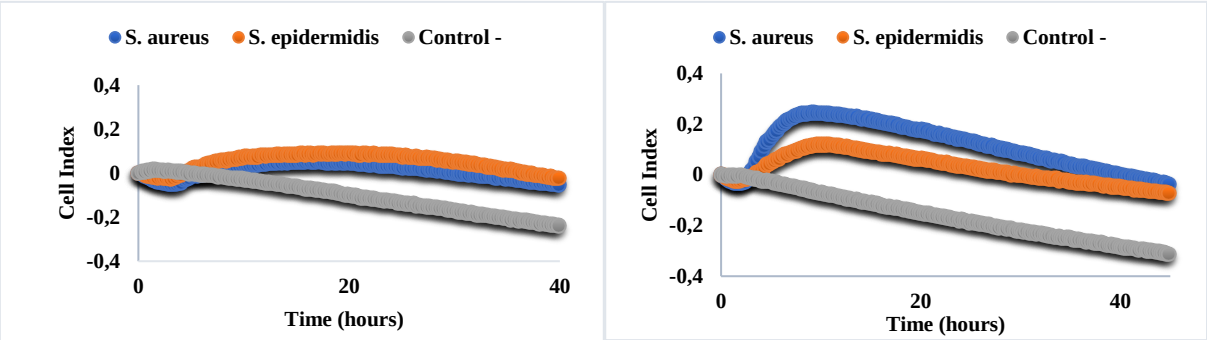

Figure 2.21. *S. aureus and S. epidermidis biofilm growths in MHB (left) and in 0.25% glucose/BHB (right). The corresponding broth was used as negative control.*

After determining that the best medium to grow the *S. aureus* biofilm was 0.25% glucose/BHB, we decided to incubate the bacteria in this broth, inoculate it in a 96-well flat-bottom cell culture plates and incubate it at 37ºC for 24 h to create the biofilm. After the corresponding washes with PBS, wells were refilled with MHB. The procedure with the peptide is the same independently of the medium used. The activity of the compounds against mature *S. aureus* biofilm is summarized in Table 2.9. All peptides with the short chain show the same activity, with a minimal biofilm inhibitory concentration (MBIC) of 320 µg/mL. Although the MBIC are quite high, we should emphasize that this activity against the biofilm is "only" 20-fold the concentration against planktonic bacteria, whereas the MBIC for other antibiotics, as is the case of rifampicin, that is more than 800-fold the MIC.[423]

Code	peptide	MIC (µg/mL)	
		S. aureus	***S. aureus biofilm***
CP-A4-C10	*c*-[QKZ^{C10}WSKSR]	16	320
CP-A4-C14	*c*-[QKZ^{C14}WSKSR]	16	1250
CP-A6-C10	*c*-[QKZ^{C10}WSKSX]	8	320
CP-A6-C14	*c*-[QKZ^{C14}WSKSX]	32	2500
CP-A-C10	*c*-[QKZ^{C10}WSKSK]	16	320
CP-A-C14	*c*-[QKZ^{C14}WSKSK]	16	1250

ND = not detected. Z = propargylglycine. X = 2,3-diaminopropionic acid.

Table 2.9. *Activity of the cyclic peptides against S. aureus and its biofilm.*

We also compared the activity of our cyclic peptide with commercial antibiotics, vancomycin and ampicillin (Figure 2.13). Although these antibiotics do not have the same mechanism of action, vancomycin is used to treat MRSA infections. The vancomycin reduces the biofilm at many concentrations, from 500 µg/mL to 16 µg/mL, but we did not find a concentration under 500 µg/mL in which all the biofilm disappears in presence of the

[423] Salem, A. H.; Elkhatib, W. F.; Noreddin, A. M., *J. Pharm. Pharmacol.*, **2011**, 63, 73-79.

commercial antibiotic. In the case of ten carbons cyclic peptides, the biofilm disappears completely at 625 µg/mL.

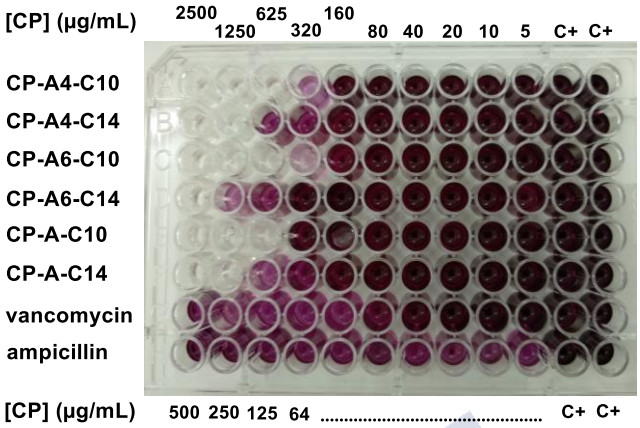

Figure 2.22. *Inhibition of the biofilm of the cyclic peptides CP-A4, CP-A6 and CP-A with their alkyl chains compare with the commercial antibiotics, vancomycin and ampicillin.*

Experiments of inhibition of the formation of *S. aureus* biofilm was also carried out using the xCELLigence® System RTCA with the cyclic peptides. The bacteria (10^7 CFU/mL) was incubated in the presence of the cyclic peptides at different concentrations (Figure 2.23). At 250 µg/mL, all the peptides tested inhibit the formation of the biofilm. At 125 µg/mL, **CP-A4$_{10}$**, **CP-A4$_{14}$** and **CP-A6$_{14}$** also inhibit the formation of the biofilm, but **CP-A$_{10}$** and **CP-A6$_{10}$** present high cell index after 20 hours. Moreover, at 64 µg/mL (Figure 2.23C), **CP-A$_{10}$** and **CP-A4$_{14}$** still inhibit the biofilm formation. Although the experiment was carried out at lower concentrations (32 µg/mL, Figure 2.23D), no inhibition was observed. Despite the inhibition of the biofilm formation can be a result of the death of the bacteria at these concentrations, that are much higher than the MICs, these experiments confirm that the peptides can be used to prevent the formation of the biofilm.

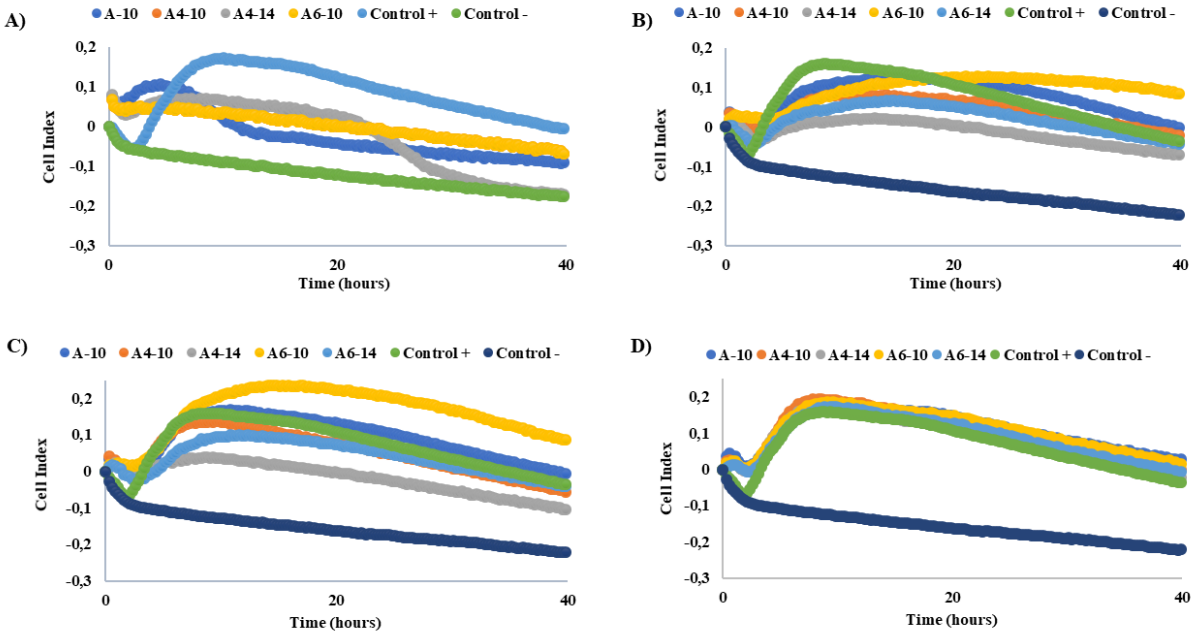

Figure 2.23. *Inhibition of the formation of the biofilm at A) 250 µg/mL, B) 125 µg/mL, C) 64 µg/mL, D) 32 µg/mL.*

2.5. Glycopeptides with a saccharide in its structure.

During the course of this work, Dr. Veronica Prado, working under Prof. Concepcion Bello supervision, synthesized a saccharide derivative (compound **18**, Figure 2.24) protected with Fmoc on the amino group. The trans diol was protected as a trans dimethoxy derivate acetal of 2,3-butanedione. The chirality of this residue would be equivalent to a *D*-α-residue based on the previously stablish for structural analogues.[424] This fully protected amino acid can be used in solid phase synthesis using Fmoc/^{t}Bu methods.

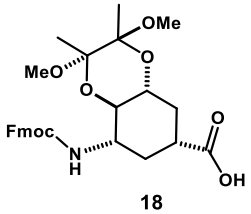

18

Figure 2.24. *Structure of the compound **18**.*

[424] Amorín, M.; Castedo, L.; J. R. Granja, *Chem. Eur. J.*, **2008**, 14, 2100-2111.

γ-Amino acids have been used by our group in the formation of nanotubes.[313a,424,425] This new amino acid would substitute one of the *D*-residues of the active compounds. In this case, we considered to substituted one of the Ser for this new γ-residue, leading to an additional hydroxy group. The incorporation of the γ-residue restrict the inter-ring rotation characteristic of *D,L-α*-cyclic peptide nanotubes. This nanotube face would be decorated by hydroxy groups that could mimic the saccharide properties. Therefore, cyclic peptides derived from previous studies, **CP-A6** and **CP-A7**, were designed and, as mentioned, the ser was substituted by the γ-amino acid. Lysine in the four position was also substituted by an arginine in **CP-A7**. Alkyl chains having ten and fourteen carbons were attached to these cyclic peptides. The structures are shown in Figure 2.25. In addition, we also considered Ghadiri´s model, *c*-[WLWKSKZK] (entry 5, Table 16), in which Z residue represent the serine in which a glycoside was formed on its side chain. Based on this peptide, we proposed two cyclic peptides, **CP-C1** and **CP-C2** (Figure 2.25). In these peptides, one or two serines were substituted by the γ-amino acid **18**. **CP-C1** and **CP-C2** were tested against bacteria and compared with cyclic peptide *c*-[WLWKSKZK]. The results are summarized in Table 2.10. Both cyclic peptides were less active than Ghadiri´s model against *S. aureus*. Interestingly, **CP-C1** shown a quite promising activity against *S. epidermidis* and is more active than the one with two γ-residues (**CP-C2**).

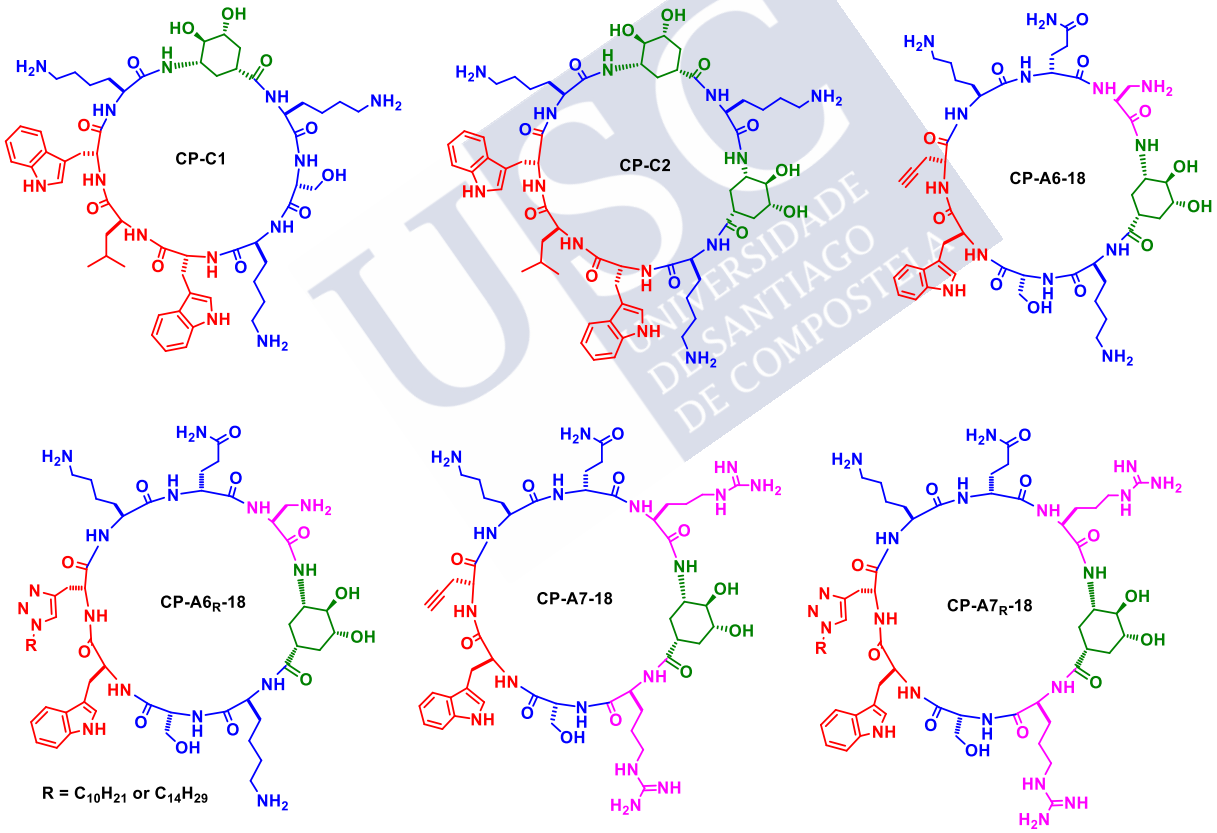

Figure 2.25. *Structure of the compounds with the saccharide in its sequence.*

[425] a) Rodríguez-Vázquez, N.; Amorín, M.; Granja, J. R., *Org. Biomol. Chem.*, **2017**, 15, 4490-4505. b) Fuertes, A.; Ozores, H. L.; Amorín, M.; Granja, J. R., *Nanoscale*, **2017**, 9, 748-753.

Code	peptide	MIC (μg/mL)		
		S. aureus	***S. epidermidis***	***E. coli***
entry 5 (Table 16)	*c*-[WLWKSKZK]	10	---	---
CP-C1	*c*-[WLWKSK18K]	64	8	64
CP-C2	*c*-[WLWK18K18K]	125	32	125

--- = not measured.

Table 2.10. *Activity of the compounds* ***CP-C1*** *and* ***CP-C2*** *compared with the analogue c-[WLWKSKZK].*

In summary, in this chapter we synthesized and tested a library of peptide. In general, the peptides, in which several alkyl chains were attached, were very soluble in aqueous conditions, allowing to carry out the biological assays with aqueous solutions and non-organic solvent (DMSO) or any other reagents were required. From these studies, we found that alkyl chains of ten and fourteen are the more effective, although we do not know the reason. Twelve carbon chains have shown a reduced activity compared with ten and fourteen carbons chains. Peptide with fourteen carbon chains are more effective against the Gram-negative bacteria, while the shorter chain provides stronger Gram-positive antibacterial activities.

The incorporation of the saccharide reduces the activities of the cyclic peptides. Fortunately, these saccharides seem not necessary in terms of toxicity (haemolysis) because all the peptides derived from **CP-A** presented very low haemolytic activity even at concentrations as high as 250 μg/mL. These initial studies suggest to us that the second residue of the CP structure was playing an important role in term of antimicrobial activity. Therefore, a new set of cyclic peptides were synthesized, in which this lysine residue was substituted by arginine, ornithine and 2,3-diaminopropionic acid. These peptides exhibit a relevant activity against Gram-positive bacteria, specially *S. epidermidis*. The most active peptides were tested against *S. aureus* biofilm, achieving MBIC values not so far from the MIC levels for planktonic *S. aureus*.

Finally, a new kind of cyclic peptides were also designed and tested. These peptides incorporate a new non-natural residue, a γ-amino acid, that can resemble a hybrid structure between saccharide and an amino acid. This substitution provides cyclic peptides with good antimicrobial activity against Gram-positive bacteria. New studies about nanotube formation, mode of action and activities incorporating different alkyl chains should be carried out.

USC
UNIVERSIDADE
DE SANTIAGO
DE COMPOSTELA

Chapter 3: Drug delivery systems for anticancer therapy

USC
UNIVERSIDADE
DE SANTIAGO
DE COMPOSTELA

3.1. Introduction.

Cancer is expected to rank as the leading cause of death and the single most important barrier to increasing life expectancy in every country of the world in the 21st century.[426] According to the WHO in 2015, cancer is the first or second leading cause of death before age 70 years in 91 of 172 countries, ranking third or fourth in additional 22 countries (Figure 3.1). The rising incidence in developing countries is likely due to the increasing adaptation of risk factors associated with the Western lifestyle,[427] yet the differing cancer profiles in individual countries and between regions signify that market geographic diversity still exists, with a persistence of local risk factors in populations at quite different phases of social and economic transition.

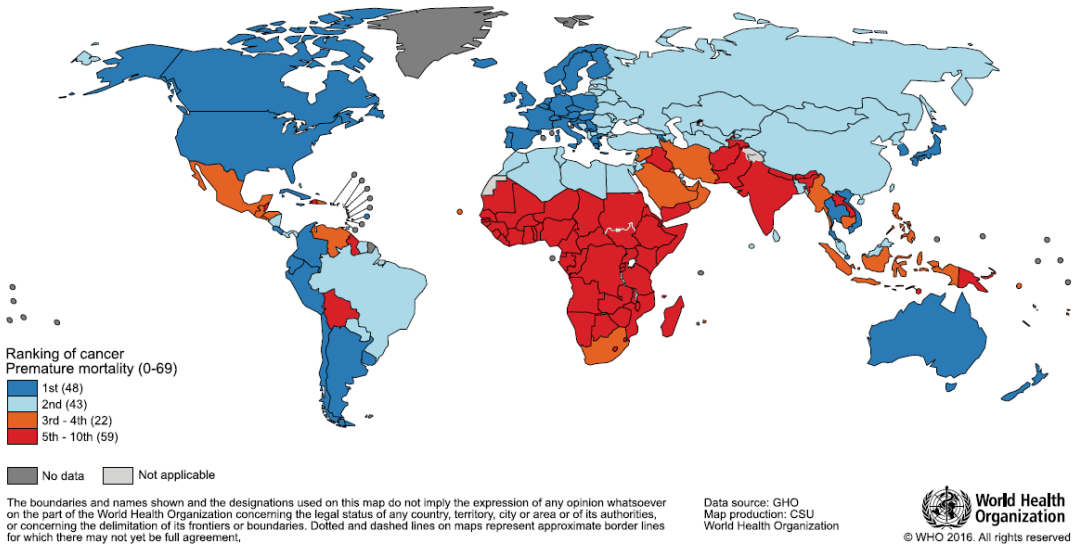

Figure 3.1. *Global map presenting the national ranking of cancer as a cause of death at ages below 70 years in 2015. In brackets are the numbers of countries represented in each ranking. Source: World Health Organization.*

It has been estimated that there were 18.1 million new cases and 9.6 million cancer deaths worldwide in 2018 (Table 3.1). Lung cancer is the most commonly diagnosed cancer (11.6% of the total cases) and the leading cause of cancer death (18.4% of the total cancer deaths), closely followed by female breast cancer (11.6%). By sex, lung cancer is the most commonly diagnosed cancer and the leading cause of cancer death in males, followed by prostate and colorectal cancer for incidence, and liver and stomach cancer for mortality (Figure 3.2). Among females, breast cancer is the most commonly diagnosed cancer, followed by colorectal and lung cancer. Cervical cancer ranks fourth for both incidence and mortality (Figure 3.2).

[426] Bray, F. *et al*, *CA Cancer J. Clin*., **2018**, 68, 394-424.
[427] a) Gersten, O.; Wilmoth, J. R., *Demogr. Res*., **2002**, 7, 271-306. b) Bray, F. in Stewart BW, Wild CP, eds. World Cancer Report **2014**. Lyon: IARC Press; 2014, 42-55. c) Maule, M.; Merletti, F., *Lancet Oncol*., **2012**, 13, 745-746.

Cancer site	Nº of new cases (% of all sites)	Nº of deaths (% of all sites)
Lung	2,093,876 (11.6)	1,761,007 (18.4)
Breast	2,088,849 (11.6)	626,679 (6.6)
Prostate	1,276,106 (7.1)	358,989 (3.8)
Colon	1,096,601 (6.1)	551,269 (5.8)
Nonmelanoma of skin	1,042,056 (5.8)	65,155 (0.7)
Stomach	1,033,701 (5.7)	782,685 (8.2)
Liver	841,080 (4.7)	781,631 (8.2)
Rectum	704,376 (3.9)	310,394 (3.2)
Esophagus	572,034 (3.2)	508,585 (5.3)
Cervix uteri	569,847 (3.2)	311,365 (3.3)
Thyroid	567,233 (3.1)	41,071 (0.4)
Bladder	549,393 (3.0)	199,922 (2.1)
Non-hodgkin lymphoma	509,590 (2.8)	248, 724 (2.6)
Pancreas	458,918 (2.5)	432,242 (4.5)
Leukemia	437,033 (2.4)	309,006 (3.2)
Kidney	406,262 (2.2)	175,098 (1.8)
Corpus uteri	382,069 (2.1)	89,929 (0.9)
Lip, oral cavity	354,864 (2.0)	177,384 (1.9)
Brain, nervous system	296,851 (1.6)	241,037 (2.5)
Ovary	295,414 (1.6)	184,799 (1.9)
Melanoma of skin	287,723 (1.6)	60,712 (0.6)
Gallbladder	219,420 (1.2)	165,087 (1.7)
Larynx	177,422 (1.0)	94,771 (1.0)
Multiple myeloma	159,985 (0.9)	106,105 (1.1)
Nasopharynx	129,079 (0.7)	72,987 (0.8)
Oropharynx	92,887 (0.5)	51,005 (0.5)
Hypopharynx	80,6088 (0.4)	34,984 (0.4)
Hodgkin lymphoma	79,990 (0.4)	26,167 (0.3)
Testis	71,105 (0.4)	9,507 (0.1)
Salivary glands	52,799 (0.3)	22,176 (0.2)
Anus	48,541 (0.3)	19,129 (0.2)
Vulva	44,235 (0.2)	15,222 (0.2)
Kaposi sarcoma	41,799 (0.2)	19,902 (0.2)
Penis	34,475 (0.2)	15,138 (0.2)
Mesothelioma	30,443 (0.2)	25,576 (0.3)
Vagina	17,600 (0.1)	8,062 (0.1)

Table 3.1. *New cases and deaths for 36 cancers and all cancers combined in 2018.*

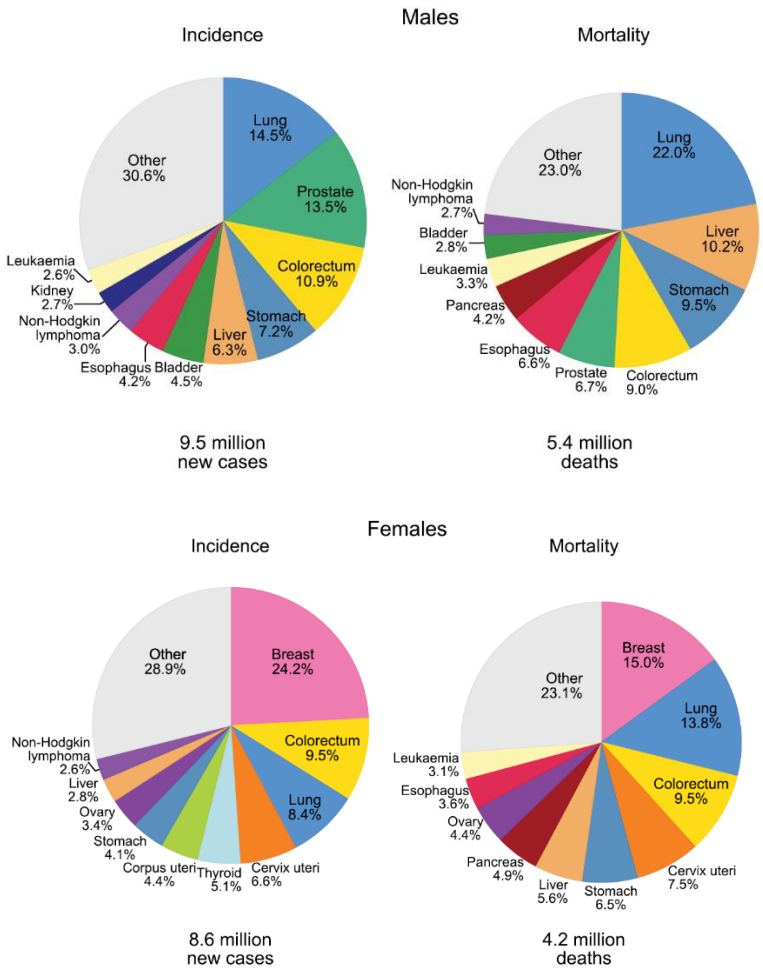

Figure 3.2. *Pie charts present the distribution of cases and deaths for the 10 most common cancers in 2018 for males (top) and females (bottom). For each sex, the area of the pie chart reflects the proportion of the total number of cases or deaths; nonmelanoma skin cancers are included in the 'other' category. Source: GLOBOCAN 2018.*

3.1.1. Breast cancer.

Humankind has struggled to understand and treat breast cancer since the earliest documentation more than 3500 years ago. The visible signs and symptoms of breast cancer and the palpability and tangibility of the lumps at later stages of the disease have enabled easy diagnosis by physicians in almost every period of recorded history. From the ancient civilizations and through the 18th and 19th centuries, it was recognized that breast cancer could not be cured once the cancer had spread.[428] Breast cancer is characterized by uncontrolled growth of malignant cells in the mammary epithelial tissue. It is the most frequent type of cancer in women worldwide (although can affect both genders), with an incidence that rises dramatically with age. A much modern description of the breast cancer is "a heterogenous disease that displays diversity in histopathology, genetic variation, molecular subtype and clinical outcome". Since 1999, incidence rates of breast cancer have stabilized among women aged 50 or over, which may reflect trends in mammography screening rates. However, in most countries, breast cancer incidence rates are increasing, including in countries with historically higher rates, such as those in

[428] Lukong, K. E., *BBA Clinical*, **2017**, 7, 64-77.

Europe, as well as regions with historically lower incidence rates like many countries in Latin America, Asia and Africa.[429] One in every eight women confronts a breast cancer diagnosis throughout her lifetime in developed countries.[430] This rise is generally due to changes in reproductive patterns such as age at menarche, age at first pregnancy, number of births, and duration of breastfeeding.[431] Moreover, recurrent or metastatic disease develops in 20-30% of patients.[432]

Estrogens are hormones that regulate mammary gland development and the female menstrual cycle and are essential for successful reproduction. The estrogen was discovered in 1929 but was not until 1960s, when it was demonstrated that estrogen bound to a molecule,[433] which was later identified as the estrogen receptor.[434] These were significant discoveries because in the 1970s it was demonstrated that breast tumors grew in response to estrogen, which intensified the quest for antiestrogen drugs. The FDA approved tamoxifen for the treatment of metastatic estrogen receptor-positive breast cancer in 1977. The FDA later approved tamoxifen as adjuvant therapy for post-menopausal women (1986) and for prophylactic use in women at high risk of breast cancer (1998).[435] Almost 40 years since its approval, tamoxifen is still considered as the gold standard for the treatment of all stages of estrogen-receptor-positive breast cancers.

Several significant events took place during the 90s:

1) Emergence of taxanes as important chemotherapeutic drugs for breast cancer treatment (1994).

2) The introduction of bone-building drugs that helped to reduce complications of breast cancer (1995).

3) The approval of capecitabine, an oral chemotherapeutic drug (1998).

4) The identification of specific inherited mutations in tumour suppressor genes *BRCA1* and *BRCA2* that increased the risks of breast and ovarian cancers (1994).[436]

Carriers of the cancer-associated genes *BRCA1* and *BRCA2* have been shown to display between a 40% and 80% risk of developing breast cancer by age 70.[437] Families with a history of both breast and ovarian cancers are usually associated with inherited *BRCA1* mutations, whereas families that include male breast cancer cases are more commonly linked to *BRCA2* mutations.

[429] DeSantis, C. E., *Cancer Epidemiol. Biomark. Prev*., **2015**, 24, 1495-1506.
[430] Aktas, B. Y.; Guner, G.; Guven, D. C.; Arslan, C.; Dizdar, O., *Expert Rev. Anticancer Ther*., **2019**, 19, 589-601.
[431] Gonzalez-Jimenez, E.; Garcia, P. A.; Aguilar, M. J.; Padilla, C. A.; Alvarez, J., *J. Clin. Nurs*., **2014**, 23, 2397-2403.
[432] O´Shaughnessy, J., *Oncologist*, **2005**, 10, Suppl 3:20-29.
[433] Jensen, E. V.; Jacobson, H. I.; Walf, A. A.; Frye, C. A., *Physiol. Behav*., **2010**, 99, 151-162.
[434] Gorski, J.; Toft, D.; Shyamala, G.; Smith, D.; Notides, A., *Recent Prog. Horm. Res*., **1968**, 24, 45-80.
[435] Jordan, V. C., *Nat. Rev. Drug Discov*., **2003**, 2, 205-213.
[436] a) Narod, S. A.; Foulkes, W. D., *Nat. Rev. Cancer*, **2004**, 4, 665-676. b) Miki, Y. *et al*, *Science*, **1994**, 266, 66-71. c) Wooster, R.; Bignell, G.; Lancaster, J.; Swift, S.; Seal, S., *Nature*, **1995**, 378, 789-792.
[437] Cornejo-Moreno, B. A.; Uribe-Escamilla, D.; Salamanca-Gomez, F., *Isr. Med. Assoc. J*., **2014**, 16, 787-792.

In 2000, breast cancer has been classified in four molecular subtypes: basal-like, human epidermal growth factor receptor 2-positive (HER2), luminal A and luminal B. Both luminal A and B are estrogen receptor positive, whereas the basal-like breast cancers are usually ER-negative, progesterone-receptor negative, and HER2-negative tumors (hence, "triple-negative" breast cancers or TNBCs). This TNBC accounts for the 10-20% of all breast cancers, which is the most aggressive and invasive tumour subtype of breast cancer.[438,439] Considerable number of breast cancer deaths, especially TNBCs, are due to metastasis. TNBCs are resistant to common therapies of breast cancer such as endocrine therapy and/or therapies that target HER2.

3.1.2. Therapy of breast cancer.

It is well known that, as a result of various types of DNA mutations and genomic instability are related to most steps of carcinogenesis, invasion, metastasis and immune escape mechanisms.[429,440] There are several therapies to treat breast cancer, such as immunotherapy or target therapy. However, the most common one is the chemotherapy, which include the platinum salts and the anthracyclines.

Platinum salts cause covalent crosslinks between DNA bases and are used for the treatment of a various type of cancers.[441] The common action mechanism of cisplatin is damage DNA, blocking cell division that leads in an apoptotic death.[442] All of them are accompanied and potentiated by oxidative stress, where the mitochondria is the primary target. Cisplatin produce acute kidney injury in 30-60% of patients.[443] Renal dysfunction is developed as consequence of the apoptosis and necrosis mediated by oxidative stress.[444]

Current breast cancer treatment options are associated with cardiovascular toxicities that can offset expected therapeutic benefits, disrupt the cancer treatment course, and adversely affect quality of life.[445] Anthracyclines are the most widely used family of chemotherapeutic agents for the treatment of breast cancer,[446] which includes the doxorubicin, daunorubicin, epirubicin and idarubicin (Figure 3.3).[447] Chronic progressive dose-dependent cardiomyopathy is the characteristic presentation of anthracycline-induced cardiotoxicity. Inhibition of topoisomerase-2β leads to oxidative stress, mitochondrial dysfunction and cardiomyocyte apoptosis.[448] An analysis of three studies comprised mostly of breast cancer patients showed a 5% incidence of symptomatic heart failure at a cumulative doxorubicin dose of 400 mg/m^2, increasing to 48% at 700 mg/m^2.[449] Cumulative anthracycline dose is a well-recognized risk factor for development of cardiotoxicity. A recent guideline from the American Society of Clinical Oncology

[438] Tajbakhsh, A.; Rivandi, M.; Adedini, S.; Pasdar, A.; Sahebkar, A., *Crit. Rev. Oncol. Hematol*., **2019**, 140, 17-27.
[439] Stuart, E. C.; Jarvis, R. M.; Rosengren, R. J., *Oncol. Rep*., **2010**, 24, 779-785.
[440] Hanahan, D.; Weinberg, R. A., *Cell*, **2011**, 144, 646-674.
[441] Teo, M. Y. *et al*, *Clin. Cancer Res*., **2017**, 23, 3610-3618.
[442] Negrette-Guzmán, M., *Eur. J. Pharm*., **2019**, 859, 172513.
[443] Sooriyaarachchi, M.; George, G. N.; Pickering, I. J.; Narendran, A.; Gailer, J., *Metall*, **2016**, 8, 1170-1176.
[444] Gómez-Sierra, T.; Eugenio-Pérez, D.; Sánchez-Chinchillas, A.; Pedraza-Chaverri, J., *Food Chem. Toxicol*., **2018**, 120, 230-242.
[445] Lee Chuy, K.; Yu, A. F., *Curr. Treat. Options Oncol*., **2019**, 20, 51-67.
[446] Blum, J.L. *et al*, *J. Clin. Oncol*., **2017**, 35, 2647-2655.
[447] Octavia, Y. *et al*, *J. Mol. Cell. Cardiol*., **2012**, 52, 1213-1225.
[448] a) Zhang, S. *et al*, *Nat. Med*., **2012**, 18, 1639-1642.
[449] Swain, S. M.; Whaley, F. S.; Ewer, M. S., *Cancer*, **2003**, 97, 2869-2879.

states that "high dose" is regarded as a cumulative dose of doxorubicin ≥ 250 mg/m^2 or epirubicin ≥ 600 mg/m^2.[450]

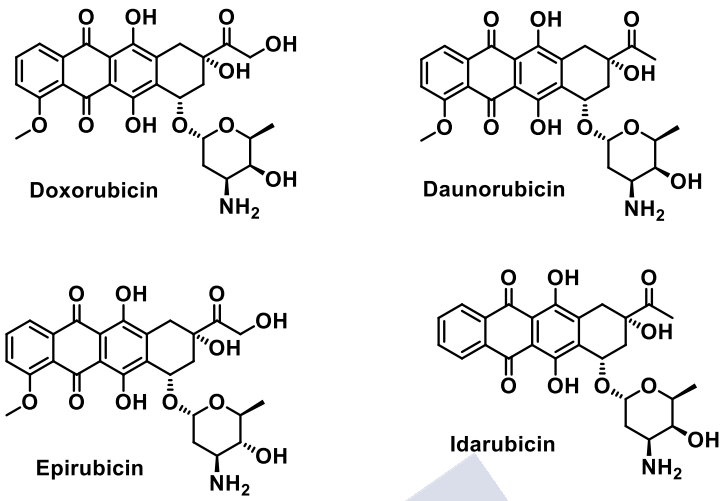

Figure 3.3. *Anthracyclines structures.*

The broad mechanisms underlying DOX-induced cardiotoxicity are: i) oxidative stress, ii) DNA damage and iii) autophagy dysfunction or impaired autophagic flux.[451] The large accumulation of reactive oxygen species caused by DOX, which take places in the mitochondria and cytoplasm, has been recognized as the main source of the cardiac damage. Under DOX treatment, hydrogen peroxide and superoxide radicals are formed. This process leads to the production of the highly reactive and toxic hydroxyl radical by the iron-catalyzed Haber-Weiss reaction.[452] The toxic effects of doxorubicin are, among others, hematopoietic suppression, nausea, vomiting, extravasation, alopecia and, the most feared side effect, cardiotoxicity.[453] Strategies to mitigate anthracycline-induced cardiotoxicity including continuous versus bolus administration, liposomal formulation of doxorubicin, and cardioprotective agents (such as dexrazoxane) can reduce the risk of cardiotoxicity and should be considered in patients with metastatic breast cancer requiring high doses of anthracyclines.[450] Dexrazoxane, which chelates iron and prevents free radical generation, afforded about a 65-80% lower risk of left ventricular dysfunction among patients receiving high doses of anthracyclines with no clear effect on treatment efficacy.[454]

[450] Armenian, S. H. *et al*, *J. Clin. Oncol*., **2017**, 35, 893-911.
[451] Xiao, B. *et al*, *Oncol. Lett*., **2019**, 18, 2165-2172.
[452] a) Shabalala, S.; Muller, C. J. F.; Louw, J.; Johnson, R., *Life Sci*, **2017**, 180, 160-170. b) Cappetta, D. *et al*, *Oxid. Med. Cell Longev*., **2017**, 1521020.
[453] Tassone, P. *et al*, *Br.J. Cancer*, **2003**, 88, 1285-1291.
[454] a) Marty, M. *et al*, *Ann. Oncol*., **2006**, 17, 614-622. b) Swain, S. M. *et al*, *J. Clin. Oncol*., **1997**, 15, 1318-1332.

Although there is a dilemma about promoting or suppressing oxidative stress, using or not using antioxidants for cancer treatment,[455] there are reports that suggest antioxidants as promising chemotherapeutics.[456] Antioxidants exhibit cell-specific effects such as apoptosis and cell cycle arrest as well as cytoprotection or negligible effects in normal cells.[457] Sulforaphane and curcumin (Figure 3.4) are natural compounds with protective effects against oxidative damage induced by toxic drugs, and has been combined with cisplatin and doxorubicin in order to reduce its side effects.[442]

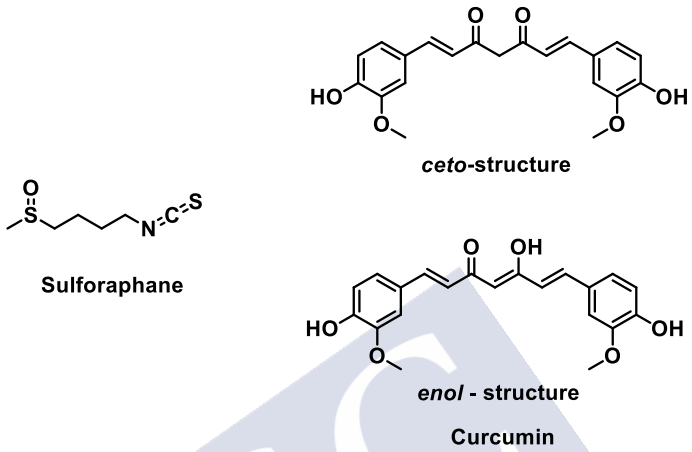

Figure 3.4. *Structure of Sulforaphane and Curcumin.*

Trastuzumab is a humanized monoclonal antibody that binds to the extracellular domain IV of HER2. Cardiotoxicity with trastuzumab was first recognized in patients with metastatic breast cancer undergoing concurrent treatment with anthracyclines.[458] The combination of chemotherapy with trastuzumab for adjuvant treatment was associated with a twofold increased risk of late-onset heart failure.[459] Importantly, treatment interruption occurs in 15-20% of patients due to cardiotoxicity.[460] Cardiac dysfunction most commonly occurs within 2 years of treatment iniciation.[460a,461] In contrast to anthracyclines, partial to complete left ventricular ejection fraction recovery is common and can be seen in up to 80% of patients by 6-7 months with treatment interruption, spontaneously or with medical treatment.[460b,462]

[455] Galadari, S.; Rahman, A.; Pallichankandy, S.; Thayyullathil, F., *Free Radic. Biol. Med*., **2017**, 104, 144-164.
[456] Salehi, B. *et al*, *Biomolecules*, **2018**, 8, 124.
[457] Zubair, H. *et al*, *Nutr. Canc*., **2017**, 69, 932-942.
[458] Slamon, D. J. *et al*, *N. Engl. J. Med*., **2001**, 344, 786-792.
[459] Banke, A. *et al*, *JACC Heart Fail*., **2019**, 7, 217-224.
[460] a) Romond, E. H. *et al*, *J. Clin. Oncol*., **2012**, 30, 3792-3799. b) Yu, A. F. *et al*, *Breast Cancer Res. Treat.*, **2015**, 149, 489-495.
[461] Cameron, D. *et al*, *Lancet*, **2017**, 389, 1195-1205.
[462] a) Seidman, A. *et al*, *J. Clin. Oncol*., **2002**, 20, 1215-1221. b) de Azambuja, E. *et al*, *J. Clin. Oncol.*, **2014**, 32, 2159-2165.

3.1.3. Nanocarriers for DOX delivery systems.

Nanomedicine is an emerging field where the use of knowledge and techniques of nanoscience are implemented in biomedicine and disease prevention and remediation.[463] Nanostructures can be utilized as delivery agents by encapsulation drugs or attaching therapeutic drugs and deliver them to target tissues with a controlled release.[464] Nanomaterials can be defined as a material with sizes ranged between 1 and 100 nm. The first generation of nanoparticle-based therapy were consisted on lipid systems, such as liposomes and micelles, which are now approved by the FDA.[465] In the current medical nanotechnology scenario, there are more than fifty products based on this technology.[466] Due to their nano-size, these structures penetrate in the tissue system, facilitate easy uptake of the drug by cells, permit an efficient drug delivery and ensure action at the targeted location.

Although there are several nanocarriers with different drug release profiles, drug delivery systems are usually formulated to reduce the immunogenicity through their coating or chemical functionalization with several substances, such as polymers,[467] natural polysaccharides,[468] antibodies,[469] tuneable surfactants,[470] peptides,[471] etc.[472] The nanocarriers have been used to pass through the cell membrane and allow a programmed drug delivery in a particular environment. Stimuli-responsive nanocarriers have shown the ability to control the release profile of drugs using external factors such as ultrasound,[473] heat,[474] magnetism,[475] light,[476] pH[477] and ionic strength.[478] As a wide variety of biological sites involve pH gradients, such as the acidic pH found in various tumour tissues, endosomes, liposomes, and inflammatory tissues, pH is a useful external stimulus to trigger drug release in these locations.[479] pH-sensitive nanocarriers have attracted much interest for two reasons. One is that the endosomes into which carriers are incorporated through endocytosis present a more acidic environment (pH 4.5-5.5). The

[463] Patra *et al*, *J. Nanobiotechnol*., **2018**, 16, 71.
[464] a) Jahangirian, H.; Lemraski, E. G.; Webster, T. J.; Rafiee-Moghaddam, R.; Abdollahi, Y., *Int. J. Nanomed*., **2017**, 12, 2957-2978. b) Lam, P. L.; Wong, W. Y.; Bian, Z. Chui, C. H.; Gambari, R., *Nanomedicine*, **2017**, 12, 357-385.
[465] Shi, X; Sun, K. Baker, J.R Jr., *J. Phys. Chem. C*., **2008**, 112, 8251-8258.
[466] a) Ventola, C. L., *Pharm. Ther*., **2017**, 42, 742-755. b) Sainz, V. *et al*, *Biochem. Biophys. Res. Commun*., **2015**, 468, 504-510. c) Hassan, S. *et al*, *Nano Today*, **2017**, 15, 91-106. d) Agrahari, V.; Agrahari, V., *Drug Discov. Today*, **2018**, 23, 974-991.
[467] Pelaz, B. *et al*, *ACS Nano*., **2015**, 9, 6996-7008.
[468] a) Almalik, A. *et al*, *Sci. Rep*., **2017**, 7, 10542. b) Martens, T. F. *et al*, *J. Control Release*, **2015**, 202, 83-92.
[469] Kolhar, P. *et al*, *Proc. Natl. Acad. Sci U.S.A*., **2013**, 110, 10753-10758.
[470] Muller, J. *et al*, *Biomaterials*, **2017**, 115, 1-8.
[471] Gao, H. *et al*, *Sci. Rep*., **2013**, 3, 2534.
[472] Sharma, P. *et al*, *Chemico-Biological Int*., **2019**, 309, 108720.
[473] Anirudhan, T. S.; Nair, A. S., *J. Mater. Chem. B*, **2018**, 6, 428-439.
[474] a) Al-Ahmady, Z.; Kostarelos, K., *Chem. Rev*., **2016**, 116, 3883-3918. b) Bai, Y.; Xie, F. Y.; Tian, W., *Chin. J. Polym. Sci*., **2018**, 36, 406-416. c) Zhang, Z. *et al*, *Coll. Surf. B*, **2017**, 159, 905-912.
[475] a) Guo, Y. *et al*, *J. Control Release*, **2017**, 272, 145-158. b) Hervault, A.; Thanh, N. T., *Nanoscale*, **2014**, 6, 11553-11573.
[476] Mathiyazhakan, M.; Wiraja, C.; Xu, C. J., *Nanomicro. Lett*., **2018**, 10, 10.
[477] Xu, L. *et al*, *J. Mater. Chem. B*, **2018**, 6, 510-517.
[478] Ma, G. L. *et al*, *J. Mater. Chem. B*, **2017**, 5, 935-943.
[479] Gu, L. *et al*, *J. Bioact. Compat. Polym*., **2017** ,32, 3-16.

second reason is that acidosis in tumour tissue may be exploitable for selective targeting of tumour over normal tissues.[480]

The release of the drug for an external stimulus is usually based on dynamic bonds, which can reversibly break and reform.[481] The condensation reaction between an aldehyde and a primary amine to give an imine plus water is widely a known organic reaction. One of the disadvantages of imine chemistry is the hydrolytic instability of the imine bond.[482] Nevertheless, examples of drug delivery systems of DOX through an imine bond can be found in literature.[483] The susceptibility to hydrolysis can be avoided by using more stable acylhydrazones or oximes. Acylhydrazones and oximes can be formed by reacting aldehyde with hydrazide and hydroxylamine (also known as alkoxyamine) respectively.[484] Both hydrazone and oxime formation are "click" reactions.[485]

Hydrazones are small, organic molecules where the imine (N=C) is cleavage via a hydrolysis reaction, so the drug can be released in a controlled manner.[486,487] Hydrazones are stable in blood, which has neutral pH. However, near the tumour sites or within the endosomes of cells and the cargo can be released due to their lower pH, leading to the active drug.[488] These characteristics have allowed hydrazones to be linked to many drugs, including cisplatin.[489] Doxorubicin was conjugated through a pH-sensitive hydrazone to avoid toxicity, which has resulted in a high survival rate.[490] DOX-loaded micelle, where the hydrazone bond is between DOX and polyethylene glycol chain (PEG) bearing a hydrazone moiety at the end of the chain, enhanced circulation times in the bloodstream. Other micelles are based on polymers that are biodegradable, where the DOX is still connected to the nanoparticles by an hydrazone bond.[491] The system DOX-hydrazone was also applied in gold nanoparticles.[492]

The application of oxime bond in bioconjugation is limited due to its greater thermodynamic stability, which delays the release of drug at acidic targets.[480] Oximes are ideally suited for preparing bioconjugates that are stable at physiological pH. Moreover, oxime exchange may be useful for applications in which covalent capture and controlled release are needed.[493] Thus, bioconjugates of DOX and daunorubicin were prepared by covalently attaching drug to gonadotropin-releasing hormone-III (GnRh-III) hormone.[494]

---

[480] Kanamala, M.; Wilson, W. R.; Yang, M.; Palmer, B. D.; Wu, Z., *Biomaterials*, **2016**, 85, 152-167.
[481] Chakma, P.; Konkolewicz, D., *Angew. Chem. Int. Ed.*, **2019**, 58, 9682-9695.
[482] Godoy-Alcántar, C.; Yatsimirsky, A. K.; Lehn, J. M., *J. Phys. Org. Chem.*, **2005**, 18, 979-985.
[483] a) Li, Y.; Bui, Q. N.; Duy, L. T. M.; Yang, H. Y.; Lee, D. S., *Biomacromolecules*, **2018**, 19, 2062-2070. b) Han, X.; Meng, X.; Wu, Z.; Wu, Z.; Qi, X., *Mater. Sci. Eng. C*, **2018**, 93, 1064-1072.
[484] Jin, Y.; Yu, C.; Denman, R. J.; Zhang, W., *Chem. Soc. Rev.*, **2013**, 42, 6634-6654.
[485] Xi, W.; Scott, T. F.; Kloxin, C. J.; Bowman, C. N., *Adv. Func. Mater.*, **2014**, 24, 2572-2590.
[486] Wahbeh, J.; Milkowski, S., *SLAS Technology*, **2019**, 24, 161-168.
[487] Kolmel, D.; Tool, E., *Chem. Rev.*, **2017**, 117, 10358-10376.
[488] Sonaware, S.; Kalhapure, R.; Govender, T., *Eur. J. Pharm. Sci.*, **2017**, 99, 45-65.
[489] Dhar, S.; Gu, F. X.; Langer, R.; Farokhza, O. C.; Lippard, S. J., *Proc. Natl. Acad. Sci. U. S. A.*, **2008**, 17356-17361.
[490] a) Cheng, Y. *et al*, *Small*, **2014**, 10, 5137-5150. b) Crisalli, P.; Kool, E.; *Org. Lett.*, **2013**, 15, 1646-1649. c) Ye, W. *et al*, *Nat. Res. J.*, **2015**, 5, 14614.
[491] Gatti, S. *et al*, *Nanotechnology*, **2018**, 29, 305602.
[492] Liyanage, P. Y. *et al*, *Biochim. Biophys. Acta Rev. Cancer*, **2019**, 1871, 419-433.
[493] a) Ulrich, S.; Boturyn, D.; Marra, A.; Renaudet, O.; Dumy, P., *Chem. Eur. J.*, **2014**, 20, 34-41. b) Rashidian, M.; Song, J. M.; Pricer, R. E.; Distefano, M. D., *J. Am. Chem. Soc.*, **2012**, 134, 8455-8467. c) Haney, C. M.; Loch, M. T.; Horne, W. S., *Chem. Commun.*, **2011**, 47, 10915-10917.
[494] a) Szabó, I. *et al*, *Bioconjug. Chem.*, **2009**, 20, 656-665. b) Jin, Y. *et al*, *Biomacromolecules*, **2011**, 12, 3460-3468.

3.2. Objective.

Peptides are most versatile tools with immense potential for the development of cancer diagnosis and therapies.[495] Anticancer peptides is a term used to distinguish a group of peptides that are derived from antimicrobial peptides but show cancer-selective toxicity by membranolytic activity.[496] They are able to distinguish cancer cells due to abnormalities in cancer cell membrane composition.

On the other hand, the peptides used as drug delivery systems are usually cell penetrating peptides (CPPs). They are typically short peptides of less than 30 amino acids that can pass through cell membranes and transport attached cargoes along with them. Classically, cargoes were attached to CPPs by covalent conjugation or by fusion of the cargo with the CPP.[495]

In this chapter we proposed to exploit the antimicrobial behaviour of our peptides as anticancer transporting agents, using them as drug delivery systems of an anticancer drug in a combinatorial therapy manner. Therefore, we decided to take advantage of the alkoxyamine present in our cyclic peptide skeletons to attach an anticancer compound and delivery it to the cancer cell. The dynamic bond could allow the release of the cytotoxic compound inside the cell (or at the membrane) and reduce the toxicity associated with the drug itself.

For this purpose, we proposed to test the best antimicrobial cyclic peptides as anticancer compounds as well as combine them with the doxorubicin in order to facilitate its transport to improve the anticancer properties of the anthracyclines against breast cancer and reduce its toxicity. To achieve this purpose, we planned to incorporate the alkoxyamine on **CP-A4** and **CP-A6**. Based on the result of the alkoxyamines in each of remaining lysine amino acids against bacteria, we decide to introduce it in the fourth position (*c*-[QRSK^{Ox}SWZ^{10}K] and *c*-[QXSK^{Ox}SWZ^{10}K], Figure 3.5).

[495] Kurrikoff, K.; Aphkhazava, D.; Langel, Ü., *Curr. Opin. Pharmacol*., **2019**, 47, 27-32.
[496] Gaspar, D.; Veiga, A. S.; Castanho, M. A., *Front. Microbiol*., **2013**, 4, 294.

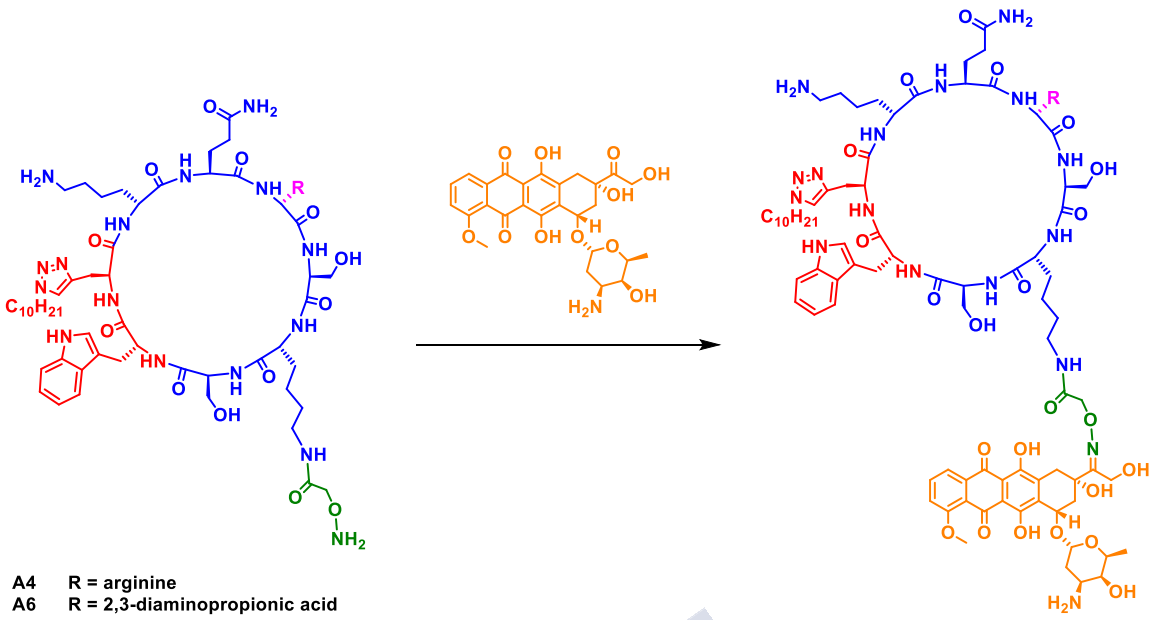

Figure 3.5. *Combination of the cyclic peptide with the doxorubicin by an oxime bond reaction.*

3.3. Synthesis and activity of the cyclic peptides with and without doxorubicin by oxime bond attachment.

The cyclic peptides were synthesis following the same strategy previously optimized and reported on chapter 1. After the peptide purification, the doxorubicin was attached to the cyclic peptide in 10% acetic acid/H_2O at room temperature for 12 hours (overnight). With this method, we prepared the cyclic peptides **CP-A4$_{10}$-DOX**, **CP-A6$_{10}$-DOX** in quantitative yields as was determined by HPLC analysis, in which only the peak of the product was observed. In order to determine if the aliphatic tail plays also an important role in the anticancer activity, in the same way that the antimicrobial activity, we also prepared the **CP-A1-DOX** and **CP-A2-DOX** (Figure 3.6).

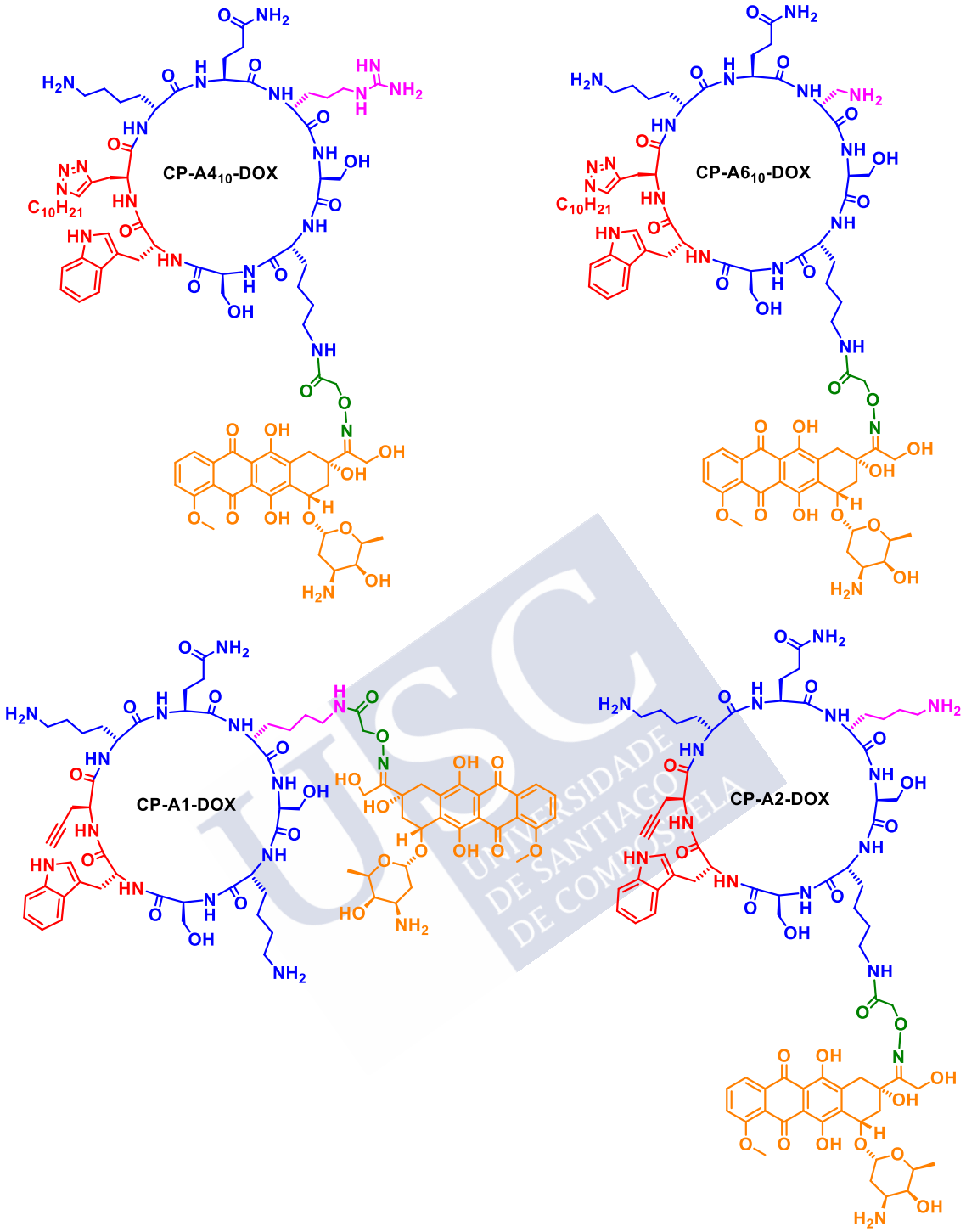

Figure 3.6. *Peptides prepared with DOX in the lysine-oxime side chain.*

All cyclic peptides were characterized before tested against breast cancer cells. STEM images show some kind of fibres of the cyclic peptides containing DOX. The cyclic peptide **CP-A4$_{10}$-DOX** at 0.005 mg/mL form fibres (Figure 3.7a) whereas at higher concentrations, big sheets was also observed (Figure 3.7b), demonstrating that the tubular structure formation depends on the concentration of the sample. For the rest of the peptides, the tubular structures were obtained at the highest concentration tested (0.5 mg/mL). TEM images was also obtained for **CP-A2-DOX** (Figure 3.7f).

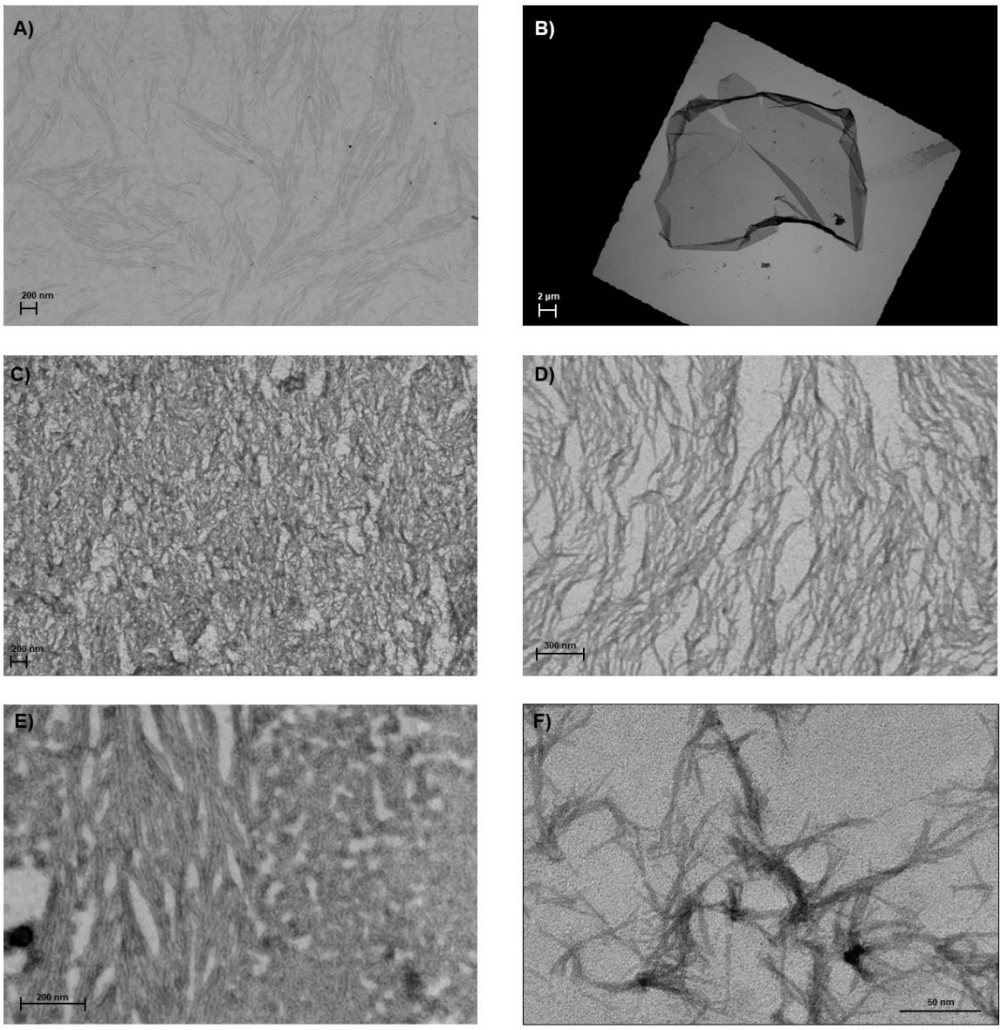

Figure 3.7. *STEM images (A-E) of the cyclic peptides prepared with doxorubicin and dissolved in water. A)* ***A4-C10-DOX*** *(0.005 mg/mL). B)* ***A4-C10-DOX*** *(0.5 mg/mL). C)* ***A6-C10-DOX*** *(0.5 mg/mL). D)* ***A1-DOX*** *(0.5 mg/mL). E)* ***A2-DOX*** *(0.5 mg/mL). F) TEM images of* ***A2-DOX*** *(0.5 mg/mL).*

The ^{1}H-NMR of compounds **CP-A4$_{10}$-DOX** and **CP-A6$_{10}$-DOX** (0.5 mg/mL) show not-defined signals that correspond with highly aggregate structures. On the other hand, ^{1}H-NMR of **CP-A1-DOX** and **CP-A2-DOX** (0.5 mg/mL, Figure 3.8) are well defined confirming the importance of the alkyl chain in the aggregation properties.

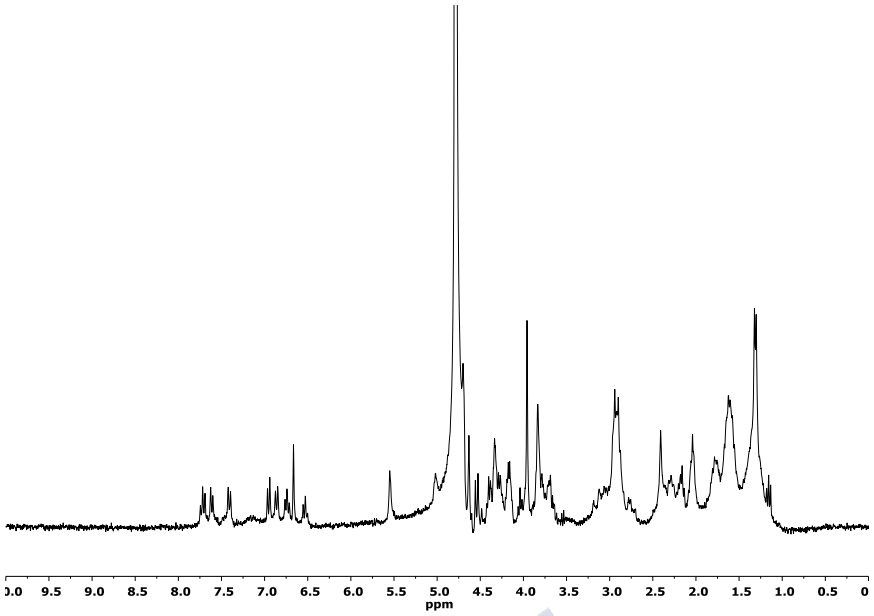

Figure 3.8. *^{1}H-NMR of peptide* ***CP-A2-DOX****.*

With the collaboration of Prof. Mabel Loza group, the compounds with and without **DOX** were tested against breast cancer cell line MCF-7. The cytotoxicity studies were carried out by MTT assays and summarized in Table 3.2. The activity of the compounds is directly related with the cell growth inhibition. In other words, the low inhibition means that the peptide has not activity against cancer cells. For the peptides **A1** and **A2**, the activity is small, confirming previous results related with toxicity in mammalian cells. Opposed to the antimicrobial activities, **CP-A4$_{10}$** present less activity than **CP-A6$_{10}$**, with 40% of inhibition. Moreover, the activity of peptides **CP-A6$_{10}$** and **CP-A6$_{10}$-DOX** are quite the similar, with 46% inhibition of cell growth at a peptide concentration of 100 μM. Therefore, from this initial evaluation, it seems that **DOX** incorporation is not playing an important role in the anticancer efficacy. In any case, the most active compounds are those having **DOX** covalent linked. Interestingly, one of the active peptides is the 2,3-diaminopropionic acid derivative having the ten carbons chain while the second one, **CP-A2-DOX**, has not the alkyl chain.

Code	Conc. (μM)	% cell growth inhibition ± standard error
CP-A4$_{10}$	100	29 ± 4
CP-A1	100	6 ± 3
CP-A2	100	9 ± 2
CP-A6$_{10}$	100	40 ± 2
CP-A2-DOX	100	46 ± 2
CP-A6$_{10}$-DOX	100	46 ± 2

Table 3.2. *Percentage of cell growth inhibition.*

The more potent peptides, **CP-A1-DOX** and **CP-A4$_{10}$-DOX**, were measured at different concentrations to determine the IC_{50} and the maximum percentage of inhibition and compare with doxorubicin activity. The results of these studies are shown in Table 3.3. **CP-A1-DOX** present moderate inhibition efficiency against breast cancer cell. However, the compound **CP-A4$_{10}$-DOX** is more efficiency than the control. Unfortunately, they are less potent than the **DOX** by itself. In fact, they are between 5 and 10 times less active than **DOX**.

Code	Emax (%inhibition)	± standard error	IC_{50} (μM)	± standard error (μM)	Figure 3.9
CP-A1-DOX	68	2	4.10	0.17	A
CP-A4$_{10}$-DOX	91	1	8.33	0.39	B
DOX	86	1	0.82	0.07	C

Table 3.3. *Inhibitory efficiency of the MCF-7 cell growth.*

The inhibition curves as a function of the concentration of these three compounds are shown in Figure 3.9.

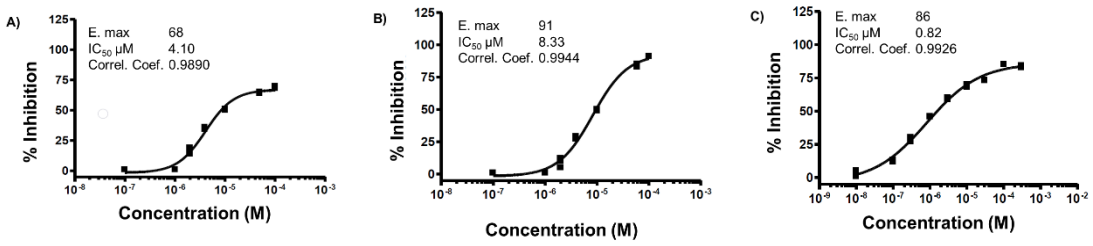

Figure 3.9. *Cell line MCF-1 growth inhibition as a function of concentration for A)* ***CP-A1-DOX****, B)* ***CP-A4$_{10}$-DOX****, C)* ***DOX*** *(control).*

The same peptides were also tested against the ovarium cell line NCI/ADR-RES, which is a doxorubicin resistant cell line. The results of the MTT assays are summarized in Table 3.5. In this case, all peptides showed low cell growth inhibition, with the exception of **CP-A4$_{10}$-DOX**, which was the only peptide with higher inhibition than **DOX** itself. Unfortunately, it was not possible to determine the curve of inhibition as a function of the concentration as these activities are smaller than 50%.

Code	Conc. (μM)	% cell growth inhibition ± standard error
CP-A4$_{10}$	100	28 ± 3
CP-A1	100	13 ± 1
CP-A2	100	20 ± 2
CP-A6$_{10}$	100	1 ± 1
CP-A1-DOX	100	6 ± 2
CP-A2-DOX	100	8 ± 3
CP-A4$_{10}$-DOX	100	48 ± 2
CP-A6$_{10}$-DOX	100	38 ± 3
DOX	100	43 ± 3

Table 3.4. *Percentage of NCI/ADR-RES cell growth inhibition.*

For these cell line, they determined the inhibition efficiency and the inhibition power of the cisplatin. Cisplatin show an Emax of 91%, same value that **CP-A4$_{10}$-DOX** achieved with the breast cancer cells and showed an IC_{50} of 13 μM (Figure 3.10).

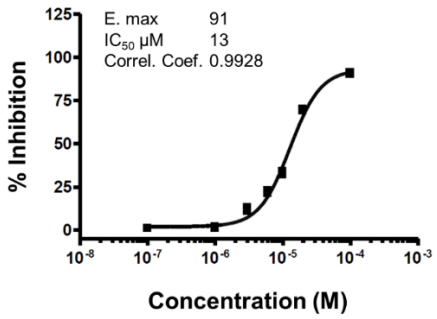

Figure 3.10. *Cell growth inhibition of the NCI/ADR-RES ovarian cell induced by cisplatin.*

The results obtained with **DOX** attached to the cyclic peptides suggest that **DOX** liberation must be playing an important role because in all the cases the cell grow inhibition is always smaller that the drug by itself. Many studies reported that within the early stages of the endosome to the lysosome maturation, the pH drops from 6.2 to 5.0,[497] so we decided to measure the released of the **DOX** at different pH over time. The release of **DOX** could be follow by HPLC. They can be distinguished by HPLC as it is indicated in figure 3.11. One important point of this study is the stability of the **DOX-CP** conjugates. They were stable to the HPLC conditions. Compound **CP-A2-DOX** was incubated at pH 4 at room temperature and the solution was followed by HPLC for 12 h. As it is shown in Figure 3.12, the trace of **DOX** formation was almost negligible. This study confirms the high stability of oxime bond and, consequently, the difficulties to

[497] a) Schmaljohann, D., *Adv. Drug Deliv. Rev*., **2006**, 58, 1655-1670. b) Hu, R.; Zheng, H.; Cao, J.; Davoudi, Z.; Wang, Q., *J. Biomed. Nanotechnol*., **2017**, 13, 1097-1105.

release the drug at the endosome, which might explain the low activity observed in the cytotoxicity studies.

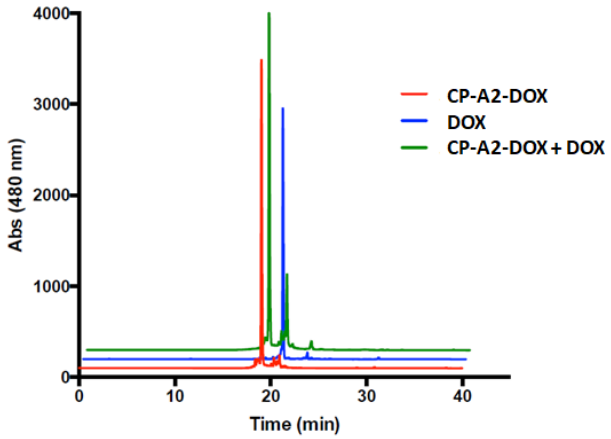

Figure 3.11. *Measurements of the peptide* ***CP-A2-DOX***, ***DOX*** *and a mixture of* ***CP-A2-DOX*** *and* ***DOX****. Method: [Agilent C18 column, H_2O (0.1% TFA)/ACN (0.1% TFA). 100:0 →100:0 (5 min) and 100:0 → 5:95 (30 min)]*

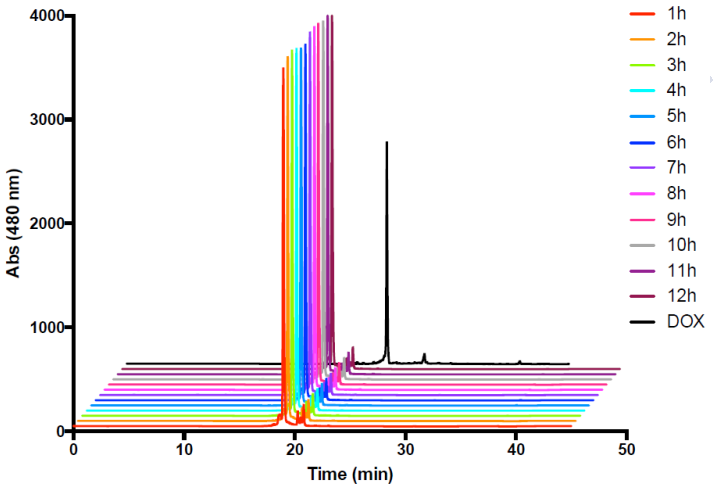

Figure 3.12. *Measurements of the peptide* ***CP-A2-DOX*** *at pH 4 for 12 hours.* ***DOX*** *is measured as control. No release is observed. Method: [Agilent C18 column, H_2O (0.1% TFA)/ACN (0.1% TFA). 100:0 →100:0 (5 min) and 100:0 → 5:95 (30 min)]*

In summary, in this chapter we proposed the most active cyclic peptide developed in the previous chapter as drug delivery systems. We attached **DOX** to four different peptides and we tested them against breast and ovarium cancer cells. Two cyclic peptides, **CP-A1-DOX** and **CP-A4$_{10}$-DOX** present activity against the breast cancer cell line. Interestingly, one of these peptides do not have an alkyl chain. Unfortunately, any of the peptides tested were active against ovarian cell line. At the view of the results, we concluded that the drug delivery system was not working as we expected due to the cargo was not released.

USC
UNIVERSIDADE
DE SANTIAGO
DE COMPOSTELA

Conclusions

USC
UNIVERSIDADE
DE SANTIAGO
DE COMPOSTELA

Throughout this Ph.D., we have proposed and developed a synthetic strategy for the preparation of cyclic peptides with antimicrobial properties. For this purpose, we have planned a divergent strategy that allows the preparation of a library of cyclic peptides starting form a common basic platform. This platform would have an amphipathic structure that contain two reactive moieties. Each of these reactants would be placed in different environments, one at the hydrophilic core and the other one in the hydrophobic side. As reactive groups we selected two orthogonal click-type reactions, the copper catalysed [3+2] cycloaddition and the formation of an oxime bond.

The platforms proposed in this project were composed by eight α-amino acids with an alternating chirality that allow the flat conformation of the cyclic peptide. Moreover, the amphipathic structures contained only two hydrophobic amino acids, which provides them a very good solubility in aqueous media. Two different platforms were designed, **CP-A** and **CP-B**, in which the reactive ends are placed at different environments of the amphipathic peptides.

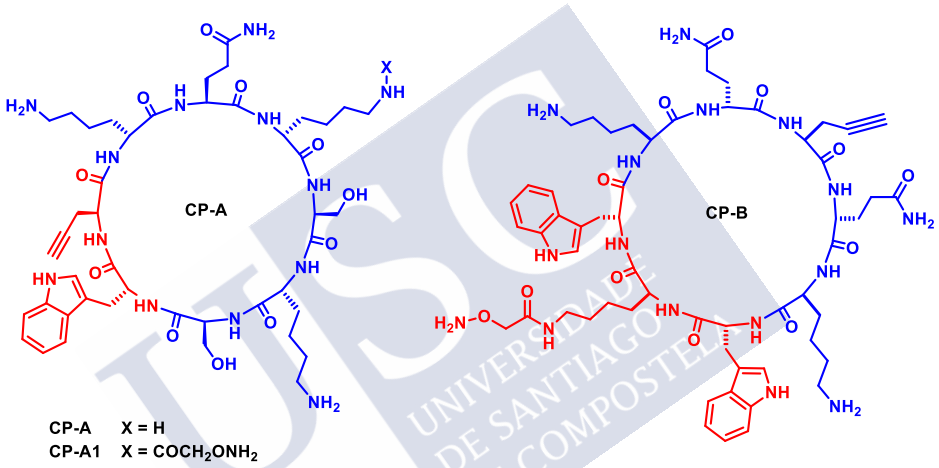

Our first approach implied the studies to attach the saccharide by a [3+2] cycloaddition reaction in the hydrophilic side of platform **CP-B**. Unfortunately, this reaction was not very successful due to the limited solubility of both components in the studied conditions. On the other hand, the condensation of **CP-B** with different aldehydes took place with good yields, although the purification of derivatives with long alkyl chains was tedious and difficult.

The antibacterial assays were optimized using some of the peptides of the series **CP-B**, which were tested against two Gram-positive bacteria, *S. aureus* and *S. epidermidis*, and one Gram-negative bacteria, *E. coli*. These cyclic peptides showed low activity against the Gram-positive bacteria and no detectable activity against Gram-negative.

At the view of these results, we decided to change the strategy for platform **CP-A**. This peptide presented the triple bond in the hydrophobic core of the molecule. CuAAC transformation and alkoxyamine incorporation were optimized to be carried out on the solid support. On the other hand, the alkoxyamine was incorporated at different positions of the platform, which would allow the optimization of the properties of the cyclic peptide, **CP-A1**, **CP-A2** and **CP-A3**.

In the second chapter of this manuscript, biological assays of derivatives with alkyl chains of different lengths in **CP-A1** and **CP-A2** were carried. These studies showed an improvement of the activity upon increase of alkyl chain, achieving the highest activities with lengths of ten and fourteen carbon atoms. Moreover, **CP-A1$_{14}$** showed no toxicity under 125 μg/mL and only a 25% of toxicity at a concentration of 500 μg/mL. The introduction of saccharides reduces the toxicity of this compound, specially the cyclic peptide with glucose, **CP-A1$_{14}$-Glu**, which showed no toxicity at the highest concentration tested, leading to a therapeutic window of 15 folds the MIC for Gram-positive bacteria and 7.8 folds the MIC for Gram-negative bacteria. In addition, **CP-A2$_{10}$** show no toxicity at any concentration tested, even in absence of saccharides, showing a therapeutic window of at least 15 folds the MIC.

The substitution of the lysine amino acid in the cyclic peptide skeleton for another cationic residues (**CP-A4**, **CP-A5** and **CP-A6**) showed a general improvement in the activity. However, the toxicity was also increased specially for **CP-A4$_{14}$** and **CP-A6$_{14}$**, leading to a smaller therapeutic window for these compounds (4 folds the MIC).

Bactericidal studies were also carried out against *S. aureus* biofilm. The cyclic peptides show bactericidal activity around 20 folds the MIC. Inhibition of the formation of the biofilm studies were also tested. However, the results showed a reduction of the biofilm more according to the fast death of the bacteria cells than to a mechanism of inhibition of biofilm formation by itself. To sum up, in the presence of the cyclic peptide, the size of the resulting biofilm is smaller than control, therefore the peptides could be used in the prevention of the biofilm formation.

In the third and last chapter of this manuscript, we proposed the use of these cyclic peptide as drug delivery systems using a dynamic bond (alkoxyamine) for the release of the drug, doxorubicin, for the treatment of breast and ovarium cancer. Preliminary results showed a general pattern of low activity. Only two cyclic peptides, **CP-A1-DOX** and **CP-A4$_{10}$-DOX** present some activity against the breast cancer cell line. The lack of activity could be related to the release process of the doxorubicin as suggested by the kinetic studies of oxime stability. In order to improve the release of the doxorubicin, furthers studies will be carried out with the hydrazone as dynamic bond, which is more labile than the oxime bond.

Experimental Section

USC
UNIVERSIDADE
DE SANTIAGO
DE COMPOSTELA

Materials and methods

1-[Bis(dimethylamino)methylene]-1H-1,2,3-triazolo[4,5-b]pyridinium 3-oxid hexafluorophosphate or Hexafluorophosphate Azabenzotriazole Tetramethyl Uronium (*N*-HATU), 2-(1H-benzotriazol-1-yl)-1,1,3,3-tetramethyluronium hexafluorophosphate or Hexafluorophosphate Benzotriazole Tetramethyl Uronium (*N*-HBTU), 2-(1H-benzotriazol-1-yl)-1,1,3,3-tetramethyluronium tetrafluoroborate (*N*-TBTU), (7-azabenzotriazol-1-yloxy)tripyrrolidinophosphonium hexafluorophosphate (PyAOP), hydroxybenzotriazole (HOBt), *N*-(3-dimethylaminopropyl)-*N´*-ethylcarbodiimide hydrochloride (EDC·HCl), 4-dimethylaminopyridine (DMAP) and the α-amino acids were purchased from Iris Biotech, Novabiochem, Advanced Chemtech, Aldrich, and/or GL Biochem (Shangai) Ltd. Rink Amide resin was purchased from Novabiochem and chlorotrityl chloride (CTC) resin was purchased from Iris Biotech. Triisopropylsilane (TIS) and diisopropylethyl amine (DIEA) were purchased from Sigma-Aldrich. Trifluoroethanol and 1,1,1,3,3,3-hexafluoroisopropanol (HFIP) were purchased from TCI. All solvents were HPLC grade purchased from Aldrich or Fisher Scientific, using without additional purification, except the dry DCM, which were distilled with CaH_2. We used synthesis grade DMF to synthesize the peptides in solid phase. Broth cultures and broth agars were purchased from Boente. The 96-well microplates and erythrocytes were purchased from Proquinorte.

Thin-layer chromatography (TLC) were used by pieces of 2 x 5 cm of TLC silicagel 60 F_{254} plates, purchased from Merk, which thickness is 0.2 mm. The analysis of the TLC were carried out by UV at 254 nm for the compounds which absorb at that wavelength, and/or by heating the TLC after treating with a ninhydrin solution (2% in EtOH) or Ce/Mo (200 mg of cerium nitrate and ammonium, 9.6 g of ammonium molybdate, 11.2 mL H_2SO_4, 200 mL H_2O). Silica gel (high-purity grade, pore size 60 Å, 230-400 mesh particle size) was used for flash column chromatography. HPLC semi-preparative purification was carried out on Hitachi D-7000 and Jasco LC-4000 with an Agilent Eclipse XDB-C18 column. High-performance liquid chromatography coupled with mass spectrometry (HPLC-MS) analysis were carried out on Agilent Technologies 1260 Infinity II associated with a 6120 Quadrupole LC-MS using an Agilent SB-C18 column.

Nuclear Magnetic Resonance (NMR) spectra were recorded on a Varian Mercury 250, Varian Mercury 300 MHz and a Varian Inova 500 MHz. $CDCl_3$, D_2O, and H_2O/D_2O were the solvents employed to obtain the NMR. Chemical shifts are reported in ppm referenced to TMS ($\delta = 0.00$ ppm) or to the solvent signals, HOD ($\delta = 4.79$ ppm). Spin multiplicities are reported as a singlet (s), doublet (d), triplet (t), multiplet (m) or broad (b). The coupling constants (*J*) are given in Hz.

Accurate mass determination (HR-MS) were carried out in "Servicio de Espectroscopía de Masas de la Universidad de Santiago de Compostela" (USC), using a Bruker MicroTof to realize the ESI-MS. The data is expressed in units of mass per unit of load (m/z).

STEM experiments were carried out in "Microscopía Electrónica e Confocal" which is part of "Servicio de Microscopía Electrónica e Confocal e de Apoio ás Especialidades Biolóxicas" (USC), using a ZEISS FESEM ULTRA Plus with EDX with a resolution of 0.8 nm at 30 kV for STEM mode.

Bacterial assays were carried out in "Departamento de Microbioloxía de la Facultad de Medicina (USC)". The bacteria strains used in this work were: *S. aureus* CECT 794, *S. epidermidis* CECT 231, *E. coli* CECT 101, *E. faecalis* CECT 795, *S. mutans* CECT 479T, and MRSA isolated from the "Santiago de Compostela" university hospital. They assays were measured by Biochrom EZ Read 400 Elisa and Galapagos software for EZ Read microplate (Biochrom) was used to export the data as xls file. Inhibition of biofilm quantification was done using the xCELLigence® System RTCA (ACEA, Biosciences Inc.). The increase in the cell adherence is expressed into a dimensionless parameter called cell index. E-plates 16 were used to execute the experiment.

A Tecan Ultra Evolution microplate reader (595 nm) was used to measure directly in cell culture 96-well plates UV-Vis absorbance for the MTT viability assays carried out by Prof. Mabel Loza group. Tecan Infinity F200 Pro (450 nm and 570 nm) (CIQUS) was used to measure directly in cell culture 96-well plates UV-Vis absorbance for the MTT viability assays.

Chapter 1

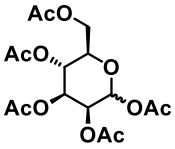

2

1,2,3,4,6-penta-O-acetyl-*D*-mannose (2). *D*-mannose (1.13 g, 6.25 mmol) was solved in acetic anhydride (16 mL) in an ice bath. Iodine (107 mg, 0.42 mmol) was added slowly. After 1 h of stirring, the ice bath was removed, and the reaction was stirred another 2 h at room temperature. Then, the reaction was cooled again at 0 ºC and MeOH was added slowly, after which the reaction was stirred for 12 h. The MeOH was removed under high vacuum and the precipitate was solved in DCM (30 mL) and the solution was made up with $Na_2S_2O_3$ (1 M, 3 x 50 mL) to remove the iodine. The organic phase was dried with anhydride Na_2SO_4, filtered and concentrated under high vacuum to obtain the compound 1,2,3,4,6-penta-O-acetyl-*D*-mannose (**2**) as a white lather [2.39 g, 90%, R_f = 0.47 (50% EtOAc/hexane)]. **^{1}H-NMR** ($CDCl_3$, 250 MHz, δ): 6.00-5.99 (d, 2H, H-1), 5.27-5.25 (m, 2H, H-2 and H-3), 5.18-5.17 (m, 1H, H-4), 4.23-4.16 (m, 1H, H-5), 4.04-3.96 (m, 2H, C$\underline{H}_2$OAc), 2.09 (2s, 6H, OAc), 2.02 (s, 3H, OAc), 2.01 (s, 3H, OAc), 1,97 (s, 3H, OAc), 1.92 (s, 3H, OAc).

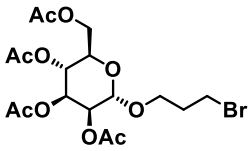

3

2,3,4,6-tetra-O-acetyl-α-*D*-mannopyranoside of 3-bromopropyl (3). Compound **2** (0.73 g, 1.87 mmol) was solved in dry DCM (12 mL) under argon atmosphere. Trimethylene bromohydrin (250 µL, 2.76 mmol) and boron trifluoride diethyl etherate (1.3 mL, 10.26 mmol) were added and stirred in dark for 4 h at room temperature. Then, DCM (40 mL) was added and the reaction was made up with an aqueous solution of $NaHCO_3$ (40 mL) and H_2O (3 x 20 mL). The organic phase was dried with anhydride Na_2SO_4, filtered and concentrated under high vacuum. The crude was purified by silica gel column chromatography (20-50% EtOAc/hexane) to obtain the compound 2,3,4,6-tetra-O-acetyl-α-*D*-mannopyranoside of 3-bromopropyl (**3**) as a light-yellow oil [398 mg, 45%, R_f= 0.69 (50% EtOAc/hexane)]. **^{1}H-NMR** ($CDCl_3$, 250 MHz, δ): 5.07-5.01 (m, 3H, H-2, H-3, H-4), 4.63 (s, 1H, H-1), 4.10-4.03 (m, 2H, 2H-6), 3.93-3.68 (m, 3H, H-5 and C$\underline{H}_2$OAc), 3.43-3.30 (m, 4H, CH_2-CH_2-Br), 1.95 (s, 3H, OAc), 1.89 (s, 3H, OAc), 1.85 (s, 3H, OAc), 1.78 (s, 3H, OAc).

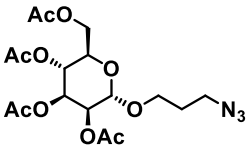

4

2,3,4,6-tetra-O-acetyl-α-*D*-mannopyranoside of 3-azidopropyl (4). Compound **3** (188 mg, 0.4 mmol) was solved in DMF (7 mL) and heated to 60 º C under argon atmosphere. Sodium azide (153 mg, 2.35 mmol) was added slowly and the reaction was stirred for 1.5h at 60 ºC. Then, the solvent was removed under high vacuum. The crude was solved in DCM (15 mL) and made up with MilliQ H_2O (4 x 5 mL), dried with anhydride Na_2SO_4, filtered and concentrated under high vacuum. The crude was purified by silica gel column chromatography (10-50% EtOAc/hexane) to obtain the compound 2,3,4,6-tetra-O-acetyl-α-*D*-mannopyranoside of 3-azidopropyl (**4**) as a light-yellow oil [118 mg, 69%, R_f= 0.73 (50% EtOAc/hexane)]. **^{1}H-NMR** ($CDCl_3$, 250 MHz, δ): 5.27-5.26 (m, 2H, H-3 and H-4), 5.16 (m, 1H, H-2), 4.75 (s, 1H, H-1), 4.21 (dd, *J* = 12,2; 5,4 Hz, 2H, C$\underline{H}_2$OAc), 4.04 (dd, *J* = 12,2; 2,4 Hz, 1H, H-5), 3.79-3.70 (m, 1H, O-$\underline{CH}_2$-CH_2-CH_2-N_3), 3.50-3.46 (m, 1H,

O-CH$_2$-CH$_2$-CH$_2$-N$_3$), 3.44-3.34 (m, 2H, O-CH$_2$-CH$_2$-CH$_2$-N$_3$), 2.08 (s, 3H, OAc), 2.03 (s, 3H, OAc), 1.98 (s, 3H, OAc), 1.92 (s, 3H, OAc), 1.77 (m, 2H, CH$_2$-CH$_2$-CH$_2$).

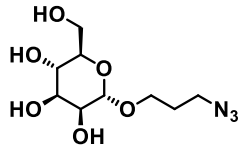

5

α-*D*-mannopyranoside of 3-azidopropyl (5). Compound **4** (60 mg, 0.14 mmol) was solved in HPLC MeOH (1 mL) and treated with an aqueous solution of NH_3 (25%, 250 μL). The reaction was stirred for 1 hour at room temperature. Then, solvent was removed at high vacuum and H_2O was added and the solution was lyophilized several times until all ammonium acetate was completely removed, leading to a non-colour oil (24 mg, 60%).**^{1}H-NMR** ($CDCl_3$, 300 MHz, δ): 4.96 (ancho, OH), 4.83 (s, 1H, H-1), 3.93 (s, 1H, H-1), 3.81-3.74 (m, 6H, H-2, H-3, H-4, H-5, CH$_2$OAc), 3.51-3.49 (m, 1H, O-CH$_2$-CH$_2$-CH$_2$-N$_3$), 3.40-3.36 (m, 2H, O-CH$_2$-CH$_2$-CH$_2$-N$_3$), 1.88-1.83 (m, 2H, CH$_2$-CH$_2$-CH$_2$).

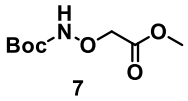

7

(Boc-aminooxy)acetyl methyl ester (7). A solution of (Boc-aminooxy)acetic acid (1.0 g, 5.24 mmol) in dry MeOH (52.4 mL) was purged with argon. The solution was treated with EDC·HCl (1.5 g, 7.85 mmol), HOBt (1.0 g, 7.85 mmol) and DMAP (0.96 g, 7.85 mmol). The resulting mixture was stirred for 3 h at room temperature. Then, the reaction was worked up with an aqueous solution of HCl at 5% (3 x 15 mL). The organic phase was dried with Na_2SO_4, filtered and the solvent was removed under high vacuum. The crude was purified by silica gel column chromatography (0-20% EtOAc/hexane) to obtain the (Boc-aminooxy)acetyl methyl ester (**7**) as a white solid [1.05 g, 95%, R_f = 0.83 (50% EtOAc/hexane)]. **^{1}H-NMR** ($CDCl_3$, 300 MHz, δ): 7.91 (s, 1H, NH), 4.42 (s, 2H, CH$_2$COOCH$_3$), 3.75 (s, 3H, CH$_2$COOCH$_3$), 1.44 (s, 9H, Boc).

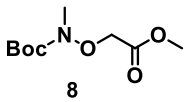

8

(Boc-methyl-aminooxy)acetyl methyl ester (8). A solution of (Boc-aminooxy)acetyl methyl ester (**7**) (1.05 g, 5.12 mmol) in DMF (5 mL) was treated with NaH (0.16 g, 6.66 mmol) and stirred for 15 min. Then, MeI (0.87 g, 6.15 mmol) was added and the mixture was stirred for 2.5 h at room temperature. The solvent was removed under high vacuum and the crude was solved in DCM and mixture with silica gel to create a silica powder with the compound. The powder was purified by silica gel column chromatography (0-10% EtOAc/hexane) to obtain the (Boc-methyl-aminooxy)acetyl methyl ester (**8**) as a white solid [0.72 g, 65%, R_f = 0.91 (50% EtOAc/hexane)]. **^{1}H-NMR** ($CDCl_3$, 300 MHz, δ): 4.34 (s, 2H, CH$_2$COOCH$_3$), 3.64 (s, 3H, CH$_2$COOCH$_3$), 3.07 (s, 3H, N-CH$_3$), 1.44 (s, 9H, Boc).

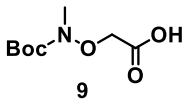

9

(Boc-methyl-aminooxy)acetic acid (9). The (Boc-methyl-aminooxy)acetyl methyl ester (**8**) (0.48 g, 2.2 mmol) was solved in a solution MeOH/H_2O (75:25) (22 mL) cooled in a ice bath. A solution of 28% w/w NaOMe in MeOH was added and the mixture was stirred for 1 h. Then, the ice bath was removed, and amberlite (H^+), previously washed with MeOH, was added until pH = 5 was achieved. The solution was filtered and dried under high vacuum to obtain the (Boc-methyl-aminooxy)acetic acid (**9**) as a impure white solid [0.40 g, 90%, R_f = 0.0

(50% EtOAc/hexane)]. **^{1}H-NMR** ($CDCl_3$, 300 MHz, δ): 8.5 (broad s, 1H, COOH), 4.48 (22 H, CH_2COOCH_3 + H_2O), 3.09 (s, 3H, N-CH_3), 1.44 (s, 9H, Boc).

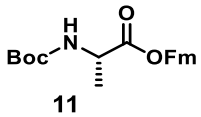

11

Boc-*L*-Ala-OFm (11): A solution of Boc-*L*-Ala-OH (0.5 g, 2.6 mmol) in dry DCM (26 mL) was purged with argon. The solution was treated with EDC·HCl (0.77 g, 4 mmol), HOBt (0.54 g, 4 mmol), DMAP (0.49 g, 4 mmol) and 9-fluorenylmethanol (0.78 g, 4 mmol). The resulting mixture was stirred for 4 h at room temperature. Then, the reaction was worked up with an aqueous solution of HCl at 5% (3 x 15 mL) and saturated solution of Na_2CO_3 (3 x 15 mL). The organic phase was dried with Na_2SO_4, filtered and the solvent was removed under high vacuum. The crude was purified by silica gel column chromatography (0-10% EtOAc/hexane) to obtain the Boc-*L*-Ala-OFm (**11**) as a pure white solid [0.78 g, 82%, R_f = 0.46 (25% EtOAc/hexane)]. **^{1}H-NMR** ($CDCl_3$, 300 MHz, δ): 7.77 (d, *J* = 7.5 Hz, 2H, Ar Fm), 7.60 (t, *J* = 7.2 Hz, 2H, Ar Fm), 7.44-7.29 (m, 4H, Ar Fm), 5.04 (d, 1H, Hα), 4.48 (m, 2H, CH_2 Fm), 4.23 (m, 1H, CH Fm), 1.45 (s, 9H, Boc), 1.32 (d, 3H, CH_3).

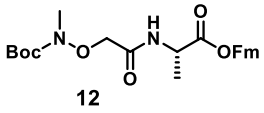

12

(Boc-methyl-aminooxy)CH_2CO-Ala-OFm (12): A solution of Boc-*L*-Ala-OFm (**11**) (0.18 g, 0.49 mmol) in a mixture of TFA and DCM (1:1, 4 mL) was stirred for 20 min at room temperature. The solution was dried under high vacuum and the residue was solved in DCM and dried several times in order to remove all the TFA. The resulting salt was dissolved in dry DCM (5 mL), follow by the addition of DIEA (230 µL, 0.51 mmol), (Boc-methyl-aminooxy)acetic acid (**9**) (0.1 g, 0.49 mmol), y *N*-HBTU (0.2 g, 0.54 mmol). The mixture was stirred for 2 h at room temperature under argon. The reaction was worked up with an aqueous solution of 5% HCl (3 x 4 mL). The organic phase was dried with Na_2SO_4, filtered and the solvent was removed under high vacuum. The crude was purified by silica gel column chromatography (0-30% EtOAc/hexane) to obtain the (Boc-methyl-aminooxy)CH_2CO-Ala-OFm (**12**) as a pure white solid [0.17 g, 79%, R_f = 0.42 (50% EtOAc/hexane)]. **^{1}H-NMR** ($CDCl_3$, 300 MHz, δ): 8.58 (broad s, 1H, NH), 7.77 (d, *J* = 7.47 Hz, 2H, Ar Fm), 7.60 (t, *J* = 7.6 Hz, 2H, Ar Fm), 7.42-7.28 (m, 4H, Ar Fm), 4.67 (m, 1H, Hα), 4.46 (m, 2H, CH_2 Fm), 4.35 (s, 2H, CH_2), 4.24 (m, 1H, CH Fm), 3.12 (s, 3H, N-CH_3), 1.45 (s, 9H, Boc), 1.42 (d, 3H, CH_3). **^{13}C-NMR** ($CDCl_3$, 300 MHz, δ): 172.3 (CO), 168,6 (CO), 143.8 (C), 143.4 (C), 141 (CO), 127.8 (CH), 127.1 (CH), 125.1 (CH), 120.0 (CH), 82.9 (C), 73.3 (CH_2), 67.0 (CH_2), 47.8 (CH), 46.8 (CH), 37.4 (CH_3), 28.1 (CH_3), 17.5 (CH_3).

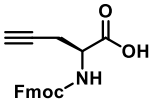

Fmoc-*L*-Prg-OH: A solution of Boc-*L*-Prg-OH (1 g, 4,7 mmol) in a mixture of TFA and DCM (1:1, 4 mL) was stirred for 20 min at room temperature. The solution was dried under high vacuum and the residue was solved in DCM and dried several times in order to remove all the TFA. The resulting salt was dissolved in 10% Na_2CO_3/dioxane (1:1, 20 mL), follow by the dropwise addition of a solution of Fmoc-OSu (1,75 g, 5.2 mmol) in dioxane (10 mL). The mixture was stirred for 12 h at room temperature, after which the dioxane was removed under high vacuum. The aqueous solution was treated with 10% HCl to afford a pH ≈ 3. The **Fmoc-*L*-Prg-OH** was extracted in DCM (4 x 10 mL), dried with Na_2SO_4, filtered and the solvent was removed under high vacuum. The crude was purified by silica gel column

chromatography (0-3% MeOH/DCM) to obtain the compound **Fmoc-*L*-Prg-OH** as a pure white solid [1.1 g, 70%, R_f= 0,71 (MeOH/DCM/AcOH 5:95:0,04)]. **^{1}H-NMR** ($CDCl_3$, 300 MHz, δ): 7,77 (d, *J* = 7,4 Hz, 2H, Ar-H); 7,61 (d, *J* = 7,2 Hz, 2H, Ar-H); 7,43-7,26 (m, 4H, Ar-H); 5,60 (d, *J* = 8,0 Hz, 1H, NH); 4,60 (broad s, 1H, H_α); 4,43 (d, *J* = 7,1 Hz, 2H, CH_2-Fmoc); 4,25 (t, *J* = 7,0 Hz, 1H, CH-Fmoc); 2,85 (broad s, 2H, H_β); 2,11 (s, 1H, C≡C-H).

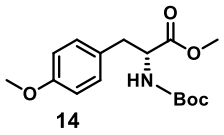

14

Boc-D-Tyr(Me)-OMe (14): A solution of Boc-*D*-Tyr(Me)-OH (0.6 g, 2.0 mmol) in dry MeOH (20 mL) was purged with argon. The solution was treated with EDC·HCl (0.59 g, 3.0 mmol), HOBt (0.41 g, 3.0 mmol) and DMAP (0.37 g, 3.0 mmol). The resulting mixture was stirred for 4 h at room temperature. Then, the solvent was removed under high vacuum and the crude was solved in DCM. The reaction was worked up with an aqueous solution of HCl at 5% (3 x 15 mL) and saturated solution of Na_2CO_3 (3 x 15 mL). The organic phase was dried with Na_2SO_4, filtered and the solvent was removed under high vacuum. The crude was purified by silica gel column chromatography (0-20% EtOAc/hexane) to obtain the Boc-*D*-Tyr(Me)-OMe (**14**) as a pure white solid [0.21 g, 34%, R_f = 0.75 (50% EtOAc/hexane)]. **^{1}H-NMR** ($CDCl_3$, 300 MHz, δ): 7.03-7.00 (d, 2H, H-Ar), 6.82-6.79 (d, 2H, H-Ar), 5.02-4.99 (d, 1H, Hα), 3.75 (s, 3H, Ar-OC<u>H</u>$_3$), 3.68 (s, 3H, COOC<u>H</u>$_3$), 3.02-2.97 (t, 2H, C<u>H</u>$_2$CHα), 1.41-1.39 (s, 9H, Boc).

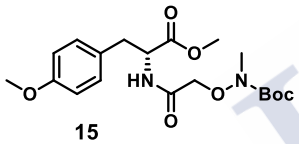

15

(Boc-methyl-aminooxy)CH2CO-Tyr(Me)-OMe (15): A solution of Boc-*D*-Tyr(Me)-OMe (**14**) (0.2 g, 0.65 mmol) in a mixture of TFA and DCM (1:1, 4 mL) was stirred for 20 min at room temperature. The solution was dried under high vacuum and the residue was solved in DCM and dried several times in order to remove all the TFA. The resulting salt was dissolved in dry DCM (10 mL), follow by the addition of DIEA (330 µL, 2.6 mmol), (Boc-methyl-aminooxy)acetic acid (**9**) (0.1 g, 0.48 mmol), y *N*-HBTU (0.27 g, 0.72 mmol). The mixture was stirred for 2 h at room temperature under argon. The reaction was worked up with an aqueous solution of 5% HCl (3 x 4 mL). The organic phase was dried with Na_2SO_4, filtered and the solvent was removed under high vacuum. The crude was purified by silica gel column chromatography (0-60% EtOAc/hexane) to obtain the (Boc-methyl-aminooxy)CH_2CO-*D*-Tyr(Me)-OMe (**15**) as a pure white solid [0.77 g, 30%, R_f = 0.38 (50% EtOAc/hexane)].

General protocol for the SPPS

All peptides were synthesized by manual Fmoc solid phase peptide synthesis, using Fmoc-Rink Amide resin (100 mg, loading 0.7 mmol/g) or CTC resin (200 mg, loading 0.45 mmol/g). The resin was swelled in DCM (HPLC, 3 mL) for 1 hour in a peptide synthesis vessel prior synthesis. Coupling cycle consisted on the removal of the Fmoc protecting group with a solution of piperidine in DMF (25%, 2 mL) for 15 min and then the mixture was filtered, and the resin was washed with DMF (6 x 2 mL). The amino acid coupling was carried out by treatment with a solution of α-amino acids (3 equiv), *N*-HBTU (3 equiv) in DMF (2 mL), which was mixed with DIEA (6 equiv) for 1 min before the addition to the resin. The coupling was shaken for 40 min and washed with DMF (3 x 2 mL). The efficiency of each amino acid coupling and deprotection was monitored employing the TNBS test.

Deprotection of the C-terminal group: The allyl group was removed using a solution of $[Pd(PPh_3)_4]$ prepared *in situ* as a result of mixing $Pd(OAc)_2$ (0.25 equiv) and PPh_3 (1.25 equiv) in dry DCM. Phenylsilane (7 equiv) and 4-methylmorpholine (7 equiv) were added, and the mixture was degassed, through over the resin and shaken for 4-5 hours. After that, the resin was washed with DCM (3 x 2 mL), DMF (3 x 2 mL), 0.5% sodium diethyldithiocarbamate in DMF (2 x 2 mL x 15 min), DMF (2 x 2 mL), 10% DIEA/DMF (2 x 2 mL), DMF (3 x 2 mL).

Deprotection of the N-terminal group: The Fmoc was removed with 25% piperidine/DMF (1 x 2 mL x 30 min). Then, the resin was washed with DMF (6 x 2 mL), 5% DIEA/DMF (3 x 2 mL), 0.8 M LiCl in DMF (3 x 2 mL), DMF (3 x 2 mL).

Cyclization: *N*-TBTU (3 equiv) and DIEA (6 equiv) in DMF (3 mL) were employed in the cyclization reaction (12 hours). The resin was washed DMF (3 x 2 mL) and DCM (3 x 2 mL). For the sequence that one cyclization was not enough to obtain the full product, PyAOP (3 equiv) and DIEA (6 equiv) in DMF (3 mL) were also used, after which the resin was washed in the same way as using *N*-TBTU.

Alkoxyamine: The 4-methyltrityl protecting group was removed with a cocktail of DCM/HFIP/TFE/TIS (0.65:0.2:0.1:0.05; 3 x 3 mL x 2 h), which is prepared freshly before using. Then, the alkoxyamine (2.5 equiv) and *N*-HATU (2.5 equiv) are solved in DMF (3 mL) and add to the resin. DIEA (5 equiv) is directly through over the resin and the mixture is shaken for 30 min.

Cleavage and purification: The peptides were deprotected and cleaved from the resin by standard TFA cleavage procedure at room temperature by using the TFA/TIS/H_2O (95:2.5:2.5, 1 mL per 50 mg of resin) cocktail for 2 hours. Then, the mixture was filtered, washed with TFA (1 mL) and the peptide was precipitated with Et_2O (20 mL of Et_2O for 1 mL of TFA). The precipate was centrifuged and dissolved in H_2O (5-10 mL depending on the solubility in each case). Peptides were purified by semi-preparative high-performance liquid chromatography (HPLC) with a method that would be specified in each case. Finally, the corresponding fractions were lyophilised to afford the pure peptides as white solids.

Synthesis of CP-B:

Following the general protocol of the SPPS, the **CP-B** was grown, cycled and alkoxyamine was introduced in the solid support. Then, the cleavage of the resin was carried out and the resulting powder was solubilized in ACN/H_2O (1:1) and purified in reverse phase HPLC [Phenomenex Luna C18 (2) 100A column, H_2O (0.1% TFA)/ ACN (0.1% TFA) 95:5 → 95:5 (0 → 5 min), 95:5 → 5:95 (5 → 35 min) with an overall yield of 22% (20.2 mg) [Agilent C18 column, H_2O (0.1% TFA)/ACN (0.1% TFA), 75:25 →75:25 (5 min) and 75:25 → 5:95 (30 min)] (R_t = 19.1 min). **MS** (ESI, H_2O): 1180.6 (100, $[M+1H]^+$), 591.0 (45, $[M+2H]^{2+}$). **HRMS** (ESI): Calcd for: $C_{57}H_{80}N_{16}O_{12}$ $[M+1H]^+$: 1180.6283; found 1180.6262.

Synthesis of CP-BAc:

Following the general protocol of the SPPS, the **CP-B** was grown, cycled and alkoxyamine was introduced in the solid support. Then, the cleavage of the resin was carried out and the resulting powder was solubilized in ACN/H_2O (1:1). The addition of acetone lead to the final compound **CP-BAc**, which was purified in reverse phase HPLC [Phenomenex Luna C18 (2) 100A column, H_2O (0.1% TFA)/ ACN (0.1% TFA) 95:5 → 95:5 (0 → 5 min), 95:5 → 5:95 (5 → 35 min) with an overall yield of 10% (9.5 mg). [Agilent C18 column, H_2O (0.1% TFA)/ACN (0.1% TFA). 75:25 →75:25 (5 min) and 75:25 → 5:95 (30 min)] (R_t = 22.7 min). **MS** (ESI, H_2O): 1222.4 (100, $[M+1H]^+$), 611.9 (38, $[M+2H]^{2+}$). **HRMS** (ESI): Calcd for: $C_{60}H_{84}N_{16}O_{12}$ $[M+H]^+$: 1222.6731; found 1222.6731.

Synthesis of CP-BAc-Man:

Following the general protocol of the SPPS, the **CP-B** was grown, cycled and alkoxyamine was introduced in the solid support. Then, the cleavage of the resin was carried out and the resulting powder was solubilized in H_2O. The addition of acetone lead to the compound **CP-BAc**, which was purified in the conditions described above. The **CP-BAc** (8 mg, 6.4 x 10^{-3} mmol) was solved in THF/H_2O and treated with the azide **5** (1.68 mg, 6.4 x 10^{-3} mmol, 0.053 M), $CuSO_4$ (1.6 mg, 6.4 x 10^{-3} mmol), sodium ascorbate (5.1 mg, 25.6 x 10^{-3} mmol) and TBTA (6.8 mg, 12.8 x 10^{-3} mmol). The mixture was stirred overnight under argon atmosphere. The mixture was treated with QuadraSil™-AP resin for 30 min to remove all the copper in the solution, which achieve a final yellow colour. Then, the resin was filtered, and the solution was dried under vacuum to remove the THF. The aqueous solution was purified by reverse phase HPLC [Phenomenex Luna C18 (2) 100A column, H_2O (0.1% TFA)/ ACN (0.1% TFA) 95:5 → 95:5 (0 → 5 min), 95:5 → 25:75 (5 → 35 min) with an overall yield of 4% (4.6 mg).

Synthesis of CP-B_6:

Following the general protocol of the SPPS, the **CP-B** was grown, cycled and alkoxyamine was introduced in the solid support. Then, the cleavage of the resin was carried out and the resulting powder was solubilized in DMSO. Hexyl aldehyde and a 5% acetic acid was added and stirred for 2 hours at 60 ºC, leading to the final compound **CP-B_6**, which was purified in reverse phase HPLC [Phenomenex Luna C18 (2) 100A column,

H_2O (0.1% TFA)/ ACN (0.1% TFA) 75:25 → 75:25 (0 → 5 min), 75:25 → 5:95 (5 → 35 min) with an overall yield of 8% (7.9 mg).

Synthesis of CP-B_{10}:

Following the general protocol of the SPPS, the **CP-B** was grown, cycled and alkoxyamine was introduced in the solid support. Then, the cleavage of the resin was carried out and the resulting powder was solubilized in DMSO. Decyl aldehyde and a 5% acetic acid was added and stirred for 2 hours at 60 ºC, leading to the final compound **CP-B_{10}**, which was purified in reverse phase HPLC [Phenomenex Luna C18 (2) 100A column, H_2O (0.1% TFA)/ ACN (0.1% TFA) 75:25 → 75:25 (0 → 5 min), 75:25 → 5:95 (5 → 35 min) with an overall yield of 5% (5.2 mg). [Agilent C18 column, H_2O (0.1% TFA)/ACN (0.1% TFA). 75:25 →75:25 (5 min) and 75:25 → 5:95 (30 min)] (R_t = 22.8 min). **MS** (ESI, H_2O): 1319.8 (92, $[M+1H]^+$), 660.2 (100, $[M+2H]^{2+}$).

Synthesis of CP-B_{16}:

Following the general protocol of the SPPS, the **CP-B** was grown, cycled and alkoxyamine was introduced in the solid support. Then, the cleavage of the resin was carried out and the resulting powder was solubilized in DMSO. Hexadecyl aldehyde and a 5% acetic acid was added and stirred for 2 hours at 60 ºC, leading to the final compound **CP-B_{16}**, which was purified in reverse phase HPLC [Phenomenex Luna C18 (2) 100A column, H_2O (0.1% TFA)/ ACN (0.1% TFA) 75:25 → 75:25 (0 → 5 min), 75:25 → 5:95 (5 → 35 min) with an overall yield of 6% (6.5 mg). [Agilent C18 column, H_2O (0.1% TFA)/ACN (0.1% TFA). 75:25 →75:25 (5 min) and 75:25 → 5:95 (30 min)] (R_t = 25.8 min). **MS** (ESI, H_2O): 1404.1 (25, $[M+1H]^+$), 702.7 (100, $[M+2H]^{2+}$), 468.2 (8, $[M+3H]^{3+}$).

Synthesis of CP-B-Leu:

Following the general protocol of the SPPS, the cyclic peptide was grown and cycled in the solid support. Then, the cleavage of the resin was carried out and the resulting powder was solubilized in H_2O/ACN. The solution was purified by reverse phase HPLC [Phenomenex Luna C18 (2) 100A column, H_2O (0.1% TFA)/ ACN (0.1% TFA) 95:5 → 95:5 (0 → 5 min), 95:5 → 5:95 (5 → 35 min) with an overall yield of 15% (12.8 mg). [Agilent C18 column, H_2O (0.1% TFA)/ACN (0.1% TFA). 75:25 →75:25 (5 min) and 75:25 → 5:95 (30 min)] (R_t = 20.2 min). **MS** (ESI, H_2O): 1093.3 (75, $[M+1H]^+$), 547.5 (100, $[M+2H]^{2+}$). **HRMS** (ESI): Calcd for: $C_{55}H_{77}N_{14}O_{10}$ $[M+1H]^+$: 1093.5944; found 1093.5942.

Synthesis of *c*-[W<u>L</u>W<u>L</u>W<u>K</u>S<u>K</u>] (code 8 in table 10):

The cyclic peptide was grown in the CTC resin. For that, the first coupling is the reaction of the lysine (0.33 mmol for 200 mg of resin) in DCM (dry) with DIEA (4 equiv, 0.1 ml). After the first coupling, the loading of the resin is calculated by Fmoc test, which consist on deprotected an amount of resin in a determined concentration with 25%

piperidine/DMF and measure the Fmoc release from the resin in the UV at 290 nm and 310 nm. The absorbance can be related with the load of the resin following the equation:

$$\text{Load (resin)} = \frac{\text{Absorbance*Volume (sample, μL)*1000}}{\varepsilon\text{*Volume (fraction, μL)*}\omega\text{(mg)*l(cm)}}$$

$$\varepsilon = 5800\ M^{-1}cm^{-1} \text{ at } 290 \text{ nm and } 7100\ M^{-1}cm^{-1} \text{ at } 301 \text{ nm.}$$

where the volume of the sample and the ω is the determined concentration of the deprotection step and volume (fraction) is the dilution for the UV.

Once the load of the resin is obtained, the rest of the peptide is grown in the same way that we carried out in the Rink Amide resin. After the cyclization, the cleavage of the resin was carried out and the resulting powder was solubilized in H_2O/ACN. The solution was purified by reverse phase HPLC [Phenomenex Luna C18 (2) 100A column, H_2O (0.1% TFA)/ ACN (0.1% TFA) 95:5 → 95:5 (0 → 5 min), 95:5 → 5:95 (5 → 35 min) with an overall yield of 20% (17.6 mg). **HRMS** (ESI): Calcd for: $C_{60}H_{82}N_{13}O_9$ $[M+1H]^+$: 1128.6393; found 1128.6353.

General protocol for the SPPS of serie CP-A:

Serie **CP-A** include an additional step, the introduction of the aliphatic tail by click chemistry reaction before the cleavage of the resin. Furthermore, for the peptides that have a saccharide derived with an aldehyde, this is attached after the cleavage of the resin.

Click chemistry reaction: This step is carried out before cleavage the resin. Firstly, the azide (6 equiv) and the aliphatic bromide (6 equiv) are mixed in DMF (1 mL) for 24 hours at 40 ºC. Then, DMF (0.2 mL) and piperidine (0.3 mL) are added to the resulting aliphatic azide. CuI (5 equiv), sodium ascorbate (5 equiv) and DIEA (10 equiv) are added, and the mixture is purged with argon before. The reaction was shaken at room temperature for 36 hours. Then, the reaction was washed with DCM (3 x 2 mL), DMF (3 x 2 mL), 20% piperidine/DMF (2 x 3 mL x 15 min), DMF (3 x 2 mL), MilliQ H_2O (2 x 2 mL x 10 min), DMF (3 x 2 mL) and DCM (3 x 2 mL).

Introduction of the aldehyde: After the cleavage of the resin, a solution of the CP (10 mM) in H_2O was treated with the aldehyde (120 mM) and shaken for 30 min, after which the reaction was checked for HPLC-MS and purified by reverse phase HPLC. The corresponding fractions were lyophilised to afford the pure peptide as a white solid.

Introduction of the commercial saccharide: After the cleavage of the resin, a solution of the CP (5 mM) in 5% acetic acid/H_2O was treated with the saccharide (120 mM) and shaken for 2 h at 60 ºC, after which the reaction was checked for HPLC-MS and purified by reverse phase HPLC. The corresponding fractions were lyophilised to afford the pure peptide as a white solid.

Synthesis of CP-A:

Following the general protocol of the SPPS, the cyclic peptide was grown and cycled in the solid support. Then, the cleavage of the resin was carried out and the resulting powder was solubilized in H_2O, purified in reverse phase HPLC [Phenomenex Luna C18 (2) 100A column, H_2O (0.1% TFA)/ ACN (0.1% TFA) 100:0 → 100:0 (0 → 5 min), 100:0 → 60:40 (5 → 35 min) with an overall yield of 32% (24.2 mg). [Agilent SB-C18 column, H_2O (0.1% TFA)/ACN (0.1% TFA). 100:0 →100:0 (2 min) and 100:0 → 25:75 (19 min)] (R_t = 9.1 min). **MS** (ESI, H_2O): 968.5 (25, $[M+1H]^+$), 484.9 (100, $[M+2H]^{2+}$), 323.6 (8, $[M+3H]^{3+}$). **HRMS** (ESI): Calcd for: $C_{45}H_{70}N_{13}O_{11}$ $[M+1H]^+$: 968.5316; found 968.5312. **FTIR (neat)**: ν = 3273 (amide A), 1669, 1623 (amide I), 1535 cm^{-1} (amide II).

Synthesis of CP-A1:

Following the general protocol of the SPPS, the cyclic peptide was grown, cycled and alkoxyamine was introduced in the solid support. Then, the cleavage of the resin was carried out and the resulting powder was solubilized in H_2O, purified in reverse phase HPLC [Phenomenex Luna C18 (2) 100A column, H_2O (0.1% TFA)/ ACN (0.1% TFA) 100:0 → 100:0 (0 → 5 min), 100:0 → 60:40 (5 → 35 min) with an overall yield of 28% (22.7 mg). [Agilent SB-C18 column, H_2O (0.1% TFA)/ACN (0.1% TFA). 100:0 →100:0 (2 min) and 100:0 → 25:75 (19 min)] (R_t = 9.3 min). **MS** (ESI, H_2O): 1065.4 (10, $[M+Na]^+$), 1042.5 (25, $[M+1H]^+$), 521.3 (100, $[M+2H]^{2+}$), 348.5 (5, $[M+3H]^{3+}$). **HRMS** (ESI): Calcd for: $C_{47}H_{72}N_{14}O_{13}$ $[M+1H]^+$: 1041.5482; found 1041.5476. **FTIR (neat)**: ν = 3279 (amide A), 1662, 1626 (amide I), 1541 cm^{-1} (amide II).

Synthesis of CP-A2:

Following the general protocol of the SPPS, the cyclic peptide was grown, cycled and alkoxyamine was introduced in the solid support. Then, the cleavage of the resin was carried out and the resulting powder was solubilized in H_2O, purified in reverse phase HPLC [Phenomenex Luna C18 (2) 100A column, H_2O (0.1% TFA)/ ACN (0.1% TFA) 100:0 → 100:0 (0 → 5 min), 100:0 → 60:40 (5 → 35 min) with an overall yield of 27% (21.9 mg). [Agilent SB-C18 column, H_2O (0.1% TFA)/ACN (0.1% TFA). 100:0 →100:0 (2 min) and 100:0 → 25:75 (19 min)] (R_t = 9.5 min). **MS** (ESI, H_2O): 1042.7 (20, $[M+1H]^+$), 521.3 (100, $[M+2H]^{2+}$), 347.9 (10, $[M+3H]^{3+}$). **HRMS** (ESI): Calcd for: $C_{47}H_{72}N_{14}O_{13}Na$ $[M+Na]^+$: 1063.5302; found 1063.5295. **FTIR (neat)**: ν = 3273 (amide A), 1668, 1620 (amide I), 1535 cm^{-1} (amide II).

Synthesis of CP-A3:

Following the general protocol of the SPPS, the cyclic peptide was grown, cycled and alkoxyamine was introduced in the solid support. Then, the cleavage of the resin was carried out and the resulting powder was solubilized in H_2O, purified in reverse phase HPLC [Phenomenex Luna C18 (2) 100A column, H_2O (0.1% TFA)/ ACN (0.1% TFA) 100:0 → 100:0 (0 → 5 min), 100:0 → 60:40 (5 → 35 min) with an overall yield of 28% (22.5 mg). [Agilent SB-C18 column, H_2O (0.1% TFA)/ACN (0.1% TFA). 100:0 →100:0 (2 min) and 100:0 → 25:75 (19 min)] (R_t = 9.4 min). **MS** (ESI, H_2O): 1042.6 (30, $[M+1H]^+$), 521.3 (100, $[M+2H]^{2+}$). **HRMS** (ESI): Calcd for: $C_{47}H_{72}N_{14}O_{13}$ $[M+1H]^+$:

1041.5479; found 1041.5476. **FTIR (neat)**: ν = 3273 (amide A), 1662, 1626 (amide I), 1541 cm^{-1} (amide II).

Synthesis of CP-A1-17:

Following the general protocol of the SPPS, the cyclic peptide was grown, cycled and alkoxyamine was introduced in the solid support. Then, the cleavage of the resin was carried out and the resulting powder was solubilized in H_2O. The solution with **CP-A1** was treated with aldehyde **17**, as it was described above, before purifying in reverse phase HPLC [Phenomenex Luna C18 (2) 100A column, H_2O (0.1% TFA)/ ACN (0.1% TFA) 100:0 → 100:0 (0 → 5 min), 100:0 → 60:40 (5 → 35 min) with an overall yield of 6% (5.8 mg). [Agilent SB-C18 column, H_2O (0.1% TFA)/ACN (0.1% TFA). 100:0 →100:0 (2 min) and 100:0 → 25:75 (19 min)] (R_t = 8.8 min). **MS** (ESI, H_2O): 1245.6 (20, $[M+1H]^+$), 623.4 (85, $[M+2H]^{2+}$), 521.3 (10, $[M+2H-17]^{2+}$). **HRMS** (ESI): Calcd for: $C_{56}H_{86}N_{14}O_{18}$ $[M+1H]^+$: 1245.6122; found 1245.6110. **FTIR (neat)**: ν = 3272 (amide A), 1680, 1626 (amide I), 1541 cm^{-1} (amide II).

Synthesis of CP-A1-Man:

Following the general protocol of the SPPS, the cyclic peptide was grown, cycled and alkoxyamine was introduced in the solid support. Then, the cleavage of the resin was carried out and the resulting powder was solubilized in H_2O. The solution with **CP-A1** was treated with *D*-mannose, as it was described above, before purifying in reverse phase HPLC [Phenomenex Luna C18 (2) 100A column, H_2O (0.1% TFA)/ ACN (0.1% TFA) 100:0 → 100:0 (0 → 5 min), 100:0 → 60:40 (5 → 35 min) with an overall yield of 8% (7.5 mg). [Agilent SB-C18 column, H_2O (0.1% TFA)/ACN (0.1% TFA). 100:0 →100:0 (2 min) and 100:0 → 25:75 (19 min)] (R_t = 9.6 min). MS (ESI, H_2O): 1203.7 (10, $[M+1H]^+$), 968.5 (5, $[M+H\text{-}Man]^+$), 603.0 (100, $[M+2H]^{2+}$), 485.5 (15, $[M+2H\text{-}Man]^{2+}$).**HRMS** (ESI): Calcd for: $C_{53}H_{82}N_{14}O_{18}$ $[M+H]^+$: 1203.6010; found 1203.6004.

Synthesis of CP-A1-*N*AcGlc:

Following the general protocol of the SPPS, the cyclic peptide was grown, cycled and alkoxyamine was introduced in the solid support. Then, the cleavage of the resin was carried out and the resulting powder was solubilized in H_2O. The solution with **CP-A1** was treated with *N*-acetyl-*D*-glucosamine, as it was described above, before purifying in reverse phase HPLC [Phenomenex Luna C18 (2) 100A column, H_2O (0.1% TFA)/ ACN (0.1% TFA) 100:0 → 100:0 (0 → 5 min), 100:0 → 60:40 (5 → 35 min) with an overall yield of 7% (6.8 mg). [Agilent SB-C18 column, H_2O (0.1% TFA)/ACN (0.1% TFA). 100:0 →100:0 (2 min) and 100:0 → 25:75 (19 min)] (R_t = 9.5 min). **MS** (ESI, H_2O): 1244.6 (18, $[M+1H]^+$), 622.9 (100, $[M+2H]^{2+}$), 347.8 (5, $[M+2H\text{-}Man]^{2+}$). **HRMS** (ESI): Calcd for: $C_{55}H_{85}N_{15}O_{18}Na$ $[M+Na]^+$: 1266.6082; found 1266.6089. **FTIR (neat)**: ν = 3285 (amide A), 1680, 1626 (amide I), 1547 cm^{-1} (amide II).

Synthesis of CP-A2-*N*AcGlc:

Following the general protocol of the SPPS, the cyclic peptide was grown, cycled and alkoxyamine was introduced in the solid support. Then, the cleavage of the resin was carried out and the resulting powder was solubilized in H_2O. The solution with **CP-A2** was treated with *N*-acetyl-*D*-glucosamine, as it was described above, before purifying in reverse phase HPLC [Phenomenex Luna C18 (2) 100A column, H_2O (0.1% TFA)/ ACN (0.1% TFA) 100:0 → 100:0 (0 → 5 min), 100:0 → 60:40 (5 → 35 min) with an overall yield of 9% (8.6 mg). [Agilent SB-C18 column, H_2O (0.1% TFA)/ACN (0.1% TFA). 100:0 →100:0 (2 min) and 100:0 → 25:75 (19 min)] (R_t = 9.6 min). **MS** (ESI, H_2O): 1246.7 (12, $[M+1H]^+$), 1063.4 (8, [M+Na- *N*AcGlc]$^+$), 623.0 (100, $[M+2H]^{2+}$), 521.4 (25, [M+2H- *N*AcGlc]$^{2+}$). **HRMS** (ESI): Calcd for: $C_{55}H_{85}N_{15}O_{18}$ $[M+H]^+$: 1244.6268; found 1244.6270. **FTIR (neat)**: ν = 3273 (amide A), 1668, 1620 (amide I), 1535 cm^{-1} (amide II).

Synthesis of CP-A2-Man:

Following the general protocol of the SPPS, the cyclic peptide was grown, cycled and alkoxyamine was introduced in the solid support. Then, the cleavage of the resin was carried out and the resulting powder was solubilized in H_2O. The solution with **CP-A2** was treated with *D*-mannose, as it was described above, before purifying in reverse phase HPLC [Phenomenex Luna C18 (2) 100A column, H_2O (0.1% TFA)/ ACN (0.1% TFA) 100:0 → 100:0 (0 → 5 min), 100:0 → 60:40 (5 → 35 min) with an overall yield of 9% (8.4 mg). [Agilent SB-C18 column, H_2O (0.1% TFA)/ACN (0.1% TFA). 100:0 →100:0 (2 min) and 100:0 → 25:75 (19 min)] (R_t = 9.5 min). **MS** (ESI, H_2O): 1203.6 (20, $[M+1H]^+$), 602.4 (100, $[M+2H]^{2+}$). **HRMS** (ESI): Calcd for: $C_{53}H_{82}N_{14}O_{18}$ $[M+H]^+$: 1203.6010; found 1203.6004. **FTIR (neat)**: ν = 3273 (amide A), 1674, 1620 (amide I), 1541 cm^{-1} (amide II).

Synthesis of CP-A3-*N*AcGlc:

Following the general protocol of the SPPS, the cyclic peptide was grown, cycled and alkoxyamine was introduced in the solid support. Then, the cleavage of the resin was carried out and the resulting powder was solubilized in H_2O. The solution with **CP-A3** was treated with *N*-acetyl-*D*-glucosamine, as it was described above, before purifying in reverse phase HPLC [Phenomenex Luna C18 (2) 100A column, H_2O (0.1% TFA)/ ACN (0.1% TFA) 100:0 → 100:0 (0 → 5 min), 100:0 → 60:40 (5 → 35 min) with an overall yield of 6% (6.0 mg). [Agilent SB-C18 column, H_2O (0.1% TFA)/ACN (0.1% TFA). 100:0 →100:0 (2 min) and 100:0 → 25:75 (19 min)] (R_t = 9.6 min). **MS** (ESI, H_2O): 1244.7 (20, $[M+1H]^+$), 622.8 (100, $[M+2H]^{2+}$). **HRMS** (ESI): Calcd for: $C_{55}H_{85}N_{15}O_{18}Na$ $[M+Na]^+$: 1266.6092; found 1266.6089. **FTIR (neat)**: ν = 3273 (amide A), 1680, 1620 (amide I), 1541 cm^{-1} (amide II).

Synthesis of CP-A3-Man:

Following the general protocol of the SPPS, the cyclic peptide was grown, cycled and alkoxyamine was introduced in the solid support. Then, the cleavage of the resin was carried out and the resulting powder was solubilized in H_2O. The solution with **CP-A3** was treated with *D*-mannose, as it was described above, before purifying in reverse phase HPLC [Phenomenex Luna C18 (2) 100A column, H_2O (0.1% TFA)/ ACN (0.1% TFA) 100:0 → 100:0 (0 → 5 min), 100:0 → 60:40 (5 → 35 min) with an overall yield of 12% (11.0 mg). [Agilent SB-C18 column, H_2O (0.1% TFA)/ACN (0.1% TFA). 100:0 →100:0 (2 min) and 100:0 → 25:75 (19 min)] (R_t = 9.6 min). **MS** (ESI, H_2O): 1204.6 (30, $[M+1H]^+$), 602.3 (100, $[M+2H]^{2+}$). **HRMS** (ESI): Calcd for: $C_{53}H_{82}N_{14}O_{18}Na$ $[M+Na]^+$: 1225.5826; found 1225.5824. **FTIR (neat)**: ν = 3273 (amide A), 1674, 1620 (amide I), 1541 cm^{-1} (amide II).

Synthesis of CP-14 (RRKWLWLW):

The peptide was grown in CTC resin in the same way that ***c*-[WLWLWKSK]**. After the cyclization, the cleavage of the resin was carried out and the resulting powder was solubilized in H_2O and purified in reverse phase HPLC [Phenomenex Luna C18 (2) 100A column, H_2O (0.1% TFA)/ ACN (0.1% TFA) 70:30 → 70:30 (0 → 5 min), 70:30 → 50:50 (5 → 35 min) with an overall yield of 28% (26.6 mg). [Agilent SB-C18 column, H_2O (0.1% TFA)/ACN (0.1% TFA). 100:0 →100:0 (2 min) and 100:0 → 25:75 (19 min)] (R_t = 9.0 min). **MS** (ESI, H_2O): 1226.7 (10, $[M+1H]^+$), 613.5 (100, $[M+2H]^{2+}$). **HRMS** (ESI): Calcd for: $C_{63}H_{88}N_{18}O_8$ $[M+H]^+$: 1225.7114; found 1225.7105. **FTIR (neat)**: ν = 3279 (amide A), 1650 (amide I), 1529 cm^{-1} (amide II).

Antibacterial assays:

A colony of bacteria is diluted in 4 mL of MHB to achieve a concentration of 1-5 x 10^8 CFU/mL (McFarland 0.5 turbidity, absorption from 0.08 to 0.10 at 625 nm). Then, the solution is diluted 100 times to afford a concentration of 10^6 CFU/mL.

On the other hand, the cyclic peptide is diluted in MHB in the 96-well microplates. Usually, one line is filled with one peptide. For the dilution, the line is filled with 50 µL of MHB, then 50 µL of cyclic peptide is introduced in the first well of the line, mixed and 50 µL of that mixture is introduced in the next well. We repeat the mixture with the new 50 µL of the second well and, again, 50 µL of that mixture is introduced in the next well. At the end, the peptide is diluted to half in each well. Later, 40 µL of fresh MHB is introduced in all wells and 10 µL of bacteria is introduced as well to achieve a final volume of 100 µL. The microplate is incubated overnight at 37 ºC. The microplate is read at 492 nm and 620 nm to determine the turbidity of each well. The wells that does not show turbidity represents inhibitory concentrations for every peptide. The MIC is the lower concentration with no turbidity.

Chapter 2

STEM assays:

Samples were solubilized in water or in 9 g/L NaCl (specify in each case) and 10 µL of the sample were dropped over the grid and left there for 5 minutes. Then the drop is removed from below (using the grid as a filter). The sample is covered to avoid contaminations and powder. After drying, the sample was stained with uranyl acetate (2% w/w, 5 µL), which is removed after a 1 min. Then, the sample was washed once with H_2O (10 µL). The sample is covered again and, when it is completely dried, the measure can be done.

Introduction of the carboxyl-aldehyde: After the cleavage of the resin, a solution of the CP (5 mM) in 5% acetic acid/H_2O was treated with the corresponding carboxyl-aldehyde (120 mM) and shaken for 30 min at room temperature, after which the reaction was checked for HPLC-MS and purified by reverse phase HPLC. The corresponding fractions were lyophilised to afford the pure peptide as a white solid.

Haemolysis assays:

To prepare the solution of the erythrocytes, 4.5 mL the commercially available erythrocytes were centrifuged, and the supernatant is removed from the medium. The erythrocytes were washed with PBS (PBS was added, centrifuged and removed from the erythrocytes solution; 3 x 10 mL) and, finally, the erythrocytes are solved in PBS to achieve a concentration of 8% erythrocytes/PBS.

The microplate was filled with 50 µL of PBS and the peptide was introduced in the first well to dilute in the same way that in the antibacterial assays. 50 µL of the 8% erythrocytes/PBS are introduced in each well (final volume of 100 µL) and the microplate is incubated for 1 h at 37 ºC. After the incubation, the microplate is centrifuged at 2000 rpm for 5 minutes. Then, the supernatant is removed to another microplate for reading in the plate reader at 405 y 450 nm. The toxicity of the peptide increases with the red colour of the supernatant. The positive control are the erythrocytes with a 0.1% of Triton in PBS and the negative control is PBS.

Biofilm assays:

A solution of bacteria was incubated overnight in a 0.25% glucose/BHB, diluted 1:100, inoculated in a 96-well-flat-bottom cell culture plates and incubated overnight at 37 ºC to obtain the mature biofilm. The supernatant was removed, and biofilm was washed with PBS (3 x 200 µL). Several dilutions of the peptide in MHB, prepared in other microplate as in the normal antibacterial assays, are added over the biofilm and the microplate is incubated for 24 h at 37 ºC. Then, the supernatant is removed again and a solution of 0.5% MTT in PBS is added and incubated for 2 h at 37 ºC. The supernatant is removed and DMSO is added to the microplate, which is read in the microplate reader at 405 nm.

Synthesis of CP-A6*:

Following the general protocol of the SPPS, the cyclic peptide was grown, cycled and alkoxyamine was introduced in the solid support. Then, the click chemistry was carried out with benzyl azide and, finally, the cleavage of the resin. The resulting powder was solubilized in H_2O and purified in reverse phase HPLC [Phenomenex Luna C18 (2) 100A column, H_2O (0.1% TFA)/ ACN (0.1% TFA) 100:0 → 100:0 (0 → 5 min), 100:0 → 40:60 (5 → 35 min) with an overall yield of 11% (9.8 mg). [Agilent SB-C18 column, H_2O (0.1% TFA)/ACN (0.1% TFA). 100:0 →100:0 (2 min) and 100:0 → 25:75 (19 min)] (R_t = 11.2 min). **MS** (ESI, H_2O): 1222.6 (10, $[M+2Na]^+$), 1200.6 (15, $[M+2H+Na]^+$), 600.9 (100, $[M+2H+Na]^{2+}$), 401.0 (10, $[M+2H+Na]^{3+}$). **HRMS** (ESI): Calcd for: $C_{54}H_{79}N_{17}O_{13}$ $[M+1H]^+$: 1174.6116; found 1174.6116. **FTIR (neat)**: ν = 3273 (amide A), 1674, 1626 (amide I), 1541 cm^{-1} (amide II).

Synthesis of CP-A16:

Following the general protocol of the SPPS, the cyclic peptide was grown, cycled and alkoxyamine was introduced in the solid support. Then, the click chemistry was carried out with hexyl azide and, finally, the cleavage of the resin. The resulting powder was solubilized in H_2O and purified in reverse phase HPLC [Phenomenex Luna C18 (2) 100A column, H_2O (0.1% TFA)/ ACN (0.1% TFA) 100:0 → 100:0 (0 → 5 min), 100:0 → 40:60 (5 → 35 min) with an overall yield of 14% (12.8 mg). [Agilent SB-C18 column, H_2O (0.1% TFA)/ACN (0.1% TFA). 100:0 →100:0 (2 min) and 100:0 → 25:75 (19 min)] (R_t = 11.8 min). **MS** (ESI, H_2O): 1168.6 (18, $[M+1H]^+$), 585.0 (100, $[M+2H]^{2+}$), 390.1 (10, $[M+3H]^{3+}$). **HRMS** (ESI): Calcd for: $C_{53}H_{85}N_{17}O_{13}$ $[M+1H]^+$: 1168.6585; found 1168.6586. **FTIR (neat)**: ν = 3273 (amide A), 1668, 1632 (amide I), 1535 cm^{-1} (amide II).

Synthesis of CP-A19:

Following the general protocol of the SPPS, the cyclic peptide was grown, cycled and alkoxyamine was introduced in the solid support. Then, the click chemistry was carried out with nonyl azide and, finally, the cleavage of the resin. The resulting powder was solubilized in H_2O and purified in reverse phase HPLC [Phenomenex Luna C18 (2) 100A column, H_2O (0.1% TFA)/ ACN (0.1% TFA) 95:5 → 95:5 (0 → 5 min), 95:5 → 25:75 (5 → 35 min) with an overall yield of 20% (19.0 mg). [Agilent SB-C18 column, H_2O (0.1% TFA)/ACN (0.1% TFA). 100:0 →100:0 (2 min) and 100:0 → 25:75 (19 min)] (R_t = 13.6 min). **MS** (ESI, H_2O): 1211.7 (20, $[M+1H]^+$), 606.0 (100, $[M+2H]^{2+}$), 404.4 (12, $[M+3H]^{3+}$). **HRMS** (ESI): Calcd for: $C_{56}H_{91}N_{17}O_{13}$ $[M+1H]^+$: 1210.7052; found 1210.7055.

Synthesis of CP-A110:

Following the general protocol of the SPPS, the cyclic peptide was grown, cycled and alkoxyamine was introduced in the solid support. Then, the click chemistry was carried out with decyl azide and, finally, the cleavage of the resin. The resulting powder was solubilized in H_2O and purified in reverse phase HPLC [Phenomenex Luna C18 (2) 100A column, H_2O (0.1% TFA)/ ACN (0.1% TFA) 95:5 → 95:5 (0 → 5 min), 95:5 → 25:75 (5

→ 35 min) with an overall yield of 19% (18.2 mg). [Agilent SB-C18 column, H_2O (0.1% TFA)/ACN (0.1% TFA). 100:0 →100:0 (2 min) and 100:0 → 25:75 (19 min)] (R_t = 14.2 min). **MS** (ESI, H_2O): 1225.7 (25, $[M+1H]^+$), 613.0 (100, $[M+2H]^{2+}$), 409.1 (15, $[M+3H]^{3+}$). **HRMS** (ESI): Calcd for: $C_{57}H_{93}N_{17}O_{13}$ $[M+1H]^+$: 1224.7213; found 1224.7212. **FTIR (neat)**: ν = 3273 (amide A), 1656 (amide I), 1529 cm^{-1} (amide II).

Synthesis of CP-A1$_{10*}$:

Following the general protocol of the SPPS, the cyclic peptide was grown, cycled and alkoxyamine was introduced in the solid support. Then, the click chemistry was carried out with geranyl azide and, finally, the cleavage of the resin. The resulting powder was solubilized in H_2O and purified in reverse phase HPLC [Phenomenex Luna C18 (2) 100A column, H_2O (0.1% TFA)/ ACN (0.1% TFA) 20:80 → 20:80 (0 → 5 min), 20:80 → 5:95 (5 → 35 min) with an overall yield of 10% (9.7 mg). [Agilent SB-C18 column, H_2O (0.1% TFA)/ACN (0.1% TFA). 100:0 →100:0 (2 min) and 100:0 → 5:95 (19 min)] (R_t = 11.3 min). **MS** (ESI, H_2O): 1246.7 (15, $[M+H+Na]^+$), 619.9 (100, $[M+2H+Na]^{2+}$), 583.5 (10, $[M+2H+Na\text{-}COCH_2ONH_2]^{2+}$), 416.0 (25, $[M+2H+Na]^{3+}$), 407 (10, $[M+3H]^{3+}$). **FTIR (neat)**: ν = 3273 (amide A), 1656 (amide I), 1529 cm^{-1} (amide II).

Synthesis of CP-A1$_{11}$:

Following the general protocol of the SPPS, the cyclic peptide was grown, cycled and alkoxyamine was introduced in the solid support. Then, the click chemistry was carried out with undecyl azide and, finally, the cleavage of the resin. The resulting powder was solubilized in H_2O and purified in reverse phase HPLC [Phenomenex Luna C18 (2) 100A column, H_2O (0.1% TFA)/ ACN (0.1% TFA) 100:0 → 100:0 (0 → 5 min), 100:0 → 25:75 (5 → 35 min) with an overall yield of 8% (7.7 mg). [Agilent SB-C18 column, H_2O (0.1% TFA)/ACN (0.1% TFA). 100:0 →100:0 (2 min) and 100:0 → 25:75 (19 min)] (R_t = 14.7 min). **MS** (ESI, H_2O): 1239.7 (25, $[M+H]^+$), 1167.6 (5, $[M+1H\text{-}COCH_2ONH_2]^+$), 620.0 (100, $[M+2H]^{2+}$), 583.5 (20, $[M+2H\text{-}COCH_2ONH_2]^{2+}$), 389.6 (5, $[M+3H\text{-}COCH_2ONH_2]^{3+}$). **HRMS** (ESI): Calcd for: $C_{58}H_{95}N_{17}O_{13}$ $[M+1H]^+$: 1238.7369; found 1238.7368.

Synthesis of CP-A1$_{12}$:

Following the general protocol of the SPPS, the cyclic peptide was grown, cycled and alkoxyamine was introduced in the solid support. Then, the click chemistry was carried out with dodecyl azide and, finally, the cleavage of the resin. The resulting powder was solubilized in H_2O and purified in reverse phase HPLC [Phenomenex Luna C18 (2) 100A column, H_2O (0.1% TFA)/ ACN (0.1% TFA) 75:25 → 75:25 (0 → 5 min), 75:25 → 25:75 (5 → 35 min) with an overall yield of 6% (5.8 mg). [Agilent SB-C18 column, H_2O (0.1% TFA)/ACN (0.1% TFA). 100:0 →100:0 (2 min) and 100:0 → 25:75 (19 min)] (R_t = 15.3 min). **MS** (ESI, H_2O): 1252.7 (15, $[M+H]^+$), 1181.7 (6, $[M+1H\text{-}COCH_2ONH_2]^+$), 627.0 (100, $[M+2H]^{2+}$), 590.5 (40, $[M+2H\text{-}COCH_2ONH_2]^{2+}$), 418.4 (15, $[M+3H]^{3+}$) 394.6 (5, $[M+3H\text{-}COCH_2ONH_2]^{3+}$). **HRMS** (ESI): Calcd for: $C_{59}H_{97}N_{17}O_{13}$ $[M+1H]^+$: 1252.7528; found 1252.7525. **FTIR (neat)**: ν = 3285 (amide A), 1656 (amide I), 1535 cm^{-1} (amide II).

Synthesis of CP-A1$_{14}$:

Following the general protocol of the SPPS, the cyclic peptide was grown, cycled and alkoxyamine was introduced in the solid support. Then, the click chemistry was carried out with tetradecyl azide and, finally, the cleavage of the resin. The resulting powder was solubilized in H_2O and purified in reverse phase HPLC [Phenomenex Luna C18 (2) 100A column, H_2O (0.1% TFA)/ ACN (0.1% TFA) 75:25 → 75:25 (0 → 5 min), 75:25 → 25:75 (5 → 35 min) with an overall yield of 17% (16.9 mg). [Agilent SB-C18 column, H_2O (0.1% TFA)/ACN (0.1% TFA). 100:0 →100:0 (2 min) and 100:0 → 25:75 (19 min)] (R_t = 17.1 min). **MS** (ESI, H_2O): 1281.7 (10, $[M+1H]^+$), 641.0 (100, $[M+2H]^{2+}$), 604.5 (45, $[M+2H\text{-}COCH_2ONH_2]^{2+}$), 427.7 (15, $[M+3H]^{3+}$). **HRMS** (ESI): Calcd for: $C_{61}H_{101}N_{17}O_{13}$ $[M+1H]^+$: 1280.7835; found 1280.7838.

Synthesis of CP-A1$_{16}$:

Following the general protocol of the SPPS, the cyclic peptide was grown, cycled and alkoxyamine was introduced in the solid support. Then, the click chemistry was carried out with hexadecyl azide and, finally, the cleavage of the resin. The resulting powder was solubilized in H_2O and purified in reverse phase HPLC [Phenomenex Luna C18 (2) 100A column, H_2O (0.1% TFA)/ ACN (0.1% TFA) 80:20 → 80:20 (0 → 5 min), 80:20 → 5:95 (5 → 35 min) with an overall yield of 12% (12.2 mg). [Agilent SB-C18 column, H_2O (0.1% TFA)/ACN (0.1% TFA). 100:0 →100:0 (2 min) and 100:0 → 5:95 (19 min)] (R_t = 17.5 min). **MS** (ESI, H_2O): 1309.8 (25, $[M+H]^+$), 655.2 (100, $[M+2H]^{2+}$), 618.8 (25, $[M+2H\text{-}COCH_2ONH_2]^{2+}$), 437.1 (18, $[M+3H]^{3+}$) 413.2 (5, $[M+3H\text{-}COCH_2ONH_2]^{3+}$). **HRMS** (ESI): Calcd for: $C_{63}H_{105}N_{17}O_{13}$ $[M+1H]^+$: 1308.8150; found 1308.8151.

Synthesis of CP-A1$_{18}$:

Following the general protocol of the SPPS, the cyclic peptide was grown, cycled and alkoxyamine was introduced in the solid support. Then, the click chemistry was carried out with octadecyl azide and, finally, the cleavage of the resin. The resulting powder was solubilized in H_2O and purified in reverse phase HPLC [Phenomenex Luna C18 (2) 100A column, H_2O (0.1% TFA)/ ACN (0.1% TFA) 80:20 → 80:20 (0 → 5 min), 80:20 → 5:95 (5 → 35 min) with an overall yield of 14% (14.6 mg). [Agilent SB-C18 column, H_2O (0.1% TFA)/ACN (0.1% TFA). 80:20 →80:20 (2 min) and 80:20 → 5:95 (19 min)] (R_t = 12.2 min). **MS** (ESI, H_2O): 1337.8 (25, $[M+1H]^+$), 669.0 (100, $[M+2H]^{2+}$), 632.7 (5, $[M+2H\text{-}COCH_2ONH_2]^{2+}$), 446.5 (25, $[M+3H]^{3+}$). **HRMS** (ESI): Calcd for: $C_{65}H_{109}N_{17}O_{13}$ $[M+1H]^+$: 1336.8459; found 1336.8464. **FTIR (neat)**: ν = 3273 (amide A), 1668,1626 (amide I), 1541 cm^{-1} (amide II).

Synthesis of CP-A1$_{20}$:

Following the general protocol of the SPPS, the cyclic peptide was grown, cycled and alkoxyamine was introduced in the solid support. Then, the click chemistry was carried out with eicosyl azide and, finally, the cleavage of the resin. The resulting powder was solubilized in H_2O and purified in reverse phase HPLC [Phenomenex Luna C18 (2) 100A column, H_2O (0.1% TFA)/ ACN (0.1% TFA) 80:20 → 80:20 (0 → 5 min), 80:20 → 5:95 (5 → 35 min) with an overall yield of 9% (9.5 mg). [Agilent SB-C18 column, H_2O (0.1%

TFA)/ACN (0.1% TFA). 80:20 →80:20 (2 min) and 80:20 → 5:95 (19 min)] (R_t = 19.8 min). **MS** (ESI, H_2O): 1365.8 (18, $[M+H]^+$), 1293.9 (4, $[M+1H-COCH_2ONH_2]^+$), 683.2 (100, $[M+2H]^{2+}$), 646.8 (10, $[M+2H-COCH_2ONH_2]^{2+}$), 455.8 (14, $[M+3H]^{3+}$) 431.4 (3, $[M+3H-COCH_2ONH_2]^{3+}$). **HRMS** (ESI): Calcd for: $C_{67}H_{113}N_{17}O_{13}$ $[M+1H]^+$: 1364.8776; found 1364.8777.

Synthesis of CP-A2$_6$:

Following the general protocol of the SPPS, the cyclic peptide was grown, cycled and alkoxyamine was introduced in the solid support. Then, the click chemistry was carried out with hexyl azide and, finally, the cleavage of the resin. The resulting powder was solubilized in H_2O and purified in reverse phase HPLC [Phenomenex Luna C18 (2) 100A column, H_2O (0.1% TFA)/ ACN (0.1% TFA) 100:0 → 100:0 (0 → 5 min), 100:0 → 40:60 (5 → 35 min) with an overall yield of 16% (14.4 mg). [Agilent SB-C18 column, H_2O (0.1% TFA)/ACN (0.1% TFA). 100:0 →100:0 (2 min) and 100:0 → 25:75 (19 min)] (R_t = 12.0 min). **MS** (ESI, H_2O): 1168.6 (35, $[M+1H]^+$), 1096.0 (10, $[M+H-COCH_2ONH_2]^+$), 585.0 (100, $[M+2H]^{2+}$), 548.5 (20, $[M+2H-COCH_2ONH_2]^{2+}$), 390.4 (25, $[M+3H]^{3+}$), 366 (5, $[M+3H-COCH_2ONH_2]^{3+}$). **HRMS** (ESI): Calcd for: $C_{53}H_{85}N_{17}O_{13}$ $[M+1H]^+$: 1168.6585; found 1168.6586.

Synthesis of CP-A2$_{10}$:

Following the general protocol of the SPPS, the cyclic peptide was grown, cycled and alkoxyamine was introduced in the solid support. Then, the click chemistry was carried out with decyl azide and, finally, the cleavage of the resin. The resulting powder was solubilized in H_2O and purified in reverse phase HPLC [Phenomenex Luna C18 (2) 100A column, H_2O (0.1% TFA)/ ACN (0.1% TFA) 100:0 → 100:0 (0 → 5 min), 100:0 → 40:60 (5 → 35 min) with an overall yield of 18% (17.1 mg). [Agilent SB-C18 column, H_2O (0.1% TFA)/ACN (0.1% TFA). 100:0 →100:0 (2 min) and 100:0 → 25:75 (19 min)] (R_t = 14.4 min). **MS** (ESI, H_2O): 1225.7 (30, $[M+1H]^+$), 1151.7 (10, $[M+H-COCH_2ONH_2]^+$), 613.0 (100, $[M+2H]^{2+}$), 576.5 (20, $[M+2H-COCH_2ONH_2]^{2+}$), 409.0 (20, $[M+3H]^{3+}$), 384.8 (5, $[M+3H-COCH_2ONH_2]^{3+}$). **HRMS** (ESI): Calcd for: $C_{57}H_{93}N_{17}O_{13}$ $[M+1H]^+$: 1224.7213; found 1224.7212. **FTIR (neat)**: ν = 3291 (amide A), 1656 (amide I), 1535 cm^{-1} (amide II).

Synthesis of CP-A2$_{12}$:

Following the general protocol of the SPPS, the cyclic peptide was grown, cycled and alkoxyamine was introduced in the solid support. Then, the click chemistry was carried out with dodecyl azide and, finally, the cleavage of the resin. The resulting powder was solubilized in H_2O and purified in reverse phase HPLC [Phenomenex Luna C18 (2) 100A column, H_2O (0.1% TFA)/ ACN (0.1% TFA) 75:25 → 75:25 (0 → 5 min), 75:25 → 25:75 (5 → 35 min) with an overall yield of 12% (11.8 mg). [Agilent SB-C18 column, H_2O (0.1% TFA)/ACN (0.1% TFA). 100:0 →100:0 (2 min) and 100:0 → 5:95 (19 min)] (R_t = 9.4 min). **MS** (ESI, H_2O): 1253.7 (30, $[M+1H]^+$), 627 (100, $[M+2H]^{2+}$), 418.4 (20, $[M+3H]^{3+}$). **HRMS** (ESI): Calcd for: $C_{59}H_{97}N_{17}O_{13}Na$ $[M+Na]^+$: 1274.7338; found 1274.7344. **FTIR (neat)**: ν = 3273 (amide A), 1674, 1626 (amide I), 1535 cm^{-1} (amide II).

Synthesis of CP-A2$_{14}$:

Following the general protocol of the SPPS, the cyclic peptide was grown, cycled and alkoxyamine was introduced in the solid support. Then, the click chemistry was carried out with tetradecyl azide and, finally, the cleavage of the resin. The resulting powder was solubilized in H_2O and purified in reverse phase HPLC [Phenomenex Luna C18 (2) 100A column, H_2O (0.1% TFA)/ ACN (0.1% TFA) 75:25 → 75:25 (0 → 5 min), 75:25 → 25:75 (5 → 35 min) with an overall yield of 18% (17.8 mg). [Agilent SB-C18 column, H_2O (0.1% TFA)/ACN (0.1% TFA). 100:0 →100:0 (2 min) and 100:0 → 25:75 (19 min)] (R_t = 16.9 min). **MS** (ESI, H_2O): 1281.7 (12, $[M+1H]^+$), 641.0 (100, $[M+2H]^{2+}$), 604.5 (40, $[M+2H\text{-}COCH_2ONH_2]^{2+}$), 427.7 (15, $[M+3H]^{3+}$). **HRMS** (ESI): Calcd for: $C_{61}H_{101}N_{17}O_{13}$ $[M+1H]^+$: 1280.7835; found 1280.7838. **FTIR (neat)**: ν = 3285 (amide A), 1656 (amide I), 1535 cm^{-1} (amide II).

Synthesis of CP-A2$_{16}$:

Following the general protocol of the SPPS, the cyclic peptide was grown, cycled and alkoxyamine was introduced in the solid support. Then, the click chemistry was carried out with hexadecyl azide and, finally, the cleavage of the resin. The resulting powder was solubilized in H_2O and purified in reverse phase HPLC [Phenomenex Luna C18 (2) 100A column, H_2O (0.1% TFA)/ ACN (0.1% TFA) 80:20 → 80:20 (0 → 5 min), 80:20 → 5:95 (5 → 35 min) with an overall yield of 14% (14.5 mg). [Agilent SB-C18 column, H_2O (0.1% TFA)/ACN (0.1% TFA). 100:0 →100:0 (2 min) and 100:0 → 25:75 (19 min)] (R_t = 17.9 min). **MS** (ESI, H_2O): 1309.8 (22, $[M+1H]^+$), 655.1 (100, $[M+2H]^{2+}$), 618.5 (8, $[M+2H\text{-}COCH_2ONH_2]^{2+}$), 437.1 (20, $[M+3H]^{3+}$). **HRMS** (ESI): Calcd for: $C_{63}H_{105}N_{17}O_{13}Na$ $[M+Na]^+$: 1330.7965; found 1330.7970.

Synthesis of CP-A2$_{18}$:

Following the general protocol of the SPPS, the cyclic peptide was grown, cycled and alkoxyamine was introduced in the solid support. Then, the click chemistry was carried out with octadecyl azide and, finally, the cleavage of the resin. The resulting powder was solubilized in H_2O and purified in reverse phase HPLC [Phenomenex Luna C18 (2) 100A column, H_2O (0.1% TFA)/ ACN (0.1% TFA) 80:20 → 80:20 (0 → 5 min), 80:20 → 5:95 (5 → 35 min) with an overall yield of 9% (9.3 mg). [Agilent SB-C18 column, H_2O (0.1% TFA)/ACN (0.1% TFA). 100:0 →100:0 (2 min) and 100:0 → 25:75 (19 min)] (R_t = 19.1 min). **MS** (ESI, H_2O): 1337.8 (50, $[M+H]^+$), 1265.8 (4, $[M+1H\text{-}COCH_2ONH_2]^+$), 669.0 (100, $[M+2H]^{2+}$), 446.5 (34, $[M+3H]^{3+}$). **HRMS** (ESI): Calcd for: $C_{65}H_{109}N_{17}O_{13}$ $[M+1H]^+$: 1336.8466; found 1336.8464. **FTIR (neat)**: ν = 3279 (amide A), 1656 (amide I), 1535 cm^{-1} (amide II).

Synthesis of CP-A1$_{14}$-Glu:

Following the general protocol of the SPPS, the cyclic peptide was grown, cycled and alkoxyamine was introduced in the solid support. Then, the click chemistry was carried out with tetradecyl azide and, finally, the cleavage of the resin. The solution with **CP-A1$_{14}$** was treated with *D*-glucose aldehyde, as it was described above, before purifying in reverse phase HPLC [Phenomenex Luna C18 (2) 100A column, H_2O (0.1% TFA)/ ACN

(0.1% TFA) 75:25 → 75:25 (0 → 5 min), 75:25 → 25:75 (5 → 35 min) with an overall yield of 6% (7.0 mg). [Agilent SB-C18 column, H_2O (0.1% TFA)/ACN (0.1% TFA). 100:0 →100:0 (2 min) and 100:0 → 25:75 (19 min)] (R_t = 16.8 min). **MS** (ESI, H_2O): 1485.8 (12, $[M+1H]^+$), 743.1 (100, $[M+2H]^{2+}$), 495.7 (5, $[M+3H]^{3+}$). **HRMS** (ESI): Calcd for: $C_{69}H_{113}N_{17}O_{19}Na$ $[M+Na]^+$: 1506.8281; found 1506.8291. **FTIR (neat)**: ν = 3279 (amide A), 1674, 1626 (amide I), 1535 cm^{-1} (amide II).

Synthesis of CP-A1$_{14}$-Man (17):

Following the general protocol of the SPPS, the cyclic peptide was grown, cycled and alkoxyamine was introduced in the solid support. Then, the click chemistry was carried out with tetradecyl azide and, finally, the cleavage of the resin. The solution with **CP-A1$_{14}$** was treated with compound **17**, as it was described above, before purifying in reverse phase HPLC [Phenomenex Luna C18 (2) 100A column, H_2O (0.1% TFA)/ ACN (0.1% TFA) 75:25 → 75:25 (0 → 5 min), 75:25 → 25:75 (5 → 35 min) with an overall yield of 5% (5.8 mg). [Agilent SB-C18 column, H_2O (0.1% TFA)/ACN (0.1% TFA). 100:0 →100:0 (2 min) and 100:0 → 25:75 (19 min)] (R_t = 16.9 min). **MS** (ESI, H_2O): 1484.8 (13, $[M+1H]^+$), 743.2 (100, $[M+2H]^{2+}$), 495.9 (7, $[M+3H]^{3+}$). **HRMS** (ESI): Calcd for: $C_{69}H_{113}N_{17}O_{19}Na$ $[M+Na]^+$: 1506.8292; found 1506.8291.

Synthesis of CP-A1$_{14}$-Gal:

Following the general protocol of the SPPS, the cyclic peptide was grown, cycled and alkoxyamine was introduced in the solid support. Then, the click chemistry was carried out with tetradecyl azide and, finally, the cleavage of the resin. The solution with **CP-A1$_{14}$** was treated with *N*-acetyl-*D*-galactosamine aldehyde, as it was described above, before purifying in reverse phase HPLC [Phenomenex Luna C18 (2) 100A column, H_2O (0.1% TFA)/ ACN (0.1% TFA) 75:25 → 75:25 (0 → 5 min), 75:25 → 25:75 (5 → 35 min) with an overall yield of 7% (8.4 mg). [Agilent SB-C18 column, H_2O (0.1% TFA)/ACN (0.1% TFA). 100:0 →100:0 (2 min) and 100:0 → 25:75 (19 min)] (R_t = 16.9 min). **MS** (ESI, H_2O): 1525.8 (10, $[M+1H]^+$), 763.7 (100, $[M+2H]^{2+}$), 509.4 (8, $[M+3H]^{3+}$). **HRMS** (ESI): Calcd for: $C_{71}H_{116}N_{18}O_{19}Na$ $[M+Na]^+$: 1547.8561; found 1547.8556. **FTIR (neat)**: ν = 3279 (amide A), 1668, 1626 (amide I), 1535 cm^{-1} (amide II).

Synthesis of CP-A1$_{14}$-Mal:

Following the general protocol of the SPPS, the cyclic peptide was grown, cycled and alkoxyamine was introduced in the solid support. Then, the click chemistry was carried out with tetradecyl azide and, finally, the cleavage of the resin. The solution with **CP-A1$_{14}$** was treated with *D*-maltose aldehyde, as it was described above, before purifying in reverse phase HPLC [Phenomenex Luna C18 (2) 100A column, H_2O (0.1% TFA)/ ACN (0.1% TFA) 75:25 → 75:25 (0 → 5 min), 75:25 → 25:75 (5 → 35 min) with an overall yield of 5% (6.5 mg). [Agilent SB-C18 column, H_2O (0.1% TFA)/ACN (0.1% TFA). 100:0 →100:0 (2 min) and 100:0 → 25:75 (19 min)].

Synthesis of CP-A2$_{10}$-Glu:

Following the general protocol of the SPPS, the cyclic peptide was grown, cycled and alkoxyamine was introduced in the solid support. Then, the click chemistry was carried out with decyl azide and, finally, the cleavage of the resin. The solution with **CP-A2$_{10}$** was treated with *D*-glucose aldehyde, as it was described above, before purifying in reverse phase HPLC [Phenomenex Luna C18 (2) 100A column, H_2O (0.1% TFA)/ ACN (0.1% TFA) 75:25 → 75:25 (0 → 5 min), 75:25 → 25:75 (5 → 35 min) with an overall yield of 7% (7.9 mg). [Agilent SB-C18 column, H_2O (0.1% TFA)/ACN (0.1% TFA). 100:0 →100:0 (2 min) and 100:0 → 25:75 (19 min)] (R_t = 14.6 min). **MS** (ESI, H_2O): 1428.8 (15, $[M+1H]^+$), 1153.6 (5, $[M+1H\text{-Glu-}COCH_2ONH_2]^+$), 715.0 (100, $[M+2H]^{2+}$), 576.5 (27, $[M+2H\text{-Glu-}COCH_2ONH_2]^{2+}$), 476.9 (5, $[M+3H]^{3+}$). **HRMS** (ESI): Calcd for: $C_{65}H_{105}N_{17}O_{19}Na$ $[M+Na]^+$: 1450.7668; found 1450.7665. **FTIR (neat)**: ν = 3273 (amide A), 1674, 1632 (amide I), 1541 cm^{-1} (amide II).

Synthesis of CP-A2$_{10}$-Man (17):

Following the general protocol of the SPPS, the cyclic peptide was grown, cycled and alkoxyamine was introduced in the solid support. Then, the click chemistry was carried out with decyl azide and, finally, the cleavage of the resin. The solution with **CP-A2$_{10}$** was treated with compound **17**, as it was described above, before purifying in reverse phase HPLC [Phenomenex Luna C18 (2) 100A column, H_2O (0.1% TFA)/ ACN (0.1% TFA) 75:25 → 75:25 (0 → 5 min), 75:25 → 25:75 (5 → 35 min) with an overall yield of 4% (4.5 mg). [Agilent SB-C18 column, H_2O (0.1% TFA)/ACN (0.1% TFA). 100:0 →100:0 (2 min) and 100:0 → 25:75 (19 min)] (R_t = 14.6 min). **MS** (ESI, H_2O): 1428.8 (20, $[M+1H]^+$), 1151.7 (5, $[M+1H\text{-Man-}COCH_2ONH_2]^+$), 715.0 (100, $[M+2H]^{2+}$), 576.5 (18, $[M+2H\text{-Man-}COCH_2ONH_2]^{2+}$), 384.7 (5, $[M+3H\text{-Man-}COCH_2ONH_2]^{3+}$). **HRMS** (ESI): Calcd for: $C_{65}H_{105}N_{17}O_{19}Na$ $[M+Na]^+$: 1450.7659; found 1450.7665. **FTIR (neat)**: ν = 1674, 1632 (amide I), 1541 cm^{-1} (amide II).

Synthesis of CP-A2$_{10}$-Gal:

Following the general protocol of the SPPS, the cyclic peptide was grown, cycled and alkoxyamine was introduced in the solid support. Then, the click chemistry was carried out with decyl azide and, finally, the cleavage of the resin. The solution with **CP-A2$_{10}$** was treated with *N*-acetyl-*D*-galactosamine aldehyde, as it was described above, before purifying in reverse phase HPLC [Phenomenex Luna C18 (2) 100A column, H_2O (0.1% TFA)/ ACN (0.1% TFA) 75:25 → 75:25 (0 → 5 min), 75:25 → 25:75 (5 → 35 min) with an overall yield of 5% (5.9 mg). [Agilent SB-C18 column, H_2O (0.1% TFA)/ACN (0.1% TFA). 100:0 →100:0 (2 min) and 100:0 → 25:75 (19 min)] (R_t = 15.0 min). **MS** (ESI, H_2O): 1469.8 (20, $[M+1H]^+$), 1152.7 (8, $[M+1H\text{-Gal-}COCH_2ONH_2]^+$), 735.7 (100, $[M+2H]^{2+}$), 576.7 (18, $[M+2H\text{-Gal-}COCH_2ONH_2]^{2+}$), 490.9 (7, $[M+3H]^{3+}$), 384.7 (5, $[M+3H\text{-Gal-}COCH_2ONH_2]^{3+}$). **HRMS** (ESI): Calcd for: $C_{67}H_{108}N_{18}O_{19}Na$ $[M+Na]^+$: 1491.7937; found 1491.7930. **FTIR (neat)**: ν = 3273 (amide A), 1674, 1632 (amide I), 1541 cm^{-1} (amide II).

Synthesis of CP-A2$_{10}$-Mal:

Following the general protocol of the SPPS, the cyclic peptide was grown, cycled and alkoxyamine was introduced in the solid support. Then, the click chemistry was carried out with decyl azide and, finally, the cleavage of the resin. The solution with **CP-A2$_{10}$** was treated with *D*-maltose aldehyde, as it was described above, before purifying in reverse phase HPLC [Phenomenex Luna C18 (2) 100A column, H_2O (0.1% TFA)/ ACN (0.1% TFA) 75:25 → 75:25 (0 → 5 min), 75:25 → 25:75 (5 → 35 min) with an overall yield of 7% (8.8 mg). [Agilent SB-C18 column, H_2O (0.1% TFA)/ACN (0.1% TFA). 100:0 →100:0 (2 min) and 100:0 → 25:75 (19 min)] (R_t = 14.2 min). **MS** (ESI, H_2O): 1592.8 (18, $[M+1H]^+$), 1152.7 (10, $[M+1H\text{-Mal-}COCH_2ONH_2]^+$), 796.2 (100, $[M+2H]^{2+}$), 576.5 (25, $[M+2H\text{-Mal-}COCH_2ONH_2]^{2+}$), 531.2 (7, $[M+3H]^{3+}$), 384.6 (8, $[M+3H\text{-Mal-}COCH_2ONH_2]^{3+}$). **HRMS** (ESI): Calcd for: $C_{71}H_{115}N_{17}O_{24}Na$ $[M+Na]^+$: 1612.8203; found 1612.8193. **FTIR (neat)**: ν = 3279 (amide A), 1674, 1632 (amide I), 1541 cm^{-1} (amide II).

Synthesis of CP-A4:

Following the general protocol of the SPPS, the **CP-A4** was grown and cycled in the solid support. Then, the cleavage of the resin was carried out, the resulting powder was solubilized in H_2O and purified in reverse phase HPLC [Phenomenex Luna C18 (2) 100A column, H_2O (0.1% TFA)/ ACN (0.1% TFA) 100:0 → 100:0 (0 → 5 min), 100:0 → 25:75 (5 → 35 min) with an overall yield of 30% (23.1 mg). (R_t = 9.6 min). **MS** (ESI, H_2O): 996.5 (20, $[M+1H]^+$), 499.0 (100, $[M+2H]^{2+}$), 333.1 (10, $[M+3H]^{3+}$). **HRMS** (ESI): Calcd for: $C_{45}H_{69}N_{15}O_{11}$ $[M+1H]^+$: 996.5373; found 996.5374. **FTIR (neat)**: ν = 3279 (amide A), 1668, 1620 (amide I), 1535 cm^{-1} (amide II).

Synthesis of CP-A5:

Following the general protocol of the SPPS, the **CP-A5** was grown and cycled in the solid support. Then, the cleavage of the resin was carried out, the resulting powder was solubilized in H_2O and purified in reverse phase HPLC [Phenomenex Luna C18 (2) 100A column, H_2O (0.1% TFA)/ ACN (0.1% TFA) 100:0 → 100:0 (0 → 5 min), 100:0 → 25:75 (5 → 35 min) with an overall yield of 33% (24.5 mg). (R_t = 9.1 min). **MS** (ESI, H_2O): 973.5 (20, $[M+H_2O+H]^+$), 486.9 (100, $[M+H_2O+2H]^{2+}$). **HRMS** (ESI): Calcd for: $C_{44}H_{67}N_{13}O_{11}$ $[M+1H]^+$: 954.5148; found 954.5156.

Synthesis of CP-A6:

Following the general protocol of the SPPS, the **CP-A6** was grown and cycled in the solid support. Then, the cleavage of the resin was carried out, the resulting powder was solubilized in H_2O and purified in reverse phase HPLC [Phenomenex Luna C18 (2) 100A column, H_2O (0.1% TFA)/ ACN (0.1% TFA) 100:0 → 100:0 (0 → 5 min), 100:0 → 25:75 (5 → 35 min) with an overall yield of 29% (21.0 mg). (R_t = 9.1 min). **MS** (ESI, H_2O): 948.5 (5, $[M+Na]^+$), 926.5 (35, $[M+1H]^+$), 463.8 (100, $[M+2H]^{2+}$), 309.8 (5, $[M+3H]^{3+}$). **HRMS** (ESI): Calcd for: $C_{45}H_{69}N_{15}O_{11}$ $[M+1H]^+$: 926.4839; found 926.4843. **FTIR (neat)**: ν = 3279 (amide A), 1674, 1626 (amide I), 1535 cm^{-1} (amide II).

Synthesis of CP-A4$_{10}$:

Following the general protocol of the SPPS, **CP-A4** was grown and cycled in the solid support. Then, the click chemistry was carried out with decyl azide and, finally, the cleavage of the resin. The resulting powder was solubilized in H_2O and purified in reverse phase HPLC [Phenomenex Luna C18 (2) 100A column, H_2O (0.1% TFA)/ ACN (0.1% TFA) 100:0 → 100:0 (0 → 5 min), 100:0 → 25:75 (5 → 35 min) with an overall yield of 17% (15.5 mg). [Agilent SB-C18 column, H_2O (0.1% TFA)/ACN (0.1% TFA). 100:0 →100:0 (2 min) and 100:0 → 25:75 (19 min)] (R_t = 14.5 min). **MS** (ESI, H_2O): 1180.7 (20, $[M+1H]^+$), 590.6 (100, $[M+2H]^{2+}$), 394.1 (25, $[M+3H]^{3+}$). **HRMS** (ESI): Calcd for: $C_{55}H_{90}N_{18}O_{11}Na$ $[M+Na]^+$: 1201.6926; found 1201.6929.

Synthesis of CP-A4$_{14}$:

Following the general protocol of the SPPS, **CP-A4** was grown and cycled in the solid support. Then, the click chemistry was carried out with tetradecyl azide and, finally, the cleavage of the resin. The resulting powder was solubilized in H_2O and purified in reverse phase HPLC [Phenomenex Luna C18 (2) 100A column, H_2O (0.1% TFA)/ ACN (0.1% TFA) 100:0 → 100:0 (0 → 5 min), 100:0 → 25:75 (5 → 35 min) with an overall yield of 13% (12.8 mg). [Agilent SB-C18 column, H_2O (0.1% TFA)/ACN (0.1% TFA). 100:0 →100:0 (2 min) and 100:0 → 25:75 (19 min)] (R_t = 16.8 min). **MS** (ESI, H_2O): 1235.7 (15, $[M+1H]^+$), 618.5 (100, $[M+2H]^{2+}$), 412.8 (22, $[M+3H]^{3+}$). **HRMS** (ESI): Calcd for: $C_{59}H_{98}N_{18}O_{11}Na$ $[M+Na]^+$: 1257.7554; found 1257.7555.

Synthesis of CP-A5$_{10}$:

Following the general protocol of the SPPS, **CP-A5** was grown and cycled in the solid support. Then, the click chemistry was carried out with decyl azide and, finally, the cleavage of the resin. The resulting powder was solubilized in H_2O and purified in reverse phase HPLC [Phenomenex Luna C18 (2) 100A column, H_2O (0.1% TFA)/ ACN (0.1% TFA) 100:0 → 100:0 (0 → 5 min), 100:0 → 70:30 (5 → 25 min), 70:30 → 25:75 (25 → 45 min), with an overall yield of 18% (16.3 mg). [Agilent SB-C18 column, H_2O (0.1% TFA)/ACN (0.1% TFA). 100:0 →100:0 (2 min) and 100:0 → 25:75 (19 min)] (R_t = 14.6 min). **MS** (ESI, H_2O): 1138.7 (20, $[M+1H]^+$), 569.5 (100, $[M+2H]^{2+}$), 380.0 (20, $[M+3H]^{3+}$). **HRMS** (ESI): Calcd for: $C_{54}H_{88}N_{16}O_{11}Na$ $[M+Na]^+$: 1159.6708; found 1159.6711.

Synthesis of CP-A5$_{14}$:

Following the general protocol of the SPPS, **CP-A5** was grown and cycled in the solid support. Then, the click chemistry was carried out with tetradecyl azide and, finally, the cleavage of the resin. The resulting powder was solubilized in H_2O and purified in reverse phase HPLC [Phenomenex Luna C18 (2) 100A column, H_2O (0.1% TFA)/ ACN (0.1% TFA) 100:0 → 100:0 (0 → 5 min), 100:0 → 25:75 (5 → 35 min) with an overall yield of 16% (15.0 mg). [Agilent SB-C18 column, H_2O (0.1% TFA)/ACN (0.1% TFA). 100:0 →100:0 (2 min) and 100:0 → 25:75 (19 min)] (R_t = 16.6 min). **MS** (ESI, H_2O): 1193.8 (20, $[M+1H]^+$), 597.5 (100, $[M+2H]^{2+}$), 398.8 (22, $[M+3H]^{3+}$). **HRMS** (ESI): Calcd for:

$C_{58}H_{96}N_{16}O_{11}$ $[M+H]^+$: 1193.7518; found 1193.7517. **FTIR (neat)**: ν = 3273 (amide A), 1674, 1626 (amide I), 1535 cm^{-1} (amide II).

Synthesis of CP-A6$_{10}$:

Following the general protocol of the SPPS, **CP-A6** was grown and cycled in the solid support. Then, the click chemistry was carried out with decyl azide and, finally, the cleavage of the resin. The resulting powder was solubilized in H_2O and purified in reverse phase HPLC [Phenomenex Luna C18 (2) 100A column, H_2O (0.1% TFA)/ ACN (0.1% TFA) 100:0 → 100:0 (0 → 5 min), 100:0 → 25:75 (5 → 35 min), with an overall yield of 25% (21.3 mg). **^{1}H-NMR** (2 mM, H_2O/D_2O, 500 MHz, δ): 10.09 (s, 1H, NH $_{Trp}$), 8.37-8.34 (d, 3H, CH-triazole + 2 NH), 8.25-8.24 (d, 1H, NH), 8.21-8.20 (d, 1H, NH), 8.15-8.13 (d, 1H, NH $_{Ser}$), 8.06-8.05 (d, 1H, NH), 7.49-7.38 (m, 7H, 2 NH +NH_2 Gln), 7.30-7.29 (d, 1H, CH $_{Trp}$), 7.18-7.15 (t, 1H, CH $_{Trp}$), 7.09-7.07 (d, 1H, CH Trp), 7.02 (s, 1H, CH Trp), 4.28-4.25 (m, 2H, N=N-N-C$\underline{H}_2$-CH_2), 3.80 (s, 2H, 2 OH $_{Ser}$), 3.72-3.63 (m, 2H, CH_2 $_{Ser}$), 3.03-2.86 (m, 12H, CH_2-triazole-aliphatic tail + 2 NH_2 $_{Lys}$ + NH_2 $_{Dap}$), 1.71-1.52 (m, 19H, CH_2 $_{aliphatic\ tail}$), 1.32-1.25 (m, 6H, 2 CH_2 $_{Lys}$ + CH_2 $_{Dap}$), 1.16-0.99 (m, 22H, 2 CH_2 Gln + 5 CH_2 $_{Lys}$), 0.76-0.75 (t, 3H, CH_3 aliphatic tail). [Agilent SB-C18 column, H_2O (0.1% TFA)/ACN (0.1% TFA). 100:0 →100:0 (2 min) and 100:0 → 25:75 (19 min)] (R_t = 14.6 min). **MS** (ESI, H_2O): 1110.7 (20, $[M+1H]^+$), 555.5 (100, $[M+2H]^{2+}$), 370.8 (13, $[M+3H]^{3+}$). **HRMS** (ESI): Calcd for: $C_{52}H_{84}N_{16}O_{11}$ $[M+H]^+$: 1109.6580; found 1109.6578. **FTIR (neat)**: ν = 3270 (amide A), 1660, 1629 (amide I), 1535 cm^{-1} (amide II).

Synthesis of CP-A6$_{14}$:

Following the general protocol of the SPPS, **CP-A6** was grown and cycled in the solid support. Then, the click chemistry was carried out with tetradecyl azide and, finally, the cleavage of the resin. The resulting powder was solubilized in H_2O and purified in reverse phase HPLC [Phenomenex Luna C18 (2) 100A column, H_2O (0.1% TFA)/ ACN (0.1% TFA) 100:0 → 100:0 (0 → 5 min), 100:0 → 25:75 (5 → 35 min) with an overall yield of 20% (18.1 mg). [Agilent SB-C18 column, H_2O (0.1% TFA)/ACN (0.1% TFA). 100:0 →100:0 (2 min) and 100:0 → 25:75 (19 min)] (R_t = 16.5 min). **MS** (ESI, H_2O): 1165.7 (20, $[M+1H]^+$), 583.5 (100, $[M+2H]^{2+}$), 389.5 (13, $[M+3H]^{3+}$). **HRMS** (ESI): Calcd for: $C_{56}H_{92}N_{16}O_{11}$ $[M+H]^+$: 1165.7194; found 1165.7204. **FTIR (neat)**: ν = 3270 (amide A), 1672, 1629 (amide I), 1535 cm^{-1} (amide II).

Synthesis of CP-A4$_{10}$-Ox^4:

Following the general protocol of the SPPS, **CP-A4** was grown, cycled and alkoxyamine was introduced in the solid support. Then, the click chemistry was carried out with decyl azide and, finally, the cleavage of the resin. The resulting powder was solubilized in H_2O and purified in reverse phase HPLC [Phenomenex Luna C18 (2) 100A column, H_2O (0.1% TFA)/ ACN (0.1% TFA) 100:0 → 100:0 (0 → 5 min), 100:0 → 25:75 (5 → 35 min) with an overall yield of 13% (12.6 mg). [Agilent SB-C18 column, H_2O (0.1% TFA)/ACN (0.1% TFA). 100:0 →100:0 (2 min) and 100:0 → 25:75 (19 min)] (R_t = 14.6 min). **MS** (ESI, H_2O): 1252.7 (18, $[M+1H]^+$), 1180.6 (5, $[M+1H\text{-}COCH_2ONH_2]^+$), 627.2 (100, $[M+2H]^{2+}$), 590.6 (5, $[M+2H\text{-}COCH_2ONH_2]^{2+}$). **HRMS** (ESI): Calcd for:

$C_{57}H_{93}N_{19}O_{13}$ $[M+1H]^+$: 1252.7265; found 1252.7273. **FTIR (neat)**: ν = 3273 (amide A), 1662, 1632 (amide I), 1541 cm^{-1} (amide II).

Synthesis of CP-A4$_{14}$-Ox^{4}:

Following the general protocol of the SPPS, **CP-A4** was grown, cycled and alkoxyamine was introduced in the solid support. Then, the click chemistry was carried out with tetradecyl azide and, finally, the cleavage of the resin. The resulting powder was solubilized in H_2O and purified in reverse phase HPLC [Phenomenex Luna C18 (2) 100A column, H_2O (0.1% TFA)/ ACN (0.1% TFA) 100:0 → 100:0 (0 → 5 min), 100:0 → 25:75 (5 → 35 min) with an overall yield of 14% (14.1 mg). [Agilent SB-C18 column, H_2O (0.1% TFA)/ACN (0.1% TFA). 100:0 →100:0 (2 min) and 100:0 → 25:75 (19 min)] (R_t = 16.7 min). **MS** (ESI, H_2O): 1309.6 (20, $[M+1H]^+$), 655.1 (100, $[M+2H]^{2+}$), 437.1 (25, $[M+3H]^{3+}$). **HRMS** (ESI): Calcd for: $C_{61}H_{101}N_{19}O_{13}$ $[M+1H]^+$: 1308.7895; found 1308.7899. **FTIR (neat)**: ν = 3273 (amide A), 1662, 1626 (amide I), 1541 cm^{-1} (amide II).

Synthesis of CP-A4$_{10}$-Ox^{8}:

Following the general protocol of the SPPS, **CP-A4** was grown, cycled and alkoxyamine was introduced in the solid support. Then, the click chemistry was carried out with decyl azide and, finally, the cleavage of the resin. The resulting powder was solubilized in H_2O and purified in reverse phase HPLC [Phenomenex Luna C18 (2) 100A column, H_2O (0.1% TFA)/ ACN (0.1% TFA) 100:0 → 100:0 (0 → 5 min), 100:0 → 25:75 (5 → 35 min) with an overall yield of 18% (17.4 mg). [Agilent SB-C18 column, H_2O (0.1% TFA)/ACN (0.1% TFA). 100:0 →100:0 (2 min) and 100:0 → 25:75 (19 min)] (R_t = 14.5 min). **MS** (ESI, H_2O): 1254.7 (8, $[M+1H]^+$), 1180.7 (33, $[M+1H\text{-}COCH_2ONH_2]^+$), 626.9 (25, $[M+2H]^{2+}$), 590.5 (100, $[M+2H]^{2+}$), 418.5 (5, $[M+3H]^{3+}$), 394.0 (27, $[M+3H\text{-}COCH_2ONH_2]^{3+}$). **HRMS** (ESI): Calcd for: $C_{57}H_{93}N_{19}O_{13}$ $[M+1H]^+$: 1252.7272; found 1252.7273. **FTIR (neat)**: ν = 3273 (amide A), 1668, 1632 (amide I), 1535 cm^{-1} (amide II).

Synthesis of CP-A4$_{14}$-Ox^{8}:

Following the general protocol of the SPPS, **CP-A4** was grown, cycled and alkoxyamine was introduced in the solid support. Then, the click chemistry was carried out with tetradecyl azide and, finally, the cleavage of the resin. The resulting powder was solubilized in H_2O and purified in reverse phase HPLC [Phenomenex Luna C18 (2) 100A column, H_2O (0.1% TFA)/ ACN (0.1% TFA) 100:0 → 100:0 (0 → 5 min), 100:0 → 25:75 (5 → 35 min) with an overall yield of 20% (20.2 mg). [Agilent SB-C18 column, H_2O (0.1% TFA)/ACN (0.1% TFA). 100:0 →100:0 (2 min) and 100:0 → 25:75 (19 min)] (R_t = 17.0 min). **MS** (ESI, H_2O): 1308.0 (10, $[M+1H]^+$), 655.0 (100, $[M+2H]^{2+}$), 619.0 (65, $[M+2H\text{-}COCH_2ONH_2]^{2+}$), 437.0 (30, $[M+3H]^{3+}$), 412.6 (18, $[M+3H\text{-}COCH_2ONH_2]^{3+}$). **HRMS** (ESI): Calcd for: $C_{61}H_{101}N_{19}O_{13}$ $[M+1H]^+$: 1308.7898; found 1308.7899. **FTIR (neat)**: ν = 3267 (amide A), 1662, 1626 (amide I), 1535 cm^{-1} (amide II).

Synthesis of CP-A$_{10}$:

Following the general protocol of the SPPS, **CP-A** was grown and cycled in the solid support. Then, the click chemistry was carried out with decyl azide and, finally, the cleavage of the resin. The resulting powder was solubilized in H_2O and purified in reverse phase HPLC [Phenomenex Luna C18 (2) 100A column, H_2O (0.1% TFA)/ ACN (0.1% TFA) 100:0 → 100:0 (0 → 5 min), 100:0 → 25:75 (5 → 35 min) with an overall yield of 29% (26.1 mg). **^{1}H-NMR** (2 mM, H_2O/D_2O, 500 MHz, δ): 10.09 (s, 1H, NH $_{Trp}$), 8.36-8.34 (d, 3H, CH-triazole + 2 NH), 8.25-8.24 (d, 1H, NH), 8.21-8.20 (d, 1H, NH), 8.15-8.13 (d, 1H, NH $_{Ser}$), 8.06-8.05 (d, 1H, NH), 7.49-7.38 (m, 7H, 2 NH +NH_2 Gln), 7.30-7.29 (d, 1H, CH $_{Trp}$), 7.18-7.15 (t, 1H, CH $_{Trp}$), 7.09-7.07 (d, 1H, CH Trp), 7.02 (s, 1H, CH Trp), 4.28-4.25 (m, 2H, N=N-N-C$\underline{H}_2$-CH_2), 3.80 (s, 2H, 2 OH $_{Ser}$), 3.72-3.69 (m, 2H, CH_2 $_{Ser}$), 3.03-2.86 (m, 12H, CH_2-triazole-aliphatic tail + 3 NH_2 $_{Lys}$), 1.71-1.52 (m, 19H, CH_2 $_{aliphatic\ tail}$), 1.32-1.25 (m, 6H, 3 CH_2 $_{Lys}$), 1.16-0.99 (m, 22H, 2 CH_2 Gln + 9 CH_2 $_{Lys}$), 0.76-0.75 (t, 3H, CH_3 aliphatic tail). [Agilent SB-C18 column, H_2O (0.1% TFA)/ACN (0.1% TFA). 100:0 →100:0 (2 min) and 100:0 → 25:75 (19 min)] (R_t = 14.6 min). **MS** (ESI, H_2O): 1151.7 (20, $[M+1H]^+$), 576.5 (100, $[M+2H]^{2+}$), 384.8 (20, $[M+3H]^{3+}$). **HRMS** (ESI): Calcd for: $C_{55}H_{90}N_{16}O_{11}$ $[M+H]^+$: 1151.7054; found 1151.7048. **FTIR (neat)**: ν = 3273 (amide A), 1668, 1626 (amide I), 1535 cm^{-1} (amide II).

Synthesis of CP-A$_{14}$:

Following the general protocol of the SPPS, **CP-A** was grown and cycled in the solid support. Then, the click chemistry was carried out with tetradecyl azide and, finally, the cleavage of the resin. The resulting powder was solubilized in H_2O and purified in reverse phase HPLC [Phenomenex Luna C18 (2) 100A column, H_2O (0.1% TFA)/ ACN (0.1% TFA) 100:0 → 100:0 (0 → 5 min), 100:0 → 25:75 (5 → 35 min) with an overall yield of 26% (24.5 mg). [Agilent SB-C18 column, H_2O (0.1% TFA)/ACN (0.1% TFA). 100:0 →100:0 (2 min) and 100:0 → 25:75 (19 min)] (R_t = 16.5 min). **MS** (ESI, H_2O): 1208.8 (28, $[M+1H]^+$), 604.5 (100, $[M+2H]^{2+}$), 403.5 (25, $[M+3H]^{3+}$). **HRMS** (ESI): Calcd for: $C_{59}H_{98}N_{16}O_{11}$ $[M+H]^+$: 1207.7678; found 1207.7674. **FTIR (neat)**: ν = 3273 (amide A), 1668, 1626 (amide I), 1535 cm^{-1} (amide II).

Synthesis of peptide CP-C1:

Following the general protocol of the SPPS, the cyclic peptide was grown and cycled in the solid support. Then, the cleavage of the resin was carried out and the resulting powder was solubilized in H_2O/ACN. The solution was purified by reverse phase HPLC [Phenomenex Luna C18 (2) 100A column, H_2O (0.1% TFA)/ ACN (0.1% TFA) 80:20 → 80:20 (0 → 5 min), 80:20 → 5:95 (5 → 35 min) with an overall yield of 8% (7.0 mg). [Agilent SB-C18 column, H_2O (0.1% TFA)/ACN (0.1% TFA). H_20 (0.1% TFA)/ACN (0.1% TFA). 80:20 →80:20 (2 min) and 80:20 → 5:95 (19 min)] (R_t = 11.6 min). **MS** (ESI, H_2O): 1115.6 (38, $[M+1H]^+$), 558.0 (100, $[M+2H]^{2+}$), 372.5 (25, $[M+3H]^{3+}$). **HRMS** (ESI): Calcd for: $C_{56}H_{83}N_{13}O_{11}$ $[M+1H]^+$: 1114.6408; found 1194.6408. **FTIR (neat)**: ν = 3273 (amide A), 1674, 1626 (amide I), 1529 cm^{-1} (amide II).

Synthesis of peptide CP-C2:

Following the general protocol of the SPPS, the cyclic peptide was grown and cycled in the solid support. Then, the cleavage of the resin was carried out and the resulting powder was solubilized in H_2O/ACN. The solution was purified by reverse phase HPLC [Phenomenex Luna C18 (2) 100A column, H_2O (0.1% TFA)/ ACN (0.1% TFA) 80:20 → 80:20 (0 → 5 min), 80:20 → 5:95 (5 → 35 min) with an overall yield of 9% (8.3 mg). [Agilent SB-C18 column, H_2O (0.1% TFA)/ACN (0.1% TFA). H_20 (0.1% TFA)/ACN (0.1% TFA). 80:20 →80:20 (2 min) and 80:20 → 5:95 (19 min)] (R_t = 11.3 min). **MS** (ESI, H_2O): 1185.7 (25, $[M+1H]^+$), 592.9 (100, $[M+2H]^{2+}$), 395.8 (35, $[M+3H]^{3+}$). **HRMS** (ESI): Calcd for: $C_{60}H_{89}N_{13}O_{12}$ $[M+1H]^+$: 1183.6846; found 1184.6826. **FTIR (neat)**: ν = 3285 (amide A), 1674, 1620 (amide I), 1535 cm^{-1} (amide II).

Synthesis of CP-A6-18:

Following the general protocol of the SPPS, **CP-A6-18** was grown and cycled in the solid support. Then, the resulting powder was solubilized in H_2O and purified in reverse phase HPLC [Phenomenex Luna C18 (2) 100A column, H_2O (0.1% TFA)/ ACN (0.1% TFA) 100:0 → 100:0 (0 → 5 min), 100:0 → 25:75 (5 → 35 min) with an overall yield of 10% (7.6 mg). [Agilent SB-C18 column, H_2O (0.1% TFA)/ACN (0.1% TFA). 100:0 →100:0 (2 min) and 100:0 → 25:75 (19 min)] (R_t = 9.2 min). **MS** (ESI, H_2O): 996.5 (30, $[M+1H]^+$), 498.9 (100, $[M+2H]^{2+}$), 332.8 (8, $[M+3H]^{3+}$). **HRMS** (ESI): Calcd for: $C_{46}H_{69}N_{13}O_{12}$ $[M+H]^+$: 996.5266; found 996.5261. **FTIR (neat)**: ν = 3273 (amide A), 1668, 1626 (amide I), 1535 cm^{-1} (amide II).

Synthesis of CP-A6$_{10}$-18:

Following the general protocol of the SPPS, **CP-A6** was grown and cycled in the solid support. Then, the click chemistry was carried out with decyl azide and, finally, the cleavage of the resin. The resulting powder was solubilized in H_2O and purified in reverse phase HPLC [Phenomenex Luna C18 (2) 100A column, H_2O (0.1% TFA)/ ACN (0.1% TFA) 100:0 → 100:0 (0 → 5 min), 100:0 → 25:75 (5 → 35 min) with an overall yield of 9% (8.2 mg). [Agilent SB-C18 column, H_2O (0.1% TFA)/ACN (0.1% TFA). 100:0 →100:0 (2 min) and 100:0 → 25:75 (19 min)] (R_t = 13.9 min). **MS** (ESI, H_2O): 1180.7 (27, $[M+1H]^+$), 590.5 (100, $[M+2H]^{2+}$), 394.0 (35, $[M+3H]^{3+}$). **HRMS** (ESI): Calcd for: $C_{56}H_{90}N_{16}O_{12}$ $[M+H]^+$: 1179.6996; found 1179.6997. **FTIR (neat)**: ν = 3279 (amide A), 1662, 1626 (amide I), 1529 cm^{-1} (amide II).

Synthesis of CP-A6$_{14}$-18:

Following the general protocol of the SPPS, **CP-A6** was grown and cycled in the solid support. Then, the click chemistry was carried out with tetradecyl azide and, finally, the cleavage of the resin. The resulting powder was solubilized in H_2O and purified in reverse phase HPLC [Phenomenex Luna C18 (2) 100A column, H_2O (0.1% TFA)/ ACN (0.1% TFA) 100:0 → 100:0 (0 → 5 min), 100:0 → 25:75 (5 → 35 min) with an overall yield of 10% (9.6 mg). [Agilent SB-C18 column, H_2O (0.1% TFA)/ACN (0.1% TFA). 100:0 →100:0 (2 min) and 100:0 → 25:75 (19 min)] (R_t = 16.4 min). **MS** (ESI, H_2O): 1237.7 (10, $[M+1H]^+$), 618.6 (100, $[M+2H]^{2+}$), 412.6 (16, $[M+3H]^{3+}$). **HRMS** (ESI): Calcd for:

$C_{60}H_{98}N_{16}O_{12}$ $[M+H]^+$: 1235.7622; found 1235.7623. **FTIR (neat)**: *v* = 3279 (amide A), 1668, 1626 (amide I), 1535 cm^{-1} (amide II).

Synthesis of CP-A7-18:

Following the general protocol of the SPPS, **CP-A7-18** was grown and cycled in the solid support. Then, the resulting powder was solubilized in H_2O and purified in reverse phase HPLC [Phenomenex Luna C18 (2) 100A column, H_2O (0.1% TFA)/ ACN (0.1% TFA) 100:0 → 100:0 (0 → 5 min), 100:0 → 25:75 (5 → 35 min) with an overall yield of 8% (6.8 mg). [Agilent SB-C18 column, H_2O (0.1% TFA)/ACN (0.1% TFA). 100:0 →100:0 (2 min) and 100:0 → 25:75 (19 min)] (R_t = 9.2 min). **MS** (ESI, H_2O): 1096.6 (15, $[M+1H]^+$), 547.9 (100, $[M+2H]^{2+}$), 365.6 (25, $[M+3H]^{3+}$). **HRMS** (ESI): Calcd for: $C_{49}H_{75}N_{17}O_{12}$ $[M+H]^+$: 1094.5859; found 1094.5854. **FTIR (neat)**: *v* = 3279 (amide A), 1656, 1626 (amide I), 1535 cm^{-1} (amide II).

Synthesis of CP-A7$_{10}$-18:

Following the general protocol of the SPPS, **CP-A7** was grown and cycled in the solid support. Then, the click chemistry was carried out with decyl azide and, finally, the cleavage of the resin. The resulting powder was solubilized in H_2O and purified in reverse phase HPLC [Phenomenex Luna C18 (2) 100A column, H_2O (0.1% TFA)/ ACN (0.1% TFA) 100:0 → 100:0 (0 → 5 min), 100:0 → 25:75 (5 → 35 min) with an overall yield of 9% (9.0 mg). [Agilent SB-C18 column, H_2O (0.1% TFA)/ACN (0.1% TFA). 100:0 →100:0 (2 min) and 100:0 → 25:75 (19 min)] (R_t = 14.1 min). **MS** (ESI, H_2O): 1277.8 (18, $[M+1H]^+$), 639.6 (100, $[M+2H]^{2+}$), 426.8 (45, $[M+3H]^{3+}$). **HRMS** (ESI): Calcd for: $C_{59}H_{96}N_{20}O_{12}$ $[M+H]^+$: 1277.7589; found 1277.7589. **FTIR (neat)**: *v* = 3279 (amide A), 1662, 1626 (amide I), 1529 cm^{-1} (amide II).

Synthesis of CP-A7$_{14}$-18:

Following the general protocol of the SPPS, **CP-A7** was grown and cycled in the solid support. Then, the click chemistry was carried out with tetradecyl azide and, finally, the cleavage of the resin. The resulting powder was solubilized in H_2O and purified in reverse phase HPLC [Phenomenex Luna C18 (2) 100A column, H_2O (0.1% TFA)/ ACN (0.1% TFA) 100:0 → 100:0 (0 → 5 min), 100:0 → 25:75 (5 → 35 min) with an overall yield of 7% (9.1 mg). [Agilent SB-C18 column, H_2O (0.1% TFA)/ACN (0.1% TFA). 100:0 →100:0 (2 min) and 100:0 → 25:75 (19 min)] (R_t = 16.3 min). **MS** (ESI, H_2O): 1333.8 (20, $[M+1H]^+$), 667.6 (100, $[M+2H]^{2+}$), 445.5 (42, $[M+3H]^{3+}$). **HRMS** (ESI): Calcd for: $C_{63}H_{104}N_{20}O_{12}$ $[M+H]^+$: 1333.8220; found 1333.8215. **FTIR (neat)**: *v* = 3279 (amide A), 1662, 1626 (amide I), 1529 cm^{-1} (amide II).

Chapter 3

MTT assay in cell lines NCI/ADR-RES and MCF-7:

Cell line and broth conditions: Both cell lines (doxorubicin resistant ovarium cancer cells, NCI/ADR-RES, and breast cancer cells, MCF-7) were grown in RPMI 1640 broth with a 10% of fetal bovine serum (FBS) and 2 mM of L-glutamine in an atmosphere of 95% air and 5% CO_2 at a temperature of 37 ºC.

Cytotoxicity assays: The cell growth inhibition for the peptides was evaluated by MTT assay due to it allow to determine the metabolic active cells in the experiment. Cell were incubated in a 96-well plate with a concentration of 1500 cells per well for 24 h. Later, the peptides solved in MilliQ water were added, keeping the same proportion of MilliQ water in each well. After 48 h of incubation (in atmosphere of 5% CO_2/95% air at 37 ºC), 10 µL of MTT was added to each well and incubated for another 4 h. The MTT was diluted to a concentration of 5 mg/mL in PBS (same concentration of MTT used in bacteria in chapter 2). 100 µL of SDS at 10% HCl (0.01 M) was added and incubated for 12-14 h under same experimental conditions. Finally, the plate was read at a wavelength of 595 nm.

All experiments were repeated with triplicate points.

Controls were carried out with a well of 1500 cells in RPMI 1640 as positive control and other with only RPMI 1640 as negative control. Moreover, control with the same amount of MilliQ water used for diluting the peptides was also tested. This control did not show growth inhibition of the cell compare with the positive control.

Analysis and expression of the results: data was expressed as growth inhibition percentage. This percentage was calculated based on the equation:

$$\% \text{ inhibition} = 100 - ((AO*100)/AT)$$

where AO is the absorbance observed for the peptides in the wells and AT is the absorbance observed for MilliQ water in the wells.

The inhibitory power of the compounds was evaluated by the calculation of the concentration curve with the percentage of inhibition, adjusting to the equation:

$$y = \frac{\text{Emax}}{1+\left(\frac{\text{IC50}}{\text{x}}\right)^{\text{n}}}$$

where **y** is the effect observed at the **x** concentration, **Emax** is the maximum effect, **IC_{50}** is the concentration that achieves the 50% of the growth and **n** is the gradient of the curve. This no linear adjust was carried out with the regression program GraphPad Prism Version 2.01, 1996, (GraphPad Software Inc.).

The parameters used in the evaluation of the compounds were the inhibitory power (inverse of IC_{50}) and the efficiency (express as the maximum percentage of inhibition achieved by the compound). Both parameters were also used for the *cis*-platin.

Synthesis of CP-A4$_{10}$-DOX:

Following the general protocol of the SPPS, **CP-A4** was grown, cycled and alkoxyamine was introduced in the solid support. Then, the click chemistry was carried out with decyl azide and, finally, the cleavage of the resin. The resulting powder (0.078 mmol) was solubilized in H_2O (10 mM) and mixed with a solution of DOX (45 mg, 0.078 mmol, 120 mM). Acetic acid was added until final concentration 0.1% acetic acid/H_2O. The reaction was stirred for 2 h at room temperature and then purified in reverse phase HPLC [Phenomenex Luna C18 (2) 100A column, H_2O (0.1% TFA)/ ACN (0.1% TFA) 100:0 → 100:0 (0 → 5 min), 100:0 → 25:75 (5 → 35 min) with an overall yield of 18% (24.8 mg). [Agilent SB-C18 column, H_2O (0.1% TFA)/ACN (0.1% TFA). 100:0 →100:0 (2 min) and 100:0 → 25:75 (19 min)] (R_t = 15.2 min). **MS** (ESI, H_2O): 1781.6 (12, $[M+1H]^+$), 889.8 (100, $[M+2H]^{2+}$), 593.5 (42, $[M+3H]^{3+}$). **HRMS** (ESI): Calcd for: $C_{84}H_{121}N_{20}O_{23}$ $[M+1H]^+$: 1777.8893; found 1777.8908. **FTIR (neat)**: ν = 3277 (amide A), 1662, 1632 (amide I), 1542 cm^{-1} (amide II).

Synthesis of CP-A6$_{10}$-Ox^4:

Following the general protocol of the SPPS, **CP-A6** was grown, cycled and alkoxyamine was introduced in the solid support. Then, the click chemistry was carried out with decyl azide and, finally, the cleavage of the resin. The resulting powder was solubilized in H_2O and purified in reverse phase HPLC [Phenomenex Luna C18 (2) 100A column, H_2O (0.1% TFA)/ ACN (0.1% TFA) 100:0 → 100:0 (0 → 5 min), 100:0 → 25:75 (5 → 35 min) with an overall yield of 22% (20.2 mg). [Agilent SB-C18 column, H_2O (0.1% TFA)/ACN (0.1% TFA). 100:0 →100:0 (2 min) and 100:0 → 25:75 (19 min)] (R_t = 14.4 min). **MS** (ESI, H_2O): 1183.7 (30, $[M+1H]^+$), 592.0 (100, $[M+2H]^{2+}$), 395.1 (12, $[M+3H]^{3+}$). **HRMS** (ESI): Calcd for: $C_{54}H_{87}N_{17}O_{13}$ $[M+1H]^+$: 1182.6740; found 1182.6742. **FTIR (neat)**: ν = 3277 (amide A), 1668, 1632 (amide I), 1535 cm^{-1} (amide II).

Synthesis of CP-A6$_{10}$-DOX:

Following the general protocol of the SPPS, **CP-A6** was grown, cycled and alkoxyamine was introduced in the solid support. Then, the click chemistry was carried out with decyl azide and, finally, the cleavage of the resin. The resulting powder (0.078 mmol) was solubilized in H_2O (10 mM) and mixed with a solution of DOX (45 mg, 0.078 mmol, 120 mM). Acetic acid was added until final concentration 0.1% acetic acid/H_2O. The reaction was stirred at room temperature for 2 h and then purified in reverse phase HPLC [Phenomenex Luna C18 (2) 100A column, H_2O (0.1% TFA)/ ACN (0.1% TFA) 100:0 → 100:0 (0 → 5 min), 100:0 → 25:75 (5 → 35 min) with an overall yield of 15% (19.9 mg). [Agilent SB-C18 column, H_2O (0.1% TFA)/ACN (0.1% TFA). 100:0 →100:0 (2 min) and 100:0 → 25:75 (19 min)] (R_t = 15.1 min). **MS** (ESI, H_2O): 1708.8 (14, $[M+1H]^+$), 854.7 (100, $[M+2H]^{2+}$). **HRMS** (ESI): Calcd for: $C_{81}H_{114}N_{18}O_{23}$ $[M+1H]^+$: 1707.8372; found 1707.8377. **FTIR (neat)**: ν = 3277 (amide A), 1668, 1632 (amide I), 1542 cm^{-1} (amide II).

Synthesis of CP-A1-DOX:

Following the general protocol of the SPPS, **CP-A1** was grown, cycled and alkoxyamine was introduced in the solid support before the cleavage of the resin. The resulting powder (0.078 mmol) was solubilized in H_2O (10 mM) and mixed with a solution of DOX (45 mg, 0.078 mmol, 120 mM). Acetic acid was added until final concentration 0.1% acetic acid/H_2O. The reaction was stirred at room temperature for 2 h and then purified in reverse phase HPLC [Phenomenex Luna C18 (2) 100A column, H_2O (0.1% TFA)/ ACN (0.1% TFA) 100:0 → 100:0 (0 → 5 min), 100:0 → 25:75 (5 → 35 min) with an overall yield of 22% (26.7 mg). [Agilent SB-C18 column, H_2O (0.1% TFA)/ACN (0.1% TFA). 100:0 →100:0 (2 min) and 100:0 → 25:75 (19 min)] (R_t = 11.9 min). **MS** (ESI, H_2O): 1566.7 (22, $[M+1H]^+$), 784.2 (100, $[M+2H]^{2+}$). **HRMS** (ESI): Calcd for: $C_{74}H_{100}N_{15}O_{23}$ $[M+1H]^+$: 1566.7111; found 1566.7111. **FTIR (neat)**: ν = 3271 (amide A), 1668, 1626 (amide I), 1542 cm^{-1} (amide II).

Synthesis of CP-A2-DOX:

Following the general protocol of the SPPS, **CP-A2** was grown, cycled and alkoxyamine was introduced in the solid support before the cleavage of the resin. The resulting powder (0.078 mmol) was solubilized in H_2O (10 mM) and mixed with a solution of DOX (45 mg, 0.078 mmol, 120 mM). Acetic acid was added until final concentration 0.1% acetic acid/H_2O. The reaction was stirred at room temperature for 2 h and then purified in reverse phase HPLC [Phenomenex Luna C18 (2) 100A column, H_2O (0.1% TFA)/ ACN (0.1% TFA) 100:0 → 100:0 (0 → 5 min), 100:0 → 25:75 (5 → 35 min) with an overall yield of 20% (24.4 mg). [Agilent SB-C18 column, H_2O (0.1% TFA)/ACN (0.1% TFA). 100:0 →100:0 (2 min) and 100:0 → 25:75 (19 min)] (R_t = 11.9 min). **MS** (ESI, H_2O): 1567.6 (25, $[M+1H]^+$), 784.2 (100, $[M+2H]^{2+}$). **HRMS** (ESI): Calcd for: $C_{74}H_{100}N_{15}O_{23}$ $[M+1H]^+$: 1566.7093; found 1566.7111. **FTIR (neat)**: ν = 3277 (amide A), 1668, 1626 (amide I), 1536 cm^{-1} (amide II).

Appendage I: Characterization of CPs

USC
UNIVERSIDADE
DE SANTIAGO
DE COMPOSTELA

Chapter 1

Peptide CP-A: *c*-[QKSKSWZK]

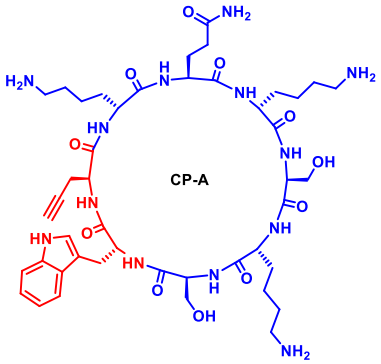

RP-HPLC: [Agilent SB-C18 column, H_20 (0.1% TFA)/ACN (0.1% TFA). 100:0 →100:0 (2 min) and 100:0 → 25:75 (19 min)] (R_t = 9.1 min). Absorbance at 222 nm.

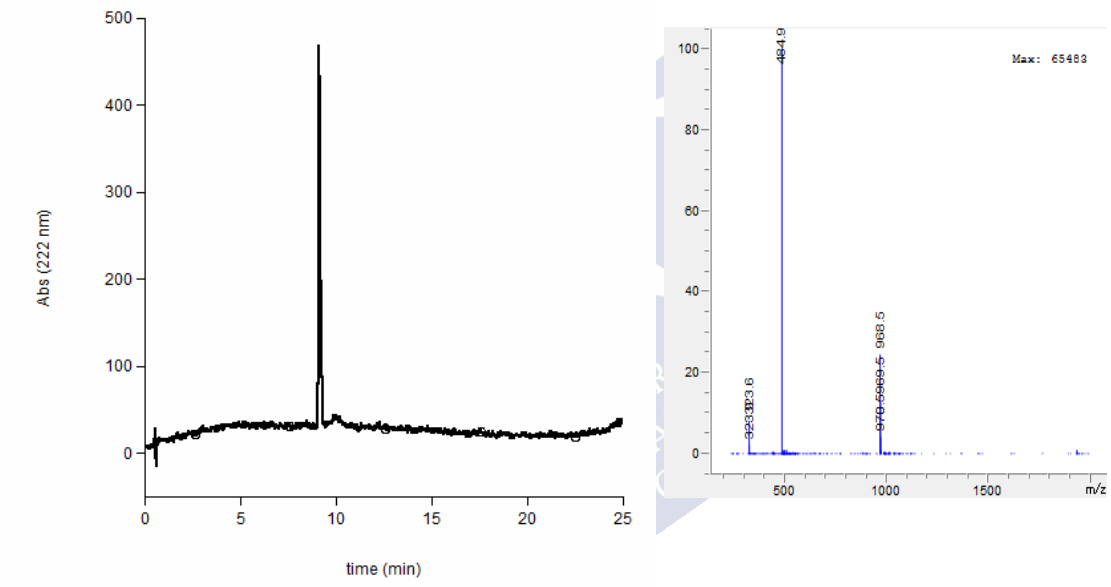

FT-IR (neat, 298 K)

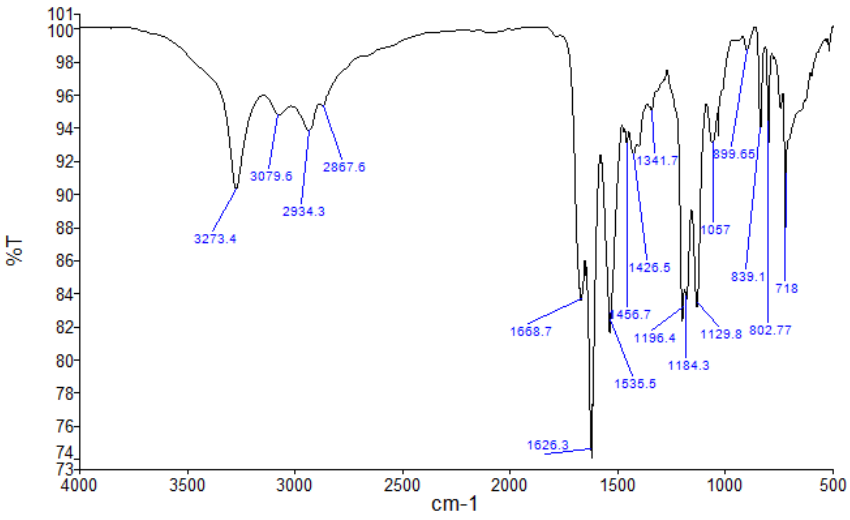

Peptide CP-A1: *c*-[QK^{Ox}SKSWZK]

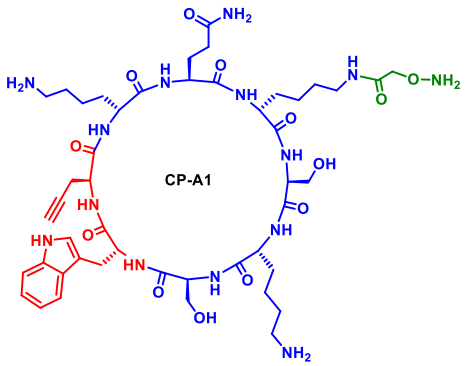

RP-HPLC: [Agilent SB-C18 column, H_20 (0.1% TFA)/ACN (0.1% TFA). 100:0 →100:0 (2 min) and 100:0 → 25:75 (19 min)] (R_t = 9.3 min). Absorbance at 222 nm.

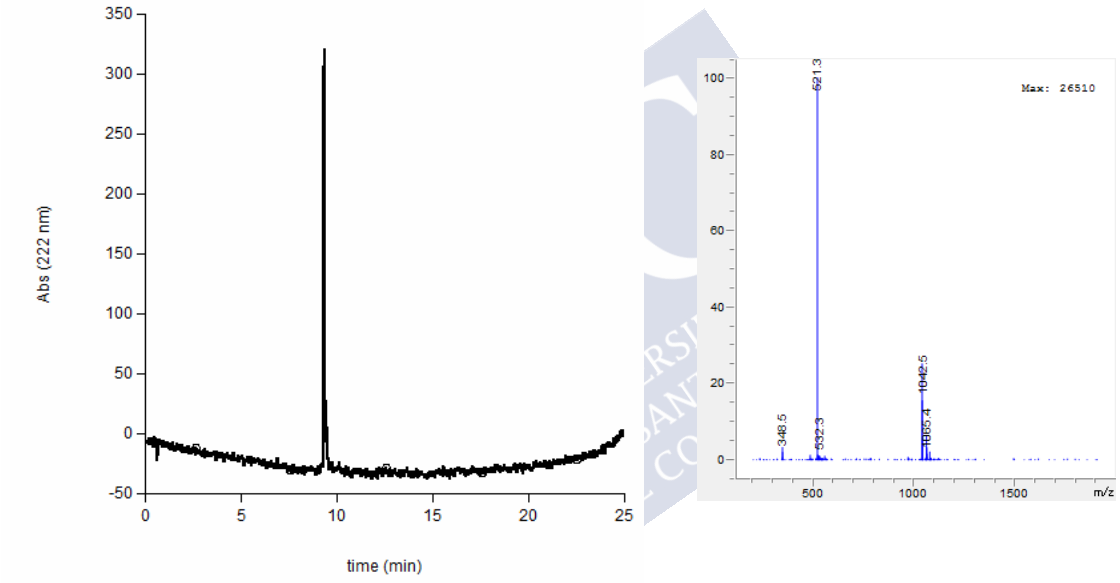

FT-IR (neat, 298 K)

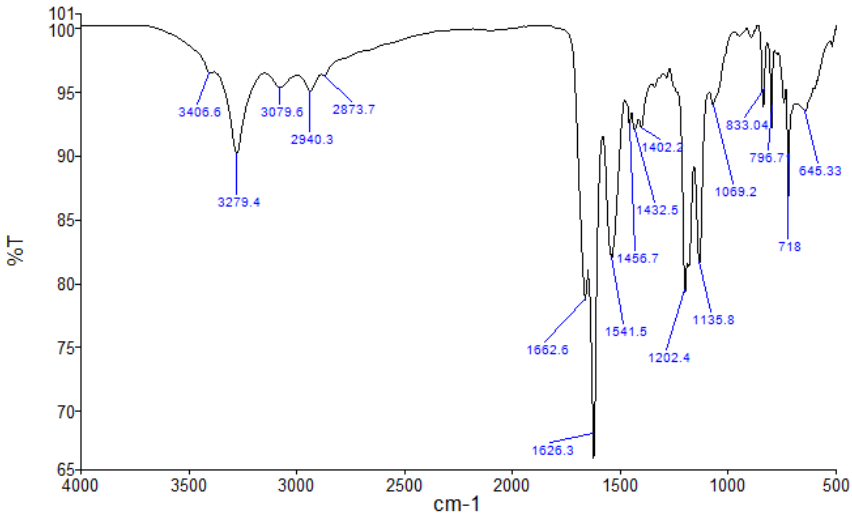

^{1}H-NMR: (H_2O/D_2O, 500 MHz)

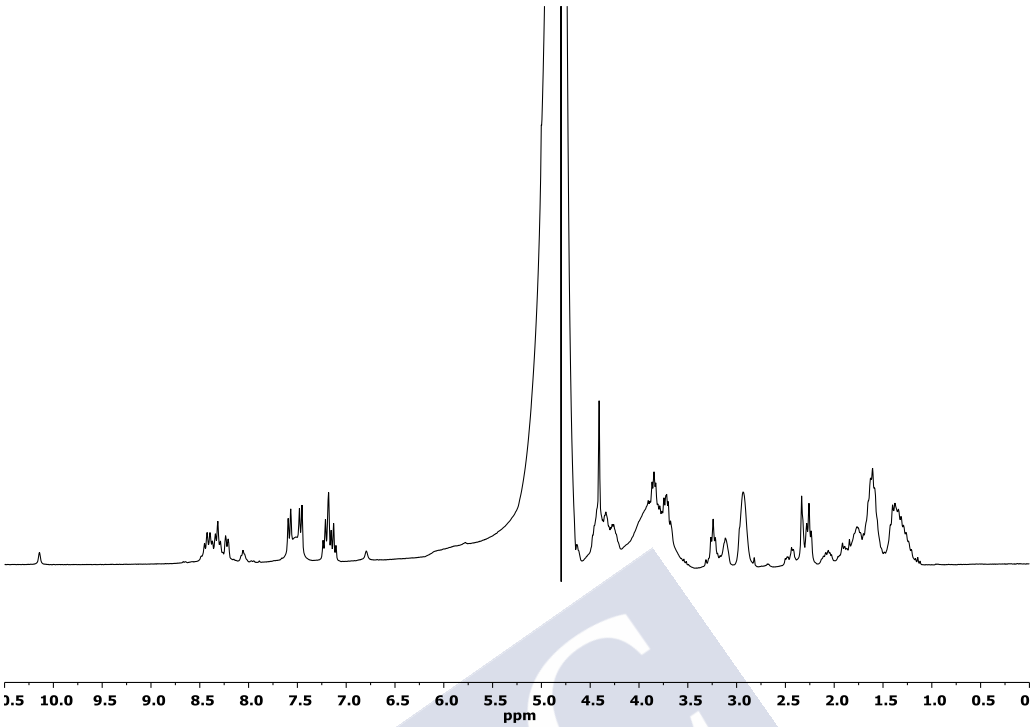

Peptide CP-A2: *c*-[QKSK^{Ox}SWZK]

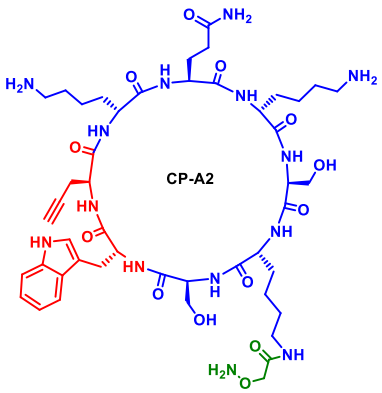

RP-HPLC: [Agilent SB-C18 column, H_20 (0.1% TFA)/ACN (0.1% TFA). 100:0 →100:0 (2 min) and 100:0 → 25:75 (19 min)] (R_t = 9.5 min). Absorbance at 222 nm.

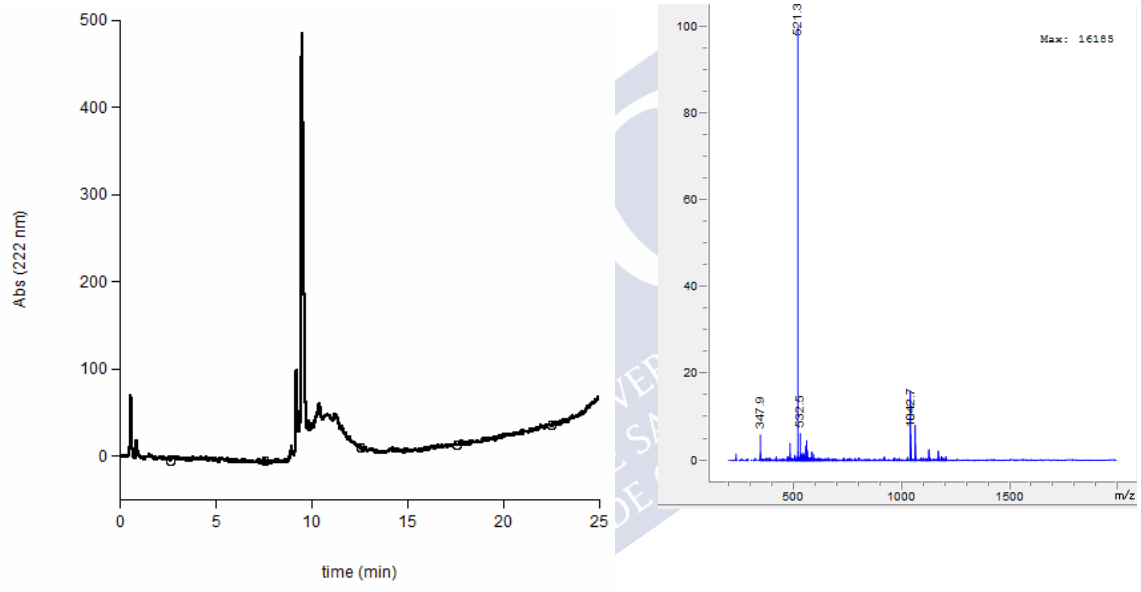

FT-IR (neat, 298 K)

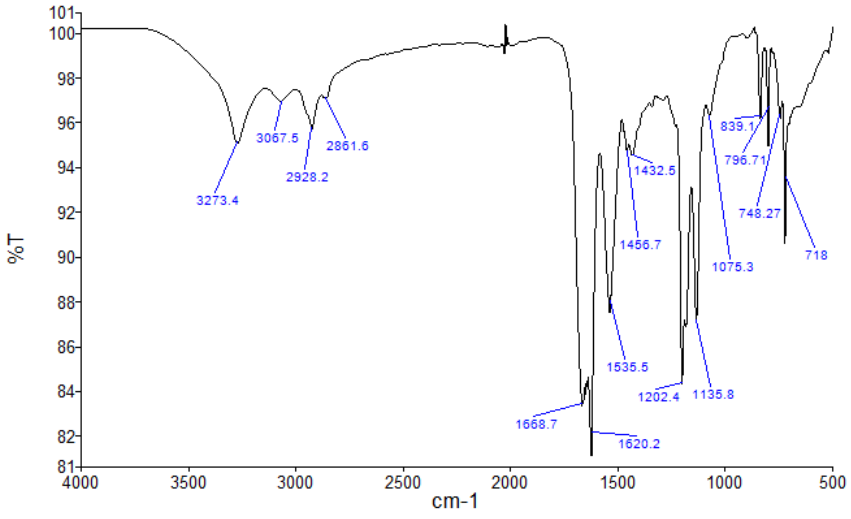

^{1}H-NMR: (H_2O/D_2O, 500 MHz)

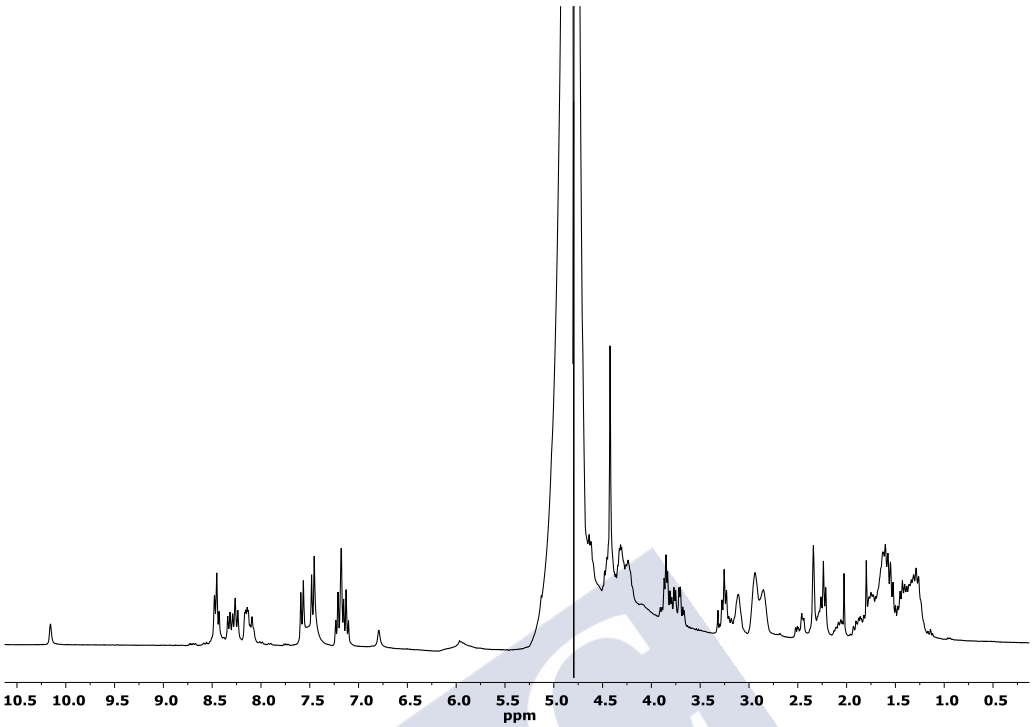

Peptide CP-A3: *c*-[QSK^{Ox}KSWZK]

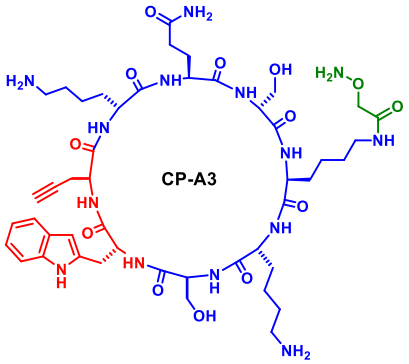

RP-HPLC: [Agilent SB-C18 column, H_20 (0.1% TFA)/ACN (0.1% TFA). 100:0 →100:0 (2 min) and 100:0 → 25:75 (19 min)] (R_t = 9.5 min). Absorbance at 222 nm.

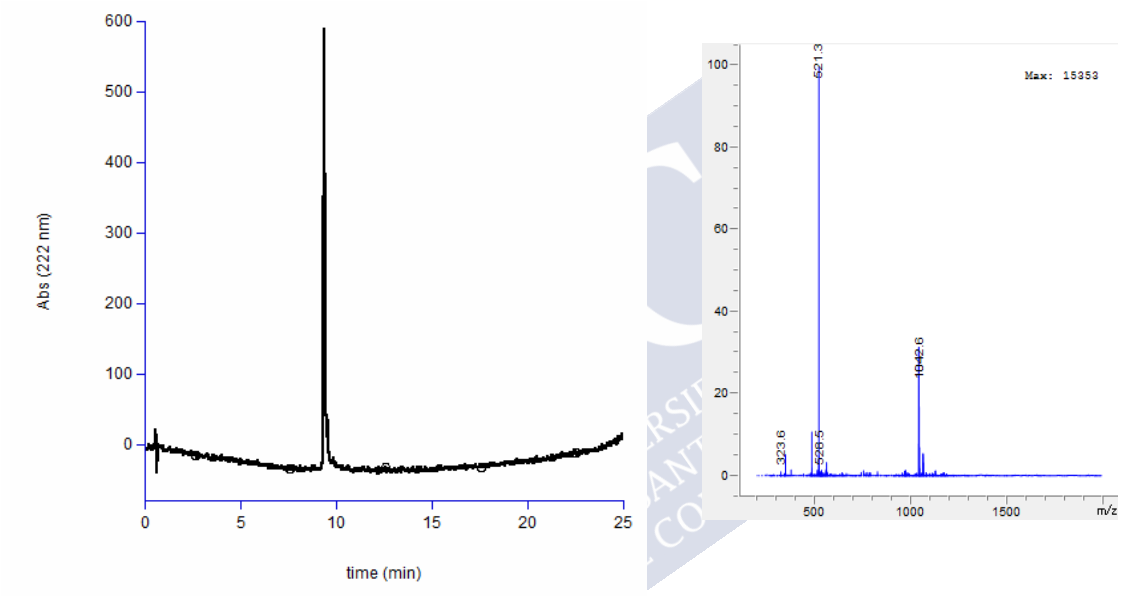

FT-IR (neat, 298 K)

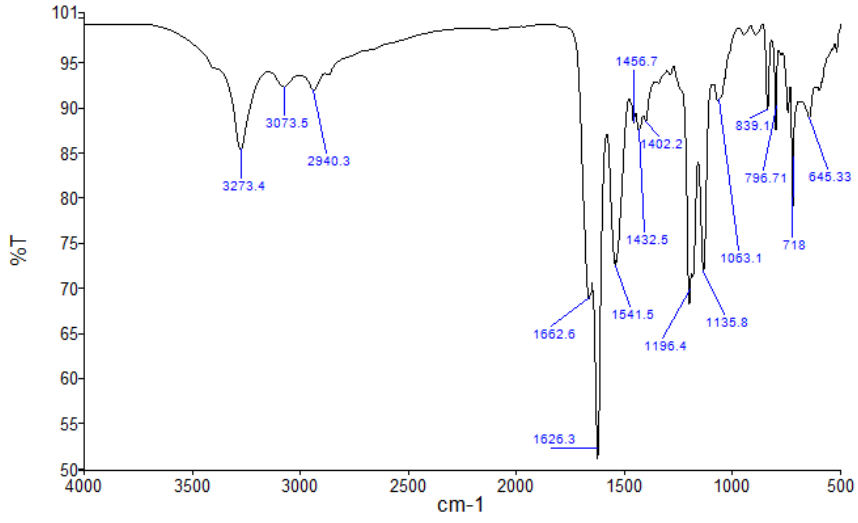

Chapter 2

Peptide CP-A1$_{10}$: *c*-[QK^{Ox}SKSWZ^{10}K]

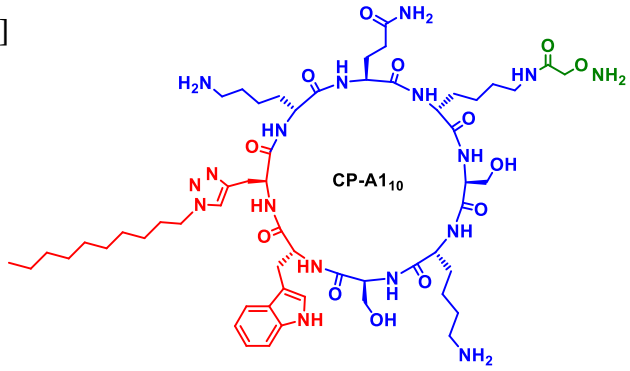

RP-HPLC: [Agilent SB-C18 column, H_20 (0.1% TFA)/ACN (0.1% TFA). 100:0 →100:0 (2 min) and 100:0 → 25:75 (19 min)] (R_t = 14.2 min). Absorbance at 222 nm.

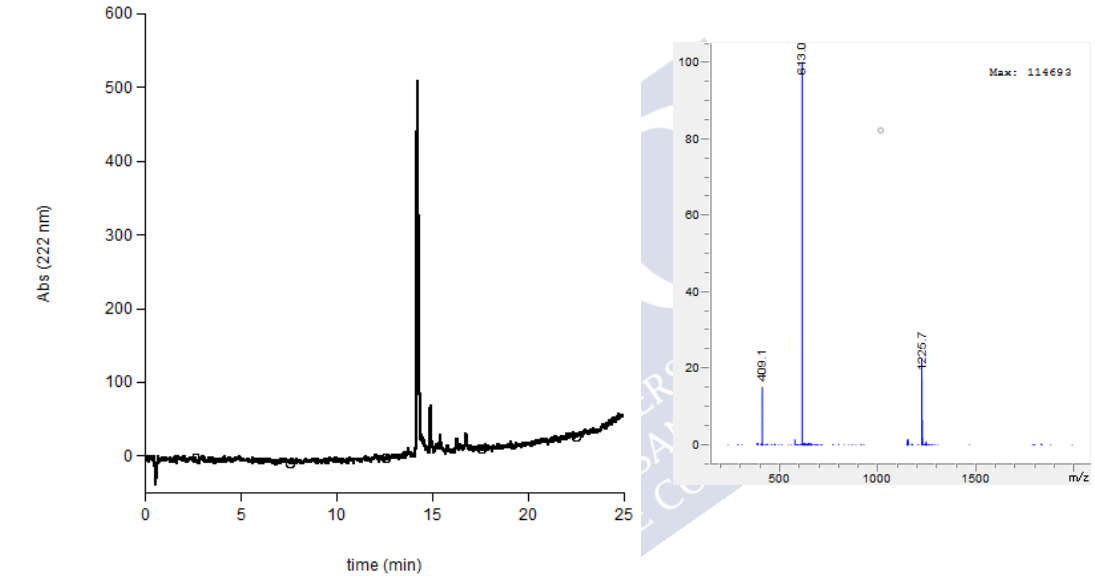

FT-IR (neat, 298 K)

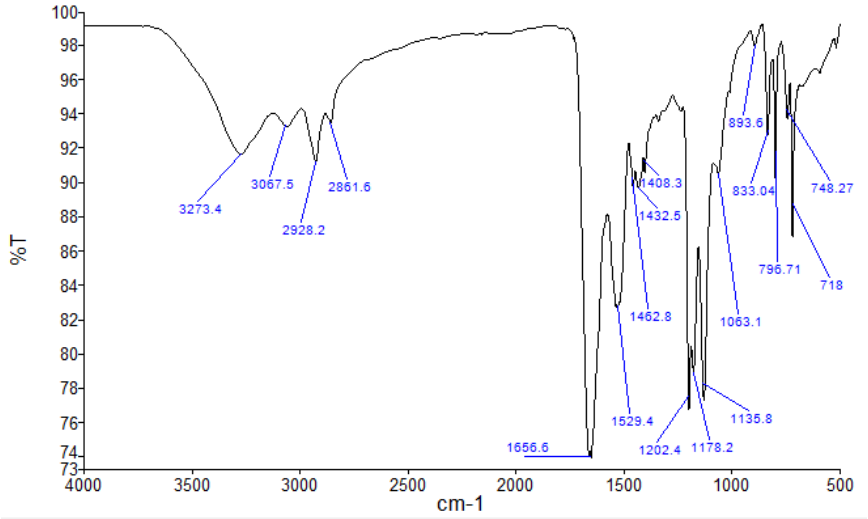

Peptide CP-A1$_{14}$: *c*-[Q$\underline{\text{K}}^{\text{Ox}}S\underline{\text{K}}S\underline{\text{W}}Z^{14}\underline{\text{K}}$]

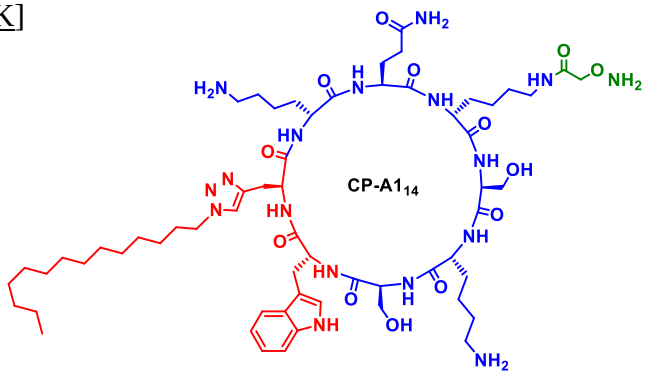

RP-HPLC: [Agilent SB-C18 column, H_20 (0.1% TFA)/ACN (0.1% TFA). 100:0 →100:0 (2 min) and 100:0 → 25:75 (19 min)] (R_t = 17.1 min). Absorbance at 222 nm.

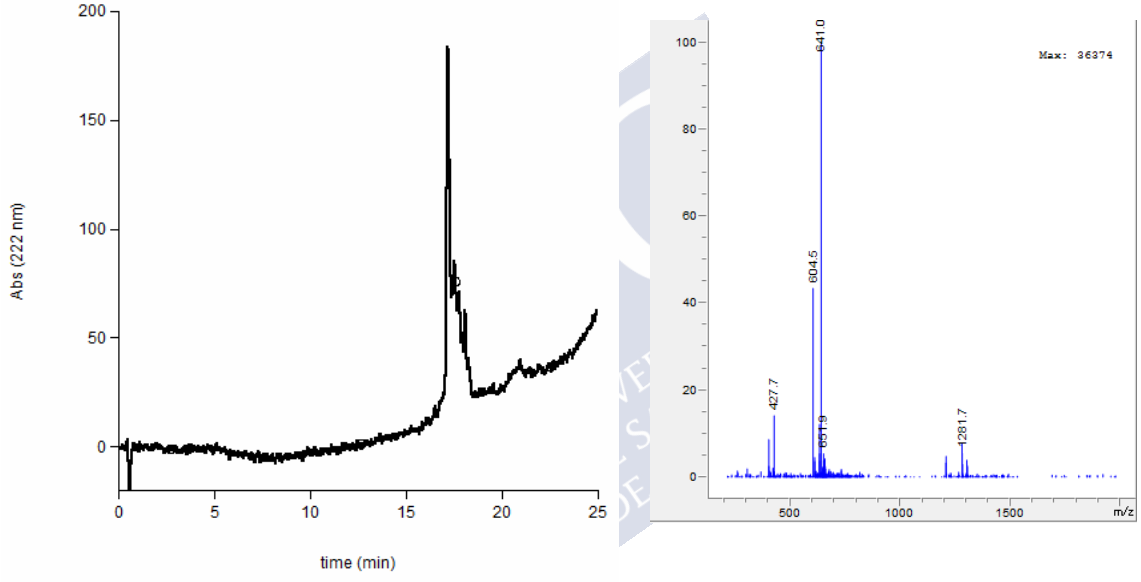

Peptide CP-A2$_{10}$: *c*-[QKSK^{Ox}SWZ^{10}K]

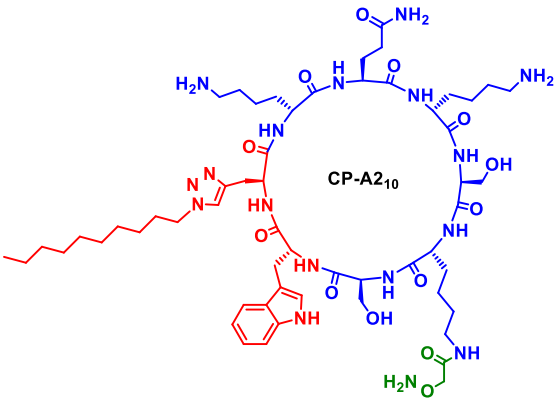

RP-HPLC: [Agilent SB-C18 column, H_20 (0.1% TFA)/ACN (0.1% TFA). 100:0 →100:0 (2 min) and 100:0 → 25:75 (19 min)] (R_t = 14.4 min). Absorbance at 222 nm.

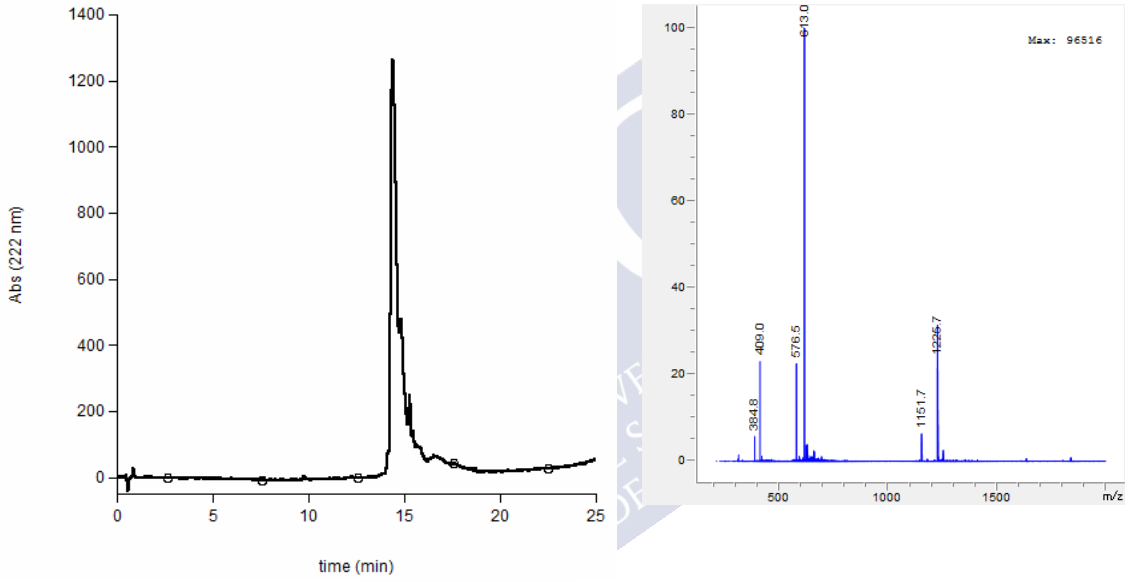

FT-IR (neat, 298 K)

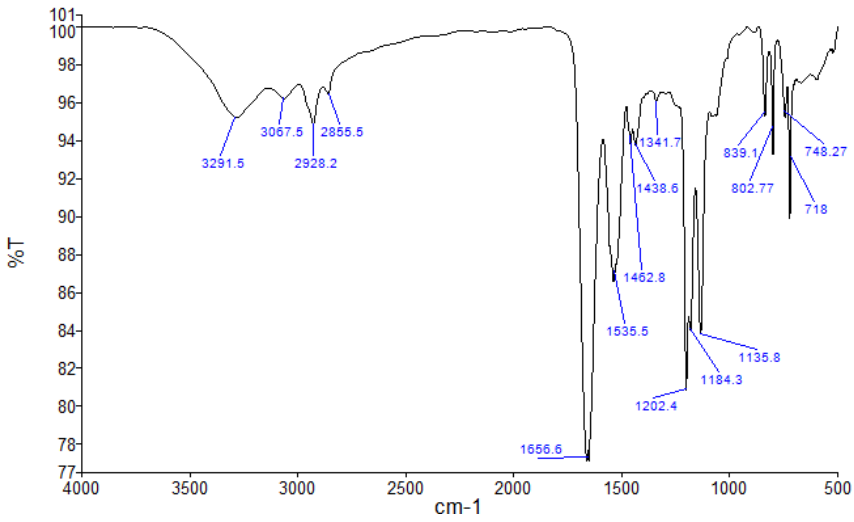

Peptide CP-A2$_{14}$: *c*-[QKSK^{Ox}SWZ^{14}K]

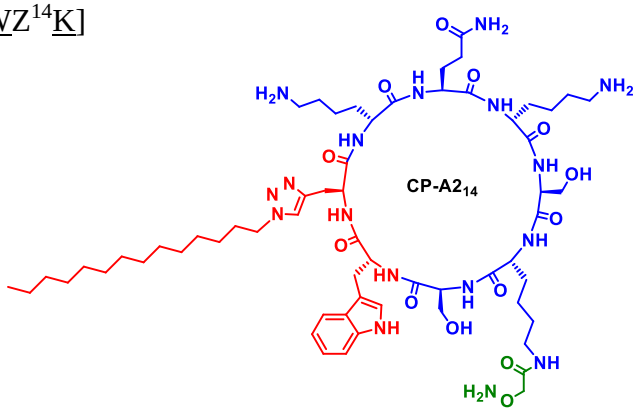

RP-HPLC: [Agilent SB-C18 column, H_20 (0.1% TFA)/ACN (0.1% TFA). 100:0 →100:0 (2 min) and 100:0 → 25:75 (19 min)] (R_t = 16.9 min). Absorbance at 222 nm.

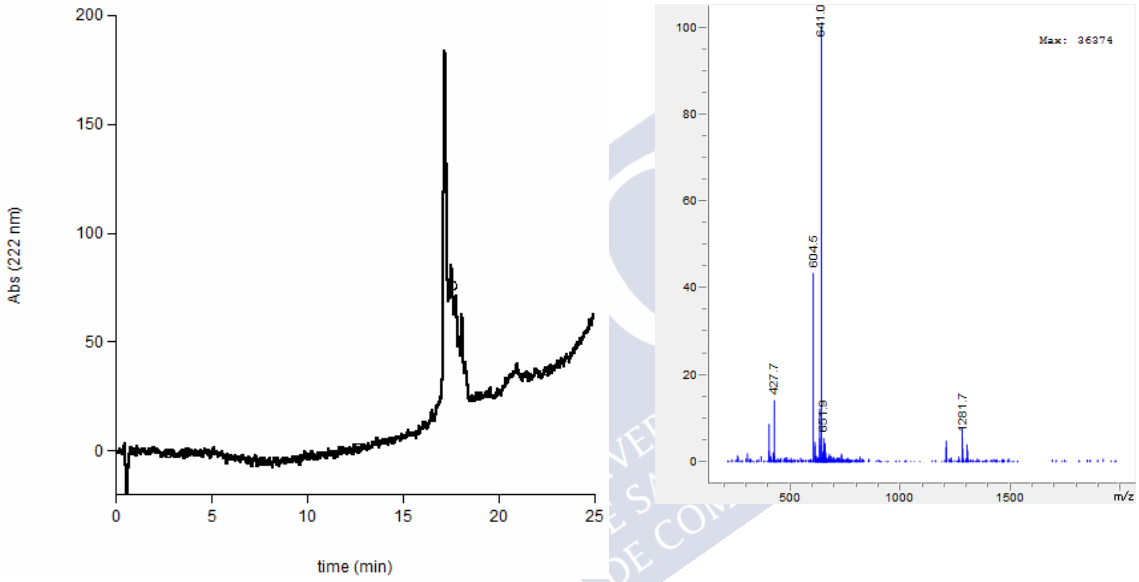

FT-IR (neat, 298 K)

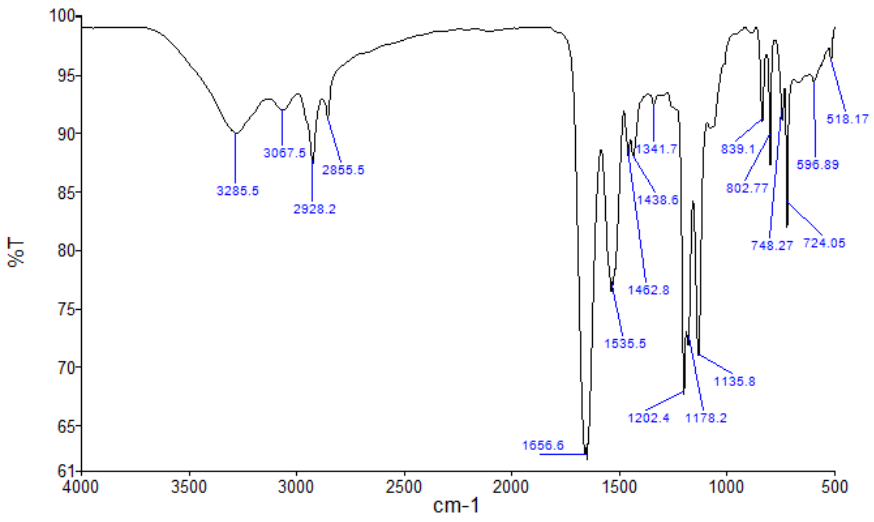

Peptide CP-A4: *c*-[QRSKSWZK]

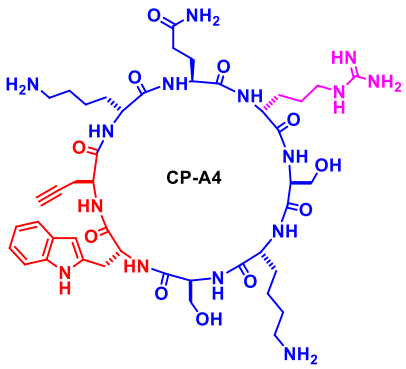

RP-HPLC: [Agilent SB-C18 column, H_20 (0.1% TFA)/ACN (0.1% TFA). 100:0 →100:0 (2 min) and 100:0 → 25:75 (19 min)] (R_t = 9.6 min). Absorbance at 222 nm.

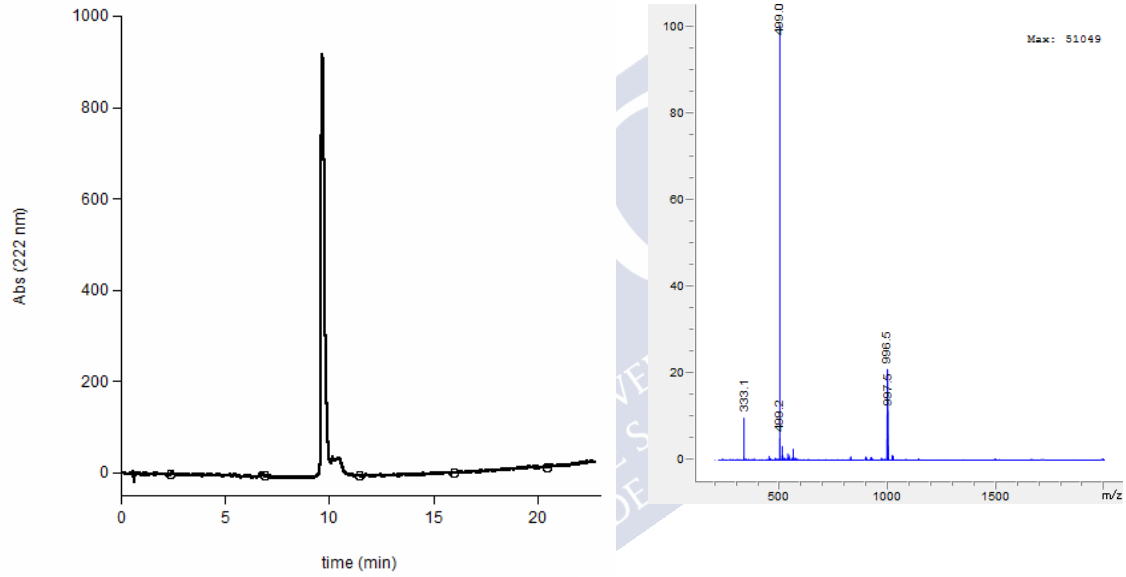

FT-IR (neat, 298 K)

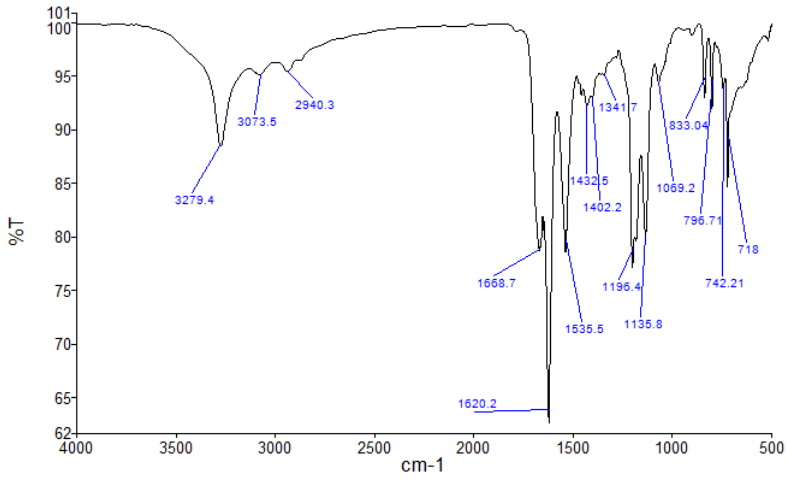

Peptide CP-A5: *c*-[QOSKSWZK]

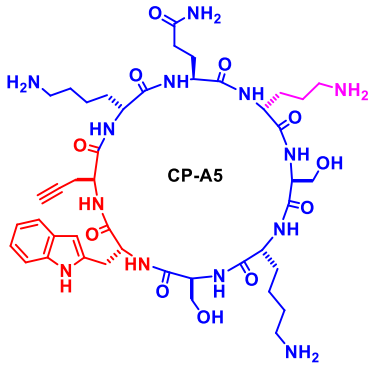

RP-HPLC: [Agilent SB-C18 column, H_20 (0.1% TFA)/ACN (0.1% TFA). 100:0 →100:0 (2 min) and 100:0 → 25:75 (19 min)] (R_t = 9.1 min). Absorbance at 222 nm.

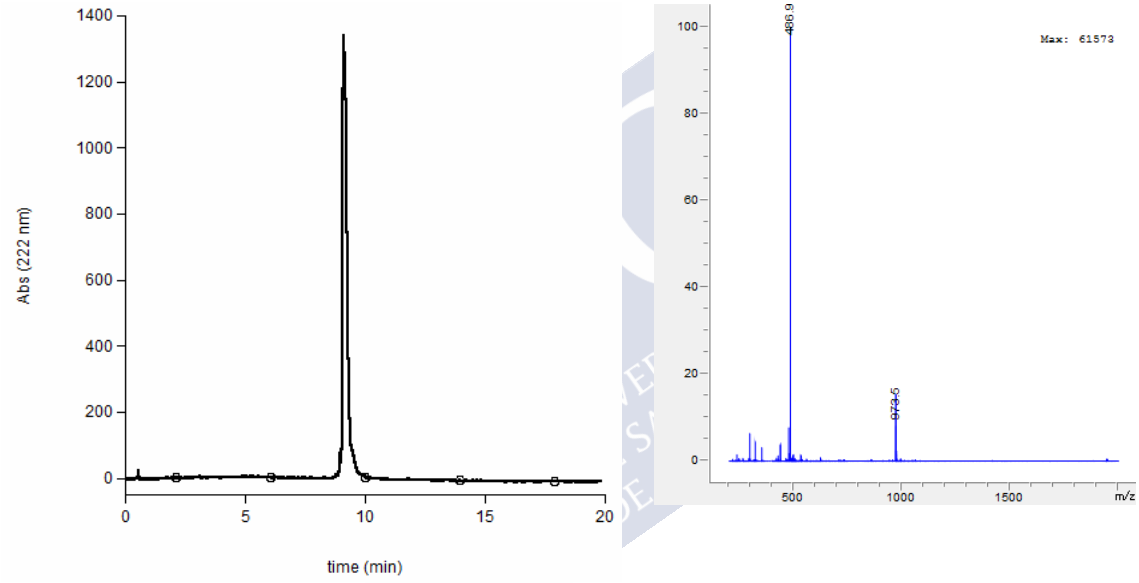

Peptide CP-A6: *c*-[QXSKSWZK]

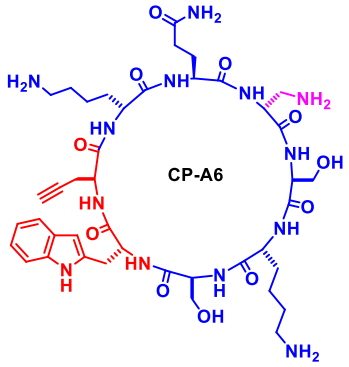

RP-HPLC: [Agilent SB-C18 column, H_20 (0.1% TFA)/ACN (0.1% TFA). 100:0 →100:0 (2 min) and 100:0 → 25:75 (19 min)] (R_t = 9.7 min). Absorbance at 222 nm.

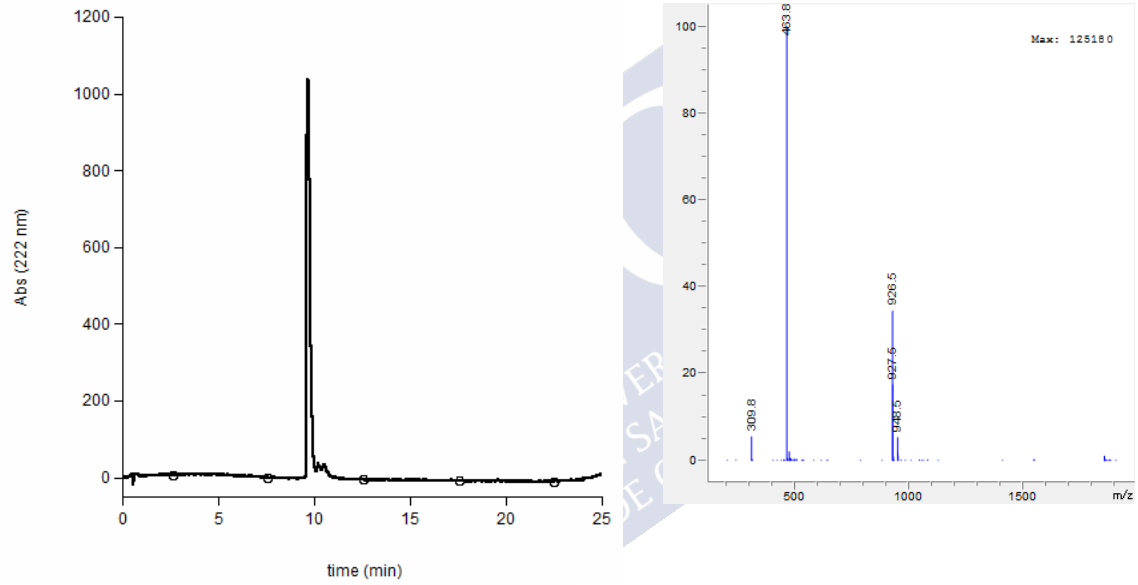

FT-IR (neat, 298 K)

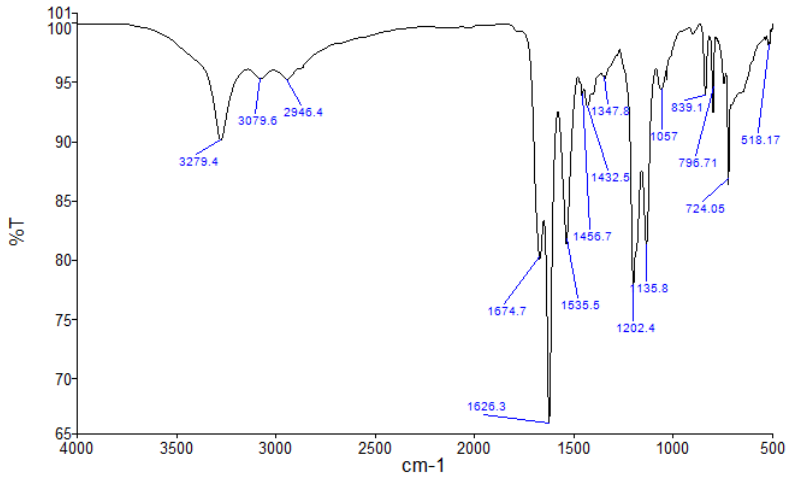

Peptide CP-A4$_{10}$: *c*-[QRSKSWZ^{10}K]

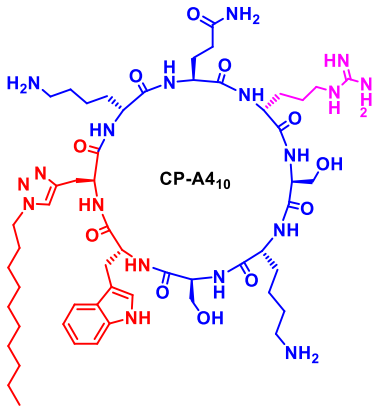

RP-HPLC: [Agilent SB-C18 column, H_20 (0.1% TFA)/ACN (0.1% TFA). 100:0 →100:0 (2 min) and 100:0 → 25:75 (19 min)] (R_t = 14.5 min). Absorbance at 222 nm.

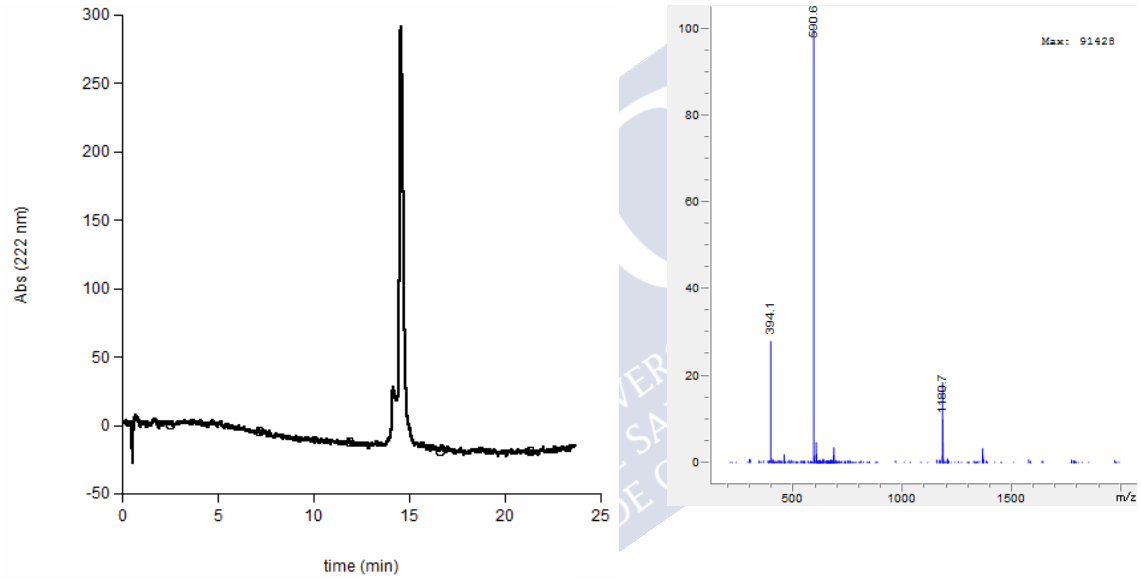

^{1}H-NMR: (2 mM, H_2O/D_2O, 300 K, 500 MHz)

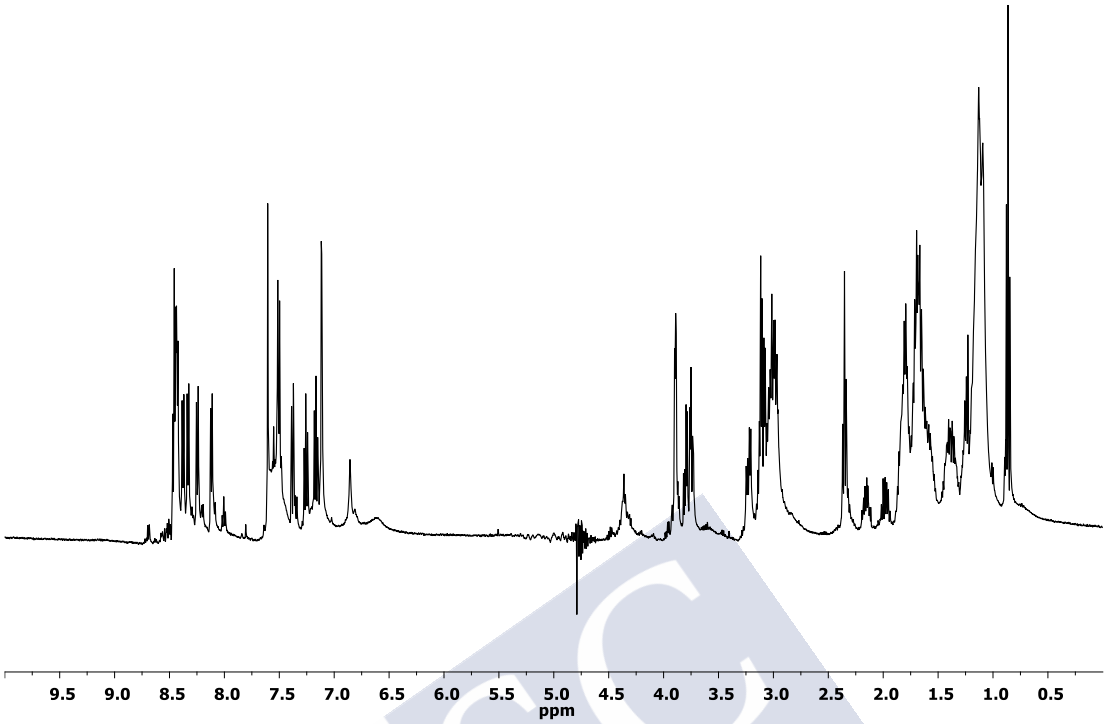

TOCSY: (2 mM, H_2O/D_2O, 300 K, 500 MHz)

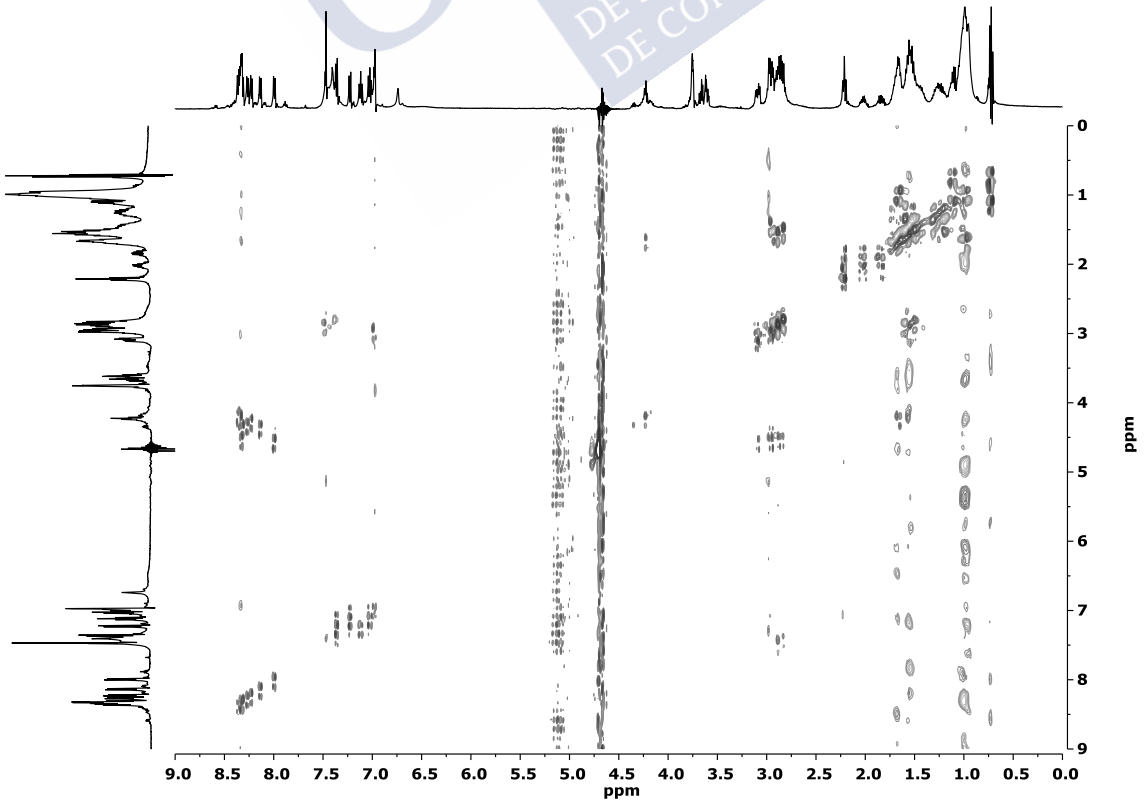

COSY: (2 mM, H_2O/D_2O, 300 K, 500 MHz)

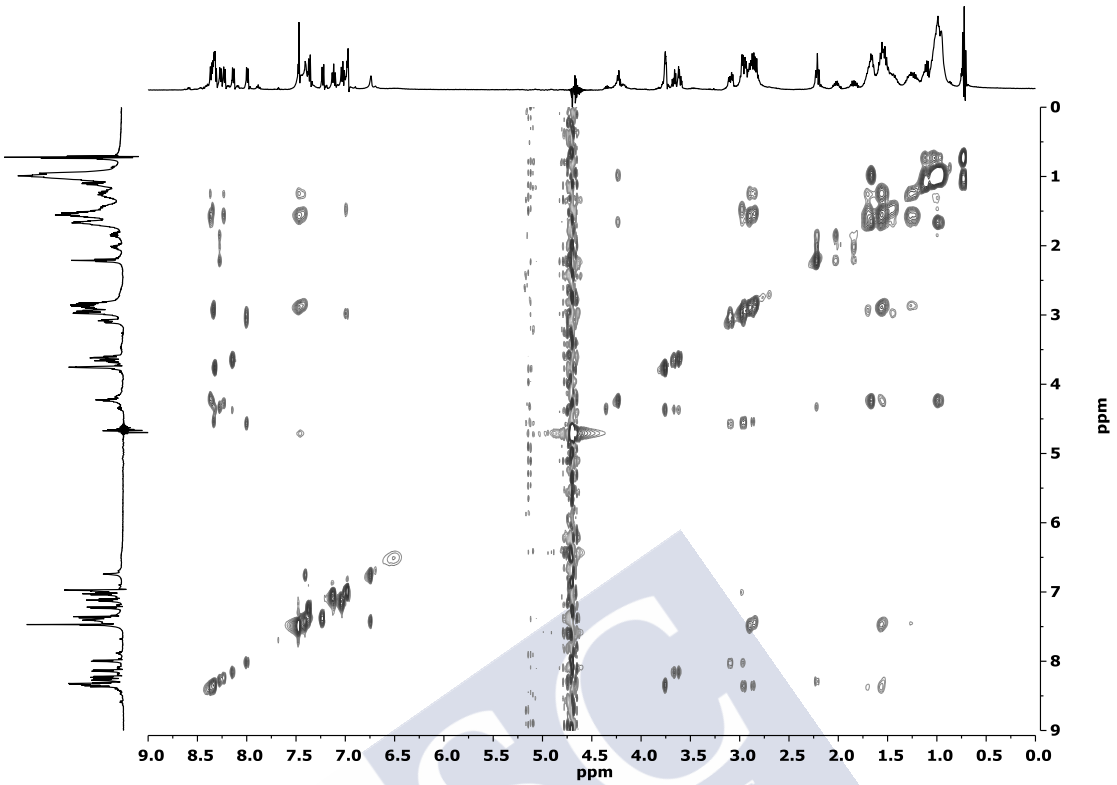

Peptide CP-A4$_{14}$: *c*-[QRSKSWZ^{14}K]

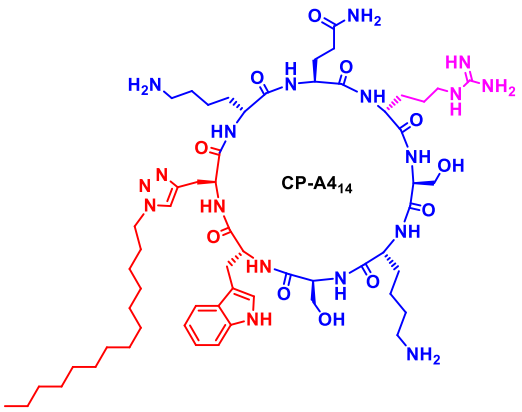

RP-HPLC: [Agilent SB-C18 column, H_20 (0.1% TFA)/ACN (0.1% TFA). 100:0 →100:0 (2 min) and 100:0 → 25:75 (19 min)] (R_t = 16.8 min). Absorbance at 222 nm.

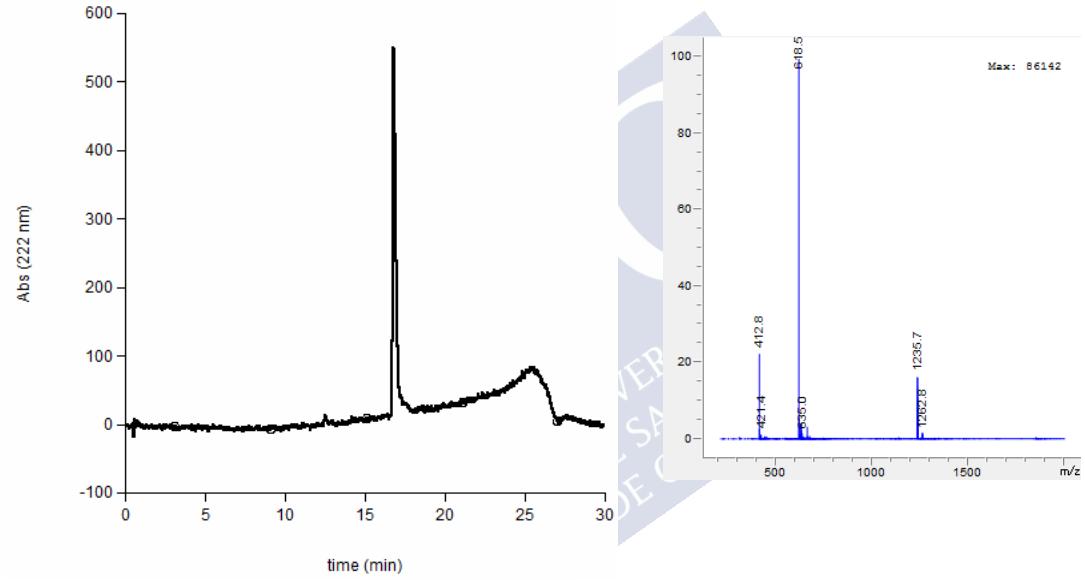

^{1}H-NMR: (2 mM, H_2O/D_2O, 300 K, 500 MHz)

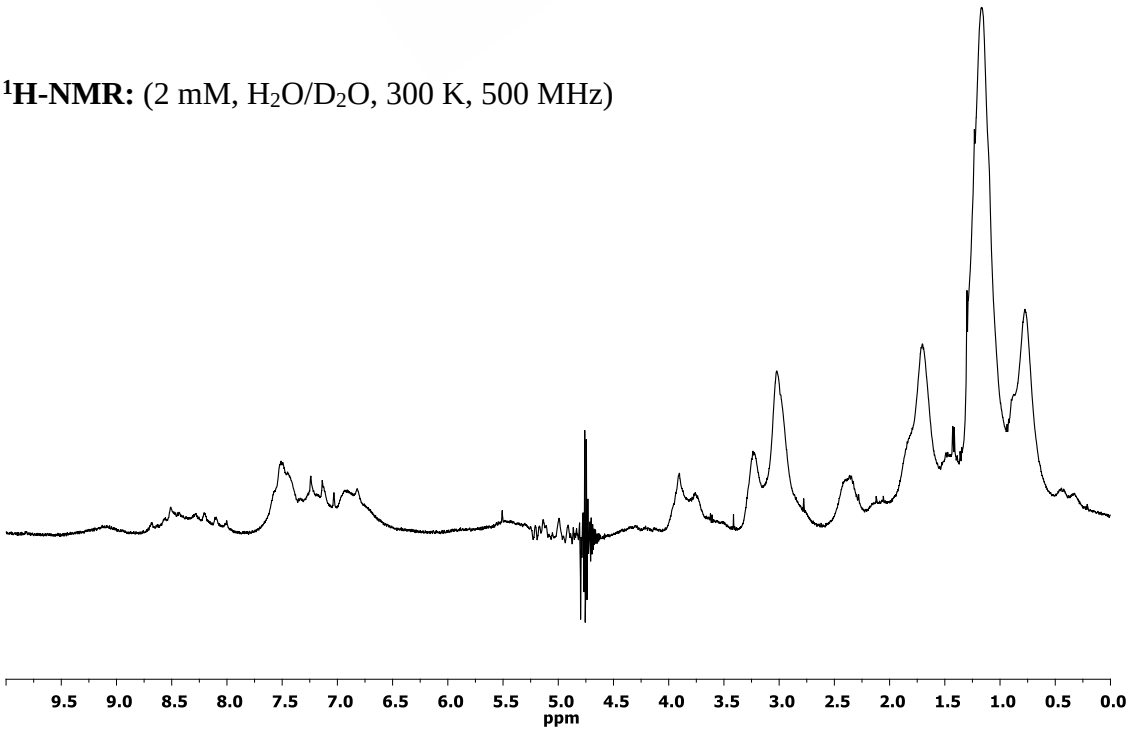

Peptide CP-A5$_{10}$: *c*-[QOSKSWZ^{10}K]

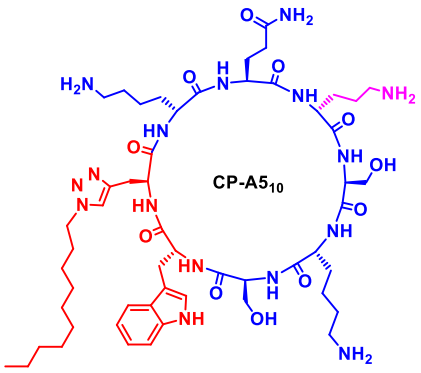

RP-HPLC: [Agilent SB-C18 column, H_20 (0.1% TFA)/ACN (0.1% TFA). 100:0 →100:0 (2 min) and 100:0 → 25:75 (19 min)] (R_t = 14.6 min). Absorbance at 222 nm.

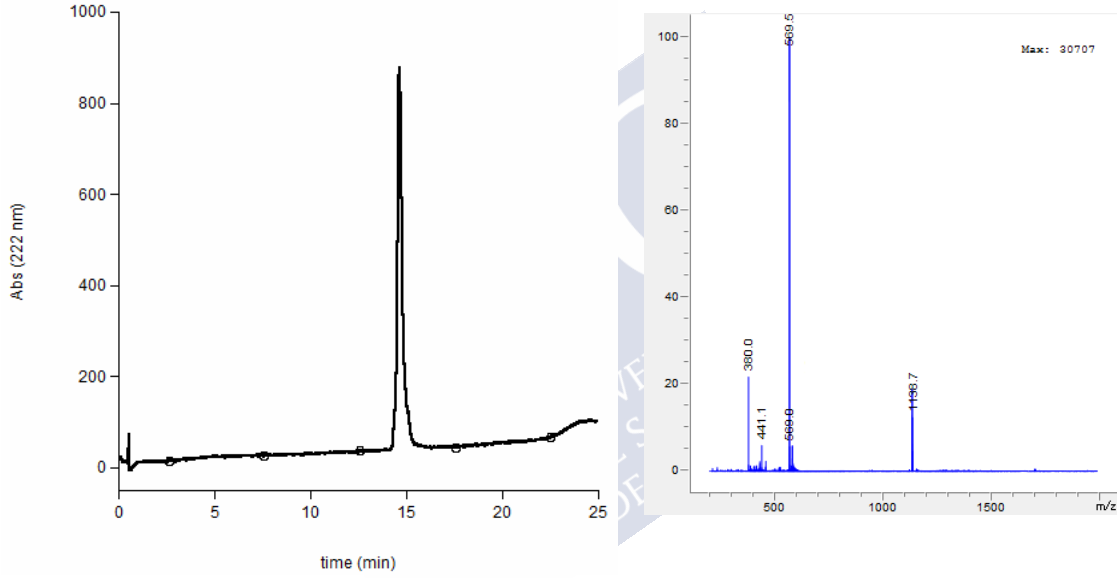

Peptide CP-A5$_{14}$: *c*-[QOSKSWZ^{14}K]

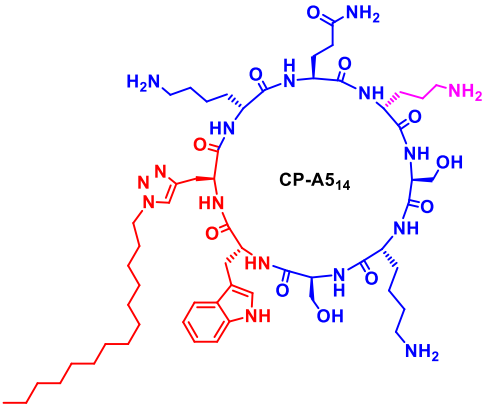

RP-HPLC: [Agilent SB-C18 column, H_20 (0.1% TFA)/ACN (0.1% TFA). 100:0 →100:0 (2 min) and 100:0 → 25:75 (19 min)] (R_t = 16.6 min). Absorbance at 222 nm.

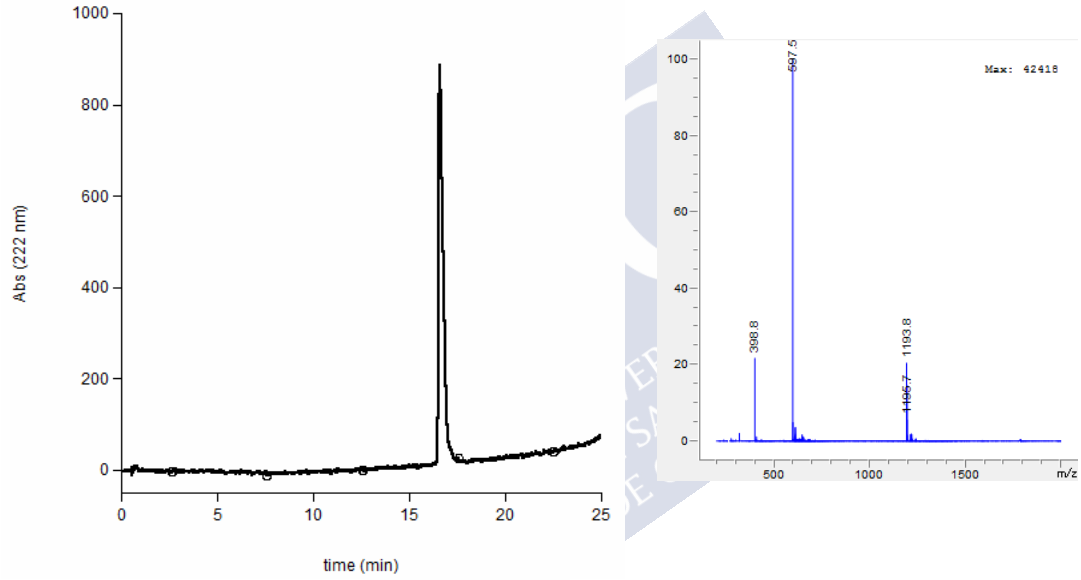

FT-IR (neat, 298 K)

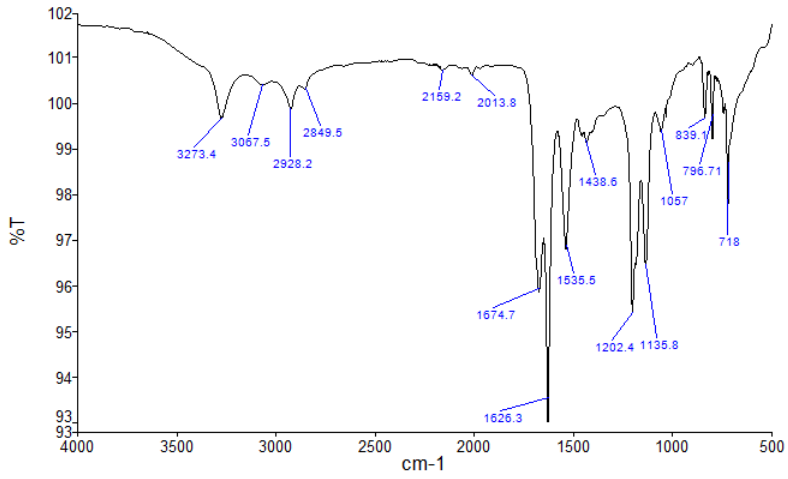

Peptide CP-A6$_{10}$: *c*-[QXSKSWZ^{10}K]

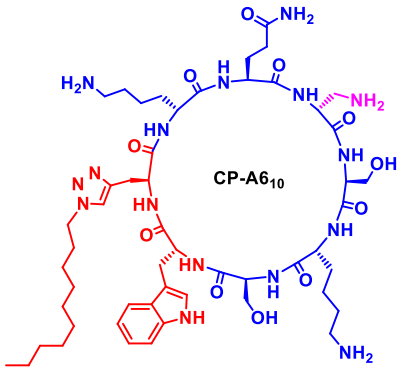

RP-HPLC: [Agilent SB-C18 column, H_20 (0.1% TFA)/ACN (0.1% TFA). 100:0 →100:0 (2 min) and 100:0 → 25:75 (19 min)] (R_t = 14.6 min). Absorbance at 222 nm.

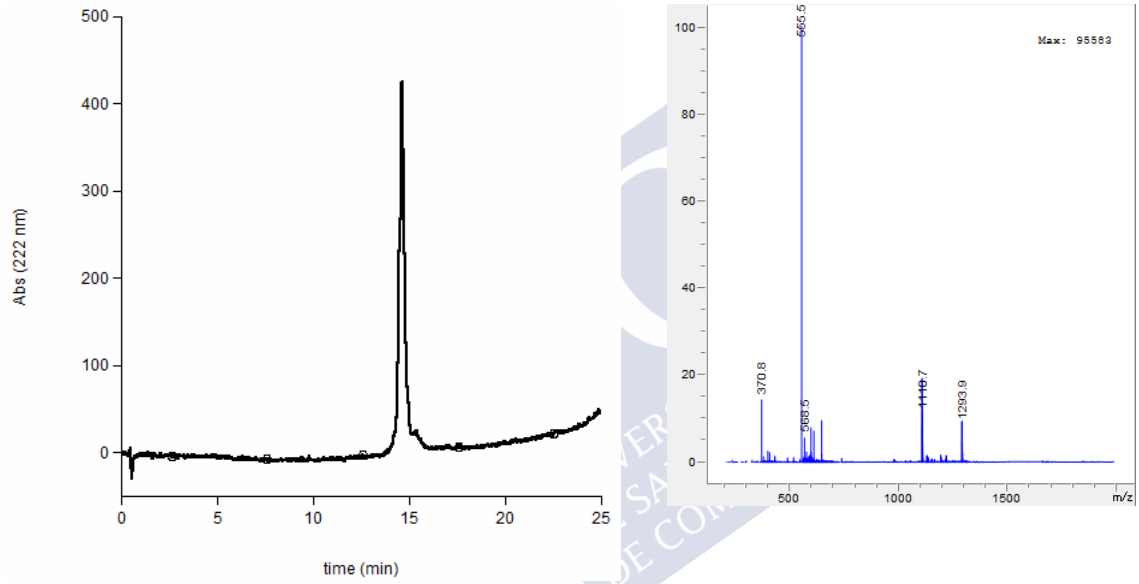

FT-IR (neat, 298 K)

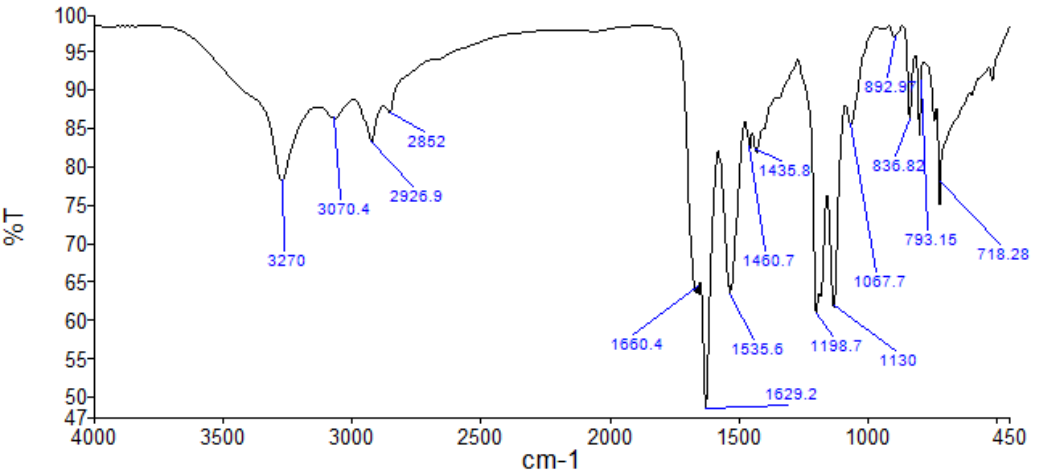

^{1}H-NMR: (2 mM, H_2O/D_2O, 300 K, 500 MHz)

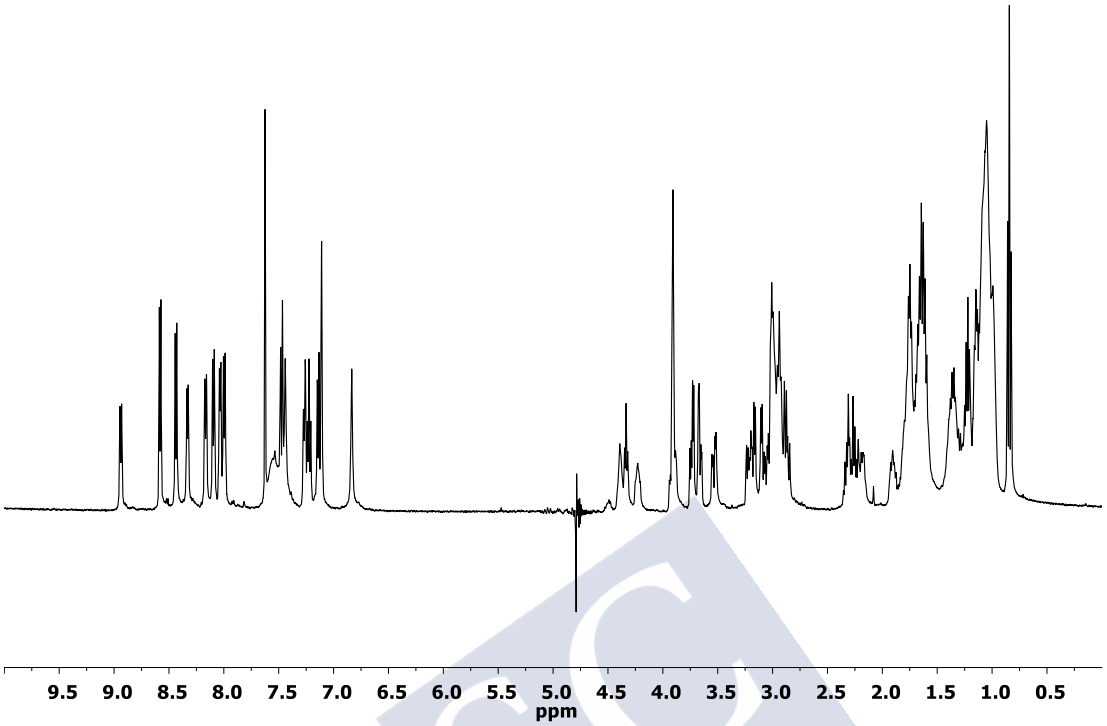

TOCSY: (2 mM, H_2O/D_2O, 300 K, 500 MHz)

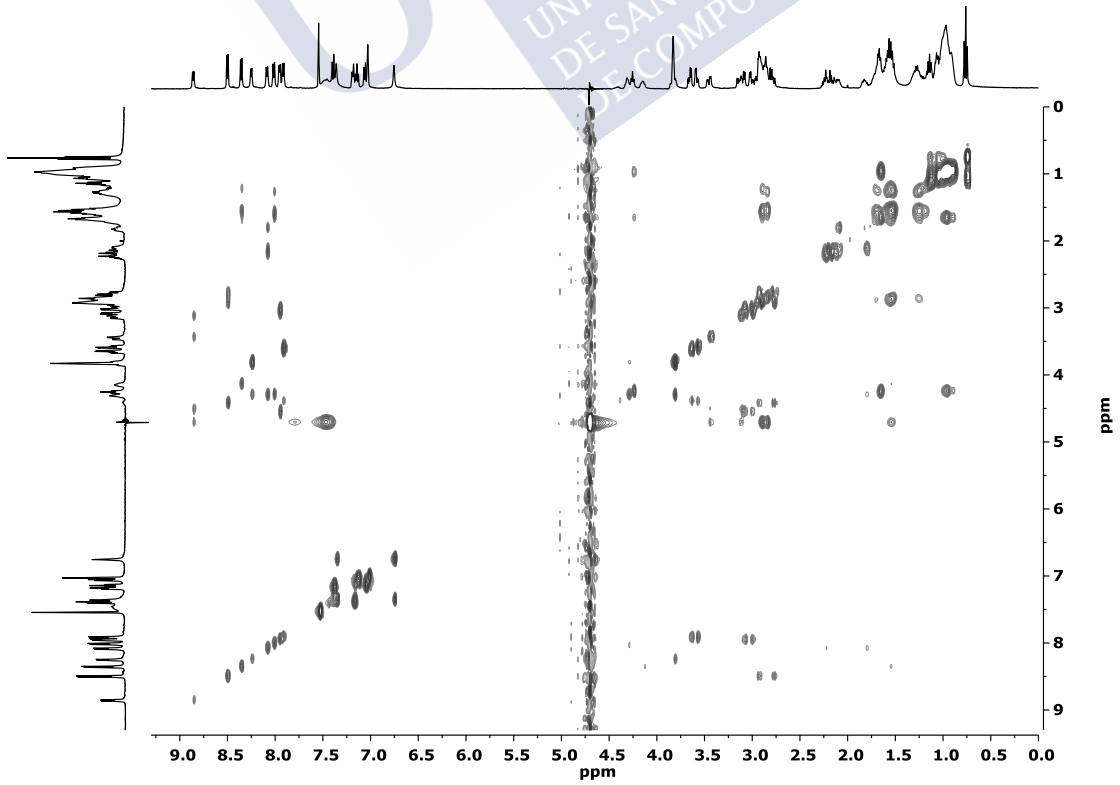

COSY: (2 mM, H_2O/D_2O, 300 K, 500 MHz)

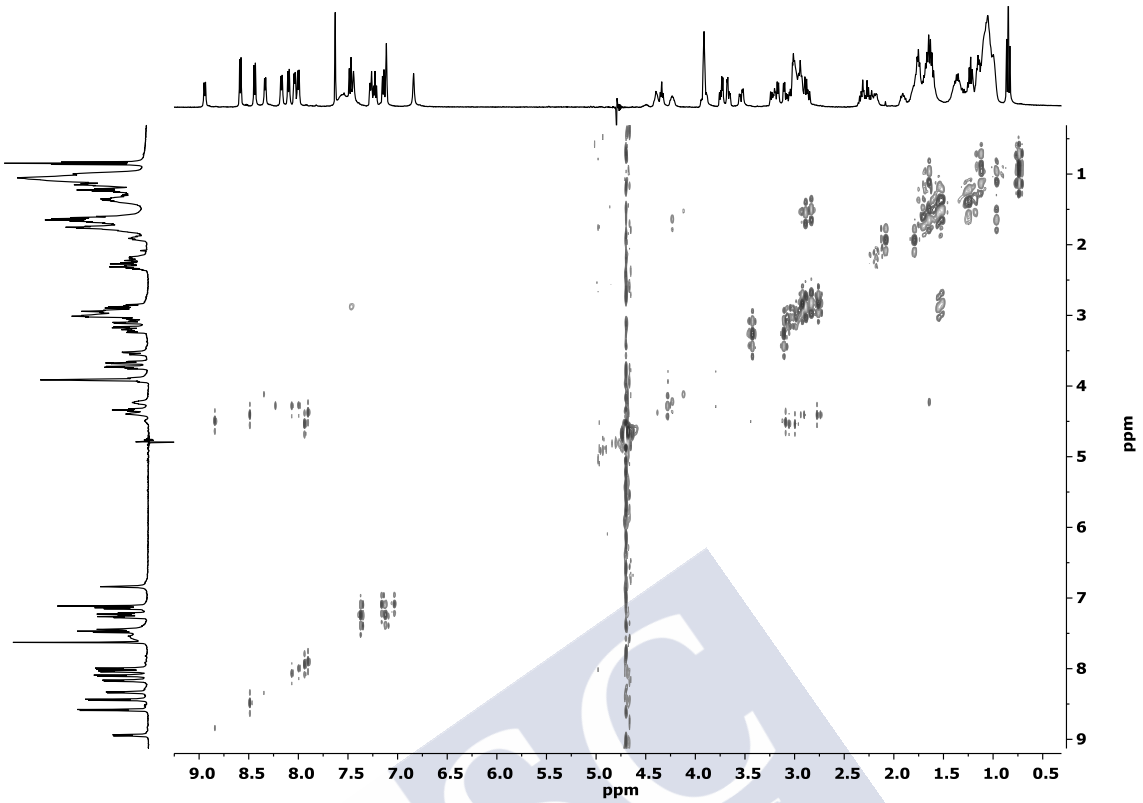

Peptide CP-A6$_{14}$: *c*-[QXSKSWZK]

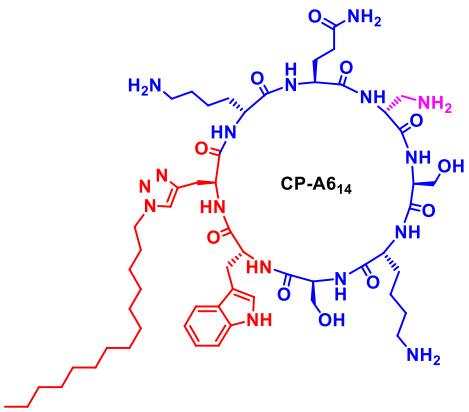

RP-HPLC: [Agilent SB-C18 column, H_20 (0.1% TFA)/ACN (0.1% TFA). 100:0 →100:0 (2 min) and 100:0 → 25:75 (19 min)] (R_t = 16.5 min). Absorbance at 222 nm.

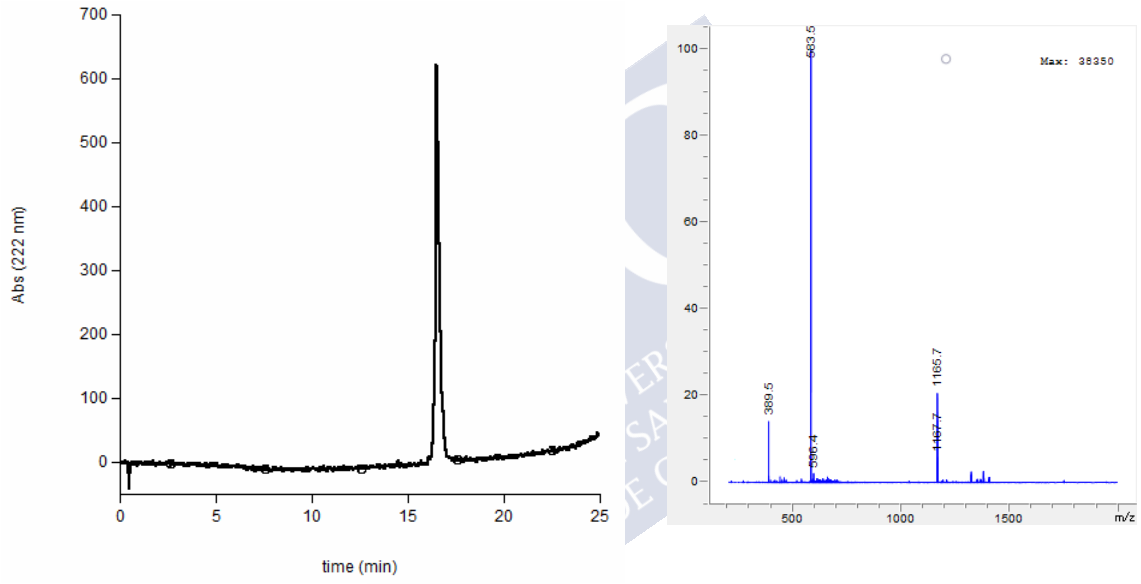

FT-IR (neat, 298 K)

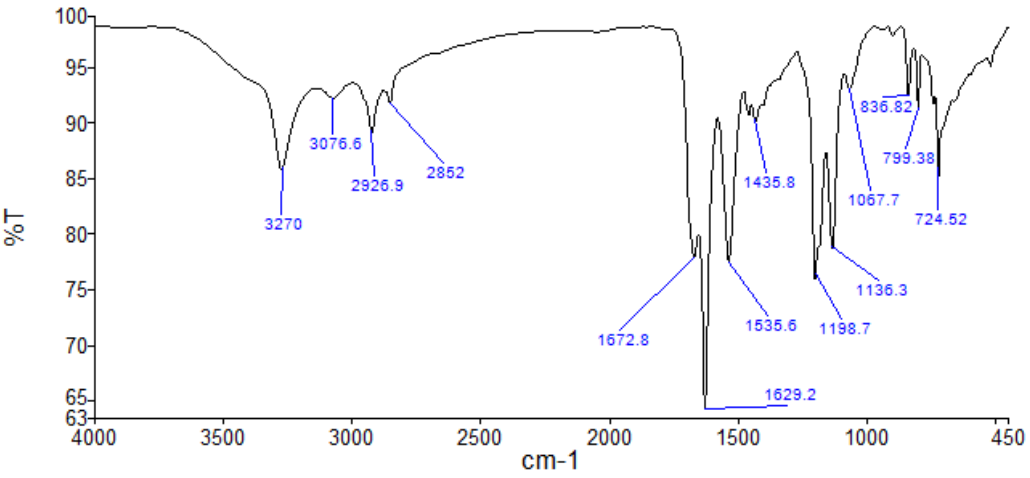

^{1}H-NMR: (2 mM, H_2O/D_2O, 300 K, 500 MHz)

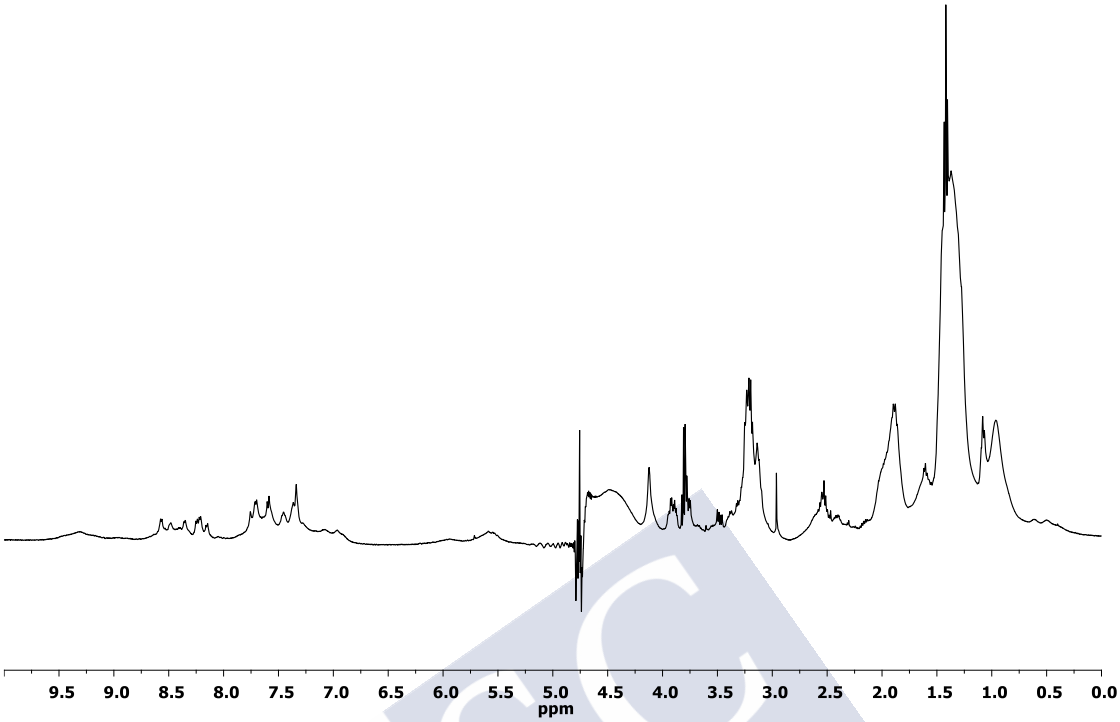

Peptide CP-A4$_{10}$-Ox^4: *c*-[QRSK^{Ox}SWZ^{10}K]

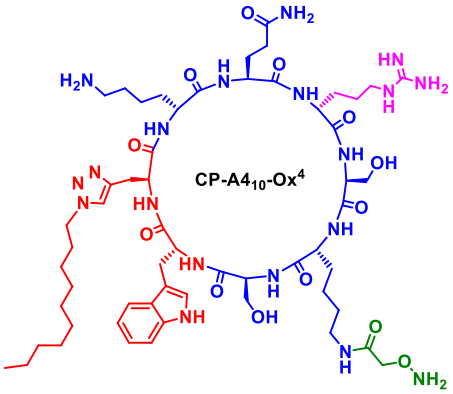

RP-HPLC: [Agilent SB-C18 column, H_20 (0.1% TFA)/ACN (0.1% TFA). 100:0 →100:0 (2 min) and 100:0 → 25:75 (19 min)] (R_t = 14.5 min). Absorbance at 222 nm.

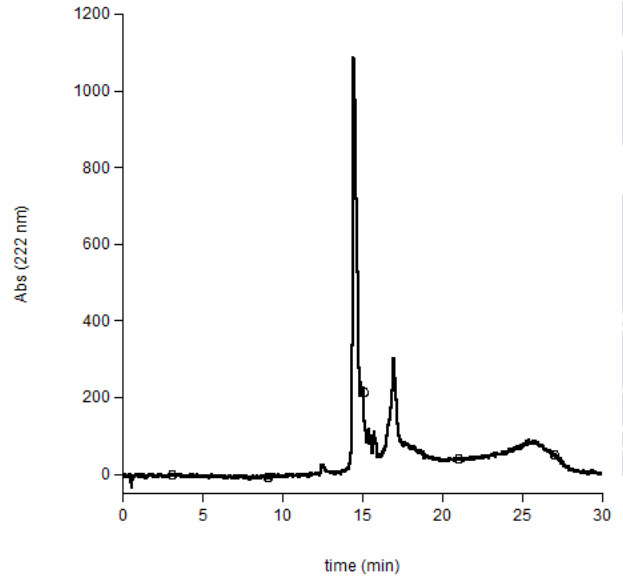

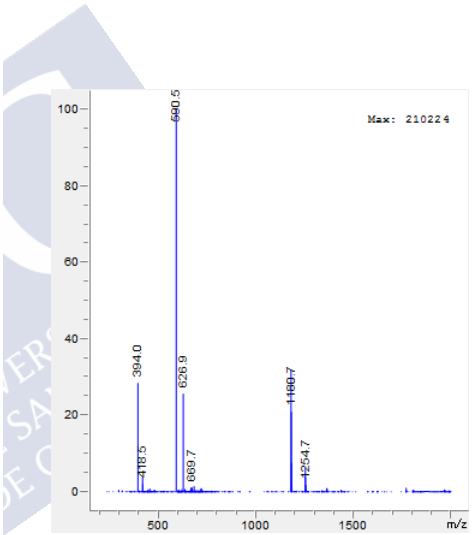

FT-IR (neat, 298 K)

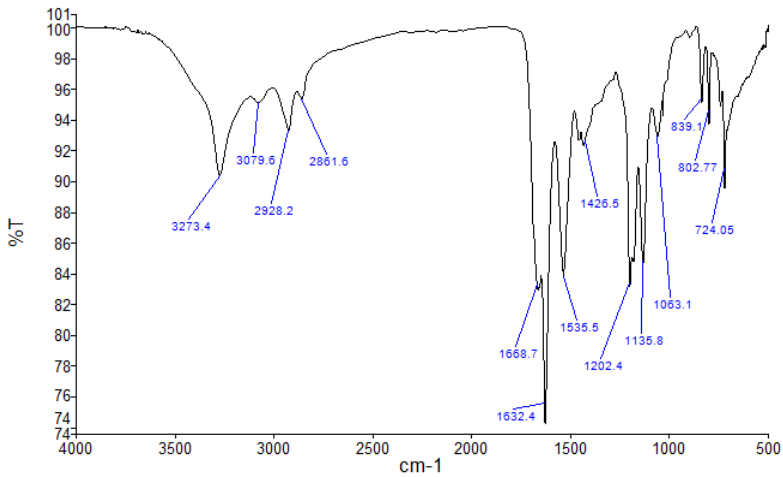

Peptide CP-A4$_{10}$-Ox^{8}: *c*-[QRSKSWZ^{10}K^{Ox}]

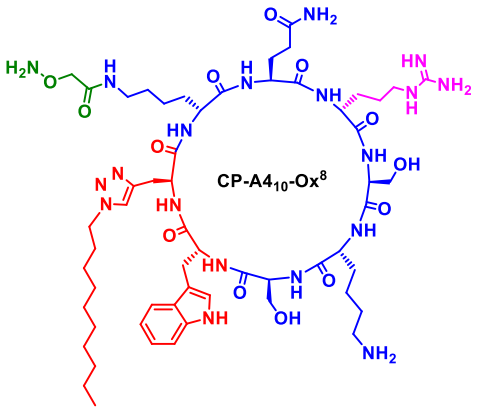

RP-HPLC: [Agilent SB-C18 column, H_20 (0.1% TFA)/ACN (0.1% TFA). 100:0 →100:0 (2 min) and 100:0 → 25:75 (19 min)] (R_t = 14.7 min). Absorbance at 222 nm.

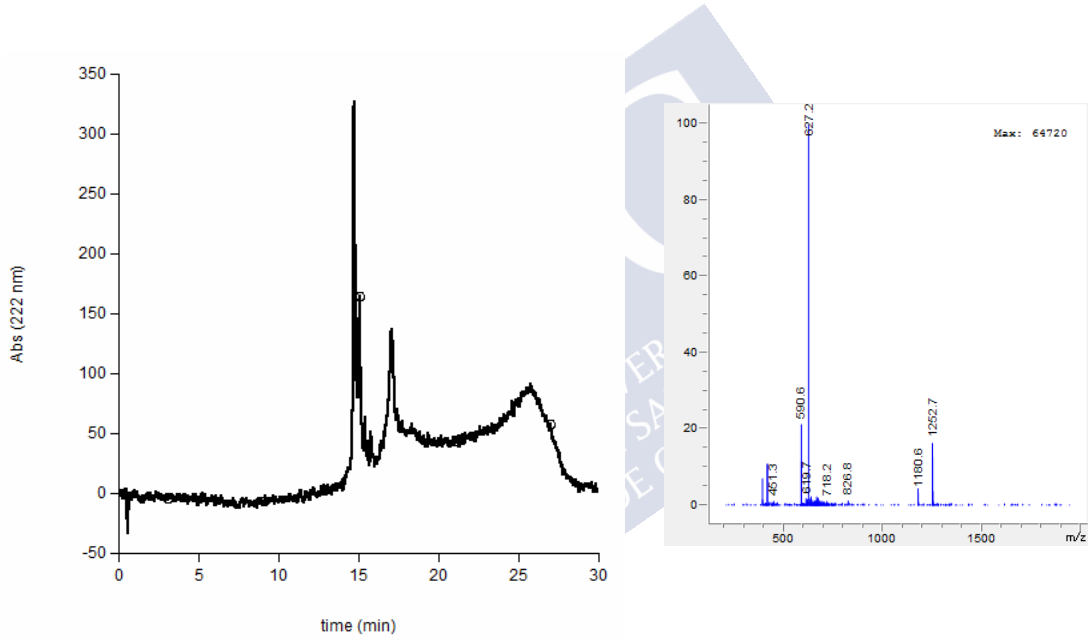

FT-IR (neat, 298 K)

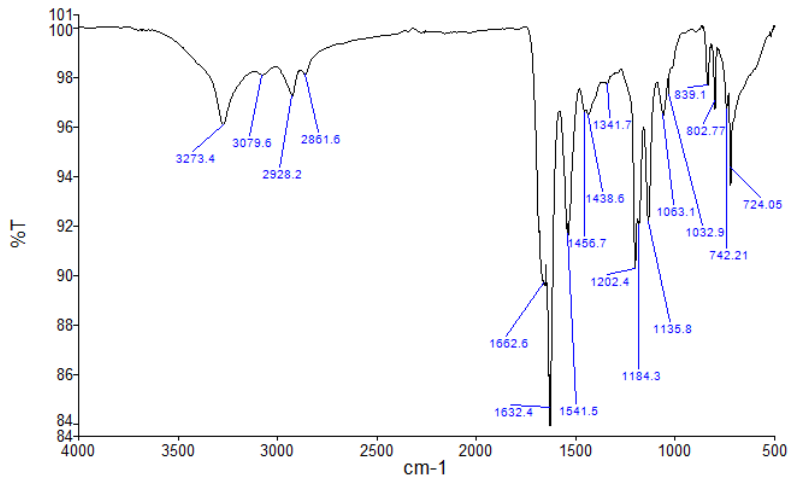

Peptide CP-A$_{10}$: *c*-[QKSKSWZ^{10}K]

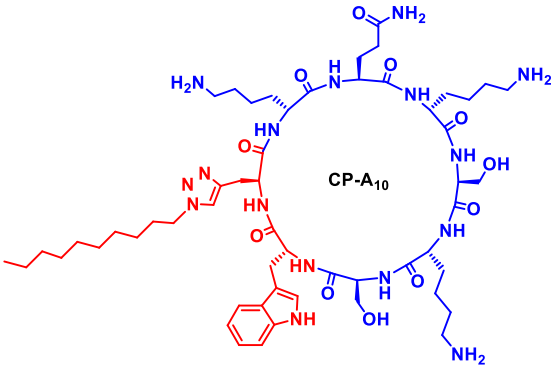

RP-HPLC: [Agilent SB-C18 column, H_20 (0.1% TFA)/ACN (0.1% TFA). 100:0 →100:0 (2 min) and 100:0 → 25:75 (19 min)] (R_t = 14.6 min). Absorbance at 222 nm.

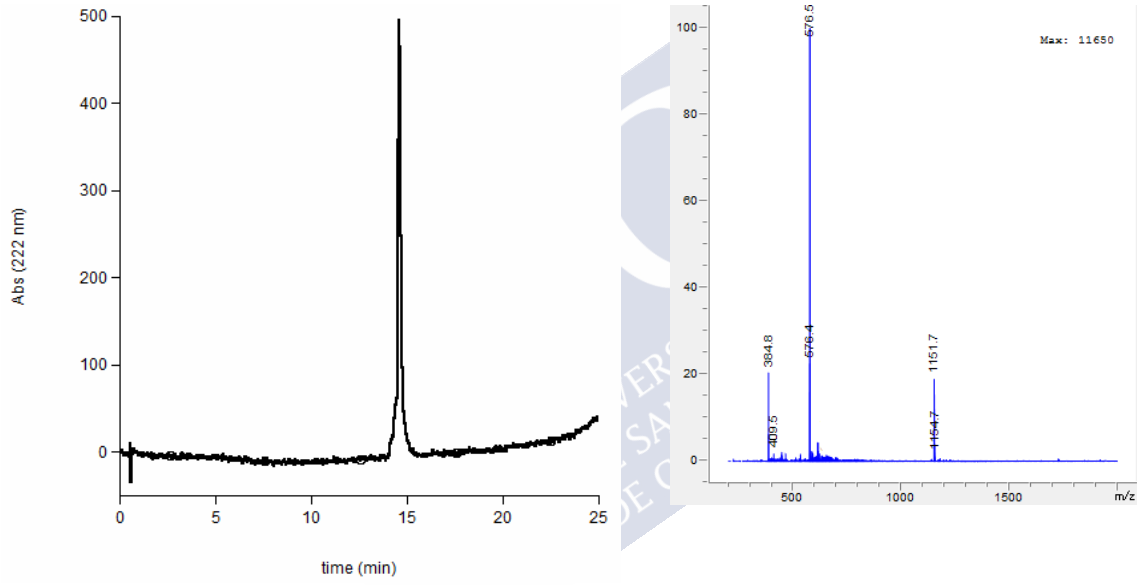

FT-IR (neat, 298 K)

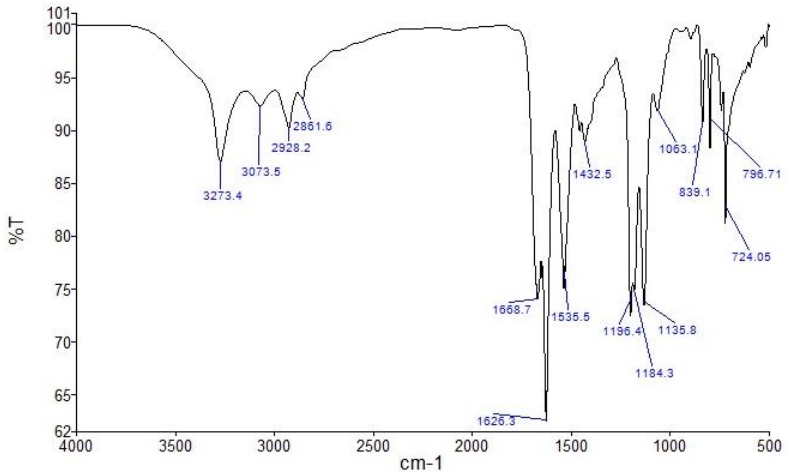

^{1}H-NMR: (2 mM, H_2O/D_2O, 300 K, 500 MHz)

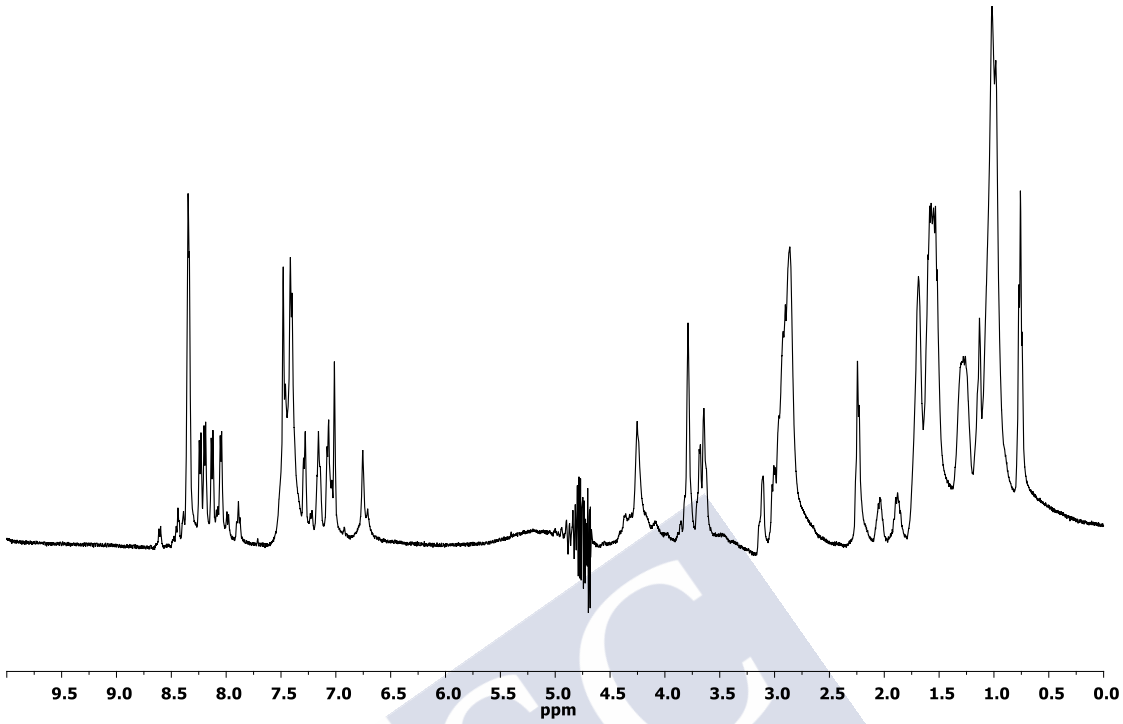

TOCSY: (2 mM, H_2O/D_2O, 300 K, 500 MHz)

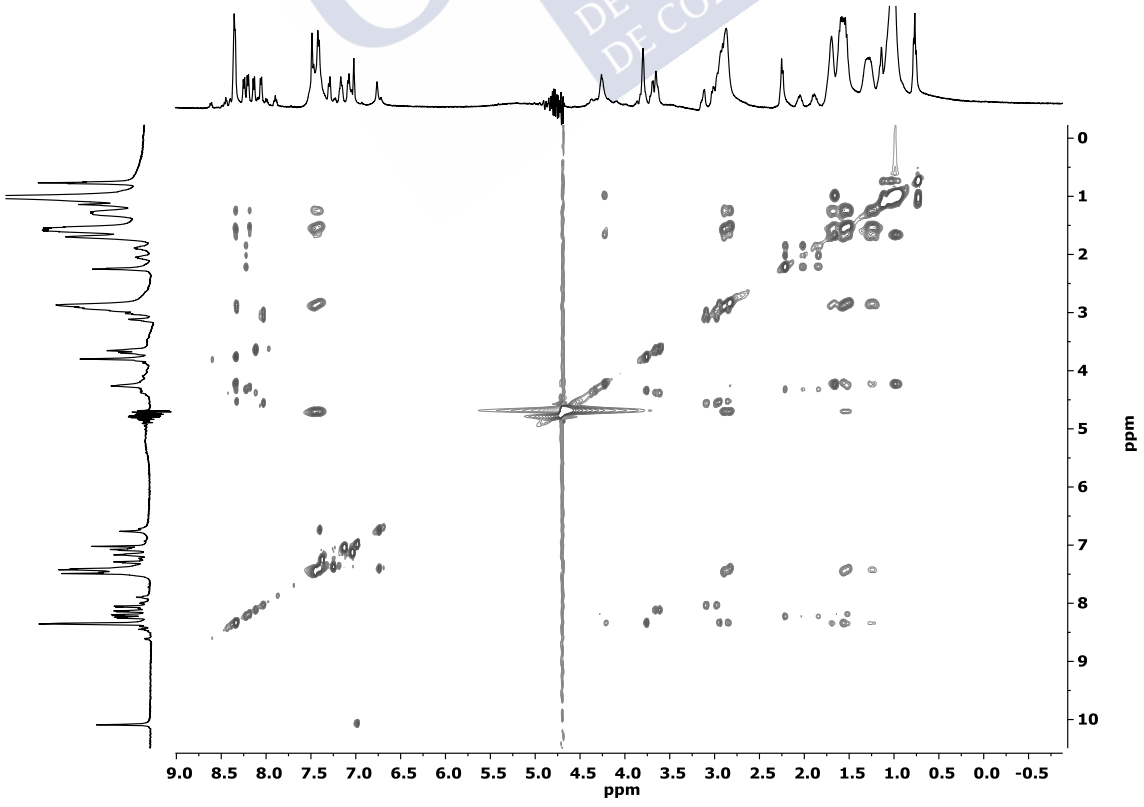

COSY: (2 mM, H_2O/D_2O, 300 K, 500 MHz)

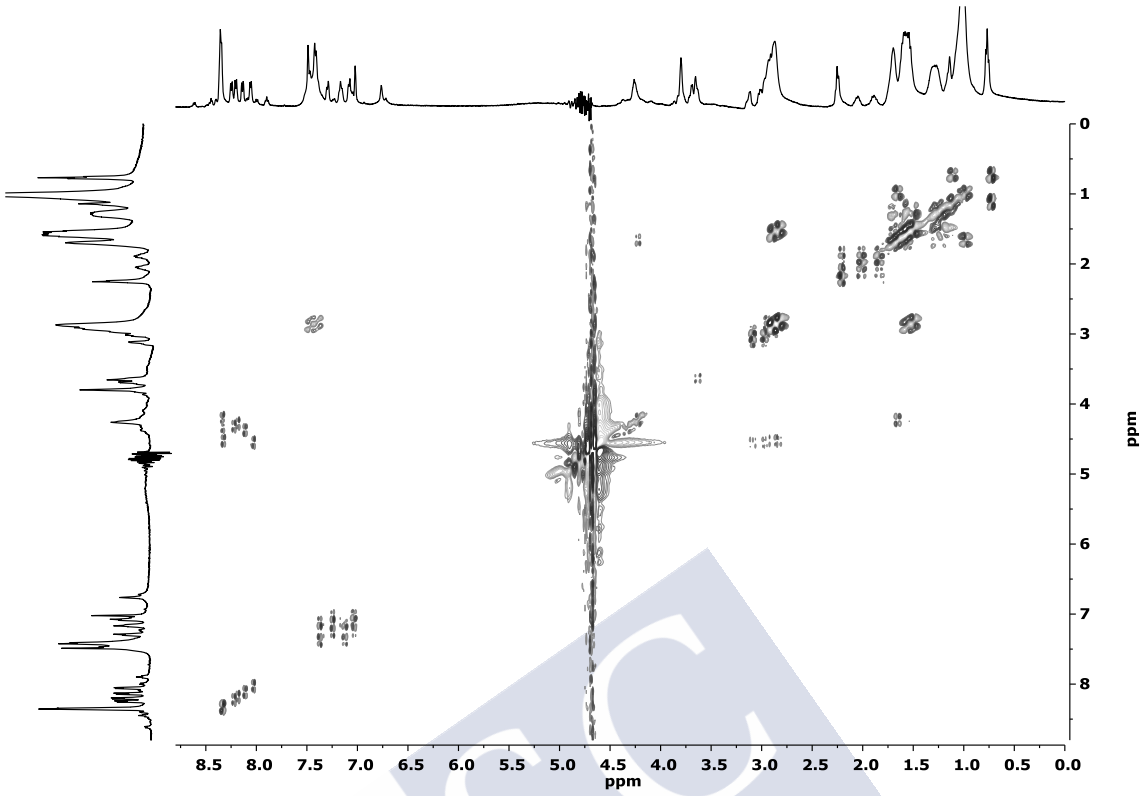

Peptide CP-A$_{14}$: *c*-[QKSKSWZ^{14}K]

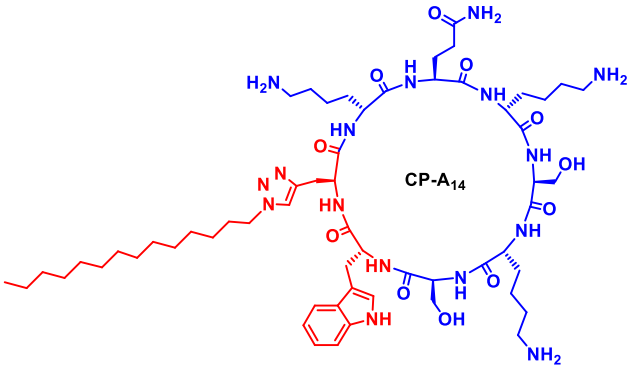

RP-HPLC: [Agilent SB-C18 column, H_20 (0.1% TFA)/ACN (0.1% TFA). 100:0 →100:0 (2 min) and 100:0 → 25:75 (19 min)] (R_t = 16.5 min). Absorbance at 222 nm.

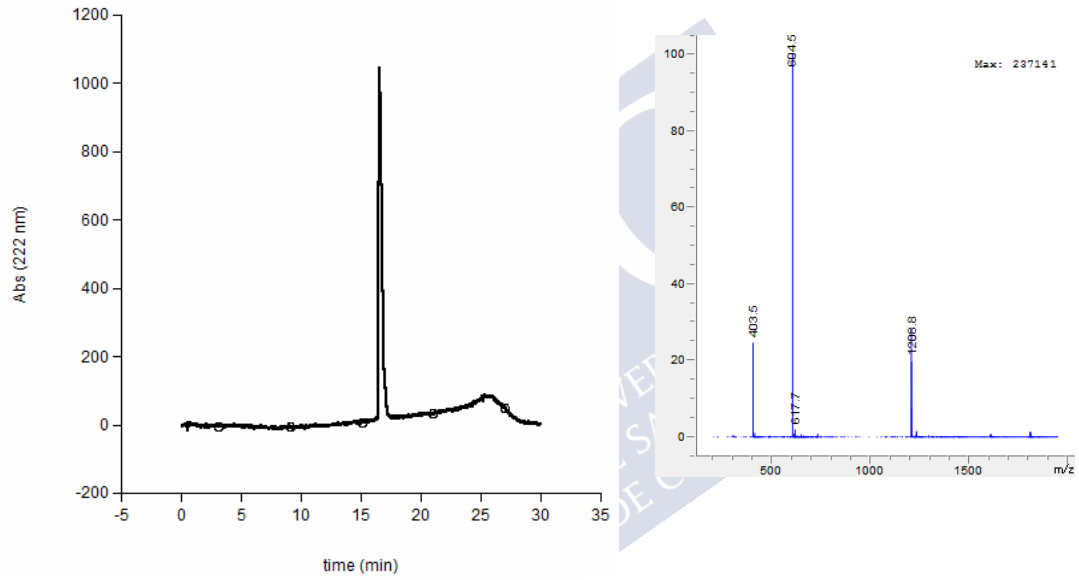

FT-IR (neat, 298 K)

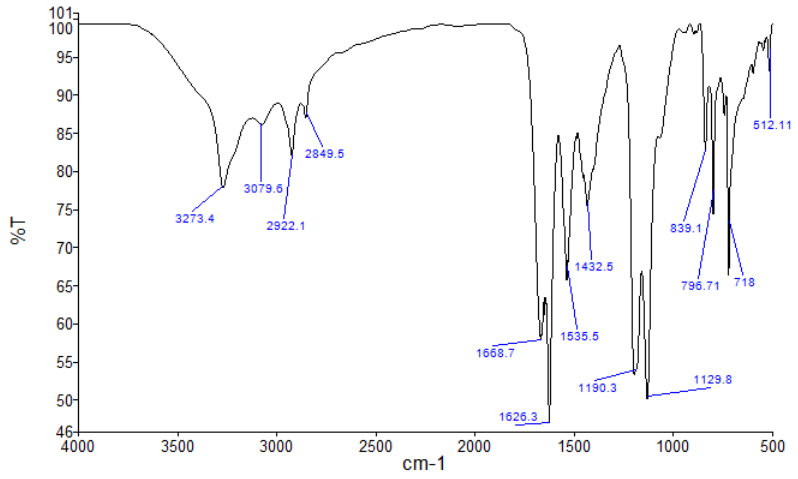

^{1}H-NMR: (2 mM, H_2O/D_2O, 300 K, 500 MHz)

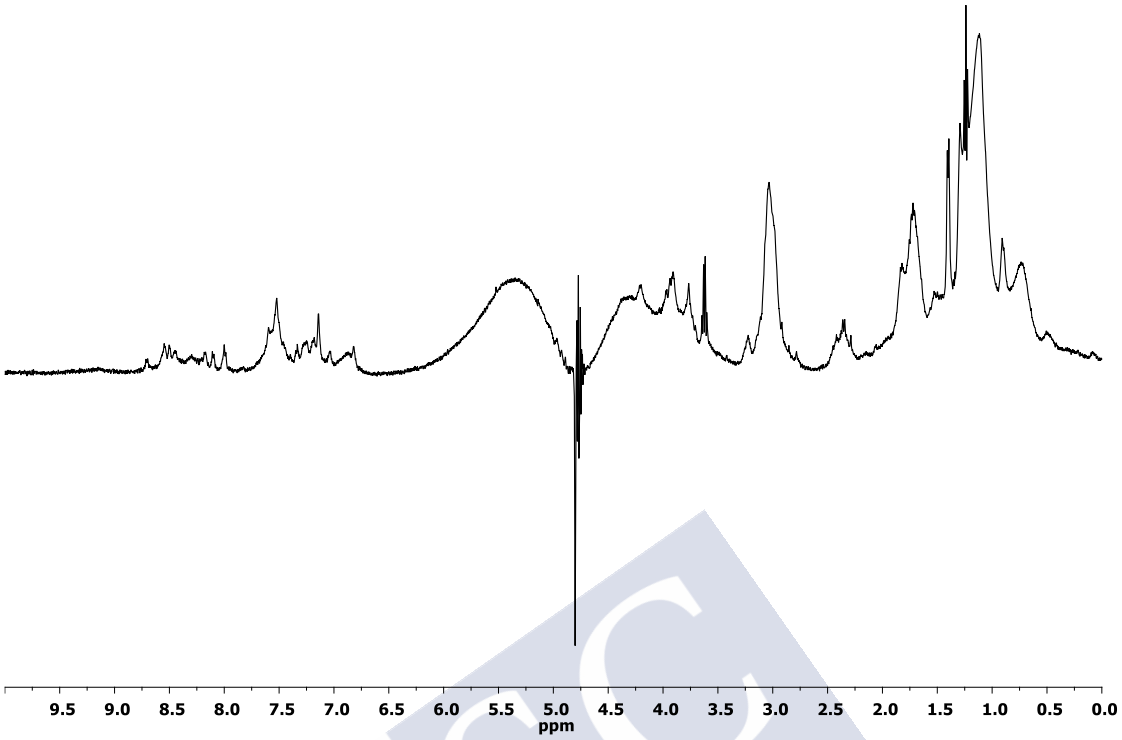

Chapter 3

Peptide CP-A4$_{10}$-DOX: *c*-[QRSK^{DOX}SWZ^{10}K]

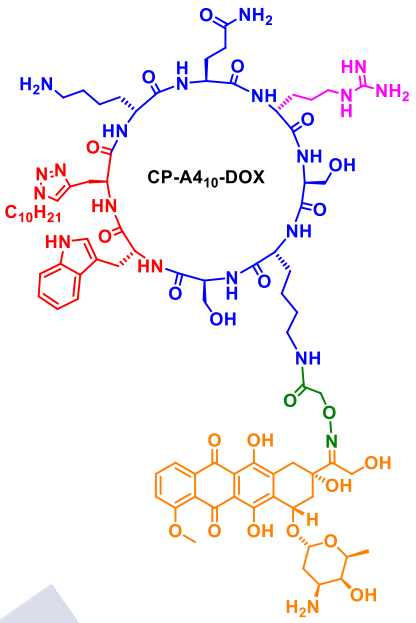

RP-HPLC: [Agilent SB-C18 column, H_20 (0.1% TFA)/ACN (0.1% TFA). 100:0 →100:0 (2 min) and 100:0 → 25:75 (19 min)] (R_t = 15.2 min). Absorbance at 222 nm.

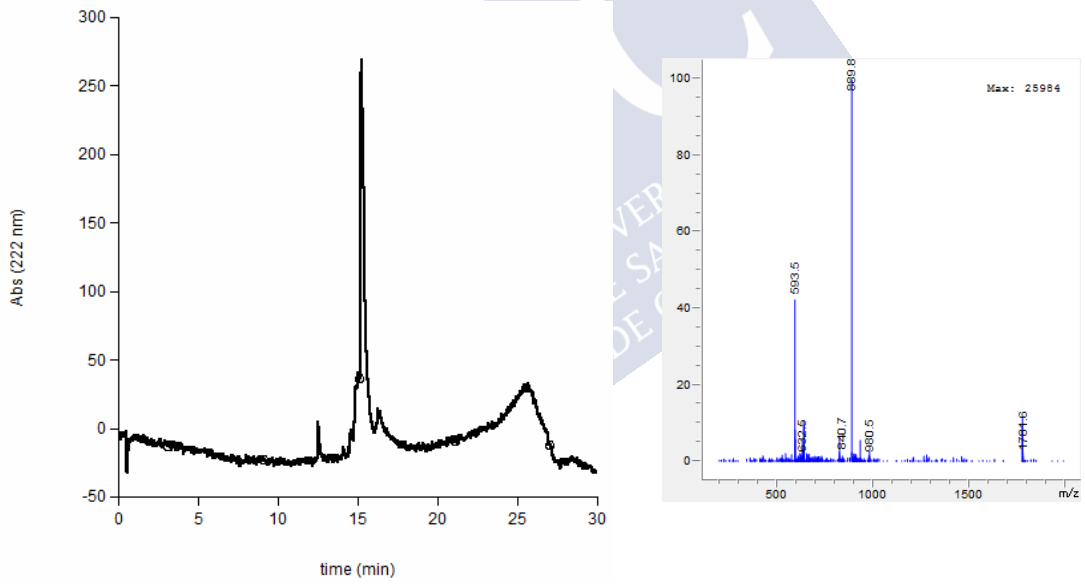

FT-IR (neat, 298 K)

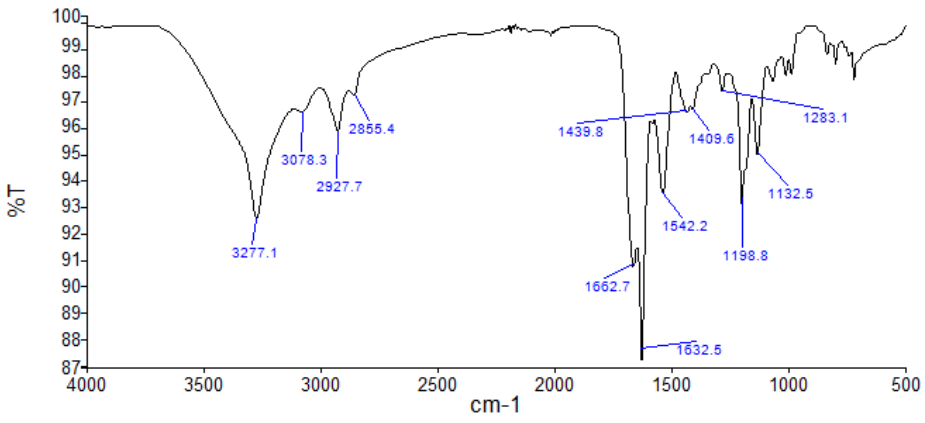

Peptide CP-A6$_{10}$-Ox^4: *c*-[QXSK^{Ox}SWZ^{10}K]

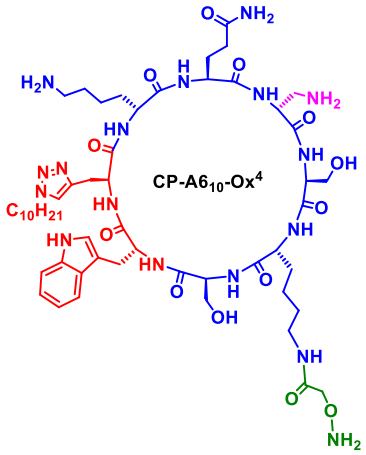

RP-HPLC: [Agilent SB-C18 column, H_20 (0.1% TFA)/ACN (0.1% TFA). 100:0 →100:0 (2 min) and 100:0 → 25:75 (19 min)] (R_t = 14.4 min). Absorbance at 222 nm.

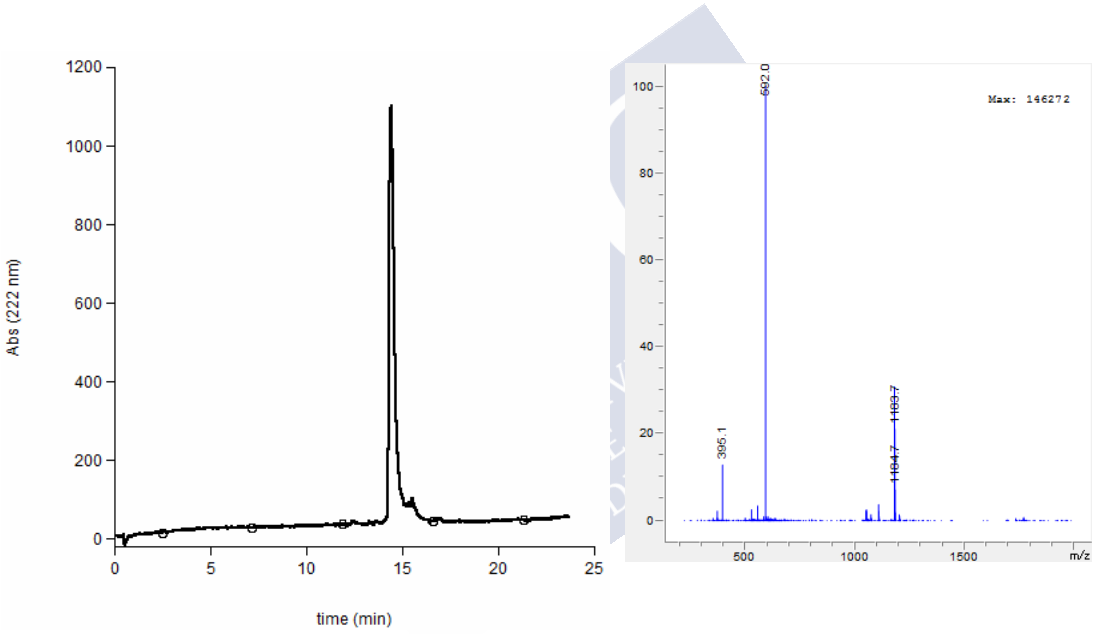

FT-IR (neat, 298 K)

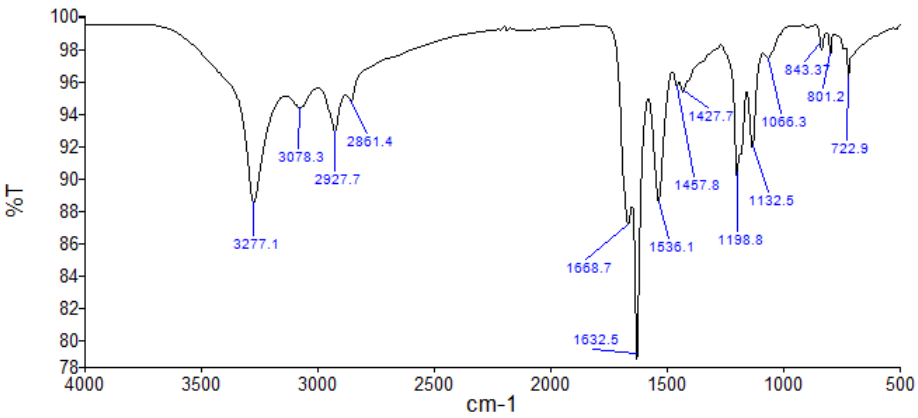

^{1}H-NMR: (H_2O/D_2O, 500 MHz)

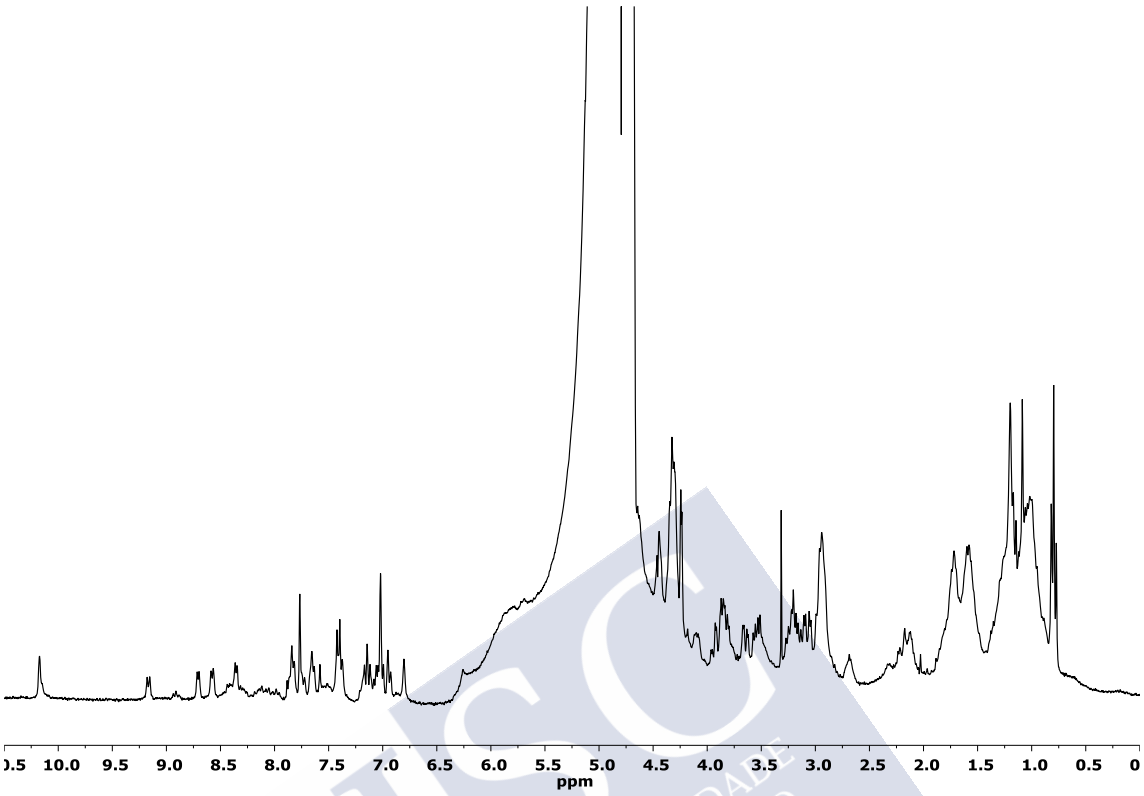

Peptide CP-A6$_{10}$-DOX: *c*-[QXSK^{DOX}SWZ^{10}K]

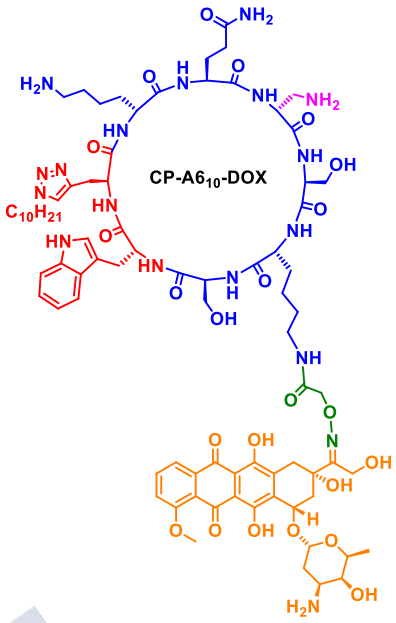

RP-HPLC: [Agilent SB-C18 column, H_20 (0.1% TFA)/ACN (0.1% TFA). 100:0 →100:0 (2 min) and 100:0 → 25:75 (19 min)] (R_t = 15.1 min). Absorbance at 222 nm.

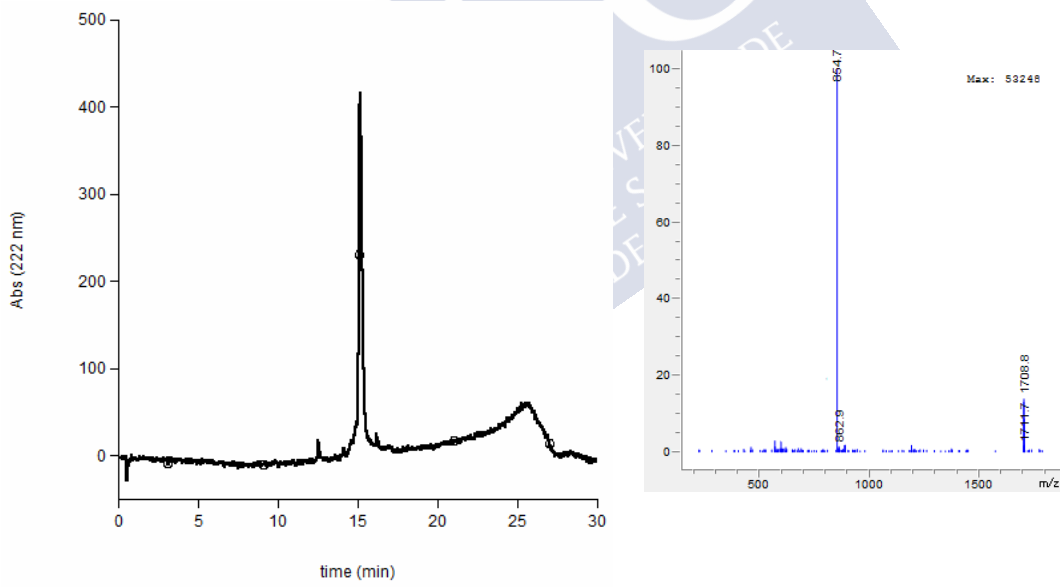

FT-IR (neat, 298 K)

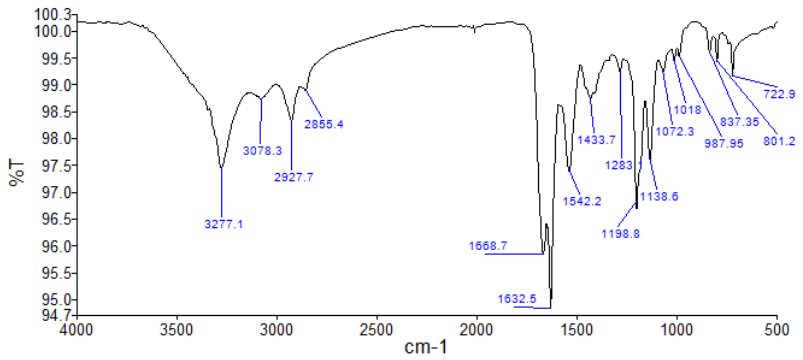

Peptide CP-A1-DOX: *c*-[Q$\underline{K^{DOX}}$S$\underline{K}$S$\underline{W}$Z$\underline{K}$]

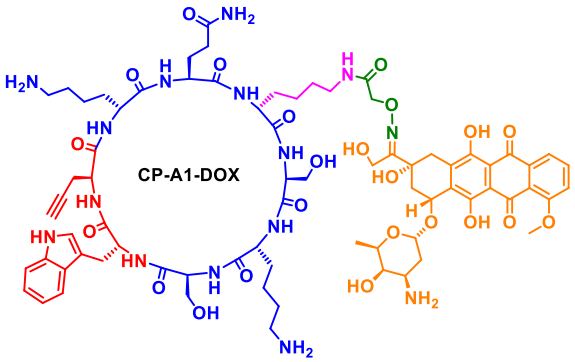

RP-HPLC: [Agilent SB-C18 column, H_20 (0.1% TFA)/ACN (0.1% TFA). 100:0 →100:0 (2 min) and 100:0 → 25:75 (19 min)] (R_t = 11.9 min). Absorbance at 222 nm.

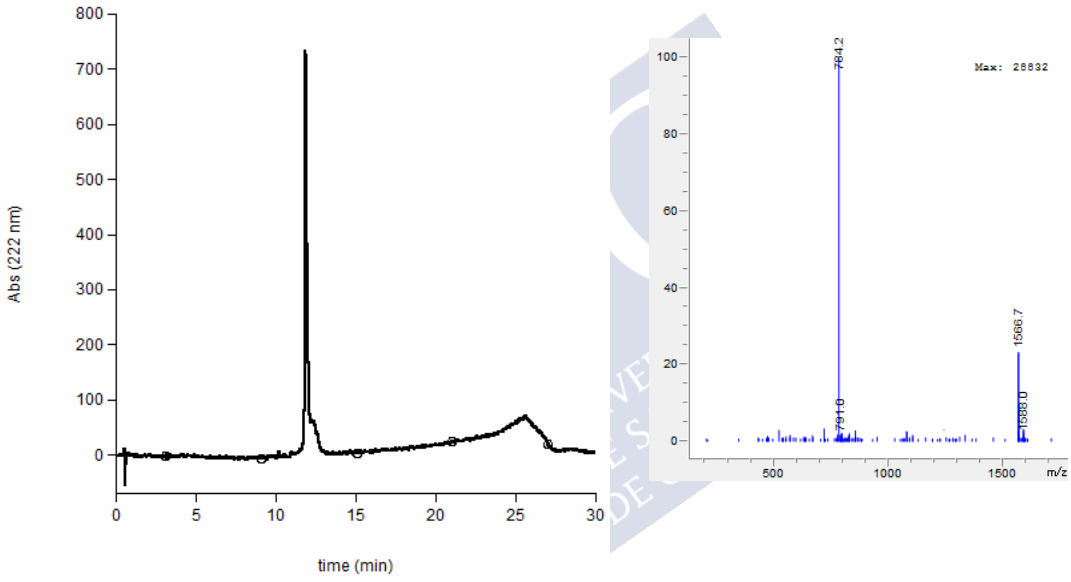

FT-IR (neat, 298 K)

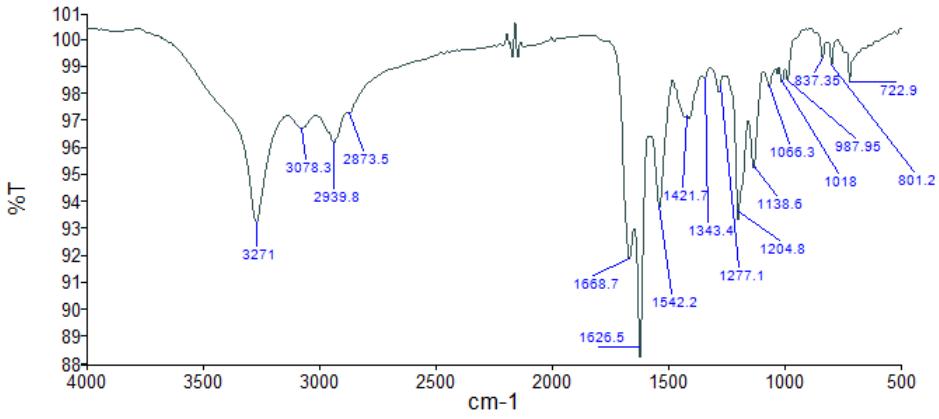

Peptide CP-A2-DOX: *c*-[QKSK^{DOX}SWZK]

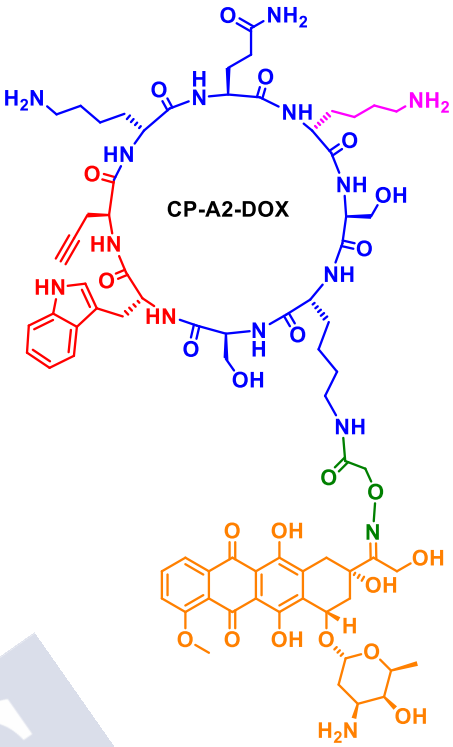

RP-HPLC: [Agilent SB-C18 column, H_20 (0.1% TFA)/ACN (0.1% TFA). 100:0 →100:0 (2 min) and 100:0 → 25:75 (19 min)] (R_t = 11.9 min). Absorbance at 222 nm.

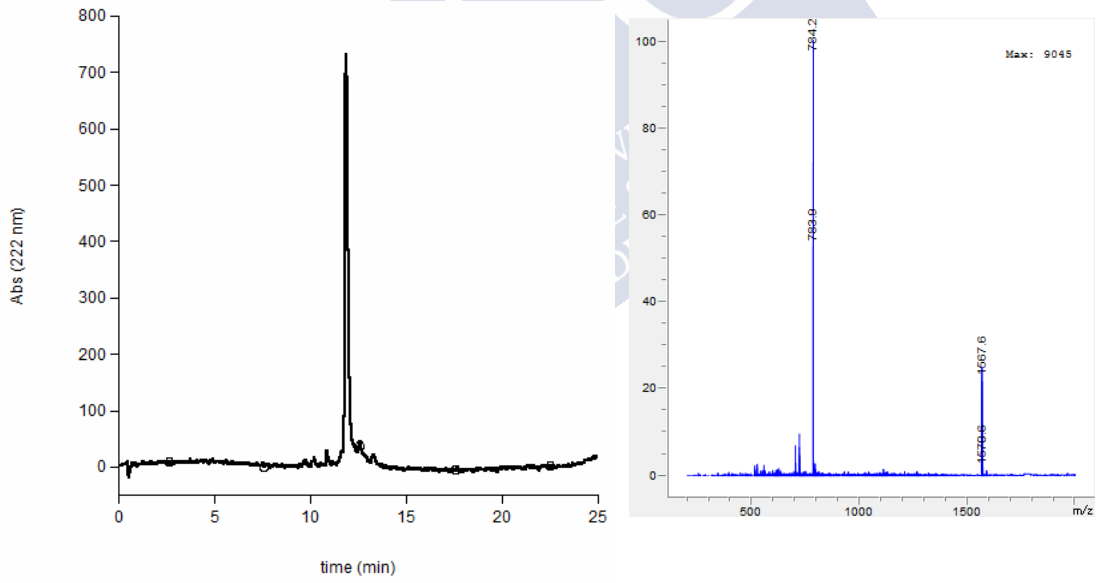

FT-IR (neat, 298 K)

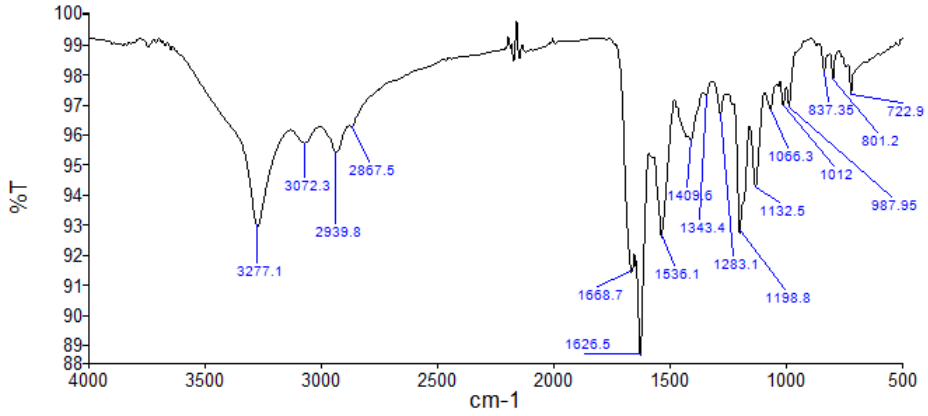

^{1}H-NMR: (H_2O/D_2O, 500 MHz)